Order N° 41582 Confidential until 11th December 2019

University Lille 1

Ecole doctorale des Sciences de la Matière, du Rayonnement et de l'Environnement

University Regensburg

Naturwissenschaftliche Fakultät IV – Chemie und Pharmazie

Dissertation as co-tutelle

for the degree

Doctor of the University Lille 1 (*Molécules et matière condensée*)

and **Doctor of the University Regensburg** (*Naturwissenschaften, Dr. rer. nat.*)

Andrea MÜHLBAUER

Synthesis and physicochemical characterization of novel biocompatible ionic liquids for the solubilization of biopolymers

PhD thesis under the supervision of:

Prof. Véronique NARDELLO-RATAJ and Prof. Werner KUNZ

Defense on 11th December 2014

Members of the jury:

Dr. François Jérôme	CNRS, University Poitiers	**Reviewers**
Prof. Stefan Stolte	University Bremen	
Prof. Dirk de Vos	University Leuven	**Examiners**
Prof. Dominik Horinek	University Regensburg	
Dr. Boris Estrine	Company A.R.D.	
Prof. Véronique Nardello-Rataj	University Lille 1	**Supervisors**
Prof. Werner Kunz	University Regensburg	

Acknowledgements

The work described in this PhD thesis has been carried out as collaboration between the *laboratory of molecular chemistry and formulation* (director of the laboratory: Prof. Dr. Jean-Marie Aubry, *University of Lille*, France) under the supervision of Prof. Dr. Véronique Nardello-Rataj, and at the *institute of physical and theoretical chemistry* (*University of Regensburg*, Germany) under the co-supervision of Prof. Dr. Werner Kunz. Additionally, this PhD thesis was part of an industrial project financed by the society *A.R.D. – Agro-industrie recherches et développements* (CIFRE, co-financed by ANRT) under the direction of Dr. Boris Estrine. I would like to express my honest thanks to them for having welcomed me in their laboratories and teams, and for having given me the opportunity to work on this interesting project.

I would like to express my sincere gratitude to Prof. Dr. Veronique Nardello-Rataj who supervised my thesis during the last three years. Thank you for guiding my work in an ambitious way and having faith in my work and decisions. Furthermore, I would like to thank deeply my co-supervisor Prof. Dr. Werner Kunz for his scientific advices. I extend these thanks to my industrial supervisor Dr. Boris Estrine from A.R.D. not only for the helpful discussions but also for the financial support.
I am grateful to the jury members, the reviewers Dr. François Jérôme and Prof. Stefan Stolte, and the examiners Prof. Dr. Dirk de Vos and Prof. Dr. Dominik Horinek, for having accepted to take their time and to bring their experience to evaluate this manuscript.

I would like to acknowledge the team of A.R.D. for their experimental support, especially Dr. Sinisa Marinkovic for some syntheses and Marianne Dargelos for the biodegradation tests. Furthermore, I am grateful to Dr. François Jérôme and his team for the fruitful cooperation of the study on cellulose solubilization. I would like to thank Prof. Stefan Stolte and Marta Markiewicz for carrying out several biodegradation and toxicity tests. I thank the team of Cosmo*logic*, especially Dr. Andreas Klamt, Dr. Micheal Diedenhofen and Dr. Jens Reinisch, for their advices, help and discussions in support of COSMO-RS calculations. I am also grateful to the assistant professor Dr. Frédéric Cazaux for using the equipment for the TGA- and DSC- measurements. I would like to express my thanks to Estelle, Bingyu, Marie and Remi for their contribution and cooperative efforts on helping me with some experiments throughout the scope of this work.

I would like to thank the assistant professors Valérie Molinier, Christel Pierlot, Loïc Leclercq and Raphael Lebeuf for supporting this project with their generous help and inspiring discussions.

I would like to express my sincere gratitude to my colleagues and friends of the lab for sharing this special atmosphere and their extraordinary support, without going into details: Adrien B., Adrien M., Aurélie, Benjamin, Bing, Christophe, Clémentine, Delphine, Fermin, Mickael, Laura, Laurianne, Maxime N., Maxime R., Roberto, Romain, Thomas.

Finally, I would like to express my deepest thanks to my family, especially my mother, sister and grandmother for their inestimable support. And very special tanks go to Jérémie - thank you infinitely for everything - especially for giving me strength and incredible encouragement in hard times.
I dedicate this manuscript to my father.

Abstract

During the last fifteen years, green chemistry became a central topic of academic and industrial research which is still progressively growing. In this context, many researchers are interested in alternative solvents which are environmentally friendly. Among them, there are ionic liquids (ILs) and deep eutectic solvents (DESs). The aim of the thesis was to development of new biocompatible ILs and DESs for the solubilization of biopolymers, such as cellulose. Short-chain two- and three-tailed quaternary alkylammonium (C_3 - C_6) associated with various biosourced carboxylates (*e.g.* itaconate, lactate, levulinate) have been good candidates and the identification of structural key factors for cellulose solubilization was realizable. This systematic approach coupled with extensive physicochemical study of ILs, resulted in the levulinates of [DiC_3], [DiC_4] and [$TriC_4$] and [DiC_4]itaconate as the most efficient with a solubilization of cellulose up to 10 %, or even 20 % in the presence of the bio-based co-solvent γ-valerolactone. Despite their good biodegradability in comparison with that of imidazolium, quaternary ammonium are not naturally resourced. They were therefore, in a second step, substituted by derivatives of choline, betaine and carnitine as biocompatible cations, associated with the above carboxylates. The ether- and ester-derivatives are ILs, and ethyl-choline ether levulinate is able to solubilize 10 % cellulose. Moreover, urea combined with dibutylammonium salts or betaine esters behave as DESs with melting temperatures around 30 to 40 °C. In the same way, DESs based on sugar-derivatives having an ether function on the anomeric carbon has been obtained in the presence of salts of choline, betaine and carnitine. Finally, a theoretical approach using the COSMO-RS software was used to model the properties of ILs and DESs and for predictions of cellulose solubilization.

Keywords: biocompatible solvents, ionic liquid, deep eutectic solvent, cellulose, biopolymer, solubilization, biodegradability, hydrotrope, COSMO-RS, choline, betaine, carnitine, levulinate, itaconate.

Résumé

Depuis une quinzaine d'années, la chimie verte, devenue un axe prioritaire des recherches académiques et industrielles, connait un développement considérable. Dans ce contexte, de nombreuses recherches s'intéressent aux solvants alternatifs, respectueux de l'environnement. Parmi eux, on trouve les liquides ioniques (LIs) et les eutectiques profonds (DESs). L'objectif de la thèse était de développer de nouveaux LIs et DESs biocompatibles pour la solubilisation de biopolymères tels que la cellulose. Les alkylammonium quaternaires à chaîne courte (C_3 à C_6) bi- et tricaténaires associés à divers carboxylates d'origine naturelle (*e.g.* itaconate, lactate, lévulinate) se sont révélés être de bons candidats et ont permis d'identifier les effets structuraux clés pour la solubilisation de la cellulose. Par cette approche systématique couplée à une étude physicochimique approfondie des LIs, les lévulinates de [DiC_3], [DiC_4] et [$TriC_4$] et l'itaconate de [DiC_4] sont les plus efficaces et permettent de solubiliser jusqu'à 10 % de cellulose, voire 20% en présence d'un co-solvant biosourcé, la γ-valérolactone. Malgré leur très bonne biodégradabilité en comparaison à celle des imidazolium, les ammonium quaternaires ne sont pas naturels. Ils ont donc été, dans un second temps, substitués par des cations biocompatibles dérivés de la choline, de la bétaïne et de la carnitine, associés aux carboxylates précédents. Les dérivés de type éther et ester sont des liquides ioniques et l'éthyl-choline éther lévulinate permet de solubiliser 10% de cellulose. Par ailleurs, en présence d'urée, les sels de dibutylammonium et les esters de bétaïne se comportent comme des DESs dont les températures de fusion sont de l'ordre de 30 à 40 °C. De même, des DESs à base de dérivés de sucre possédant une fonction éther sur le carbone anomérique ont été obtenus en présence des sels de choline, de bétaïne et de carnitine. Enfin, une approche théorique utilisant le logiciel COSMO-RS a été utilisée pour la modélisation des propriétés des LIs et des DESs ainsi que pour la solubilisation de la cellulose afin de la prédire.

Mots clés : solvants biocompatibles, liquide ionique, eutectique profonde, cellulose, biopolymère, solubilisation, biodégradabilité, hydrotrope, COSMO-RS, choline, bétaïne, carnitine, lévulinate, itaconate.

Abbreviations

Ace	Acetate
Cit	Citrate
CMC	Critical micelle concentration
[C_n-Bet]	Alkyl betaine ester
[C_n-Carn]	Alkyl carnitine ester
[C_n-Chol]	Alkyl choline ether
COSMO-RS	Conductor-like screening model for real solvents
DES	Deep eutectic solvent
DG	Degree of polymerization
DMSO	Dimethylsulfoxide
DSC	Differential scanning calorimetry
For	Formate
Fum	Fumarate
Gly	Glycolate
GVL	γ-Valerolactone
HBA	Hyrogen bond acceptor
HBD	Hydrogen bond donor
5-HMF	5-Hydroxymethylfurfural
HSP	Hansen solubility parameter
IL	Ionic liquid
Ita	Itaconate
Lac	Lactate
Lev	Levulinate
LTTM	Low transition temperatur mixture
MAC	Minimal aggregation concentration
Mala	Malate
Male	Maleate
Mand	Mandelate
MCC	Microcrystalline cellulose
NMMO	*N*-Methylmorpholine-*N*-oxide
QACIL	Quaternary ammonium carboxylate ionic liquid
RTIL	Room temperature ionic liquid
Sal	Salicylate

Sor	Sorbate
Suc	Succinate
SXS	Sodium xylene sulfonate
Tar	Tartrate
T_b	Boiling temperature
T_{deg}	Degradation temperature
T_f	Freezing temperature
T_g	Glass transition temperature
TGA	Thermogravimetric analysis
T_m	Melting temperature
wt%	Mass fraction

INTRODUCTION

In recent years, the research on novel eco-friendly classes of solvents has gained more and more importance with the consciousness of "greener" processing. The term *"green" chemistry* has been defined as "*the invention, design and application of chemical products and processes to reduce or to eliminate the use and generation of hazardous substances*".[1] In the context of the development of sustainable solvent media, especially ionic liquids (ILs)[2] and deep eutectic solvents (DESs)[3] have appeared very promising for the replacement of volatile organic solvents. **Figure I.1** illustrates the most important milestones in the field of ILs and DESs.[4] Even though the first IL was introduced in 1914, this discovery had no real impact until the end of the 20th century. However, research on these so-called designer solvents has become a hot topic in various scientific and technological areas during the last twenty years.

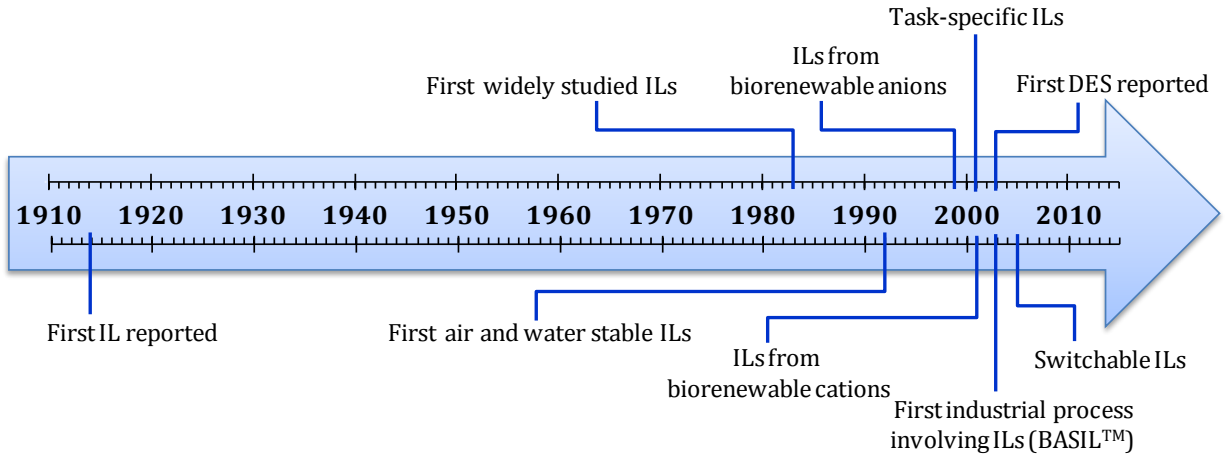

Figure I.1 Milestones in the development of knowledge in the field of ILs and DESs.[4]

The use and transformation of renewable raw materials, *i.e.* biomass and biopolymers, is a further important aspect of "green" chemistry with the aim to replace petro-sourced products. For biomass processing, the main focus lies on cellulose because it is the major natural resourced biopolymer produced by plants' photosynthesis.[5] This raw-material, built of a rich structure, is of high interest for many different applications and transformation processes due to its high occurrence, renewability and biodegradability (**Figure I.2**).

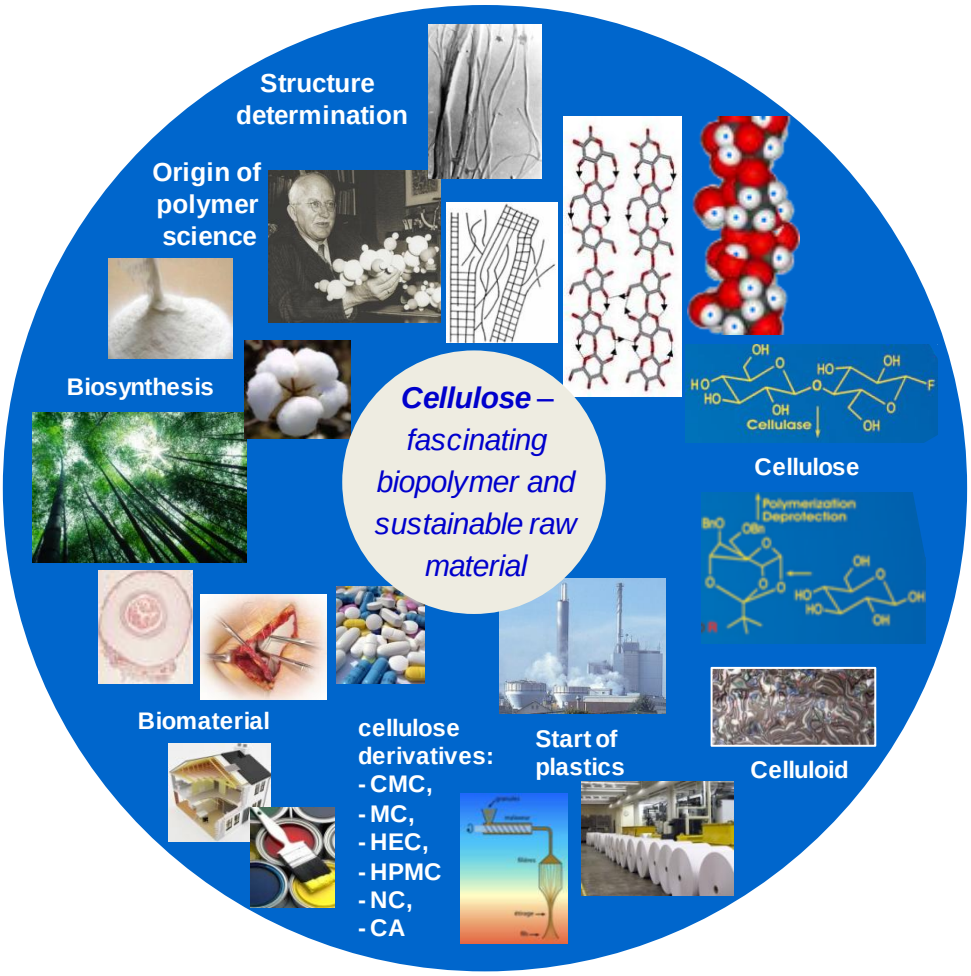

Figure I.2 Overview for cellulose: discovery, structure, biosynthesis, applications.[6]

A resistant fibrous solid was described in 1838 by the French chemist Anselme Payen using the term "cellulose".[6] The detailed polymeric structure of cellulose was determined by Hermann Staudinger in 1920.[7] Thousands of years prior to the discovery of the "sugar of the plant cell wall", cellulose was used in the form of wood, cotton, and other plant fibers as an energy source, for building materials, and for clothing.[6] Today, most of the cellulose is used for the production of paper and cardboard. Furthermore, the production of cellulose fibers and films, as well as the synthesis of a large number of cellulose-derivatives (CMC: carboxymethyl cellulose, MC: methyl cellulose, HEC: hydroxyethyl cellulose, HPCM: hydroxypropylmethyl cellulose, NC: nitrocellulose, CA: cellulose acetate) are important sectors. On an industrial scale, cellulose is used for coatings, laminates, optical films and sorption media, and furthermore for property-determining additives in building materials, pharmaceuticals, foodstuffs, and cosmetics. Some new applications in the field of biomaterials have been reported, such as immobilization of proteins, antibodies and heparin. Well-known cellulose-derived thermoplastics based on nitrocellulose and camphor are celluloids.[8] Celluloid is easily molded and shaped, and it found generally its application for movie

and photography films. However, it is highly flammable, and difficult and expensive to produce, thus today it is no longer widely used.

In our days, the research on cellulose as a renewable raw material is still a growing field of interest. For the production of platform molecules or cellulose derivatives, cellulose has to be extracted from biomass before its solubilization and / or reduction of polymerization degree (**Figure I.3**). In this project, we focused on the solubilization of biopolymers, especially cellulose, with novel biocompatible solvents with regard to the principles of "green" chemistry. In the course of this study, mainly ILs were applied as cellulose solvents.

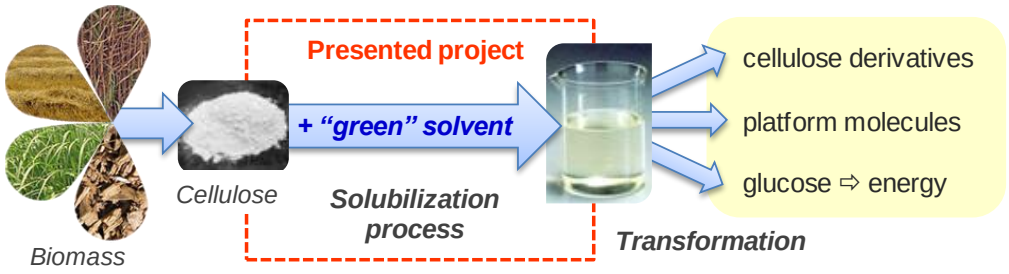

Figure I.3 The presented project in the context of biomass transformation.

The project of this PhD thesis deals with the synthesis and characterization of novel biocompatible solvents for the solubilization of biopolymers, mainly cellulose. As schematically represented in **Figure I.4**, the PhD thesis was carried out within the frame of a cotutelle between the University of Lille1 (France) and the University of Regensburg (Germany), as well as in the context of an industrial project with the French company A.R.D. – *Agro-industrie recherches et développements*.

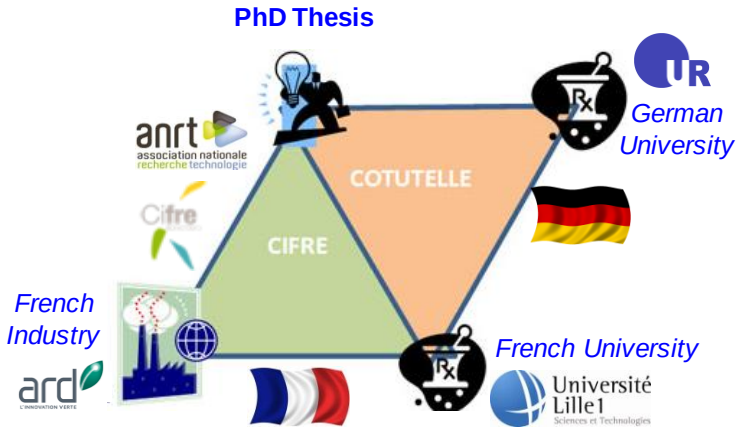

Figure I.4 Situation of the PhD thesis as Cotutelle (France, Germany) and industrial project (Cifre) with A.R.D.

First of all, ILs with alkyl-chained quaternary ammonium cations were tested with the aim to determine their structural effect, like size and number of alkyl-chains on both their physicochemical properties and their capacity to solubilize cellulose. The counter anions were

constituted of various natural carboxylates, which were screened in combination with different cations in order to evaluate their cellulose dissolution power.

In a further step, the targeted ILs were changed with regard to the optimization of their properties being in unison with the "green" chemistry principles. We concentrated on ILs cations derived from natural products, such as choline, betaine and carnitine. The synthesized ether- and ester-derivatives of choline, betaine and carnitine were combined with natural carboxylates, similar to the first part of the study, to give ILs which were studied for the cellulose dissolution process.

An additional part of the project deals with DESs, another class of "green" solvents which shows a growing potential for various applications. Therefore, bio-based sugar-derivatives, which could be obtained from cellulose, were used for the formation of DES and low melting mixtures. For the moment, their main application is the decrease melting temperature of salts and solids, thus the simplification for several processes.

In the context of "green" chemistry, theoretical modeling also becomes more and more important to support or even avoid experimental work. Consequently, chemicals, energy and waste could be saved or prevented. Hence, in this project, the software COSMO-RS was used to carry out theoretical calculations with the aim to assist experimental results.

CHAPTER 1 - Molten salts and ionic liquids for biopolymer solubilization: State of the art

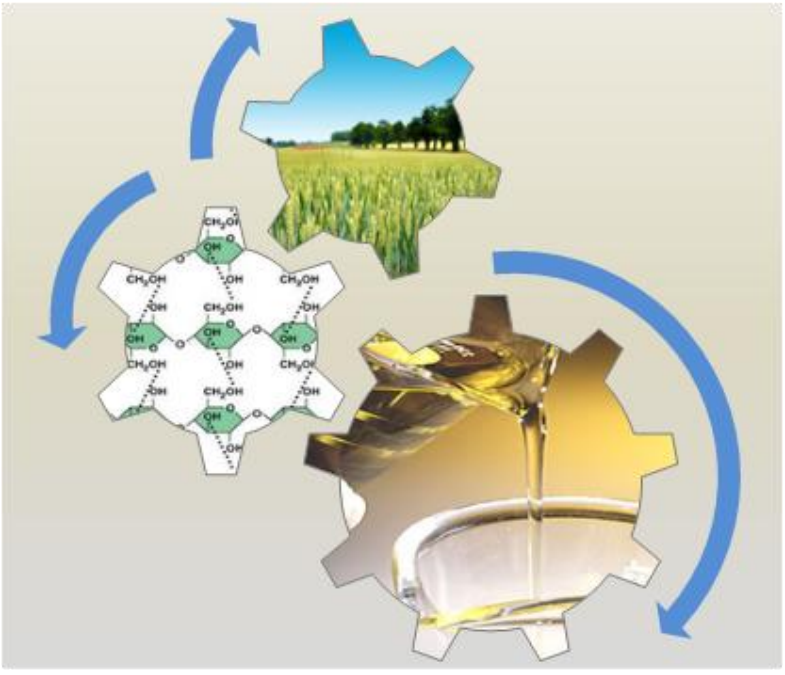

1.1 Biomass and biopolymers

Biomass gains more and more importance as an alternative to fossil resources in the course of "green" chemistry.[9] It is a renewable source from natural raw materials and it occurs often as waste product during transformation processes, thus its use as alternative to petrochemicals is of huge interest.[10] A survey of the literature with the keyword "biomass" highlights a huge and exponential development during the last decade. **Figure 1.1** shows the great increase of publications dealing with "biomass" during the last thirty-five years (the bibliometric analysis was carried out with the database Scifinder®). In 1980, we find ≈ 850 publications against ≈ 1300 publications in 1990, ≈ 3300 publications in 2000 to reach ≈ 20500 publications in the year 2013.

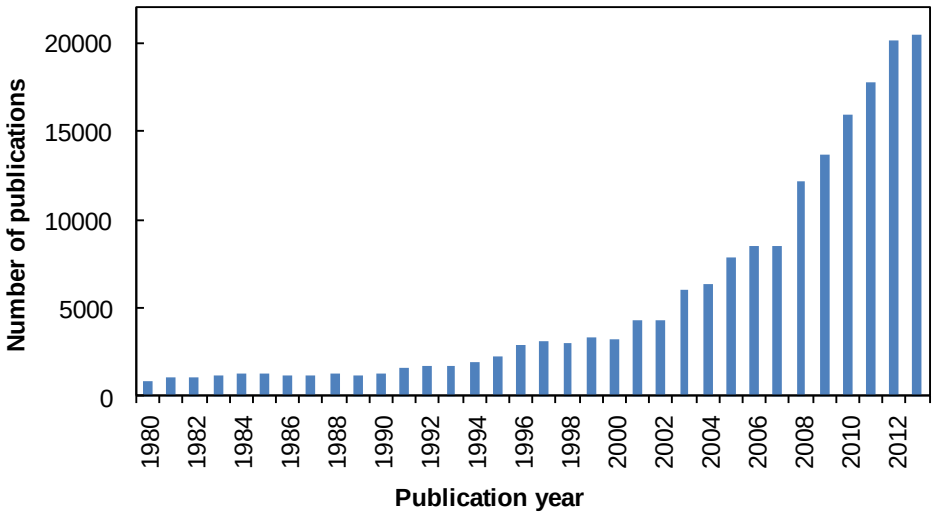

Figure 1.1 Number of publications dealing with "biomass" as a function of the publication year (analyzed with the database Scifinder®)

1.1.1 Biomass - Natural sources and structures of biopolymers

Biomass is obtained from different natural sources such as forestry, agricultural and industrial crops and residues, municipal solid waste, animal residues and sewage.[11] During pretreatment and extraction processes, various biopolymers can be gained from crude biomass. These biopolymers can be used as renewable resources for further transformation processes to obtain biofuels or fine chemicals. The most important biopolymers are found in three different polymer families, namely **polasaccharides**, **polypeptides** and **polyesters** (**Figure 1.2**).[10] The most important polysaccharides are **cellulose**, **starches** (namely amylose and amylopectin), **chitin**, **chitosan** and **pectins**. The main natural resourced polypeptides are **casein**, **wheat gluten**,

keratin and **collagen**. In the the group of polyesters, we find **polylactic acid**, **polyhydroxybutyrate** or **polyhydroxyalkanoates**.

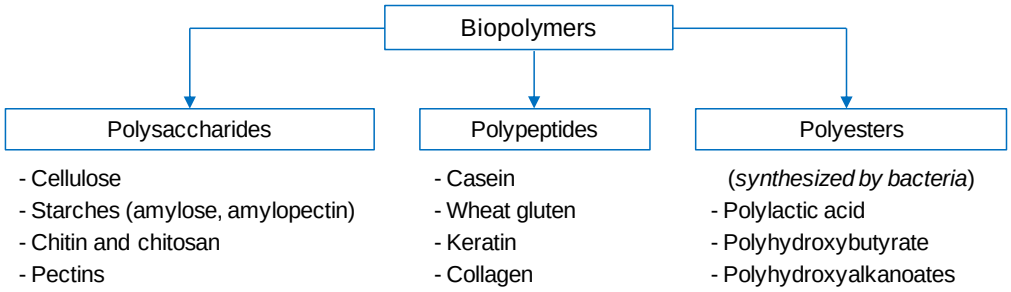

Figure 1.2 Schematic overview of the most important families of biopolymers: polysaccharides, polypeptides and polyesters.[10]

In general, ligno-cellulosic biomass is the most used natural raw material because of its high world-wide occurrence. In fact, 170 billion tons of biomass per year are produced by photosynthesis in nature; 75% of them are carbohydrates.[9] Ligno-cellulosic biomass is composed of **40-50 % cellulose**, **25-35 % hemicellulose** and **15-20 % lignin** (**Figure 1.3**).[12] **Cellulose** is composed of a polymeric structure of *β*-glycosidic-linked glucose units which results in a rigid cristallinity. The hemicellulose portion of lingo-cellulosic biomass contains generally five different sugar-monomers: *D*-xylose, *D*-arabinose, *D*-galactose, *D*-glucose and *D*-mannose. **Lignin** is an amorphous polymer including methoxylated phenylpropane structures, such as coniferyl alcohol, sinapyl alcohol and coumaryl alcohol.[12] The major carbohydrate produced by plant photosynthesis is cellulose, so this is the most plentiful organic polymer on Earth.[13] Accordingly, its use as a renewable resource for further conversions to chemical products is more and more important for "green" performances. Intended for further transformation processes, biomass has to be fractioned into its single components, namely cellulose, lignin and hemicellulose. Different pretreatment techniques are used for the isolation of biomass fractions. Most of the pretreatment processes contain physical, chemical or

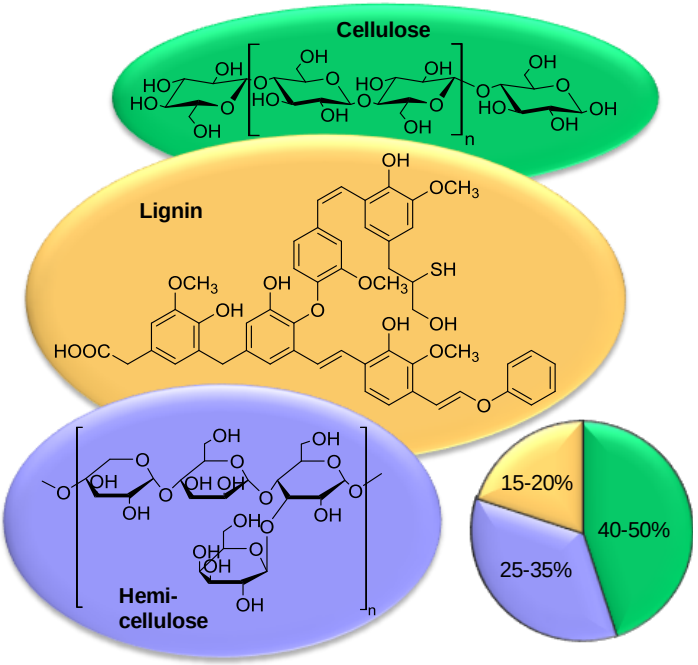

Figure 1.3 Composition of lignocellulosic biomass: cellulose (40-50%), hemicelluloses (25-35%) and lignin (15-20%).[4]

biological procedures.[14] The physical pretreatment method deals mainly with the mechanical size reduction obtained by milling, comminuting or steam.[12] These processes augment the available specific surface area, and decrease both the degree of polymerization and the cellulose crystallinity.[14] For chemical pretreatment ways, mainly acids, alkali and organic solvents are used. Thereby, the native structure of lingo-cellulosic biomass is not influenced. Biological pretreatment ways include essentially the action of enzymes that can degrade lignin, hemicelluloses and polyphenols.[14]

1.1.2 Application of biopolymers and their transformation to platform chemicals

Biopolymers are more and more used as alternatives to petro-chemistry in the course of biorefining processes.[15] Ligno-cellulosic biomass can be transformed into biomolecules and bioderivatives *via* different pathways, as shown in **Figure 1.4**, which give platform molecules for fine chemicals, *e.g.* **furfural**, **5-hydroxymethylfurfural** or **levulinic acid**.[16] Cellulose is particularly interesting for biorefining industries because of its high appearance in nature and its potential for various transformations.

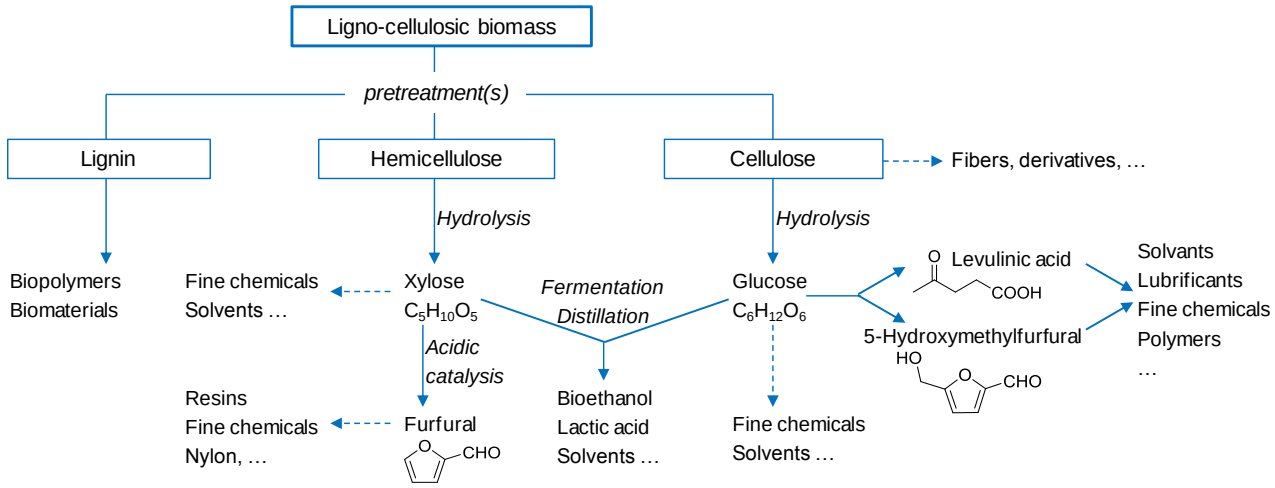

Figure 1.4 Overview of biorefining processes for lingo-cellulosic biomass.[15]

In **Figure 1.5**, the most important platform molecules obtained by cellulose transformations are shown.[17,18] Possible reactions of cellulose to glucose contain enzymatic or acid catalyzed hydrolysis, with a further transformation of glucose to ethanol *via* fermentation. Further products obtainable by biocatalytic transformation processes of glucose are **succinic**, **itaconic**, **glutamic**, **glutaric** and **lactic acids**. Other chemocatalytic transformations of glucose include the hydrogenation to sorbitol or the direct hydrogenolysis of cellulose to sugar alcohols. As a result, sorbitol can be first dehydrated to sorbitan and then to isosorbide or reacted *via* further reactions to glycerol and propylene or ethylene glycol, as well as various C_1 to C_6 mono- and

polyols and even alkanes. Otherwise, 5-hydroxymethylfurfural (5-HMF) can be obtained by acid catalyzed dehydration of glucose, which can be further transformed to levulinic acid.[19]

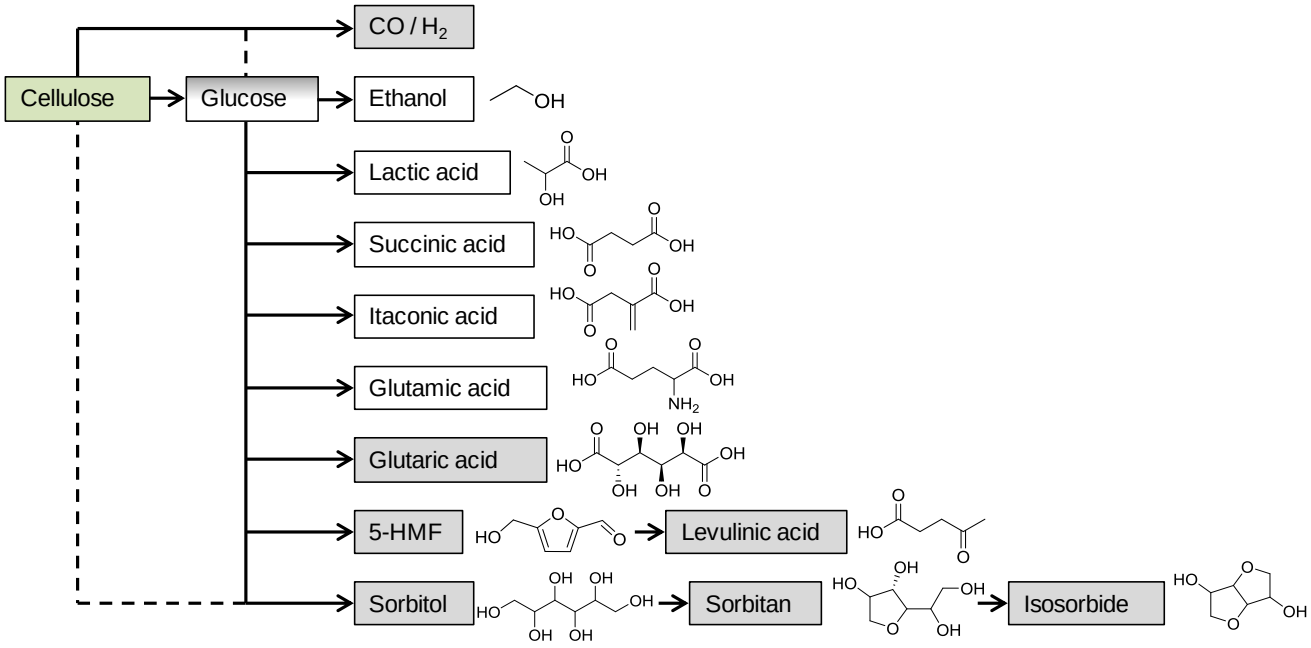

Figure 1.5 Schematic overview of cellulose transformation to platform chemicals *via* biocatalytic (white) or chemocatalytic (grey) processes.[17]

A highly efficient hydrolysis process of cellulose to glucose was described by Wang *et al.* using heteropoly acids ($H_3PW_{12}O_{40}$) as catalyst under hydrothermal conditions.[20] With this process, a high yield of glucose (50.5%) and selectivity higher than 90% are achieved at 180 °C for 2 h with a mass ratio of cellulose to $H_3PW_{12}O_{40}$ of 0.42. Up to this, different methods with solid acid catalysts have already been described for the dissolution of cellulose. Another example shows the hydrolysis of saccharides, like cellulose and starch, with the layered transition metal oxide $HNbMoO_6$ which exhibited a significant catalytic performance.[21]

1.1.3 Classical solvents and solubilization processes

Generally, the solubilization of polymers is a complex process because of the various and numerous interactions within the polymer and between polymer molecules which play important roles for their rigid structure.[22] However, solubilization of lignocellulosic biomass, native lignin, for instance, can be very useful for its conversion into aromatics, phenols and saturated cyclic derivatives.[23] The general process consists of chemical pulping (*e.g.* Kraft pulping) including strong acids or bases under high pressure at high temperature.[24,25] In particular, the biopolymer cellulose is complex to dissolve because of its very stable supra-molecular structure resulting from strong interactions, especially hydrogen bonds (**Figure 1.6**).[26] Cellulose consists of polydisperse linear glucose chains, where *D*-glucopyranoside-units

are linked together by β-1,4-glycosidic bonds. The size of the molecule is depending on the degree of polymerization (DP) and can vary between 20 – 10 000 units, according to the type of cellulose (*e.g.* 10 for laboratory-synthesized cellulose or 10 000 or more for bacterial cellulose).[26] Between the glucose-chains, there are inter- and intra-molecular hydrogen bonds which cause the highly stable structure. For these structural properties, the hydrolysis process, and therefore the solubilization of cellulose, is very complex. For many decades, the research for ideal cellulose solvents (high dissolution capacity, cheap, low viscous, stable, non-toxic, ecologically friendly, easy to recycle) is a great challenge both for academics and industrials.

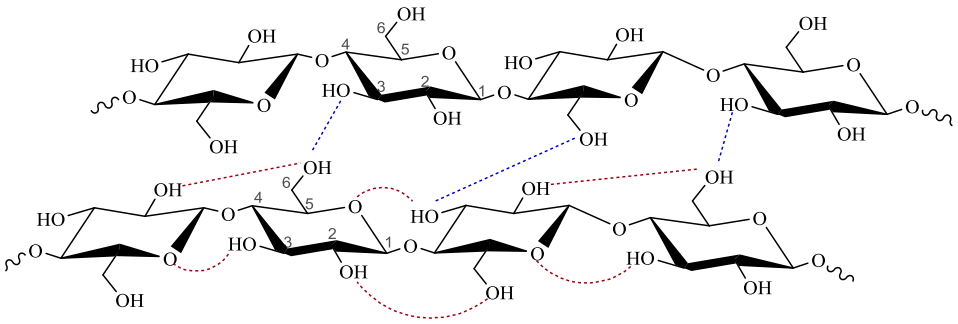

Figure 1.6 Structure of cellulose with its intramolecular (- - -) and intermolecular (- - -) hydrogen bonds.[26]

Usually, successful cellulose solvents must possess the ability to compete for existing intermolecular hydrogen bond interactions, in order to separate the polymer chains from each other, resulting in the dissolution of the biopolymer.[27] So far, different classical solvents are used for the solubilization of cellulose, which are classified as **derivatizing** and **non-derivatizing solvents**, depending on their interactions with the polysaccharide.[2] In contrast to non-derivatizing solvents which dissolve the polymer only by intermolecular interactions, derivatizing ones interact chemically with the cellulose hydroxyl groups and form intermediates.[27] Some traditional solvent systems were found to be efficient, such as *N*-methylmorpholine oxide,[28] *N*,*N*-dimethylacetamide / lithium chloride,[29] 1,3-dimethyl-2-imidazolidinone / lithium chloride,[30] *N*,*N*-dimethylformamide / nitrous tetroxide,[31] dimethyl sulfoxide / tetrabutylammonium fluoride,[32] and some molten salt hydrates (*e.g.* $LiClO_4$, LiSCN, $ZnCl_2$).[33] **Figure 1.7** gives an overview of the structure of the most traditional cellulose solvents: 1) *N*,*N*-dimethylacetamide / lithium chloride (DMA / LiCl); 2) dinitrogen tetroxide / dimethylformamide (N_2O_2 / DMF); 3) *N*-methylmorpholine-*N*-oxide (NMMO); 4) mineral acids: sulfuric acid, phosphoric acid, etc.; 5) sodium hydroxide; 6) dimethylsulfoxide / tetrabutylammonium fluoride (DMSO / TBAF); 7) dimethylimidazolone / lithium chloride; 8) molten salt hydrates : $LiClO_4$, LiSCN, $ZnCl_2$.

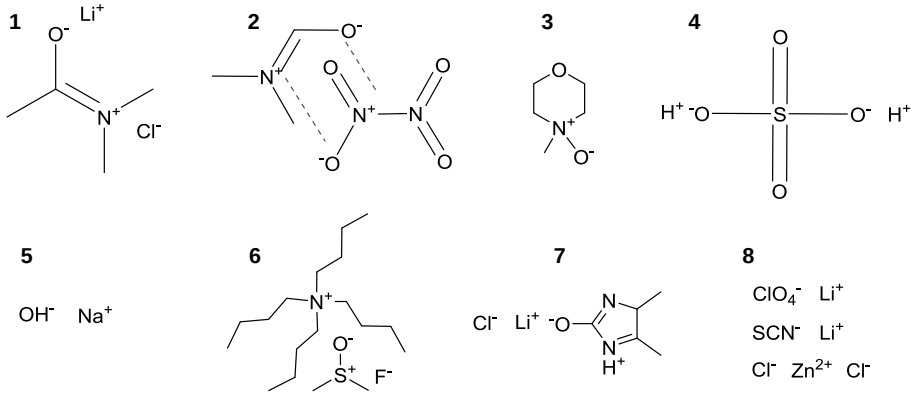

Figure 1.7 Classical cellulose solvents: 1) DMA / LiCl; 2) N_2O_2 / DMF; 3) NMMO; 4) mineral acids: H_2SO_4, H_3PO_4, etc.; 5) NaOH; 6) DMSO / TBAF; 7) dimethylimidazolone / LiCl; 8) molten salt hydrates : $LiClO_4$, LiSCN, $ZnCl_2$.[34]

It has been shown that all non-derivatizing solvents can hypothetically be arranged in cyclic structures (**Figure 1.8**).[26] Small ions or polar characteristics assist in the ring-formation of five- or six-ring geometries; larger cations, such as NMMO or TBA seem to be less-suited for this purpose. However, fluoride is a very small anion and the involvement of an additional dipolar molecule (DMSO) can compensate for the unfavorable steric geometry of the cation. Therefore, one expects that larger anions, such as chloride or bromide, are less capable to dissolve cellulose. The ion size governs the ion mobility, and therefore influences the ion's ability to penetrate and attack the cellulose network; the smaller the ion, the more favorable. This explains why the addition of salts composed of small ions, such as lithium chloride, is favorable for the cellulose dissolution.[26]

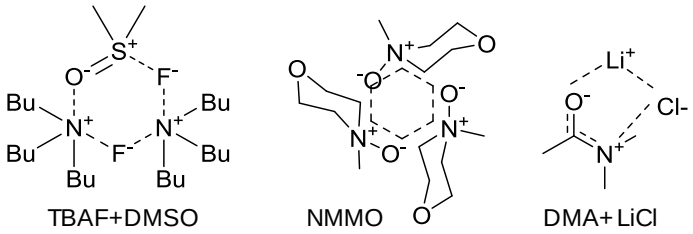

Figure 1.8 Hypothetical ability of traditional non-derivatizing cellulose solvents to arrange in cyclic formations: TBAF + DMSO (6-ring geometry); NMMO (6-ring geometry); DMA + LiCl (5-ring geometry).[26]

At first sight, from their solubilization capacity of cellulose, these solvents are satisfactory but from an ecological point of view, they are not ideal. All of the traditional cellulose solvents suffer from some drawbacks like toxicity, volatility, high cost, recovery, or insufficient solvation power.[35,36] Hence, the development of alternative cellulose solvents, containing notably "greenness" and high efficiency, persists as an active field of research. For the general evaluation of eco-friendly solvents, both the **toxicity** (the degree at which a substance can damage an organism) and the **biodegradation** (the decomposition of materials by micro-organisms) have

become essential criteria.[37] In 1998, Paul Anastas and John Warner have stated the "twelve principles of green chemistry" as guidelines for sustainable chemistry and processes (**Figure 1.9**).[38] These rules guide the design of new chemical products and processes, holding all features of the process life-cycle from the raw materials to the efficiency and safety of the transformation, the toxicity and biodegradability of products and reagents. First, waste should be avoided. Second, the incorporation of starting materials in the final product of syntheses should be maximized (atom economy). Third, the used and generated products of chemical syntheses should have little or no toxicity to human health and the environment. Safer chemicals should be designed, and used auxiliary substances should be safe or avoided. Energy efficiency should be respected during chemical processes, thus syntheses should be carried out at ambient temperature and pressure if possible. The seventh principle recommends the use of renewable feedstock as raw material. The eighth rule deals with the reduction of derivatives during processes due to the minimization of auxiliaries and waste. Catalytic procedures are preferred, especially very selective ones. The tenth rule prescribes design of degradation of chemical products, so that they do not persist in the environment. Real-time analysis methods are avoided with the aim to control directly the formation of hazardous substances. The twelfth principle deals with processes working with a minimal potential for chemical accidents, including releases, explosions, and fires.

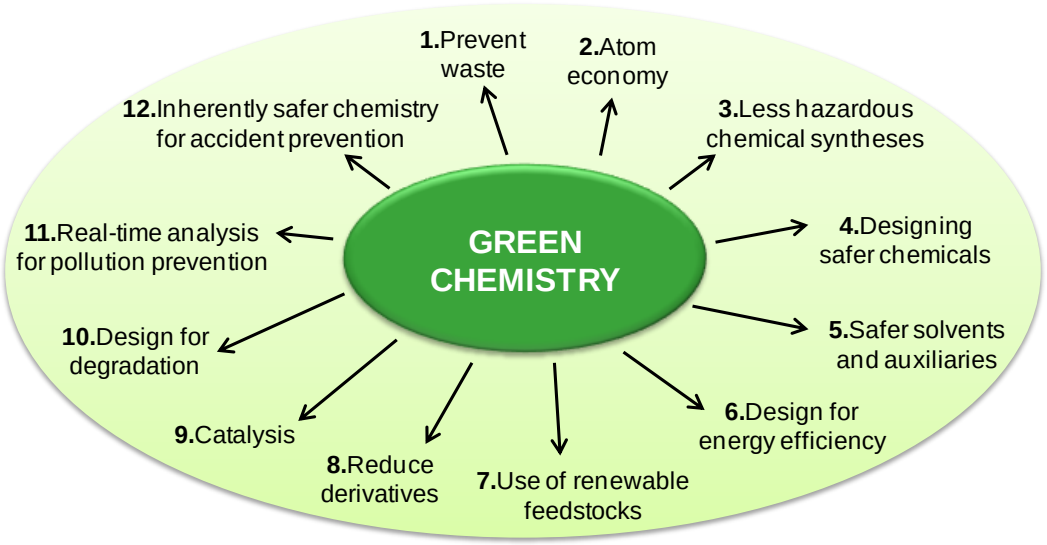

Figure 1.9 The twelve principles of "green" chemistry.[38]

Regarding the main guidelines for "green" chemistry, alternative solvents and solubilization processes for cellulose or other biopolymers are necessary to take benefit from renewable feedstock in a sustainable way. With the development of alternative processing ways, a new class of "green" solvents, namely **ionic liquids**, was introduced to the field of cellulose dissolution.

1.2 Ionic liquids

Since a while, a new class of solvents, called **ionic liquids (ILs)**, has emerged. These solvents are composed of ionic species and their melting temperature is below 100 °C by definition.[2]

In 1914, the first room temperature IL was discovered by Walden, namely **ethylammonium nitrate [$EtNH_3$][NO_3]**, with a melting temperature of 12 °C.[39] However, more research on ILs only really started some decades later. In 1975, research work on room temperature liquid chloro-aluminate melts was published with the focus on electrochemical applications.[40] In the 1980s, **alkyl-substituted imidazolium** and **pyridinium molten salts** were developed for their application as battery electrolytes.[41] A bibliometric analysis with the database Scifinder® was carried out with the keyword "ionic liquid" which shows a great increase of scientific interest during the past years (**Figure 1.10**). In 1990, only 39 publications were found, ten years later ≈ 200, and further ten years later, in 2010, already ≈ 5600. There is a continual growing interest in ILs, especially in **room temperature ILs (RTILs)** because of their special properties and various applications.

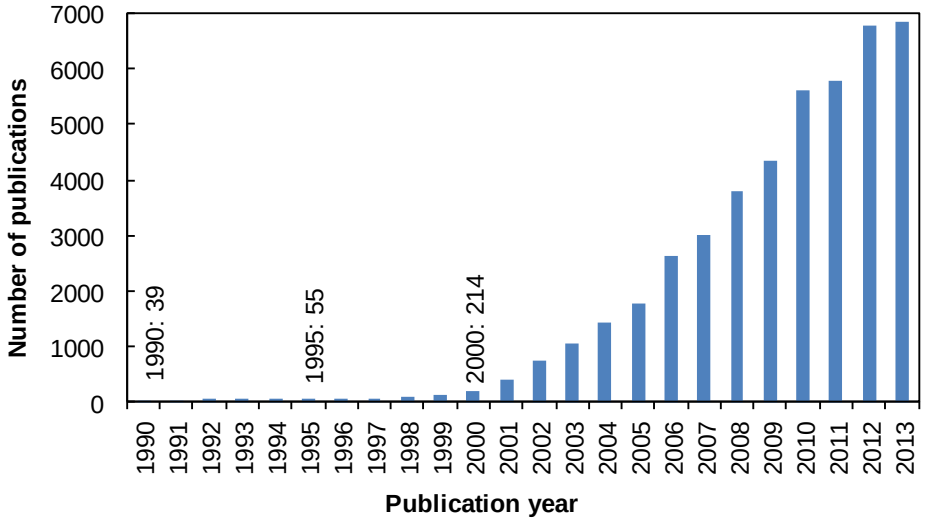

Figure 1.10 Number of publications dealing with "**ionic liquid**" as a function of the publication year (analyzed with the database Scifinder®).

Regarding the huge number of publications on ILs, the whole range of IL's research cannot be discussed at this point. Thus, only a brief overview about their structure, physicochemical properties, applications and ecological aspects is given.

1.2.1 Types and structures of ionic liquids

In general, two main classes of ILs have been defined: **protic** and **aprotic ILs**. **Protic ILs (PILs)** are formed by proton transfer from a Brønsted acid to a Brønsted base.[42] **Aprotic ionic liquids (AILs)** hold other substituents than a proton, such as alkyl groups at the position occupied by a labile proton in an analogous PIL. Because of the acid-base reaction of PILs, neutral acid or base species can be present in the PIL system. Therefore, a guideline was proposed according to which ILs should contain less than 1% of neutral species.[43]

Generally, the formation of ILs depends on structural reasons. For example, a low degree of symmetry is preferred which prevents regular crystalline packing, thus the solid crystalline state becomes less favorable, leading to a low melting temperature.[44] Therefore, common ILs contain typically organic bulky cations, such as imidazolium, pyridinium, quaternary ammonium, pyrrolidinium, piperidinium, tetraalkylphosphonium or trialkylsulfonium. The effect of melting point depression can be further improved with the choice of an anion with a delocalized charge, resulting in decreased inter-ionic interactions.[45] Some examples for typical IL anions are halogenides, nitrate, acetate, sulfate, thiocyanate, tetrafluoroborate, hexafluorophosphate, tosylate, bis(trifluoromethyl sulfonyl)imide. **Table 1.1** gives an overview of the most common IL cations and anions.

Table 1.1 Some classical cations and anions for ILs.

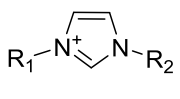	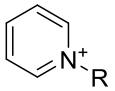	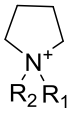	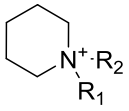	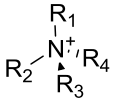	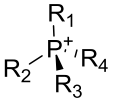	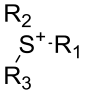
Br-	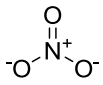		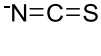	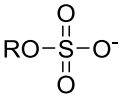	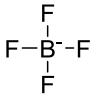	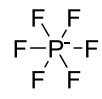	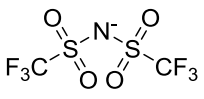

Depending on the choice of ions, ILs can be either hydrophobic or hydrophilic.[46] With the widely used cation imidazolium, **hydrophilic ILs** can be obtained with **halides**, **acetate**, **nitrate** or **ethylsulfate** as anions, whereas **hexafluorophosphate** or **bis(trifluoromethylsulfonyl)imide** give **hydrophobic** ones. But most of the ILs are hygroscopic, even hydrophobic ones. As they can consist of various different combinations of a cation with an anion, ILs are also called "**designer solvents**" or "**task-specific**" with regard to their tunable properties.[47] Accordingly, their properties like thermal and electrochemical stability, melting point, viscosity, polarity, solvent ability or surface tension can be targeted by structural variation.

1.2.2 Physical and chemical properties

The physical and chemical properties of ILs vary strongly depending on their cation and/or anion, as already mentioned. These properties are notably influenced by traces of impurities in the IL. Another important "impurity" in ILs is water, as they are very hygroscopic, so their water content should always be measured. Thus, ILs must be as purified as possible and characterizations should be carried out under inert atmosphere.

1.2.2.1 Thermal properties: stability, liquid range and melting temperature

The liquid range of a compound is defined by its thermal properties, *i.e.* the **melting temperature (T_m)** or **glass transition (T_g)** as lower limits and the **boiling temperature (T_b)** or **decomposition temperature (T_{dec})** as upper limits.[48] Water, for example, has a liquid range of 100 °C (0 to 100 °C) and dichloromethane 135 °C (-95 to +40 °C). ILs, however, can have large liquid ranges, due to their low melting or glass transition and their high thermal stability.

The theoretical correlation between melting temperature and structure of ILs is discussed in several studies.[2,48] But experimental examination of melting temperatures is often more difficult due to their recurrent super-cooling behavior. This phenomenon results typically in different phase transitions depending on the observation during a heating or a cooling event.[49,50] Generally, the crystal packing and thus the melting point of ILs is influenced by several factors, *i.e.* size, charge, charge distribution, intermolecular interactions and symmetry of the ions.[48] A very strong force in ILs is the Coulomb attraction E_C between ions, which is only short-ranged for ILs due to the size, charge distribution and flexible substituents (**Eq. 1.1**):

$$E_C = \frac{MZ^+Z^-}{4\pi\varepsilon_0 r^2} \qquad \textbf{Eq. 1.1}$$

where M is the Madelung constant, which represents the packing efficiency of ions in salts, Z^+ and Z^- are the ion charges and r is the inter-ion separation.[48] The whole lattice energies of ionic salts depend on the product of the net ion charges, the ion-ion separation and the packing efficiency of the ions. Consequently, low melting salts are supposed to consist of single charged ions with a large size, hence the inter-ion separation is also large. Additionally, large ions facilitate charge delocalization which reduces overall charge density. The effect of ion's size on melting temperatures can be illustrated by the comparison of simple sodium (Na^+) and 1-ethyl-3-methyl-imidazolium (**EMIm**) salts (**Table 1.2**). The melting point of the different sodium salts decreases from 801 to 185 °C by increasing the thermochemical radius from Cl^- (1.7 Å) to BF_4^- (2.2 Å) to PF_6^- (2.4 Å) and finally to $AlCl_4^-$ (2.8 Å). An extrapolation of these values shows that an anion with a radius of 3.4 – 4 Å would be necessary to form a room temperature liquid sodium salt.[48] ILs with organic cations, that are large compared to inorganic ones, have reduced melting

temperatures due to the increased ion size. This effect is shown in **Table 1.2** for the salts with the large non-symmetric $EMIm^+$ cation compared to the Na^+ salts.

Table 1.2 Comparison of melting points T_m and thermochemical radii r of different anions for their Na- and EMIm-salts; the ionic radii of the cations are 1.2 Å for Na^+ and 2 x 2.7 Å for the non-spherical $EMIm^+$.[48]

Anion X^-	r [Å]	T_m of NaX [°C]	T_m of EMImX [°C]
Cl^-	1.7	801	87
BF_4^-	2.2	384	6
PF_6^-	2.4	>200	60
$AlCl_4^-$	2.8	185	7

Many, but not all, ILs show glass transition in addition or instead of crystal formation. Glass formation is the result of the very unfavorable packing efficiency of some ILs in the solid state. Accordingly, the glass transition temperature T_g of ILs occurs often at extremely low temperatures, principally below -50 °C.[51,52]

1.2.2.2 Vapor pressure

ILs are famous for their negligible vapor pressure which results from their salt character. For a long time, this non-volatility was the main reason to call ILs "green" solvents. From a processing point of view, this feature is rather disadvantageous for efficient product isolation due to the lacking possibility of separation of reaction mixtures by distillation.[47] Nevertheless, some distillable ILs are known which show a boiling point before thermal decomposition, especially protic ILs.[51,53] During a back-protonation of the anion, the original acid, thus the neutral species is reformed. Therefore, the condition for the distillation of a protic IL is a low proton-transfer energy. A few examples of distillable aprotic ILs have been reported, but the conditions are very rigorous: very low pressure and high temperature are necessary,-while decomposition has to be avoided.[54]

1.2.2.3 Viscosity and ionic conductivity

In general, the dynamic (shear) viscosity η of a fluid is the measurement of its resistance to gradual deformation by shear stress τ which arises from the fluid's internal friction. The shear stress τ is the force F acting on area A to effect a movement in the liquid element between two plates (**Eq. 1.2**). The velocity of the movement at a given force is controlled by the internal forces of the material.

$$\tau = \frac{F}{A}\left[\frac{Newton}{m^2} = Pa\right] \qquad \textbf{Eq. 1.2}$$

By applying shear stress, a laminar shear flow is generated between the two plates. The uppermost layer moves at the maximum velocity v_{max}, the lowermost layer remains at rest. The shear rate is defined as follows (**Eq. 1.3**)

$$\dot{\gamma} = \frac{dv}{dh} \approx \frac{v}{h} \left[\frac{m/s}{m} = s^{-1} \right] \qquad \textbf{Eq. 1.3}$$

If the dynamic viscosity η of a fluid is independent of shear rate and shear stress its flow behavior is Newtonian (**Eq. 1.4**).

$$\eta = \frac{shear\ stress\ \tau}{shear\ rate\ \dot{\gamma}} \left[\frac{Pa}{s^{-1}} = Pa \cdot s \right] \qquad \textbf{Eq. 1.4}$$

Two different behaviors of fluids are well-known: Newtonian and non-Newtonian.[55] Newtonian fluids have a constant viscosity independent of the applied shear stress or shear rate. Non-Newtonian fluids, however, do not have a constant viscosity, thus they show either thickening or thinning behavior with changing shear stress or shear rate. ILs show usually Newtonian fluid behavior.[2]

Some examples for viscosities of common ILs are given in **Table 1.3**.

Table 1.3 Dynamic viscosities η [cP] at 25°C of common ILs.

Cation	**Anion**	**η [cP], 25°C**
$EMIm^+$	$CH_3CO_2^-$	162 [48]
$EMIm^+$	BF_4^-	34 [48]
$EMIm^+$	$(CF_3SO_2)_2N^-$	34 [48]
$BMIm^+$	$CH_3CO_2^-$	440 [48]
$BMIm^+$	BF_4^-	115 [48]
$BMIm^+$	$(CF_3SO_2)_2N^-$	52 [48]
BPy^+	BF_4^-	223 [56]
BPy^+	$CF_3SO_3^-$	86 [56]
monoC3-N^+	$(CF_3SO_2)_2N^-$	72 [57]
monoC4-N^+	$(CF_3SO_2)_2N^-$	132 [57]
monoC6-N^+	$(CF_3SO_2)_2N^-$	153 [57]
$P4448^+$	BF_4^-	1240 [58]
$P4448^+$	$(CF_3SO_2)_2N^-$	250 [58]
$P4448^+$	PF_6^-	1720 [58]

Most ILs have a much higher viscosity than water (0.890 cP) or classical organic solvents. The typical dynamic viscosity η of ILs is found between 10 and 500 cP. The viscosity of ILs is basically influenced by the formation of hydrogen bonds and the strengths of their van der

Waals interactions. Both cations and anions play an important role in the IL viscosity. To obtain low viscosity, ILs should contain large fluorinated asymmetric anions with good charge delocalization and weakened hydrogen bonds. Thus, for ILs with the same cation, the viscosity increases in the order: bis(trifluoromethylsulfonyl)imide < tetrafluoroborate < hexafluorophosphate < chloride. The viscosity of ILs is also influenced by the choice of the cation. Larger cations with long-chained alkyl substituents give higher viscosities due to their stronger van der Waals interactions.[48]

As ILs contain only ionic species, high conductivities κ are expected. However, ILs hold mediocre but not excellent conductivities around 1 $S \cdot m^{-1}$.[48] These values are comparable to good non-aqueous solvents-electrolyte systems but they are significantly lower than those for concentrated aqueous electrolytes. The reduced conductivity can be explained by the formation of ion pairs or ion aggregations.

Both viscosities η and conductivities κ of ILs are strongly influenced by temperature. The temperature dependence is often expressed by the empiric Vogel-Tamman-Fulcher equation (**Eq. 1.5**, **Eq. 1.6**) which shows the decrease of viscosity with increasing temperature.[59]

$$\eta = \eta^0 \cdot \exp\left(\frac{B}{T - T^0}\right) \qquad \textbf{Eq. 1.5}$$

$$\kappa = \kappa^0 \cdot \exp\left(\frac{B}{T - T^0}\right) \qquad \textbf{Eq. 1.6}$$

The equations imply η^0, κ^0, B and T^0 as represent fitting parameters depending on the studied system at temperature T in K.

The relationship between viscosity and conductivity of ILs can be described with the Walden rule (**Eq. 1.7**)[60]

$$\Lambda\eta = const. \qquad \textbf{Eq. 1.7}$$

where Λ is the molar conductivity ($\Lambda = \kappa M/\rho$ with M as molecular weight and ρ the mass density). The Walden rule relates the ionic mobility, which is represented by the molar conductivity Λ, to the fluidity of the medium. For a liquid that can be described by independently moving ions, the Walden plot (log Λ versus $\log(1/\eta)$) corresponds closely to the ideal line (**Figure 1.11**).[53] This ideal line can be represented using aqueous potassium chloride solutions at high dilutions. The first Walden plots for ILs have been described by Angell *et al.* in 2003[53] and later by MacFarlane *et al.* in 2007.[61] Depending on the deviation from the ideal KCl line, ILs can be classified in the following subgroups: superionic liquids, good ILs, poor ILs and non-ionic liquids, as shown in **Figure 1.11**.[53]

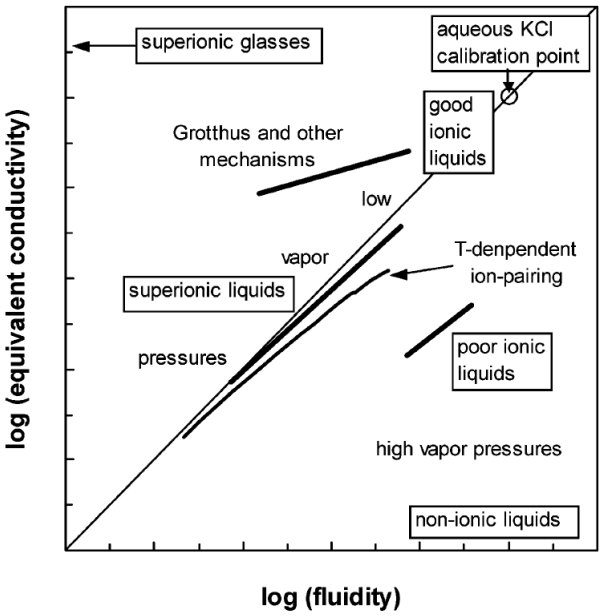

Figure 1.11 Classification diagram for ILs, based on the classical Walden rule, and deviations thereof.[53]

1.2.2.4 Surface tension

In general, surface tension measurements give information about the cohesive forces between liquid molecules present at the surface.[62] For ideal liquids composed on spherical molecules (*e.g.* liquid argon or methane), surface tension σ correlates well with the intermolecular interactions in the bulk. However, liquids composed of non-spherical molecules with polar and non-polar parts show strong orientation. Especially ILs, which are generally composed of strongly anisotropic ions referring to structure and charge, have quite different structure and molecular distribution at the surface and in the bulk. The intermolecular interaction potential energy and the liquid interfacial microstructure are the main factors leading to the surface tension.[63] The surface tension of a liquid is an important physicochemical property for its application. Usually, ILs have higher surface tensions than most common molecular solvents (*e.g.* ethanol: 22 $mN \cdot m^{-1}$, acetone: 23 $mN \cdot m^{-1}$, diethyl ether: 17 $mN \cdot m^{-1}$), but lower surface tensions than water (72 $mN \cdot m^{-1}$).[64,65] The choice of the cation and anion influences the surface tension for the reason that generally both ions are present at the surface.[66,67] Cations with long alkyl-chains decrease the IL surface tension because of the increased amount of hydrocarbons situated at the surface. Larger anions, however, lead to high IL surface tension values. As the anion radius is increased, the cations are shoved apart, therefore the surface tension increases due to the reduction of the hydrocarbon amount present at the liquid surface.[63] Consequently, the surface tension of ILs is strongly dependent on the length and the packing efficiency of the hydrocarbons of the IL's surface.[68] The surface tension of pure ILs is also dependent on temperature. The surface tension decreases with increasing temperature as a result of the change of the internal cohesive energy

as the sum of molecular interactions, namely hydrogen bonding, electrostatic and van-der-Waals interactions.[62]

ILs containing long alkyl-chains, thus hydrophobic tails, and a charged hydrophilic headgroup resemble conventional surfactants and can form aggregates.[69] Because of their structure and intrinsic charge, they can self-assemble not only in pure form leading to thermotropic liquid crystal formation, but also in binary mixtures with water.[70] Some studies have shown that the critical micelle concentration (cmc) of long-chain imidazolium ILs are lower than those of typical cationic surfactants, the alkyltrimethylammonium bromides. Therefore, the surface activity of long-chain imidazolium ILs seems superior, and could be explained by a favored packing and a higher hydrophobicity of the planar aromatic headgroup.[69,71,72]

1.2.2.5 Polarity and solubility

The polarity is one of the most important properties for solvents. Molecular solvents can be classified and compared due to their dielectric constant ε, but this is not useful for ILs because of their charges. Thus, other scales were developed for ILs, like the assignation *via* solvatochromic or fluorescent dyes; well-known dyes are Nile red and Reichardt's dye.[73,74] In 1965, Reichardt defined solvent polarity as a complex salvation capability depending on all non-specific and specific intermolecular solute-solvent interactions.[75] And interactions leading to definite chemical modifications of the ions or molecules of the solute are excluded. An empirical polarity scale, called $E_T(30)$, has been developed using the molar transition energies of the standard betaine dye 30, called Reichardt's dye, measured in different solvents at ambient temperature and pressure (**Eq. 1.8**),

$$E_T(30)/kcal\ mol^{-1} = h\tilde{\upsilon}_{max}\, cN_A = \frac{28951}{\lambda_{max}\ /nm} \qquad \textbf{Eq. 1.8}$$

where $\tilde{\upsilon}_{max}$ is the wavenumber and λ_{max} the wavelength of the maximum of the long wavelength solvatochromic intramolecular change transfer (CT) absorption band of the Reichardt's dye, and h, c and N_A are Planck's constant, the speed of light and Avogadro's constant.[73] With increasing $E_T(30)$ values, the polarity of the solvent increases. The dimensionless scale E_T^N was introduced using water and tetramethylsilane (TMS) as reference solvents leading to the fixed scale with $E_T^N(H_2O)$ = 1.00 and E_T^N(TMS) = 0.00.[76] **Figure 1.12** shows the polarity scale of some traditional organic solvents and common ILs.

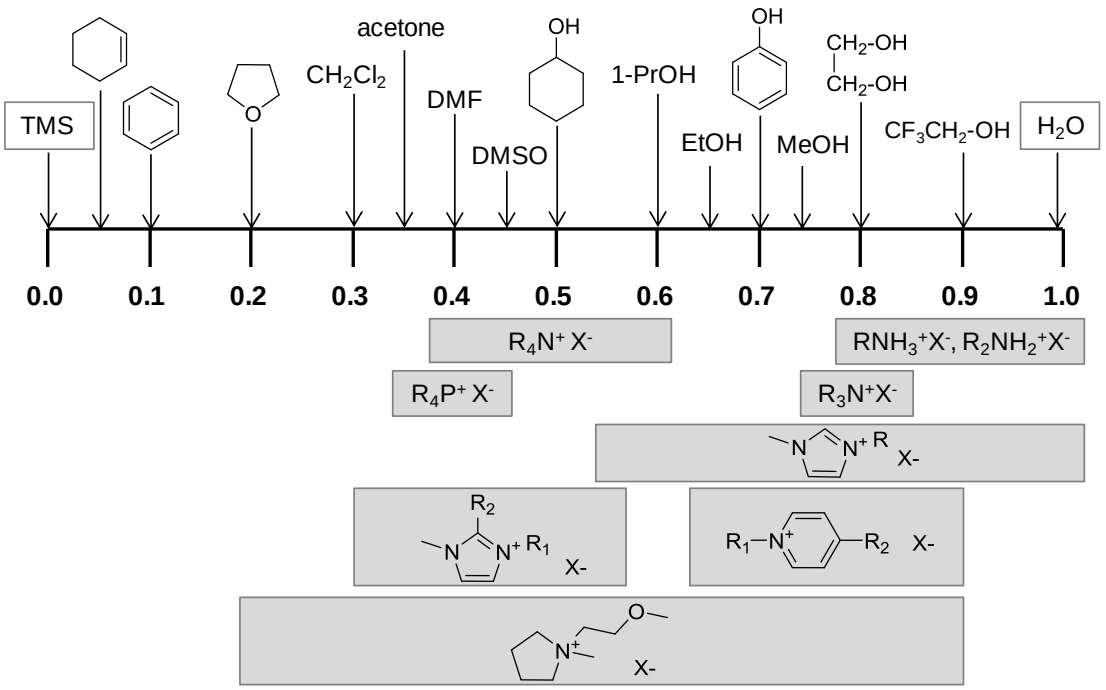

Figure 1.12 Normalized solvent polarity scale E_T^N for several organic solvents compared to the most common groups of ILs.[73]

The polarity of ILs can be modified task-specifically, thus the solvent properties can be adjusted by the choice of cation – anion combination. The variation from hydrophobic to hydrophilic ILs is possible which enables the solubilization of either non-polar or polar solutes.[47] Depending on the chain length of the IL cation, the type of the anion shows, in case of longer chains, more or less impact on the total polarity. The polarity decreases with the effective charge density of the anion and its size.[74] The solvent properties of imidazolium ILs, especially their solubility in water, are mostly influenced by the anion. ILs with hexafluorophosphate and bis(trifluoromethylsulfonyl)imide are hydrophobic, and therefore insoluble in water. Highly hydrophilic ILs are formed with anions like acetate or nitrate (**Figure 1.13**).[77]

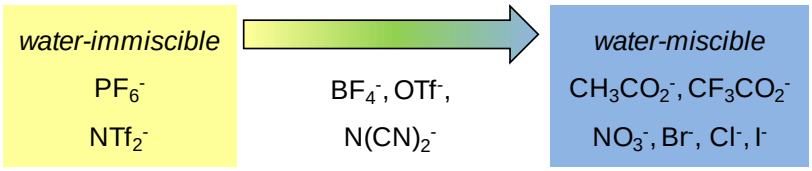

Figure 1.13 Effect of some common anions on ILs with the same cation (*e.g.* imidazolium) resulting in water-miscible or –immiscible ILs.[77]

In this context, the octanol/water partition coefficient $P_{O/W}$ gives important information about partitioning of solvents, which is an important and fundamental property of a chemical.[78] Only few studies on this property for ILs have been done. In general, the partition coefficient is

defined as the ratio of the equilibrium concentration of a dissolved substance in a biphasic system (*e.g.* octanol and water)[79]

$$P_{O/W} = \frac{c(solute\ in\ octanol - phase)}{c(solute\ in\ water - phase)} \quad \textbf{Eq. 1.9}$$

For ionic solutes, the intrinsic (true) partition coefficient is the ratio of the concentrations of the undissociated species in the two phases; therefore, the measurement is quite difficult. So, the apparent partition coefficient is generally used, which is involves the undissociated and dissociated species for the concentrations. This lack of clarity leads to $P_{O/W}$ values for ILs which vary due to the measurement in different studies.[79] A study on imidazolium-based ILs showed that values change strongly with the variation of counter anions (0.003 to 11.1 at RT).[80]

For the estimation of solubilization processes, the Hildebrand solubility parameter δ can be used. It attempts to measure the energy required during solubilization due to the significant change in the molar volume of the solute(s) which involves a change in the separations of the solvent species (**Eq. 1.10**).[81]

$$\delta^2 = \frac{\Delta U_V}{V_m} \approx \frac{\Delta H_V - RT}{V_m} \quad \textbf{Eq. 1.10}$$

where V_m is the molar volume of the solvent, and ΔU_V and ΔH_V are the molar energy and enthalpy of vaporization. For a long time, ILs were thought to be completely non-volatile, thus measurements of Hildebrand parameters were impossible. But today, we know that evaporation is possible for some ILs.[54] Thus, the enthalpies of vaporization have been determined for several ILs, and the δ values were obtained.[82] The δ values for some imidazolium, pyrrolidinium and ammonium ILs were found in the range of 16.3 – 26.5 $(J \cdot cm^{-3})^{1/2}$, which are comparable to those for short- to medium-chained alcohols. The Hildebrand parameter of ILs seems to depend on the nature of anion and cation. It decreases with increasing chain length of the cation. Compared to this method, δ values could also be derived from surface tension measurements,[83] from viscosity measurements,[84] or chemical reactivity.[85]

1.2.3 "Green" ionic liquids – toxicity and biodegradability

In general, the design of "green" compounds is supported by a full risk management study.[86] A comparative risk evaluation of chemical substances has been devised in five risk indicators forming eco-toxicological risk-profiles for each substance. These risk indicators and their interrelations with the development cycle of chemical substances are illustrated in **Figure 1.14**: release, spatiotemporal range, bioaccumulation, biological activity, uncertainty.

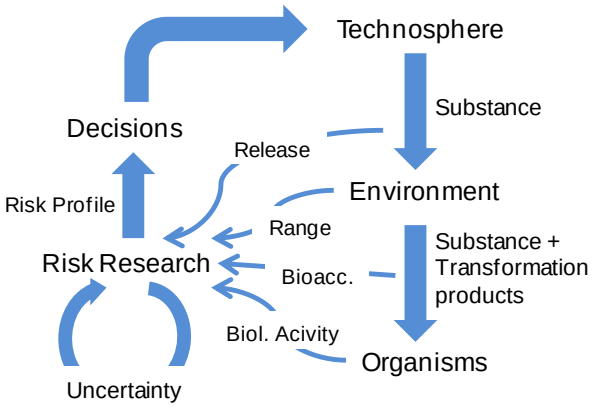

Figure 1.14 Graphical illustration of the risk management cycle and its correlation with the eco-toxicological risk indicators.[86]

When the research of ILs began the whole substance class was discussed in an undifferentiated way to be "green" and environmentally benign. Those statements were justified with the negligible vapor pressure which results in reduced air emission, non-flammability, and non-explosiveness.[87] But these properties are not sufficient to classify all ILs as "green", so in the past few years, the image of ILs has changed.

As a first step, "greenness" of the synthesis of an IL should be evaluated. Therefore, a synthesis tree (as a family tree) should be prepared with the IL at the bottom and its "parents" above, as shown in **Figure 1.15** for $[BMIm]BF_4$.[88] With this method, all generations are demonstrated back to the original compounds that were extracted from the ground, air or sea.

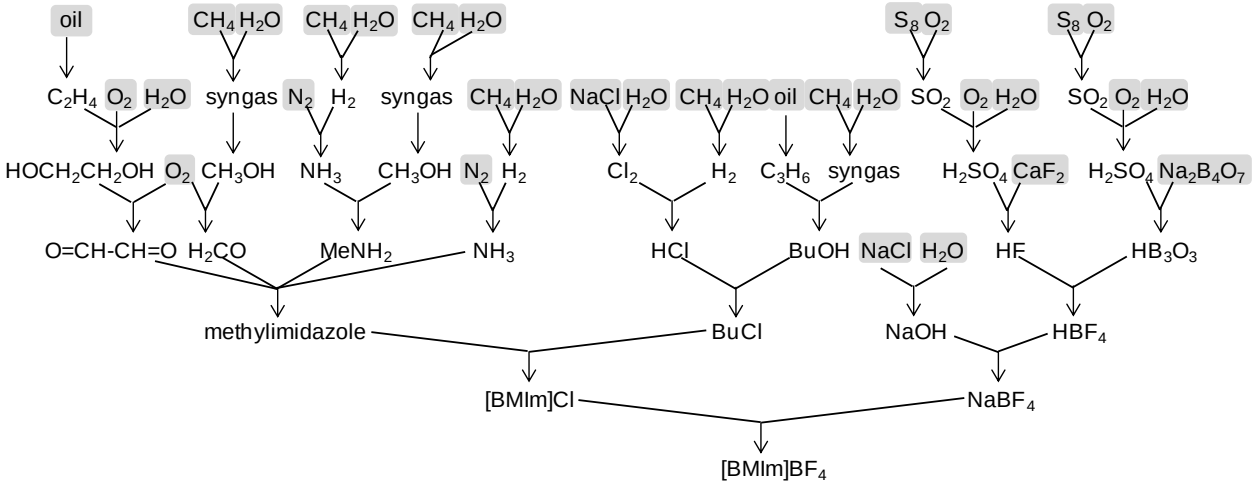

Figure 1.15 Synthesis tree for the IL $[BMIm]BF_4$.[88]

In general, one can establish rules for the structural composition of ILs to obtain more eco-friendly solvents. Therefore, two different concepts have to be considered – the **toxicity** and the **biodegradation**.[89] In general, a product is more toxic when its molecular structure is more hydrophobic.[90] The (eco)toxicity seems to be predominantly determined by the structure of the

cation. [86,91–93] Therefore, the general tendency for the toxicity of the cationic head group is as following:

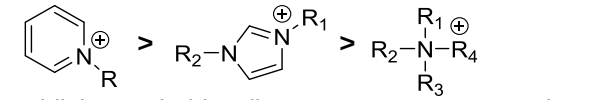

pyridinium imidazolium quaternary ammonium

Additionally, the side chains R play a very important role for the toxicity of an IL. Compounds which contain shorter alkyl side chains (number of carbons < 4) are less hydrophobic, and therefore less toxic.[90] Moreover, the introduction of polar functional groups (*e.g.* ether, hydroxyl, amine, amide) has a large reducing effect on ILs toxicity.[92] Most of the common ILs anions are not significantly toxic, with the following exceptions: hydrophobic and fluorinated species, like trifluoroacetate, trifluoro[tris(pentafluoroethyl)]phosphate, bis(trifluoromethanesulfonyl)imide. Biodegradation is the second important factor for giving evidence of the "greenness" of products. This is the microbial breakdown of chemical compounds, in contrast to the chemical decomposition.[92] Usually, the presence of certain sites, which allow the decomposition of a substance by microorganisms, is necessary.[94–98] There are important parameters including the potential sites of enzymatic hydrolysis (*e.g.* esters, amides), and oxygen in form of hydroxyl, aldehyde or carboxylic acid groups as well as unsubstituted linear alkyl chains and phenyl rings, which represent possible sites for attack by oxygenase. With respect to the cation, the pyridinium core exhibits in general a higher degree of biodegradation than the imidazolium derivatives. The imidazolium-ring and C-substituted derivatives are completely biological degradable, but *N*-substituted derivatives (*N*-alkylimidazole) are not.[95] Furthermore, an increased biodegradability is found with elongated alkyl side chains (number of carbons ≥ 6).

Regarding the anions for ILs, naturally sourced compounds are preferred, like sulfate, sulfonate, phosphate, nitrate, nitrite, and salts from organic acids (*e.g.* acetate, lactate, etc.). Anions with fluorinated groups are not biodegradable. One of the new trends in IL's chemistry is the research of bio-sourced cations and anions, for instance from **natural organic acids** (*e.g.* lactic acid, levulinic acid, salicylic acid),[98,99] **amino acids** (*e.g.* valine, proline, leucine),[100–102] **non-nutritive sweeteners** (*e.g.* saccharinate and acesulfamate),[103] or natural compounds like choline or betaine.[104–106] **Figure 1.16** shows the most famous examples for bio-based and renewable ions which have been used for the design of new "greener" ILs.

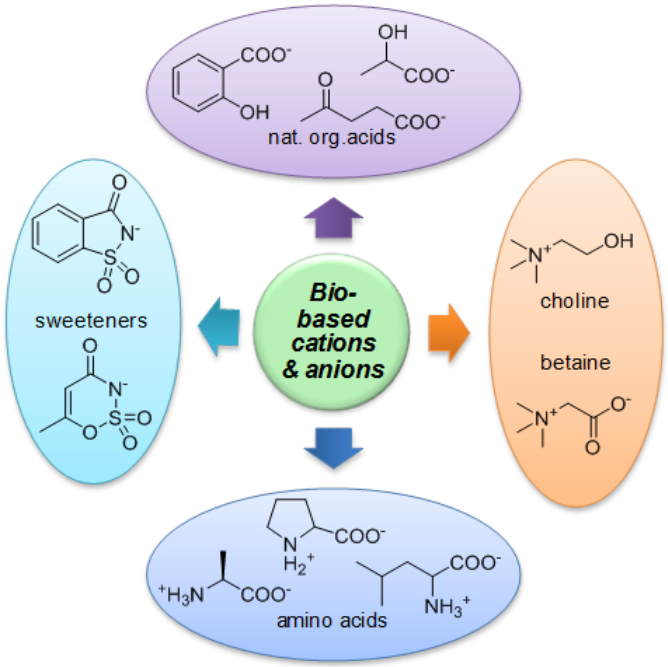

Figure 1.16 Examples for bio-based IL cations and anions.

1.2.4 Applications

Due to the unlimited number of IL combinations and their exceptional physicochemical properties, their potential for diverse applications in research and industry is indubitable. Generally, about 600 conventional solvents are used in industry, compared to at least 10^6 possible simple ILs.[77] **Table 1.4** gives a short overview of the most important properties of organic solvents compared to ILs.

Table 1.4 Comparison of organic solvents and ionic liquids.[77]

Property	Organic solvents	Ionic liquids
Number of solvents	> 1000	> 1 000 000
Applicability	single function	multifunction
Catalytic ability	rare	common and tunable
Vapor pressure	Clausius-Clapeyron-equation	negligible
Flammability	usually flammable	usually non-flammable
Solvation	weakly solvating	strongly solvating
Polarity	conventional polarity concepts	polarity concept questionable
Tunablity	limited range	unlimited (“designer” solvents)
Cost	usually cheap	expensive
Recyclability	green imperative	economic imperative
Viscosity /cP	0.2 - 100	20 – 40 000

An overview of the most important (potential) ILs applications is given in **Figure 1.17**. ILs can replace conventional solvents in organic synthesis or catalysis,[107] and they can also be used for extraction processes.[108,109] Another important field of ILs applicability concerns electrochemistry,[110] including ILs as electrolytes in batteries,[111] electroplating processes,[112] or solar cells.[113] Due to their advantage in formulation technology and in colloid science, ILs find further applications as lubricants,[114] additives in paintings,[115] or templates in nano-technology.[116] The use of ILs for biopolymer processing is of great interest, like the dissolution of cellulose (detailed in ***section 1.2.5***),[117] lignin,[118] suberin,[119,120] or chitin.[121] ILs are also applied in extraction processes of proteins.[122]

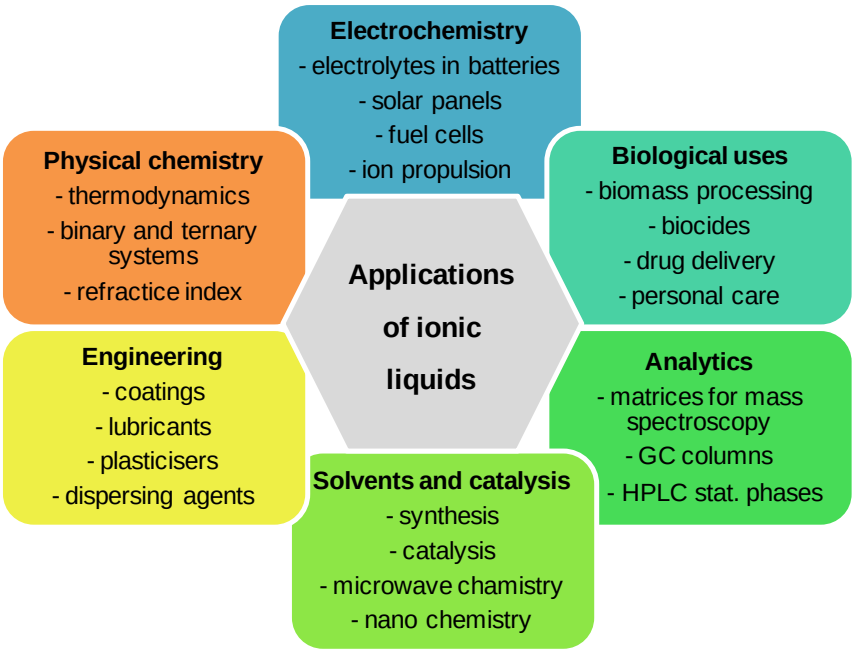

Figure 1.17 Applications of ionic liquids: different fields and some examples.[77]

Up to now, the most popular and well established example for an industrial process involving an IL is the BASIL™ (**b**iphasic **a**cid **s**cavenging utilizing **i**onic **l**iquids) process, which was introduced by BASF AG in 2002.[123] This process deals with the production of alkoxyphenylphosphines which are generic photoinitiator precursors.

1.2.5 Ionic liquids as cellulose solvents

Apart from the traditional cellulose solvents (***section 1.1.3***), ILs were found to have a high potential for the solubilization of biopolymers (*e.g.* cellulose, hemicelluloses, lignin).[117,124–127]
A bibliometric analysis with the database Scifinder® was carried out with the combination of the keywords “ionic liquid” + “biomass” and “ionic liquid” + “cellulose” (**Figure 1.18**) showing a great increase of scientific interest during the past years. In 2000, only one publication was

found for both keyword combinations. For "ionic liquid" + "biomass", ten years later, in 2010, we find ≈ 130 publications, and 2013, already ≈ 210 (**Figure 1.18.a**). For "ionic liquid" + "cellulose", some more publications have been found, ≈ 315 publications in 2010, and in 2013, already ≈ 430 (**Figure 1.18.b**). This analysis shows that there is a continual growing interest in ILs for biomass and / or cellulose treating and transformation.

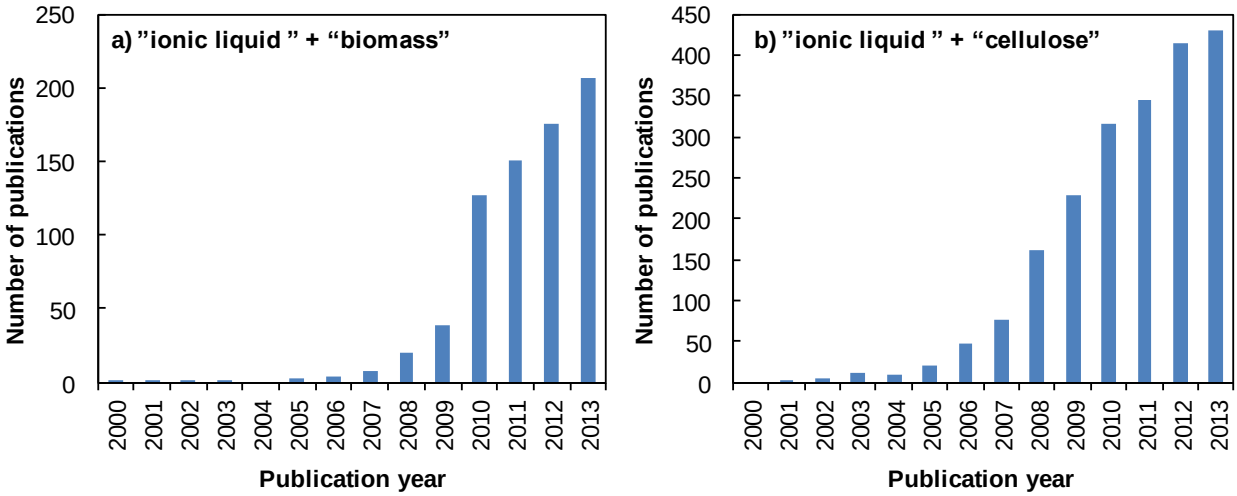

Figure 1.18 Number of publications dealing with **a)** "**ionic liquid" and "biomass"**, **b) "ionic liquid" and "cellulose"** as a function of the publication year (analyzed with the database Scifinder®)

Table 1.5 Overview for the solubility of cellulose with different degrees of polymerization (DP) in ILs.

Ionic liquid	Solubility (wt%)	DP	T (°C)
[BMIm]Cl	25	1000	110 (MW)[117]
[BMIm]Cl	10	1000	100 [117]
[BMIm]SCN	5-7	1000	110 (MW)[117]
[BMIm]BF_4	0	1000	110 (MW)[117]
[BMIm]PF_6	0	1000	110 (MW)[117]
[AMIm]Cl	14.5	650	80 [127]
[AMMIm]Br	4	593	80 [128]
[AMIm]For	22	250	85 [129]
[EMIm]Cl	6	593	80 [128]
[EMIm]Ace	20	795	80 [130]
[BMPy]Cl	39	286	105 [131]
[Bu_4P]For	6	225	110 [132]
[Bu_4N]For	1.5	225	110 [132]
[Me$(OEt)_2$EtIm]Ace	12	225	110 [132]
[Me$(OEt)_2Et_3$N]Ace	10	225	110 [132]
[$(MeOEt)_2NH_2$]Ace	0	225	110 [132]

Table 1.5 gives an overview for the most famous examples of cellulose dissolution in ILs. One can observe that the solubilization process is strongly influenced by several factors, like the degree of polymerization (DP) of cellulose, the temperature *T* and microwave heating (MW).

1.2.5.1 Structural aspects and mechanism for cellulose dissolution

In literature, most of the studies deal with 1,3-alkyl-imidazolium ILs with different alkyl chain lengths and different counter anions. For instance, a screening of 1-butyl-3-methylimidazolium ILs with a range of anions showed that small H-bond accepting anions (like Cl^-) are the most efficient ones.[117] Furthermore, ILs with longer-chain substituted cations, like 1-hexyl-3-methylomidazolium or 1-octyl-3-methylimidazolium were found to be less efficient for dissolving cellulose. This fact was accounted for by the reduced effective anion concentration within these longer chain ILs. Some of the most important ILs cations and anions for cellulose solubilization are shown in **Table 1.6**.[133] The cation of the IL does not play the predominant role, whereas the choice of the anion is all-important. Common IL anions with a strong potential to dissolve cellulose have a basic character, such as chloride, carboxylates (*e.g.* acetate, formate) and dialkylphosphates.[126]

Table 1.6 IL cations (1,3-dialkyl-imidazolium, 1,3-dialkyl-pyridinium) and anions (dialkylphosphate, thiocyanate, formate, acetate, chloride, bromide) with the potential for cellulose dissolution.[133]

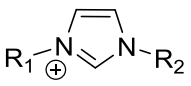	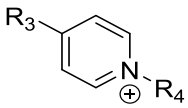				R_1 = Me R_2 = Et, Bu R_3 = Me R_4 = Bu R_5 = Me, Et
imidazolium	pyridinium				
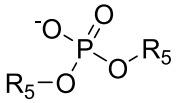				Cl^-	Br^-
dialkylphosphate	thiocyanate	formate	acetate	chloride	bromide

In addition, an IL solvent for cellulose dissolution should not only have high dissolution capacity, but also low melting point, low viscosity, high stability, and low or even no toxicity. In order to dissolve cellulose, the IL has to disrupt a great number of inter- and intramolecular hydrogen bonds; therefore, a high concentration and activity of the anion in the IL plays the key role for this process.[117] Studies show that the solubility of cellulose decreases with increasing size of the cations, such as the length of alkyl groups substituted on the cation. Investigations of the dissolution of cellulose with ILs in connection with the structural properties of the solvents, a dissolution mechanism is proposed (**Figure 1.19**).[26,134] Above a critical temperature, the ion pairs of the IL dissociate to individual cations and anions. So, the free anions (electron-donor center) associate with the cellulose hydroxyl protons, and the free cations (electron-acceptor

center) complex with the cellulose hydroxyl oxygens, which disrupts hydrogen bonding in cellulose and results in the dissolution of the polymer.

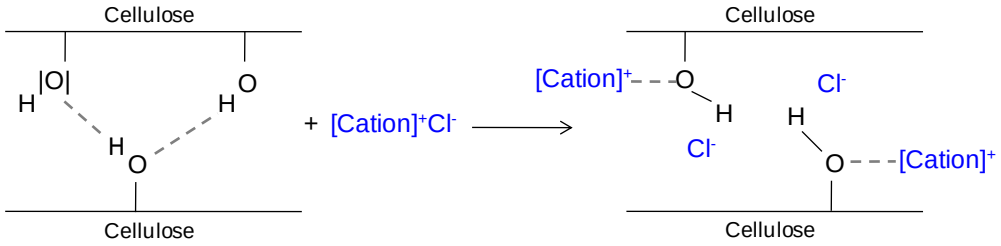

Figure 1.19 Possible mechanism of cellulose dissolution with chloride ILs.[134]

Other investigations showed that some ILs are not able to dissolve cellulose (**Table 1.7**).[26] Especially ILs containing non-aromatic ammonium- and phosphonium-based cations have poor dissolution power, thus they can only dissolve cellulose with a low degree of polymerization, or form only fine dispersions of undissolved cellulose. The anions, which are not successful for dissolving cellulose, seem to be too voluminous and symmetric for the interaction with the hydroxyl-groups between the glucose-chains of the cellulose polymer.

Table 1.7 IL cations (pyrrolidinium, piperidinium) and anions (bis(trifluoromethanesulfonyl)amide Tf_2N, tosylate, tetrafluoroborate, hexafluorophosphate) without cellulose dissolving abilities.[26]

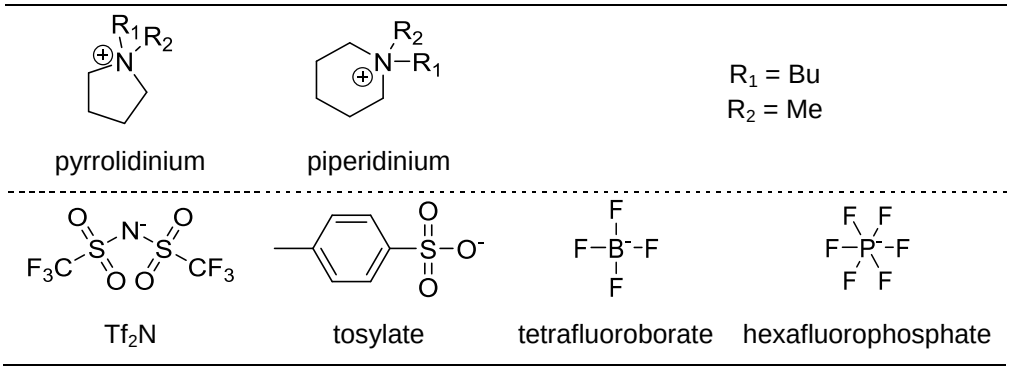

In contrast to the poorly dissolving cations (**Table 1.7**), dissolving cations (**Table 1.6**) seem to consist of planar, nitrogen-containing rings with the ability to delocalize their positive charge within their aromatic π-system. The non-aromatic ring structure of the non-dissolving compounds results in a tetrahedral-like nitrogenium heteroatom (sp^3-hybridized center) without the possibility to delocalize the positive charge. A wide structural variety of cellulose-dissolving anions is determined, covering trigonal planar (formate, acetate), tetrahedral (dialkylphosphate), linear (thiocyanate), and spherical (chloride, bromide) structures. Non-dissolving anions are primarily hexagonal (tetrafluoroborate, hexafluorophosphate) or tetrahedral with bulky substituents (Tf_2N, tosylate). Differences are also found with regard to their H-bond ability: the non-dissolving anions display poor to negligible H-bond donor- or acceptor-characteristics. In contrast, the cellulose-dissolving anions are moderate to excellent H-

bond acceptors, and this ability is partially reflected in their dissolution power: thiocyanate < bromide < dialkylphosphate < chloride ≈ acetate ≈ formate. **Table 1.8** summarizes the structural properties for ILs ions with good or poor dissolution power for cellulose.

Table 1.8 Overview of the structural properties of IL cations and anions with regard to their dissolution power for cellulose.

GOOD SOLUBILITY	POOR SOLUBILITY
imidazolium, pyridinium	**pyrrolidinium, piperidinium**
• planar, *N*-containing ring with the ability to delocalize the positive charge within their aromatic π–system (sp^2 *N*-heteroatom) • H-bond ability because of the aromatic character (ring protons for H-bonding) • polarity of the cation: heteroatoms induce polar character	• non-aromatic ring tetrahedral-like *N*-heteroatom without ability to delocalize the positive charge (⊕ at sp^3-center) • no H-bond ability for tetrahedral non-dissolving cations
acetate, formate, dialkylphosphate, thiocyanate, chloride, bromide	**tetrafluoroborate, hexafluorophosphate, bis(trifluoromethanesulfonyl)imide, tosylate**
• trigonal planar, tetrahedral, linear, spherical • moderate to excellent H-bond acceptors (basicity): SCN^- < Br^- < dialkylphosphate < formate ≈ OAc^- < Cl^-	• poor to negligible H-bond donor or acceptor characteristics • too bulky and symmetric (no interaction with cellulose H-bond network)

Another important structural factor for the dissolution of cellulose is the dipolar character of the solvent. The configuration of a four-, five- or six-membered ring-structure seems favorable (**Figure 1.20**). To form a six-membered cyclic state, a dipolar character with favorably n = 2 bridging atoms is necessary. Fewer bridging atoms result in five-membered (n = 1) or four-membered (n = 0) arrangements.[26,135]

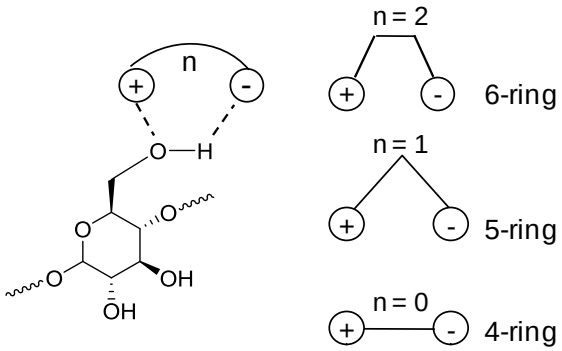

Figure 1.20 Scheme for possible interactions of a cellulose hydroxyl group with a solvent dipole: the amount of bridging molecules n determines the size of the resulting cyclic state.[26]

Based on these considerations, Pinkert *et al.* have discussed the structural design for ILs for dissolving cellulose.[26] Generally, salts with low melting temperatures must include certain structural criteria for decreasing the attractive Coulombic forces between their cations and anions (***section 1.2.2***), thus at least one ion cannot be very small anymore. Requiring that one ion (usually the cation) should be of larger size, can result in a hindered dissolution power for cellulose, because of its reduced ability to penetrate the cellulosic H-bond network and to adjust its dipole in a favorable position. The important advantage of ILs compared to traditional cellulose solvents is their ability to delocalize the charge of their more bulky ion and improve their ability to adapt the geometrical arrangement of their dipoles for a favorable H-bond interaction with cellulose. The presence of two good H-bond acceptors (*e.g.* oxygen) in intermediate proximity on one side of the molecule, and the non-favorable substituents on the reverse side can explain why those ions are still found in cellulose-dissolving solvents. One should come to a compromise between ion size and the ability to present its H-bond at a favorable location to form thermodynamically stable H-bonds with cellulose. In a further step, Pinkert *et al.* proposed further ions which are expected to be efficient (**Table 1.9**) for cellulose dissolution.[26]

Table 1.9 Proposed IL cations (oxazolium, oxaphospholium) and anions (phosphate, dimethylcarbamate, nitrate, nitrite) for enhanced cellulose dissolution.[26]

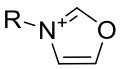		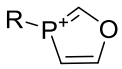	
oxazolium		oxaphospholium	
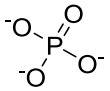	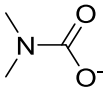	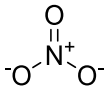	
phosphate	dimethylcarbamate	nitrate	nitrite

Two different cases for well-known cellulose solvents are identified: (a) structure with two heteroatoms that are more electronegative than the connecting C-atoms (*e.g.* imidazolium cations), or (b) structure with two heteroatoms with a very large difference in electronegativity (*e.g.* NMMO). If the difference in electronegativity of the heteroatoms is larger, the resulting dipole of the molecule is larger (**Figure 1.21**). Consequently, oxazolium and oxaphospholium are conceivable as IL cations. Suitable anions are good H-bond acceptors, preferably small in size, and without any hydrophobic substituents. The presence of several H-bond acceptor sites can be favorable; possibilities include fluoride, chloride, formate, acetate, phosphate derivatives, peroxide, superoxide, hydroxide, nitrate or nitrite. Moreover, the mesomeric effect of the *N*-atom in the structure of dicarbamate offers the possibility of two H-bond acceptor sites. The phosphate anion can offer multiple sites that qualify as H-bond acceptors; the triple negative charge enables the anion to be paired with three cations.

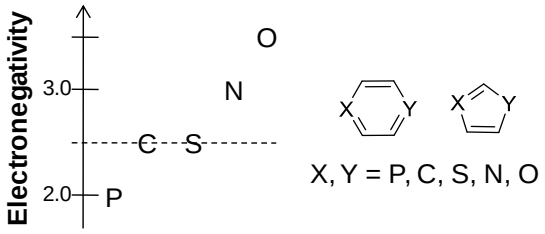

Figure 1.21 Dipolar character in aromatics introduced through heteroatoms; electronegativities increase from phosphor to oxygen.[15]

1.2.5.2 Conversion of cellulose to platform chemicals in ionic liquids

As already mentioned in ***section 1.1.2***, the transformation of biopolymers to platform chemicals is an important possibility to use renewable feedstock as alternative to petro-chemicals. Tao *et al.* showed a simple and effective route for the production of 5-hydroxymethyl furfural (HMF), furfural and levulinic acid from microcrystalline cellulose (MCC) with the catalyst $CoSO_4$ in the IL 1-(4-sulfonic acid) butyl-3-methylimidazolium hydrogen sulfate (**Figure 1.22**).[136] This cellulose hydrolysis process at 150 °C led to 84% conversion of MCC after 5 h. Yields of HMF and furfural were up to 24% and 17%, respectively, and a small amount of levulinic aid (8%) and reducing sugars (4%) were generated.

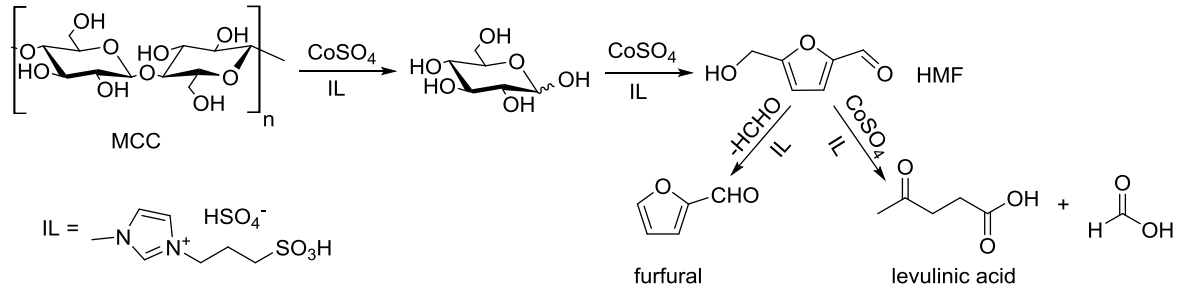

Figure 1.22 Catalytic process for the transformation of microcrystalline cellulose (MCC) to 5-hydroxymethyl furfural (HMF), furfural, and levulinic acid in an IL.[136]

A similar route for the conversion of cellulose to HMF in a single-step-reaction was shown using a pair of metal chlorides ($CuCl_2$ and $CrCl_2$) as catalyst and the IL [EMIm]Cl at 80-120 °C.[137] For this type of processing, catalytic ILs have been synthesized and applied on cellulose transformation, *e.g.* heteropolyacid (HPA) ILs $[MImPSH]_nH_{3-n}PW_{12}O_{40}$ (**Figure 1.**23).[138]

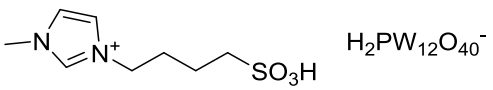

Figure 1.23 Structure of $[MImPSH]H_2PW_{12}O_{40}$.[138]

In this context, Villandier *et al.* published a one-pot conversion route for the conversion of cellulose to biodegradable surfactants with an acid catalyst in IL media.[139,140] As shown in **Figure 1.24**, by working in IL media with Amberlyst 15Dry as acid catalyst and coupling the rate of cellulose hydrolysis and the rate of glycosidation of the monosaccharides formed with C_4- to C_8-alcohols, 82% mass yield of octyl-α,β-glycoside and octyl-α,β-xyloside was obtained.

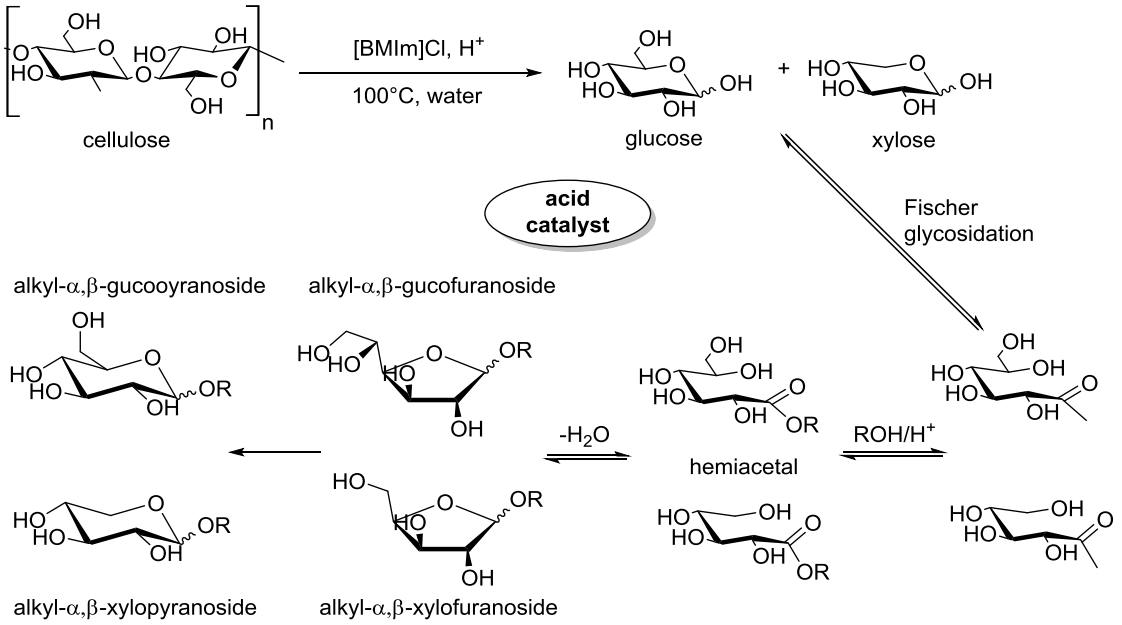

Figure 1.24 One step conversion of cellulose into alkyl-α,β-glycoside surfactants.[139]

1.3 Deep eutectic solvents

Deep eutectic solvents (DESs) based on biosourced compounds represent a new class of alternative solvents. The analysis of published literature by means with the database Scifinder® gave only a limited number of results due to the recent development of such compounds. In 2004, we identify only 11 publications with the keyword "**deep eutectic solvents**", whereas in 2012, the limit of 100 hits was passed, and in 2013, we can find already 150 ones. This shows that the research on DES is quite recent but already knows a growing interest.

1.3.1 Theoretical background and structure

Deep eutectic solvents (DESs) are composed of salts which form an eutectic with a melting point much lower than either of the individual compounds.[141] The phase diagram of an eutectic mixture of two solids A and B (**Figure 1.25**) shows different regions: below a certain temperature (isothermal line *c* - *d*), both solids co-exist. Above this temperature, the mixture is either liquid or a liquid-solid-mixture, which depends on the composition of the mixture. The eutectic point *e* is the intersection of the liquid-solid lines of A and B at a certain ratio and temperature, which is the common freezing temperature defining the DES.

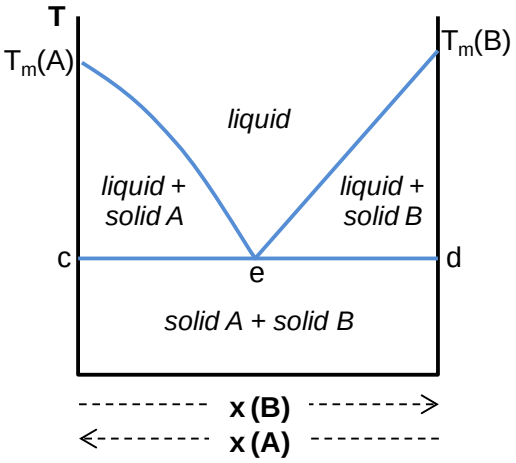

Figure 1.25 Phase diagram for an eutectic mixture of solid A and solid B with T_m: melting temperature of pure solid; c – d: isothermal line, e: eutectic point.

Generally, DESs are formed between quaternary ammonium salts and a hydrogen bond donor (HBD), like carboxylic acids, amides, amines or alcohols.[141] The formation of DES takes place because of the stronger interactions of the quaternary ammonium counter anion (*e.g.* chloride) with the HBD than with the quaternary ammonium cation. Thus, non-Coulomb interactions are stronger in this case than Coulomb interactions.

The eutectic mixture of **choline chloride with urea** was the first metal-free DES example, and it results in a liquid with a freezing point of 12 °C. The charge delocalization during mixing these compounds is achieved through rearrangement of the structure by changing the hydrogen bonding.

The term DES was coined for eutectics of mixtures of two components, but unlike the most molecular eutectic mixtures, the interaction between the ammonium salt and the HBD results in a very large depression of freezing point (up to 200 °C).[142] Recently, DES has also been called "**low transition temperature mixture**" **(LTTM)**.[143] **Figure 1.26** gives an overview of the possible structures for HBDs and hydrogen bond acceptors (HBAs) which can be combined for the formation of DES or LTTM.

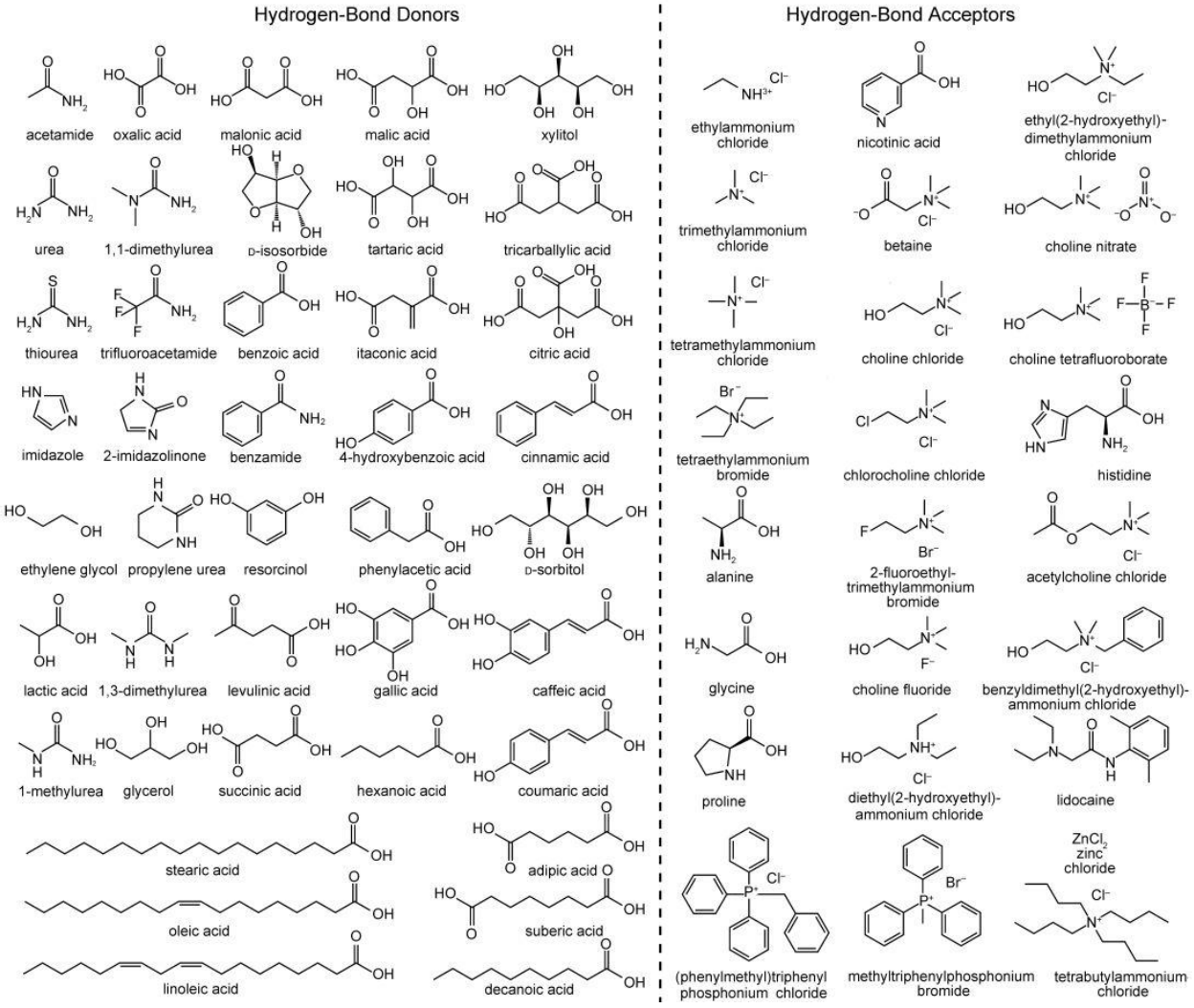

Figure 1.26 Molecular structures of hydrogen bond donors (HBDs) and hydrogen bond acceptors (HBAs) that can be combined to form a DES or a LTTM.[144]

Unlike apparently similar, DESs are different from ILs for two main reasons: 1) DESs are not wholly composed of ionic species and 2) DESs can be formed from ionic, but also from non-ionic species.[3] The comparison of DESs (derived from choline chloride) to classical ILs shows many

advantages: low price, chemical inertness with water, simple preparation (mixing of two compounds), mostly biodegradable, biocompatible and non-toxic.

1.3.2 Physical and chemical properties

As ILs, DESs are designable due to the huge possibility of combinations of HBDs and HBAs (**Figure 1.26**). Consequently, their physical and chemical properties can be tuned depending on the choice of compounds used for the DES formation.[3]

The liquid nature of the salt mixtures is ascribed to a reduction of Coulomb forces which decrease with a large volume and asymmetric charge distribution of the molecular ions.[145] As already mentioned, DESs are formed by mixing two solids which generate, at a certain molar ratio, a new liquid phase by self-association due to hydrogen bonding. The out-coming mixture is characterized by a lower freezing point T_f than that of the individual salts. All reported DES have freezing points below 150 °C.[3]

Table 1.10 Some examples for DES with choline chloride (ChCl; T_m = 303 °C) and different HBDs.

Hydrogen bond donor (HBD)	**ChCl : HBD (molar ratio)**	**T_m(HBD) /°C**	**T_f /°C**
Urea	1 : 2	134	12 [146]
Thiourea	1 : 2	175	69 [146]
Acetamide	1 : 2	80	51 [146]
Benzamide	1 : 2	129	92 [146]
Ethylene glycol	1 : 2	-12.9	-66 [147]
Glycerol	1 : 2	17.8	-40 [148]
Imidazole	3 : 7	89	56 [149]
Adipic acid	1 : 1	153	85 [141]
Citric acid	1 : 1	149	69 [141]
Malonic acid	1 : 1	135	10 [141]
Oxalic acid	1 : 1	190	34 [141]
Succinic acid	1 : 1	185	71 [141]
Phenylacetic acid	1 : 1	77	25 [141]
Levulinic acid	1 : 2	32	lq at RT [150]
Itaconic acid	1 : 1	166	57 [150]
L-(+)-Tartaric acid	1 : 0.5	171	47 [150]
Xylitol	1 : 1	96	lq at RT [150]
D-Sorbitol	1 : 1	99	lq at RT [150]
D-Isosorbide	1 : 2	62	lq at RT [150]

Table 1.10 summarizes the properties (molar ratio of the mixture and its freezing point T_f) of some DES formed between **choline chloride** (ChCl) and various HBDs, such as **urea**, **polyols** (*e.g.* glycerol), **carboxylic acids** (*e.g.* citric acid, levulinic acid, itaconic acid), **sugar-derived polyols** (*e.g.* xylitol, *D*-sorbitol, *D*-isosorbide).

Recently, not only binary but also ternary low-melting systems were reported in literature.[151] Mixtures of ChCl with urea, and glucose or sorbitol as sugar showed melting temperatures with melting points below RT. Thus, sugars could be made liquid at RT without caramelization.

In general, the physicochemical properties of DESs, such as viscosity, conductivity, and surface tension, are similar to ambient temperature ILs and can be explained with the hole-theory.[152,153] The reason for the high viscosity of RTILs and DESs lies in the relatively large radii (≈ 3-4 Å) of the solvent species (ions) compared to the average radius of the voids (≈ 2 Å). The viscosity of a fluid is correlated to the free volume and the probability to find holes of appropriate dimensions for the solvent molecules or ions to move into.[153] The free volume of a liquid can be increased by decreasing the surface tension, and the conductivity of an ionic fluid can be increased by using smaller ions. Thus, less viscous liquids with higher conductivities can be obtained using small quaternary ammonium cations (*e.g.* ethylammonium) and fluorinated hydrogen-bond donors (*e.g.* trifluoroacetamide).

The polarity, which is an important solvent property, can be evaluated as its polarity scale $E_T(30)$, as explained in ***section 1.2.2.5***. Up to now, only few data on solvent properties of DESs are reported. Abbot *et al.* studied the solvent polarity parameters of various ChCl-glycerol mixtures ($E_T(30)$ between 57.17 to 58.49 kcal·mol^{-1}) resulting in a linear increase of $E_T(30)$ with the ChCl concentration.[154]

1.3.3 Aspects of "green" chemistry for DESs

The preparation of DESs is simple and 100% atom economic, occurs without any solvent, and no waste is produced.[3] Thus, producing DESs follows the principles of "green" chemistry (***section 1.1.3***).

In addition, most of the starting materials for metal-free DES are bio-sourced, natural and renewable products which comprise no risk for human or environment. A recent study reports various natural DES, called NADES, wholly formed from natural products, *e.g.* organic acids, sugars and amino acids.[155] All the resulting DE mixtures are not volatile and not flammable and furthermore, they are biocompatible, biodegradable and non-toxic.[145] Moreover, the potential for recycling of DES after an application process is promising.[3] In the context of eco-friendly processing, DESs could replace classical organic solvents, which include various risks. Some

more developments and future perspectives are conceivable, such as biocatalysis, carbon dioxide capture or biomedical applications.[156]

1.3.4 Applications

Despite the novelty of this research field, DESs have already found various (potential) applications in different areas such as material preparation, electrochemistry, synthesis, separation processes, bio applications and catalysis.[144] In **Figure 1.27**, the distribution of publications dealing with DESs in the main sectors of application is represented.

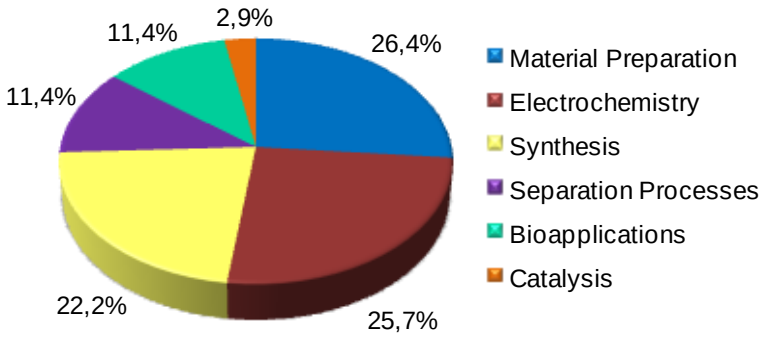

Figure 1.27 Relative distribution of publications on DESs due to their (potential) application field.[144]

The first applications of DES were in **electrochemistry**, especially in the field of **metal electrodeposition**.[157] An appropriate solvent for metal electrodeposition or electrochemical reactions needs to fit the obligatory redox-potential window. ILs were used in this field to avoid the limitations of using aqueous solutions as solvents.[158] DESs have several advantages, like water-tolerance, biodegradability and being cheap, thus they were successfully applied to metal and alloy electrodeposition,[159] electropolishing,[152] and preparation of electrolytes.[144]

The application of DESs for **material preparation** is also of huge interest. They have been used as solvents and/or dispersion media for the preparation of nanoparticles which allows the control of the size, shape, and surface structure of dispersed nanoparticles.[160] Furthermore, new open-framework structures, like metal phosphates, metal-organic frameworks, and new organic-inorganic structures highlighting polyoxometalate-based hybrid materials, were successfully produced in DESs.[144]

A variety of DESs, mainly ChCl-urea mixtures, have already been applied to **organic synthesis**, *e.g.* bromination,[161] Perkin reaction,[162] Knoevenagel condensation,[163] reduction of epoxides and carbonyl compounds.[164] A diversity of C-C coupling reactions in "sweet" low melting mixtures based on sugars or sugar alcohols combined with urea as reaction media have been reported, namely Diels-Alder,[165] Suzuki coupling,[166] Heck reaction and Sonogashira reaction.[167] DESs have

also found application in the field of catalysis.[3] Especially some examples for base-catalyzed, acid-catalyzed, transition-metal catalyzed, and biocatalysis processes were studied.

A further field of DES application is their use in **separation and dissolution processes**.[3] The solubility of carbon dioxide CO_2 in a ChCl-urea mixture has been reported.[168] This procedure, which could be used for CO_2 capturing, depends on three different factors: pressure, temperature, and the molar ratio of the ChCl-urea mixture. Another example for solubilization processing in DES is the dissolution of metal oxides. DESs are able to donate or accept electrons or protons to form hydrogen bonds which explains their excellent dissolution properties.[3] Different metal oxides, e.g. ZnO, CuO, Fe_3O_4, have been dissolved in ChCl-DES with different carboxylic acids, such as malonic, propionic and phenylpropionic acid.[142] Another imposing example for the application of DES in separation processes is the **purification of biodiesel**. Because of their high polarity, DESs have been used for the separation of residual glycerol, a side product after transesterification of vegetable oils, from raw biodiesel.[147] Due to the ability of various quaternary ammonium salts to form eutectic mixtures with glycerol, this was extracted from the biodiesel phase.

Francisco *et al.* have studied LTTMs as solvents for biopolymers, *e.g.* lignin, cellulose and starch.[143] As starting materials, natural HBAs (ChCl, betaine, alanine, glycine, histidine and proline) and natural HBDs (nicotinic acid, oxalic acid, lactic acid and malic acid) have been combined. Some of the mixtures were able to dissolve lignin (up to 15 wt% with malic acid-proline 1:3) and starch (up to 7.6 wt% with malic acid-glycine 1:3), but not cellulose.

Summing up, DESs and LTTMs are a new class of “green”, designable solvents with a great potential for many different applications due to their tunable properties.

1.4 Conclusions

In the field of biopolymers as renewable resources, especially ligno-cellulosic biomass, **cellulose** is the **most produced natural feedstock**. Thus, the processing and solubilization for cellulose are important steps to gain access for its further use as alternative resource. Furthermore, cellulose can be transformed to numerous different platform chemicals, such as 5-hydroxymethylfurfural or levulinic acid as the most important ones. However, the research on an ideal solvent for this complex structured polymer rests a huge challenge for academics and industrials. An ideal solvent should comply with the following requests: high dissolution capacity, cheap, low viscous, stable, non-toxic, ecologically friendly and easy to recycle.

In the course of this research, **ionic liquids** (ILs) have been widely studied as solvent for biopolymers, especially cellulose, showing a high dissolution power. For the solubilization of cellulose, short-chain imiazolium cations combined with small basic anions, such as chloride and acetate, are described as very efficient.
ILs represent a quite new class of alternative solvents with special physicochemical properties which can be tuned due to the choice of cations and anions. Therefore, ILs find many different applications, *e.g.* in the field of electrochemistry, as solvents and catalysts, biological uses, analytics, engineering and formulation, physical chemistry.
Generally, ILs are considered as "green" solvents due to their negligible vapor pressure and their high potential for recyclability. However, real benign solvents should fulfill some more properties and principles, especially biodegradability, non-toxicity and easy synthesis from biogenic material. The research on eco-friendly ILs, which are ideally based on renewable materials, is still a great challenge.

Deep eutectic solvents (DESs) are another class of low-melting salts which represent a new class of "green" solvents. They can be obtained from natural raw materials (*i.e.* choline chloride and urea) by a simple and efficient way of preparation. As ILs, DESs have a high potential for various applications, such as electrochemistry, material preparation and synthesis, separation processes, bioapplications and catalysis.

In this project, we focus on the dissolution of cellulose with novel solvents, mainly low-melting salt mixtures, such as ILs or DESs. In the context of this study, the principles of "green" chemistry play a major role, and the use of natural resourced species is applied.

CHAPTER 2 – Short-chain quaternary ammonium ionic liquids (QACILs) with biosourced carboxylate counter anions

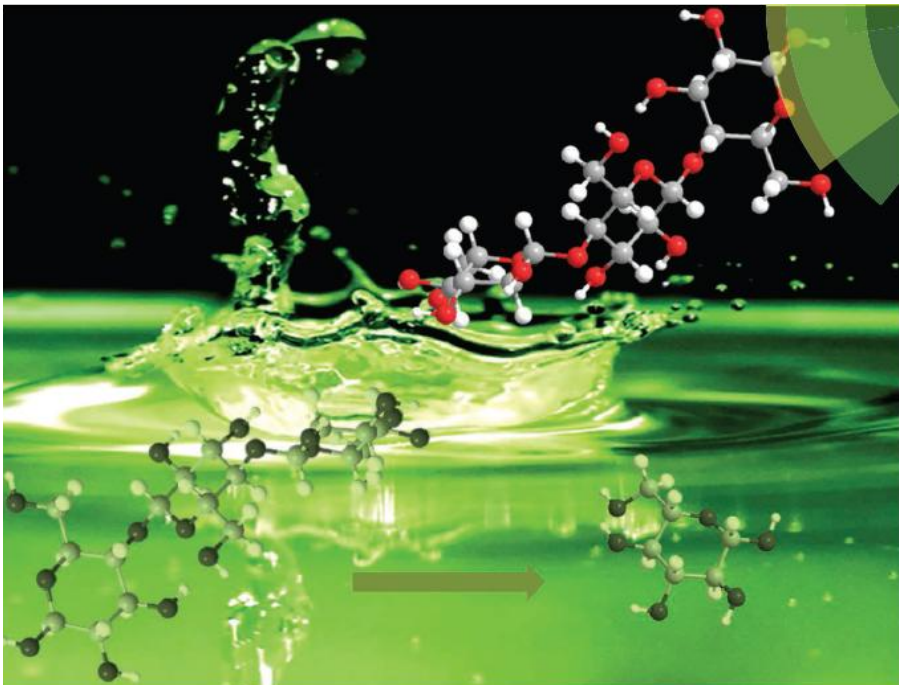

PAPER – ***Green Chem.***, 2014,**16**, 2463-2471
Véronique Nardello-Rataj, François Jérôme *et al.*
Transition of cellulose crystalline structure in biodegradable mixtures of renewably-sourced levulinate alkyl ammonium ionic liquids, γ-valerolactone and water

2.1 Introduction

In the design of ILs, both the cationic and anionic counterparts must be carefully taken into account because they both play an important role in the IL properties and, accordingly, in its potential applications. As far as cellulose solubilization in ILs is concerned a great field of ILs application, numerous cations have been investigated. A survey of the literature combining "cellulose" and "ionic liquid" as keywords highlights the high occurrence of **imidazolium-based ILs** with more than 400 related publications, as illustrated in **Figure 2.1** (the bibliometric analysis was carried out with the Scifinder® database and it includes all documents such as scientific journals, patents, etc.). The second mostly used IL cation is the **pyridinium** with about 230 publications, followed by **quaternary ammonium** (≈ 75 publications) and **phosphonium** (≈ 45 publications). With about 20 publications, **pyrrolidinium**, **piperidinium** and **morpholinium** are not really much studied as IL cations for cellulose treatment.

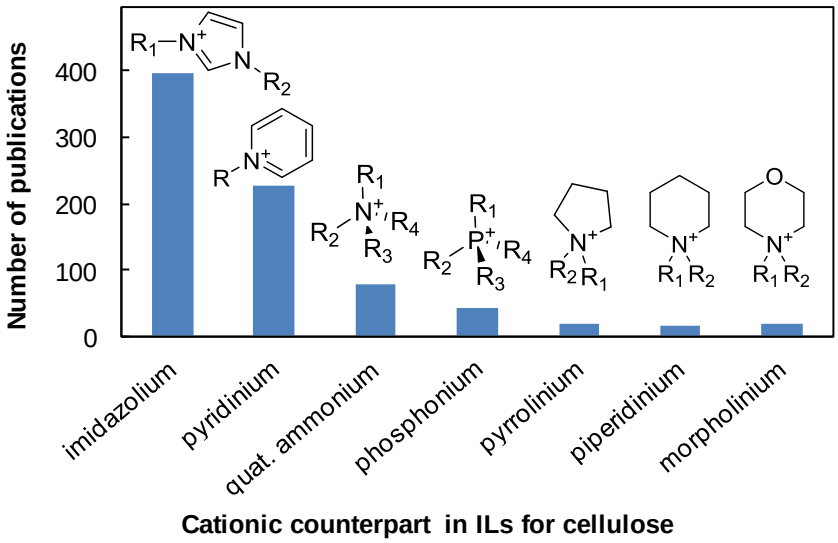

Figure 2.1 Number of publications dealing with "**ionic liquid**" for "**cellulose**" highlighting their cationic counterpart (analyzed with the Scifinder® database).

The group "Oxidation & Formulation" has a long experience in alkyl quaternary ammonium for several years ago, especially in their behavior as catalytic surfactants for the elaboration of microemulsions. As an example, the self-aggregation behavior of dimethyldioctylammonium salts in water has been thoroughly studied as a function of various counter anions, as depicted in **Figure 2.2**.[169]

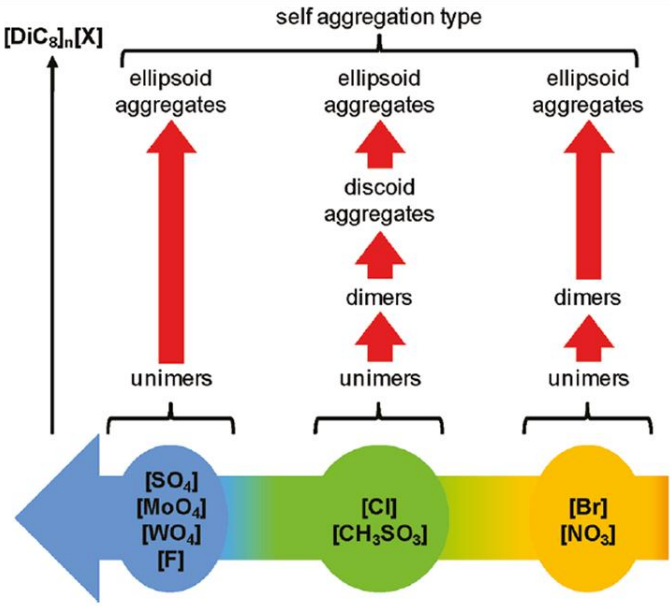

Figure 2.2 Self-aggregation behavior of dimethyldioctylammonium [DiC_8] in water as a function of the counter anion [X].[169]

During the numerous investigations, researchers have noticed that some of them were liquid at room temperature. In line with such findings, the group has decided to go deeper in the search of ILs based on alkyl quaternary ammonium salts. Furthermore, quaternary ammonium is the simplest cation allowing a tuning of the number and length of alkyl chains in order to assess the impact of the IL chemical structure on its physicochemical properties and capacity for cellulose solubilization. Therefore, short chain quaternary ammonium salts were first used in the present work as a model to investigate a series of organic cationic counter parts with further attempts to rationalize the rules making that their combination leads to an IL. Other advantages of quaternary ammonium cations is that they are less toxic than imidazolium and pyridinium which have also been much more investigated.[92] Besides, they are expected to be more biodegradable than ILs with heteroaromatic counterparts at cations, *e.g.* imidazolium and pyridinium.[170]

Regarding the anions commonly encountered for the cellulose solubilization application, up to now, mainly **chloride**, **bromide** and **acetate** have been used.[34] One of our aims was to develop novel biocompatible ILs for the cellulose solubilization. Indeed, a remaining challenge in the search for novel Ils is a 100% biosourced origin and within this context, biosourced IL anions, such as **natural carboxylates**, appear as good candidates from an ecological point of view. Thus, to get closer to the "Graal", the quaternary ammonium bearing various short alkyl chains were combined with various biosourced carboxylate anions, which are much more common than their cationic counterpart. In the literature, several quaternary ammonium carboxylates have already been described, such as the **diethyldimethylammonium carboxylates** (acetate, formate,

propionate, butyrate, maleate, succinate) or cyclohexyl-based ammonium in combination with formate and acetate.[171,172]

In this work, we performed a systematic investigation of 15 organic anions: **formate**, **acetate**, **lactate**, **glycolate**, **levulinate**, **sorbate**, **salicylate**, **mandelate**, **succinate**, **itaconate**, **maleate**, **fumarate**, **malate**, **tartrate** and **citrate** as natural-sourced anions, as shown in the following (**Figure 2.3**). Besides their biosourcing, they have also been retained both for their easy accessibility and relatively low price.[173]

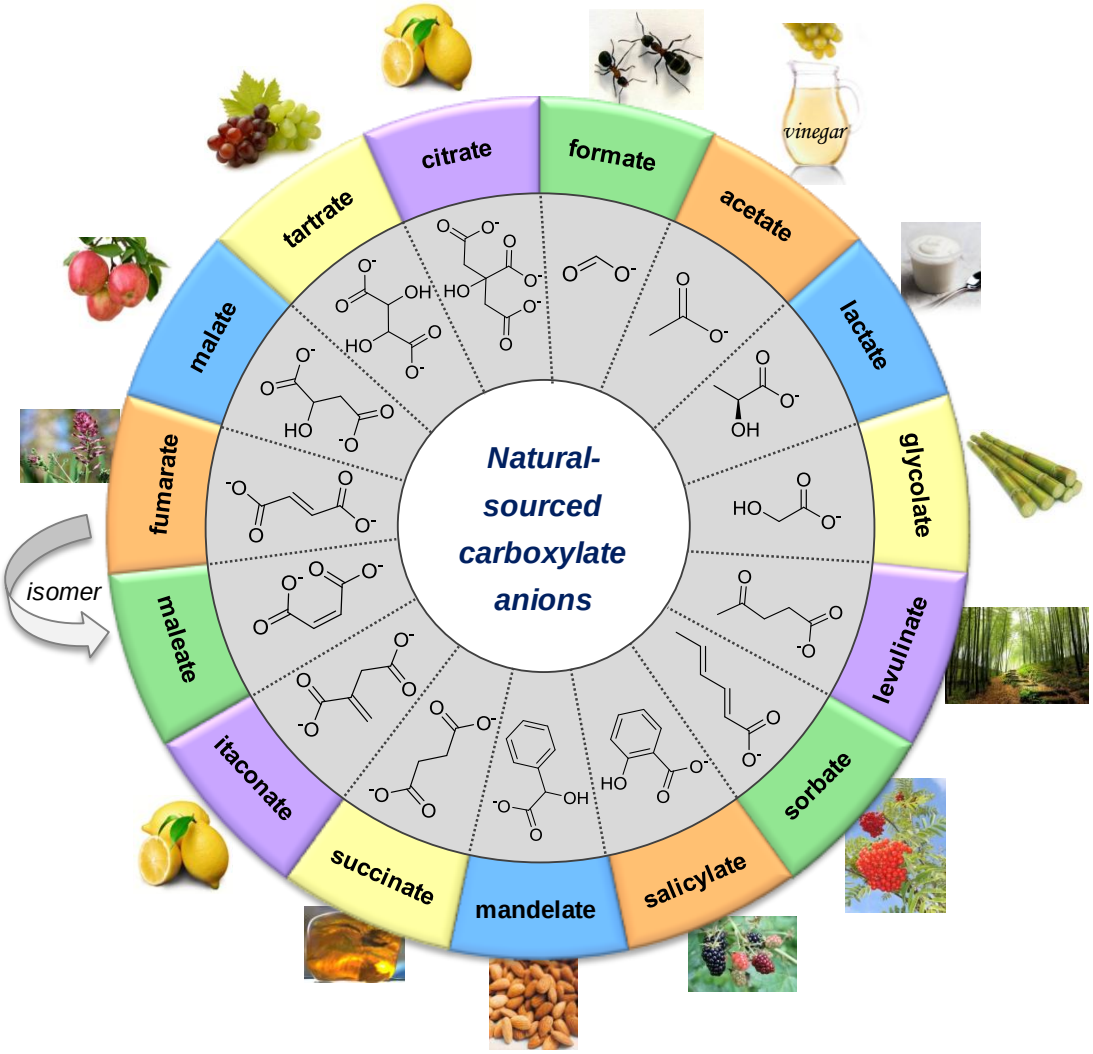

Figure 2.3 Overview for the used natural-sourced carboxylate anions and their natural sources.

In nature, **formic acid (For; pka 3.77)** is found in the venom of ants. **Acetic acid (Ace; pka 4.76)** is the main component of vinegar (4 – 8%) apart from water. The primary natural sources for **lactic acid (Lac; pka 3.86)** are milk products, *e.g.* yogurt, cheese. **Glycolic acid (Gly; pka 3.83)** is found in some sugar-crops. **Levulinic acid (Lev; pka 4.64)** is derived from degradation of cellulose. **Sorbic acid (Sor; pka 4.76)** was first isolated from rowanberry oil by distillation. Unripe fruits and vegetables are natural sources for **salicylic acid (Sal; pka 2.97)**, in particular

blackberries, blueberries, etc. **Mandelic acid (Mand; pka 3.41)** was discovered in an extract of bitter almonds. **Succinic acid (Suc; pka_1 4.16, pka_2 5.61)**, which is historically known as spirit of amber, was originally obtained from amber. **Itaconic acid (Ita; pka_1 3.84, pka_2 5.55)** is produced by distillation of **citric acid (Cit; pka_1 3.13, pka_2 4.76, pka_3 6.39)**, which is mainly found in citrus fruits. **Maleic acid (Male; pka_1 1.83, pka_2 6.59)** is the *trans*-isomer of **fumaric acid (Fum; pka_1 3.03, pka_2 4.44)**, which is found in nature in fumitory, bolete mushrooms or Iceland moss. **Malic acid (Mala; pka_1 3.40, pka_2 5.20)** was first isolated from apple juice. **Tartaric acid (Tar; pka_1 2.89, pka_2 4.40)** occurs naturally in many plants, mainly in grapes, bananas and tamarinds.

Two main approaches were undertaken: one physicochemical approach during which all the synthesized ILs have been fully characterized by several descriptors and parameters, and one practical approach aiming at assessing the maximum percentage of cellulose solubilized in each IL, searching *in fine* for a correlation between physicochemistry and solubilization. As a progressive evolution of the work and to reach "the Graal", the third chapter will be devoted to biosourced cations **choline**, **betaine** and **carnitine** combined with the most relevant biosourced anions. The screening and investigation of many different carboxylate anions expanded the model for this work and helped us to understand the structural effects on the physicochemical properties and cellulose solubilization capacity. In other words, before finding a new biosourced and biocompatible IL able to dissolve a high percentage of cellulose, our approach was to understand which structural parameters drive this property.

Short-chain two- and three-tailed quaternary ammonium cations have been combined with various natural carboxylate anions to give ILs of the type $[(C_nH_{2n+1})_2N(CH_3)_2]X$ or $[(C_nH_{2n+1})_3N(CH_3)]X$ (n = 3, 4, 6; X = carboxylate anion), abbreviated as **QACILs**. The physicochemical characterization of these compounds as novel potential ILs, *i.e.* thermal phase transitions, thermal stability, viscosity, surface activity and hydrotropic behavior, have been investigated, and their ability for dissolving cellulose was studied. As an additional aspect, Hansen solubility parameters of the ILs have also been investigated with the aim to support the result for cellulose dissolution. To assess their use as potential "green" solvents, their biodegradability has also been studied.

2.2 Synthesis of QACILs

The QACILs were synthesized according to two reaction steps. During the first step, the quaternary ammonium halide salt was prepared starting from the corresponding amine. The second step consisted in an anion exchange providing directly the pure ILs with a carboxylate anion as a counterpart.

2.2.1 Preparation of quaternary ammonium halide salts

The two- or three-tailed quaternary ammonium compounds $[(C_nH_{2n+1})_2N(CH_3)_2]X$ or $[(C_nH_{2n+1})_3N(CH_3)]X$, abbreviated as **[DiC$_n$]** or **[TriC$_n$]** respectively (n = 3, 4, 6; X = Br, I), were synthesized *via* a nucleophilic substitution, namely an alkylation of *N,N,N*-alkyldimethylamines or *N,N,N*- dialkylmethylamines with 1-haloalkanes (**Eq. 2.1**) with yields around 90-99 %.

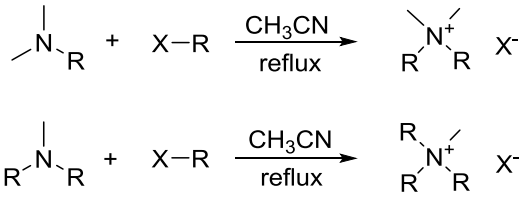

Eq. 2.1

2.2.2 Preparation of quaternary ammonium carboxylates via anion exchange

By varying the nature of the organic anion and the number and chain length of the ammonium 46 compounds were synthesized. The first step of the synthesis was followed by an anion metathesis to obtain the quaternary ammonium carboxylates (**Eq. 2.2**). Therefore, the salt with a halide anion $[(C_nH_{2n+1})_2N(CH_3)_2]X$ or $[(C_nH_{2n+1})_3N(CH_3)]X$ was transformed to a hydroxide salt over an exchange resin (Amberlite® IRA-400(Cl) followed by neutralization with the corresponding biosourced carboxylic acid with yields around 90 %.[174]

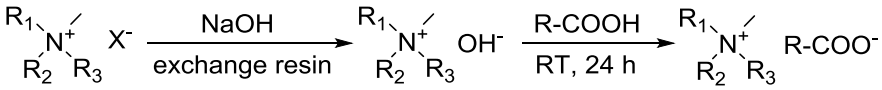

Eq. 2.2

$R_1 = R_2 = CH_3$ or C_nH_{2n+1} with n = 3, 4 or 6; R_3 = H or CH_3

Water was then removed by lyophilization of the synthesized ILs using a freeze dryer for at least 72 h. Residual water content was determined with a coulometric Karl-Fischer titration. The **QACILs** are very hygroscopic. Moreover, some of them contain water in their structure, as crystallization water. Thus, the quaternary ammonium compounds can contain water between 0.7 for *e.g.* $[DiC_4]Br$ until 12.8 wt% for *e.g.* $[DiC_4]_2Ita$ (details are given in the ***experimental section***), even after freeze drying for several days. This is an important point since residual

water can modify the physicochemical properties of the compounds, especially its behavior as an IL. This is a recurrent problem for these compounds which have many times been pointed out in the literature. However, it is noteworthy that this is not straightforward at all to synthesize ILs free of residual water. It is nevertheless important to determine this "water impurity" and to be aware of it. Thus, before determining their physicochemical properties, the **QACILs** have been dried as much as possible and stored under an atmosphere of argon. The purity of the synthesized products was confirmed by ^{1}H- and ^{13}-C-NMR. The anion exchange was followed by pH-control with a pH-meter, and the good agreement between integrations of the cation and of the anion in the ^{1}H-NMR spectrum of the final products was a proof of the total anion exchange. The chemical structures of the quaternary ammonium cations and carboxylate anions as well as their abbreviations are given in **Table 2.1**. The ^{1}H- and ^{13}C-NMR data of the 46 synthesized QACILs are detailed in the ***experimental section*** of this chapter.

Table 2.1 Cations and anions investigated for the preparation of the 46 QACILs.

Cations				
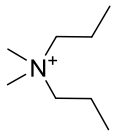	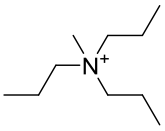	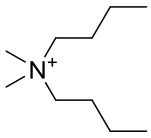	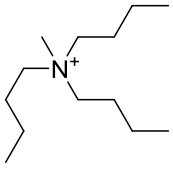	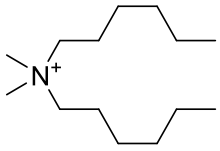
[DiC$_3$]	**[TriC$_3$]**	**[DiC$_4$]**	**[TriC$_4$]**	**[DiC$_6$]**
Anions				
	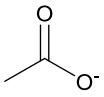	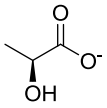	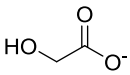	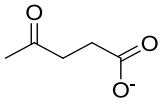
Formate	Acetate	Lactate	Glycolate	Levulinate
For	**Ace**	**Lac**	**Gly**	**Lev**
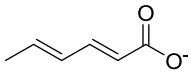	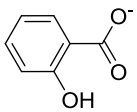	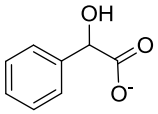	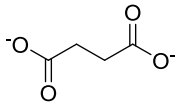	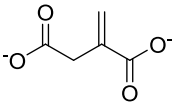
Sorbate	Salicylate	Mandelate	Succinate	Itaconate
Sor	**Sal**	**Mand**	**Suc**	**Ita**
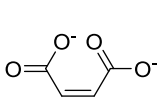	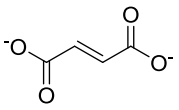	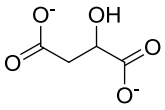	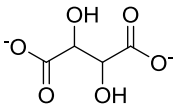	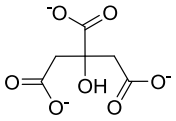
Maleate	Fumarate	Malate	Tartrate	Citrate
Male	**Fum**	**Mala**	**Tar**	**Cit**

2.3 Physicochemical properties of QACILs

The investigation of physicochemical properties is an essential step to understand the characteristics of a compound with regard to its application potential. **Figure 2.4** summarizes some of the most important properties required for pure ILs, which have already been explained in detail in the first chapter, ***section 1.1.2***, *e.g.* degradation temperature, melting temperature, glass transition, viscosity and surface tension.

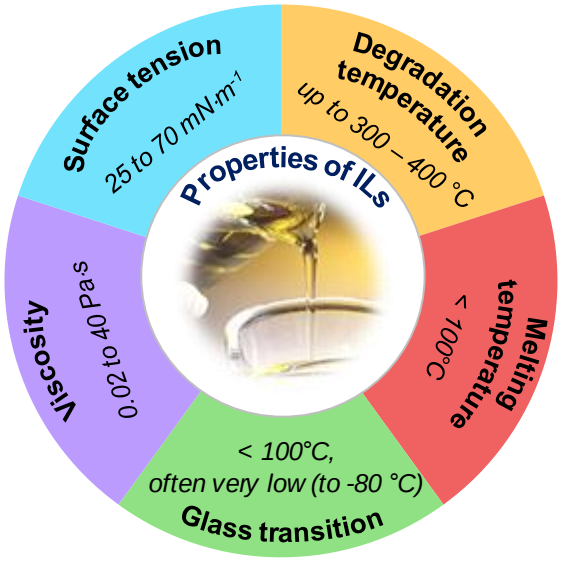

Figure 2.4 Schematic overview of the most important properties required for ILs.

Based on this, the most important physicochemical properties of the **QACILs** previously prepared have been studied. **Thermal analyses** have been carried out with the aim to determine the **decomposition temperatures** and **thermal phase transitions**, such as **glass transition** and **melting temperature**. **Viscosities** were measured at different temperatures. Additionally, **surface tensions** of the pure **QACILs** have also been determined. Finally, because of their chemical structure, their ability to act as **hydrotropes** was also examined by measuring their critical aggregation concentration to assess their possible self-aggregation and their capacity to solubilize a hydrophobic solute in water.

2.3.1 Thermal analyses

2.3.1.1 Thermal stability

Thermogravimetric analysis (TGA) was used to determine the thermal degradation temperatures, abbreviated as T_{deg}, and therefore the thermal stability of the **QACILs**. The degradation ranges (temperature range of the peak of the derivative weight loss curve) for the

different compounds are given in **Table 2.2** (TGA curves are shown in the ***experimental section)***. For all compounds, decomposition started at temperatures from 135 to 230 °C in agreement with data found in the literature for similar compounds (*e.g.* **[DiC$_4$]Br**: 225 °C; **[DiC$_6$]Br**: 215 °C).[175] Generally, the halogenated ILs are stable until higher temperatures compared to their carboxylate analogues. In particular, the acetate IL series shows an early loss of weight (**Figure 2.5.a**) which could be explained by a degradation mechanism involving dealkylation of the cation by nucleophilic attack from the anion to form the corresponding amine, as already proposed in the literature.[176,177] Such phenomenon mainly appears in the presence of rather nucleophilic anions like acetate.[178] The comparison of TGA curves of the acetate-based ILs highlights some similarity, irrespective of the cations.

Figure 2.5.b, however, shows huge differences of TGA curves due to different anions with the same cation [DiC$_4$]. As already mentioned, halogenide ILs (**[DiC$_4$]Br**) are thermally more stable than carboxylate ones. The salicylate-based IL is more stable than the ILs with simple carboxylates which could be fact of the aromatic part in the structure. The QACIL **[DiC$_4$]Gly** exhibits an early weight loss (starting at ca 60 °C) which seems to be similar to the decomposition phenomenon of acetate ILs. **[DiC$_4$]$_2$Suc** is the less stable QACIL in this serie. The lower thermal stability of this divalent-anion-based IL is probably due to the weaker cation-anion Coulombic interaction freeing up the anions to act as stronger nucleophiles.[176] Generally, the thermostability data and the comparison of the TGA curves indicate that this property is mainly dependent on the anion of ILs series.

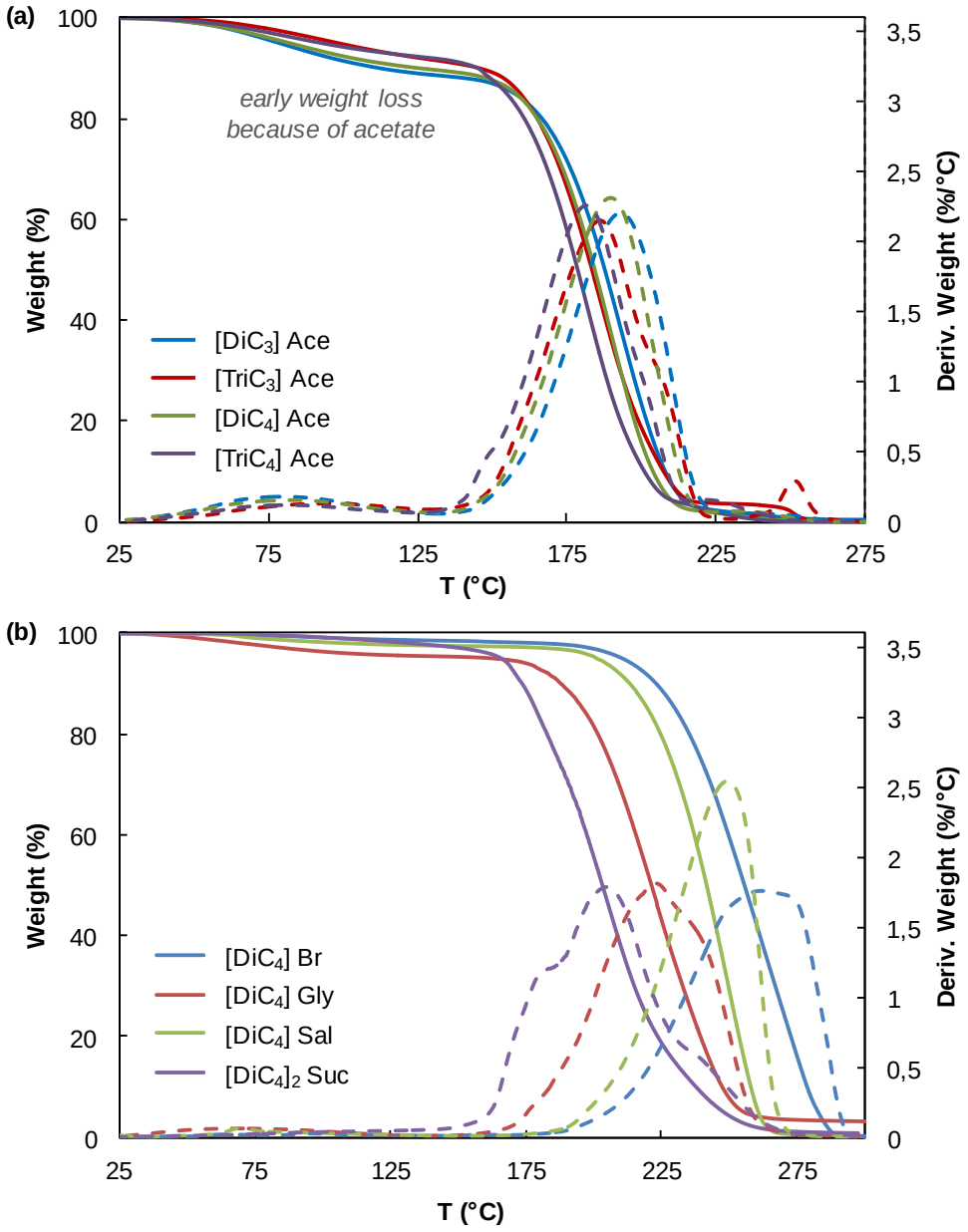

Figure 2.5 Comparison of TGA-curves (continuous line: weight %; dashed line: derivative weight % / °C): **(a)** of acetate ILs with different cations: [DiC_3], [$TriC_3$], [DiC_4], [$TriC_4$], and **(b)** [DiC_4] ILs with different anions: Br, Gly, Sal, Suc.

2.3.1.2 Thermal transitions

Thermal phase transitions were determined by differential scanning calorimetry (DSC), providing the **glass transition** (T_g, as the midpoint of a small endothermic heat capacity change from the amorphous glass state to a liquid state), the **cold crystallization** (T_c, as onset of an exothermic peak on heating from a supercooled liquid state to a crystalline solid state), the **melting temperature** (T_m, as onset of an endothermic peak on heating) and the **freezing temperatures** (T_f, as onset of an exothermic peak on cooling).[179,180] In **Table 2.2**, the glass transition temperatures T_g and the melting temperatures T_m of the **QACILs** are listed.

Table 2.2 Thermal properties of QACILs: degradation ranges T_{deg}, glass transition temperatures T_g and melting temperatures T_m.

Compound	T_{deg} (°C)	T_g (°C)	T_m (°C)	DSC-behavior [a]
[DiC$_3$]Cl	178-273	-	145	I
[DiC$_3$]I	187-275	-	180 (175.6[175])	I
[DiC$_3$]Ace	140-228	-	-	IV
[DiC$_3$]Lac	156-263	-	-	IV
[DiC$_3$]Lev	143-254	-13.0	-	II
[DiC$_3$]$_2$Ita	150-260	-55.3	-	II
[TriC$_3$]Cl	222-275	-	127.2	I
[TriC$_3$]Br	232-274	-	137.9	I
[TriC$_3$]Ace	140-260	-64.0	-	II
[TriC$_3$]Lac	150-256	-68.4	-	II
[TriC$_3$]Lev	140-250	-66.8; -11.9	-	II
[TriC$_3$]$_2$Ita	136-252	-47.4; -12.2	-	II
[DiC$_4$]Cl	177-272	-	126	I
[DiC$_4$]Br	183-293	-	130.1	I
[DiC$_4$]For	157-255	-	-	IV
[DiC$_4$]Ace	138-248	-	-	IV
[DiC$_4$]Lac	162-262	-	14.6	III
[DiC$_4$]Gly	155-272	-62.4	-	II
[DiC$_4$]Lev	140-258	-	-	IV
[DiC$_4$]Sor	144-245	-64.3	51.9	III
[DiC$_4$]Sal	186-273	-59.5	45.2	III
[DiC$_4$]Mand	173-281	-52.0	-	II
[DiC$_4$]$_2$Suc	146-276	-54.7; -7.2	-	II
[DiC$_4$]$_2$Ita	142-260	-53.4; 5.4	-	II
[DiC$_4$]$_2$Male	140-250	-56.6	-	II
[DiC$_4$]$_2$Fum	153-262	-53.5; 3.1	-	II
[DiC$_4$]$_2$Mala	157-256	-46.4	-	II
[DiC$_4$]$_2$Tar	170-260	-36.9	-	II
[DiC$_4$]$_3$Cit	135-250	-41.8; -1.1	-	II
[TriC$_4$]Cl	156-244	-	114 (110[181])	I
[TriC$_4$]Br	172-267	-	123 (120[182])	I
[TriC$_4$]Ace	132-247	-55.7	-	II
[TriC$_4$]Lac	152-252	-13.5	67.3	I

[TriC$_4$]Gly	153-270	-13.7	-	II
[TriC$_4$]Lev	139-245	-64.9	-	II
[TriC$_4$]$_2$Ita	144-260	-39.5	-	II
[DiC$_6$]Br	179-298	-	55 (53.9[175])	I
[DiC$_6$]Ace	140-249	-	-	IV
[DiC$_6$]Lac	166-253	-34.0	-	II
[DiC$_6$]Gly	161-265	-68.1	-	II
[DiC$_6$]Lev	143-247	-	-	IV
[DiC$_6$]Sal	179-269	-	66.7	III
[DiC$_6$]Mand	183-269	-59.2	-	II
[DiC$_6$]$_2$Ita	144-263	-59.2; 1.7	-	II
[DiC$_6$]$_2$Tar	167-251	-0.4	-	II
[DiC$_6$]$_3$Cit	129-239	-51.9	37.9	III

[a] **Group I**: classical crystallization of salts; **Group II**: only glass transition; **Group III**: with cold crystallization; **Group IV**: no transition.

Four different thermal behaviors can be identified during the cooling and heating scans for the **QACILs** (**Figure 2.6**). The first behavior (group I, **Figure 2.6.a**) is characterized by a melting point upon heating and a freezing point upon cooling. This behavior, which is typical of *classic crystallization processes of salts* is specific of halogenated compounds, such as dialkyldimethylammonium bromides and iodides.[175] **[TriC$_4$]Lac** is the only carboxylate compound exhibiting such a behavior. This unexpected behavior remains unexplained. Suspecting an ideal arrangement between the anion and the cation of this IL, caused on their structural and electronic properties, the crystallization arises with a classic melting transition peak and a freezing transition peak in the DSC thermogram. The second behavior (group II, **Figure 2.6.b**) shows only a glass transition without melting or freezing, and *almost all of the RT-liquid QACILs* reveal this behavior pattern. Further compounds of this class, such as **[DiC$_4$]$_2$Suc**, **[DiC$_4$]$_2$Fum**, **[DiC$_4$]$_3$Cit**, are gels, pastes or waxes at RT. Because of the reduced packing efficiency, the formation of an amorphous glass takes place instead of an ordered crystalline state.[178] So-called overshoot peaks, which are detected in many thermograms with a typical heat flow jump at one side of the peak (**Figure 2.7**), come up from a structural relaxation.[183] The thermograms of **[DiC$_3$]$_2$Ita, [TriC$_3$]Ace, [TriC$_3$]$_2$Ita, [DiC$_4$]Mand, [DiC$_4$]$_2$Male, [TriC$_4$]Ace** and **[TriC$_4$]Lev** contain overshoot peaks for the glass transition. The third type shows cold crystallization between the glass transition and the melting points on heating (group III, **Figure 2.6.c**) which was found for **[DiC$_4$]Sor** and **[DiC$_4$]Sal**, and also for **[DiC$_4$]Lac** with a cold crystallization between two melting transitions. The last behavior holds DSC thermograms

without any phase transition (group IV, **Figure 2.6.d**). **[DiC$_3$]Ace**, **[DiC$_3$]Lac, [DiC$_4$]Ace** and **[DiC$_4$]Lev** are liquid at RT, and in the range from -80 until 50 °C, no transition peak was found with DSC measurements. The DSC curves for the other compounds are given in the ***experimental section***.

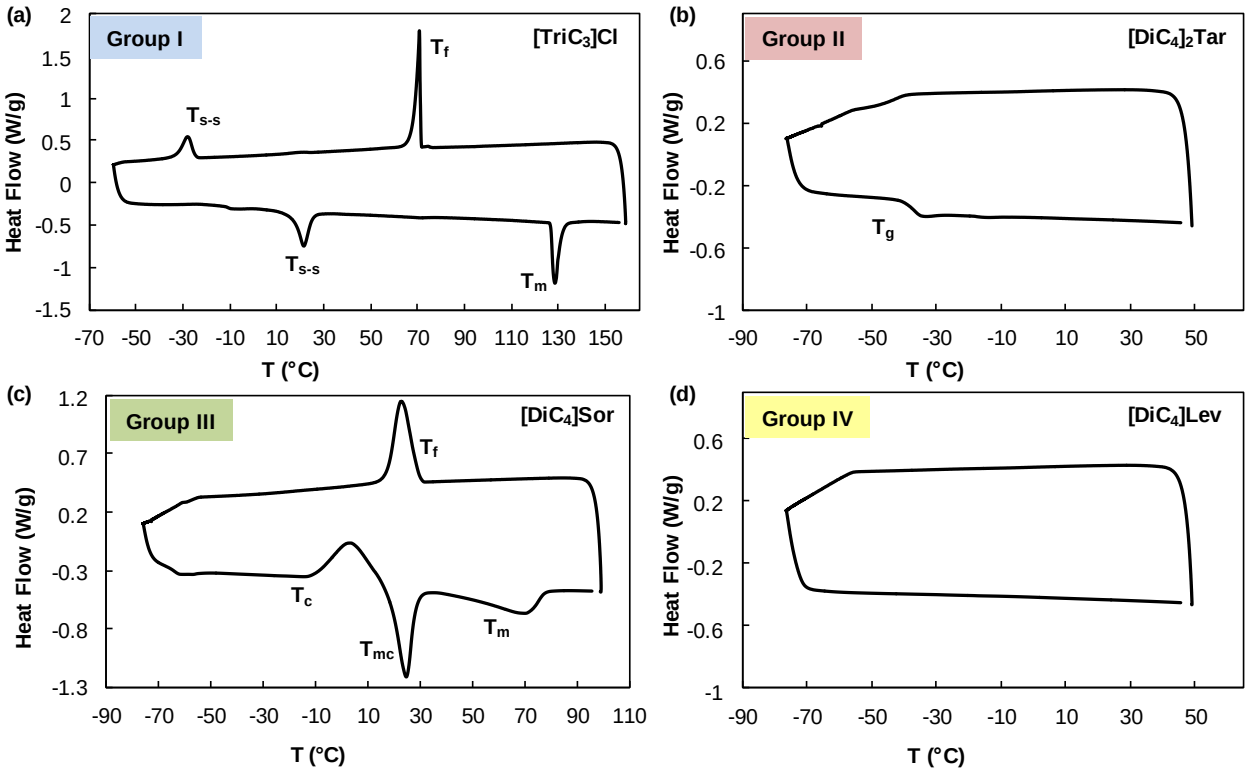

Figure 2.6 DSC curves of **(a) [TriC$_3$]Cl**, with a solid-solid transition $T_{s\text{-}s}$ and a melting transition T_m on heating, and a freezing point T_f and a solid-solid transition $T_{s\text{-}s}$ on cooling, **(b) [DiC$_4$]$_2$Tar**, with a glass transition T_g on heating, **(c) [DiC$_4$]Sor**, with a cold crystallization T_c and two melting transitions T_{mc} and T_m on heating, and a freezing transition T_f on cooling, and **(d) [DiC$_4$]Lev**, without a phase transition. The exothermic events are pointing up in the DSC curves; the upper curve represents the cooling scan and the lower curve the heating scan.

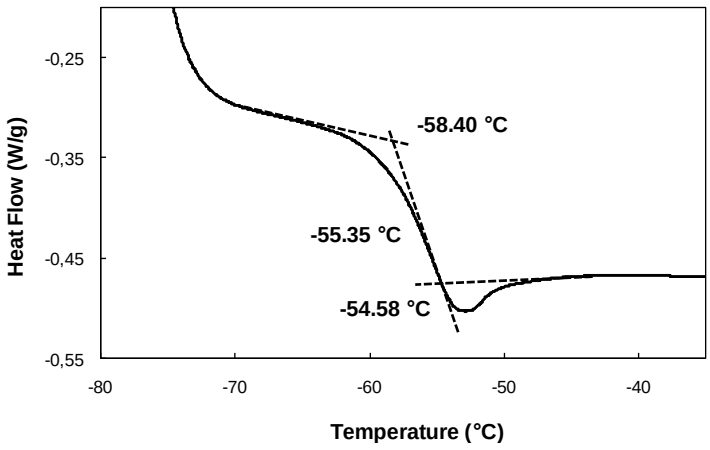

Figure 2.7 Glass transition with an overshoot peak on DSC heating scan for **[DiC$_3$]$_2$Ita** with T_{onset} = -58.40 °C, T_g = -55.35 °C (midpoint), and T_{end} = -54.58 °C.

2.3.2 Viscosity of QACILs

The **dynamic viscosity** η of ILs depends on different factors, such as the molecular symmetry, the ion size and the ion interactions, and on the whole, it is mainly governed by van der Waals interactions and H-bonding.[184] Minimal viscosities are obtained with the use of small ion weights which show a high mobility.[52] Alkyl chain lengthening or fluorination, for instance, make an IL more viscous due to increased van der Waals interactions. Alkyl chain ramification (from butyl to isobutyl for instance) has the same effect due to minimized rotation freedom. Increasing the number of H-bonding of cations and anions leads to an increase of IL viscosity.[52] Viscosity is probably one of the most important physical properties considering the application of ILs because of its strong effect on the rate of mass transport.[64,185]

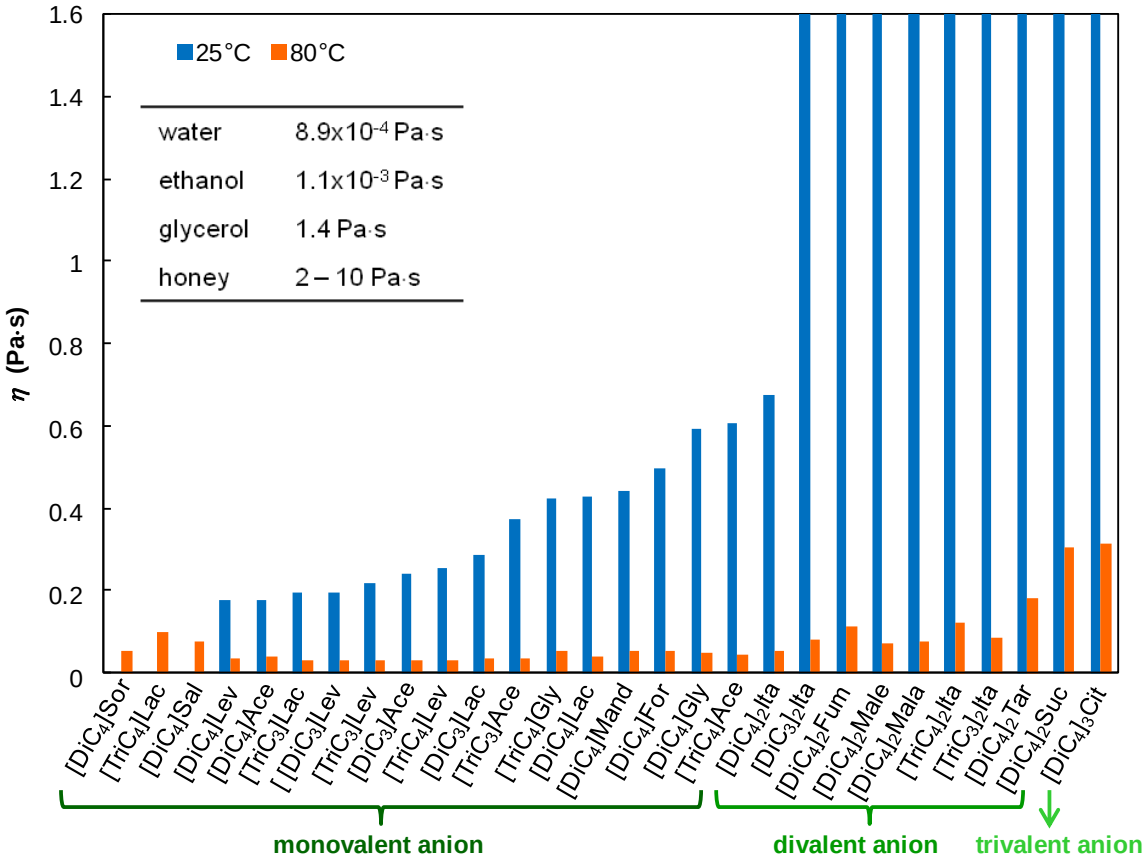

Figure 2.8 Dynamic viscosities η of QACILs at 25 and 80 °C (values are given in the experimental section); $[DiC_4]$Sor, $[TriC_4]$Lac and $[DiC_4]$Sal are solid at RT.

The dynamic viscosity η of the **QACILs** was measured with a Kinexus rotational rheometer with cone plate geometry (CP 20/2°), equipped with a Peltier temperature-controlled plate (see ***experimental section***). All the measured viscosity data of **QACILs** at 25, 40, 60 and 80 °C are given in the ***experimental section***. We mainly focused on ILs based on propyl- and butyl-chain quaternary ammonium cations because they showed promising results for the application as cellulose solvents. **Figure 2.8** reports the dynamic viscosities of **QACILs** at 25 and 80 °C. At RT,

the measured viscosity values are found in the wide range of 0.17-19.2 Pa·s. In the series of the [DiC$_4$] cation, the viscosity decreases in the following order: **Cit > Suc > Tar > Male > Ita > Fum > Gly > For > Mand > Lac > Ace > Lev**. The viscosity is higher for tri- and divalent anions than for ILs with a 1:1 cation-to-anion ratio. This phenomenon is essentially attributed to the lack of conformational degrees of freedom, involving stronger intermolecular interactions than for the 1:1 ion pairs which are more flexible, and give therefore a less viscous IL.

The temperature dependence of viscosity was investigated over a temperature range of 25 to 80 °C for the different **QACILs** (see ***experimental section***). The examined viscosities decreases with increasing temperature due to the higher mobility of ions at elevated temperatures, as expected.[7] However, a great difference in the decreasing rate of viscosity between the ILs was found. In general, the viscosity of the more viscous compounds decreases more rapidly with increasing temperature. As shown in **Figure 2.9**, the viscosity of **[DiC$_4$]Lev** could be decreased 4.8 times from 0.174 Pa·s to 0.036 Pa·s, 8.5 times from 0.442 Pa·s to 0.052 Pa·s for **[DiC$_4$]Mand**, 31.2 times from 6.525 Pa·s to 0.209 Pa·s for **[DiC$_4$]$_2$Tar** and 54.7 times from 16.790 Pa·s to 0.307 Pa·s for **[DiC$_4$]$_2$Suc**.

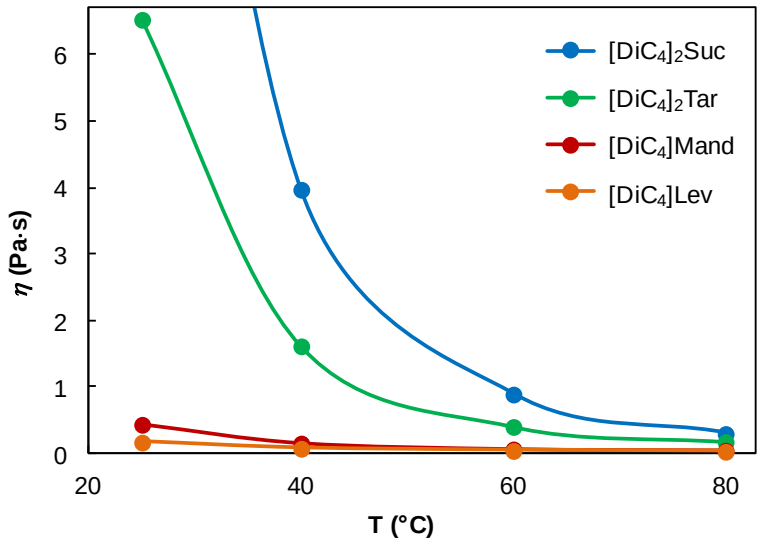

Figure 2.9 Temperature dependence of dynamic viscosities η of **QACILs**.

2.3.3 Surface tension of pure QACILs

Surface tension σ is a contractive propensity of the surface of a liquid that permits it to resist an external force. It is defined as the ratio of required energy for the transport of a molecule from the bulk to the surface of a liquid, leading to the increase of the liquid surface area, which is represented by surface free energy per unit surface area in thermodynamics.[186] So, this property of pure liquids is interesting for the determination of cohesive forces among liquid molecules

present at the surface.[62] Especially ILs, which are generally composed of strongly anisotropic ions referring to structure and charge, have quite different structure and molecular distribution at the surface and in the bulk.[62] The intermolecular interaction potential energy and the liquid interfacial microstructure are the main factors leading to the surface tension.[63] Water, for instance, has a high surface tension (72.7 $mN \cdot m^{-1}$) because of its high molecular attraction. As a visible result, a liquid with high surface tension forms spherical droplets because a sphere offers the smallest area for a definite volume. Liquids with low surface tension, however, have the tendency to form films. Generally, ILs have higher surface tensions than most common molecular solvents (*e.g.* ethanol: 22.0 $mN \cdot m^{-1}$, acetone: 23.5 $mN \cdot m^{-1}$, diethyl ether: 16.6 $mN \cdot m^{-1}$), but lower ones than water (72 $mN \cdot m^{-1}$ at 25 °C).[64,65]

Surface tensions of **QACILs** (with propyl- and butyl-chains on the cation) have been determined at 25 and 80 °C. As expected, the values are found in the range of 30 to 47 $mN \cdot m^{-1}$ at 25 °C, thus higher than organic solvents and lower than water. The lowest values were found for **[DiC$_4$]$_2$Mala** (29.9 $mN \cdot m^{-1}$), **[DiC$_4$]$_2$Tar** (30.5 $mN \cdot m^{-1}$), **[TriC$_4$]Ace** (33.9 $mN \cdot m^{-1}$), and **[DiC$_4$]Ace** (34.7 $mN \cdot m^{-1}$). The **QACILs** with the highest surface tensions were **[DiC$_3$]$_2$Ita** (46.8 $mN \cdot m^{-1}$), **[TriC$_3$]Lac** (42.8 $mN \cdot m^{-1}$), **[TriC$_3$]$_2$Ita** (42.6 $mN \cdot m^{-1}$), **[DiC$_4$]$_2$Fum** (42.3 $mN \cdot m^{-1}$), and **[DiC$_4$]Gly** (41.6 $mN \cdot m^{-1}$). Generally, the increase of the size of molecules or ions leads to a decrease of surface tensions related to the lowered intermolecular interaction.[187] However, ILs are complex compounds where Coulombic forces, hydrogen bondings and van der Waals forces all are present in the interactions between the ions. Thus, it is not evident to edict simple rules for ILs surface tensions. In our case, we found that **Ita** combined with **[DiC$_3$]** and **[TriC$_3$]**, **[TriC$_3$]Lac**, **[DiC$_4$]$_2$Fum** and **[DiC$_4$]Gly** had the highest surface tensions, which means that there are strong interactions between these ions which could be attributed to a favored arrangement of their size and charge distributions. **Ita** and **Fum** are divalent anions which contain C=C double bonds which can play an important role in the surface tension. **Lac** and **Gly** contain hydroxyl groups affecting the hydrogen bond interactions in the ILs leading to elevated surface tensions.

Taking a closer look at the change of the surface tension σ with the variation of IL cations, a certain influence can be highlighted. The difference of surface tension with anion variation is much higher for **[DiC$_3$]** > **[TriC$_3$]** > **[DiC$_4$]** > **[TriC$_4$]**, as shown in **Figure 2.10**. Obviously, the more the cation is hydrophobic, the less the variation of anion affects the ILs surface tension.

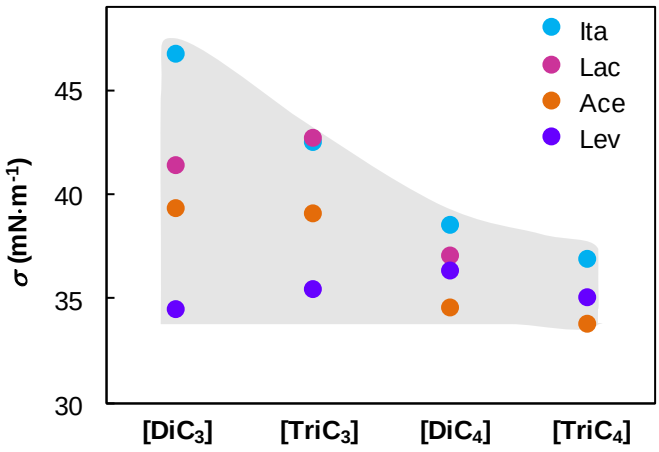

Figure 2.10 Surface tension σ of **QACILs** based on various cations, [DiC$_3$], [TriC$_3$], [DiC$_4$], [TriC$_4$], and anions (Ace, Lac, Lev, Ita) at 25 °C; for **[TriC$_4$]Lac**: no data point because it is solid at RT.

Regarding the temperature dependence, the surface tension σ at the liquid/air interface decreases generally with increasing temperatures as a result of the change of the internal cohesive energy (the sum of molecular interactions, like hydrogen bonding, electrostatic and van der Waals interactions).[62] The amount of the slope of the temperature dependence of the surface tension σ of a pure liquid is the surface entropy S^{σ} which is the degree of surface disorder relating to the bulk liquid (**Eq. 2.3**).[188]

$$S^{\sigma} = -\left(\frac{\mathrm{d}\sigma}{\mathrm{d}T}\right) \qquad \textbf{Eq. 2.3}$$

As the surface entropy is reported to be primarily ruled by the anion nature,[189] we took a closer look at the cation **[DiC$_4$]** series with different anions (**Figure 2.11**). As a result, the surface tension decreases with the following sequence: **Fum > Mand > Ita > Lac > Lev > Ace** at 25 °C, whereas at 80 °C the order changes for Ace, Ita and Lev. The surface entropy S^{σ} has been calculated for each **[DiC$_4$] IL**, and the values are given in **Table 2.3**. The **QACILs [DiC$_4$]Ace**, **[DiC$_4$]Lac**, **[DiC$_4$]Mand** and **[DiC$_4$]$_2$Fum** show low entropy values, which indicates a high degree of surface ordering.[190] However, two **QACILs**, namely **[DiC$_4$]Lev** and **[DiC$_4$]$_2$Ita**, stand out with very high values around 15 J·m^{-2}·K^{-1}. Such high values have already been reported in the literature, but no real structural reason was addressed.[62]

Table 2.3 Surface entropy S^{σ} of **QACILs**.

QACIL	**[DiC$_4$]Ace**	**[DiC$_4$]Lac**	**[DiC$_4$]Lev**	**[DiC$_4$]Mand**	**[DiC$_4$]$_2$Ita**	**[DiC$_4$]$_2$Fum**
S^{σ} (J·m^{-2}·K^{-1}) x 10^{-5}	4.10	3.96	15.31	4.74	15.57	3.69

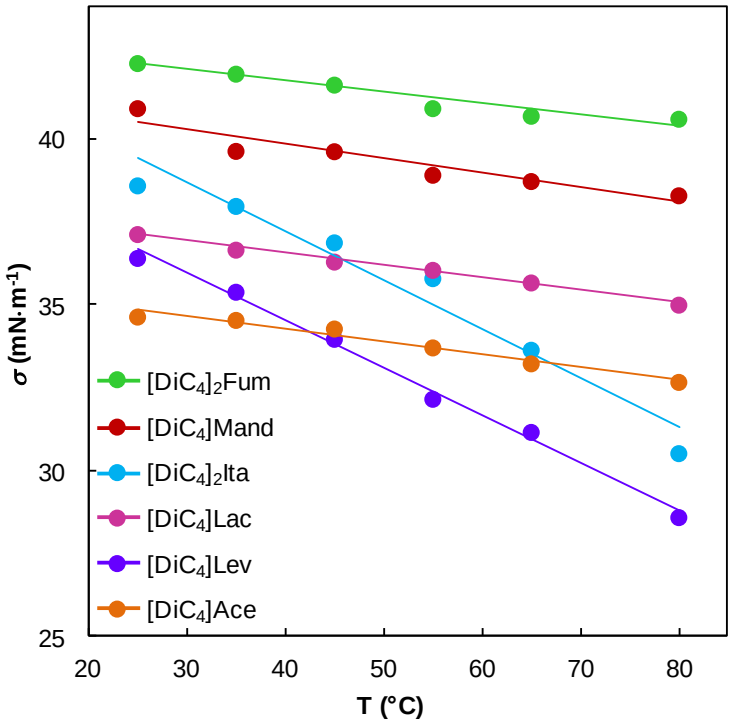

Figure 2.11 Temperature dependence of the surface tensions σ of **QACILs** with [DiC_4] cation and various anions.

2.3.4 Hydrotropic behavior of QACILs

2.3.4.1 Minimal aggregation concentration (MAC)

The study of surface tensions of binary mixtures with water are very useful for the evaluation of self-assembly properties of amphiphilic cations or anions, and their combination, i.e. of ILs.[191]

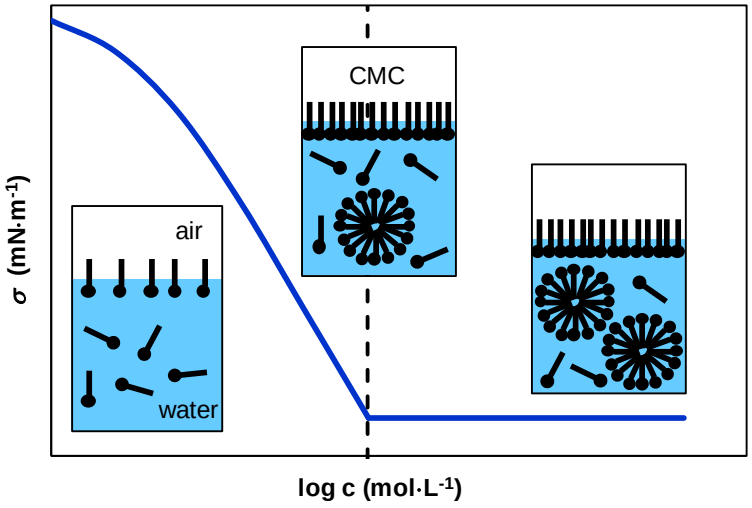

Figure 2.12 Surface tension σ as a function of surfactant concentration c of a surfactant with ideal self-assembly behavior showing micelle formation from the critical micelle concentration (CMC).[191,192]

As shown in **Figure 2.12**, surface tension changes significantly as a function of the concentration of surface active compounds. At the minimal aggregation concentration (MAC) or critical micelle concentration (CMC), the surface of the solution is completely saturated and the formation of aggregates or micelles initiates.[192] The surface tension changes strongly due to the massive change of the liquid's surface. Above the CMC or MAC, the surface tension remains constant and a plateau is reached, as shown in **Figure 2.12**. The term MAC is used for different kind of bulk complexation or aggregations, however the term CMC is only used for surfactants which form defined structures called micelles.[193] In this study, we use the term MAC (minimal aggregation concentration) because the formation of defined micelles is not assumed.[194,195]

The surface tensions of aqueous solutions containing increasing concentrations of **QACILs** have been measured. Some significant results are shown in **Figure 2.13 a)** for [DiC_4] and **b)** for [DiC_6] cations in combination with different anions (*e.g.* Br, Lev, Sal, Tar), and the MAC for all compounds is given in **Table 2.4**. The maximal concentration for aqueous surface tension measurements was fixed at 2 mol·L^{-1} for practical reasons. In the case of **[DiC_6]Sal**, the measurement was limited by the low water solubility of the IL. Regarding the series with [DiC_4] cations, some ILs have high MAC values ($\geq$ 1 mol·L^{-1}), namely Br, Ace, Lac, Gly and Lev. Thus, the combination of short-chain quaternary ammonium with small hydrophilic anions results in a structure composition which has not a typical amphiphilic character, and the formation of aggregates does only take place at elevated concentrations. However, aggregates of [DiC_4] combined with aromatic, di- or trivalent anions (*e.g.* Sal, Mand, Ita, Tar and Cit) occured above a certain concentration, which was defined as MAC (**Table 2.4**). The MAC at lower than 1 mol·L^{-1} for [DiC_4] shows the following order: **Br > Ace > Lev > Gly > Lac > Mand > Tar > Ita > Cit > Sal**.

Table 2.4 Minimal aggregation concentrations (MACs) with corresponding surface tensions (σ_{MAC}) of **QACILs**.

[DiC_4]	**Br**	**Ace**	**Lac**	**Gly**	**Lev**	**Sal**	**Mand**	**Ita**	**Tar**	**Cit**
MAC (mol·L^{-1})	1.97	1.93	1.02	1.32	1.38	0.13	0.64	0.21	0.34	0.14
σ_{MAC} (mN·m^{-1})	48.1	44.7	43.2	46.3	39.9	40.4	41.2	41.6	42.0	34.0
[DiC_6]	**Br**	**Ace**	**Lac**	**Gly**	**Lev**	**Sal**	**Mand**	**Ita**	**Tar**	**Cit**
MAC (mol·L^{-1})	0.20	0.23	0.24	0.27	0.24	0.04	0.19	0.17	0.08	0.04
σ_{MAC} (mN·m^{-1})	33.5	32.5	32.7	38.2	34.0	27.0	33.4	33.5	31.7	32.9

Regarding the surface tension graphs for aqueous solutions of [DiC_6] ILs with the same counter anions (**Figure 2.13.b**), the typical curve of surface-active compounds was perceived. Thus, all of the compounds aggregate (**Table 2.4**). The MACs for [DiC_6] compounds are in the following order: **Gly > Lev ≥ Lac > Ace > Br > Mand > Ita > Tar > Cit > Sal**. Remarkably, this series is

significantly different from the corresponding [DiC_4] series. The MACs for the [DiC_6] cation combined with small hydrophilic anions, such as Ace, Lac, Gly and Lev are much higher (of about 0.2 mol·L^{-1}) than the MACs obtained with the aromatic, di- or trivalent anions, like Sal, Mand, Ita, Tar, Cit, Sal (**Table 2.4**) due to their elevated hydrophobic part, which results also in a lower aqueous solubility. These **QACILs** exhibit thus a hydrotropic behavior.

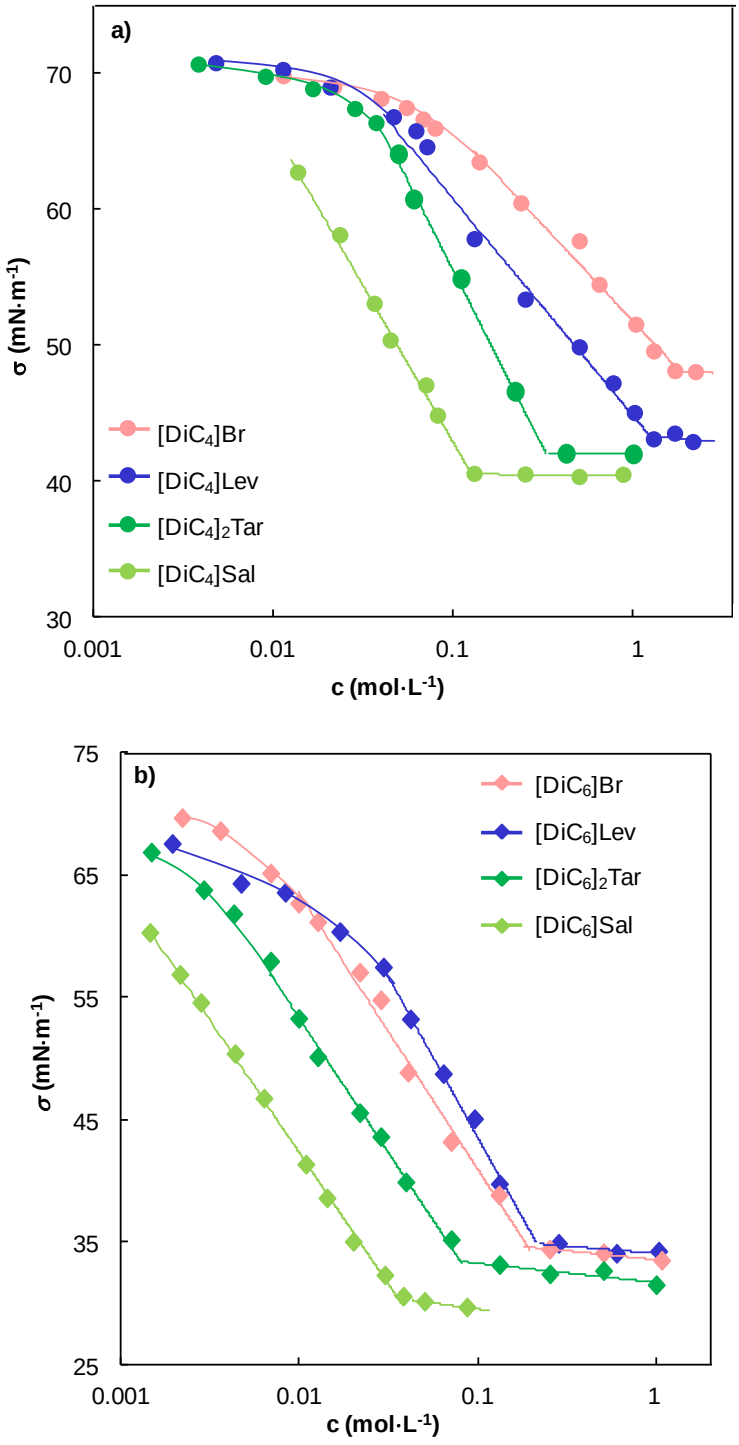

Figure 2.13 Surface tension σ as a function of **QACIL** concentration in aqueous solutions at RT: **a)** [DiC_4] cation and **b)** [DiC_6] cation combined with different anions.

2.3.4.2 Hydrotropic solubilization capacity

In 1916, Neuberg described hydrotropes as water-soluble compounds that greatly enhance the aqueous solubility of organic composites.[196] Original hydrotropes had an anionic hydrophilic group linked to a hydrophobic aromatic ring, such as sodium benzoate and salicylate. Later on, the definition was extended to cationic (*e.g. p*-aminobenzoic acid hydrochloride, procaine hydrochloride) and nonionic (*e.g.* resorcinol, pyrogallol) organic compounds.[197] Today, the class of hydrotropes has been enlarged to a wide range of compounds, namely from simple organic molecules, *e.g.* ethanol and glycols, to various amphiphilic compounds with a quite small polar part and a bulky non-polar group, such as sodium benzene sulfonate, sodium cumene sulfonate or caffeine.[198] Even if hydrotropes are a class of amphiphilic molecules, they cannot form well organized structures, such as micelles, in water but they are able to increase the aqueous solubility of organic hydrophobic molecules.[199] Compared to surfactants, hydrotropes have a less pronounced hydrophobic character and therefore exhibit higher water solubility. At high concentrations, they do not form liquid crystals, as typical surfactants. Whereas the mechanism of hydrotropic solubilization by aromatic hydrotropes has been ascribed to the self-association of the compounds *via* the plane-to-plane stacking of hydrophobic part of molecules, it is not entirely explained for other types of hydrotropes without a bulky aromatic part in their structures. Hydrotropes form aggregates at higher concentrations, but they differ from surfactant micelles, as already mentioned.[200] They could rather be regarded as dimers or trimers or movable structures connected *via* weak interactions like hydrogen bonding.[201] Due to their properties as solubilizing agents, hydrotropes are of great interest for industrial applications, particularly for the formulation of cleaning products, for drugs solubilization, and for painting and coating industries.[202]

For some of the prepared **QACILs**, their hydrotropic behavior has been investigated. Sodium xylenesulfonate (SXS), which is a well-known hydrotrope, was used as reference in this study (**Figure 2.14.a**).[203] The hydrotropic behavior of **QACILs** has been evaluated by means of the solubilization of a hydrophobic dye in aqueous solutions. Therefore, **Disperse Red 13** (**Figure 2.14.b**) has been used as a model organic molecule, which can imitate active pharmaceutical ingredients or perfumes. Its concentration in aqueous IL solutions was measured by UV-visible spectroscopy at λ = 503 nm, corresponding to a maximum absorption. In **Figure 2.14.c**, the UV-visible spectra of Disperse Red 13 in acetone and in ethanol are shown. The concentration of Disperse Red 13 in aqueous QACIL solutions was determined by means of a calibration curve in ethanol (shown in the ***experimental section***).

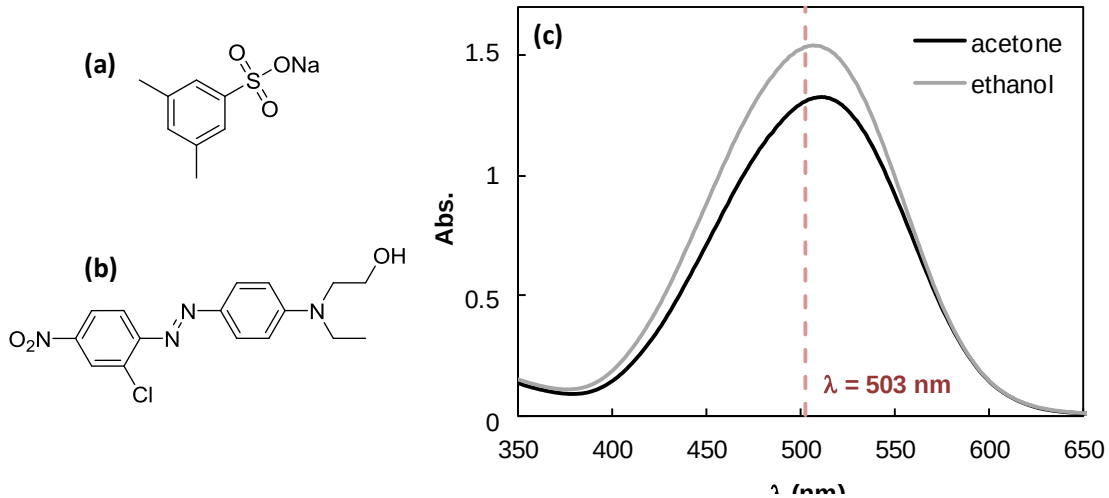

Figure 2.14 Structure of **(a)** the common hydrotrope sodium xylenesulfonate (SXS) and **(b)** the hydrophobic dye Disperse Red 13, and **(c)** UV-Vis spectrum of Disperse Red 13.

The results of the solubilization of Disperse Red 13 as a function of **QACILs** concentration are shown in **Figure 2.15**. Cations are represented with different forms of markers: ✱ = Na, ▲ = [TriC3], ● = [DiC4], — = [TriC4], ◆ = [DiC6], and anions with different colors: XS = red, Sal = green, Lev = violet, Ita = light-blue.

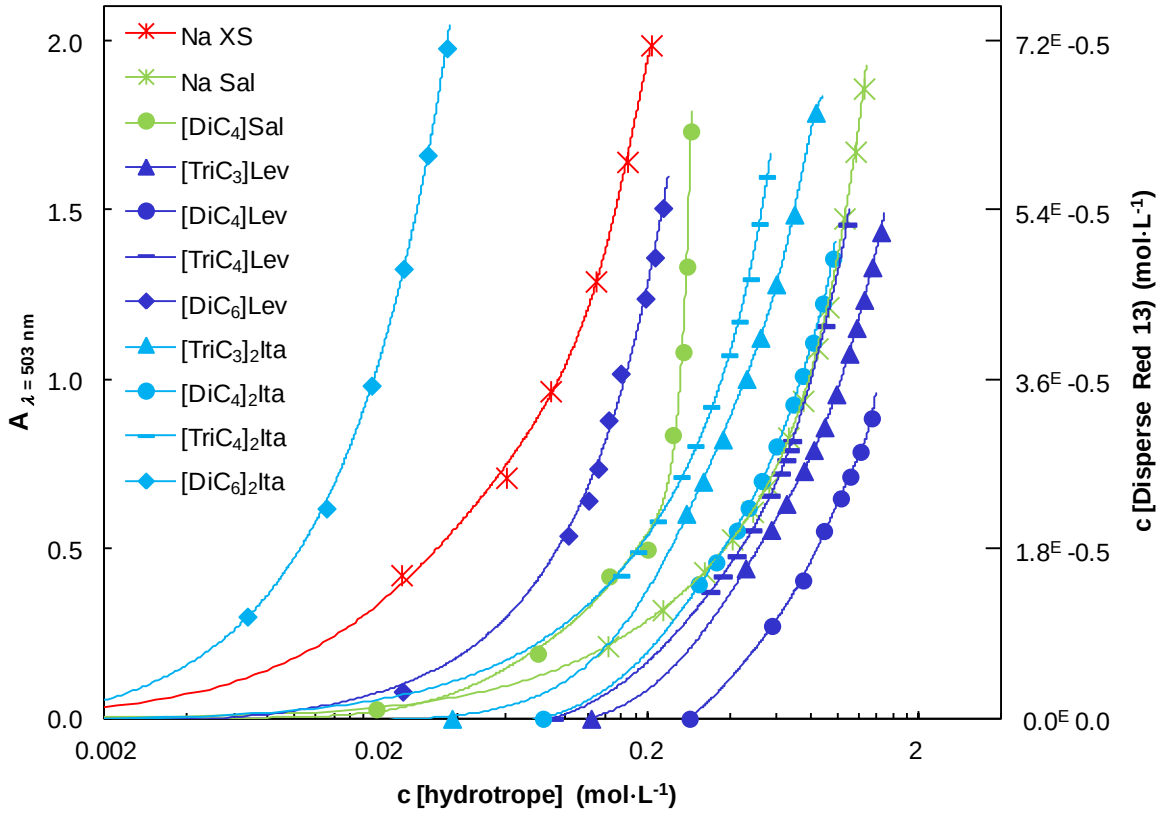

Figure 2.15 Solubilization of Disperse Red 13 measured by UV/visible spectroscopy at λ = 503 nm, in aqueous solutions of **QACILs** and SXS used as a reference.

First of all, the comparison of the anions (represented by different colors in **Figure 2.15**) highlights great differences in the hydrotropic behavior of ILs. For the studied **QACILs**, the following trend for anions combined with the same cation can be noticed: **Sal > Ita > Lev**. Unfortunately, the measure could not be performed with **[DiC$_6$]Sal** owing to its poor water solubility (< 0.03 mol·L^{-1}). On the other hand, **[DiC$_4$]Sal** acts as a very efficient hydrotrope compared to the well-known SXS. It is noteworthy that sodium salicylate itself also gives good results, which is already reported as hydrotrope in literature.[204] Hydrotropes containing an aromatic ring were reported to be very efficient due to their association *via* ring stacking into ellipsoidal structures.[198] In general, hydrotropes form three-dimensional aggregates with localized hydrophobic regions which are responsible for the increased aqueous solubility of hydrophobic compounds.

Ita is more efficient than Lev for all tested cations. In particular, **[DiC$_6$]$_2$Ita** shows the highest efficiency, compared to [DiC$_6$]Lev but also compared to SXS. This phenomenon could be explained by the structure of Ita-ILs which are composed of two cations and one anion, due to the divalent nature of the anion. Thus, ILs based on 2:1 ion pairs contains a higher carbon-content which increases the hydrophobic part of the structure. As a result, they are efficient for the solubilization of organic compounds in an aqueous milieu.

Finally, within a same anion series, notably Lev and Ita, the same tendency of hydrotrope efficiency can be found for both anions: **[DiC$_6$] > [TriC$_4$] > [TriC$_3$] > [DiC$_4$]**. This trend shows that the ILs are more efficient if their cation is more hydrophobic. Consequently, increasing alkyl chain length or increasing number of alkyl chains up to a specific limit leads to enhanced effectiveness as hydrotrope. The same general trend has already been described for the MACs of **QACILs** which has been determined by aqueous surface tension measurements.

2.4 Biodegradation of QACILs

The biodegradability of compounds expresses the ability of microorganisms to degrade molecules. Biodegradation studies are a powerful method to assess the fade in environment of organic contaminants of anthropogenic origin. According to appropriate legislation of novel compounds, the environmental risk assessment is required, called REACH (**r**egistration, **e**valuation, **a**uthorization and restriction of **ch**emicals). In pursuance of the OECD (**o**rganization for **e**conomic **c**ooperation and **d**evelopment), a compound is defined as biodegradable if 60% of the substances has been degraded, so converted to CO_2, after a period of 28 days.

Biodegradation tests were performed following the OECD 301F standard, which requires the biological oxygen consumption (BOC) and the theoretical oxygen demand ($ThOD$).[205] The $ThOD$ (in mg of oxygen per mg of product) corresponds to the amount of oxygen necessary to oxidize the compound into its final oxidation products. Sodium acetate was used as a reference. With the average number of each element in the structure and the average molar weight (MW) of the compound, the $ThOD$ can be calculated according to **Eq. 2.4** when no nitrification occurs.

$$ThOD = \frac{2C + 0.5(H - Cl - 3N) + 3S + 2.5P + 0.5Na - O}{\overline{MW}} \qquad \textbf{Eq. 2.4}$$

The biological oxygen consumption (BOC) was determined by means of an IBUK respirometer, which identifies the oxygen consumption all along the degradation process. Experiments were conducted at 20 °C over a period of 28 days in a medium containing various mineral substances (sodium and potassium phosphates, ammonium, calcium and iron chlorides, magnesium sulfate) and bacteria collected from a local wastewater treatment plant. The starting pH was 7.4. The percentage of biodegradation or biodegradability (% B) values were obtained according to the following equation (**Eq. 2.5**):

$$\%B = \frac{BOC}{ThOD} \cdot 100 \qquad \textbf{Eq. 2.5}$$

The biodegradation test OECD 301F standard was carried out for ILs based on the [DiC_4] cation with different anions by means of comparing the influence of the anion on the biodegradability of the **QACILs**. In the ***experimental part***, the detailed graphs over the whole period are shown for chloride, acetate, levulinate, lactate, sorbate, mandelate, itaconate, succinate, tartrate and citrate as counter-anions, and sodium acetate as reference. In **Table 2.5**, the results are summarized for the two most important moments, namely after 10 and 28 days.

Table 2.5 Biodegradation (after 10 and 28 days) of **QACILs** and the mass fraction (wt%) of the anion; biodegradation values > 60% are marked in green.

Compound	% Biodegradation		wt% of anion
	10 days	28 days	
[DiC$_4$]Ace	65	77	27
[DiC$_4$]Lac	41	72	36
[DiC$_4$]Lev	21	66	42
[DiC$_4$]Sor	16	54	41
[DiC$_4$]Mand	27	78	49
[DiC$_4$]$_2$Suc	65	69	27
[DiC$_4$]$_2$Ita	36	45	29
[DiC$_4$]$_3$Cit	65	69	28

After 28 days, most of the tested ILs have passed the biodegradation limit of 60% apart from [DiC$_4$]Sor (54%), [DiC$_4$]$_2$Ita (45%) and [DiC$_4$]Cl with only 5% biodegradation. The poor biodegradability of ILs based on Cl anion has already been reported in previous studies on [BMIm]Cl. However, the presence of a renewably-sourced anion greatly enhanced the biodegradation of [DiC$_4$] ILs. The biodegradation after 28 days of the studied ILs can be classified as follows: **[DiC$_4$]Mand ≥ [DiC$_4$]Ace > [DiC$_4$]Lac > [DiC$_4$]$_3$Cit = [DiC$_4$]$_2$Suc > [DiC$_4$]Lev > [DiC$_4$]Sor > [DiC$_4$]$_2$Ita**.

Interestingly, the anion is not the only part of the IL which enters into the biodegradation process. In particular, we have noticed that the anion also exerts an influence on the biodegradation of the quaternary ammonium cation. Indeed, if one may consider only the renewably-sourced anion is biodegraded, the biodegradability would have followed the wt% proportion of the anion in the IL (**Table 2.5**). For most of the investigated ILs in this study, the biodegradation exceeds the wt% of the anions, implying that the cation is concomitantly biodegraded. In particular, this is clearly highlighted by the good biodegradation of [DiC$_4$]Ace, keeping in mind that the reference material of the test is sodium acetate. In literature, very few studies or data are available on the biodegradation of organic acid-derived quaternary ammonium compounds. The short set of data available attests that the biodegradation of ammonium cation also obviously depends on the cation structure, such as the number of methyl groups or the length alkyl groups,[206] but also on the absence of the toxicity generated by the biodegradation of the anions.

Furthermore, the studied **QACILs** are assumed to be less toxic than classical ILs based on pyridinium or imidazolium cations with the same side chain length. For a same alkyl chain length and a same counter anion, toxicity of ILs shows the following trend with cation type of ammonium < pyridinium < imidazolium < triazolium < tetrazolium.[90,207] This tendency is based on the fact that toxicity increases with the number of nitrogen atoms in an aromatic cation ring. In general, the lipophilicity of chemical substances is considered to be the mediator of non-specific toxic effects induced by membrane interactions.[93] As the toxicity increases with increasing lipophilicity, shorter alkyl chain lengths on the cation of ILs are favored. In the literature, a clear difference has been pointed out between shorter alkyl substituted chains (C_1 – C_4) and C_8 – C_{18} substituted chains which show respectively low and high toxicity.[90]

The anion of ILs, however, is supposed to have a negligible influence on the ILs toxicity.[93] Apart from fluorinated anions, such as bis(trifluoromethanesulfone)imide, tetrafluoroborate, or hexafluorophosphate, the typical anions do not exhibit any intrinsic effect.
Consequently, we expect lowered toxicity for the studied short-chain **QACILs** due to their lower lipophilicity (short alkyl chains and additionally without an aromatic group) and the reduced number of nitrogen atoms in their structure.[92,93,207]

2.5 QACILs as solvents for cellulose solubilization

As already discussed in the first chapter, the solubilization of cellulose, which is the major carbohydrate produced by plant photosynthesis, and its further conversion to chemical products is more and more important for "green" chemistry based on renewable feedstock (***Chapter 1 – section 1.1.2***).[13,34,117,208–212] Cellulose is composed of a polymeric structure of β-glycosidic linked glucose units resulting in a rigid crystallinity which plays an important role as a material benefit for cell walls (**Figure 2.16**).[12]

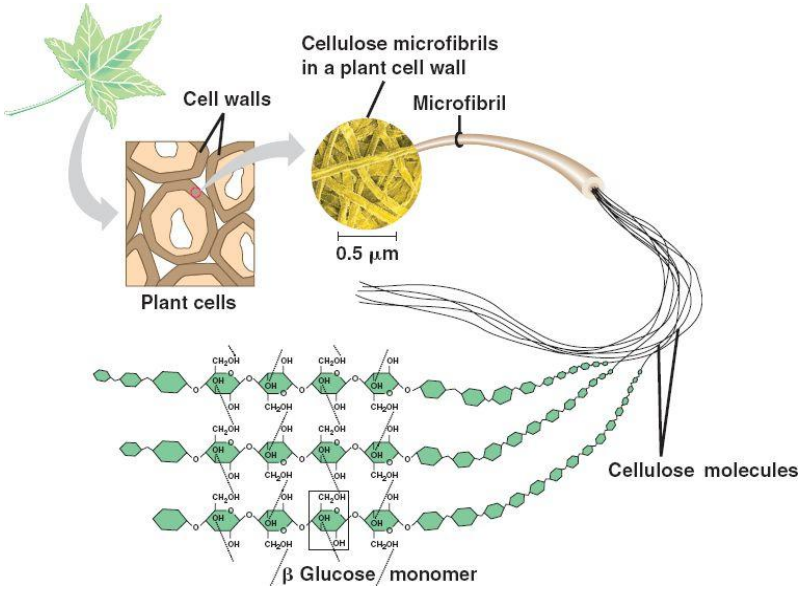

Figure 2.16 Cellulose scaffolding [http://bio1151.nicerweb.com/Locked/media/ch05/cellulose.html].

Because of this highly structured organization with strong interactions, hydrolysis of cellulose is hindered and its dissolution is complex. For many decades, the research for ideal cellulose solvents (high dissolution capacity, cheap, low viscous, stable, non-toxic, and ecologically friendly, easy to recycle) is a great competition in science and industry.[126,134,171,213,214] As already explained in ***Chapter 1 – section 1.2.5***, ILs play an important role as cellulose solvents (**Figure 2.17**).

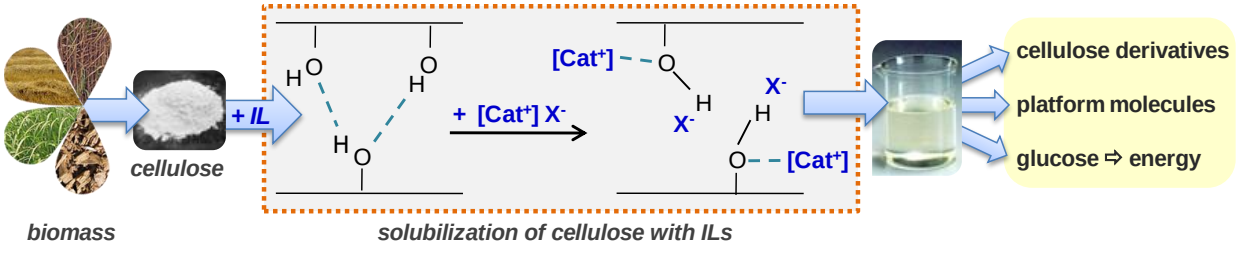

Figure 2.17 Schema for cellulose solubilization with ILs and its further transformation.

The application of **QACILs** for cellulose solubiilzation was carried out in the framework of a common project with the working group *Laboratoire de catalyse en chimie organique* of the

University of Poitiers, the results have been published in the journal *Green Chemistry*, and we have designed the inside front cover of the issue may 2014 (volume 16, number 5; see title page of Chapter 2).[215] The cellulose dissolution experiments have been done by the third year PhD student Florent Boissou under the supervision of Dr. François Jérôme.

2.5.1 Solubilization of cellulose in QACILs

All cellulose dissolution experiments were performed using **microcrystalline cellulose (MCC)** of the type AVICEL PH 200. AVICEL PH 200 has a glucose content higher than 99% along with a degree of polymerization (DP) of 200, a particle size of 150 μm and a water content of 5 wt%. In a typical experiment, a solution of IL containing 2 wt% of MCC was heated at 90–115 °C. When MCC was dissolved, an extra amount of MCC was progressively added until the limit of solubility was reached. Considering that the total removal of water from ILs is a costly and energy consuming step, we decided here to not extensively dry ILs prior to dissolving cellulose and to evaluate their performances as collected after synthesis. Results on solubility measurements are summarized in **Table 2.6**.

Among all tested renewably-sourced anions, it appears that **Lev** is the most promising one allowing up to 10 wt% of MCC to be dissolved within only 2 h of stirring at 90 °C.

In a first approximation independently of the cation, the efficiency of anions for cellulose dissolution can be classified as follows:

Lev > Ita, Ace > Lac > Sor, Suc, Cit > Gly, Mand, Male, Fum, Tar

It was observed that anions with a higher pKa value of their corresponding acid (4.5 to 5) are more efficient due to their elevated basicity. As a general trend, it appears that anions bearing a hydroxyl group such as Tar, Cit, Mand, Gly and Lac are not favorable for the dissolution of cellulose. The reason for this phenomenon is probably the interaction between the anion and the cellulose hydroxyl group which hinders the anion's reaction capacity. The presence and substitution of a carbon–carbon double bond on the structure of anions also exerted an influence on the cellulose dissolution. Whereas anions with di-substituted C=C bonds, such as Male and Fum, are incapable of dissolving cellulose, 10 wt% of cellulose can be dissolved in the presence of Ita which exhibits a terminal C=C bond. For all eligible anions, it is noteworthy that the difference in dissolution ability was obviously observed according to the nature of the cation, confirming that the cation also participates in the dissolution mechanism. Except Lev which was able to dissolve rather large amounts of cellulose whatever the cation, the [DiC_4] cation afforded the best result in terms of both dissolution ability and dissolution rate for all tested anions. The [DiC_6] cation, however, which is only able to dissolve a small amount of cellulose (3 wt%) as IL in

combination with Lev or Ita, seems to be the worst of the quaternary ammonium cations. This phenomenon is mainly influenced by the reason of size to the longer chain alkyl ammonium.

Table 2.6 Solubilization of cellulose S_{cell} with the rate in **QACILs** and the water content X_{water}.[a]

Anion	pKa	Cation	X_{water} (wt%)	S_{cell} (wt%)[b]	Rate of S_{cell} (g·h^{-1})
Lev	4.64	[TriC$_3$]	3.5	**10**	5
		[TriC$_3$]	15.5	**10**	5
		[DiC$_4$]	2.5	**10**	2
		[DiC$_4$]	14	**10**	2
		[DiC$_3$]	2.6	**10**	2
		[TriC$_4$]	6.7	5	1.7
		[DiC$_6$]	2.1	3	0.1
Ita	3.84; 5.55	[DiC$_4$]	12.8	**10**	1.4
		[DiC$_3$]	5.9	6	0.9
		[DiC$_6$]	4.2	3	0.6
		[TriC$_3$]	8.3	0	0
		[TriC$_4$]	6.6	0	0
Ace	4.76	[DiC$_4$]	10.8	**9.5**	2.4
		[DiC$_4$]	16.8	**9.5**	1.3
		[TriC$_4$]	6.5	2.6	0.4
		[DiC$_3$]	10	0	0
		[TriC$_3$]	7.7	0	0
		[DiC$_6$]	5.3	0	0
Lac	3.86	[DiC$_4$]	2.8	3.3	1.7
		[TriC$_3$]	2.6	0	0
		[DiC$_6$]	1.9	0	0
Sor	4.76	[DiC$_4$]	5.5	2	0.7
Suc	4.16; 5.61	[DiC$_4$]	5.3	2	0.2
Cit	3.13; 4.76; 6.39	[DiC$_4$]	7.3	2	0.1
		[DiC$_6$]	3.2	0	0
Gly	3.83	[DiC$_4$]	5	0	0
		[TriC$_4$]	1.6	0	0
Mand	3.41	[DiC$_4$]	1.1	0	0
Male	1.83; 6.59	[DiC$_4$]	11.5	0	0
Fum	3.03; 4.44	[DiC$_4$]	9.8	0	0
Tar	2.89; 4.40	[DiC$_4$]	4.1	0	0

[a] conditions : T = 90-115 °C, magnetic stirring; [b] ± 0.2 wt%

The **QACILs** with the highest cellulose solubilization (9.5 and 10 wt%, **Table 2.6**) have been compared to classical well-known ILs given in the literature (**Figure 2.18**).[210] Only results

obtained under the same experimental conditions have been taken in consideration, using the one type of cellulose (AVICEL) at the temperature of around 100 °C. **[DiC$_3$]Lev**, **[TriC$_3$]Lev**, **[DiC$_4$]Lev**, **[DiC$_4$]$_2$Ita**, **[DiC$_4$]Ace** are better than **[EMIm]Ace** and **[BMIm]For** (8 wt%) but inferior to **[BMIm]Ace** (12 wt%) and **[BMIm]Cl** (20 wt%) which still remains the best reported ILs for cellulose solubilization. Nevertheless, imidazolium ILs are not ideal for cellulose treatment due to their lack of "greenness" and high costs.

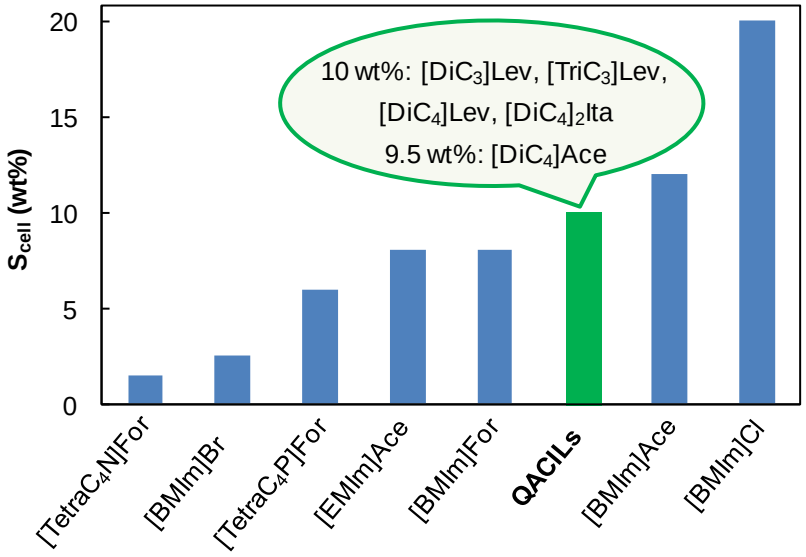

Figure 2.18 Cellulose (AVICEL) solubilities S_{cell} at around 100 °C of the best **QACILs** compared to classical ILs reported in the literature.[210]

2.5.2 Water-content and water–tolerance of QACILs and effect on cellulose solubilization

As mentioned above, water contained in commonly used imidazolium-derived ILs has an inhibiting effect on cellulose dissolution, thus requiring an extensive and energy-consuming drying of ILs before dissolution experiment. In this context, the water content of **QACILs** and its effect on the cellulose dissolution have been investigated (**Table 2.6**). The water content of each ILs was determined by means of coulometric Karl Fischer titrations (details in the ***experimental section***). Most of the ILs contain water within a range of 1.1–12.8 wt%. Although **[TriC$_3$]Lev** (the best IL in terms of dissolution ability and rate) has a lower water content (3.5 wt%) than the average of tested ILs, there is no clear relationship between the water content of ILs and their ability to dissolve cellulose. For instance, **[DiC$_4$]$_2$Ita** and **[DiC$_4$]Ace** exhibited a high water content of 12.8 and 10.8 wt%, respectively, and are capable of dissolving 10 and 9.5 wt% of cellulose whereas with a similar water content **[DiC$_4$]$_2$Male** and **[DiC$_4$]$_2$Fum** are not able to dissolve cellulose (**Table 2.6**). These results suggest that the dissolution of cellulose is more dependent on the molecular structure of the **QACILs** than on the water content of ILs.

Considering that the water-tolerance of the best ILs, *i.e.* **[TriC$_3$]Lev and [DiC$_4$]Ace**, is a remarkable advantage over imidazolium-derived ILs, we then checked their ability to dissolve cellulose when the water content was increased (**Figure 2.19**, **Table 2.6**). Remarkably, we were pleased to see that **[TriC$_3$]Lev** and **[DiC$_4$]Ace** were still able to dissolve a similar amount of cellulose (10 wt% and 9.5 wt%, respectively) at a water content of 15.5 wt% and 16.8 wt%, respectively. Interestingly, in the case of **[TriC$_3$]Lev**, the dissolution rate of cellulose was not affected by the presence of water whereas this was the case with **[DiC$_4$]Ace** for which an increase of the water content from 10.8 wt% to 16.8 wt% dramatically reduced the cellulose dissolution rate from 2.4 g h^{-1} to 1.3 g·h^{-1} (**Table 2.6**). Note that in both cases, cellulose was not dissolved anymore when the water content was higher than 18 wt%, which represents here the maximum tolerance of these ILs to water. When **[BMIm]Cl** was used as a reference IL, we found that a water content higher than 4 wt% totally inhibited the dissolution process, showing the remarkable efficiency of **[TriC$_3$]Lev** and **[DiC$_4$]Ace** in the dissolution of cellulose. Note that a similar conclusion can be drawn with **[DiC$_4$]Lev** that can dissolve up to 10 wt% of cellulose at a water content of 14 wt% (similar dissolution rate = 2 g·h^{-1}, **Table 2.6**). The temperature obviously plays also a pivotal role in the ability of ILs to dissolve cellulose. Similarly to common ILs such as **[BMIm]Cl** (solid up to 70 °C) or **[BMIm]Ace** (RTIL), below 70 °C no dissolution occurred. The dissolution process started at 70 °C and was complete only at a temperature within the range of 90–110 °C. At this stage one may conclude that the **[TriC$_3$]Lev** IL appears to be a promising IL for the dissolution of cellulose. In particular, the tolerance of **[TriC$_3$]Lev** to water is a noticeable advantage over imidazolium-derived ILs for use on a large scale.

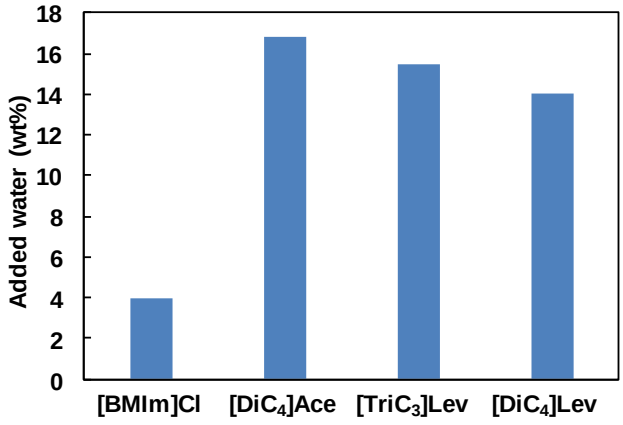

Figure 2.19 Water tolerance of tested ILs for cellulose solubilization (at 90 °C).

2.5.3 Relationship between cellulose solubility and QACILs physicochemical properties

To better understand the difference of solubilization ability observed between the alkylammonium ILs, we focused on the viscosity (η) and surface tension (σ) of ILs.
Viscosity is an important physical property considering the application of ILs because of its strong effect on the rate of mass transport.[64,185] Because dissolution experiments were performed at 80–110 °C, the variation of the viscosity versus temperature was investigated over a temperature range of 25 to 80 °C for the different ILs. As expected, the viscosities decreased with an increase of the temperature, as already discussed in ***section 2.3.2***. However, at 80 °C, one should notice that most of the ILs exhibit viscosities in a similar range (0.030–0.099 Pa·s). Only **$[DiC_4]_2$Suc**, **$[DiC_4]_2$Tar** and **$[DiC_4]_3$Cit** exhibited a slightly higher viscosity at 80 °C (0.2–0.3 Pa·s). Hence, one may conclude that viscosity of ILs is not a good descriptor to explain the greatest ability of levulinate-derived ILs to dissolve cellulose.

Next, we focused on the surface tension which provides information on the cohesive forces between liquid molecules at the surface.[62] All of the investigated ILs show this expected behavior: the reduction of the surface tension values at high temperature is noticeable and the temperature effect on average is the same for the different ILs (***section 2.3.3.1***). Although surface tension of ILs is by far not the only parameter governing the dissolution of cellulose in ILs, we experimentally observed a relationship between the ability of ILs to dissolve cellulose and their surface tensions measured at 80 °C. As a general trend, the solubilization of cellulose in ILs is higher for ILs exhibiting the lowest surface tension (**$[DiC_3]_2$Ita** is the only exception). In particular, whatever the cation ($[DiC_4]$, $[DiC_3]$ or $[TriC_3]$), we noticed that ILs exhibiting a surface tension lower than 34 $mN \cdot m^{-1}$ dissolved the highest amount of cellulose, *e.g.* 10 wt% (**Figure 2.20.a**). The same trend was also observed on the dissolution rate of cellulose, i.e. the lower the surface tension, the higher the solubilization rate (**Figure 2.20.b**). In a first approximation, one may hypothesize that ILs with a low surface tension (main feature of levulinate-derived ILs) have a low cohesive energy and are thus more prone to interact with the hydrogen bond network of cellulose.

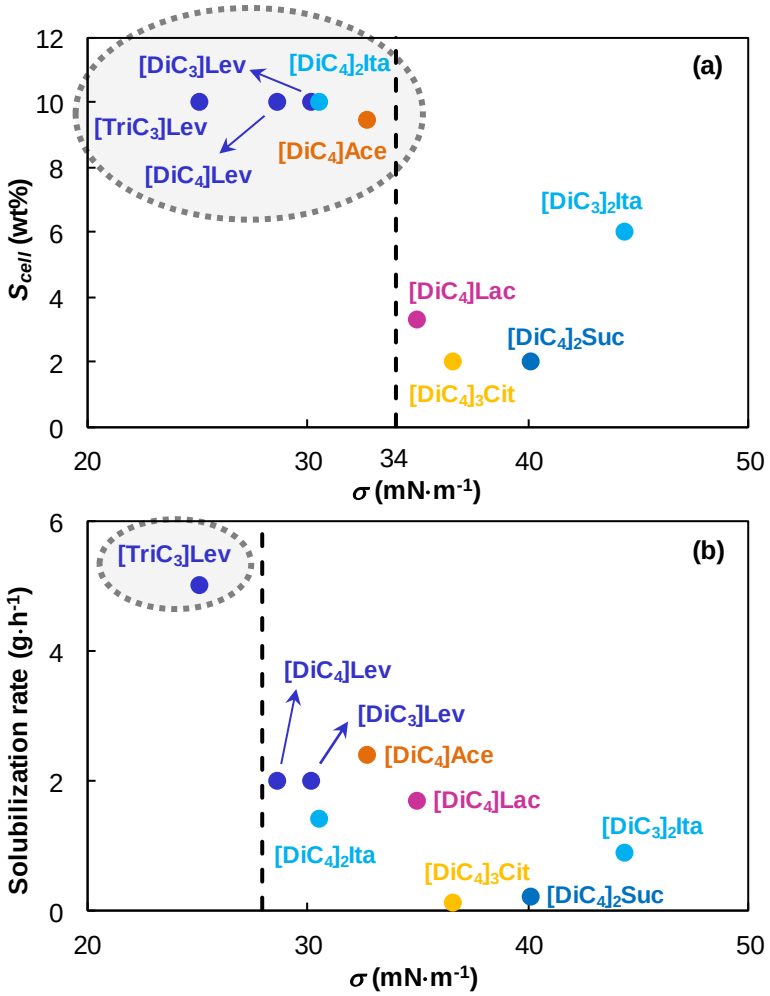

Figure 2.20 Relationship between the surface tension σ of ILs at 80 °C and **(a)** their cellulose solubilization ability and **(b)** their cellulose solubilization rate.

2.5.4 Comparison of levulinate and chloride as IL counter anions

In order to situate the Lev anion in the field of cellulose solubilization referring to the classical Cl anion, we compared the solubilization ability of **[DiC$_4$]Lev** and **[TriC$_3$]Lev** with that of **[DiC$_4$]Cl** and **[TriC$_4$]Cl**. Comparison was also carried out with the well-known **[BMIm]Cl** often used as a reference in the current literature. Results for the comparison of cellulose solubilization in ILs with Lev or Cl anions are summarized in **Table 2.7**.

[TriC$_4$]Cl and **[BMIm]Cl** are capable to dissolve similar amounts of cellulose (10 wt%) like **[TriC$_3$]Lev** and **[DiC$_4$]Lev**, while the solubility of cellulose in **[DiC$_4$]Cl** is much lower (3.5 wt%). The difference of dissolution rate was however clearly observed between chloride and levulinate-derived alkyl ammonium ILs (only **[BMIm]Cl** has similar solubilization performances as **[TriC$_3$]Lev**).

Table 2.7 Cellulose solubilization in ILs with Lev or Cl anion.

Entry	ILs	T (°C)	S_{cell} (wt%)	Rate of S_{cell} (g·h^{-1})
1	[TriC$_3$]Lev	90	10	5
2	[DiC$_4$]Lev	90	10	2
3	[TriC$_4$]Cl	110	10	0.6
4	[DiC$_4$]Cl	115	3.5	1.6
5	[BMIm]Cl	90	10	4

In particular, dissolution of cellulose in levulinate-derived alkyl ammonium ILs is faster than in chloride-derived alkyl ammonium ILs. For instance, the dissolution of cellulose is 8 times faster in **[TriC$_3$]Lev** than in **[TriC$_4$]Cl** (**Table 2.7**, entries 1, 3). This result might be here ascribed to the high viscosity of chloride-derived alkyl ammonium ILs (solid at room temperature) as compared to **[TriC$_3$]Lev** and **[DiC$_4$]Lev** (RTILs), making the stirring of the solution rather difficult. For instance, using **[TriC$_4$]Cl**, we noticed that a gel was rapidly formed after the increasing addition of cellulose, which obviously impacts not only the dissolution rate but also the cellulose dissolution ability of **[TriC$_3$]Cl**. This effect is even more pronounced with **[DiC$_4$]Cl**. Whereas **[DiC$_4$]Cl** dissolves cellulose at a higher rate than **[TriC$_3$]Cl**, only 3.5 wt% of cellulose can be dissolved in such IL. Here again, the system is limited by the formation of a highly viscous gel during the dissolution process that prevents the stirring of the mixture and thus the dissolution of a larger amount of cellulose. To circumvent this problem, co-solvents could be added to the system.

2.5.5 Effect of γ-valerolactone as a "green" co-solvent

The solubilization of cellulose in ILs may often be hindered by some limitations. Therefore, co-solvents can be used to minimize two of the major problems: (a) high viscosity of the ILs and the corresponding cellulose solutions and (b) limited miscibility of ILs with hydrophobic reagents for further cellulose processing and derivatization.[216] Solutions of cellulose in ILs have exceptionally high viscosities that rapidly increase with increasing concentration and decreasing temperature.[217]

The first necessity for a co-solvent is its miscibility with the pure IL.[216] Many different co-solvents for cellulose solubilization in ILs have already been described in the literature for the most common imidazolium ILs.[216] Hereby, the effect of various protic and aprotic co-solvents has been tested. As protic solvents tend to form hydrogen bonds with the IL anion, especially with basic ones, they form strong interactions with the IL leading to a disruption of cellulose / IL

interaction. In contrast, aprotic solvents lack this ability to form hydrogen bonds. Especially strongly dipolar, relatively basic aprotic solvents were found to be good co-solvents, such as **dimethylsulfoxide (DMSO).**[218] Mixtures of **[BMIm]Cl** or **[EMIm]Ace** with DMSO, for instance, were described as associated IL-rich clusters that are surrounded by DMSO and still possess the ability to coordinate with the hydroxyl groups of cellulose by interactions with the IL anion (**Figure 2.21**).[216,219] A detailed study of mass transport properties and additional molecular simulation for DMSO as co-solvent showed the same result: the co-solvent facilitates the mass transport leading to a lower viscosity without affecting the specific interactions between cations and anions or between the IL and cellulose.[220]

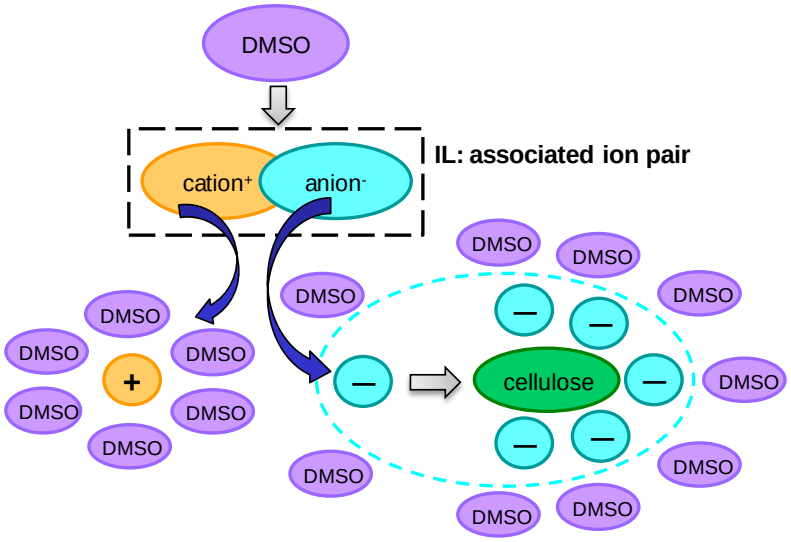

Figure 2.21 Model for the solubilization of cellulose in a binary IL-co-solvent (DMSO) system.[219]

Although DMSO can be used as a non-protic polar organic solvent to make the system more fluid, we focused our attention on the use of an aprotic solvent, **γ-valerolactone (GVL)** which is sustainable and bio-based (**Figure 2.22**), a sustainable chemical derived from levulinic acid.[221] As GVL can be derived from cellulose, it is particularly relevant due to the "greenness" of this solvent system. The results for the effect of **GVL** as co-solvent for the solubilization of cellulose in ILs with Lev or Cl anions are presented in **Table 2.8**.

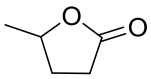

Figure 2.22 Structure of GVL.

Table 2.8 The effect of **γ–valerolactone (GVL)** as co-solvent for cellulose solubilization in ILs with Lev or Cl anions.

ILs	T (°C)	S_{cell} (wt%)	Rate of S_{cell} (g·h^{-1})
[DiC$_4$]Cl / GVL	100	10	3.3
[TriC$_3$]Lev / GVL	90	20	5
GVL	100	0	0

Interestingly, addition of **GVL** to **[DiC$_4$]Cl** helped not only in increasing the fluidity of the medium but also in increasing the cellulose dissolution ability of **[DiC$_4$]Cl**. In particular, in a mixture **[DiC$_4$]Cl–GVL** (15/1 *i.e.* 18 wt% of GVL), 10 wt% of cellulose with a dissolution rate of 3.3 g·h^{-1} was observed *vs.* 3.5 wt% at a rate of 1.6 g·h^{-1} without the assistance of GVL (**Table 2.8**). Promoting the effect of GVL on the dissolution of cellulose was then checked using **[TriC$_3$]Lev**. Remarkably, using **GVL** as a co-solvent (20 wt%) allowed also the solubilization ability of **[TriC$_3$]Lev** to be improved from 10 to 20 wt% while the dissolution rate remained constant (5 g·h^{-1}) (**Table 2.8**). It is worth noting that this is a very high dissolution capacity compared to reported ILs, demonstrating the efficiency of the proposed system.

After dissolution of cellulose in ILs, it was regenerated from the IL by precipitation with addition of anti-solvents which are typically ethanol, water or acetone. The regenerated cellulose was studied at the University of Poitiers (XRD analyses, ^{13}C CP/MAS NMR, FT-IR), leading to the result of transformation of the cellulose **crystalline structure from I to II**, which is of high interest for industrial applications (**Figure 2.23**).[215]

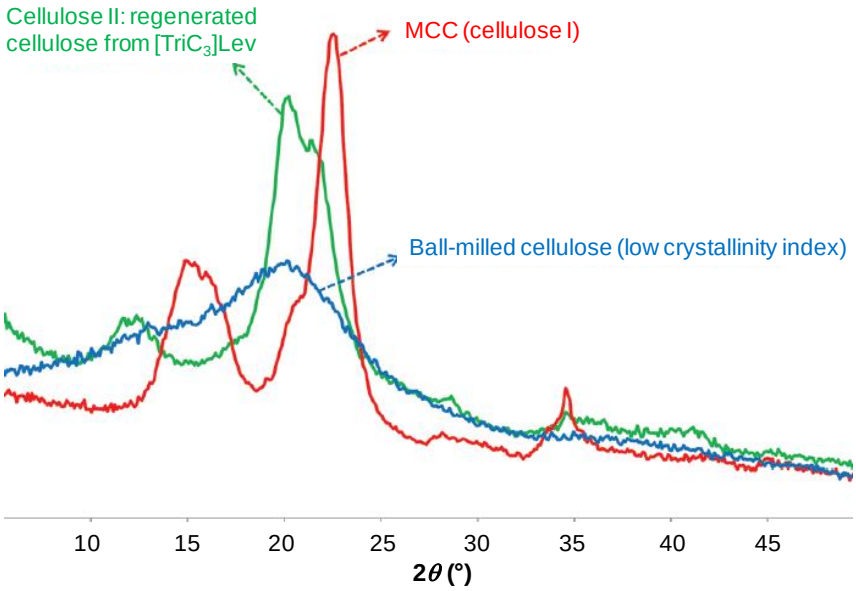

Figure 2.23 XRD patterns of MCC (cellulose I), regenerated cellulose from [TriC$_3$]Lev (cellulose II) and ball-milled cellulose ("amorphous" cellulose).[215]

Recycling experiments have been carried out for the ILs **[TriC$_3$]Lev** and **[TriC$_4$]Cl**. Cellulose dissolution experiments in **[TriC$_4$]Cl** in the second cycle have failed which could be explained by a kind of "poisoning effect" of the rests of ethanol, which was used as anti-solvent. **[TriC$_3$]Lev**, however, has been successfully recycled at least 4 times without intermediate purification. For this IL, water was used as anti-solvent because **[TriC$_3$]Lev** is highly water tolerant.

2.6 Hansen solubility parameters

2.6.1 Theoretical background

Joel Henry Hildebrand developed the solubility parameter δ as a numerical estimate of the degree of interaction between materials, which is used as indication of solubility.[222] The Hildebrand solubility parameter δ is the square root of the cohesive energy density, which is the enthalpy of vaporization ΔH_V of a compound divided by its molar volume V_m in the condensed phase (**Eq. 2.6**).

$$\delta = \sqrt{\frac{\Delta H_v - RT}{V_m}} \qquad \textbf{Eq. 2.6}$$

Charles M. Hansen has enhanced this concept for the determination of solubility parameters, based on the idea "like dissolves like" during his PhD thesis in 1967.[223] The so-called **Hansen solubility parameters (HSPs)** can be used for the prediction of solubilization behavior of solvents for a solute.[224] The basis for these HSPs is that the total energy of vaporization of a liquid consists of several individual parts. These arise from (atomic) dispersion forces, (molecular) permanent dipole-permanent dipole forces, and (molecular) hydrogen bonding (electron exchange). The total cohesive energy E can be measured by evaporating the liquid, thus breaking all the cohesive forces, and the total cohesive energy is considered as being identical to the energy of vaporization.[225] The cohesive energy E of a solvent is composed of three components: energy of dispersion E_D, polarity E_P and hydrogen bonding E_H (**Eq. 2.7**):

$$E = E_D + E_P + E_H \qquad \textbf{Eq. 2.7}$$

To scale cohesive energies in a way that molecules are more comparable with each oher, it is better to use cohesive energy density, which is connected with the cohesive energy *via* the molar volume V_m (**Eq. 2.8**):

$$E/V_m = \left(E_D/V_m\right) + \left(E_P/V_m\right) + \left(E_H/V_m\right) \qquad \textbf{Eq. 2.8}$$

The cohesive energy density is more conveniently handled in terms of the solubility parameter δ, where $\delta^2 = E/V_m$. So, the classic formula for HSPs is given by the total parameter δ (**Eq. 2.9**):

$$\delta^2 = \delta_D^2 + \delta_P^2 + \delta_H^2 \qquad \textbf{Eq. 2.9}$$

All compounds, *e.g.* materials, solvents, polymers, etc., can be characterized be three parameters, the HSPs, measured in $MPa^{0.5}$:

→ δ_D: the energy from dispersion forces between molecules (van der Waals)

→ δ_P: the energy from dipolar intermolecular forces (polarity)

→ δ_H: the energy from hydrogen bonding.

These three parameters can be treated as co-ordinates for a point in three dimensions. The HSP distance between two molecules, conventionally called *Ra*, is the measure of how alike they are. The smaller *Ra*, the more likely they are to be compatible. Materials with similar HSPs have high affinity for each other. The extent of the similarity in a given situation determines the extent of the interaction. The HSP distance *Ra* is described as follows in **Eq. 2.10**:

$$Ra^2 = 4(\delta_{D1} - \delta_{D2})^2 + (\delta_{P1} - \delta_{P2})^2 + (\delta_{H1} - \delta_{H2})^2 \qquad \textbf{Eq. 2.10}$$

The factor of 4 in front of the δ_D has aroused disagreement for decades, but plausible theoretical reasons and overwhelming experimental evidence show that it is valid. Conveniently, HSPs can be represented three-dimensionally, giving the so-called **Hansen sphere** (**Figure 2.24**). To determine if the parameters of two molecules (usually a solvent and a solute / polymer) are corresponding, a parameter called **interaction radius (R_0)** is used. Its value determines the radius of the sphere in Hansen space with δ as its center.

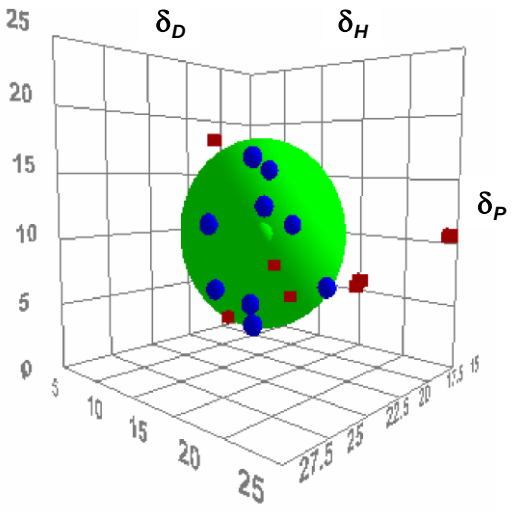

Figure 2.24 Three-dimensional representation of **HSPs (Hansen sphere)** of a compound in different solvents.

From measurements of "good" and "bad" solvents (test with a series of standard solvents), the sphere of radius R_0 can be defined. The good solvents are found inside the sphere (blue points in **Figure 2.24**), the bad ones are outside (red squares in **Figure 2.24**). It is obvious that solubility, or high affinity, requires that *Ra* be less than R_0. The combination of *Ra* and R_0 is defined as the relative energy difference *RED* which gives information about the placement in solubility space (**Eq. 2.11**):

$$RED = Ra/R_0 \qquad \textbf{Eq. 2.11}$$

For *RED* = 0 → no energy difference.

For $RED < 1$ → high affinity; the molecules are alike, and dissolution takes place.

For $RED = 1$ → the system is partially miscible.

For $RED > 1$ → no dissolution takes place.

2.6.2 Solubility parameters for the QACILs [DiC$_4$]Lev and [DiC$_4$]$_2$Ita

Up to now, HSPs for ILs are rarely found in the literature. However, the determination of HSP for ILs could be very interesting and helpful for the estimation of dissolving behavior, especially with regard to their huge variety of applications.[225–227] It has only been possible to assign HSPs to the four ILs listed in **Table 2.9** from the data in literature.

Table 2.9 Estimated HSPs for ILs.[225]

IL	δ_D (MPa$^{0.5}$)	δ_P (MPa$^{0.5}$)	δ_H (MPa$^{0.5}$)	δ (MPa$^{0.5}$)
[BMIm]Cl	19.1	20.7	20.7	35.0
[BMIm]PF_6	21.0	17.2	10.9	29.3
[BMIm]BF_4	23.0	19.0	10.0	31.5
[OMIm]PF_6	20.0	16.5	10.0	27.8

The HSPs have been determined for the **QACILs [DiC$_4$]Lev and [DiC$_4$]$_2$Ita**. Therefore, around 50 standard solvents (see ***experimental section***) were used to prepare mixtures of these ILs in all these solvents at the same concentration, namely 10 wt% as defined standard. After stirring of 24 h at RT and keeping the mixtures at a standstill for 1 h, the dissolution state was visually evaluated: miscible, partially miscible, not miscible. **[DiC$_4$]Lev** (10 wt%), for instance, was miscible with all of the tested solvents, which are not shown in **Table 2.10**. The **QACIL** was only partially miscible with *β*-pinene and 1-bomohexane, and not miscible with the ten solvents indicated in **Table 2.10**.

Table 2.10 Solvents in which 10 wt% of **[DiC$_4$]Lev** is partially or not miscible.

Partially miscible	*β*-pinene, 1-bromohexane
Not miscible	methyl oleate, geraniol, 1-chlorobutane, dipropylamine, tetralin, toluene, cyclohexane, *p*-xylene, isopropyl laurate, carbon disulfide

Based on this estimation, the parameters of **QACILs** were calculated and the Hansen sphere was drawn with the software HSPiP Edition 40.05 (**Figure 2.25**).[225] The following HSPs [MPa$^{0.5}$] were thus obtained:

[DiC$_4$]Lev: δ_D = 17.1, δ_P = 13.4, δ_H = 22.6, δ = 31.3; R_0 = 19.9;

[DiC$_4$]$_2$Ita: δ_D = 25.0, δ_P = 12.5, δ_H = 15.1, δ = 31.8; R_0 = 19.9.

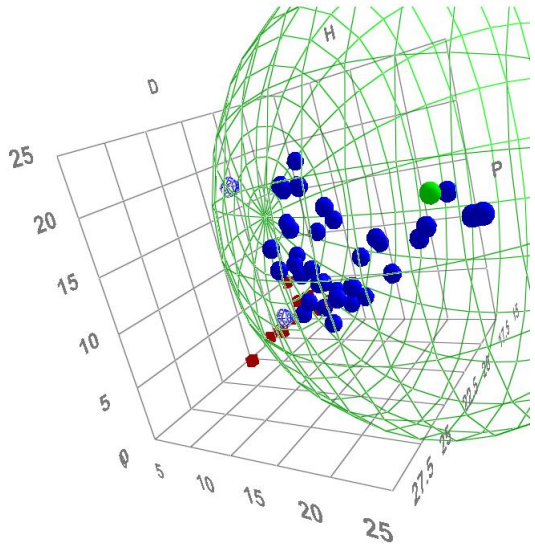

Figure 2.25 Hansen solubility sphere of the **QACIL [DiC$_4$]Lev**, determined with the software HSPiP Edition 40.05.

The main reason for the study of HSP is the information about the dissolution power of a solvent (or IL) for a certain compound (solute). The **HSPs of microcrystalline cellulose (MCC)** have already been published in the literature, and the following HSPs [MPa$^{0.5}$] have been found: δ_D = 19.4, δ_P = 12.7, δ_H = 31.3, and the total HSP δ of MCC is 39.3.[228] Using the HSPs of the QACILs (**[DiC$_4$]Lev**, **[DiC$_4$]$_2$Ita**) and MCC (**Table 2.11**), the HSP distance *Ra* was calculated as *Ra* = 9.9 for **[DiC$_4$]Lev**, and as *Ra* = 19.7 for **[DiC$_4$]$_2$Ita**. Thus, the relative energy difference *RED* was calculated for **[DiC$_4$]Lev** and cellulose as $RED = Ra/R_0$ = 0.5, and for **[DiC$_4$]$_2$Ita** and cellulose as $RED = Ra/R_0$ = 0.99. The result for **[DiC$_4$]Lev** (*RED* < 1) shows that it has a high affinity for MCC, and solubilization should take place. The result for **[DiC$_4$]$_2$Ita** (*RED* = 1) means that MCC should be partially soluble. As reported above in ***section 2.5***, **[DiC$_4$]Lev** and **[DiC$_4$]$_2$Ita** are two of the best QACILs for cellulose solubilization (10 wt%) what is more or less supported by the HSP method. However, the difference in prediction shows that this method might give an approximate idea but it cannot replace experimental results.

Table 2.11 Comparison of the HSPs of the ILs **[DiC$_4$]Lev** and **[DiC$_4$]$_2$Ita** with microcrystalline cellulose (MCC).

Compound	**δ_D (MPa$^{0.5}$)**	**δ_P (MPa$^{0.5}$)**	**δ_H (MPa$^{0.5}$)**	**δ (MPa$^{0.5}$)**
[DiC$_4$]Lev	17.1	13.4	22.6	31.3
[DiC$_4$]$_2$Ita	25.0	12.5	15.1	31.8
MCC	19.4	12.7	31.3	39.3

Summing up, the determination of HSP parameters could be a helpful tool to predict the solubility behavior of cellulose in ILs. However, this method was initially developed for organic solvents, thus its application to ILs should be used carefully and with a critical point of view. In the case of the QACILs **[DiC$_4$]Lev** and **[DiC$_4$]$_2$Ita**, the HSP method correlated well with the experimental results, even if the influence of temperature, for instance, was not taken into consideration.

2.7 Conclusions

In this work, we have synthesized 46 short-chain two- and three-tailed **QACILs** with various natural resourced carboxylates as counter anions: **formate, acetate, lactate, glycolate, levulinate, sorbate, salicylate, mandelate, succinate, itaconate, maleate, fumarate, malate, tartrate** and **citrate**. Quaternary ammonium is the simplest cation allowing a variation of the number and length of alkyl chains in order to assess the impact of the chemical structure on the physicochemical properties and power for cellulose solubilization.

The physicochemical properties of **QACILs** have been studied, and thermal phase transitions (by DSC), thermal stability (by TGA), viscosity, surface activity and hydrotropic behavior have been investigated. The thermal properties, viscosities and surface tensions of pure ILs have been identified as characteristic for ILs. Longer chain **QACILs**, namely based on [DiC_6] cations, are amphiphilic, and are therefore surface active in aqueous solutions. For some of the **QACILs**, we have tested their hydrotropic behavior which shows promising results. In particular itaconate ILs exhibit a very good solubilization capacity towards a hydrophobic dye. **[DiC_6]$_2$Ita** is even more efficient as a hydrotrope than the common sodium xylene sulfonate.

Quaternary ammonium have not only been used as cations because of their structure, but also because they are less toxic than imidazolium and pyridinium compounds. The use of bio-sourced carboxylate anions was an additional supportive aspect to obtain ILs of high "greenness". We have studied the biodegradability of **QACILs** with regard to their evaluation as "green" solvents. Most of the tested ILs, except **[DiC_4]Sor** and **[DiC_4]$_2$Ita**, have passed the limit of 60 wt% after a period of 28 days, thus they are classified as biodegradable:

[DiC_4]Mand ≥ [DiC_4]Ace > [DiC_4]Lac > [DiC_4]$_3$Cit ≈ [DiC_4]$_2$Suc > [DiC_4]Lev

The **QACILs** have finally been applied to the solubilization of cellulose. The impact of the structure of the cation and anion on the dissolution has been studied, resulting in short-chain levulinate ILs as the best cellulose solvents (up to 10 wt%), as shown in **Table 2.12**. Moreover, a system of **[$TriC_3$]Lev** combined with 20 wt% **γ-valerolactone** was able to dissolve 20 wt% of cellulose. Furthermore, the tested ILs have a high tolerance of water which is one of the main drawbacks that common ILs are currently facing for use on a large scale.

Table 2.12 Overview for the structural influence of QACILs on cellulose solubilization.

Cation structure: [DiC$_n^+$], [TriC$_n^+$]	**Effect on cellulose solubilization**
alkyl chain length: n = 3 → 4	↗↗
n = 4 → 6	↘↘↘
number of alkyl chains: di → tri	↘↘↘
⇨ *best cation structure:* 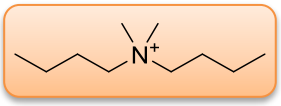	
Anion structure: R-COO$^-$	**Effect on cellulose solubilization**
R contains -OH	↘↘↘
R contains one C=C or C=O	↗↗↗
⇨ *best anion structures:* 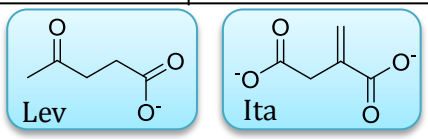	
⇨ ***best QACILs:*** 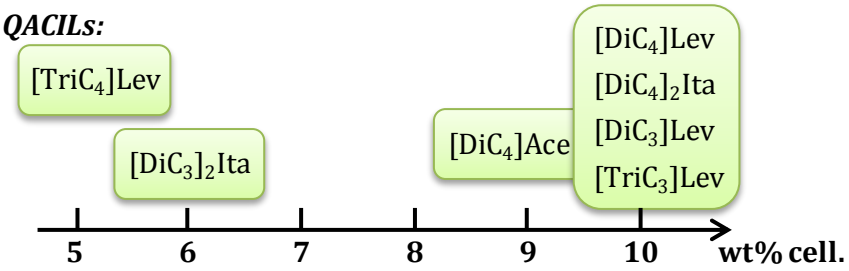	

As an additional aspect of characterization, we established the Hansen solubility parameters of **[DiC$_4$]Lev** and **[DiC$_4$]$_2$Ita** with the aim to support the results for cellulose dissolution. In this case, the experimental result (10 wt% cellulose solubilization) has been corroborated by the calculation of the relative energy difference of **[DiC$_4$]Lev** or **[DiC$_4$]$_2$Ita** and cellulose providing an interesting tool for the prediction of cellulose solubilization in ILs.

Experimental Section

1.) Preparation of quaternary ammonium halides and carboxylates

1.1) Synthesis and anion exchange

The quaternary ammonium compounds $[(C_nH_{2n+1})_2N(CH_3)_2]X$ or $[(C_nH_{2n+1})_3N(CH_3)]X$, abbreviated as $[DiC_n]$ or $[TriC_n]$ (n = 3, 4, 6; X = Br, I), were synthesized *via* nucleophilic substitution, namely an alkylation of *N,N,N*-alkyldimethylamines or *N,N,N*- dialkylmethylamines with 1-haloalkanes, followed by an anion exchange over an exchange resin (**Figure 2.26**).

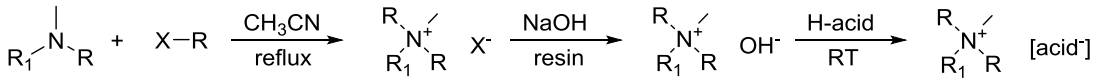

Figure 2.26 Synthesis route for quaternary ammonium carboxylate compounds; R = C_nH_{2n+1} with n = 3, 4 or 6, and R_1 = R or CH_3.

Dimethylalkylamine or methyldialkylamine (1 equiv.) and 1-bromoalkane (1.5 equiv.) were mixed with acetonitrile at RT. The reaction is carried out for min. 12 h under reflux; the end of the reaction was detected by ^{1}H-NMR. After the evaporation of the solvent, the raw product $[(C_nH_{2n+1})_2N(CH_3)_2]X$ or $[(C_nH_{2n+1})_3N(CH_3)]X$ was obtained.

This product was purified by extractions (3 to 4 times) in hexane (50 ml) followed by dichloromethane (50 ml). The extraction in hexane is for the elimination of traces of unreacted bromoalkane. The aqueous phase contains the amine, which was not reacting, and also the dimethyldioalkylammonium bromide. The procedure with dichloromethane takes out the ammonium bromide of this organic phase and the amine rests in the aqueous phase. All the organic phases were collected and evaporated to give lightly yellow oil. This oil was lyophilizated to remove traces of water.

For the ion exchange, 100 mL of the resin Amberlite IRA-400(Cl) were put in 300 ml water milipore during 10 minutes for swelling and put into a glass column (2 cm diameter). The resin has to be wet all the time. 500 ml of a sodium solution (10%) is slowly poured (2 ml per minute) in the resin. Then it is washed with water (millipore) until a neutral pH is obtained and the exit of the column.

6.0 g of $[(C_nH_{2n+1})_2N(CH_3)_2]X$ or $[(C_nH_{2n+1})_3N(CH_3)]X$ are dissolved in 100 ml water (millipore), the solution is added drop by drop to the resin and collected in a flask under argon-gas. After that, the resin is washed with water until a neutral pH is obtained at the exit of the column (≈ 250 ml water, drop by drop). 5 ml of the solution of the ammonium hydroxide are mixed with some drops bromothymol blue and it is titrated with HCl (0.02 M, which was before exactly adjusted by titration with NaOH) to determine the concentration of the product.

The aqueous solution of $[(C_nH_{2n+1})_2N(CH_3)_2]OH$ or $[(C_nH_{2n+1})_3N(CH_3)]OH$ (1 equiv.) is put in a flask and the corresponding acid (1 equiv.; with the counter-ion which is desired) and mixed under stirring (RT, ca 24 h). The water is evaporated and the obtained product is lyophilizated. The final product (hygroscopic) is conserved in a desiccator (P_2O_5, vacuum).

1.2) NMR-analysis

^{1}H- and ^{13}C-NMR spectra were recorded in the indicated solvents on a Bruker Avance 300 spectrometer. $CDCl_3$ and CD_3OD (99.95% isotopic purity) were obtained from Euriso-top. Chemical shifts (δ) are reported in parts per million (ppm) and measured relative to the HOD signal or the deuterated solvent chemical shift. The following abbreviations are used to explain the multiplicities: s = singlet, d = doublet, t = triplet, q = quartet, quint = quintet, sext = sextet, m = multiplet.

Pure products:

Dimethyldipropylammonium iodide, **[DiC$_3$]I**: $[C_8H_{20}N^+][I^-]$, M=257.16 g/mol (yield: 98 %)

^{1}H-NMR (CD_3OD): δ(ppm): 1.04 (t, *J*=7.4 Hz, 6H), 1.74-1.89 (m, 4H), 3.12 (s, 6H), 3.27-3.36 (m, 4H)

^{13}C-NMR (CD_3OD): δ(ppm): 9.6 (CH_3), 15.8 (CH_2), 50.2 (CH_3), 65.6 (CH_2)

Dimethyldipropylammonium chloride, **[DiC$_3$]Cl**: $[C_8H_{20}N^+][Cl^-]$, M=165.70 g/mol (yield: 97 %)

^{1}H-NMR ($CDCl_3$): δ(ppm): 1.01 (t, *J*=7.3 Hz, 6H), 1.66-1.85 (m, 4H), 3.36 (s, 6H), 3.40-3.49 (m, 4H)

^{13}C-NMR ($CDCl_3$): δ(ppm): 10.8 (CH_3), 16.3 (CH_2), 51.3 (CH_3), 65.2 (CH_2)

Dimethyldipropylammonium acetate, **[DiC$_3$]Ace**: $[C_8H_{20}N^+][C_3H_2O_2^-]$, M=189.29 g/mol (yield: 95 %)

^{1}H-NMR (CD_3OD): δ(ppm): 1.04 (t, *J*=7.2 Hz, 6H), 1.72-1.88 (m, 4H), 1.91 (s, 3H), 3.09 (s, 6H), 3.23-3.31 (m, 4H)

^{13}C-NMR (CD_3OD): δ(ppm): 9.7 (CH_3), 15.7 (CH_2), 22.9 (CH_3), 50.1 (CH_3), 65.5 (CH_2), 178.5 (C)

Dimethyldipropylammonium lactate, **[DiC$_3$]Lac**: $[C_8H_{20}N^+][C_3H_5O_3^-]$, M=219.32 g/mol (yield: 93 %)

^{1}H-NMR ($CDCl_3$): δ(ppm): 0.96 (t, *J*=7.4 Hz, 6H), 1.26 (d, *J*=6.9 Hz, 3H), 1.62-1.78 (m, 4H), 3.17 (s, 6H), 3.21-3.29 (m, 4H), 3.84 (q, *J*=6.7 Hz, 1H)

^{13}C-NMR ($CDCl_3$): δ(ppm): 10.8 (CH_3), 16.3 (CH_2), 21.6 (CH_3), 51.2 (CH_3), 65.4 (CH_2), 68.3 (CH), 179.6 (C)

Dimethyldipropylammonium levulinate, [DiC$_3$]Lev: [$C_8H_{20}N^+$][$C_5H_7O_3^-$], M=245.36 g/mol (yield: 95 %)

^{1}H-NMR ($CDCl_3$): δ(ppm): 0.95 (t, *J*=7.4 Hz, 6H), 1.61-1.78 (m, 4H), 2.10 (s, 3H), 2.33 (t, *J*=6.7 Hz, 2H), 2.61 (t, *J*=6.7 Hz, 2H), 3.15 (s, 6H), 3.19-3.28 (m, 4H)

^{13}C-NMR ($CDCl_3$): δ(ppm): 10.8 (CH_3), 16.1 (CH_2), 30.1 (CH_3), 31.7 (CH_2), 40.1 (CH_2), 51.2 (CH_3), 65.1 (CH_2), 177.4 (C), 210.0 (C)

Di-(dimethyldipropylammonium) itaconate, **[DiC$_3$]$_2$Ita**: [$C_8H_{20}N^+$]$_2$[$C_5H_4O_4^{2-}$], M=388.59g/mol (yield: 91 %)

^{1}H-NMR ($CDCl_3$): δ(ppm): 1.04 (t, *J*=7.3 Hz, 12H), 1.69-1.84 (m, 8H), 3.25 (s, 12H), 3.29 (s, 2H), 3.30-3.38 (m, 8H), 5.33 (s, 1H), 5.91 (s, 1H)

^{13}C-NMR (CD_3OD): δ(ppm): 9.7 (CH_3), 15.7 (CH_2), 42.6 (CH_2), 50.1 (CH_3), 65.5 (CH_2), 119.6 (CH_2), 143.1 (C), 174.2 (C), 178.5 (C)

Methyltripropylammonium bromide, **[TriC$_3$]Br**: [$C_{10}H_{24}N^+$][Br^-], M=238.21 g/mol (yield: 98 %)

^{1}H-NMR ($CDCl_3$): δ(ppm): 1.04 (t, *J*=7.2 Hz, 9H), 1.70-1.88 (m, 6H), 3.34 (s, 3H), 3.41-3.49 (m, 6H)

^{13}C-NMR ($CDCl_3$): δ(ppm): 10.8 (CH_3), 16.1 (CH_2), 48.9 (CH_3), 63.1 (CH_2)

Methyltripropylammonium chloride, **[TriC$_3$]Cl**: [$C_{10}H_{24}N^+$][Cl^-], M=193.76 g/mol (yield: 96 %)

^{1}H-NMR ($CDCl_3$): δ(ppm): 1.02 (t, *J*=7.2 Hz, 9H), 1.67-1.83 (m, 6H), 3.30 (s, 3H), 3.35-3.44 (m, 6H)

^{13}C-NMR ($CDCl_3$): δ(ppm): 10.7 (CH_3), 16.0 (CH_2), 48.8 (CH_3), 63.0 (CH_2)

Methyltripropylammonium acetate, **[TriC$_3$]Ace**: [$C_{10}H_{24}N^+$][$C_3H_2O_2^-$], M=217.35 g/mol (yield: 92 %)

^{1}H-NMR (CD_3OD): δ(ppm): 0.89 (t, *J*=7.4 Hz, 9H), 1.52-1.68 (m, 6H), 1.75 (s, 3H), 3.07 (s, 3H), 3.11-3.19 (m, 6H)

^{13}C-NMR (CD_3OD): δ(ppm): 10.7 (CH_3), 15.8 (CH_2), 24.8 (CH_3), 48.8 (CH_3), 62.9 (CH_2), 177.1 (C)

Methyltripropylammonium lactate, **[TriC$_3$]Lac**: [$C_{10}H_{24}N^+$][$C_3H_5O_3^-$], M=247.37 g/mol (yield: 93 %)

^{1}H-NMR ($CDCl_3$): δ(ppm): 0.96 (t, *J*=7.3 Hz, 9H), 1.26 (d, *J*=6.9 Hz, 3H), 1.59-1.76 (m, 6H), 3.12 (s, 3H), 3.17-3.25 (m, 6H), 3.84 (q, *J*=6.7 Hz, 1H)

^{13}C-NMR ($CDCl_3$): δ(ppm): 10.7 (CH_3), 15.9 (CH_2), 21.6 (CH_3), 48.8 (CH_3), 63.1 (CH_2), 68.1 (CH), 179.8 (C)

Methyltripropylammonium levulinate, [TriC$_3$]Lev: [$C_{10}H_{24}N^+$][$C_5H_7O_3^-$], M=273.41 g/mol (yield: 94 %)

^{1}H-NMR ($CDCl_3$): δ(ppm): 0.93 (t, *J*=7.4 Hz, 9H), 1.57-1.73 (m, 6H), 2.07 (s, 3H), 2.31 (t, *J*=6.9 Hz, 2H), 2.59 (t, *J*=6.9 Hz, 2H), 3.09 (s, 3H), 3.15-3.23 (m, 6H)

^{13}C-NMR ($CDCl_3$): δ(ppm): 10.7 (CH_3), 15.9 (CH_2), 30.2 (CH_3), 32.1 (CH_2), 40.4 (CH_2), 48.9 (CH_3), 62.9 (CH_2), 177.1 (C), 210.0 (C)

Di-(methyltripropylammonium) itaconate, **[TriC$_3$]$_2$Ita**: [$C_{10}H_{24}N^+$]$_2$[$C_5H_4O_4^{2-}$], M=444.69g/mol (yield: 90 %)

^{1}H-NMR ($CDCl_3$): δ(ppm): 0.99 (t, *J*=7.3 Hz, 18H), 1.62-1.78 (m, 12H), 3.17 (s, 18H), 3.19-3.27 (m, 12H + 2H), 5.19 (s, 1H), 5.80 (s, 1H)

^{13}C-NMR ($CDCl_3$): δ(ppm): 10.7 (CH_3), 15.9 (CH_2), 43.4 (CH_2), 49.1 (CH_3), 62.9 (CH_2), 119.4 (CH_2), 145.0 (C), 173.5 (C), 177.1 (C)

Dibutyldimethylammonium bromide, **[DiC$_4$]Br**: [$C_{10}H_{24}N^+$][Br^-], M=238.21 g/mol (yield: 99 %)

^{1}H-NMR (CD_3OD): δ(ppm): 1.03 (t, *J*=7.4 Hz, 6H), 1.44 (sext$_a$, *J*=7.5 Hz, 4H), 1.69-1.84 (m, 4H), 3.13 (s, 6H), 3.31-3.40 (m, 4H)

^{13}C-NMR (CD_3OD): δ(ppm): 12.9 (CH_3), 19.4 (CH_2), 24.2 (CH_2), 50.4 (CH_3), 64.0 (CH_2)

Dibutyldimethylammonium chloride, **[DiC$_4$]Cl**: [$C_{10}H_{24}N^+$][Cl^-], M=193.76 g/mol (yield: 94 %)

^{1}H-NMR ($CDCl_3$): δ(ppm): 0.98 (t, *J*=7.4 Hz, 6H), 1.42 (sext$_a$, *J*=7.4 Hz, 4H), 1.61-1.75 (m, 4H), 3.39 (s, 6H), 3.47-3.56 (m, 4H)

^{13}C-NMR ($CDCl_3$): δ(ppm): 13.8 (CH_3), 19.6 (CH_2), 24.7 (CH_2), 51.4 (CH_3), 63.7 (CH_2)

Dibutyldimethylammonium formate, **[DiC$_4$]For**: [$C_{10}H_{24}N^+$][CHO_2^-], M=203.32 g/mol (yield: 92 %)

^{1}H-NMR ($CDCl_3$): δ(ppm): 0.83 (t, *J*=7.4 Hz, 6H), 1.26 (sext$_a$, *J*=7.5 Hz, 4H), 1.46-1.60 (m, 4H), 3.13 (s, 6H), 3.21-3.29 (m, 4H), 8.65 (s, 1H)

^{13}C-NMR ($CDCl_3$): δ(ppm): 13.7 (CH_3), 19.5 (CH_2), 24.4 (CH_2), 50.8 (CH_3), 63.4 (CH_2), 168.0 (CH)

Dibutyldimethylammonium acetate, **[DiC$_4$]Ace**: [$C_{10}H_{24}N^+$][$C_3H_2O_2^-$], M=217.35 g/mol (yield: 93 %)

^{1}H-NMR (CD_3OD): δ(ppm): 0.96 (t, *J*=7.4 Hz, 6H), 1.38 (sext$_a$, *J*=7.5 Hz, 4H), 1.56-1.70 (m, 4H), 1.85 (s, 3H), 3.21 (s, 6H), 3.26-3.35 (m, 4H)

^{13}C-NMR (CD_3OD): δ(ppm): 13.7 (CH_3), 19.7 (CH_2), 24.6 (CH_2), 25.2 (CH_3), 51.1 (CH_3), 63.3 (CH_2), 177.3 (C)

Dibutyldimethylammonium lactate, **[DiC$_3$]Lac**: [$C_{10}H_{24}N^+$][$C_3H_5O_3^-$], M=247.37 g/mol (yield: 97 %)

^{1}H-NMR ($CDCl_3$): δ(ppm): 0.96 (t, *J*=7.3 Hz, 6H), 1.30 (d, *J*=6.7 Hz, 3H), 1.39 (sext$_a$, *J*=7.5 Hz, 4H), 1.57-1.70 (m, 4H), 3.25 (s, 6H), 3.31-3.409 (m, 4H), 3.88 (q, *J*=6.8 Hz, 1H)

^{13}C-NMR ($CDCl_3$): δ(ppm): 13.7 (CH_3), 19.8 (CH_2), 21.8 (CH_3), 24.4 (CH_2), 51.2 (CH_3), 63.7 (CH_2), 68.1 (CH), 179.5 (C)

Dibutyldimethylammonium glycolate, **[DiC$_3$]Gly**: [$C_{10}H_{24}N^+$][$C_2H_3O_3^-$], M=233.35 g/mol (yield: 97 %)

^{1}H-NMR ($CDCl_3$): δ(ppm): 0.90 (t, *J*=7.4 Hz, 6H), 1.32 (sext$_a$, *J*=7.4 Hz, 4H), 1.51-1.65 (m, 4H), 3.13 (s, 6H), 3.22-3.30 (m, 4H), 3.68 (s, 2H)

^{13}C-NMR ($CDCl_3$): δ(ppm): 13.7 (CH_3), 19.5 (CH_2), 24.4 (CH_3), 50.9 (CH_3), 62.3 (CH_2), 63.7 (CH_2), 176.6 (C)

Dibutyldimethylammonium levulinate, [DiC$_4$]Lev: [$C_{10}H_{24}N^+$][$C_5H_7O_3^-$], M=273.41 g/mol (yield: 93 %)

^{1}H-NMR ($CDCl_3$): δ(ppm): 0.95 (t, *J*=7.3 Hz, 6H), 1.37 (sext$_a$, *J*=7.4 Hz, 4H), 1.57-1.71 (m, 4H), 2.11 (s, 3H), 2.36 (t, *J*=6.7 Hz, 2H), 2.63 (t, *J*=6.7 Hz, 2H), 3.19 (s, 6H), 3.25-3.33 (m, 4H)

^{13}C-NMR ($CDCl_3$): δ(ppm): 13.8 (CH_3), 19.1 (CH_2), 24.6 (CH_2), 30.4 (CH_3), 32.1 (CH_2), 40.4 (CH_2), 51.4 (CH_3), 63.6 (CH_2), 177.5 (C), 210.4 (C)

Dibutyldimethylammonium sorbate, [DiC$_4$]Sor: [$C_{10}H_{24}N^+$][$C_6H_7O_2^-$], M=269.42 g/mol (yield: 95 %)

^{1}H-NMR (CD_3OD): δ(ppm): 1.05 (t, *J*=7.4 Hz, 6H), 1.44 (sext$_a$, *J*=7.4 Hz, 4H), 1.68-1.79 (m, 4H), 1.82 (d, *J*=6.5 Hz, 3H), 3.07 (s, 3H), 3.26-3.34 (m, 4H), 5.82 (d, *J*=15.3 Hz, 6H), 6.00 (dq, *J*=15.1 Hz, *J*=6.7 Hz,1H), 6.20 (dd, *J*=15.1 Hz, *J*=10.8 Hz,1H), 7.00 (dd, *J*=15.4 Hz, *J*=10.5 Hz,1H)

^{13}C-NMR (CD_3OD): δ(ppm): 13.9 (CH_3), 18.5 (CH_3), 20.7 (CH_2), 25.4 (CH_2), 40.1 (CH_2), 51.1 (CH_3), 65.2 (CH_2), 127.6 (CH), 131.9 (CH), 135.9 (CH), 141.4 (CH), 175.9 (C)

Dibutyldimethylammonium salicylate, [DiC$_4$]Sal: [$C_{10}H_{24}N^+$][$C_7H_5O_3^-$], M=295.42 g/mol (yield: 96 %)

^{1}H-NMR ($CDCl_3$): δ(ppm): 0.92 (t, *J*=7.3 Hz, 6H), 1.30-1.50 (m, 4H), 1.63 (sext$_a$, *J*=7.4 Hz, 4H), 3.15 (s, 6H), 3.21-3.29 (m, 4H), 6.75 (t, *J*=7.5 Hz,1H), 6.83 (d, *J*=8.0 Hz,1H), 7.26 (m,1H), 6.83 (dd, *J*=6.0 Hz, *J*=1.8 Hz,1H)
^{13}C-NMR ($CDCl_3$): δ(ppm): 13.7 (CH_3), 19.5 (CH_2), 24.4 (CH_2), 50.9 (CH_3), 64.0 (CH_2), 116.4 (CH_2), 117.6 (CH_2), 119.0 (CH), 130.7 (CH_2), 132.7 (CH_2), 162.4 (C), 173.7 (C), 210.0 (C)

Dibutyldimethylammonium mandelate, [DiC$_4$]Mand: $[C_{10}H_{24}N^+][C_8H_7O_3^-]$, M=309.44 g/mol (yield: 90 %)
^{1}H-NMR ($CDCl_3$): δ(ppm): 0.89 (t, *J*=7.3 Hz, 6H), 1.23 (sext$_a$, *J*=7.4 Hz, 4H),1.32-1.46 (m, 4H), 2.76 (s, 3H), 2.90-2.98 (m, 4H), 4.79 (s, 1H), 7.11-7.29 (m, 3H), 7.46 (d, *J*=7.3 Hz, 2H)
^{13}C-NMR ($CDCl_3$): δ(ppm): 13.7 (CH_3), 19.5 (CH_2), 24.1 (CH_2), 50.9 (CH_3), 63.4 (CH_2), 74.5 (CH), 126.87 (2xCH), 128.0 (3xCH), 143.2 (C), 176.3 (C)

Di-(dibutyldimethylammonium) succinate, **[DiC$_4$]$_2$Suc**: $[C_{10}H_{24}N^+]_2[C_4H_4O_4^{2-}]$, M=432.689 g/mol (yield: 92 %)
^{1}H-NMR ($CDCl_3$): δ(ppm): 0.88 (t, *J*=7.3 Hz, 12H), 1.31 (sext$_a$, *J*=7.4 Hz, 8H), 1.49-1.64 (m, 8H), 2.29 (s, 4H), 3.15 (s, 12H), 3.20-3.28 (m, 8H)
^{13}C-NMR ($CDCl_3$): δ(ppm): 13.7 (CH_3), 19.5 (CH_2), 24.4 (CH_2), 35.5 (CH_2), 51.2 (CH_3), 63.1 (CH_2), 119.6 (CH_2),179.2 (C)

Di-(dibutyldimethylammonium) itaconate, **[DiC$_4$]$_2$Ita**: $[C_{10}H_{24}N^+]_2[C_5H_4O_4^{2-}]$, M=444.69g/mol (yield: 95 %)
^{1}H-NMR ($CDCl_3$): δ(ppm): 0.92 (t, *J*=7.3 Hz, 12H), 1.33 (sext$_a$, *J*=7.5 Hz, 8H),1.52-1.66 (m, 8H), 3.11 (s, 2H), 3.14 (s, 12H), 3.19-3.27 (m, 8H), 5.11 (s, 1H), 5.73 (s, 1H)
^{13}C-NMR ($CDCl_3$): δ(ppm): 13.7 (CH_3), 19.8 (CH_3), 24.4 (CH_2), 43.6 (CH_2), 51.5 (CH_3), 63.4 (CH_2), 119.6 (CH_2), 144.9 (C), 173.4 (C), 176.9 (C)

Di-(dibutyldimethylammonium) maleate, **[DiC$_4$]$_2$Male**: $[C_{10}H_{24}N^+]_2[C_4H_2O_4^{2-}]$, M=430.66 g/mol (yield: 97 %)
^{1}H-NMR (CD_3OD): δ(ppm): 1.04 (t, *J*=7.3 Hz, 12H), 1.43 (sext$_a$, *J*=7.4 Hz, 8H),1.68-1.82 (m, 8H), 3.29-3.35 (m, 8H), 5.97 (s, 2H)
^{13}C-NMR (CD_3OD): δ(ppm): 13.9 (CH_3), 20.7 (CH_2), 25.5 (CH_2), 51.3 (CH_3), 65.0 (CH_2), 132.4 (CH), 175.3 (C)

Di-(dibutyldimethylammonium) fumarate, **[DiC$_4$]$_2$Fum**: $[C_{10}H_{24}N^+]_2[C_4H_2O_4^{2-}]$, M=430.66 g/mol (yield: 98 %)

^{1}H-NMR (CD_3OD): δ(ppm): 1.04 (t, *J*=7.3 Hz, 12H), 1.43 (sext$_a$, *J*=7.4 Hz, 8H), 1.68-1.81 (m, 8H), 3.08 (s, 12H), 3.26-3.35 (m, 8H), 6.67 (s, 2H)
^{13}C-NMR (CD_3OD): δ(ppm): 14.0 (CH_3), 20.7 (CH_2), 25.5 (CH_2), 51.2 (CH_3), 65.2 (CH_2), 137.1 (CH), 174.0 (C)

Di-(dibutyldimethylammonium) malate, **[DiC$_4$]$_2$Mala**: $[C_{10}H_{24}N^+]_2[C_4H_4O_5^{2-}]$, M=448.68 g/mol (yield: 92 %)
^{1}H-NMR ($CDCl_3$): δ(ppm): 0.96 (t, *J*=7.3 Hz, 12H), 1.38 (sext$_a$, *J*=7.4 Hz, 8H), 1.58-1.72 (m, 8H), 2.34 (dd, *J*=15.0 Hz, *J*=7.9 Hz, 1H), 2.66 (dd, *J*=15.1 Hz, *J*=4.9 Hz, 1H), 3.20 (s, 12H), 3.25-3.35 (m, 8H), 4.16 (dd, *J*=7.9 Hz, *J*=4.9 Hz, 1H)
^{13}C-NMR ($CDCl_3$): δ(ppm): 13.7 (CH_3), 19.8 (CH_2), 24.7 (CH_2), 43.9 (CH), 51.6 (CH_3), 63.4 (CH_2), 70.0 (CH_2), 177.1 (C), 179.0 (C)

Di-(dibutyldimethylammonium) tartrate, **[DiC$_4$]$_2$Tar**: $[C_{10}H_{24}N^+]_2[C_4H_4O_6^{2-}]$, M=464.68 g/mol (yield: 93 %)
^{1}H-NMR ($CDCl_3$): δ(ppm): 0.95 (t, *J*=7.3 Hz, 12H), 1.38 (sext$_a$, *J*=7.4 Hz, 8H), 1.55-169 (m, 8H), 3.20 (s, 12H), 3.25-3.34 (m, 8H), 4.19 (s, 2H)
^{13}C-NMR (CD_3OD): δ(ppm): 14.0 (CH_3), 19.9 (CH_2), 24.7 (CH_2), 51.9 (CH_3), 63.6 (CH_2), 73.7 (CH), 177.2 (C)

Tri-(dibutyldimethylammonium) citrate, **[DiC$_4$]$_3$Cit**: $[C_{10}H_{24}N^+]_2[C_6H_5O_7^{2-}]$, M=664.01 g/mol (yield: 98 %)
^{1}H-NMR ($CDCl_3$): δ(ppm): 0.93 (t, *J*=7.3 Hz, 18H), 1.36 (sext$_a$, *J*=7.5 Hz, 12H), 1.55-1.68 (m, 12H), 2.61 (dd, *J*=14.6 Hz, *J*=2.4 Hz, 4H), 3.25 (s, 18H), 3.26-3.35 (m, 12H)
^{13}C-NMR ($CDCl_3$): δ(ppm): 13.9 (CH_3), 19.5 (CH_2), 24.7 (CH_2), 46.7 (CH_2), 51.6 (CH_3), 63.3 (CH_2), 74.3 (C), 176.7 (C), 180.1 (C)

Tributylmethylammonium bromide, **[TriC$_4$]Br**: $[C_{13}H_{30}N^+][Br^-]$, M=280.29 g/mol, *commercial*
^{1}H-NMR ($CDCl_3$): δ(ppm): 1.02 (t, *J*=7.3 Hz, 9H), 1.47 (sext$_a$, *J*=7.5 Hz, 6H), 1.62-1.76 (m, 6H), 3.37 (s, 3H), 3.45-3.54 (m, 6H)
^{13}C-NMR ($CDCl_3$): δ(ppm): 13.8 (CH_3), 19.7 (CH_2), 24.4 (CH_2), 48.9 (CH_3), 61.4 (CH_2)

Tributylmethylammonium chloride, **[TriC$_4$]Cl**: $[C_{13}H_{30}N^+][Cl^-]$, M=235.84 g/mol (yield: 98 %)
^{1}H-NMR ($CDCl_3$): δ(ppm): 0.93 (t, *J*=7.3 Hz, 9H), 1.37 (sext$_a$, *J*=7.4 Hz, 6H), 1.54-1.69 (m, 6H), 3.23 (s, 3H), 3.33-3.42 (m, 6H)
^{13}C-NMR ($CDCl_3$): δ(ppm): 13.7 (CH_3), 19.7 (CH_2), 24.3 (CH_2), 48.9 (CH_3), 61.4 (CH_2)

Tributylmethylammonium acetate, **[TriC$_4$]Ace**: [$C_{13}H_{30}N^+$][$C_3H_2O_2^-$], M=259.43 g/mol (yield: 90 %)

^{1}H-NMR ($CDCl_3$): δ(ppm): 0.94 (t, *J*=7.3 Hz, 9H), 1.36 (sext$_a$, *J*=7.5 Hz, 6H), 1.53-1.67 (m, 6H), 1.84 (s, 3H), 3.15 (s, 3H), 3.21-3.29 (m, 6H)

^{13}C-NMR ($CDCl_3$): δ(ppm): 14.0 (CH_3), 19.9 (CH_2), 24.5 (CH_2), 25.6 (CH_3), 48.6 (CH_3), 61.2 (CH_2), 177.1 (C)

Tributylmethylammonium lactate, **[TriC$_4$]Lac**: [$C_{13}H_{30}N^+$][$C_3H_5O_3^-$], M=289.45 g/mol (yield: 93 %)

^{1}H-NMR ($CDCl_3$): δ(ppm): 1.00 (t, *J*=7.3 Hz, 9H), 1.35 (d, *J*=6.8 Hz, 3H), 1.43 (sext$_a$, *J*=7.5 Hz, 6H), 1.59-1.72 (m, 6H), 3.26 (s, 3H), 3.35-3.43 (m, 6H), 3.94 (q, *J*=6.8 Hz, 1H)

^{13}C-NMR ($CDCl_3$): δ(ppm): 13.8 (CH_3), 19.7 (CH_2), 21.8 (CH_3), 24.4 (CH_2), 48.8 (CH_3), 61.3 (CH_2), 68.3 (CH), 179.7 (C)

Tributylmethylammonium glycolate, **[TriC$_3$]Gly**: [$C_{13}H_{30}N^+$][$C_2H_3O_3^-$], M=275.43 g/mol (yield: 93 %)

^{1}H-NMR ($CDCl_3$): δ(ppm): 0.93 (t, *J*=7.3 Hz, 9H), 1.36 (sext$_a$, *J*=7.4 Hz, 6H), 1.53-1.66 (m, 6H), 3.11 (s, 3H), 3.20-3.29 (m, 6H), 3.76 (s, 2H)

^{13}C-NMR ($CDCl_3$): δ(ppm): 13.8 (CH_3), 19.8 (CH_2), 24.3 (CH_3), 48.9 (CH_3), 61.3 (CH_2), 62.5 (CH_2), 176.9 (C)

Tributylmethylammonium levulinate, [TriC$_4$]Lev: [$C_{13}H_{30}N^+$][$C_5H_7O_3^-$], M=315.49 g/mol (yield: 97 %)

^{1}H-NMR ($CDCl_3$): δ(ppm): 0.89 (t, *J*=7.3 Hz, 9H), 1.32 (sext$_a$, *J*=7.4 Hz, 6H), 1.49-1.63 (m, 6H), 2.05 (s, 3H), 2.30 (t, *J*=6.8 Hz, 2H), 2.58 (t, *J*=6.8 Hz, 2H), 3.09 (s, 3H), 3.18-3.26 (m, 6H)

^{13}C-NMR ($CDCl_3$): δ(ppm): 14.0 (CH_3), 19.8 (CH_2), 24.2 (CH_2), 29.9 (CH_3), 32.1 (CH_2), 40.6 (CH_2), 48.9 (CH_3), 61.2 (CH_2), 177.1 (C), 210.0 (C)

Di-(tributylmethylammonium) itaconate, **[TriC$_4$]$_2$Ita**: [$C_{13}H_{30}N^+$]$_2$[$C_5H_4O_4^{2-}$], M=528.85 g/mol (yield: 92 %)

^{1}H-NMR ($CDCl_3$): δ(ppm): 0.97 (t, *J*=7.3 Hz, 18H), 1.40 (sext$_a$, *J*=7.4 Hz, 12H),1.56-1.71 (m, 12H), 3.21 (s, 6H), 3.25-3.34 (m, 12H), 5.20 (s, 1H), 5.82 (s, 1H)

^{13}C-NMR ($CDCl_3$): δ(ppm): 13.7 (CH_3), 19.8 (CH_3), 24.2 (CH_2), 43.6 (CH_2), 49.15 (CH_3), 61.2 (CH_2), 119.2 (CH_2), 145.0 (C), 173.5 (C), 176.8 (C)

Dihexyldimethylammonium bromide, **[DiC$_6$]Br**: [$C_{14}H_{32}N^+$][Br^-], M=294.32 g/mol (yield: 98 %)

^{1}H-NMR (CDCl$_3$): δ(ppm): 0.80 (t, *J*=7.1 Hz, 6H), 1.12-1.39 (m, 12H),1.53-1.71 (m, 4H), 3.30 (s, 6H), 3.39-3.52 (m, 4H)

^{13}C-NMR (CDCl$_3$): δ(ppm): 13.9 (CH_3), 22.3 (CH_3), 22.7 (CH_2), 25.8 (CH_2), 31.2 (CH_2), 51.1 (CH_3), 63.9 (CH_2)

Dihexyldimethylammonium acetate, **[DiC$_6$]Ace**: [$C_{14}H_{32}N^+$][$C_3H_2O_2^-$], M=273.46 g/mol (yield: 94 %)

^{1}H-NMR (CD$_3$OD): δ(ppm): 0.96 (t, *J*=7.1 Hz, 6H), 1.32-1.47 (m, 12H), 1.69-1.83 (m, 4H), 1.91 (s, 3H), 3.08 (s, 6H), 3.26-3.36 (m, 4H)

^{13}C-NMR (CD$_3$OD): δ(ppm): 12.9 (CH_3), 22.2 (CH_2), 23.0 (CH_3), 25.7 (CH_2), 30.9 (CH_2), 49.8 (CH_3), 63.9 (CH_2), 178.6 (C)

Dihexyldimethylammonium lactate, **[DiC$_6$]Lac**: [$C_{14}H_{32}N^+$][$C_3H_5O_3^-$], M=303.49 g/mol (yield: 95 %)

^{1}H-NMR (CD$_3$OD): δ(ppm): 0.95 (t, *J*=7.1 Hz, 6H), 1.33 (d, *J*=6.8 Hz, 3H), 1.35-1.48 (m, 12H), 1.69-1.86 (m, 4H), 3.09 (s, 6H), 3.24-3.37 (m, 4H), 3.97 (q, *J*=6.8 Hz, 1H)

^{13}C-NMR (CD$_3$OD): δ(ppm): 12.9 (CH_3), 20.4 (CH_3), 22.1 (CH_2), 25.7 (CH_2), 31.0 (CH_2), 49.8 (CH_3), 63.9 (CH_2), 68.1 (CH), 180.6 (C)

Dihexyldimethylammonium glycolate, **[DiC$_6$]Gly**: [$C_{14}H_{32}N^+$][$C_2H_3O_3^-$], M=289.46 g/mol (yield: 95 %)

^{1}H-NMR (CDCl$_3$): δ(ppm): 0.77 (t, *J*=6.8 Hz, 6H), 1.11-1.32 (m, 12H), 1.49-1.64 (m, 4H), 3.12 (s, 6H), 3.18-3.31 (m, 4H), 3.69 (s, 2H)

^{13}C-NMR (CDCl$_3$): δ(ppm): 13.8 (CH_3), 22.2 (CH_2), 22.5 (CH_2), 25.8 (CH_2), 31.1 (CH_2), 50.9 (CH_3), 62.1 (CH_2), 63.9 (CH_2), 176.5 (C)

Dihexyldimethylammonium levulinate, [DiC$_6$]Lev: [$C_{14}H_{32}N^+$][$C_5H_7O_3^-$], M=329.52 g/mol (yield: 91 %)

^{1}H-NMR (CDCl$_3$): δ(ppm): 0.79 (t, *J*=7.0 Hz, 6H), 1.13-1.35 (m, 12H), 1.51-1.67 (m, 4H), 2.05 (s, 3H), 2.30 (t, *J*=6.7 Hz, 2H), 2.58 (t, *J*=6.7 Hz, 2H), 3.15 (s, 6H), 3.19-3.31 (m, 4H)

^{13}C-NMR (CDCl$_3$): δ(ppm): 13.8 (CH_3), 22.3 (CH_2), 22.5 (CH_2), 25.8 (CH_2), 29.9 (CH_3), 31.2 (CH_2), 32.2 (CH_2), 40.4 (CH_2), 51.2 (CH_3), 63.5 (CH_2), 177.1 (C), 210.0 (C)

Dihexyldimethylammonium salicylate, [DiC$_6$]Sal: [$C_{14}H_{32}N^+$][$C_7H_5O_3^-$], M=351.53 g/mol (yield: 97 %)

^{1}H-NMR ($CDCl_3$): δ(ppm): 0.87 (t, *J*=7.1 Hz, 6H), 1.22-1.35 (m, 12H), 1.55-1.69 (m, 4H), 3.25 (s, 6H), 3.27-3.37 (m, 4H), 6.73 (t, *J*=7.5 Hz,1H), 6.82 (d, *J*=8.0 Hz,1H), 7.20-7.27 (m,1H), 7.91 (dd, *J*=6.0 Hz, *J*=1.8 Hz,1H)

^{13}C-NMR ($CDCl_3$): δ(ppm): 13.9 (CH_3), 22.4 (CH_2), 22.7 (CH_2), 25.8 (CH_2), 31.2 (CH_2), 51.0 (CH_3), 63.9 (CH_2), 116.3 (CH), 117.4 (CH), 120.1 (C), 130.5 (CH), 132.1 (CH), 162.4 (C), 173.8 (C)

Dihexyldimethylammonium mandelate, [DiC$_6$]Mand: [$C_{14}H_{32}N^+$][$C_8H_7O_3^-$], M=365.56 g/mol (yield: 98 %)

^{1}H-NMR ($CDCl_3$): δ(ppm): 0.88 (t, *J*=7.0 Hz, 6H), 1.18-1.34 (m, 12H),1.39-1.53 (m, 4H), 2.88 (s, 3H), 3.01-3.11 (m, 4H), 4.81 (s, 1H), 7.09-7.29 (m, 3H), 7.49 (d, *J*=7.3 Hz, 2H)

^{13}C-NMR ($CDCl_3$): δ(ppm): 13.9 (CH_3), 22.4 (CH_2), 22.5 (CH_2), 25.9 (CH_2), 31.2 (CH_2), 50.7 (CH_3), 63.6 (CH_2), 74.4 (CH), 126.5 (2xCH), 126.7 (CH), 127.8 (2xCH), 143.7 (C), 176.1 (C)

Di-(dihexyldimethylammonium) itaconate, **[DiC$_6$]$_2$Ita**: [$C_{14}H_{32}N^+$]$_2$[$C_5H_4O_4^{2-}$], M=556.92 g/mol (yield: 97 %)

^{1}H-NMR ($CDCl_3$): δ(ppm): 0.84 (t, *J*=7.1 Hz, 12H), 1.19-1.37 (m, 24H),1.53-1.66 (m, 8H), 3.15 (s, 2H), 3.19 (s, 12H), 3.21-3.29 (m, 8H), 5.11 (s, 1H), 5.75 (s, 1H)

^{13}C-NMR ($CDCl_3$): δ(ppm): 13.9 (CH_3), 22.4 (CH_2), 22.6 (CH_2), 25.9 (CH_2), 31.3 (CH_2), 43.8 (CH_2), 51.5 (CH_3), 63.4 (CH_2), 119.2 (CH_2), 145.1 (C), 173.4 (C), 176.7 (C)

Di-(dihexyldimethylammonium) tartrate, **[DiC$_6$]$_2$Tar**: [$C_{14}H_{32}N^+$]$_2$[$C_4H_4O_6^{2-}$], M=576.90 g/mol (yield: 96 %)

^{1}H-NMR ($CDCl_3$): δ(ppm): 0.87 (t, *J*=7.0 Hz, 12H), 1.22-1.42 (m, 24H), 1.56-1.70 (m, 8H), 3.25 (s, 12H), 3.26-3.36 (m, 8H), 4.23 (s, 2H)

^{13}C-NMR (CD_3OD): δ(ppm): 13.9 (CH_3), 22.4 (CH_2), 22.6 (CH_2), 25.9 (CH_2), 31.3 (CH_2), 51.4 (CH_3), 63.5 (CH_2), 73.5 (CH), 176.9 (C)

Tri-(dihexyldimethylammonium) citrate, **[DiC$_6$]$_3$Cit**: [$C_{14}H_{32}N^+$]$_3$[$C_6H_5O_7^{2-}$], M=832.35 g/mol (yield: 98 %)

^{1}H-NMR ($CDCl_3$): δ(ppm): 0.86 (t, *J*=7.0 Hz, 18H), 1.22-1.40 (m, 36H), 1.57-1.71 (m, 12H), 2.63 (dd, *J*=14.6 Hz, *J*=3.3 Hz, 4H), 3.24 (s, 18H), 3.27-3.37 (m, 12H)

^{13}C-NMR ($CDCl_3$): δ(ppm): 14.0 (CH_3), 22.3 (CH_2), 22.6 (CH_2), 25.9 (CH_2), 31.2 (CH_2), 46.5 (CH_2), 51.8 (CH_3), 63.5 (CH_2), 74.0 (C), 176.3 (C), 179.6 (C)

1.3) Water content

After lyophilisation of the synthesized ILs using a freeze dryer Christ-Alpha 1-2LD plus, for at least 72 h, the water content was detected by means of a coulometric Karl Fischer titration (Mettler Toledo C20) with Hydranal Coulomat AG reagent. **Table 2.13** shows the water content of all synthesized quaternary ammonium compounds.

Table 2.13 Water content of **QACILs** measured by coulometric Karl Fischer titration.

Product	H_2O (wt%)	Product	H_2O (wt%)	Product	H_2O (wt%)
$[DiC_3]I$	3.4	$[TriC_3]Br$	0.7	$[TriC_4]Br$	1.9
$[DiC_3]Cl$	10.9	$[TriC_3]Cl$	3.3	$[TriC_4]Cl$	4.5
$[DiC_3]Ace$	10.0	$[TriC_3]Ace$	7.7	$[TriC_4]Ace$	6.5
$[DiC_3]Lac$	3.1	$[TriC_3]Lac$	2.6	$[TriC_4]Lac$	1.8
$[DiC_3]Lev$	2.6	$[TriC_3]Lev$	3.5	$[TriC_4]Lev$	6.7
$[DiC_3]_2Ita$	5.9	$[TriC_3]_2Ita$	8.3	$[TriC_4]_2Ita$	6.6
				$[TriC_4]Gly$	5.0
$[DiC_4]Br$	0.7	$[DiC_4]Mand$	1.1	$[DiC_6]Br$	0.5
$[DiC_4]Cl$	1.0	$[DiC_4]_2Suc$	5.3	$[DiC_6]Ace$	5.3
$[DiC_4]For$	7.7	$[DiC_4]_2Ita$	12.8	$[DiC_6]Lac$	1.9
$[DiC_4]Ace$	10.8	$[DiC_4]_2Male$	11.5	$[DiC_6]Gly$	1.2
$[DiC_4]Lac$	2.8	$[DiC_4]_2Fum$	9.8	$[DiC_6]Lev$	2.1
$[DiC_4]Gly$	1.6	$[DiC_4]_2Mala$	7.0	$[DiC_6]Sal$	1.1
$[DiC_4]Lev$	2.5	$[DiC_4]_2Tar$	4.1	$[DiC_6]Mand$	0.8
$[DiC_4]Sor$	5.5	$[DiC_4]_3Cit$	7.3	$[DiC_6]_2Ita$	4.2
$[DiC_4]Sal$	1.8			$[DiC_6]_2Tar$	2.0
				$[DiC_6]_3Cit$	3.2

2.) Physicochemical characterization of quaternary ammonium compounds

2.1) Thermogravimetric analysis (TGA)

The thermogravimetric analysis (TGA) of prepared salts was performed using a TGA Q5000 apparatus (TA Instruments) unit under a nitrogen atmosphere to determine decomposition temperatures. Samples between 5 and 10 mg were placed in aluminum pans and heated from 25 to 300 °C at a heating rate of 10 °C·min^{-1}. The degradation temperature T_{deg} is determined as starting point of the degradation (range with the highest slope of TGA curves):

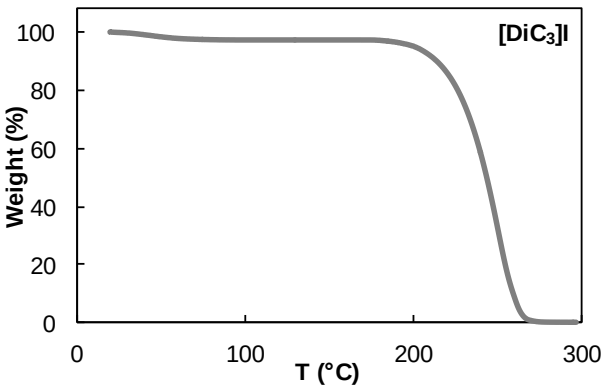
[DiC3]I
Weight (%)
T (°C)

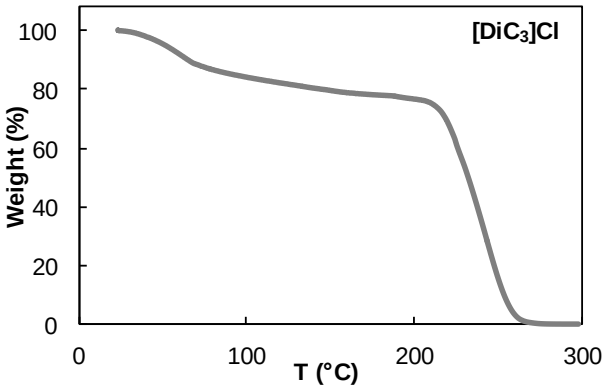
[DiC3]Cl
Weight (%)
T (°C)

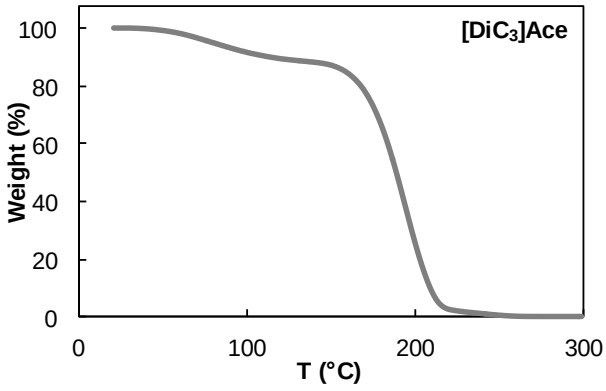
[DiC3]Ace
Weight (%)
T (°C)

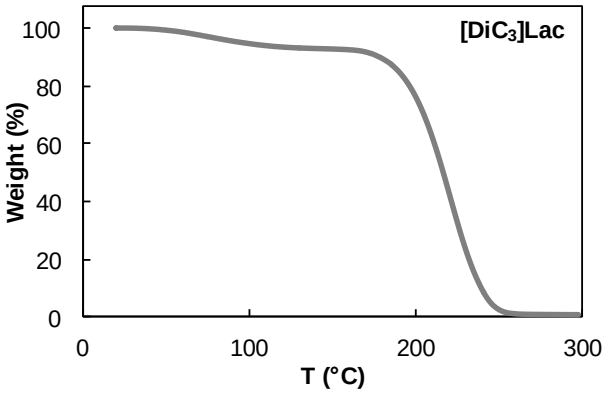
[DiC3]Lac
Weight (%)
T (°C)

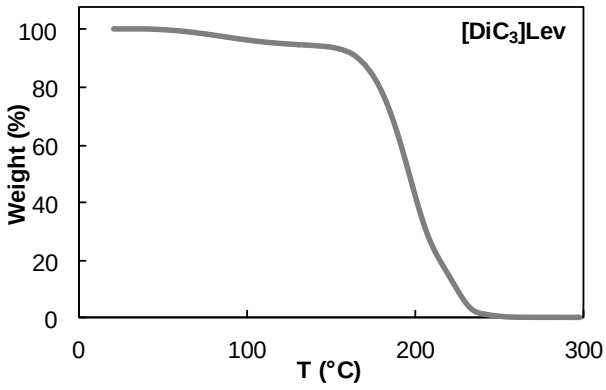
[DiC3]Lev
Weight (%)
T (°C)

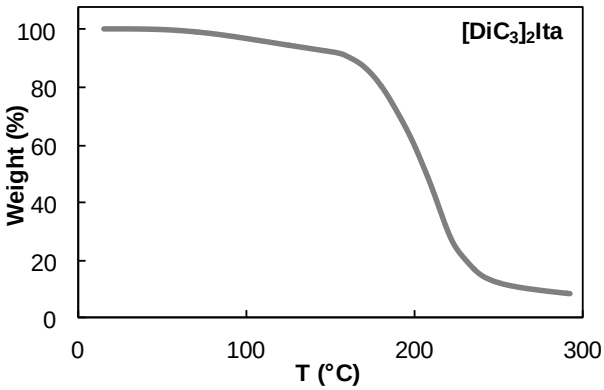
[DiC3]2Ita
Weight (%)
T (°C)

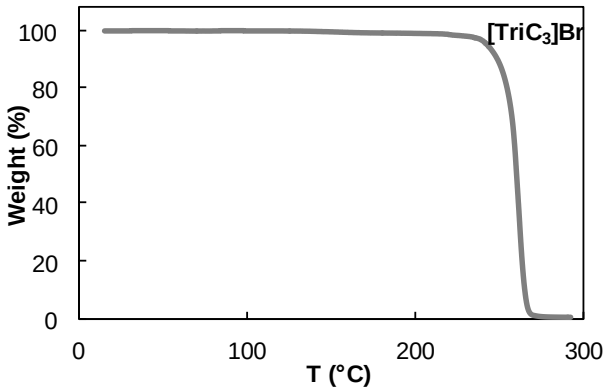
[TriC3]Br
Weight (%)
T (°C)

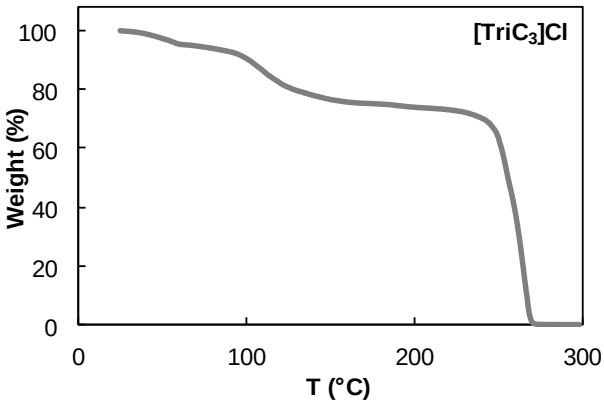
[TriC3]Cl
Weight (%)
T (°C)

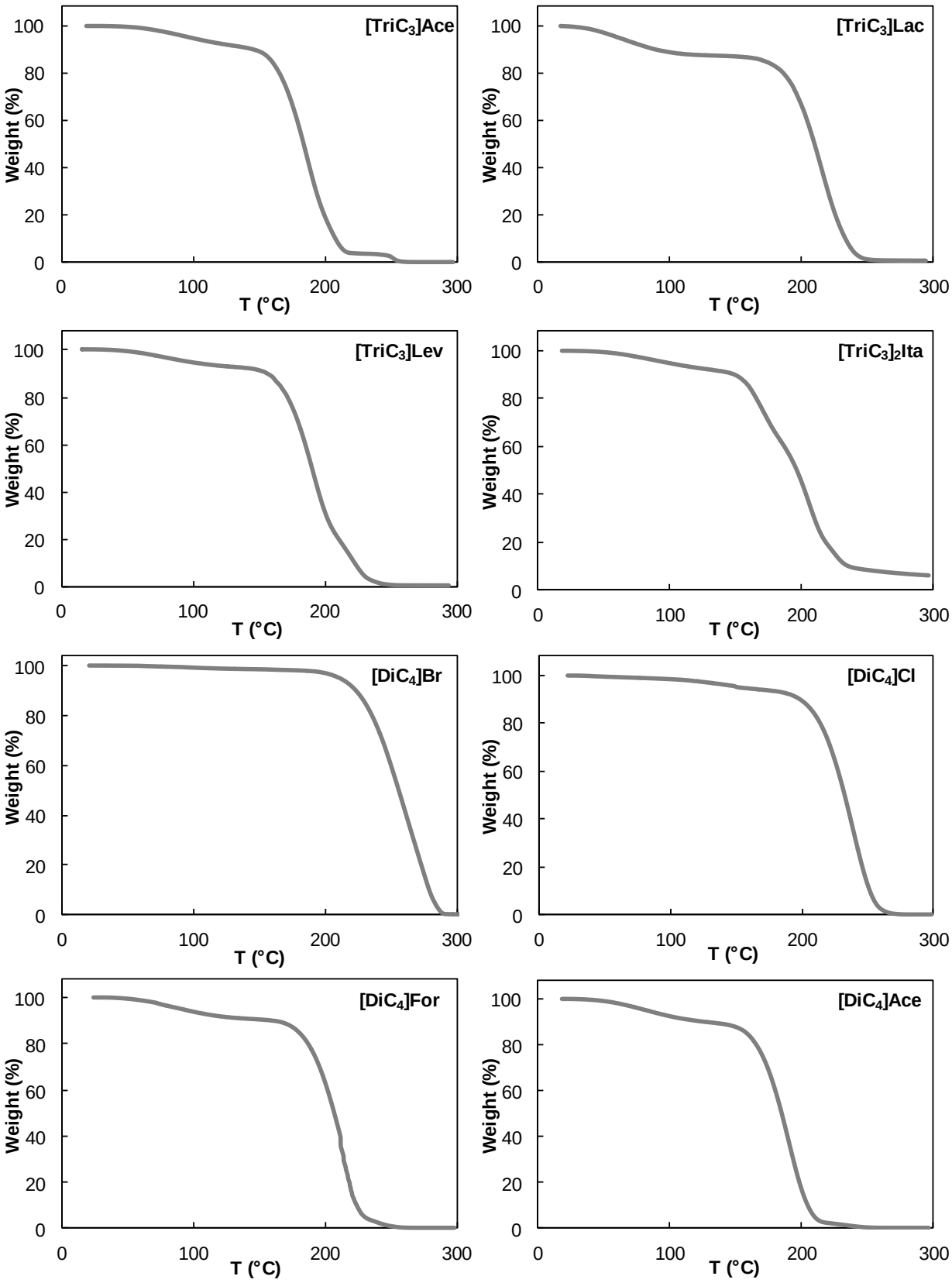
[TriC3]Ace
[TriC3]Lac
[TriC3]Lev
[TriC3]2Ita
[DiC4]Br
[DiC4]Cl
[DiC4]For
[DiC4]Ace
Weight (%)
T (°C)
0
20
40
60
80
100
0
100
200
300

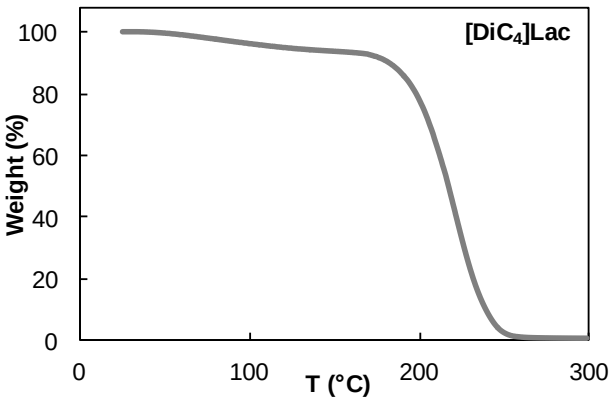
[DiC4]Lac
Weight (%)
T (°C)

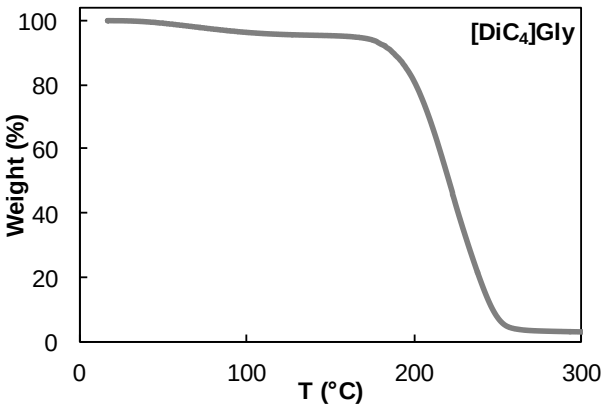
[DiC4]Gly
Weight (%)
T (°C)

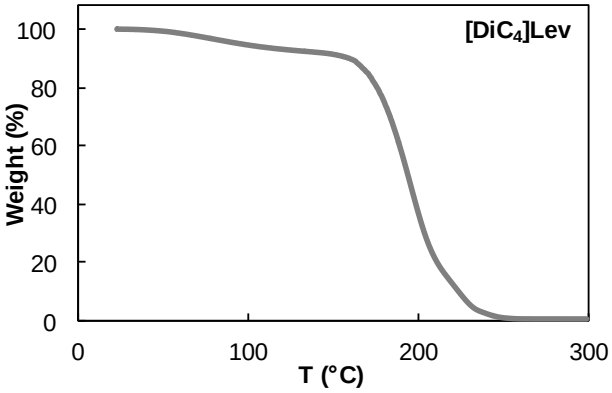
[DiC4]Lev
Weight (%)
T (°C)

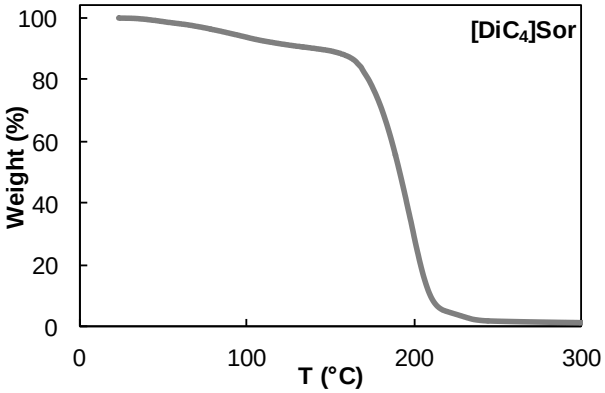
[DiC4]Sor
Weight (%)
T (°C)

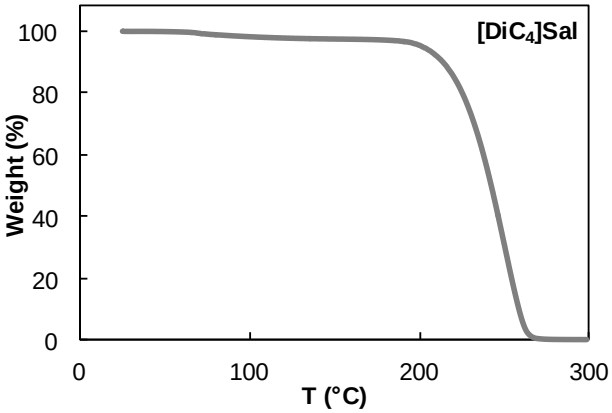
[DiC4]Sal
Weight (%)
T (°C)

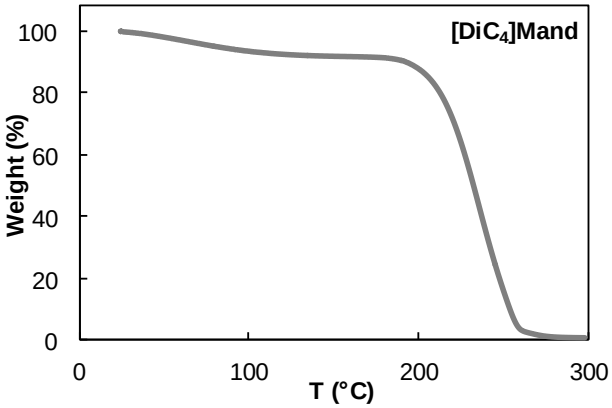
[DiC4]Mand
Weight (%)
T (°C)

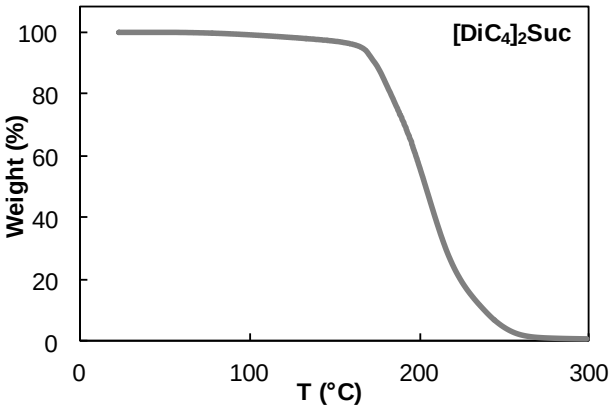
[DiC4]2Suc
Weight (%)
T (°C)

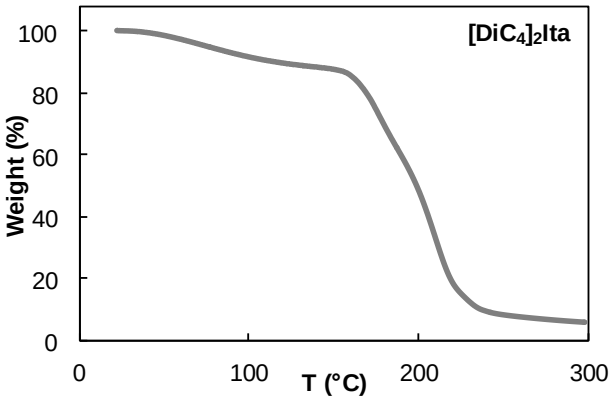
[DiC4]2Ita
Weight (%)
T (°C)

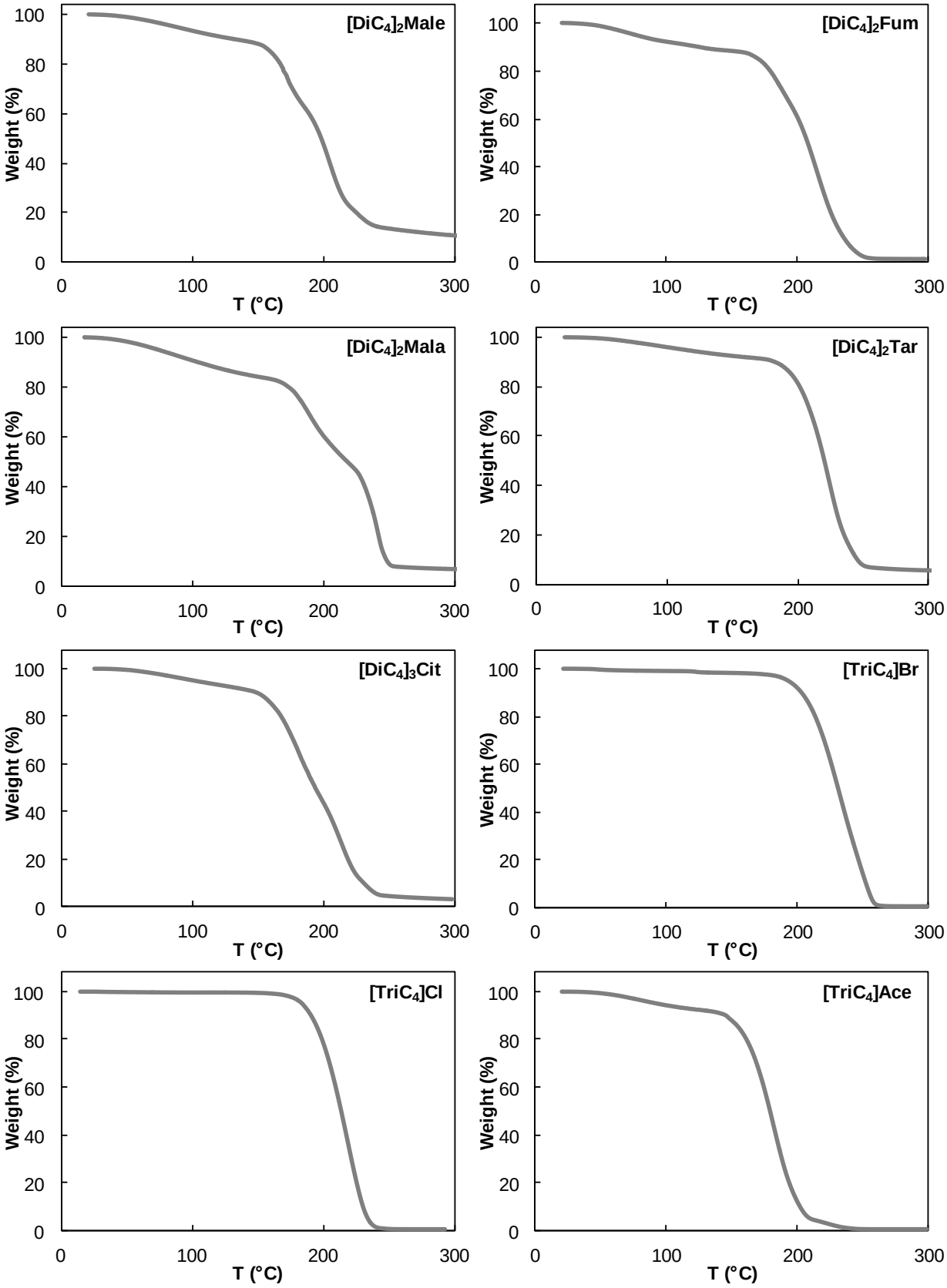
[DiC4]2Male
[DiC4]2Fum
[DiC4]2Mala
[DiC4]2Tar
[DiC4]3Cit
[TriC4]Br
[TriC4]Cl
[TriC4]Ace
Weight (%)
T (°C)
0
20
40
60
80
100
0
100
200
300

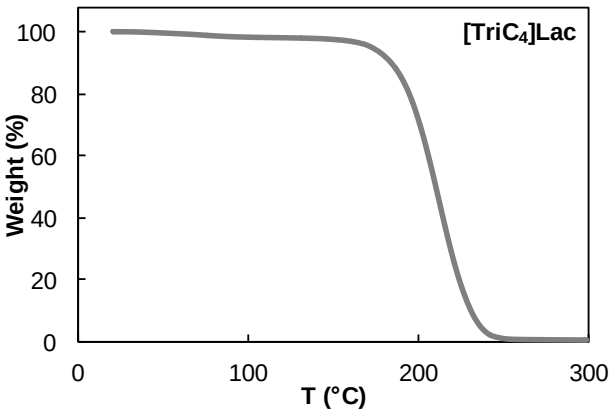
[TriC4]Lac
Weight (%)
T (°C)

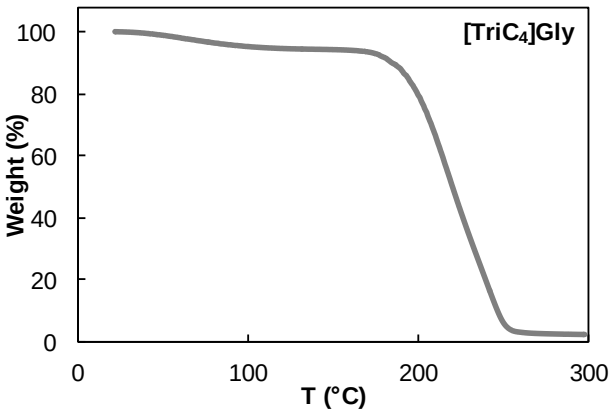
[TriC4]Gly
Weight (%)
T (°C)

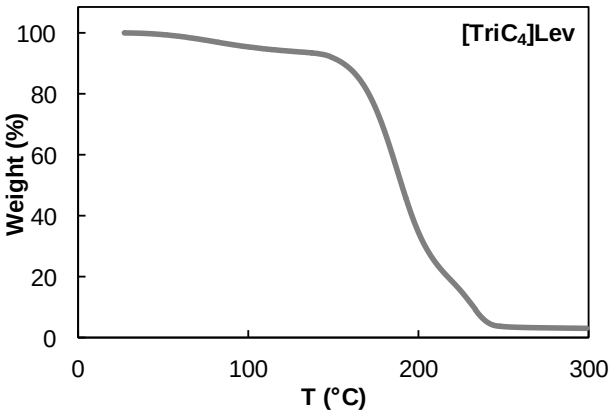
[TriC4]Lev
Weight (%)
T (°C)

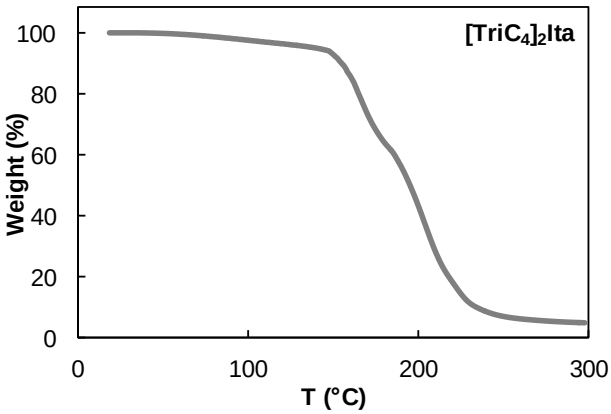
[TriC4]2Ita
Weight (%)
T (°C)

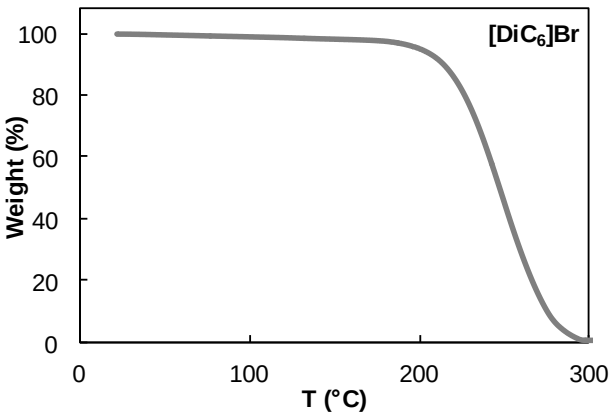
[DiC6]Br
Weight (%)
T (°C)

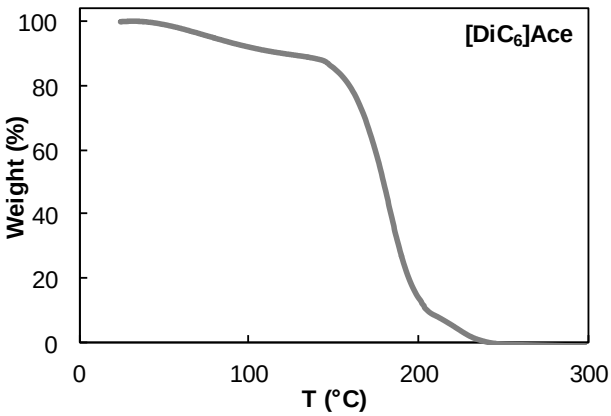
[DiC6]Ace
Weight (%)
T (°C)

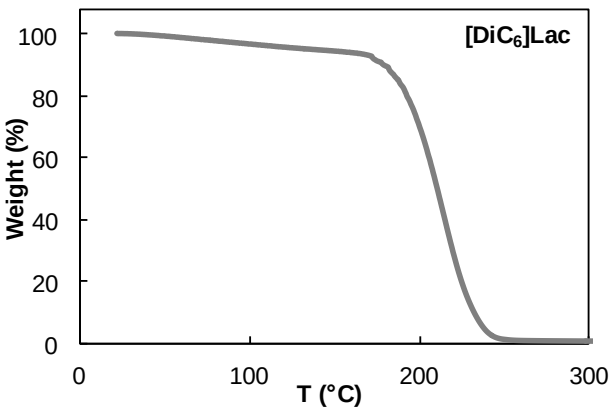
[DiC6]Lac
Weight (%)
T (°C)

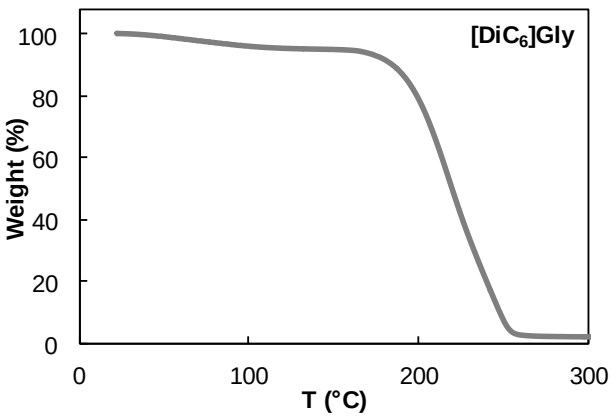
[DiC6]Gly
Weight (%)
T (°C)

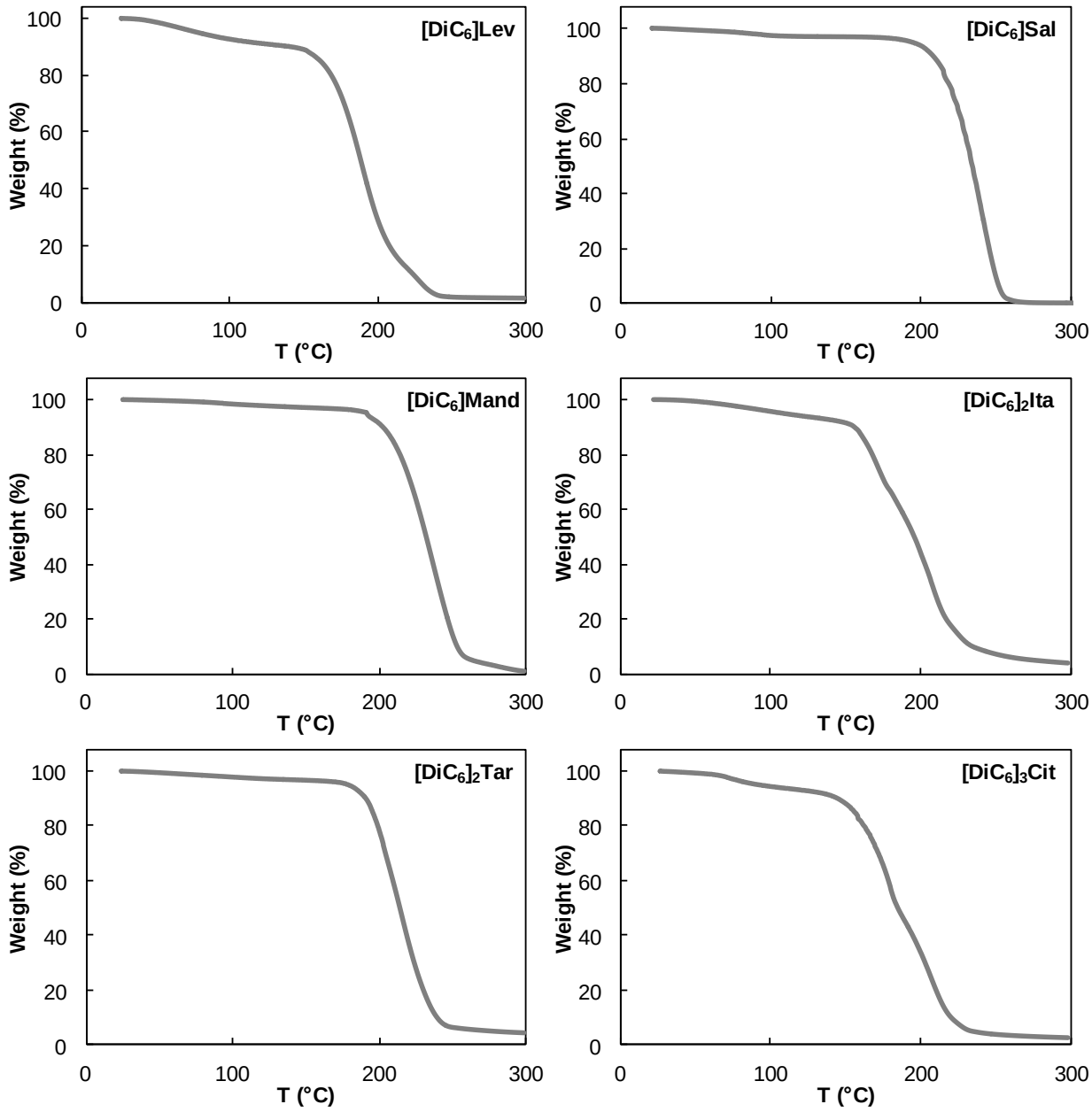

2.2) Differential scanning calorimetry (DSC)

Thermal transitions were determined by differential scanning calorimetry (DSC) with a DSC Q100 calorimeter (TA Instruments) unit under a nitrogen atmosphere, calibrated with a standard sample of indium. Samples between 5 and 10 mg were sealed in aluminum pans and measured over a temperature range of -80 °C until ca. 20 °C under the beginning of degradation with a rate of 10 °C·min^{-1}; the samples were cooled with an intercooler. The phase transitions of the products were investigated, providing the glass transition (T_g, as the midpoint of a small endothermic heat capacity change from the amorphous glass state to a liquid state), the cold crystallization (T_c, as onset of an exothermic peak on heating from a supercooled liquid state to a crystalline solid state), the melting temperature (T_m, as onset of an endothermic peak on

heating) and the freezing temperatures (T_f, as onset of an exothermic peak on cooling) with the software TA Universal Analysis. The DSC-curves (exo up) of **QACILs** are shown in the following:

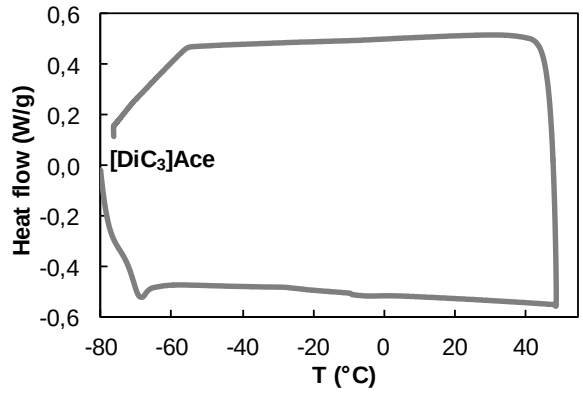

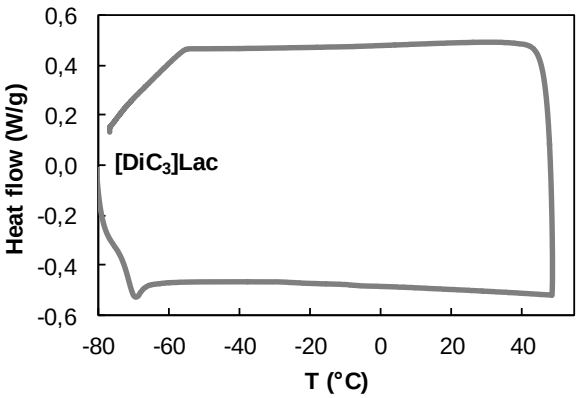

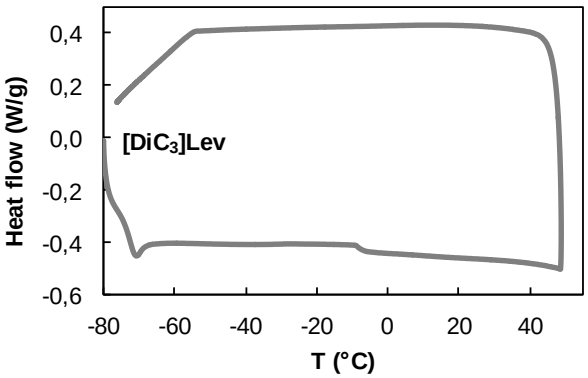

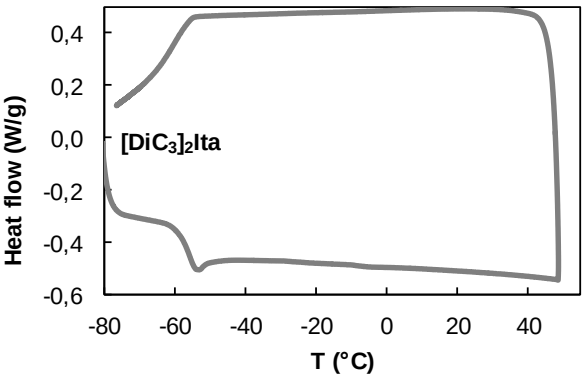

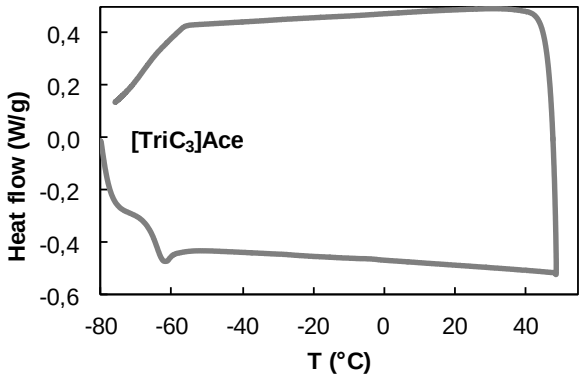

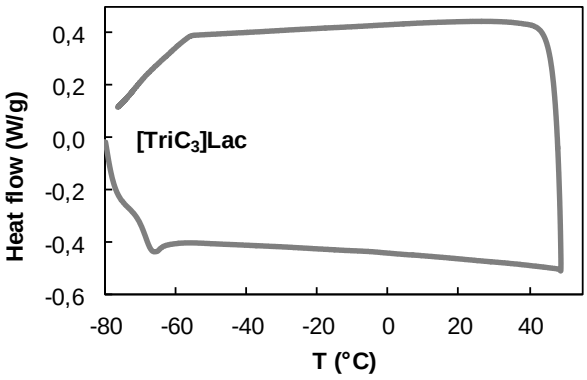

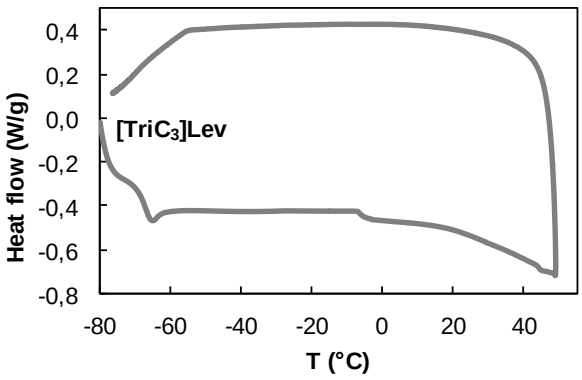

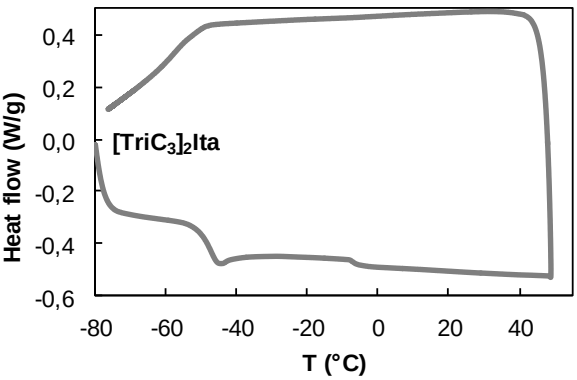

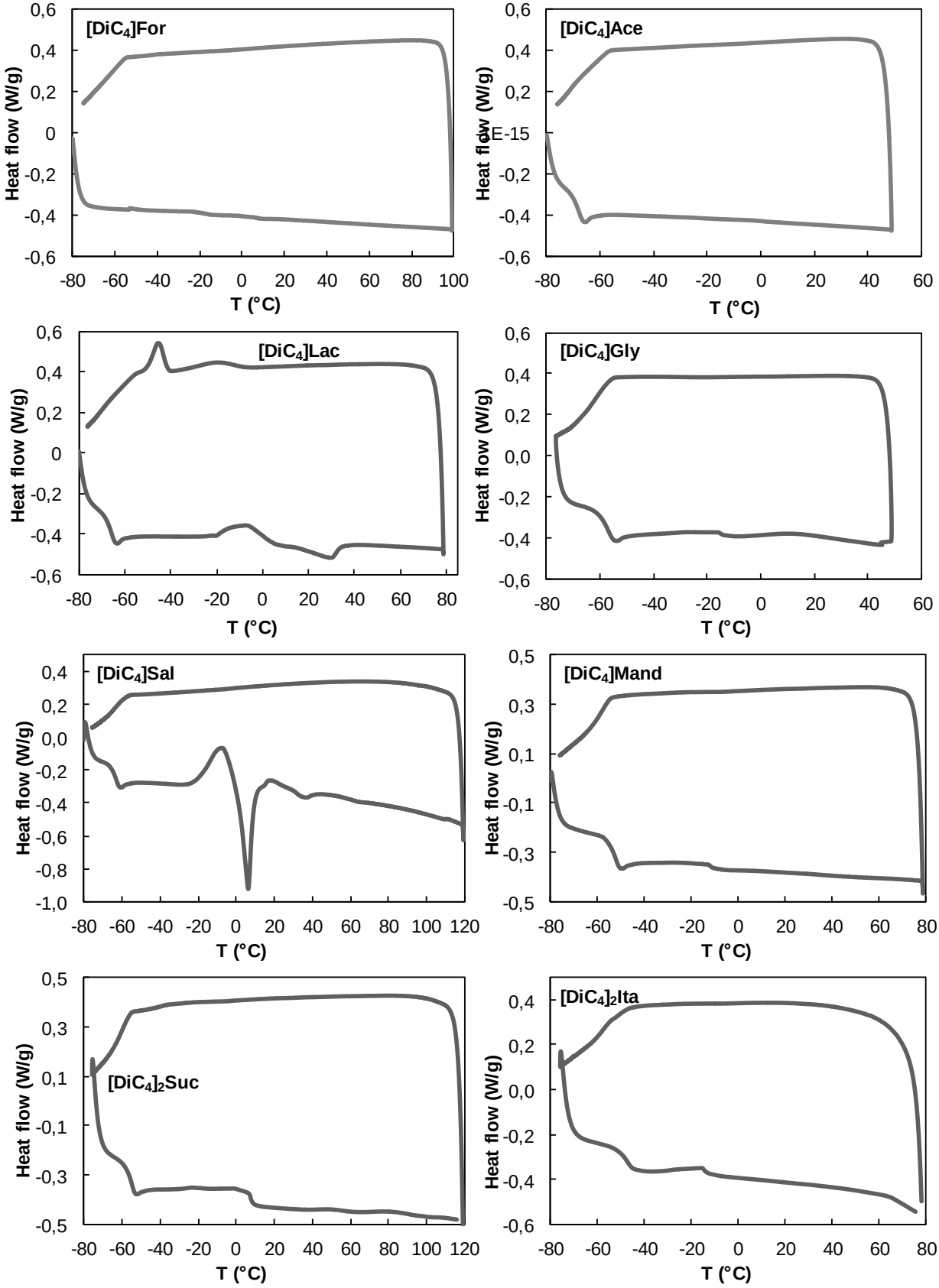
[DiC4]For
[DiC4]Ace
[DiC4]Lac
[DiC4]Gly
[DiC4]Sal
[DiC4]Mand
[DiC4]2Suc
[DiC4]2Ita
Heat flow (W/g)
T (°C)

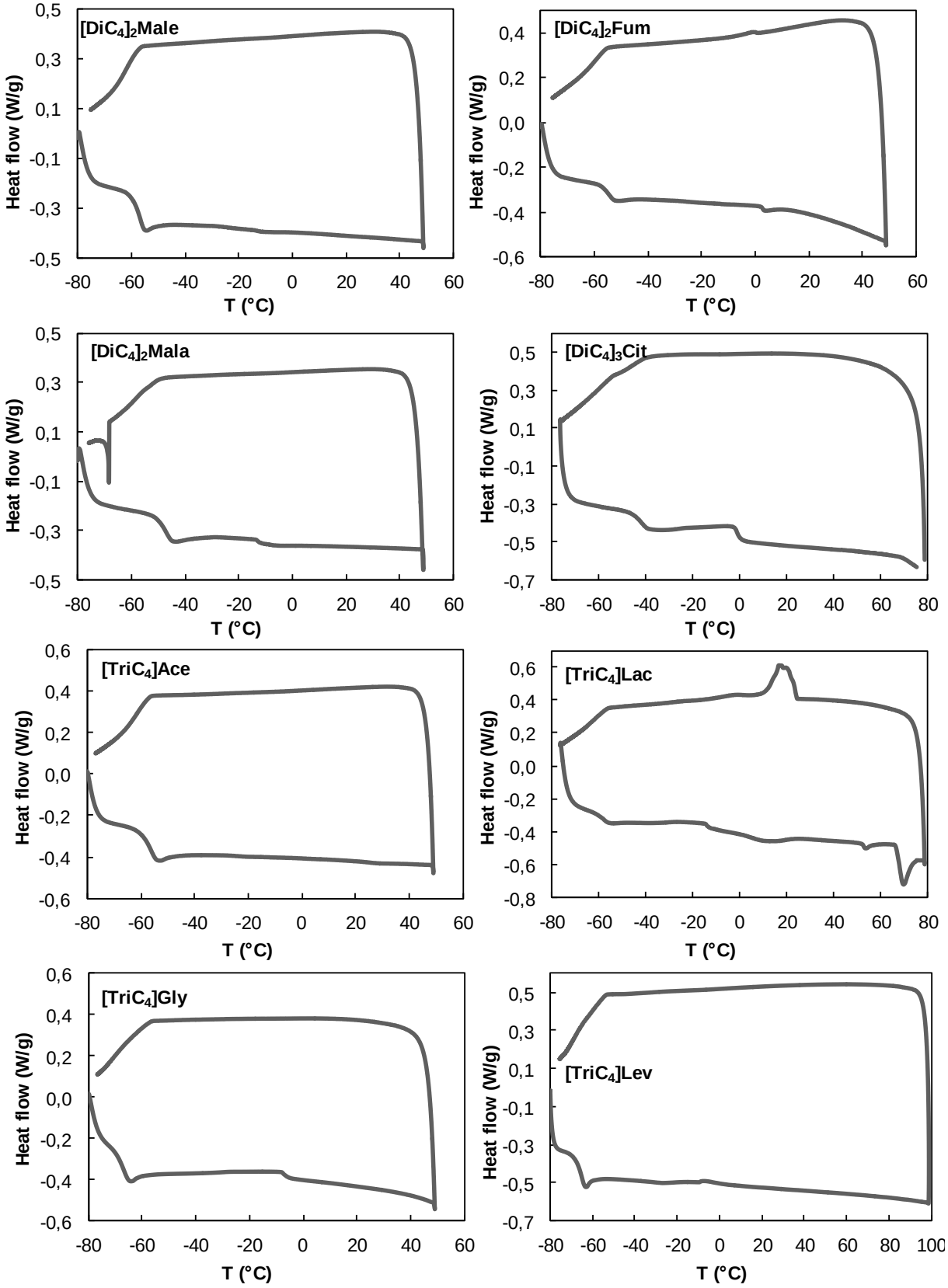
[DiC4]2Male
[DiC4]2Fum
[DiC4]2Mala
[DiC4]3Cit
[TriC4]Ace
[TriC4]Lac
[TriC4]Gly
[TriC4]Lev
Heat flow (W/g)
T (°C)

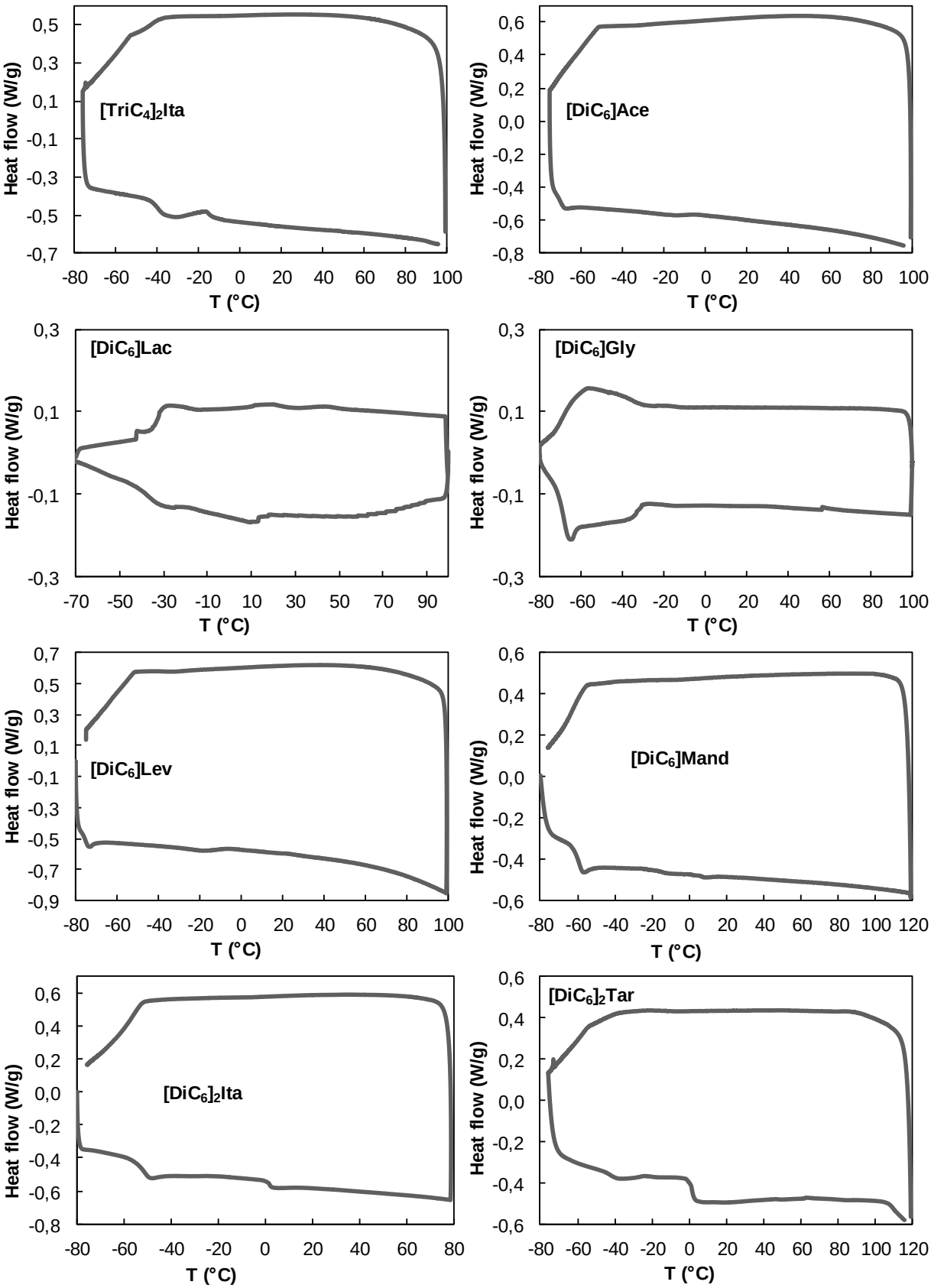
[TriC4]2Ita
[DiC6]Ace
[DiC6]Lac
[DiC6]Gly
[DiC6]Lev
[DiC6]Mand
[DiC6]2Ita
[DiC6]2Tar
Heat flow (W/g)
T (°C)

2.3) Viscosity

Viscosity measurements were carried out with a Malvern Kinexus rotational rheometer with cone plate geometry (CP 20/2°), which was equipped with a Peltier temperature-controlled plate, using a sample volume of ca. 0.1 mL. Shear rates were determined over a shear stress ramp between 1 and 2000 Pa. To study the temperature dependence of the viscosity the measurements were carried out at 25, 40, 60 and 80 °C. Samples were dried under lyophilisation, and rapidly transferred to the plates of the rheometer. Measurements were started as quickly as possible to minimize the water absorption.

The shear stress τ is the force F acting on area A to effect a movement in the liquid element between two plates (**Eq. 1.2**). The velocity of the movement at a given force is controlled by the internal forces of the material.

$$\tau = \frac{F}{A}\left[\frac{Newton}{m^2} = Pa\right] \qquad \textbf{Eq. 2.12}$$

By applying shear stress, a laminar shear flow is generated between the two plates. The uppermost layer moves at the maximum velocity v_{max}, the lowermost layer remains at rest. The shear rate is defined as follows (**Eq. 1.3**)

$$\dot{\gamma} = \frac{dv}{dh} \approx \frac{v}{h}\left[\frac{m/s}{m} = s^{-1}\right] \qquad \textbf{Eq. 2.13}$$

If the dynamic viscosity η of a fluid is independent of shear rate and shear stress its flow behavior is Newtonian (**Eq. 1.4**).

$$\eta = \frac{shear\ stress\ \tau}{shear\ rate\ \dot{\gamma}}\left[\frac{Pa}{s^{-1}} = Pa \cdot s\right] \qquad \textbf{Eq. 2.14}$$

Figure 2.27 shows the graphical representation of viscosity measurements of the IL [TriC$_3$]Lev as an example. All of the measured ILs showed Newtonian behavior.

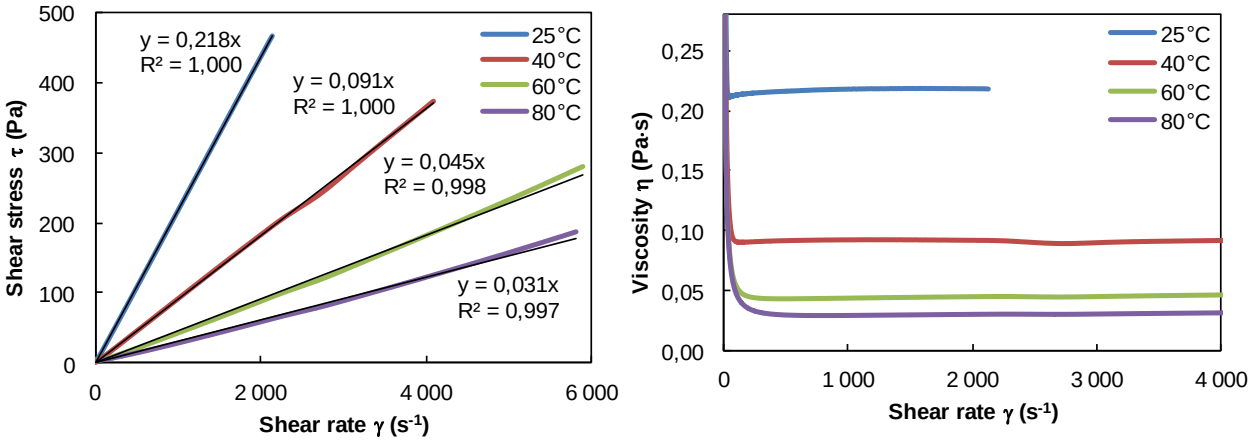

Figure 2.27 Rheograms of [TriC$_3$]Lev as representation of viscosity measurements.

Table 2.14 Dynamic viscosity η for **QACILs** at 25, 40, 60 and 80 °C.

Compounds	η (Pa·s)			
	25 °C	**40 °C**	**60 °C**	**80 °C**
[DiC_3]Ace	0.231	0.081	0.042	0.032
[DiC_3]Lac	0.284	0.110	0.054	0.037
[DiC_3]Lev	0.194	0.083	0.043	0.030
[DiC_3]$_2$Ita	1.683	0.457	0.145	0.082
[$TriC_3$]Ace	0.374	0.116	0.050	0.037
[$TriC_3$]Lac	0.196	0.081	0.047	0.036
[$TriC_3$]Lev	0.218	0.091	0.045	0.031
[$TriC_3$]$_2$Ita	4.372	0.942	0.213	0.099
[DiC_4]For	0.443	0.213	0.094	0.056
[DiC_4]Ace	0.177	0.079	0.053	0.041
[DiC_4]Lac	0.428	0.149	0.067	0.048
[DiC_4]Gly	0.585	0.228	0.099	0.058
[DiC_4]Lev	0.172	0.085	0.053	0.043
[DiC_4]Sor	solid	solid	0.264	0.064
[DiC_4]Sal	solid	solid	0.193	0.083
[DiC_4]Mand	0.448	0.170	0.094	0.071
[DiC_4]$_2$Suc	16.790	3.956	0.900	0.307
[DiC_4]$_2$Ita	0.676	0.207	0.083	0.052
[DiC_4]$_2$Male	3.317	0.901	0.242	0.092
[DiC_4]$_2$Fum	2.974	0.806	0.268	0.139
[DiC_4]$_2$Mala	3.342	0.947	0.203	0.077
[DiC_4]$_2$Tar	6.525	1.632	0.433	0.209
[DiC_4]$_3$Cit	19.185	3.806	0.813	0.316
[$TriC_4$]Ace	0.608	0.180	0.073	0.048
[$TriC_4$]Lac	solid	solid	0.229	0.100
[$TriC_4$]Gly	0.421	0.169	0.081	0.056
[$TriC_4$]Lev	0.253	0.101	0.051	0.030
[$TriC_4$]$_2$Ita	3.456	0.842	0.238	0.120

2.4) Tensiometry

The surface tension measurements of pure **QACILs** were performed using a Krüss-K11 tensiometer equipped with plate geometry. They were carried out in the temperature range from 25 to 80 °C at atmospheric pressure. The temperature was thermo-regulated thanks to a double-jacketed glass cell by means of a water bath using a Lauda RC6 circulator to control the temperature.

Table 2.15 Surface tension σ of **QACILs** at 25 and 80°C.

Ionic liquid	σ (mN·m^{-1})		Ionic liquid	σ (mN·m^{-1})	
	25 °C	80 °C		25 °C	80 °C
[DiC$_3$]Ace	39.4	36.2	**[DiC$_4$]Sal**	solid	39.3
[DiC$_3$]Lac	41.5	34.1	**[DiC$_4$]Mand**	40.95	38.3
[DiC$_3$]Lev	34.6	30.2	**[DiC$_4$]$_2$Suc**	39.9	40.1
[DiC$_3$]$_2$Ita	46.8	44.4	**[DiC$_4$]$_2$Ita**	38.6	30.5
[TriC$_3$]Ace	39.2	37.15	**[DiC$_4$]$_2$Male**	38.45	37.3
[TriC$_3$]Lac	42.8	41.6	**[DiC$_4$]$_2$Fum**	42.3	40.6
[TriC$_3$]Lev	35.5	25.05	**[DiC$_4$]$_2$Mala**	29.9	28.8
[TriC$_3$]$_2$Ita	42.6	39.0	**[DiC$_4$]$_2$Tar**	30.55	41.4
[DiC$_4$]For	37.7	37.6	**[DiC$_4$]$_3$Cit**	36.3	36.6
[DiC$_4$]Ace	34.7	32.7	**[TriC$_4$]Ace**	33.9	28.05
[DiC$_4$]Lac	37.15	35.0	**[TriC$_4$]Lac**	solid	32.7
[DiC$_4$]Gly	41.6	39.35	**[TriC$_4$]Gly**	40.9	27.9
[DiC$_4$]Lev	36.4	28.6	**[TriC$_4$]Lev**	35.2	32.9
[DiC$_4$]Sor	solid	30.6	**[TriC$_4$]$_2$Ita**	37.0	36.1

The surface tension measurements of aqueous **QACIL** solutions as a function of concentration were carried out with the same tensiometer as described before. Therefore, aqueous solutions of **QACILs** were prepared with concentrations up to 2 mol·L^{-1}; the results are shown in the following.

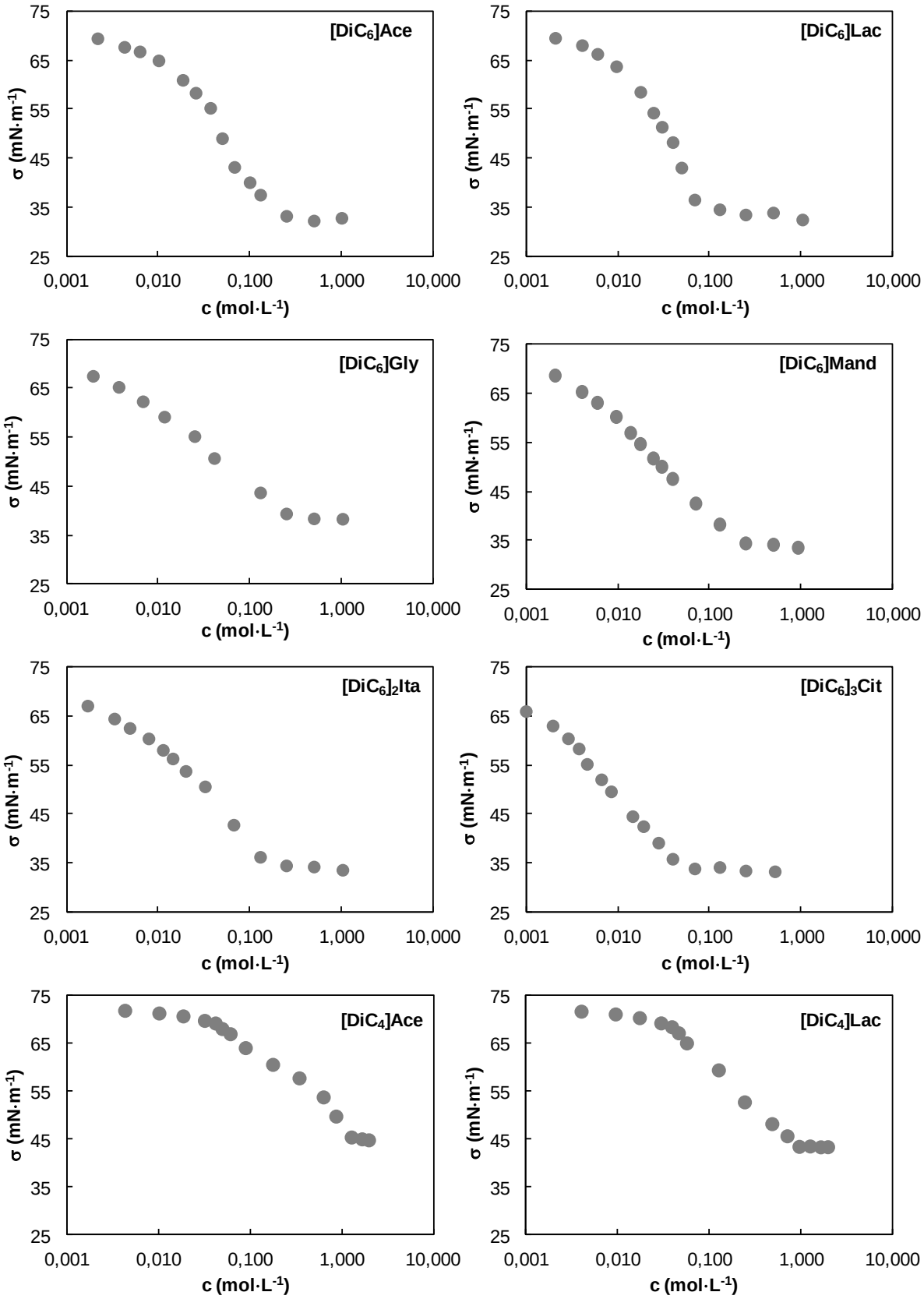
[DiC6]Ace
[DiC6]Lac
[DiC6]Gly
[DiC6]Mand
[DiC6]2Ita
[DiC6]3Cit
[DiC4]Ace
[DiC4]Lac
σ (mN·m-1)
c (mol·L-1)
75
65
55
45
35
25
0,001
0,010
0,100
1,000
10,000

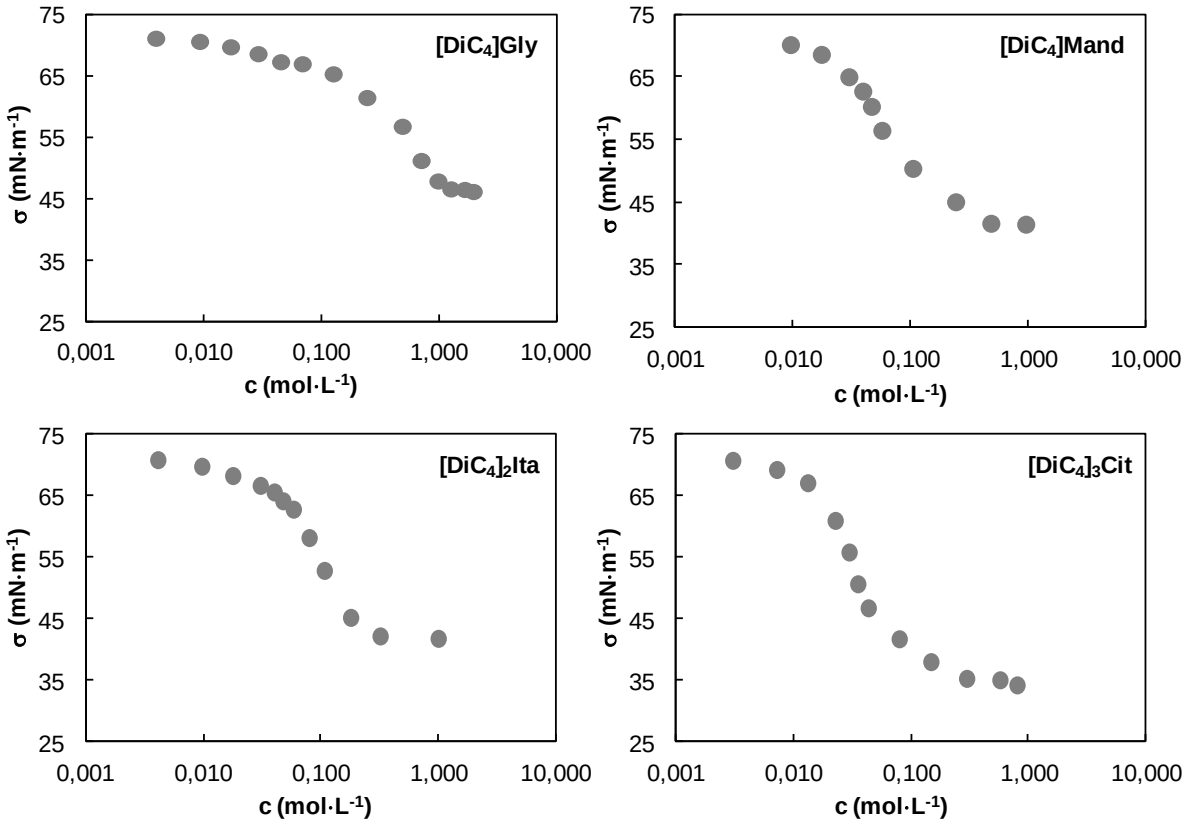

2.5) Hydrotropic behavior

The solubilization of the hydrophobic dye Disperse Red 13 was measured using a UV-visible spectrophotometer (Agilent Technologies Varian Cary 60). Therefore, aqueous stock solutions (ca 2 mol·L^{-1}) of ILs were prepared, and Disperse Red 13 was added in each solution until reaching saturation, *i.e.* until powder remained in suspension. The solutions were kept under stirring at 25 °C for 24 h. After this period of time, each solution was filtered to eliminate excess hydrophobic dye. The amount of Disperse Red 13 was determined by UV-visible absorption at 503 nm, hereby the absorbance should be in the range of 0.5 to 2. The solutions were diluted with milipore water. The concentration of Disperse Red 13 in aqueous hydrotrope solutions was detected by means of the calibration curve in ethanol:

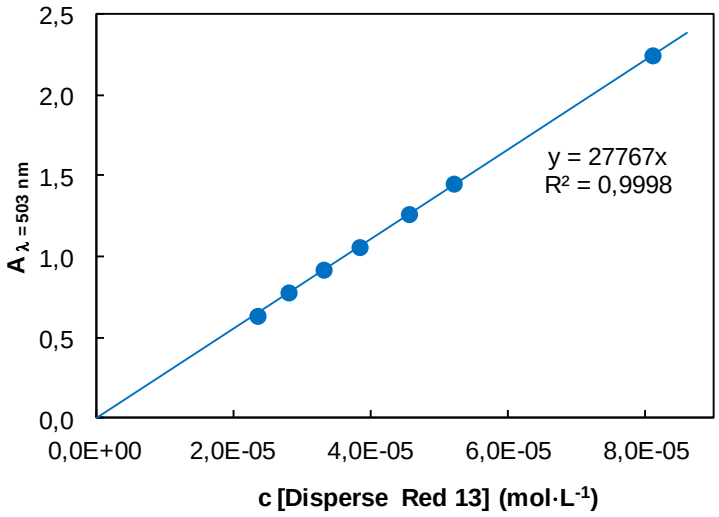

3.) Biodegradation

The Biodegradation tests were performed following the OECD 301F standard, which requires the biological oxygen consumption (BOC) and the theoretical oxygen demand (ThOD), as already described in ***section 2.4***. Thus, the percentage of biodegradation or biodegradability (% *B*) values could be calculated as ratio of BOC and ThOD.

The reliability of the experiment depends on 3 parameters. The first one is the degradation of the reference molecule (sodium acetate). Its degradation has to reach 60% after 14 days. Secondly, the mineral medium has to exhibit oxygen consumption below 60 mg·L^{-1} (ideally between 20 and 30 mg·L^{-1}) after 28 days. Finally, after 28 days, the pH should be between 6 and 8.5.[205] The resulting graphs of biodegradation as a function of time (up to 28 days) for all measured compounds are shown in **Figure 2.28**.

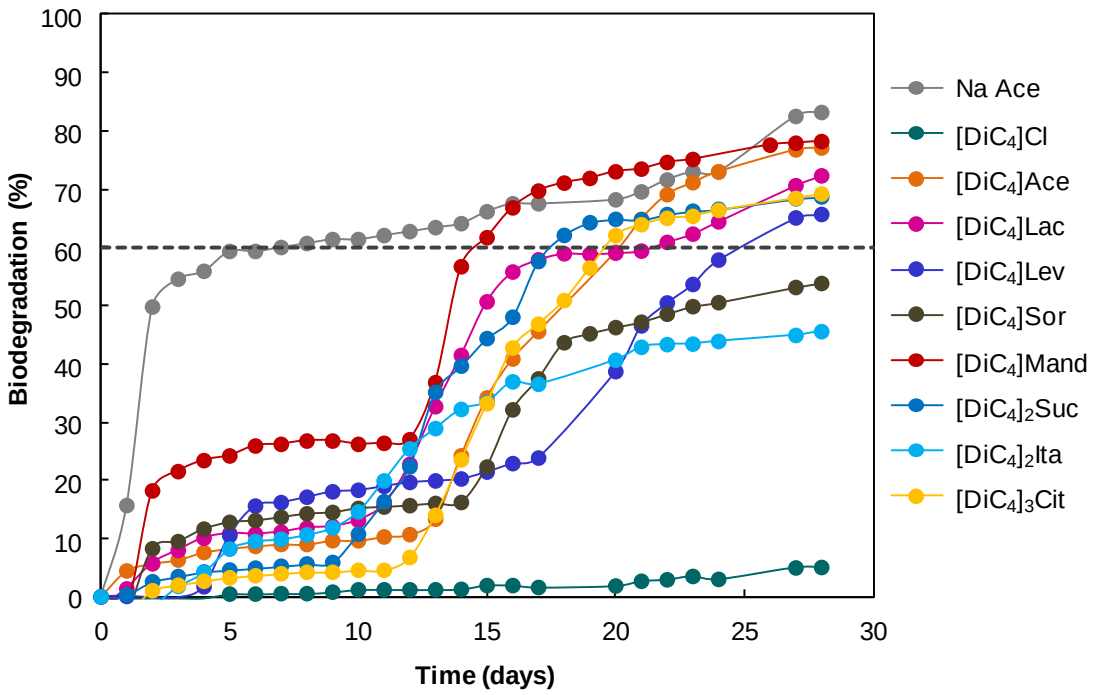

Figure 2.28 Biodegradation as a function of time of [DiC_4] carboxylate compounds, and sodium acetate as reference, during 28 days in the closed bottle test OECD 301F Standard.

4.) Solubilization of cellulose

4.1) Dissolution of cellulose

For the cellulose dissolution test, 1.5 g of IL (or mixture of the IL with a co-solvent or water) was first heated under stirring in a sealed glass vial at the desired temperature. Afterward, 2 wt% of cellulose AVICEL PH200 was added into the IL and the heating time was prolonged up to complete dissolution of cellulose was observed. When cellulose was completely dissolved, extra amounts of cellulose were then progressively added until the limit of solubility was reached. Cellulose has to be added progressively; otherwise the dissolution ability of ILs is inferior. If at least 2 wt% of cellulose was not dissolved within 10 h of heating, the IL was considered as not efficient.

4.2) Regeneration of cellulose (carried out by the group in Poitiers)

After complete dissolution of cellulose in the IL, cellulose was regenerated by addition of an anti-solvent, typically water, ethanol or acetone. 10 mL of the anti-solvent was added to the hot solution of IL (1.5 g) containing the dissolved cellulose. The regenerated cellulose was then filtered off and successively washed with water and acetone to remove residual ILs. Crystallinity and degree of polymerization of regenerated cellulose was then checked by XRD and FTIR analyses, respectively (Université de Poitiers).

4.3) Recycling of cellulose *(carried out by the group in Poitiers)*

After regeneration and filtration of cellulose, water was removed under reduced pressure. Then, the recovered IL was directly reused without any further purification using the same procedure as described above for dissolution experiments. Although tested ILs were recycled at least five times without appreciable decrease of their dissolution ability, we would like to point out that the long term recycling of ILs is more problematic like it is also observed with imidazolium derived ILs (accumulation of impurities stemming from the slight degradation of cellulose).

5.) Hansen solubility parameters

For the determination of the Hansen solubility parameters of ILs, solutions of the (10 wt%) in about 50 solvents (**Table 2.16**) have been prepared. After mixing the solutions for 24 h at RT, the samples have been left to rest for at least one hour, and the solubility has been evaluated visually. Therefore, a scale of three states was used: soluble, partially soluble or not soluble. The results were treated with the software HSPiP Edition 40.05 which gives the parameters for the tested product and its three-dimensional sphere of solubility.

Table 2.16 Solvents which have been used for the determination of Hansen parameters of ILs.

Solvent	Structure	M (g·mol^{-1})	Dipolar moment[a]
Water	H_2O	18.02	1.86
Methanol	CH_3OH	32.04	1.62
Ethanol	CH_3CH_2OH	46.07	1.55
1-Butanol	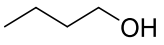	74.12	1.52
2-Ethylhexanol	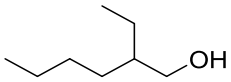	130.23	1.43
Ethylene glycol	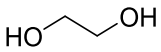	62.07	0.00
Propylene glycol	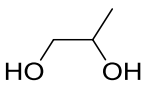	76.09	2.28
Glycerol	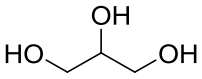	92.09	2.86
Tetraethylene glycol	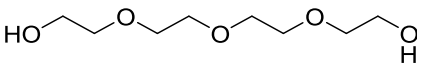	194.23	1.89
Geraniol	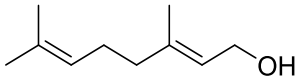	154.25	1.91
Methylal		76.09	2.83

Acetone		58.08	2.92
Acetic acid	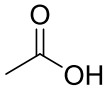	60.05	4.39
Ethyl lactate	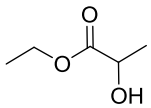	118.13	3.10
Acetic anhydride	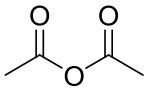	102.09	2.37
Triacetin	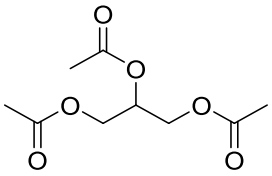	218.2	5.91
Isopropyl laurate	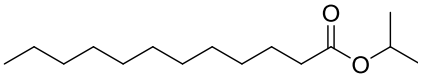	242.40	1.60
Methyl oleate	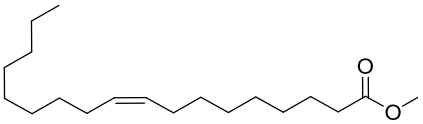	296.49	2.58
Chloroform	$CHCl_3$	153.82	1.16
Dicholoromethane	CH_2Cl_2	119.38	1.50
1-Chlorobutane	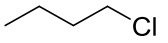	92.57	1.74
1-Bromohexane	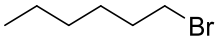	165.07	1.75
Paraffin oil	hydrocarbon mixture	14n+2	≈0.00
Acetonitrile	CH_3CN	410.50	2.89
Dipropylamine	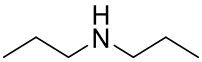	101.19	1.14
Dimethylformamide	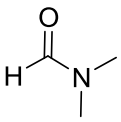	73.09	3.55
Nitroethane	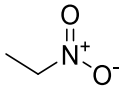	75.07	4.39
2-Nitropropane	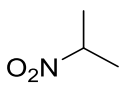	89.09	4.54
N,*N*-dimethyl decanamide	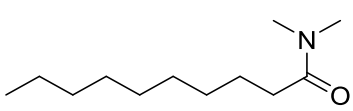	199.33	3.47

Carbon disulfide	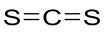	76.14	0.00
Dimethyl sulfoxide		78.13	5.75
Cyclohexane		84.16	0.00
Tetrahydrofuran		72.11	1.92
1,3 Dioxolane		74.08	1.33
1,4 Dioxane		88.11	0.00
Morpholine	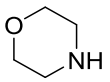	87.12	1.18
γ-Butyrolactone	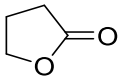	86.09	4.56
Propylene carbonate	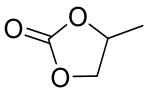	102.09	5.27
N-Metyl-2-pyrrolidine	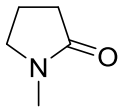	99.13	3.59
beta-Pinene	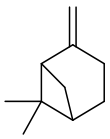	136.23	3.00
Isophorone	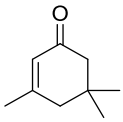	138.21	3.88
Toluene	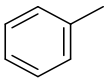	92.14	0.27
m-Xylene	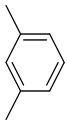	106.16	0.27
p-Xylene	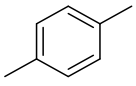	106.16	0.07
Pyridine		79.10	1.97
Benzyl alcohol	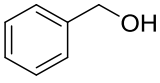	108.14	2.03

Anisole	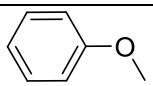	108.14	1.25
Dimethyl phthalate	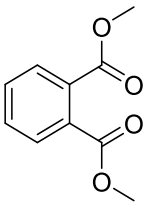	194.18	2.42
Tetralin	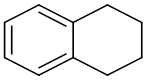	132.20	0.49

[a] The dipolar moments have been calculated with the software Spartan 08 V20 with the following parameters : theoretic semi-empiric method AM1, fundamental state, equilibrated geometry, zero charge, singular multiplicity.

CHAPTER 3 –Derivatives of choline, betaine and carnitine with biosourced carboxylate anions

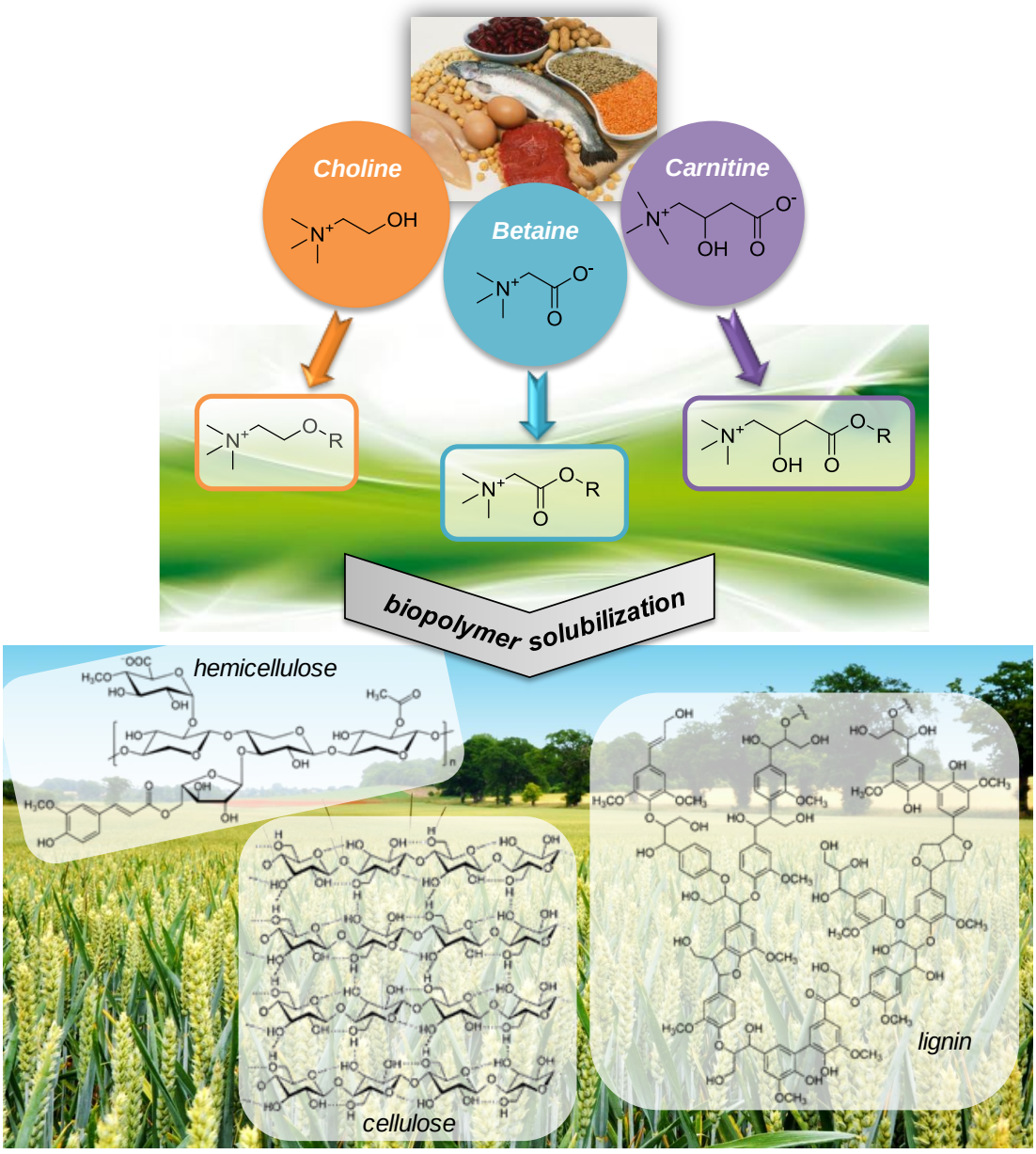

3.1 Introduction

Choline, betaine and carnitine are naturally resourced quaternary ammonium compounds which occur mainly in food, such as vegetables, eggs, milk, fish or meat.[229–231] Choline and betaine are structurally very similar, and choline is largely oxidized to betaine in the body.[232] These bio-based ammonium gain more and more interest for the design of "green" compounds. Mainly choline and its derivatives have already been used as cations for ILs. A survey of the literature combining "ionic liquid" with "choline", "betaine" or "carnitine" as keywords highlights the highest occurrence of choline-based ILs with around 600 related publications, as illustrated in **Figure 3.1** (the bibliometric analysis was carried out with the Scifinder® database, and it includes all documents such as scientific journals, patents, etc.). They are followed by ILs with betaine as cation with about 75 publications, and no publication was found for carnitine as IL cation.

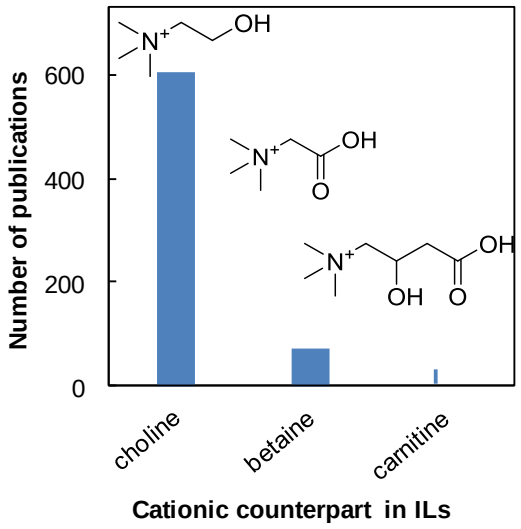

Figure 3.1 Number of publications dealing with "**ionic liquid**" for "**choline**", "**betaine**" or "**carnitine**" (analyzed with the Scifinder® database).

The choice of the compounds in this work was based on the detailed physicochemical study and the cellulose solubilization power of QACILs (see ***chapter 2***) which have been investigated on various chain lengths of the cation counterpart and various carboxylate counter anions. For QACILs, 15 different natural anions have been evaluated for cellulose solubilization resulting in **Lev, Ita, Ace, Suc, Lac** as the best ones. So, in this part of the work, only the most efficient anions have been retained.

For the cations, we focused on derivatives of choline, betaine and carnitine with the aim to obtain biocompatible and biosourced ILs. Compounds bearing an ester or an ether function, which allow the introduction of a short hydrophobic counterpart, was the main objective regarding the design of novel ILs. Thus, several **choline ethers**, **choline esters**, **betaine esters**

and **carnitine esters** were synthesized. This was also guided by the fact that esters are highly eco-friendly because their biodegradability and toxicity are optimized.[92,97] An overview of the different compounds is given in **Table 3.1**. The chain lengths of the ether- and ester-derivatives were varied from 1 to 8 carbon atoms with the aim to rationalize their structural impact on the IL properties and on cellulose solubilization. Based on the previous results obtained with QACILs (see ***chapter 2***), the focus was mainly placed on shorter chain lengths (ethyl, butyl, hexyl, octyl).

Table 3.1 Overview of ether- and ester-derivatives of choline, betaine and carnitine.

Choline		**Betaine**	**Carnitine**
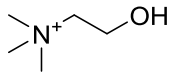		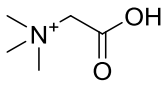	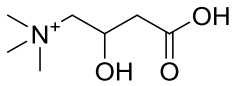
Cholineester (R= C_nH_{2n+1} with n = 1, 3, 5, 7)	**Cholineether** (R = C_nH_{2n+1} with n = 2, 4, 6, 8)	**Betaineester** (R = C_nH_{2n+1} with n = 2, 4, 6, 8)	**Carnitineester** (R = C_nH_{2n+1} with n = 2, 4, 6, 8)
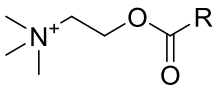	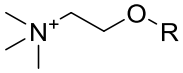	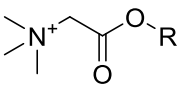	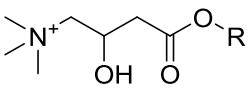

3.2 Choline derivatives

Cholinium has become a well-known natural quaternary ammonium cation for ILs. Especially in combination with biosourced counter anions, fully bio-based ILs could be obtained. As an example, Zicmanis *et al.* described biodegradable and non-toxic ILs based on (2-hydroxyethyl)ammonium carboxylates such as lactate.[233,234] Many ILs with cholinium as a cation have also been described in literature, as shown in **Figure 3.2**. Kunz *et al.* have reported cholinium oligoether carboxylates as task-specific ILs.[235] Cholinium with alkanoate counter anions or natural carboxylates, *e.g.* Ace, Gly, Fum, Suc, Mala, Tar, were described as ILs wholly composed of biomaterials, and have been studied because of their low toxicity and high biodegradability.[236,237] Some more publications describe the synthesis and the most important physicochemical properties of cholinium combined with simple carboxylates, tiglate or Male as anions.[238,239] A recent work on aqueous biphasic systems with cholinium ILs and biosourced anions (*e.g.* Ace, Lev, Gly, Suc, Sal, glutarate) for the partitioning of antibiotics has been published by Freire *et al.*[240] Furthermore, amino acid anions (*e.g.* glycine, alanine, valine, leucine, serine, etc.) have been used as counter anions to create biosourced ILs with cholinium as a cation.[241,242]

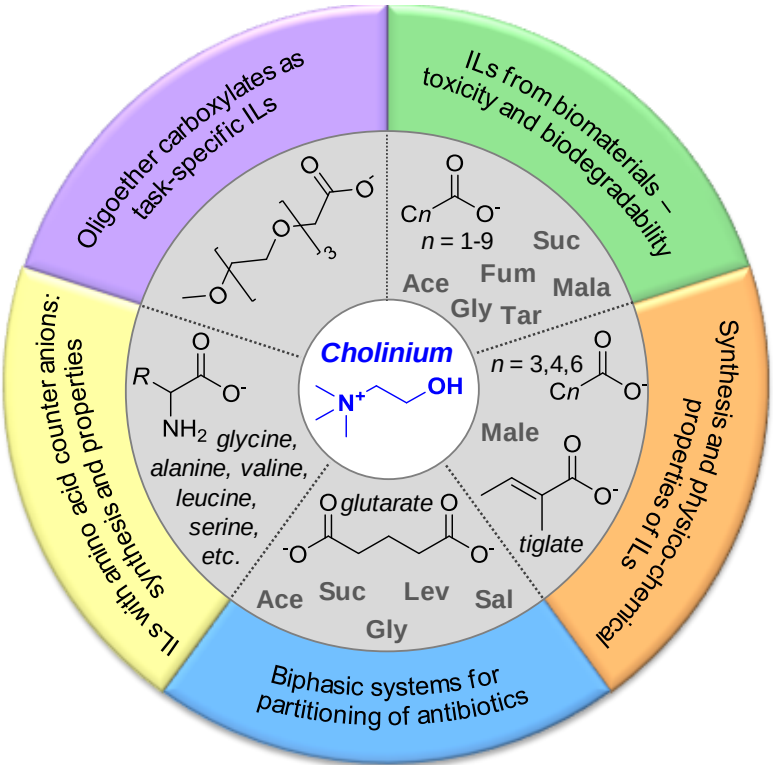

Figure 3.2 Cholinium-based ILs with different counter-anions reported in literature.

Up to now, choline-derivatives have not often been used for IL formation. There is one well-known example in literature using alkoxymethyl(2-hydroxyethyl)dimethylammonium as a

cation combined with acesulfamate or bis(trifluoromethylsulfonyl)imide (**Figure 3.3**).[105] Their physical properties, such as density, viscosity, water solubility and thermal stability were determined. The antimicrobial (cocci, rods, fungi) activities of hydrophilic acesulfamate ILs were measured, and some were found to be active. These new ILs were proposed for the application as insect feeding deterrents. The choline-derivative ILs with bis(trifluoromethylsulfonyl)imide anion were described for applications as fixatives for soft tissues and furthermore for the use as substitutes for formalin and preservatives for blood.

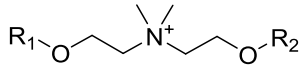

(a) R_1 = H, R_2 = from C_2H_5 to $C_{14}H_{29}$

(b) R_1 = acetyl, R_2 = from C_2H_5 to $C_{14}H_{29}$ and *c*-$C_{12}H_{23}$

(c) R_1 = C_9H_{19}, R_2 = from C_2H_5 to $C_{12}H_{25}$ and *c*-$C_{12}H_{23}$

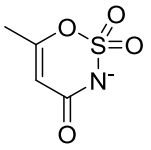

$(CF_3SO_2)_2N^-$

Figure 3.3 Structure of choline-derivative cations for ILs combined with the anions acesulfamate or bis(trifluoromethylsulfonyl)imide.

3.2.1 Preparation of ester- and ether-derivatives of choline

3.2.1.1 Choline ester compounds

Choline ester derivatives have been synthesized by esterification of the commercially available choline chloride with acyl chlorides (**Figure 3.4**). After testing other reaction pathways without success (esterification of choline chloride with acetic anhydride), choline ester chlorides (R = C_nH_{2n+1} with n = 1, 3, 5, 7) were obtained successfully *via* the reaction of acyl chlorides and choline chloride in dichloromethane under reflux. More details on the synthesis as well as ^{1}H- and ^{13}C-NMR-analysis are given in the ***experimental section***.

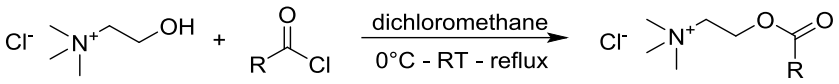

Figure 3.4 Synthesis of choline ester; R = C_nH_{2n+1} with n = 1, 3, 5, 7.

Unfortunately, the exchange of the anion *via* an exchange resin was not possible due to the highly acid- and base-sensitive ester-function which hydrolyzed.

Another method for anion exchange using silver(I) oxide Ag_2O and a corresponding carboxylic acid (**Figure 3.5**) under formation of silver chloride as precipitate.[243]

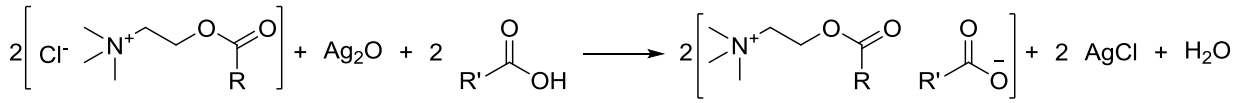

Figure 3.5 Anion exchange for choline ester compounds with silver(I) oxide.

This anion exchange method is a good alternative for ester derivatives, but it is relatively expensive. Furthermore, as time was a limiting factor in this study, and the choline esters were not the most promising products, we decided to set our priorities on more pertinent products.

3.2.1.2 Choline ether compounds

The direct etherification of choline chloride is not evident as pathway for the synthesis of choline ethers because of the low reactivity of the hydroxyl group based on the inductive electron-withdrawing effect of the quaternary ammonium. First, the dehydration of alcohols, more precisely the reaction of choline chloride with a primary alcohol catalyzed by sulfuric acid, was tested. However, this route is more adapted for generating symmetrical ethers due to the different reactivity for dissimilar alcohols. Secondly, the Williamson ether synthesis (reaction of an alcohol with an organohalide catalyzed by a strong base) was attempted, but this route was without success as well.

So, we used the way of an etherification of a chloroalkane with an alcoholate followed by the quaternization of the amine with iodomethane (**Figure 3.6**). The alcoholate was obtained by reaction of the corresponding alcohol with sodium. The second step was directly carried out by addition of 2-chloro-*N*,*N*-dimethylethylamine to the cooled mixture. This reaction was then heated under reflux for one night. For the isolation of the ether-functionalized tertiary amine, different methods were used depending on the chain-length R. For the longer ones (R = hexyl, octyl), the ether-functionalized tertiary amine has been protonated with hydrochloric acid and extracted in the aqueous phase (separation from hexanol or octanol). When this aqueous phase was neutralized with an aqueous sodium hydroxide solution, an organic phase, the pure product, was formed. For the short chain products (R = ethyl, butyl), the alcohols are miscible with water, thus such an extraction is not possible. Here, the alcohol and the ether-functionalized tertiary amine are separated by distillation at atmospheric pressure.

In the last reaction step, the ether-functionalized tertiary amine was quaternized with iodomethane in acetonitrile at room temperature for 24 h. After evaporation of the solvent, the crude product was washed several times with diethyl ether and dried over vacuum.

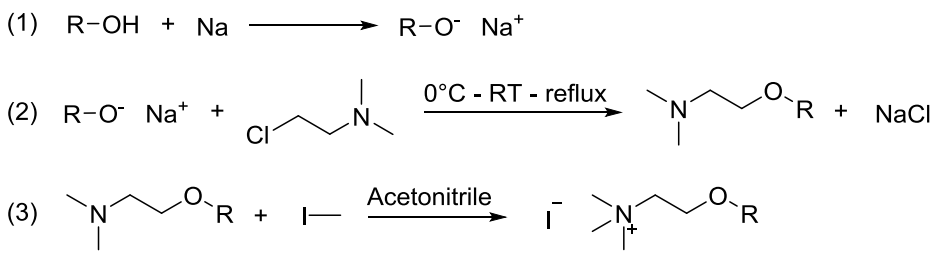

Figure 3.6. Synthesis of choline ether compounds in three steps: 1.) Formation of an alcoholate with sodium, 2.) Etherification of a chloroalkane with an alcoholate, 3.) Quaternarization of a tertiary amine with iodomethane; R = C_nH_{2n+1} with n= 2, 4, 6, 8.

To obtain the choline ether carboxylate ILs with naturally-based carboxylate counter-anions, the anion exchange was carried out with an exchange resin (Amberlite® IRA-400(Cl)), as already described in ***Chapter 2*** for classical quaternary ammonium compounds. We have chosen the anions which were the most efficient for cellulose dissolution in combination with quaternary ammonium cations, *i.e.* **Cl**, **Ace**, **Lac**, **Lev**, **Ita** and **Suc**.

After the anion exchange, water was then removed by lyophilization of the synthesized ILs using a freeze dryer for at least 72 h. Residual water content was determined with a coulometric Karl-Fischer titration. The obtained compounds are very hygroscopic, as QACILs. Moreover, some of them contain water in their structure, as crystallization water. Thus, the **choline ether carboxylate** compounds can contain water between 0.2 for *e.g.* [C_4-Chol]I until 4.2 wt% for *e.g.* [C_2-Chol]Ace (details are given in the ***experimental section***), even after freeze drying for several days. This is an important point since residual water can modify the physicochemical properties of the compounds, especially its behavior as an IL. This is a recurrent problem for these compounds which have many times been pointed out in the literature. It is nevertheless important to determine this "water impurity" and to be aware of it. Thus, before determining their physicochemical properties, the **choline ether carboxylates** have been dried as much as possible and stored under an atmosphere of argon. The purity of the synthesized products was confirmed by ^{1}H- and ^{13}-C-NMR. The anion exchange was followed by pH-control with a pH-meter, and the good agreement between integrations of the cation and of the anion in the ^{1}H-NMR spectrum of the final products was a proof of the total anion exchange.

Table 3.2 Choline ether compounds and their abbreviations for cations and anions.

Cations		
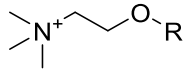		
R = C_nH_{2n+1} with n = 2, 4, 6, 8: **[C_n-Chol]**		
Anions		
Cl^-		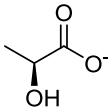
Chloride (**Cl**)	Acetate (**Ace**)	Lactate (**Lac**)
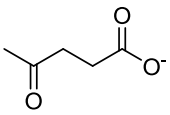	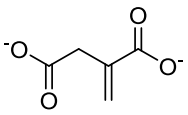	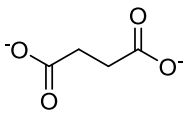
Levulinate (**Lev**)	Itaconate (**Ita**)	Succinate (**Suc**)

The chemical structures of the choline ether cations and carboxylate anions as well as their abbreviations are given in **Table 3.2**. The ^{1}H- and ^{13}C-NMR data of the 28 synthesized **choline ether carboxylates** are detailed in the ***experimental section*** of this chapter.

3.2.2 Physicochemical properties of the pure ILs

The physicochemical properties of choline derivatives have been studied, such as thermal stability, thermal phase transitions, and viscosity. In this section, we have mainly focused on ether compounds because they appear more promising regarding their potentialities regarding possible applications.

3.2.2.1 Thermal analysis

The most important thermal properties of the synthesized choline ether halogenide and carboxylate ILs have been studied (**Table 3.3**). The thermal stability (degradation temperature T_{deg}) has been assessed by thermogravimetric analysis (TGA) and the phase transitions, such as melting temperature T_m and glass transition temperature T_g, have been determined by differential scanning calorimetry (DSC). The graphs of TGA- and DSC-measurements for each product are shown in the ***experimental section***.

Roughly speaking, the T_{deg} of choline ether compounds depends more on the cation than on the anion. Indeed, T_{deg} is only slightly affected by the variation of the alkyl chain length of the cation. Even if the differences are not significant, a general trend for a same anion combined with different alkyl chain length choline ether cations can be highlighted : T_{deg} (ethyl) >T_{deg} (butyl) >T_{deg} (hexyl) >T_{deg} (octyl). As far as anions are concerned, the higher stability of halogenide compounds (I, Cl) compared to carboxylate ones (Ace, Lac, Lev, Suc, Ita) is noteworthy, as already found for QACILs in ***Chapter 2***.

Table 3.3 Thermal properties, namely degradation temperature T_{deg}, glass transition temperature T_g, melting temperature T_m, of choline ether compounds.

Cation	State at RT	T_{deg} (°C)	T_g (°C)	T_m (°C)	DSC-behavior[a]
		Iodide			
[C_2-Chol]	yellow powder	178	/	157.5	I
[C_4-Chol]	yellow powder	178	/	70.7	I
[C_6-Chol]	yellow powder	177	/	77.2	I
[C_8-Chol]	yellow powder	171	/	93.6	I
		Chloride			
[C_2-Chol]	white powder	189	/	103.9	I

[C_4-Chol]	white powder	188	/	51.0	I
[C_6-Chol]	white powder	188	/	42.5	I
[C_8-Chol]	white powder	189	/	60.3	I
Acetate					
[C_2-Chol]	yellow liquid	142	-72.2	/	II
[C_4-Chol]	colorless liquid	141	/	/	IV
[C_6-Chol]	colorless liquid	136	/	/	IV
[C_8-Chol]	colorless liquid	135	/	12.6	I
Lactate					
[C_2-Chol]	colorless liquid	154	-66.4	/	II
[C_4-Chol]	colorless liquid	156	-65.3	/	II
[C_6-Chol]	colorless liquid	149	-67.6	/	II
[C_8-Chol]	colorless liquid	144	-62.4	-11.0	V
Levulinate					
[C_2-Chol]	yellow liquid	141	-67.6	16.6	III
[C_4-Chol]	yellow liquid	141	-64.3	/	II
[C_6-Chol]	yellow liquid	139	/	14.9	I
[C_8-Chol]	yellow liquid	139	/	/	IV
Succinate					
[C_2-Chol]	yellow liquid	147	-46.8	/	II
[C_4-Chol]	colorless liquid	145	-58.8	/	II
[C_6-Chol]	colorless paste	146	-51.2	33.6	V
[C_8-Chol]	white powder	141	-56.1	65.4	V
Itaconate					
[C_2-Chol]	brown liquid	152	-48.8	/	II
[C_4-Chol]	lightly yellow liquid	149	-54.0	-30.2	III
[C_6-Chol]	white paste	146	/	16.9	I
[C_8-Chol]	white paste	145	-44.5	24.8	V

[a] **Group I**: classical crystallization of salts; **Group II**: only glass transition; **Group III**: with cold crystallization; **Group IV**: no transition; **Group V**: low glass transition and melting point

For the DSC behavior of the choline ether compounds, the same classification as already defined in ***Chapter 2*** for QACILs (**Group I – IV**) has been used with a further group of behavior (**Group V**) which shows a low glass transition and an additional melting phase transition. Regarding thermal phase transitions, choline ether halogenides (I, Cl) exhibit only melting temperatures

T_m, which indicates a classic crystallization behavior of salts.[175] **[C$_2$-Chol]** with I or Cl as counter anions show much higher T_m than their homologues with longer alkyl chains. This unexpected behavior could be explained by a much higher order of structuration, thus a higher organization in the crystalline state for the ethyl-choline ether compounds than for the ones with longer chains. The choline ether carboxylates show all the different behaviors of thermal transitions. The classic crystallization process (**group I**) has been observed for **[C$_8$-Chol]Ace**, **[C$_6$-Chol]Lev** and **[C$_6$-Chol]$_2$Ita**. The following ILs showed only a glass transition (**group II**) which is the most common behavior for ILs: **[C$_2$-Chol]Ace**, **[C$_2$-Chol]Lac**, **[C$_4$-Chol]Lac**, **[C$_2$-Chol]Lac**, **[C$_4$-Chol]Lev**, **[C$_2$-Chol]$_2$Suc**, **[C$_2$-Chol]$_4$Suc**, and **[C$_2$-Chol]$_2$Ita**. The third type of DSC behavior is characterized by a cold crystallization between the glass transition and the melting point on heating (**group III**), which was found for **[C$_2$-Chol]Lev** and **[C$_4$-Chol]$_2$Ita**. Some of the studied choline ether carboxylates hold DSC thermograms without any phase transition (**group IV**), *e.g.* **[C$_4$-Chol]Ace**, **[C$_6$-Chol]Ace**, and **[C$_8$-Chol]Lev**. For some choline ether carboxylates we have found a further DSC behavior which shows a low glass transition and also a melting temperature (**group V**). This behavior was determined for **[C$_8$-Chol]Lac**, **[C$_6$-Chol]$_2$Suc**, **[C$_8$-Chol]$_2$Suc** and **[C$_8$-Chol]$_2$Ita**, thus only for longer-chain compounds.

3.2.2.2 Viscosity

We have measured the dynamic viscosity η of choline ether levulinates with an ethyl-, butyl-, hexyl- or octyl-chain at different temperatures. The temperature dependence of viscosity was investigated over a temperature range of 25 to 80 °C for the different choline-derived ILs, as shown in **Figure 3.7**.

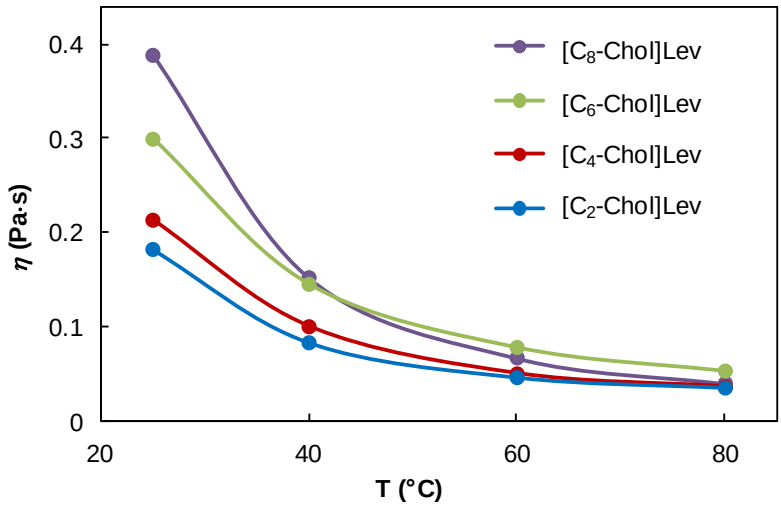

Figure 3.7 Temperature dependence of the dynamic viscosity η for levulinate ILs with different cations: [C$_n$-Chol] with n = 2, 4, 6, 8.

The examined viscosities decrease with increasing temperature due to the higher mobility of molecules or ions at higher temperatures.[244,245] In general, the viscosity of the more viscous compounds decreases more rapidly with increasing temperature. The viscosity of ILs depends on ion-ion interactions, such as van der Waals interactions and hydrogen bonding, with greater interactions leading to higher viscosities.[42] As already described in literature, the viscosity of ILs with the same anion increases with increasing alkyl-chain lengths of the cation due to stronger can der Waals interactions.[52] In our case, we found higher viscosities with increasing chain lengths from ethyl to octyl, at RT.

To situate the viscosity η of choline ether levulinate ILs, [C_n-Chol]Lev with n = 2, 4, 6, 8, the comparison with liquids (like maple syrup or motor oil) and well-known imidazolium ILs, *e.g.* [BMIm]BF_4, [BMIm]PF_6, [$CH_3CH(OH)CH_2$MIm]NTf_2, [HMIm]PF_6,[246] is illustrated in **Figure 3.8**.

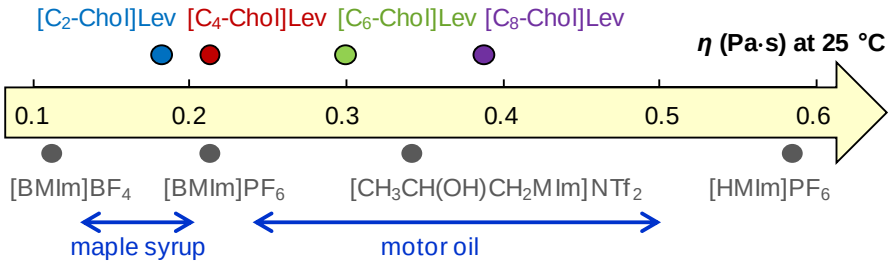

Figure 3.8 Comparison of the dynamic viscosity η for choline ether levulinate ILs with classical liquids.

3.3 Betaine derivatives

Betaine (also known as *N*,*N*,*N*-trimethyl glycine or glycine betaine) is a natural-sourced quaternary ammonium compound which is mainly present in meat, plants and microorganisms.[230] As betaine is biosourced and biodegradable,[247] this natural quaternary ammonium compound is highly interesting for the design of "green" ILs or surfactants.

The [Bet]Tf_2N ionic liquid which is composed of the protonated betaine, called betainium, as the cation and bis(trifluoromethylsulfonyl)imide as the anion has already been reported for various studies (structure in **Figure 3.9.a**). It has mainly been used for the extraction of different metals, such as palladium, rhodium and rhutenium,[248] uranium,[249] neptunium,[250] or indium and gallium.[251] Another study about [Bet]Tf_2N deals with its radiation stability of RTILs with view to electrochemical applications.[252] Furthermore, the thermo-chemical properties of this IL has been published.[253]

Another study on metal ion extraction (*e.g.* copper) was done with ILs composed of a cationic ester derivative of betaine, namely tributyl(2-ethoxy-2-oxoethyl)ammonium, and the anions [Tf_2N] or dicyanamide [Dca], as shown in **Figure 3.9.b**.[254]

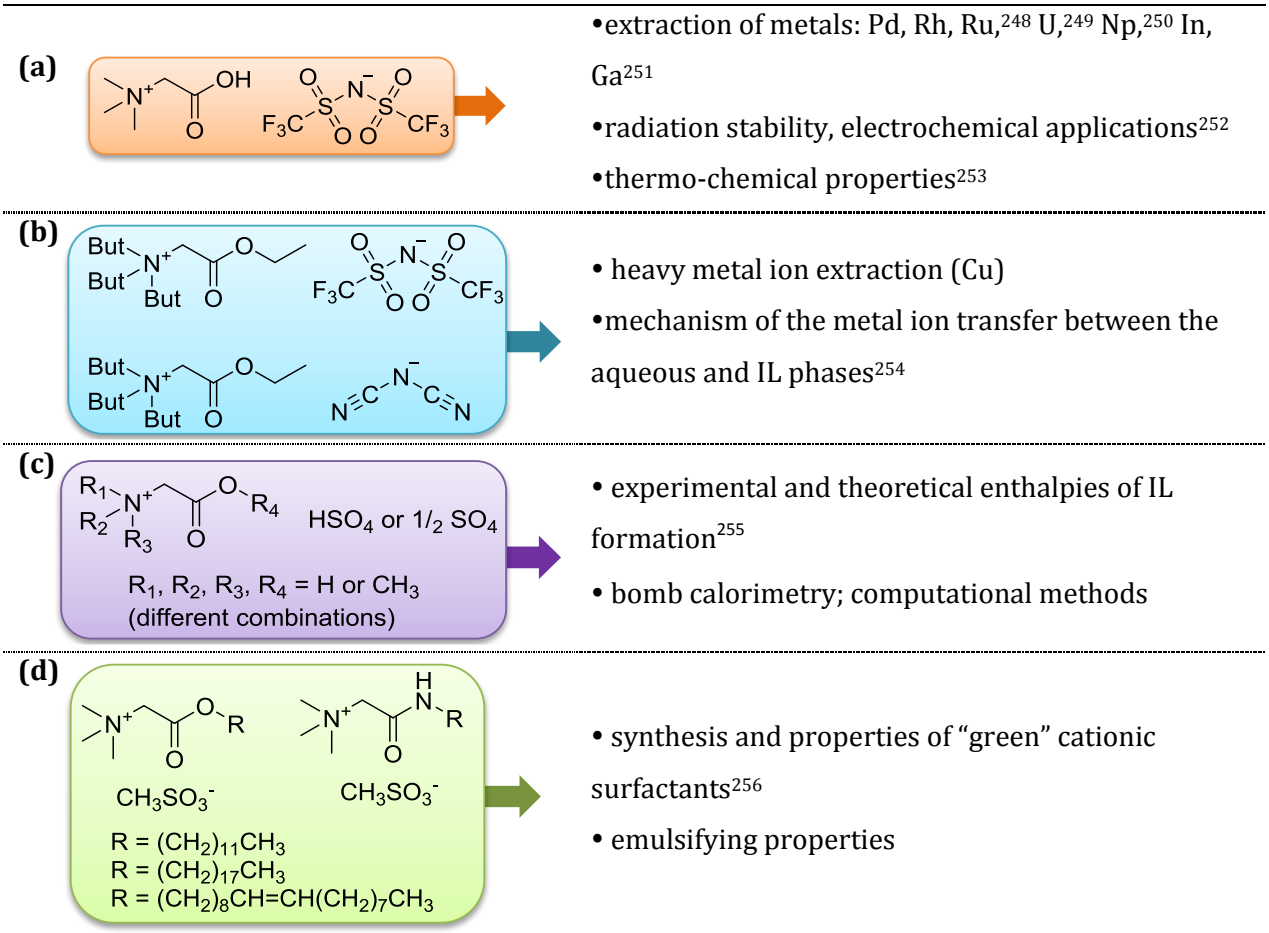

Figure 3.9 ILs or surfactants based on betaine or betaine derivatives reported in the literature.

A study of the enthalpies of formation of ILs based on ester-derivatives of betaine combined with sulfate or bisulfate has also been reported by Tao *et al.* (**Figure 3.9.c**).[255] The authors used both experimental (bomb calorimetry) and theoretical (quantum chemistry calculation using the Gaussian03 suite of programs) methods giving results which agreed well. Longer alkyl chain betaine-derived esters and amides claimed as "green" cationic surfactants has also been reported, and their emulsifying properties have been studied evaluating their application potential (**Figure 3.9.d**).[256]

In this work, a series betaine esters based on natural cations and biosourced carboxylate anions have been prepared and studied with the aim of designing novel biocompatible ILs for biopolymer solubilization. Based on the results of the detailed study on QACILs, initially chosen as model compounds (***Chapter 2***), we focused in this part on small short-chain IL cations, namely alkyl betaine ester with ethyl-, butyl-, hexyl- and octyl-chains as side chains. Only levulinate was used as a carboxylate counter anion, as we had enormous difficulties to find a suitable method for the anion exchange of ester compounds, which are readily hydrolyzed under acidic or alkaline conditions. The choice for levulinate as the anion counter part for further investigation with betaine was made in the light of the promising results obtained regarding the high rate if of cellulose solubilization when this anion was combined with some QACILs.

3.3.1 Preparation of betaine esters

The betaine esters have been synthesized *via* the reaction of betaine with 1-bromoalkanes (R = $C_nH_{2n+1}$with n = 2, 4, 6, 8) in acetonitrile under reflux (**Figure 3.10**). The cations are abbreviated as **[C_n-Bet]**. Betaine (1 equiv.) has been mixed with 1-bromoalkane (1.5 equiv.) under inert conditions before heating under reflux for at least one night. After evaporation of the solvent, the crude product was washed several times with diethyl ether, and dried under vacuum. More details as well as ^{1}H- and ^{13}C-NMR data are given in the ***experimental section*** of this chapter.

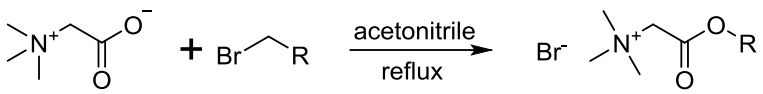

Figure 3.10 Synthesis of betaine ester bromide with R = C_nH_{2n+1} with n = 2, 4, 6, 8.

Because of the acid- and base-sensitive ester-function, the anion exchange with an exchange resin was not successful. Therefore, the method with silver(I) oxide and a corresponding carboxylic acid was used (**Figure 3.11**).[243]

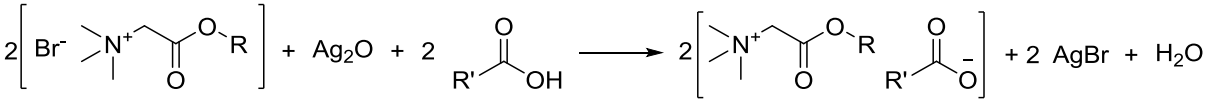

Figure 3.11 Anion exchange for betaine ester compounds with silver(I) oxide.

As this method is relatively expensive and additionally, time was a limiting factor, we decided to do the exchange only with **Lev** as anion and only for the shortest cations, *i.e.* **[C_2-Bet]** and **[C_4-Bet]**, expected to be the most promising compounds.

3.3.2 Thermal properties of betaine esters

In order to assess the interest of the betaine esters as novel ILs, their thermal stability as well as thermal phase transitions have been investigated.

All of the betaine ester bromides with different alkyl-chain lengths (ethyl, butyl, hexyl, octyl) are white powders at RT. Their degradation temperature T_{deg} was analyzed by TGA (**Table 3.4** and **Figure 3.12**) showing that the thermal stability decreases with increasing alkyl-chain length of the betaine ester cation.

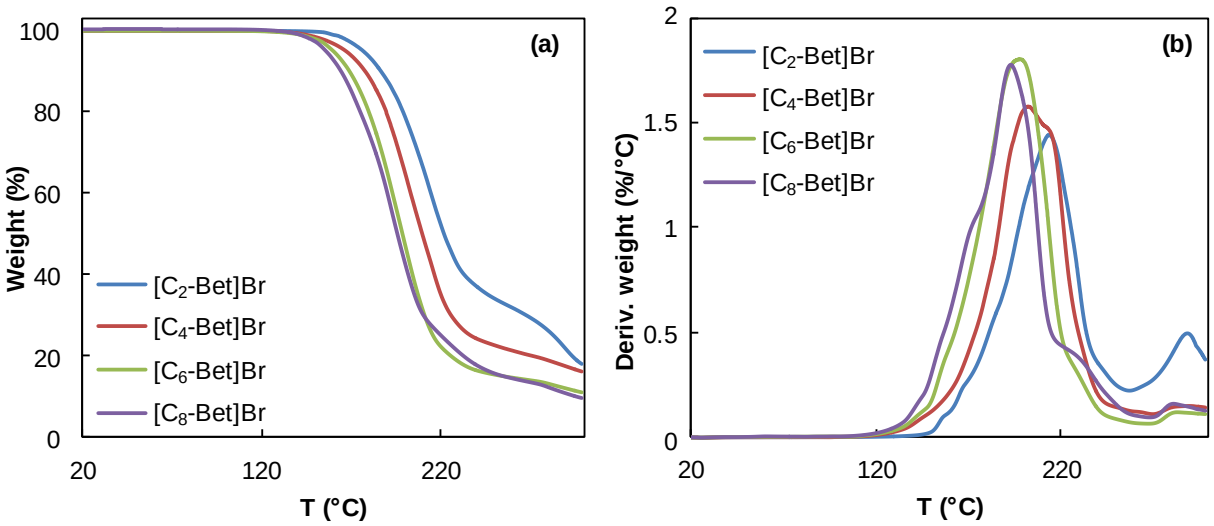

Figure 3.12 TGA-curves of betaine ester bromides (ethyl, butyl, hexyl, octyl): **(a)** weight percent as a function of temperature, **(b)** derivative weight percent as a function of temperature.

During the thermal analysis by DSC, all of the betaine ester bromides exhibited only melting temperatures T_m (as onset of an endothermic peak on heating), **Table 3.4**. The melting temperature of ethyl-betaine ester bromide of 158 °C is much higher than the other ones (between 94 and 110 °C). A same result has already been obtained with choline ether iodides

and chlorides (***section 3.2.2.1***). This phenomenon could be explained by a stronger organization of the molecular structure with a very short chain, such as ethyl. However, for betaine esters with longer alkyl side chains (butyl, hexyl, octyl), no clear tendency of T_m could be identified.

Table 3.4 Degradation temperature T_{deg}, melting temperature T_m and glass transition T_g of betaine ester compounds.

Compound	T_{deg} (°C)	T_g(°C)	T_m(°C)
[C_2-Bet]Br	149	/	158
[C_4-Bet]Br	131	/	100
[C_6-Bet]Br	128	/	110
[C_8-Bet]Br	127	/	94
[C_2-Bet]Lev	124	/	/
[C_4-Bet]Lev	120	/	/

The betaine-derivatives with Lev as a counter anion show lower thermal stability than their bromide homologues, *e.g.* 124 °C for **[C_2-Bet]Lev** compared to 149 °C for **[C_2-Bet]Br**, and 120 °C for **[C_4-Bet]Lev** compared to 131 °C for **[C_4-Bet]Br**. Both betaine ester Lev have no thermal transition (**Table 3.4**) on DSC-measurements. The graphs of TGA- and DSC-measurements are given in the ***experimental section*** of this chapter.

3.3.3 Aqueous phase behavior of betaine esters

As all these compounds exhibit an amphiphilic structure, their self-aggregation behavior in aqueous solution was studied by measuring the surface tensions and their ability to solubilize hydrophobic solutes at RT and neutral pH.

3.3.3.1 Minimal aggregation concentration (MAC) of betaine esters

The study of surface tensions σ of aqueous IL solutions gives information about the self-assembly properties due to the amphiphilic character of ILs, as already explained in detail in ***chapter 2***. The surface tensions of binary mixtures of betaine ester bromides and water containing increasing concentrations have been measured. The maximal concentration for aqueous surface tension measurements was fixed at a reasonable value of 2 mol·L^{-1} in order to not consume too much product.

Figure 3.13 shows the results for **[C_n-Bet]Br** with n = 2, 4, 6, 8. The curves of betaine ester with longer chain lengths, *i.e.* hexyl and octyl, have a distinctive form with the characteristic plateau when aggregation formation occurs. The determined MAC values are low, namely 0.04 mol·L^{-1} for **[C_8-Bet]Br** and 0.32 mol·L^{-1} for **[C_6-Bet]Br** (**Table 3.5**) indicating a well self-assembling

behavior which is characteristic for amphiphilic compounds. Compared to this result, some betaine ester surfactants with longer alkyl side chains have been reported with very low critical micelle concentration values: 1.2 mmol·L^{-1} for [C_{12}-Bet]CH_3SO_3 and 0.794 mmol·L^{-1} for [C_{18}-Bet]CH_3SO_3.[256] However, the surface tension curves of betaine ester bomides with shorter chain lengths, *i.e.* butyl and ethyl, have shapes with less significant plateaus which point to a reduced ability for self-organization due to their modest amphiphilic character. Thus, the MAC values for **[C_4-Bet]Br** (1.27 mol·L^{-1}) and **[C_2-Bet]Br** (1.71 mol·L^{-1}) are rather high based on their reduced amount of amphiphilic character (**Table 3.5**). As a result, the MAC and the σ_{MAC} for betaine ester bromides shows the following order: **[C_8-Bet] < [C_6-Bet] < [C_4-Bet] < [C_2-Bet],** as expected. The values for σ_{MAC} were relatively high (35 – 48 m·Nm^{-1}), which is typical for hydrotropes.[257] In comparison, the reduction σ with classical surfactants is much more pronounced, such as 20 – 25 m·Nm^{-1} for sodium dodecylsulfate (SDS). By the way, it should be noted that there is no dip in the surface tension curves, which is an indirect confirmation of the absence of impurities, having also an amphiphilic character.

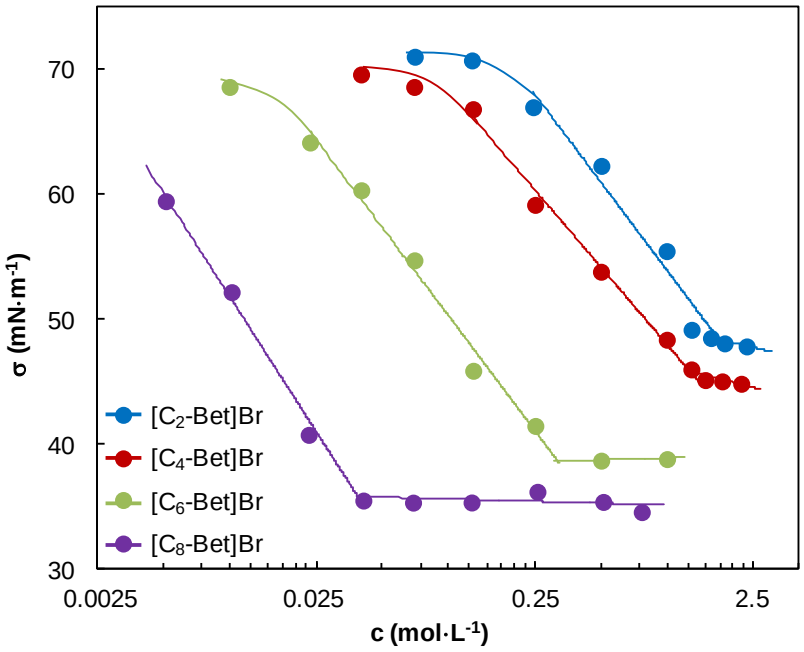

Figure 3.13 Surface tension σ as a function of alkyl-betaine ester bromide [C_n-Bet]Br with n = 2, 4, 6, 8 concentration in aqueous solutions at RT.

Table 3.5 Minimal aggregation concentrations (MACs) with corresponding surface tensions (σ_{MAC}) of alkyl-betaine ester bromides.

Br	**[C_2-Bet]**	**[C_4-Bet]**	**[C_6-Bet]**	**[C_8-Bet]**
MAC (mol·L^{-1})	1.71	1.27	0.32	0.04
σ_{MAC} (mN·m^{-1})	47.9	45.2	38.8	35.3

3.3.3.2 Hydrotropic solubilization capacity of betaine esters

Theoretical considerations regarding hydrotropes as well as details on the experimental procedure have been described previously in ***chapter 2***. The hydrotropic behavior of betaine ester bromides with different alkyl chain lengths was investigated by means of the solubilization of the hydrophobic dye Disperse Red 13 in aqueous solutions, and the results are shown in **Figure 3.14**. The comparison of betaine ester bromides with ethyl-, butyl-, hexyl- and octyl-chains shows the following trend for their hydrotropic solubilization capacity: **[C_6-Bet] > [C_4-Bet] > [C_2-Bet]**. This tendency, which is the same as the MAC values (see above), is based on their amphiphilic character which augments with increasing chain length of the betaine ester cation. **[C_2-Bet]Br** shows even no effectiveness as hydrotrope due to its very polar structure and thus its lack of amphiphilicity.

However, for **[C_8-Bet]Br** this analysis was not realizable because no clear-colored solution was obtained which is measurable with UV/visible spectroscopy. Several different concentrations have been prepared, but all the mixtures with Disperse Red 13 resulted in a kind of trouble darkly-colored solution which seems to be an emulsion. Even centrifugation has not destroyed this structuration. Apparently, **[C_8-Bet]Br** has a stronger surface active effect which effects micellar solubilization with bigger aggregates (whitish trouble solution) compared to the shorter chain betaine esters which result in small aggregates, and thus transparent solutions.

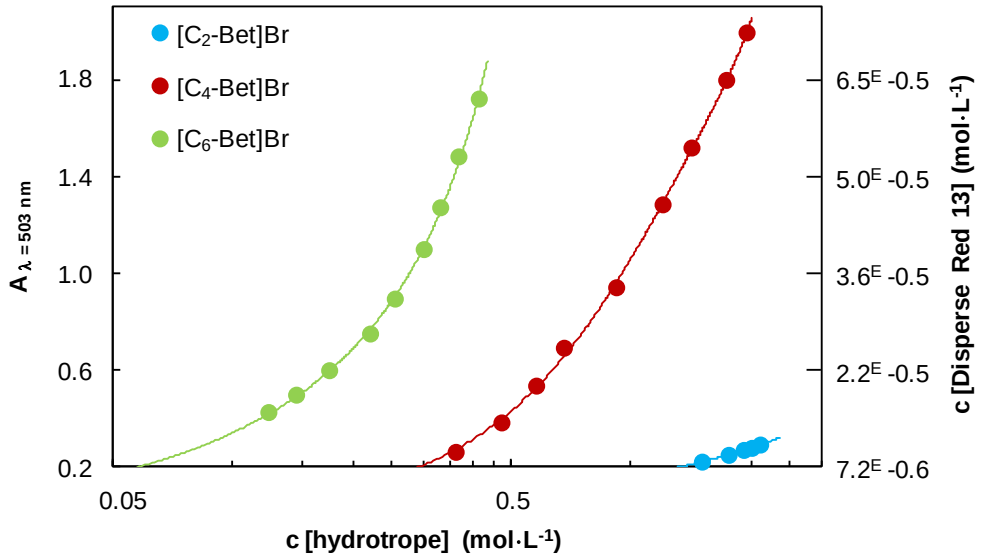

Figure 3.14 Solubilization of Disperse Red 13 measured by UV/visible spectroscopy at λ = 503 nm, in aqueous solutions of betaine ester bromides. For [C_8-Bet]Br, the measurement could not be performed due to formation of a whitish solution.

3.4 Carnitine derivatives

Carnitine, which is also called 3-hydroxy-4-*N*-trimethylammoniobutanoate, is another relevant naturally sourced quaternary ammonium compound.[258] Carnitine occurs in food, mainly in animal sources, but also in grains, fruit and vegetables. Furthermore, it can be bio-synthesized from the amino acids lysine and methionine. Only *L*-carnitine is the biologically active form, and *D*-carnitine is the biologically inactive stereoisomer. Carnitine combines the functional groups of choline (hydroxyl group) and betaine (carboxylic group) cations. This biosourced quaternary ammonium cation is a very interesting candidate for the design of "green" ILs, which is easily accessible and rather cheap. Additionnally, to the best of our knowledge, there are no examples in literature describing the use of carnitine or its derivatives as cations for ILs.

However, carnitine derivatives were used for the formation of cationic surfactants in the literature. De Maria *et al.* investigated long-chain acylcarnitine ester salts as surfactants for the formation of micelles and liposomes (**Figure 3.15.a**).[259] The aggregation behavior of the diesters have been determined resulting in more complex structures if the two chains are of comparable length. Another study dealing with a single-chain carnitine derived salt (**Figure 3.15.b**) described a detailed self-assembly study on this surfactant including spontaneous vesicle formation in water.[260]

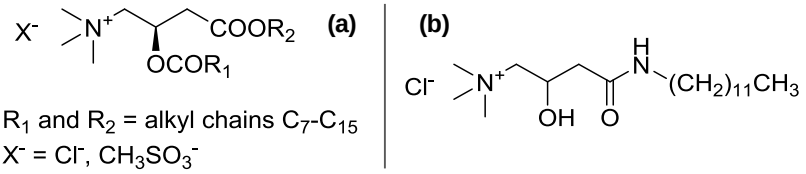

Figure 3.15 Surfactants based on carnitine derivatives reported in the literature, such as **(a)** long-chain acylcarninitine ester salts[259], and **(b)** single-chain carnitine-derived salt[260].

In the context of this study, we have prepared a series of carnitine esters, similar to the betaine ester compounds. Also in this part, only short-chain carnitine ester, *i.e.* ethyl-, butyl-, hexyl-, octyl-chains, were synthesized and studied. Lev was chosen as the carboxylate counter anion.

3.4.1 Preparation of carnitine esters

The carnitine esters have been synthesized *via* the reaction of carnitine with 1-bromoalkanes (R = $C_nH_{2n+1}$with n = 2, 4, 6, 8) in acetonitrile under reflux (**Figure 3.16**), similar to the synthesis of betaine ester. The cations are abbreviated as **[C_n-Carn]**. Carnitine (1 equiv.) and 1-bromoalkane (1.5 equiv.) have been mixed in acetonitrile under inert conditions before heating under reflux for at least one night. After evaporation of the solvent, the crude product has been washed

several times with diethyl ether, and dried under vacuum. More details and the results of ^{1}H- and ^{13}C-NMR-analysis are given in the ***experimental section*** of this chapter.

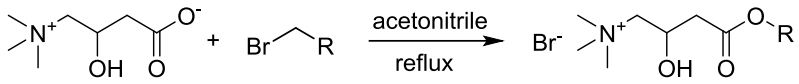

Figure 3.16 Synthesis of carnitine esters; R = C_nH_{2n+1} with n = 2, 4, 6, 8.

As already mentioned, compounds with an ester-function are acid- and base-sensitive, so the anion exchange with an exchange resin was not successful. Therefore, the method with silver(I) oxide mixed to the corresponding carboxylic acid was used (**Figure 3.17**).[243]

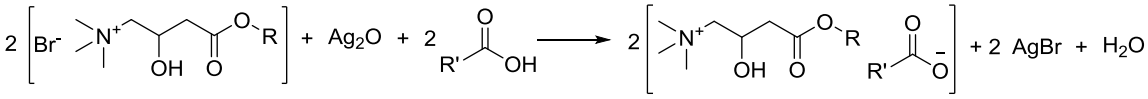

Figure 3.17 Anion exchange for carnitine ester compounds with silver(I) oxide.

In order to assess the interest to use carnitine as a counter cation for the design of biosourced ILs, and because of time, we focused on the synthesis and further physicochemical investigations of **[C_2-Carn]Lev.**

3.4.2 Thermal properties of carnitine esters

The most important thermal properties, such as thermal stability and thermal phase transitions, of the prepared carnitine ester bromides with different alkyl-chain lengths (ethyl, butyl, hexyl, octyl) have been determined. TGA measurements were carried out to study their degradation temperatures T_{deg} which are shown in **Table 3.6** and **Figure 3.18**.

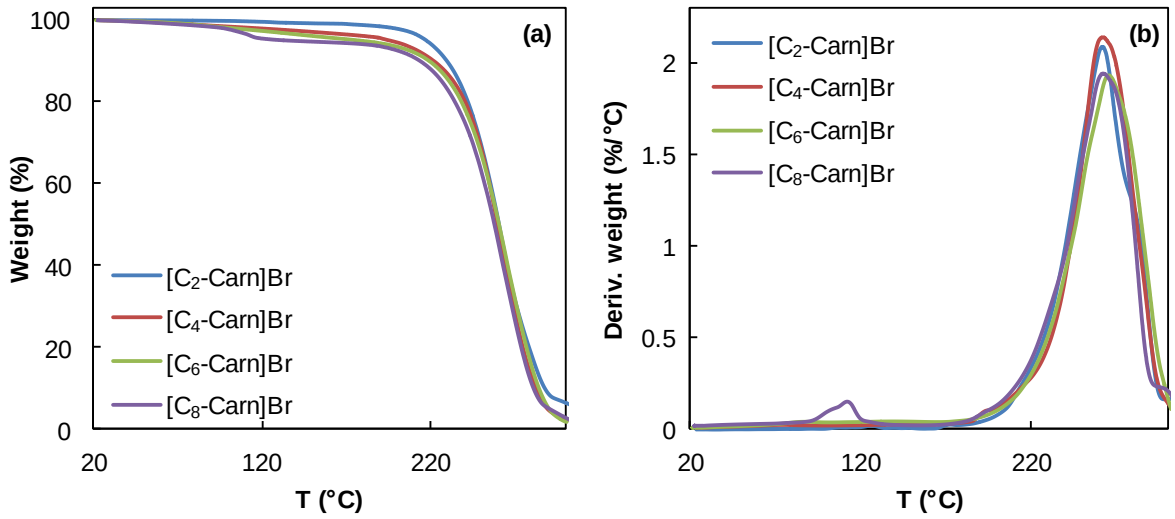

Figure 3.18 TGA-curves of carnitine ester bromides (ethyl, butyl, hexyl, octyl): **(a)** weight percent as a function of temperature, **(b)** derivative weight percent as a function of temperature.

The thermal stability decreases with increasing alkyl-chain length of the carnitine ester cation. This result is similar to the degradation behavior of betaine ester bromides, as shown before. Similar to all of the other results, the carboxylate compound **[C_2-Carn]Lev** is thermally less stable (T_{deg} 145 °C) than its halogenide homologue **[C_2-Carn]Br** (T_{deg} 190 °C).

The DSC-measurements for carnitine esters show that only the smallest carnitine ester bomide, **[C_2-Carn]Br**, had a T_m (128.5 °C), thus crystallization took place as for classical salt structures. The compounds **[C_2-Carn]Lev**, **[C_4-Carn]Br**, **[C_6-Carn]Br** and **[C_8-Carn]Br** have only low glass transitions T_g which is typical for amorphous materials (**Table 3.6**). This thermal behavior could be attributed to their large cations or anion (in the case of **[C_2-Carn]Lev**) which result in structural organizations without a defined crystalline state. The graphs of TGA- and DSC-measurements are shown in the ***experimental section*** of this chapter.

Table 3.6 Degradation temperature T_{deg}, melting temperature T_m and glass transition T_g of carnitine ester compounds.

Compound	T_{deg} (°C)	T_g (°C)	T_m(°C)
[C_2-Carn]Br	190	/	128.5
[C_4-Carn]Br	189	-43.7	/
[C_6-Carn]Br	187	-48.1	/
[C_8-Carn]Br	185	-56.1	/
[C_2-Carn]Lev	145	-44.8	/

3.4.3 Aqueous phase behavior of carnitine esters

Similar to betaine esters, carnitine esters have an amphiphilic structure. For this reason, their self-aggregation behavior in aqueous solution was studied by measuring the surface tensions and their ability to solubilize hydrophobic solutes at RT and neutral pH.

3.4.3.1 Minimal aggregation concentration (MAC) of carnitine esters

The surface tensions of aqueous carnitine ester bromide solutions with increasing concentrations have been studied with the aim to determine their self-organization behavior. As for previous measurements, the maximal concentration was fixed at 2 mol·L^{-1} for practical reasons. The surface tension curves for the compounds **[C_n-Carn]Br** with n = 2, 4, 6, 8 are shown in **Figure 3.19**. The graphs are characteristic for amphiphilic compounds reaching a plateau of surface tension with the MAC.

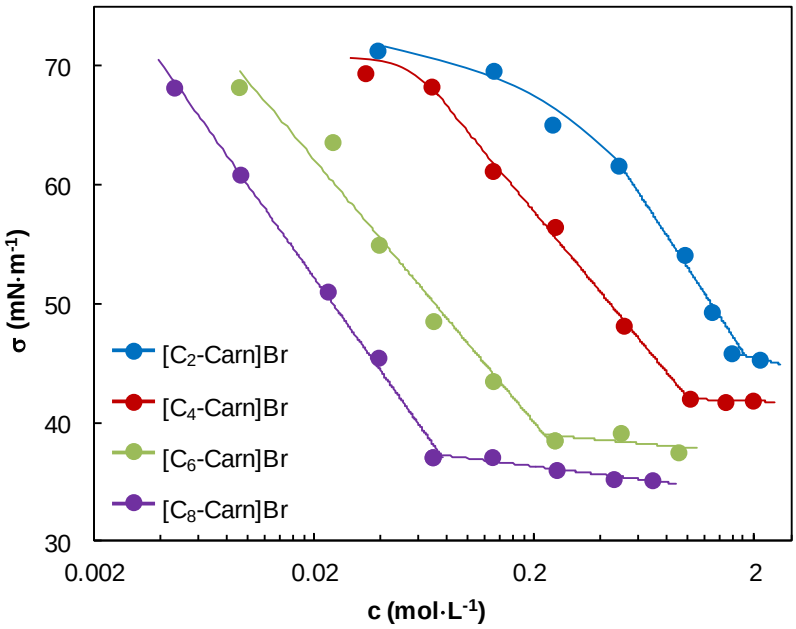

Figure 3.19 Surface tension σ as a function of alkyl-carnitine ester bromide [C_n-Carn]Br with n = 2, 4, 6, 8 concentration in aqueous solutions at RT.

Table 3.7 shows the determined MAC and σ_{MAC} values for carnitine ester bromides resulting in the following order: **[C_8-Carn] < [C_6-Carn] <[C_4-Carn] <[C_2-Carn],** as expected. So, even if the polar headgroup of carnitine ester is large, these compounds are amphiphilic and result in organized self-assembling from a certain concentration, defined as MAC.

Table 3.7 Minimal aggregation concentrations (MACs) with corresponding surface tensions (σ_{MAC}) of alkyl-carnitine ester bromides.

Br	[C_2-Carn]	[C_4- Carn]	[C_6- Carn]	[C_8- Carn]
MAC (mol·L^{-1})	1.84	1.01	0.21	0.09
σ_{MAC} (mN·m^{-1})	45.5	41.9	38.5	36.1

3.4.3.2 Hydrotropic behavior of carnitine esters

The theoretical background and the procedure of measurement have already been explained for QACILs (see ***section 2.3.4***). In this part of the work, we used the same method for the study of the hydrotropic behavior of ILs. The hydrophobic dye Disperse Red 13 (structure in ***section 2.3.4***) was dissolved in aqueous solutions of carnitine ester bromides, and its solubilization was detected by UV/visible spectroscopy.

In **Figure 3.20**, the results are shown for alkyl-carnitine ester bromides (with ethyl-, butyl-, hexyl-, octyl-chains). The following tendency has been detected for the efficiency as hydrotropes: **[C_8-Carn] > [C_6-Carn] > [C_4-Carn] > [C_2-Carn]**, as expected. However, the efficiency is not increasing linearly with growing alkyl-chain lengths. The carnitine ester compounds with hexyl- and octyl are much more efficient than the shorter chain ones. This behavior could be explained by the high polarity of short-chain carnitine esters due to its large polar head group. For compounds with longer alkyl side chain, *i.e.* hexyl and octyl, the amphiphilicity, which is important for the hydrotropic solubilization, is more pronounced.

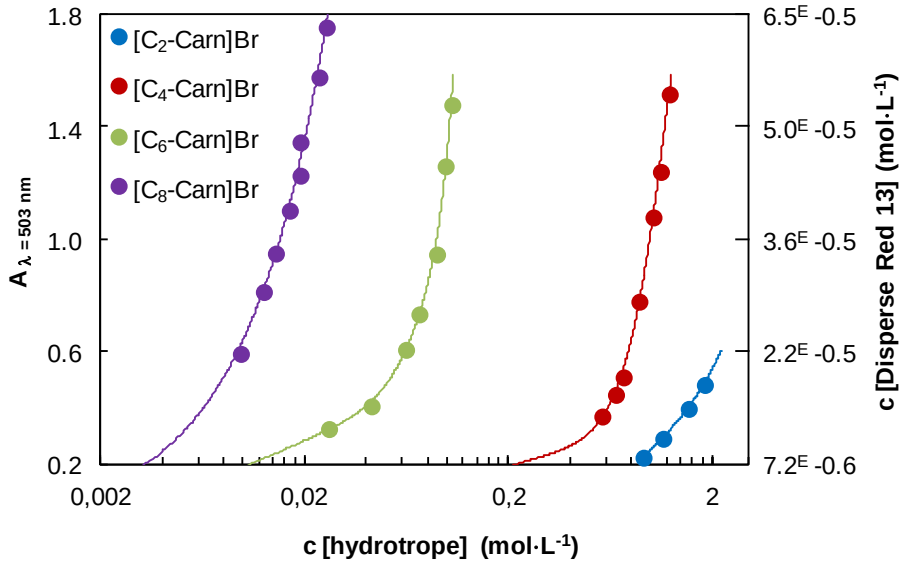

Figure 3.20 Solubilization of Disperse Red 13 measured by UV/visible spectroscopy at λ = 503 nm, in aqueous solutions of carnitine ester bromides.

3.5 Comparison of the properties of choline-, betaine- and carnitine-derivatives

To summarize the examined properties of choline-, betaine- and carnitine-based ILs, an overview is illustrated in **Table 3.8**.

Table 3.8 Overview for the properties of choline ether, betaine ester and carnitine ester.

<table>
<tr><th></th><th>Choline ether</th><th>Betaine ester</th><th>Carnitine ester</th></tr>
<tr><td>Structure</td><td> 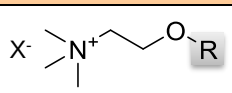 </td><td> 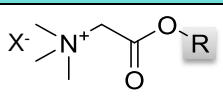 </td><td> 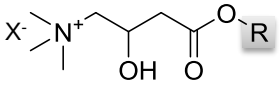 </td></tr>
<tr><td colspan="4">for all compounds: R = C_nH_{2n+1} with n = 2, 4, 6, 8</td></tr>
<tr><td colspan="4">X = I, Cl, Ace, Lac, Lev, Ita, Suc | X = Br, Lev (only n = 2, 4) | X = Br, Lev (only n = 2)</td></tr>
<tr><td>Thermal properties</td><td colspan="3"> 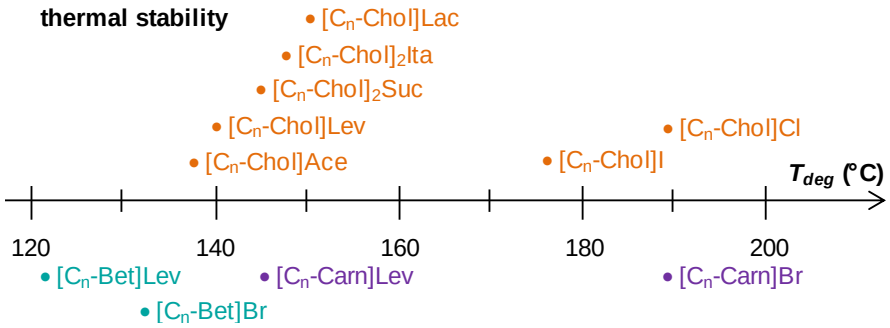
</td></tr>
<tr><td colspan="4">X = I, Cl: T_m 42 to 157 °C; X = Ace, Lac, Lev, Ita, Suc: T_m, T_g -72 to 65 °C | X = Br: T_m 94 to 158 °C; X = Lev (n=2,4): no T_m or T_g | X = Br, n=2: T_m 128 °C; X = Br (n=4-8), Lev (n=2): no T_m, T_g -56 to -44 °C</td></tr>
<tr><td>Aqueous phase behavior</td><td colspan="3"> 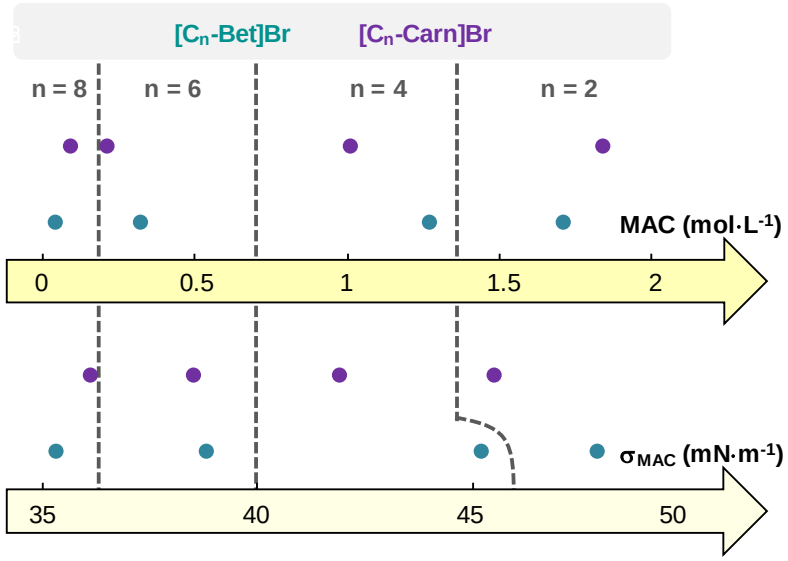
</td></tr>
</table>

Thermal properties, *i.e.* thermal stability and thermal phase transitions, of choline-, betaine- and carnitine-based compounds were compared. As the thermal stability changed mainly due to anion variation, the average values (built from the values for different alkyl chain lengths) are pointed up in **Table 3.8**. Compounds with halogenide counter anions (Cl, Br, I) are thermally more stable than with carboxylates (Ace, Lac, Lev, Suc, Ita). For the cationic part, the following trend for thermal stability could be highlighted: **[C_n-Bet] < [C_n-Chol] < [C_n-Carn]**.

The comparison of thermal phase transitions (melting temperature $\boldsymbol{T_m}$ or glass transition temperature $\boldsymbol{T_g}$) emphasizes the classical crystallization behavior with $\boldsymbol{T_m}$ for choline ether halogenides, betaine ester bromides and the short-chain [C_2-Carn]Br. The longer-chain carnitine ester bromides and choline ethers with carboxylate anions have low $\boldsymbol{T_m}$ and / or $\boldsymbol{T_g}$, indicating ILs. For the short-chain betaine ester levulinates [C_2-Bet]Lev and [C_4-Bet]Lev, no thermal phase transition was detected, which is also typical of ILs.

The aqueous phase behavior of betaine ester bromides [C_n-Bet]Br and carnitine ester bromides [C_n-Bet]Br (with n = 2, 4, 6, 8) was investigated and compiled in **Table 3.8**, expressed as minimal aggregation concentration (MAC) and its corresponding surface tension (σ_{MAC}). This representation highlights the similar surface activity of both types of compounds which is directly connected to the chain lengths n.

3.6 Biodegradability and toxicity of choline- and betaine-based ILs

Today, chemistry has evolved towards the development of greener chemicals. This means that new compounds must not only be based on renewable resources but also they must be safer for the consumer and the environment. In this context, it appears indispensable to examine the biodegradability and the toxicity of new molecules, even if they are bio-based. So, in this part, the biodegradability and the toxicity of the novel choline- and betaine-based ionic liquids have been evaluated.

3.6.1 Biodegradability of choline- and betaine-based ILs

The most important structural aspects for the design of highly biodegradable compounds are already well-known due to numerous studies. Generally speaking, biodegradability is raised with unsubstituted linear alkyl side chains (especially ≥ 4 carbons).[94] The presence of potential sites of enzymatic hydrolysis, *e.g.* esters and amides, increases the biodegradability.[94] Based on this fact, ester-derivatives of betaine and carnitine are expected to be highly biodegradable, as already proved in the literature for betaine-based surfactants.[256] Another structural amelioration for the design of biodegradable products is the introduction of oxygen in the form of hydroxyl, aldehyde or carboxylic groups. More generalities and details on biodegradability of compounds have already been described in ***chapter 1***, ***section 1.2.3***.

Table 3.9 Biodegradation (after 10 and 28 days) of levulinate compounds and the mass fraction (wt%) of the anion; biodegradation values > 60% are marked in green.

Compound	% Biodegradation		Wt% of anion
	10 days	28 days	
Na Lev	62	74	83
[Chol]Lev	57	71	52
[C_2-Chol]Lev	22	27	47
[C_2-Bet]Lev	61	76	44
[BMIm]Lev	22	25	45

Choline as a IL cation, for instance, has been reported as biodegradable.[97,236] We have investigated the biodegradability of [Chol]Lev which was excellently biodegradable after few days (71% after 28 days; **Table 3.9**). However, the choline-derived ether-functionalized cation [C_1-Ch.ether] was reported as not readily biodegradable as IL combined with the methylsulfonate [CH_3-O-SO_3] anion.[206] Thus, the choline ether compounds in this work are not

inevitably biodegradable. The biodegradation test of **[C_2-Chol]Lev**, for instance, resulted in 27% after 28 days. However, **[C_2-Bet]Lev** was excellently biodegradable (61% after only 10 days). The biodegradation test of the IL **[BMIm]Lev**, which was taken as a IL reference, ensued no biodegradability (25% after 28 days). Furthermore, the sodium salt of levulinate (Na Lev) was investigated as reference compound (62% after only 10 days). The biodegradation tests described in this project (**Table 3.9**) were carried out by Marta Markiewicz in the laboratory of Dr. Stefan Stolte at the *Department Sustainable Chemistry* (University of Bremen, Germany). Details on the experimental procedure and the graphs for biodegradation during 28 days are given in the ***experimental section*** of this chapter.

Figure 3.21 summarizes the biodegradation of the tested levulinate ILs, *i.e.* [BMIm]Lev, [C_2-Chol]Lev, [Chol]Lev, [C_2-Bet]Lev, compared to the following similar examples from the literature: [BMIm]Cl (< 5% after 28 days)[95], [C_1-Chol]CH_3SO_4 (4% after 28 days)[206], [Chol]Sal (60% after 28 days)[261], [C_{12}-Bet]Br (60% after 28 days)[262].

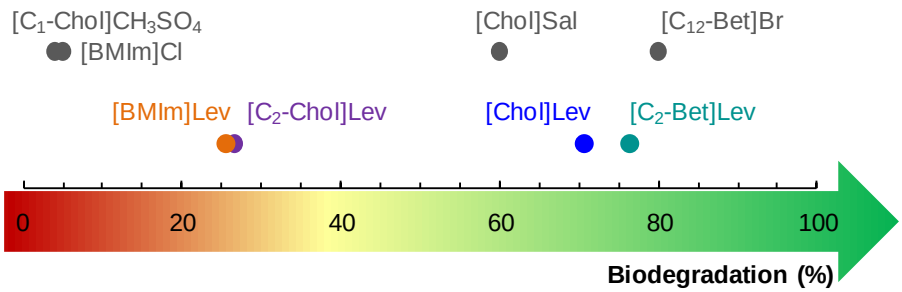

Figure 3.21 Overview for the biodegradation of levulinate ILs compared to similar examples from the literature (grey).

Summing up, for the design of biodegradable ILs both the type of head group as well as the substituted side chain of the cation have a great influence.[263]

3.6.2 Toxicity of choline- and betaine-based ILs

Generally speaking, the toxicity of ILs mainly depends on the cationic part as shown by Yun *et al.* investigating typical ILs based on imidazolium, pyridinium, pyrrolidinium, morpholinium, piperidinium, quinolinium, quaternary ammonium and quaternary phosphonium.[92] Therefore, toxicity slightly increases with the number of nitrogen atoms in an aromatic cation (ring), so the trend for toxicity is as following: ammonium < pyridinium < imidazolium < triazolium < tetrazolium.[207] Furthermore, toxicity increases with longer alkyl side chains due to possible membrane interactions evoked by the elevated lipophilicity.[93] ILs with choline as cations and acesulfamate or saccharinate as counter anions are low toxic compounds confirmed by

ecotoxicity evaluations.[264] Another study dealing with choline alkanoate ([$C_nH_{2n+1}CO_2$], n = 1-9) ILs showed that they are less toxic than their corresponding sodium salts.[236]

Some choline-like quaternary ammonium chlorides (structures in **Figure 3.22**) have been described in the literature, and their antimicrobial activity has been evaluated.[265] The results showed that the studied choline-like quaternary ammonium esters act as antimicrobial agents, unlike the alcohol quaternary derivatives. These compounds could be applied as new potential desinfectants.

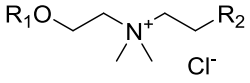

$R_1 = C_nH_{2n+1}$ *with* n = 6 to 12, 14, 16, 18

$R_2 = HOCH_2$ *or* $HOCH_2CH_2$ *or* $HO(CH_3)CH$ *or* $C_9H_{19}COOCH_2$ *or* $PhCOOCH_2$

Figure 3.22 Structure of choline-like quaternary ammonium ester- or alcohol-derivatives.[265]

Similar compounds with slightly different alkyl side chains R_1 and R_2 and acesulfamate or [Tf_2N] as counter anions also exhibit some antimicrobial activity.[105]

A former study published in 1914 showed the action of esters and ethers of choline which seems to be of muscarine-type due to their similar structure, which means that theparasympathetic nervous system could be blocked by these kind of substances.[266]

In the framework of this study, the ecotoxicity (*Daphnia magna*) and cytotoxicity (*IPC-81*), which is only one of numerous possible toxicity test, have been investigated for the same levulinate compounds as in the part of biodegradation (***section 3.6.1***). The toxicity tests were carried out by Marta Markiewicz in the laboratory of Dr. Stefan Stolte at the *Department Sustainable Chemistry* (University of Bremen, Germany). Details on the experimental procedure are given in the ***experimental section*** of this chapter.

Table 3.10 Ecotoxicity (*Daphnia magna*) of levulinate compounds.

Compound	**EC_{50} (mg·L^{-1})**	**Log EC_{50}**
Na Lev	> 500	/
[Chol]Lev	34.28	1.53
[C_2-Chol]Lev	4.32	0.64
[C_2-Bet]Lev	167.56	2.22
[BMIm]Lev	17.84	1.25

The results for the ecotoxicity tests for levulinate compounds using *Daphnia magna* (testing range: up to 500 mg·L^{-1}) are shown in **Table 3.10**. Due to the EU Directive 93/67 EEC (Commission of the European Communities, 1996), substances are classified due to their medium effective concentration (EC_{50}) values in different classes: very toxic to aquatic

organisms (< 1 mg·L^{-1}), toxic to aquatic organisms (1-10 mg·L^{-1}), harmful to aquatic organisms (10-100 mg·L^{-1}).[90] Substances with EC_{50} values above 100 mg·L^{-1} would not be classified. So, the compounds Na Lev and [C_2-Bet]Lev are not toxic to aquatic systems with EC_{50} values above 100 mg·L^{-1}. With EC_{50} values below 100 mg·L^{-1}, [C_2-Chol]Lev, [BMIm]Lev and [Chol]Lev could not be described as having low ecotoxicities.

Cytoxicty is the characteristic of being toxic to cells. As reported in the literature, the cation type of an IL is the main factor influencing the cytotoxicity of ILs, while the role of anions remains uncertain.[90] The cytotoxicity of levulinate ILs was tested using rat cells. None of the compounds showed toxic effects up to the highest tested concentrations of around 1 g·L^{-1}.

Table 3.11 Cytotoxicity (IPC-81) of levulinate compounds.

Compound	**EC_{50} (mg·L^{-1})**
Na Lev	> 1090
[Chol]Lev	> 1030
[C_2-Chol]Lev	> 1045
[C_2-Bet]Lev	> 1305
[BMIm]Lev	> 1145

3.7 Solubilization of biopolymers in choline-, betaine- and carnitine-based ILs

3.7.1 Solubilization of cellulose

In this part of the work, we focused on the capacity of the novel ILs to solubilize cellulose. First of all, non-alkylated Lev ILs were tested because Lev has provided the best results with QACILs (see ***chapter 2***). However, cholinium **[Chol]Lev**, betainium **[Bet]Lev** and carnitinium **[Carn]Lev** levulinates were not able to dissolve cellulose, as it has already been described for ILs with cholinium or alkanolamine cations.[267,268] This is accounted by the internal interactions of the hydroxyl end group of the cationic part with the cellulose hydroxyl-groups (**Figure 3.23.a**), or with the IL's anionic part which weakens the hydrogen bonding capacity of the anion, thus the dissolution of cellulose is hindered (**Figure 3.23.b**).[267,268]

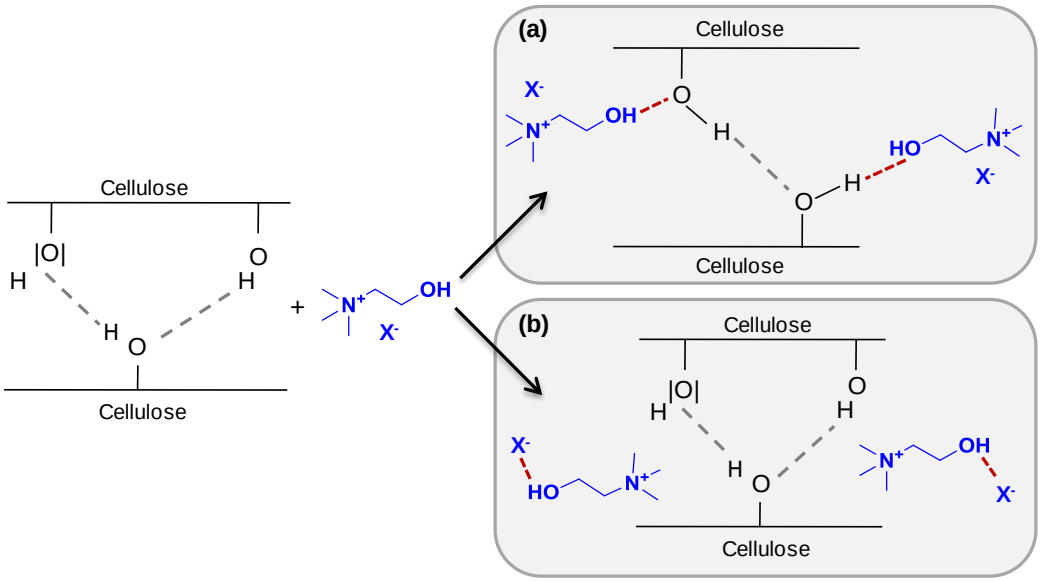

Figure 3.23 Possible mechanism for inability of choline ILs to dissolve cellulose due to **(a)** interactions between cellulose and choline or **(b)** interactions between the IL anion and choline.

Based on these considerations, we focused (as previously described) on the design of cationic derivatives with a blocked hydroxyl end group (*e.g.* choline ethers, betaine esters, carnitine esters) which were expected to be more favorable for cellulose solubilization (**Figure 3.24**).

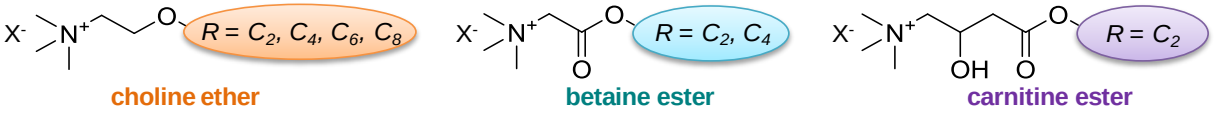

Figure 3.24 Cations with blocked hydroxyl groups: derivatives from choline, betaine and carnitine.

Based on the results of the study on QACILs, only short alkyl chains (*i.e.* ethyl, butyl, hexyl, octyl)

were linked to the ether- or ester-groups with the intention to reduce steric hindrance due to large IL cations.[210] The choice of counter anions was also derived from the previous study. Accordingly, the most important one was **Lev**, followed by **Cl**, **Ace**, **Lac**, **Ita** and **Suc**.

First, choline ether derivatives with **[C_n-Chol]**, **n = 2, 4, 6, 8**, cations and the following counter anions: **Cl**, **Ace**, **Lac**, **Lev**, **Ita** and **Suc** were investigated. The solubilization tests for cellulose were carried out for all the 24 compounds due to the same experimental procedure as explained in ***chapter 2***. As a result, **[C_2-Chol]Lev** was the only efficient IL for cellulose solubilization with up to 10 wt%, while all the other choline ether ILs with longer chain lengths on the cation and/or other carboxylate counter anions were not capable to solubilize cellulose. The inability of ILs with larger cations (n ≥ 4) could be understood from the previous results obtained with the quaternary ammonium (see ***chapter 2***) or from the literature with imidazolium ILs.[117] However, no explanation was found for the lack of solubilization power with the anions **Cl**, **Ace**, **Lac**, **Ita**, **Suc**.

With the aim to understand the role of the IL cations size, **[C_1-Chol]Lev** was prepared and tested as the smallest ether derived from cholinium, but unfortunately, and surprisingly, no cellulose solubilization was obtained. We can suppose that the structure is not enough amphiphilic for this process, with taking into consideration the model of Lindman *et al*.[269] These authors have suggested that cellulose is significantly amphiphilic, and therefore its solubililty would be facilitated in solvents that also are amphiphilic (*i.e.* have both polar and nonpolar parts, such as ILs or NMMO). Furthermore, the quaternary ammonium homologue of **[C_2-Chol]Lev**, *i.e.* **[Mono-C_4]Lev**, has been tested as cellulose solvent resulting in poor solubilization power (1.5 wt%).

In literature, several dialkoxy-functionalized quaternary ammonium ILs with **Ace** have been reported to be efficient solvents for cellulose (13-18 wt%), as shown in **Table 3.12**.[270]

Table 3.12 Solubility of cellulose S_{cell} in dialkoxy-functionalized quaternary ammonium ILs at 80 °C.[270]

IL	$S_{cellulose}$ (wt%)
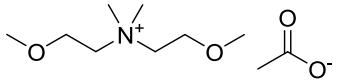	15
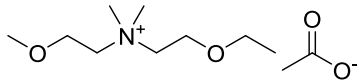	17
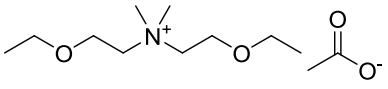	18
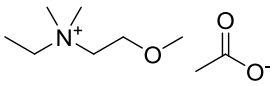	13
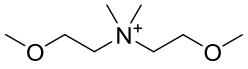	0
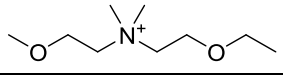	0

As **[C_2-Chol]Lev** was the most performant solvent for cellulose, the system was further investigated (**Figure 3.25**). First, the addition of co-solvents was tested (details on the background see ***chapter 2***). When the classical co-solvent DMSO (20 wt%) was used no effect on cellulose solubilization occured. With addition of more DMSO, phase separation took place. However, the "green" co-solvent γ-valerolactone (GVL; see ***chapter 2***) had a positive effect on the solubilization, with up to 13 wt% by adding 20 wt% of GVL. Up to now it is not clear why GVL is the better co-solvent for quaternary ammonium ILs. In an additional study, the 1:1-mixture of the best ILs, **[Di-C_4]Lev** and **[C_2-Chol]Lev**, was tested for the solubilization of cellulose. Contrary to the expectations, no solubilization took place. A possible explanation for this result might be a highly organized structuration between both ILs due to strong intermolecular interactions and therefore IL ions are not accessible for the solubilization process.

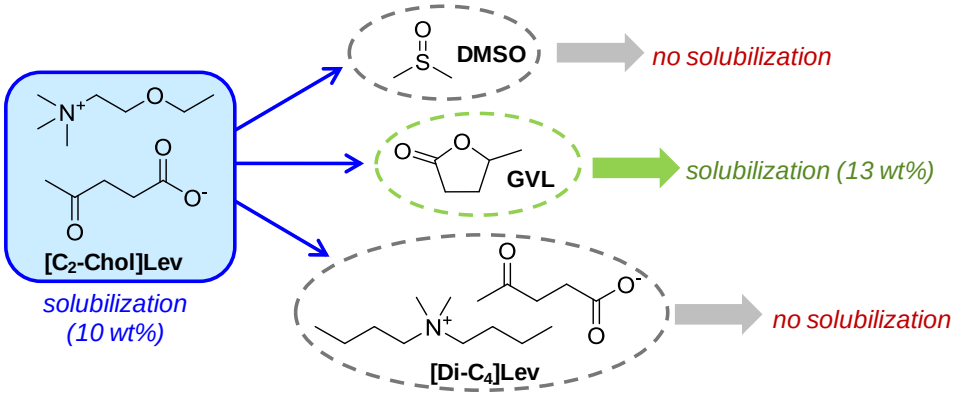

Figure 3.25 Overview for cellulose solubilization experiments with the IL [C_2-Chol]Lev.

Based on the results for choline ethers, only short-chain betaine- and carnitine-ester with Lev as counter anion were tested as cellulose solvents, *i.e.* **[C_2-Bet]Lev, [C_4-Bet]Lev, [C_2-Carn]Lev**. None of these compounds showed an effect for the solubilization of celllulose. This phenomenon could be connected to the ester-function for both, and additional to the free hydroxyl group for the carnitine-derived IL. Special interaction between the carboxylate ester group with cellulose, or with the IL anion could be imagined, which hinder the solubilization process.

The IL **[BMIm]Lev** was prepared and studied as a reference compound, since this cation is known to be very efficient for cellulose solubiliziation in combination with **Cl** or **Ace** as counter anion (up to 18 wt%).[210] However, in conjunction with **Lev**, this IL shows no effect as solvent for cellulose.

3.7.2 Solubilization of further biopolymers with levulinate ILs

Some promising Lev ILs with different small-sized cations were not only studied for the solubilization of cellulose but also for further common biopolymers, such as chitin, lignin, xylan and starch (structures in **Figure 3.26**). **Chitin** is composed of β-1,4-linked *N*-acetylglucosamine units building a polysaccharide structure similar to cellulose.[271] **Xylan**, a model compound for the group of **hemicelluloses**, is a polysaccharide mainly built from xylopyranosyl units.[272] **Starch** consists of glucose units linked by α-glycosidic bonds, in contrast to the β-linked biopolymers cellulose and chitin, which are hence much more resistant to hydrolysis. This polysaccharide contains two types of molecules: the linear and helical amylose and the branched amylopectin.[273] **Lignin** is a complex cross-linked amorphous polymer built from aromatic alcohols, called monolignols (*i.e. p*-coumaryl alcohol, coniferyl alcohol, sinapyl alcohol).[12] Its structure is variable due to the nature of the source species.

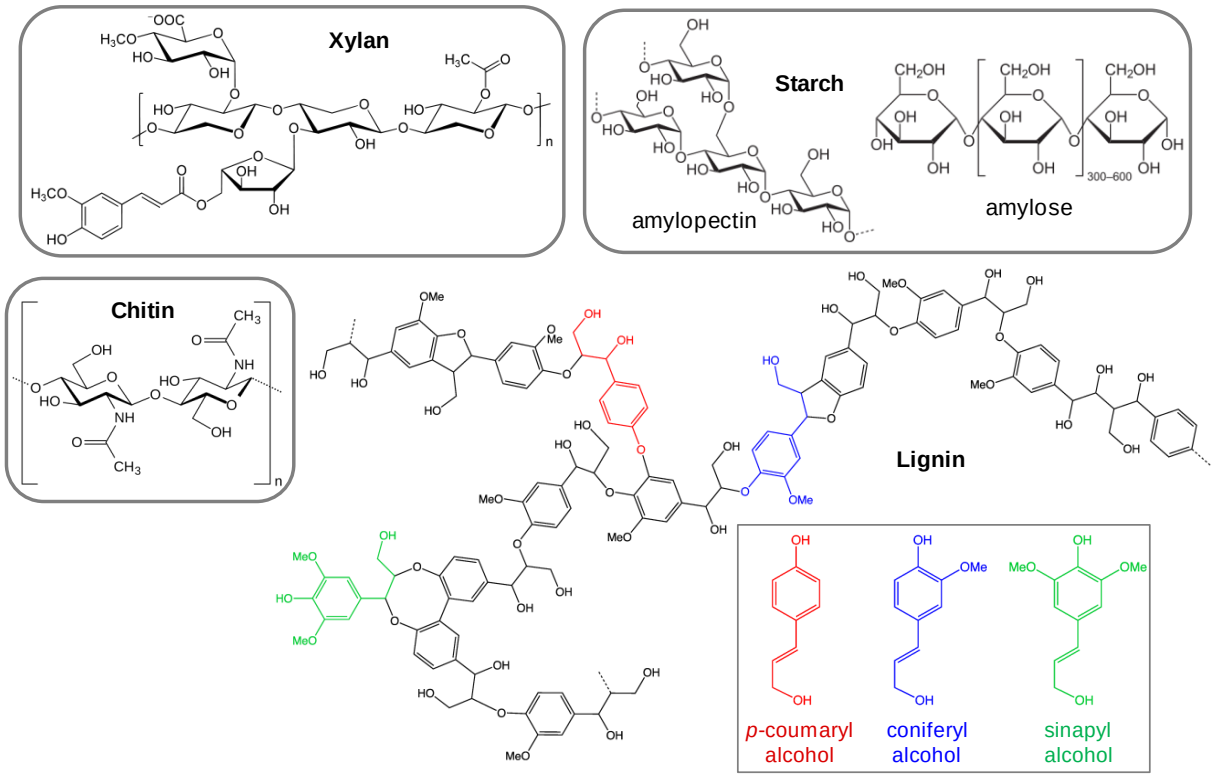

Figure 3.26 Structures of the biopolymers chitin, xylan, starch and lignin.

Table 3.13 gives an overview for the natural sources and the common solvents of these biopolymers. **Chitin** occurs in nature as structural component of crustaceans (*e.g.* shrimp, crabs), insects and fungi.[121,274] The traditional solvents for chitin are strong acids, such as HCl or H_2SO_4, or an alkaline-ice mixture (NaOH), and it is insoluble in common organic solvents.[275] In conventional methods, **xylan** is extracted from pulp with sodium or potassium hydroxide.[272] In nature, starch is used for energy storage in plants. The most important natural sources for starch

are carbohydrate food, such as potatoes, wheat, maize and rice.[273] **Starch** is one of the cheapest biopolymers which could be used as industrial raw material. However, processing is difficult due to its lack of solubility.[276] DMSO is the main well-known solvent for starch. The main natural source for **lignin** are plants and wood.[12] It can be removed from biomass *via* solubilization in alkaline-alcohol solutions, similar in effect as the Kraft paper pulping process (NaOH / Na_2S).

Table 3.13 Natural source and common solvents for the biopolymers chitin, lignin, xylan and starch.

Biopolymers	Natural sources	Common solvents
Chitin	crustaceans, insects, fungi	strong acids (HCl, H_2SO_4), alkaline ice mixture
Lignin	wood, plants	NaOH / Na_2S, alkaline-alcohol solutions
Xylan	wood, plants	NaOH, KOH
Starch	potatoes, cereals, rice	DMSO

For the solubilization of these biopolymers, we mainly focused on some **Lev-ILs** with small cations, such as **[Mono-C_4]**, **[Di-C_4]**, **[BMIm]**, **[Chol]**, **[C_2-Chol]**, **[Bet]**, **[C_2-Bet]**, **[Carn]**, and **[C_2-Carn]** (**Figure 3.27**; values are given in the ***experimental section***).

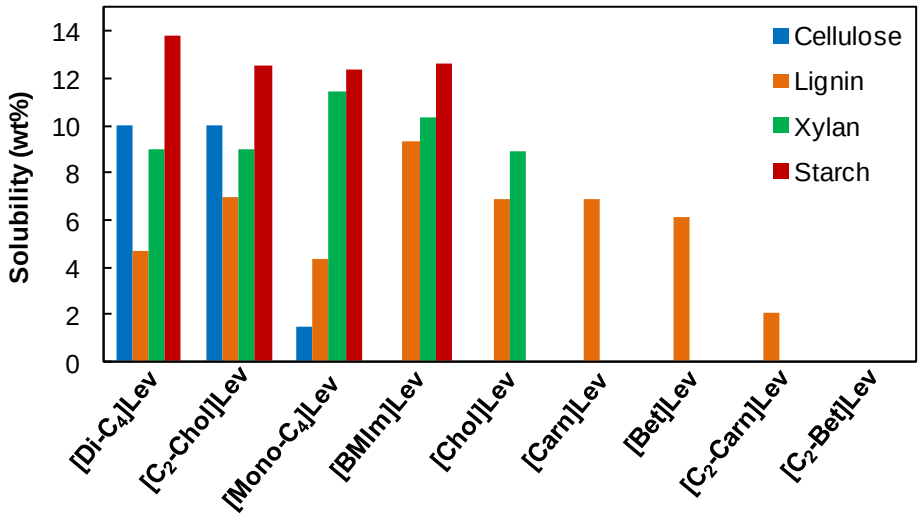

Figure 3.27 Solubility of biopolymers (cellulose, lignin, xylan, starch) in Lev-ILs at 90-100 °C.

None of the studied ILs was able to solubilize **chitin**. Studies on the solubilization of chitin in ILs explained that chitin is more difficult to dissolve than cellulose. Nevertheless, two ILs [BMIm]Cl[121] and [BMIm]Ace[277] were reported as solvents for chitin at 110 °C with 10 wt% and 6 wt% respectively.

In a previous study, **starch** was found to be soluble in ILs such as [BMIm]Cl and [BMIm]dicyanamide at 80 °C (up to 10 wt%).[276] In our study, the following ILs were efficient for the solubilization of starch at 90 °C: [Di-C_4]Lev (14 wt%), [C_2-Chol]Lev (12.5 wt%), [Mono-

C_4]Lev (12.5 wt%) and [BMIm]Lev (12.5 wt%). As starch is a polysaccharide composed of α-linked glycosidic bonds, this biopolymer is far easier to solubilize than cellulose or chitin.[12]

The solubilization experiments for **xylan** (representing hemicellulose) show that the betaine- and carnitine-derived Lev-ILs were not efficient. However, the other tested ILs had a solubilization capacity: [Di-C_4]Lev 9 wt%, [C_2-Chol]Lev 9 wt%, [Mono-C_4]Lev 11 wt% and [BMIm]Lev 10 wt%. As the structure of xylan is a little bit less complex than cellulose, it is easier to solubilize.

Nearly all of the tested Lev-ILs showed solubilization capacity for **lignin** (up to 10 wt% for [BMIm]Lev). Only [C_2-Bet]Lev had no effect on lignin. In literature, some ILs were reported to dissolve up to 20 wt% lignin, such as [HMIm][CF_3SO_3], [MMIm][CH_3SO_4] and [BMIm][CH_3SO_4].[118] For softwood Kraft lignin in ILs based on imidazolium cations, the solubility varies with the anion following the order: [CF_3SO_3] ≈ [CH_3SO_4] >> [Ace] > [For] >> [Cl] ≈ [Br] >> [BF_4] >> [PF_6].[278] Generally, ILs with a high solubilization power for lignin and a low one for cellulose are very interesting for selectively extraction of lignin from lignocellulosic biomass.[279]

Summing up, especially the ILs [C_2-Chol]Lev, [Di-C_4]Lev, and [Mono-C_4]Lev were capable to solubilize various biopolymers, such as cellulose, lignin, xylan and starch.

3.8 Conclusions

In this work, the main objective was the synthesis of novel biocompatible ILs based on choline ether, betaine ester and carnitine ester cations. First, we have focused on **choline ether** compounds with a variation of the alkyl side chain (ethyl, butyl, hexyl, octyl) and different natural resourced carboxylate counter anions: **acetate, lactate, levulinate, succinate** and **itaconate**. The impact of their chemical structure on thephysicochemical properties and power for cellulose solubilization was studied. Based on these results, the choice of further structures was made. Thus, only short-chain **betaine ester** (ethyl, butyl) and **carnitine ester** (ethyl) were prepared in combination with the natural **levulinate** anion.

The most important physicochemical properties of **choline-**, **betaine-** and **carnitine-derivatives** have been studied, such as thermal phase transitions (by DSC), thermal stability (by TGA), viscosity, surface activity and hydrotropic behavior. The thermal properties and some viscosities of pure compounds have been identified, thus the characteristic for ILs was evaluated. Compounds with longer alkyl side chains, especially based on [C_6-Bet],[C_8-Bet], [C_6-Carn], [C_8-Carn] cations, are amphiphilic, and are hence surface active in aqueous solutions. We have tested their hydrotropic behavior resulting in high solubilization capacity towards a hydrophobic dye for [C_6-Bet]Br, [C_6-Carn]Br and [C_8-Carn]Br.

As we have used derivatives from the biosourced compounds choline, betaine and carnitine for the design of sustainable ILs, the evaluation of their "greenness" plays a central role. Quaternary ammonium are less toxic than imidazolium and pyridinium compounds due to their lower lipophilicity. The eco- and cytotoxicity tests have shown that most of the tested levulinate compounds are not very toxic. Furthermore, the biodegradability of some of the used derivatives is elevated because of the incorporated oxygen sites.

The application as cellulose solvents showed that only **[C_2-Chol]Lev** had the capacity for this process (up to 10 wt%). Thus the best and only cellulose solvent was identified as short-chain levulinate IL, as already found in the study on QACILs. In addition, this IL was combined with 20 wt% **γ-valerolactone** resulting in 13 wt% cellulose solubilization. Besides, some short-chain Lev-ILs were tested for further biopolymers, *i.e.* chitin, hemicelluloses, lignin and starch, giving satisfying results for **[C_2-Chol]Lev** and two other ILs, [Mono-C_4]Lev and [Di-C_4]Lev, which were taken as reference compounds.

Experimental Section

1.) Preparation derivatives of choline, betaine and carnitine

1.1) Synthesis of choline ester

Choline ester chlorides have been synthesized by an esterification reaction of choline chloride with acyl chlorides (R =C_nH_{2n+1} with n = 1, 3, 5, 7):

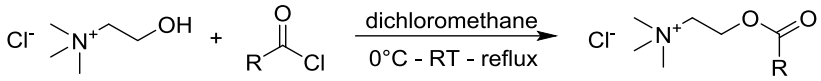

Choline chloride (1 equiv.) was mixed with acyl chloride (1.5 equiv.) at 0°C in dichloromethane. Then, the mixture was heated under reflux for at least one night. After evaporation of the solvent, the crude product was washed with diethyl ether for at least three times, and dried under high vacuum.

NMR-analysis

^{1}H- and ^{13}C-NMR spectra were recorded in the indicated solvents on a Bruker Avance 300 spectrometer. $CDCl_3$ and CD_3OD (99.95% isotopic purity) were obtained from Euriso-top. Chemical shifts (δ) are reported in parts per million (ppm) and measured relative to the HOD signal or the deuterated solvent chemical shift. The following abbreviations are used to explain the multiplicities: s = singlet, d = doublet, t = triplet, q = quartet, quint = quintet, sext = sextet, m = multiplet.

Pure products:

Acetyl-choline chloride, [C_2-Ch.ester]Cl: [$C_7H_{16}NO_2^+$][Cl^-], M=181.66 g/mol (yield: 85 %)

^{1}H-NMR (CD_3OD): δ(ppm): 2.03 (s, 3H), 3.28 (s, 9H), 3.55-3.62 (m, 2H), 3.99-4.07 (m, 2H)

^{13}C-NMR (CD_3OD): δ(ppm): 19.5 (CH_3), 35.9 (CH_2), 55.7 (CH_3), 56.0 (CH_2), 67.7 (CH_2), 172.2 (C)

Butyryl-choline chloride, [C_4-Ch.ester]Cl: [$C_9H_{20}NO_2^+$][Cl^-], M=209.71 g/mol (yield: 89 %)

^{1}H-NMR (CD_3OD): δ(ppm): 0.97 (t, *J*=7.4 Hz, 3H), 1.67 (q, *J*=7.4 Hz, 2H), 2.40 (t, *J*=7.4 Hz, 2H), 3.29 (s, 9H), 3.78-3.84 (m, 2H), 4.54-4.61 (m, 2H)

^{13}C-NMR (CD_3OD): δ(ppm): 12.7 (CH_3), 17.8 (CH_2), 35.4 (CH_2), 53.5 (CH_3), 55.8 (CH_2), 57.5 (CH_2), 64.6 (CH_2), 67.7 (CH_2), 172.6 (C)

Hexanoyl-choline chloride, [C_6-Ch.ester]Cl: [$C_{11}H_{24}NO_2^+$][Cl^-], M=237.77 g/mol (yield: 86 %)

^{1}H-NMR ($CDCl_3$): δ(ppm): 0.82 (t, *J*=6.9 Hz, 3H), 1.16-1.30 (m, 4H), 1.47-1.60 (m, 2H), 2.29 (t, *J*=7.6 Hz, 2H), 3.43 (s, 9H), 3.95-4.00 (m, 2H), 4.48-4.55 (m, 2H)

^{13}C-NMR ($CDCl_3$):δ(ppm): 13.9 (CH_3), 22.2 (CH_2), 24.4 (CH_2), 31.1 (CH_2), 34.0 (CH_2), 54.4 (CH_3), 55.8 (CH_2), 57.9 (CH_2), 64.9 (CH_2), 172.9 (C)

Octanoyl-choline chloride, [C_6-Ch.ester]Cl: [$C_{13}H_{28}NO_2^+$][Cl^-], M=265.82 g/mol (yield: 83 %)
^{1}H-NMR ($CDCl_3$): δ(ppm): 0.88 (t, *J*=6.9 Hz, 3H), 1.21-1.37 (m, 8H), 1.53-1.68 (m, 2H), 2.36 (t, *J*=7.6 Hz, 2H), 3.47 (s, 9H), 3.95-4.04 (m, 2H), 4.53-4.63 (m, 2H)
^{13}C-NMR ($CDCl_3$): δ(ppm): 14.2 (CH_3), 22.8 (CH_2), 24.7 (CH_2), 28.9 (CH_2), 29.0 (CH_2), 31.7 (CH_2), 34.1 (CH_2), 54.5 (CH_3), 58.0 (CH_2), 65.2 (CH_2), 173.1 (C)

1.2) Synthesis of choline ether

Choline ether iodides have been prepared in the following three steps: 1) preparation of the alcoholate (R = C_nH_{2n+1} with n = 2, 4, 6, 8), 2) etherification of chloroalkane with sodium alcoholate, and 3) quaternization of tertiary amine with iodomethane:

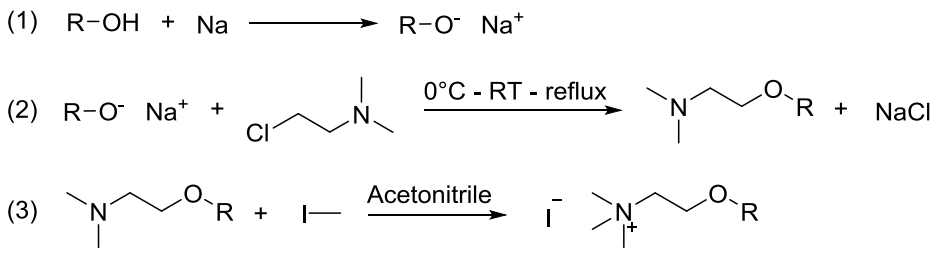

In the first step, sodium (2.5 equiv.) was added portion-wise to an excess of alcohol R-OH with R = C_nH_{2n+1} with n = 2, 4, 6, 8 under dry and inert conditions. If the mixture was too exothermic, especially for ethanol or 1-butanol, it was cooled with an ice bath. In 1-hexanol or 1-octanol, the dissolution of sodium difficult, thus the mixture was carefully heated.

When all of the sodium was completely dissolved, 2-chloro-*N*,*N*-dimethylethylamine (1 equiv.) was added portion-wise to the reaction mixture at 0°C over a 30-min. period. Then, the mixture was heated under reflux over night, and the end of the reaction is detected by a NMR-control. For the isolation of the ether-functionalized tertiary amine, different methods were used depending on the chain-length R. For R = hexyl and octyl, the ether-functionalized tertiary amine has been protonated with hydrochloric acid and extracted in the aqueous phase (separation from hexanol or octanol). When this aqueous phase was neutralized with an aqueous sodium hydroxide solution, an organic phase, the pure product, was formed. For R = ethyl and butyl, the alcohols are miscible with water, thus such an extraction is not possible. Here, the alcohol and the ether-functionalized tertiary amine are separated by distillation at atmospheric pressure.

In the third step, the ether-functionalized tertiary amine was quaternized with iodomethane (2 equiv.) in acetonitrile at room temperature for ca 24 h. After evaporation of the solvent, the crude product was washed several times with diethyl ether and dried under vacuum.
To obtain the choline ether carboxylate ILs with natural-based carboxylate counter-anions, an anion exchange with the exchange resin Amberlite® IRA-400(Cl) was carried out, as already explained in detail for QACILs in the ***experimental part of chapter 2***. From the result of the

study with QACILs, we have chosen the anions which were the most efficient for cellulose dissolution: Cl, Ace, Lac, Lev, Ita and Suc. The products were dried with a freeze dryer for at least 72 h.

NMR-analysis

The NMR analysis was carried out for all products as described before.

Pure products:

2-Ethoxyethyltrimethylammoniumiodide, [C_2-Ch.ether]I: [$C_7H_{18}NO^+$][I^-], M=259.13 g/mol (yield: 96 %)

^{1}H-NMR (CD_3OD): δ(ppm): 1.24 (t, *J*=7.0 Hz, 3H), 3.26 (s, 9H), 3.60 (t, *J*=7.0 Hz, 2H), 3.63-3.68 (m, 2H), 3.87-3.94 (m, 2H)

^{13}C-NMR (CD_3OD): δ(ppm): 14.0 (CH_3), 53.5 (CH_3), 63.9 (CH_2) , 65.6 (CH_2), 66.4 (CH_2)

2-Ethoxyethyltrimethylammonium chloride, **[C_2-Ch.ether]Cl**: [$C_7H_{18}NO^+$][Cl^-], M=167.68 g/mol (yield: 92 %)

^{1}H-NMR ($CDCl_3$): δ(ppm): 1.19 (t, *J*=7.0 Hz, 3H), 3.52 (s, 9H), 3.56 (t, *J*=7.0 Hz, 2H), 3.89 (m, 2H), 3.95 (m, 2H)

^{13}C-NMR ($CDCl_3$): δ(ppm): 15.2 (CH_3), 54.6 (CH_3), 64.6 (CH_2) , 66.1 (CH_2), 67.2 (CH_2)

2-Ethoxyethyltrimethylammonium acetate, **[C_2-Ch.ether]Ace**: [$C_7H_{18}NO^+$][$C_3H_2O_2^-$], M=191.27 g/mol (yield: 91 %)

^{1}H-NMR (CD_3OD): δ(ppm): 1.23 (t, *J*=7.0 Hz, 3H), 1.92 (s, 3H), 3.21 (s, 9H), 3.54-3.62 (m, 4H), 3.85-3.91 (m, 2H)

^{13}C-NMR (CD_3OD):δ(ppm): 14.0 (CH_3), 22.9 (CH_3), 53.5 (CH_3), 63.8 (CH_2) , 65.5 (CH_2), 66.7 (CH_2), 188.5 (C)

2-Ethoxyethyltrimethylammonium lactate, **[C_2-Ch.ether]Lac**: [$C_7H_{18}NO^+$][$C_3H_5O_3^-$], M=221.29 g/mol (yield: 95 %)

^{1}H-NMR (d-DMSO): δ(ppm): 1.07 (d, *J*=6.7 Hz, 3H), 1.11 (t, *J*=7.0 Hz, 3H), 3.15 (s, 3H), 3.43-3.52 (m, 4H), 3.56-3.61 (m, 2H), 3.74-3.81 (m, 2H)

^{13}C-NMR (d-DMSO): δ(ppm): 15.4 (CH_3), 22.3 (CH_3), 53.5 (CH_3), 64.1 (CH_2), 64.7 (CH_2), 66.1 (CH_2), 67.5 (CH),177.7 (C)

2-Ethoxyethyltrimethylammonium levulinate,[C_2-Ch.ether]Lev: [$C_7H_{18}NO^+$][$C_5H_7O_3^-$], M=247.33 g/mol (yield: 96 %)

^{1}H-NMR (d-DMSO): δ(ppm): 1.13 (t, J=7.0 Hz, 3H), 2.04 (m, 2+3H), 2.41 (t, J=7.0 Hz, 2H), 3.12 (s, 9H), 3.48 (t, J=7.0 Hz, 2H), 3.51-3.58 (m, 2H), 3.74-3.81 (m, 2H)

^{13}C-NMR (d-DMSO): δ(ppm): 15.4 (CH_3), 30.3 (CH_3), 33.2 (CH_2), 53.6 (CH_3), 63.9 (CH_2), 64.8 (CH_2), 65.9 (CH_2), 173.9 (C), 209.8 (C)

Di-(2-ethoxyethyltrimethylammonium) succinate, **[C_2-Ch.ether]$_2$Suc**: [$C_7H_{18}NO^+$]$_2$[$C_4H_4O_4^{2-}$], M=380.52 g/mol (yield: 89 %)

^{1}H-NMR (d-DMSO): δ(ppm): 1.13 (t, *J*=7.0 Hz, 6H), 2.01 (s, 4H), 3.14 (s, 18H), 3.49 (t, *J*=7.0 Hz, 4H), 3.56-3.62 (m, 4H), 3.74-3.82 (m, 4H)

^{13}C-NMR (d-DMSO): δ(ppm): 15.5 (CH_3), 53.5 (CH_3), 64.1 (CH_2), 64.8 (CH_2), 66.0 (CH_2),176.8 (C)

Di-(2-ethoxyethyltrimethylammonium) itaconate, **[C_2-Ch.ether]$_2$Ita**: $[C_7H_{18}NO^+]_2[C_5H_4O_4^{2-}]$, M=392.53 g/mol (yield: 91 %)

^{1}H-NMR (d-DMSO): δ(ppm): 1.13 (t, *J*=7.0 Hz, 6H), 2.84 (s, 2H), 3.14 (s, 18H), 3.48 (t, *J*=7.0 Hz, 4H), 3.57-3.63 (m, 4H), 3.74-3.81 (m, 4H), 4.96 (s, 1H), 5.46 (s, 1H)

^{13}C-NMR (d-DMSO): δ(ppm): 15.4 (CH_3), 44.7 (CH_2), 53.4 (CH_3), 64.1 (CH_2), 64.7 (CH_2), 65.9 (CH_2),171.7 (C)

2-Butoxyethyltrimethylammoniumiodide, [C_4-Ch.ether]I: $[C_9H_{22}NO^+][I^-]$, M=287.18 g/mol (yield: 97 %)

^{1}H-NMR (CD_3OD): δ(ppm): 1.69 (t, *J*=7.3 Hz, 3H), 1.39 (sext$_a$, *J*=7.7 Hz, 2H), 1.52-1.64 (m, 2H), 3.22 (s, 9H), 3.52 (t, *J*=6.4 Hz, 2H), 3.59-3.64 (m, 2H), 3.87-3.94 (m, 2H)

^{13}C-NMR (CD_3OD): δ(ppm): 12.9 (CH_3), 19.1 (CH_2), 31.4 (CH_2), 53.6 (CH_3), 64.3 (CH_2) , 65.7 (CH_2), 70.8 (CH_2)

2-Butoxyethyltrimethylammonium chloride, [C_4-Ch.ether]Cl: $[C_9H_{22}NO^+][Cl^-]$, M=195.73 g/mol (yield: 93 %)

^{1}H-NMR ($CDCl_3$): δ(ppm): 0.96 (t, *J*=7.3 Hz, 3H), 1.42 (sext$_a$, *J*=7.7 Hz, 2H), 1.55-1.66 (m, 2H), 3.23 (s, 9H), 3.55 (t, *J*=6.4 Hz, 2H), 3.60-3.65 (m, 2H), 3.85-3.92 (m, 2H)

^{13}C-NMR ($CDCl_3$): δ(ppm): 12.8 (CH_3), 19.1 (CH_2), 31.3 (CH_2), 53.3 (CH_3), 64.1 (CH_2) , 65.6 (CH_2), 70.8 (CH_2)

2-Butoxyethyltrimethylammonium acetate, **[C_4-Ch.ether]Ace**: $[C_9H_{22}NO^+][C_3H_2O_2^-]$, M=219.32 g/mol (yield: 95 %)

^{1}H-NMR (CD_3OD): δ(ppm): 0.96 (t, *J*=7.3 Hz, 3H), 1.42 (sext$_a$, *J*=7.7 Hz, 2H), 1.54-1.65 (m, 2H), 1.91 (s, 3H), 3.21 (s, 9H), 3.53 (t, *J*=6.4 Hz,
2H), 3.61-3.63 (m, 2H), 3.85-3.91 (m, 2H)

^{13}C-NMR (CD_3OD): δ(ppm): 12.8 (CH_3), 18.9 (CH_2), 22.9 (CH_3), 31.3 (CH_2), 53.1 (CH_3), 64.2 (CH_2) , 65.7 (CH_2), 70.8 (CH_2), 178.4 (C)

2-Butoxyethyltrimethylammonium lactate, **[C_4-Ch.ether]Lac**: $[C_9H_{22}NO^+][C_3H_5O_3^-]$, M=249.35 g/mol (yield: 94 %)

^{1}H-NMR (d-DMSO): δ(ppm): 0.88 (t, *J*=7.3 Hz, 3H), 1.07 (d, *J*=6.7 Hz, 3H), 1.31 (sext$_a$, *J*=7.7 Hz, 2H), 1.43-1.55 (m, 2H), 3.13 (s, 9H), 3.43 (t, *J*=6.5 Hz, 2H), 3.48 (d, *J*=6.6 Hz, 1H), 3.54-3.60 (m, 2H), 3.74-3.81 (m, 2H)

^{13}C-NMR (d-DMSO): δ(ppm): 14.2 (CH_3), 19.3 (CH_2), 22.1 (CH_3), 31.7 (CH_2), 53.4 (CH_3), 64.6 (CH_2), 64.9 (CH_2), 67.8 (CH), 70.4 (CH_2), 177.5 (C)

2-Butoxyethyltrimethylammonium levulinate,[C$_4$-Ch.ether]Lev: [$C_9H_{22}NO^+$][$C_5H_7O_3^-$], M=275.38 g/mol (yield: 94 %)

^{1}H-NMR (d-DMSO): δ(ppm): 0.87 (t, *J*=7.3 Hz, 3H), 1.31 (sext$_a$, *J*=7.6 Hz, 2H), 1.43-1.54 (m, 2H), 2.05 (s, 3H), 2.10 (t, *J*=6.8 Hz, 2H), 2.45 (t, *J*=6.8 Hz, 2H), 3.14 (s, 9H), 3.43 (t, *J*=6.4 Hz, 2H), 3.56-3.62 (m, 2H), 3.74-3.81 (m, 2H)

^{13}C-NMR (d-DMSO): δ(ppm): 14.1 (CH_3), 19.3 (CH_2), 30.2 (CH_3), 31.6 (CH_2), 32.7 (CH_2), 40.5 (CH_2), 53.3 (CH_3), 64.4 (CH_2), 64.7 (CH_2), 70.5 (CH_2), 174.5 (C), 209.6 (C)

Di-(2-butoxyethyltrimethylammonium) succinate, **[C$_4$-Ch.ether]$_2$Suc**: [$C_9H_{22}NO^+$]$_2$[$C_4H_4O_4^{2-}$], M=336.63 g/mol (yield: 91 %)

^{1}H-NMR (d-DMSO): δ(ppm): 0.87 (t, *J*=7.3 Hz, 6H), 1.31 (sext$_a$, *J*=7.7 Hz, 4H), 1.43-1.54 (m, 4H), 2.05 (s, 4H), 3.15 (s, 18H), 3.43 (t, *J*=6.4 Hz, 4H), 3.58-3.64 (m, 4H), 3.74-3.81 (m, 4H)

^{13}C-NMR (d-DMSO): δ(ppm): 14.2 (CH_3), 19.3 (CH_2), 31.6 (CH_2), 35.9 (CH_2), 53.4 (CH_3), 64.5 (CH_2), 64.7 (CH_2), 70.5 (CH_2),176.8 (C)

Di-(2-butoxyethyltrimethylammonium) itaconate, **[C$_4$-Ch.ether]$_2$Ita**: [$C_9H_{22}NO^+$]$_2$[$C_5H_4O_4^{2-}$], M=448.64 g/mol (yield: 93 %)

^{1}H-NMR (d-DMSO): δ(ppm): 0.88 (t, *J*=7.3 Hz, 6H), 1.31 (sext$_a$, *J*=7.7 Hz, 4H), 1.44-1.54 (m, 4H), 2.85 (s, 2H), 3.14 (s, 18H), 3.43 (t, *J*=6.4 Hz, 4H), 3.57-3.62 (m, 4H), 3.74-3.81 (m, 4H), 4.96 (s, 1H), 5.47 (s, 1H)

^{13}C-NMR (d-DMSO): δ(ppm): 14.2 (CH_3), 19.4 (CH_2), 31.5 (CH_2), 44.7 (CH_2), 53.5 (CH_3), 64.5 (CH_2), 64.9 (CH_2), 70.4 (CH_2),171.7 (C)

2-Hexyloxyethyltrimethylammoniumiodide, [C$_6$-Ch.ether]I: [$C_{11}H_{26}NO^+$][I^-], M=315.23 g/mol (yield: 96 %)

^{1}H-NMR (CD_3OD): δ(ppm): 0.88-0.96 (m, 3H), 1.28-1.46 (m, 6H), 1.55-1.68 (m, 2H), 3.24 (s, 9H), 3.54 (t, *J*=6.4 Hz, 2H), 3.54-3.66 (m, 2H), 3.85-3.93 (m, 2H)

^{13}C-NMR (CD_3OD): δ(ppm): 13.0 (CH_3), 22.2 (CH_2), 25.6 (CH_2), 29.2 (CH_2), 31.3 (CH_2), 53.4 (CH_3), 64.0 (CH_2) , 65.6 (CH_2), 70.1 (CH_2)

2-Hexyloxyethyltrimethylammonium chloride, [C$_6$-Ch.ether]Cl: [$C_{11}H_{26}NO^+$][Cl^-], M=223.78 g/mol (yield: 91 %)

^{1}H-NMR ($CDCl_3$): δ(ppm): 0.83-0.91 (m, 3H), 1.23-1.35 (m, 6H), 1.48-1.60 (m, 2H), 3.46 (t, *J*=6.6 Hz, 2H), 3.50 (s, 9H), 3.83-3.90 (m, 2H), 3.90-3.96 (m, 2H)

^{13}C-NMR ($CDCl_3$): δ(ppm): 14.1 (CH_3), 22.6 (CH_2), 25.8 (CH_2), 29.5 (CH_2), 31.6 (CH_2), 54.6 (CH_3), 64.9 (CH_2) , 65.8 (CH_2), 71.8 (CH_2)

2-Hexyloxyethyltrimethylammonium acetate, **[C$_6$-Ch.ether]Ace**: [$C_{11}H_{26}NO^+$][$C_3H_2O_2^-$], M=247.37 g/mol (yield: 95 %)

^{1}H-NMR ($CDCl_3$): δ(ppm): 0.79 (t, *J*=7.0 Hz, 3H), 1.14-1.28 (m, 6H), 1.39-1.52 (m, 2H), 1.81 (s, 3H), 3.31 (s, 9H), 3.36 (t, *J*=6.6 Hz, 2H),
3.71-3.82 (m, 4H)

^{13}C-NMR ($CDCl_3$): δ(ppm): 13.9 (CH_3), 22.4 (CH_2), 25.5 (CH_3), 25.8 (CH_2), 29.5 (CH_2), 31.5 (CH_2), 54.3 (CH_3), 64.9 (CH_2) , 65.4 (CH_2),
71.4 (CH_2), 176.9 (C)

2-Hexyloxyethyltrimethylammonium lactate, **[C_6-Ch.ether]Lac**: [$C_{11}H_{26}NO^+$][$C_3H_5O_3^-$], M=277.40 g/mol (yield: 95 %)

^{1}H-NMR (CD_3OD): δ(ppm): 0.93 (t, *J*=6.7 Hz, 3H), 1.25-1.50 (m, 6+3H), 1.57-1.68 (m, 2H), 3.23 (s, 9H), 3.53 (t, *J*=6.5 Hz, 2H), 3.59-3.66 (m, *2*H), 3.59-3.66 (m, 2H), 3.85-3.92 (m, 2H), 3.98 (q, *J*=6.7 Hz, 1H))

^{13}C-NMR (CD_3OD):δ(ppm): 17.2 (CH_3), 24.5 (CH_3), 26.4 (CH_2), 29.8 (CH_2), 33.3 (CH_2), 35.5 (CH_2), 57.4 (CH_3), 68.2 (CH_2), 69.7 (CH_2), 72.2 (CH), 75.1 (CH_2), 184.9 (C)

2-Hexyloxyethyltrimethylammonium levulinate,[C_6-Ch.ether]Lev: [$C_{11}H_{26}NO^+$][$C_5H_7O_3^-$], M=303.44 g/mol (yield: 96 %)

^{1}H-NMR (CD_3OD): δ(ppm): 0.93 (t, *J*=6.8 Hz, 3H), 1.29-1.46 (m, 6H), 1.56-1.68 (m, 2H), 2.18 (s, 3H), 2.43 (t, *J*=6.8 Hz, 2H), 2.73 (t, *J*=6.8 Hz, 2H), 3.22 (s, 9H), 3.53 (t, *J*=6.4 Hz, 2H), 3.59-3.64 (m, 2H), 3.86-3.93 (m, 2H)

^{13}C-NMR (CD_3OD): δ(ppm): 13.1 (CH_3), 22.3 (CH_2), 25.7 (CH_2), 28.5 (CH_2), 29.3 (CH_3), 30.6 (CH_2), 31.4 (CH_2), 39.0 (CH_2), 53.7 (CH_3), 64.3 (CH_2), 66.0 (CH_2), 71.3 (CH_2), 178.4 (C), 209.3 (C)

Di-(2-hexyloxyethyltrimethylammonium)succinate, **[C_6-Ch.ether]$_2$Suc**: [$C_{11}H_{26}NO^+$]$_2$[$C_4H_4O_4^{2-}$], M=492.73 g/mol (yield: 94 %)

^{1}H-NMR (CD_3OD): δ(ppm): 0.92 (t, *J*=6.9 Hz, 6H), 1.28-1.45 (m, 12H), 1.56-1.67 (m, 4H), 2.49 (s, 4H), 3.21 (s, 18H), 3.53 (t, *J*=6.4 Hz, 4H), 3.58-3.63 (m, 4H), 3.85-3.91 (m, 4H)

^{13}C-NMR (CD_3OD): δ(ppm): 13.1 (CH_3), 22.3 (CH_2), 25.8 (CH_2), 29.5 (CH_2), 31.5 (CH_2), 34.1 (CH_2), 53.4 (CH_3), 64.2 (CH_2), 65.8 (CH_2), 71.1 (CH_2),180.0 (C)

Di-(2-hexyloxyethyltrimethylammonium) itaconate, **[C_6-Ch.ether]$_2$Ita**: [$C_{11}H_{26}NO^+$]$_2$[$C_5H_4O_4^{2-}$], M=504.74 g/mol (yield: 95 %)

^{1}H-NMR (CD_3OD): δ(ppm): 0.93 (t, *J*=6.4 Hz, 6H), 1.28-1.46 (m, 12H), 1.55-1.67 (m, 4H), 3.21 (s, 18H), 3.25 (s, 2H), 3.53 (t, *J*=6.4 Hz, 4H), 3.58-3.63 (m, 4H), 3.84-3.91 (m, 4H), 5.41 (s, 1H), 5.96 (s, 1H)

^{13}C-NMR (CD_3OD): δ(ppm): 13.1 (CH_3), 22.4 (CH_2), 25.7 (CH_2), 29.3 (CH_2), 31.4 (CH_2), 42.4 (CH_2), 53.4 (CH_3), 64.3 (CH_2), 65.7 (CH_2), 71.2 (CH_2), 120.0 (CH_2), 142.4 (C), 173.9 (C), 178.2 (C)

2-Octyloxyethyltrimethylammoniumiodide, [C_8-Ch.ether]I: [$C_{13}H_{30}NO^+$][I^-], M=343.29 g/mol (yield: 98 %)

^{1}H-NMR (CD_3CN): δ(ppm): 0.87-0.95 (m, 3H), 1.25-1.39 (m, 10H), 1.51-1.64 (m, 2H), 3.16 (s, 9H), 3.45-3.55 (m, 4H), 3.78-3.85 (m, 2H)

^{13}C-NMR (CD_3CN): δ(ppm): 13.5 (CH_3), 22.5 (CH_2), 25.8 (CH_2), 28.0 (CH_2), 29.0 (CH_2), 29.1 (CH_2), 31.5 (CH_2), 54.1 (CH_3), 64.2 (CH_2) , 65.8 (CH_2), 71.1 (CH_2)

2-Octyloxyethyltrimethylammoniumchloride, **[C_8-Ch.ether]Cl**: [$C_{13}H_{30}NO^+$][Cl^-], M=251.84 g/mol (yield: 92 %)

^{1}H-NMR (CD_3OD): δ(ppm): 0.92 (t, J=6.9 Hz, 3H), 1.28-1.42 (m, 10H), 1.56-1.68 (m, 2H), 3.23 (s, 9H), 3.53 (t, J=6.5 Hz, 2H), 3.59-3.64 (m, 2H), 3.85-3.92 (m, 2H)

^{13}C-NMR (CD_3OD): δ(ppm): 13.0 (CH_3), 22.4 (CH_2), 26.0 (CH_2), 29.0 (CH_2), 29.1 (CH_2), 29.2 (CH_2), 31.7 (CH_2), 53.4 (CH_3), 64.2 (CH_2), 65.7 (CH_2), 71.2 (CH_2)

2-Octyloxyethyltrimethylammoniumacetate, **[C_8-Ch.ether]Ace**: [$C_{13}H_{30}NO^+$][$C_3H_2O_2^-$], M=275.43 g/mol (yield: 95 %)

^{1}H-NMR ($CDCl_3$): δ(ppm): 0.79 (t, *J*=6.7 Hz, 3H), 1.02-1.28 (m, 10H), 1.40-1.53 (m, 2H), 1.84 (s, 3H), 3.36 (s, 2+9H), 3.73-3.81 (m, 2H), 3.82-3.89 (m, 2H)

^{13}C-NMR ($CDCl_3$): δ(ppm): 14.0 (CH_3), 22.5 (CH_2), 25.5 (CH_3), 25.6 (CH_2), 26.1 (CH_2), 29.1 (CH_2), 29.2 (CH_2), 29.3 (CH_2), 31.7 (CH_2), 54.1 (CH_3), 64.9 (CH_2) , 65.3 (CH_2), 71.6 (CH_2), 177.1 (C)

2-Octyloxyethyltrimethylammonium lactate, **[C_8-Ch.ether]Lac**: [$C_{13}H_{30}NO^+$][$C_3H_5O_3^-$], M=305.45 g/mol (yield: 96 %)

^{1}H-NMR (CD_3CN): δ(ppm): 0.89 (t, *J*=6.9 Hz, 3H), 1.18 (d, *J*=6.9 Hz, 3H), 1.23-1.39 (m, 10H), 1.49-1.61 (m, 2H), 3.18 (s, 9H), 3.463 (t, *J*=6.5 Hz, 2H), 3.54-3.61 (m, *2*H), 3.67 (q, *J*=6.7 Hz, 1H), 3.76-3.84 (m, 2H)

^{13}C-NMR (CD_3CN): δ(ppm): 13.6 (CH_3), 21.3 (CH_3), 22.6 (CH_2), 26.0 (CH_2), 29.0 (CH_2), 29.1 (CH_2), 29.2 (CH_2), 31.6 (CH_2), 53.8 (CH_3), 64.5 (CH_2), 65.5 (CH_2), 67.9 (CH), 71.4 (CH_2), 178.8 (C)

2-Octyloxyethyltrimethylammonium levulinate,[C_8-Ch.ether]Lev: [$C_{13}H_{30}NO^+$][$C_5H_7O_3^-$], M=331.49 g/mol (yield: 96 %)

^{1}H-NMR (CD_3OD): δ(ppm): 0.89 (t, *J*=7.0 Hz, 3H), 1.22-1.38 (m, 10H), 1.49-1.61 (m, 2H), 2.10 (s, 3H), 2.25 (t, *J*=6.8 Hz, 2H), 2.56 (t, *J*=6.8 Hz, 2H), 3.17 (s, 9H), 3.46 (t, *J*=6.6 Hz, 2H), 3.55-3.61 (m, 2H), 3.76-3.84 (m, 2H)

^{13}C-NMR (d-DMSO):δ(ppm): 14.3 (CH_3), 22.6 (CH_2), 26.1 (CH_2), 29.1 (CH_2), 29.3 (CH_2), 29.5 (CH_3), 30.2 (CH_2), 31.7 (CH_2), 32.4 (CH_2), 39.9 (CH_2), 40.3 (CH_2), 53.7 (CH_3), 64.4 (CH_2), 64.8 (CH_2), 70.7 (CH_2), 174.7 (C), 209.3 (C)

Di-(2-octyloxyethyltrimethylammonium) succinate, **[C_8-Ch.ether]$_2$Suc**: [$C_{13}H_{30}NO^+$]$_2$[$C_4H_4O_4^{2-}$], M=548.85 g/mol (yield: 93 %)

^{1}H-NMR (d-DMSO): δ(ppm): 0.86 (t, *J*=6.9 Hz, 6H), 1.17-1.37 (m, 20H), 1.44-1.56 (m, 4H), 2.06 (s, 4H), 3.12 (s, 18H), 3.43 (t, *J*=6.5 Hz, 4H), 3.52-3.59 (m, 4H), 3.72-3.81 (m, 4H)

^{13}C-NMR (d-DMSO): δ(ppm): 14.4 (CH_3), 22.63 (CH_2), 26.1 (CH_2), 29.1 (CH_2), 29.2 (CH_2), 29.4 (CH_2), 31.8 (CH_2), 53.5 (CH_3), 64.3 (CH_2), 64.9 (CH_2), 70.7 (CH_2),176.7 (C)

Di-(2-octyloxyethyltrimethylammonium) itaconate, **[C_8-Ch.ether]$_2$Ita**: $[C_{13}H_{30}NO^+]_2[C_5H_4O_4^{2-}]$, M=560.85 g/mol (yield: 94 %)

^{1}H-NMR (d-DMSO): δ(ppm): 0.87 (t, *J*=6.8 Hz, 6H), 1.17-1.36 (m, 20H), 1.44-1.56 (m, 4H), 2.89 (s, 2H), 3.12 (s, 18H), 3.42 (t, *J*=6.5 Hz, 4H), 3.53-3.60 (m, 4H), 3.73-3.81 (m, 4H), 5.01 (s, 1H), 5.50 (s, 1H)

^{13}C-NMR (d-DMSO): δ(ppm): 14.4 (CH_3), 22.5 (CH_2), 26.1 (CH_2), 29.1 (CH_2), 29.2 (CH_2), 29.5 (CH_2), 31.7 (CH_2), 44.6 (CH_2), 53.4 (CH_3), 64.4 (CH_2), 64.8 (CH_2), 70.7 (CH_2), 171.7 (C)

1.3) Synthesis of betaine ester

Betaine (1 equiv.) was mixed at RT with 1-bromoalkane (R = C_nH_{2n+1} with n = 2, 4, 6, 8; 1.5 equiv.) in acetonitrile under dry and inert conditions (argon-gas). The mixture was heated under reflux at least for one night. The reaction was followed by ^{1}H-NMR to detect the end. After evaporation of the solvent, the crude product was washed with diethyl ether (at least three times) and dried under vacuum.

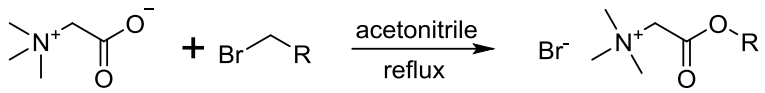

NMR-analysis

The NMR analysis was carried out for all products as described before.

<u>Pure products:</u>

(2-Ethoxy-2-oxo-ethyl)-trimethyl-ammoniumbromide, [C_2-Bet.]Br: $[C_7H_{16}NO_2^+][Br^-]$, M=226.11 g/mol (yield: 93 %)

^{1}H-NMR (CD_3OD): δ(ppm): 1.34 (t, *J*=7.1 Hz, 3H), 3.37 (s, 9H), 4.33 (q, *J*=7.1 Hz, 2H), 4.42 (s, 2H)

^{13}C-NMR (CD_3OD): δ(ppm): 12.9 (CH_3), 53.3 (CH_3), 62.2 (CH_2), 62.9 (CH_2), 164.7 (C)

(2-Butoxy-2-oxo-ethyl)-trimethyl-ammonium bromide, [C_4-Bet.]Br: $[C_9H_{20}NO_2^+][Br^-]$, M=254.16 g/mol (yield: 95 %)

^{1}H-NMR (CD_3OD): δ(ppm): 0.98 (t, *J*=7.4 Hz, 3H), 1.44 (sext$_a$, *J*=7.7 Hz, 2H), 1.70 (qint$_a$, *J*=6.9 Hz, 2H), 3.37 (s, 9H), 4.29 (q, *J*=6.6 Hz, 2H), 4.45 (s, 2H)

^{13}C-NMR (CD_3OD): δ(ppm): 12.6 (CH_3), 18.7 (CH_2), 30.2 (CH_2), 53.3 (CH_3), 62.9 (CH_2), 66.2 (CH_2), 164.7 (C)

(2-Hexyloxy-2-oxo-ethyl)-trimethyl-ammonium bromide, [C_6-Bet.]Br: $[C_{11}H_{24}NO_2^+][Br^-]$, M=282.22 g/mol (yield: 95 %)

^{1}H-NMR (CD_3OD): δ(ppm): 0.88-0.99 (m, 3H), 1.29-1.49 (m, 6H), 1.65-1.78 (m, 2H), 3.38 (s, 9H), 4.23-4.32 (m, 2H), 4.47 (s, 2H)

^{13}C-NMR (CD_3OD): δ(ppm): 12.9 (CH_3), 22.2 (CH_2), 25.5 (CH_2), 28.0 (CH_2), 31.3 (CH_2), 53.3 (CH_3), 62.9 (CH_2), 66.2 (CH_2), 164.7 (C)

(2-Octyloxy-2-oxo-ethyl)-trimethyl-ammonium bromide, [C_8-Bet.]Br: [$C_{13}H_{28}NO_2^+$][Br^-], M=310.27 g/mol (yield: 96 %)

^{1}H-NMR (CD_3OD): δ(ppm): 0.88-0.96 (m, 3H), 1.26-1.47 (m, 10H), 1.65-1.77 (m, 2H), 3.37 (s, 9H), 4.28 (t, *J*=6.7 Hz, 2H), 4.45 (s, 2H)

^{13}C-NMR (CD_3OD): δ(ppm): 13.0 (CH_3), 22.3 (CH_2), 25.5 (CH_2), 28.0 (CH_2), 28.9 (CH_2), 28.9 (CH_2), 31.5 (CH_2), 31.3 (CH_2), 53.1 (CH_3), 62.8 (CH_2), 66.2 (CH_2), 164.6 (C)

The anion exchange of betaine ester bromides to betaine ester carboxylates was carried out *via* a method with silver(I) oxide and a corresponding carboxylic acid. Therefore, silver(I) oxide (1 equiv.) was mixed with the carboxylic acid (2 equiv.) in water, and betaine ester bromide (2 equiv.) was then added at RT. Silver bromide precipitated immediately as grey salt. The mixture was stirred for further 1-2 h to complete the reaction. After filtration and washing the precipitate with water, the resulting solution was dried under lyophilization for at least 72 h. The products **[C_2-Bet.]** and **[C_4-Bet.]** were synthesized.

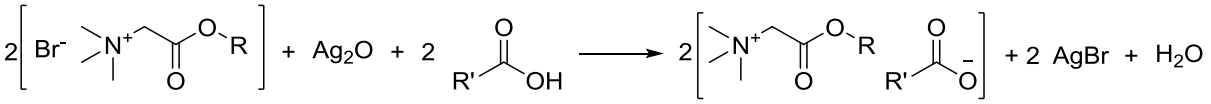

NMR-analysis

The NMR analysis was carried out for all products as described before.

<u>Pure products:</u>

(2-Ethoxy-2-oxo-ethyl)-trimethyl-ammoniumlevulinate, [C_2-Bet.]Lev: [$C_7H_{16}NO_2^+$][$C_5H_7O_3^-$], M=261.32 g/mol (yield: 95 %)

^{1}H-NMR ($CDCl_3$): δ(ppm): 0.91 (t, *J*=7.2 Hz, 3H), 1.90 (s, 3H), 2.15 (t, *J*=6.6 Hz, 2H), 2.42 (t, *J*=6.6 Hz, 2H), 3.29 (s, 9H), 4.01 (q, *J*=7.1 Hz, 2H), 4.59 (s, 2H)

^{13}C-NMR ($CDCl_3$): δ(ppm): 13.7 (CH_3), 29.8 (CH_3), 31.6 (CH_2), 39.9 (CH_2), 53.6 (CH_3), 62.1 (CH_2), 62.6 (CH_2), 164.1 (C), 176.7 (C), 209.5 (C)

(2-Butoxy-2-oxo-ethyl)-trimethyl-ammoniumlevulinate, [C_4-Bet.]Lev: [$C_9H_{20}NO_2^+$][$C_5H_7O_3^-$], M=289.37 g/mol (yield: 93 %)

^{1}H-NMR (CD_3OD): δ(ppm): 0.99 (t, *J*=7.2 Hz, 3H), 1.45 (m, 2H), 1.69 (m, 2H), 2.18 (s, 3H), 2.43 (t, 6.6 Hz, 2H), 2.72 (t, 6.7 Hz, 2H), 3.31 (s, 2H), 3.37 (s, 9H), 4.29 (m, 2H)

^{13}C-NMR (CD_3OD): δ(ppm): 12.7 (CH_3), 18.7 (CH_2), 28.6 (CH_3), 30.1 (CH_2), 30.6 (CH_2), 39.1 (CH_2), 53.3 (CH_3), 61.3 (CH_2), 65.9 (CH_2), 164.4 (C), 178.4 (C), 209.7 (C)

1.4) Synthesis of carnitine ester

Carnitine (1 equiv.) was mixed with 1-bromoalkane (R = C_nH_{2n+1} with n = 2, 4, 6, 8; 1.5 equiv.) in acetonitrile under dry and inert conditions (argon-gas). The mixture was heated under reflux for at least one night, and the reaction was controlled by NMR following. After evaporation of the solvent, the crude product was washed with diethyl ether (at least three times) and dried under vacuum.

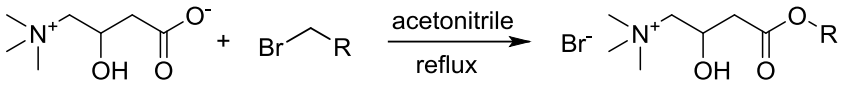

NMR-analysis

The NMR analysis was carried out for all products as described before.

Pure products:

(4-Ethoxy-2-hydroxy-4-oxobutyl)-trimethylammonium bromide, [C_2-Carn.]Br: [$C_9H_{20}NO_3^+$][Br^-], M=270.17 g/mol (yield: 96 %)

^{1}H-NMR (D_2O): δ(ppm): 1.17 (t, *J*=7.1 Hz, 3H), 2.57 (t, *J*=7.1 Hz, 2H), 3.14 (s, 9H), 3.39 (d, *J*=5.9 Hz, 2H), 4.10 (q, *J*=7.2 Hz, 2H), 4.54-4.64 (m, 1H)

^{13}C-NMR (D_2O): δ(ppm): 13.3 (CH_3), 40.2 (CH_2), 54.1 (CH_3), 62.1 (CH_2), 62.8 (CH), 69.6 (CH_2), 172.5 (C)

(4-Butoxy-2-hydroxy-4-oxobutyl)-trimethylammonium bromide, [C_4-Carn.]Br: [$C_{11}H_{24}NO_3^+$][Br^-], M=298.22 g/mol (yield: 97 %)

^{1}H-NMR (D_2O): δ(ppm): 1.04 (t, *J*=7.2 Hz, 3H), 1.43-1.59 (m, 2H), 1.70-1.85 (m, 2H), 2.74-89 (m, 2H), 3.38 (s, 9H), 3.58-3.66 (m, 2H), 4.25-4.37 (m, 2H), 4.75-4.87 (m, 1H)

^{13}C-NMR (D_2O): δ(ppm): 13.4 (CH_3), 18.8 (CH_2), 30.2 (CH_2), 40.6 (CH_2), 54.7 (CH_3), 63.2 (CH), 66.2 (CH_2), 70.2 (CH_2), 172.5 (C)

(4-Hexyloxy-2-hydroxy-4-oxobutyl)-trimethylammonium bromide, [C_6-Carn.]Br: [$C_{13}H_{28}NO_3^+$][Br^-], M=326.28 g/mol (yield: 96 %)

^{1}H-NMR (D_2O): δ(ppm): 0.97-1.07 (m, 3H), 1.39-1.57 (m, 6H), 1.73-1.86 (m, 2H), 2.82 (t, *J*=7.2 Hz, 2H), 3.39 (s, 9H), 3.61-3.68 (m, 2H), 4.24-4.34 (m, 2H), 4.76-4.87 (m, 1H)

^{13}C-NMR (D_2O): δ(ppm): 13.8 (CH_3), 22.6 (CH_2), 25.5 (CH_2), 28.3 (CH_2), 31.2 (CH_2), 40.6 (CH_2), 54.7 (CH_3), 63.2 (CH), 66.2 (CH_2), 69.9 (CH_2), 172.4 (C)

(4-Octyloxy-2-hydroxy-4-oxobutyl)-trimethylammonium bromide, [C_8-Carn.]Br: [$C_{15}H_{32}NO_3^+$][Br^-], M=354.33 g/mol (yield: 95 %)

^{1}H-NMR ($CDCl_3$): δ(ppm): 0.81 (t, *J*=7.1 Hz, 3H), 1.16-1.29 (m, 10H), 1.47-1.61 (m, 2H), 2.64 (d, *J*=6.6 Hz, 2H), 3.42 (s, 9H), 3.68 (d, *J*=5.7 Hz, 2H), 3.98 (t, *J*=6.8 Hz, 2H) 4.58-4.69 (m, 1H), 5.08-5.18 (m, 1H)

^{13}C-NMR (d-DMSO): δ(ppm): 14.4 (CH_3), 22.6 (CH_2), 25.9 (CH_2), 28.6 (CH_2), 31.7 (CH_2), 32.8 (CH_2), 35.5 (CH_2), 40.8 (CH_2), 53.8 (CH_3), 62.7 (CH), 64.7 (CH_2), 69.6 (CH_2), 170.5 (C)

The anion exchange of carnitine ester bromide to carnitine ester carboxylate was carried out *via* the method with silver(I) oxide and a corresponding carboxylic acid, which was already described for betaine ester compounds. Only the product **[C_2-Carn.]Lev** was prepared.

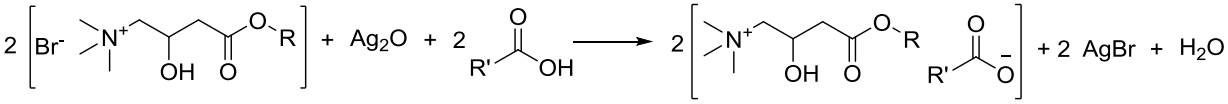

NMR-analysis

The NMR analysis was carried out for all products as described before.

Pure product:

(4-Ethoxy-2-hydroxy-4-oxobutyl)-trimethylammonium levulinate, [C_2-Carn.]Lev: $[C_9H_{20}NO_3^+][C_5H_7O_3^-]$, M=305.37 g/mol (yield: 91 %)

^{1}H-NMR (CD_3OD): δ(ppm): 1.28 (t, *J*=7.1 Hz, 3H), 2.18 (s, 2H), 2.42 (t, *J*=6.8 Hz, 2H), 2.61 (d, *J*=6.4 Hz, 2H), 2.72 (t, *J*=6.8 Hz, 2H), 3.27 (s, 9H), 3.49 (d, *J*=5.9 Hz, 2H), 4.19 (q, *J*=7.1 Hz, 2H), 4.62 (s, 1H)

^{13}C-NMR (CD_3OD): δ(ppm): 13.1 (CH_3), 28.5 (CH_3), 30.8 (CH_2), 39.2 (CH_2), 40.0 (CH_2), 53.4 (CH_3), 60.1 (CH_2), 62.7 (CH), 69.9 (CH_2), 170.6 (C), 178.7 (C), 209.8 (C)

1.4) Water content

Table 3.14 Water content of of choline-, betaine-, and carnitine-derived ILs measured measured by coulometric Karl Fischer titration.

Product	H_2O (wt%)	Product	H_2O (wt%)	Product	H_2O (wt%)
[C_2-Ch.ether]I	1.7	[C_4-Ch.ether]I	0.2	[C_2-Bet.]Br	0.9
[C_2-Ch.ether]Cl	3.6	[C_4-Ch.ether]Cl	2.3	[C_4-Bet.]Br	0.8
[C_2-Ch.ether]Ace	4.2	[C_4-Ch.ether]Ace	3.9	[C_6-Bet.]Br	0.8
[C_2-Ch.ether]Lac	4.1	[C_4-Ch.ether]Lac	4.0	[C_8-Bet.]Br	0.5
[C_2-Ch.ether]Lev	2.4	[C_4-Ch.ether]Lev	2.1	[C_2-Bet.]Lev	1.9
[C_2-Ch.ether]$_2$Ita	1.5	[C_4-Ch.ether]$_2$Ita	1.4	[C_4-Bet.]Lev	2.5
[C_2-Ch.ether]$_2$Suc	1.2	[C_4-Ch.ether]$_2$Suc	1.1		
[C_6-Ch.ether]I	0.3	[C_8-Ch.ether]I	1.1	[C_2-Carn.]Br	0.3
[C_6-Ch.ether]Cl	2.0	[C_8-Ch.ether]Cl	1.4	[C_4- Carn.]Br	0.6
[C_6-Ch.ether]Ace	3.5	[C_8-Ch.ether]Ace	1.5	[C_6- Carn.]Br	0.1
[C_6-Ch.ether]Lac	3.6	[C_8-Ch.ether]Lac	3.3	[C_8- Carn.]Br	0.9
[C_6-Ch.ether]Lev	2.5	[C_8-Ch.ether]Lev	2.8	[C_2-Carn.]Lev	1.6
[C_6-Ch.ether]$_2$Ita	1.9	[C_8-Ch.ether]$_2$Ita	0.8		
[C_6-Ch.ether]$_2$Suc	0.9	[C_8-Ch.ether]$_2$Suc	1.0		

After lyophilization of the synthesized ILs using a freeze dryer Christ-Alpha 1-2LD plus, for at least 72 h, the water content was detected by means of a coulometric Karl Fischer titration (Mettler Toledo C20) with Hydranal Coulomat AG reagent. **Table 3.14** shows the water content of all synthesized compounds.

2.) Physicochemical characterization of choline ethers, betaine esters and carnitine esters

2.1) Thermogravimetric analysis (TGA)

The thermogravimetric analysis (TGA) of prepared salts was performed with the same apparatus and method as described in the ***experimental section of chapter 2***. The degradation temperature T_{deg} is determined as starting point of the degradation (range with the highest slope of TGA curves):

Choline ether compounds:

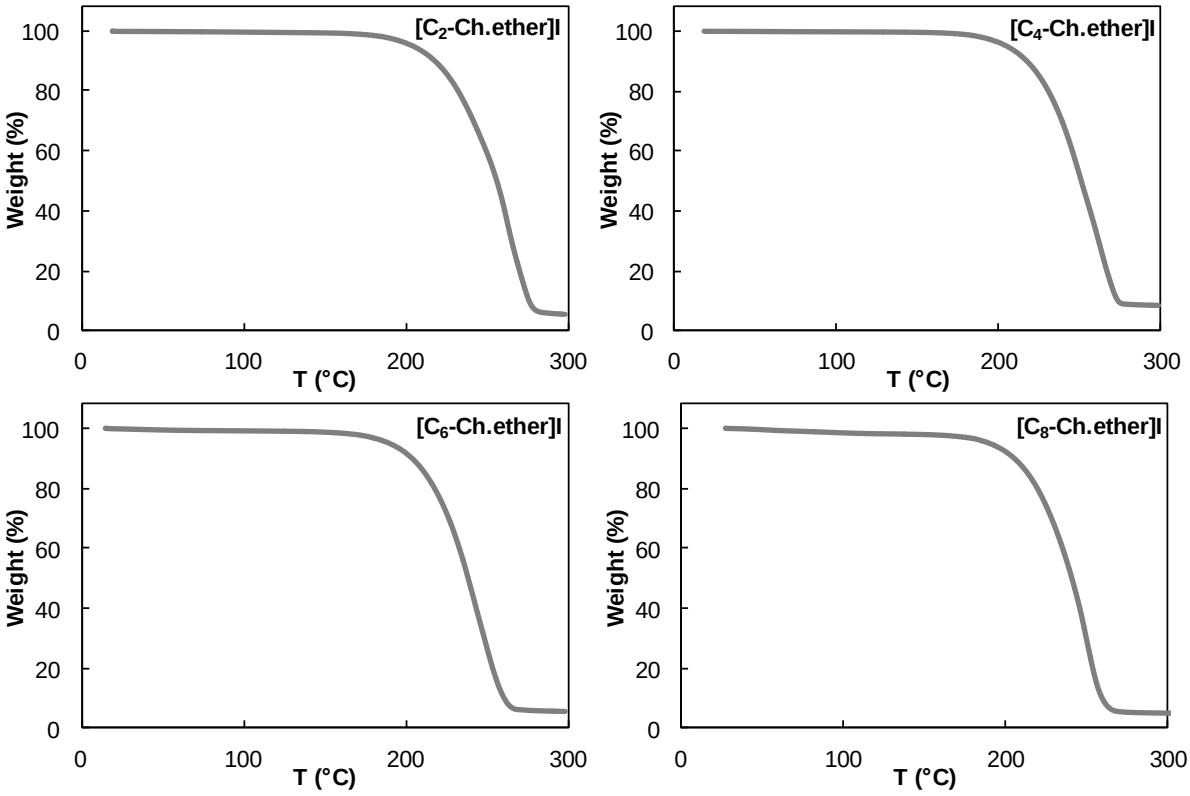

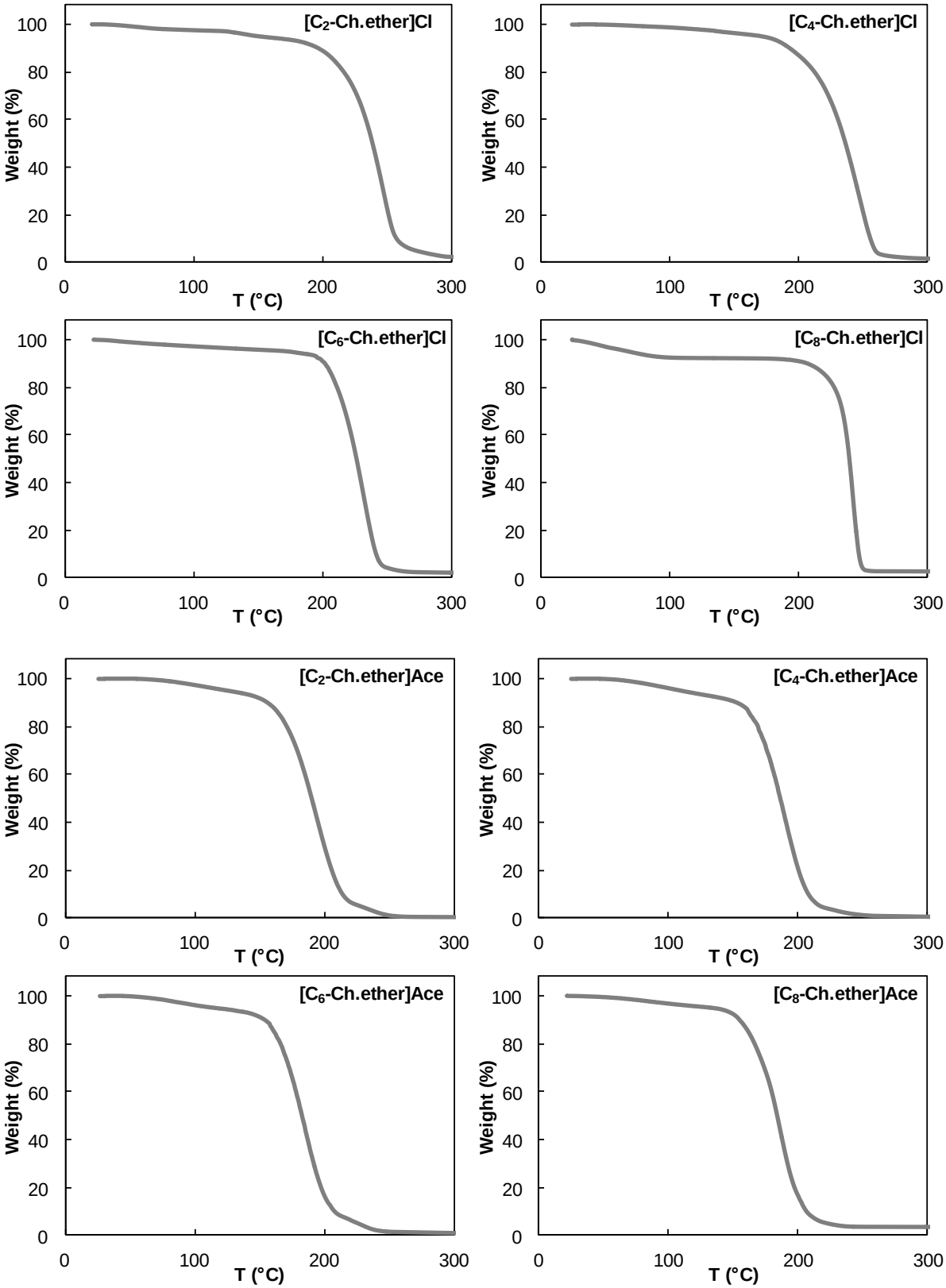
[C2-Ch.ether]Cl
[C4-Ch.ether]Cl
[C6-Ch.ether]Cl
[C8-Ch.ether]Cl
[C2-Ch.ether]Ace
[C4-Ch.ether]Ace
[C6-Ch.ether]Ace
[C8-Ch.ether]Ace
Weight (%)
T (°C)
0
20
40
60
80
100
0
100
200
300

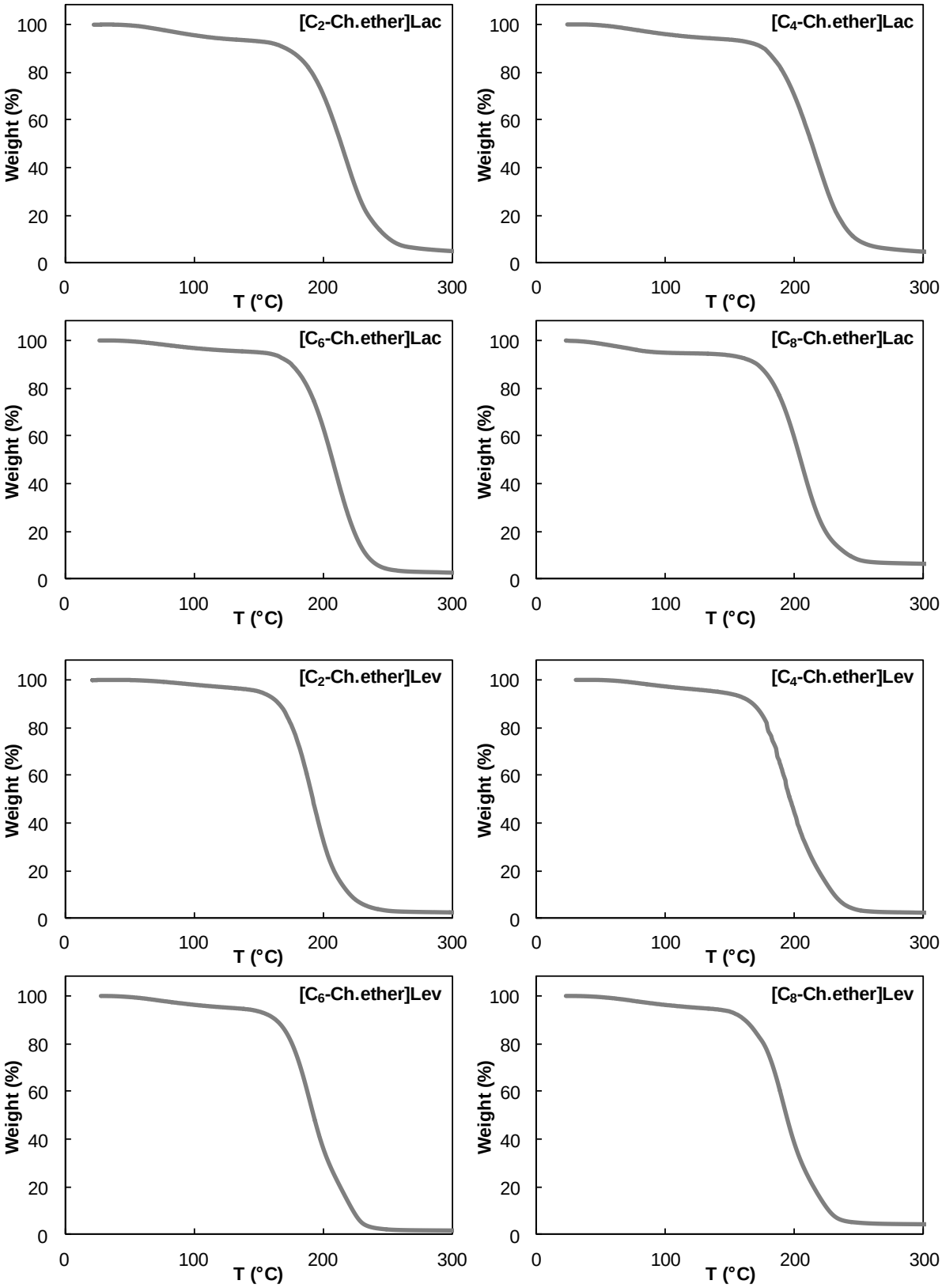
[C2-Ch.ether]Lac
[C4-Ch.ether]Lac
[C6-Ch.ether]Lac
[C8-Ch.ether]Lac
[C2-Ch.ether]Lev
[C4-Ch.ether]Lev
[C6-Ch.ether]Lev
[C8-Ch.ether]Lev
Weight (%)
T (°C)
0
20
40
60
80
100
0
100
200
300

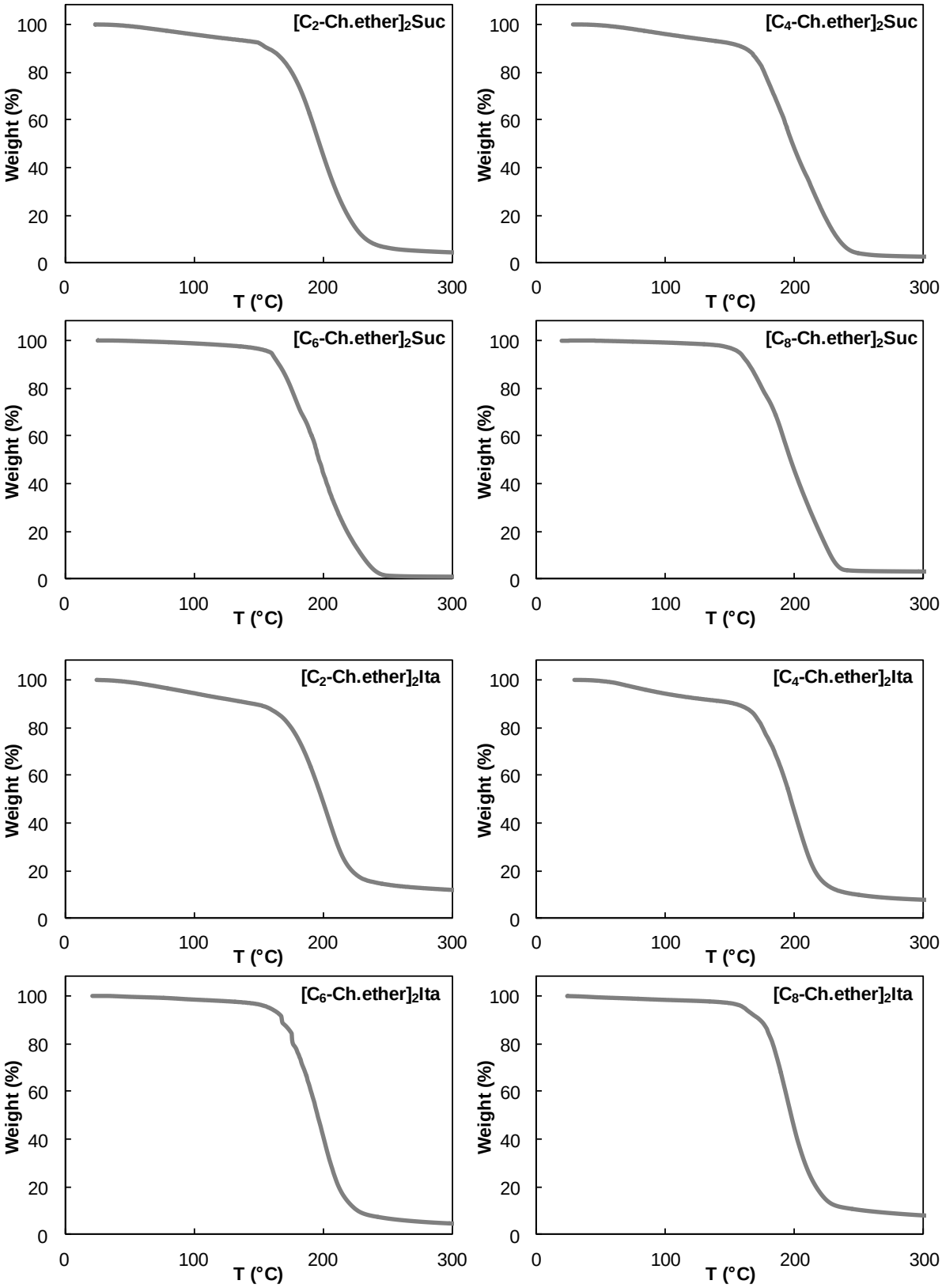
[C2-Ch.ether]2Suc
[C4-Ch.ether]2Suc
[C6-Ch.ether]2Suc
[C8-Ch.ether]2Suc
[C2-Ch.ether]2Ita
[C4-Ch.ether]2Ita
[C6-Ch.ether]2Ita
[C8-Ch.ether]2Ita
Weight (%)
T (°C)
0
20
40
60
80
100
0
100
200
300

Betaine ester compounds:

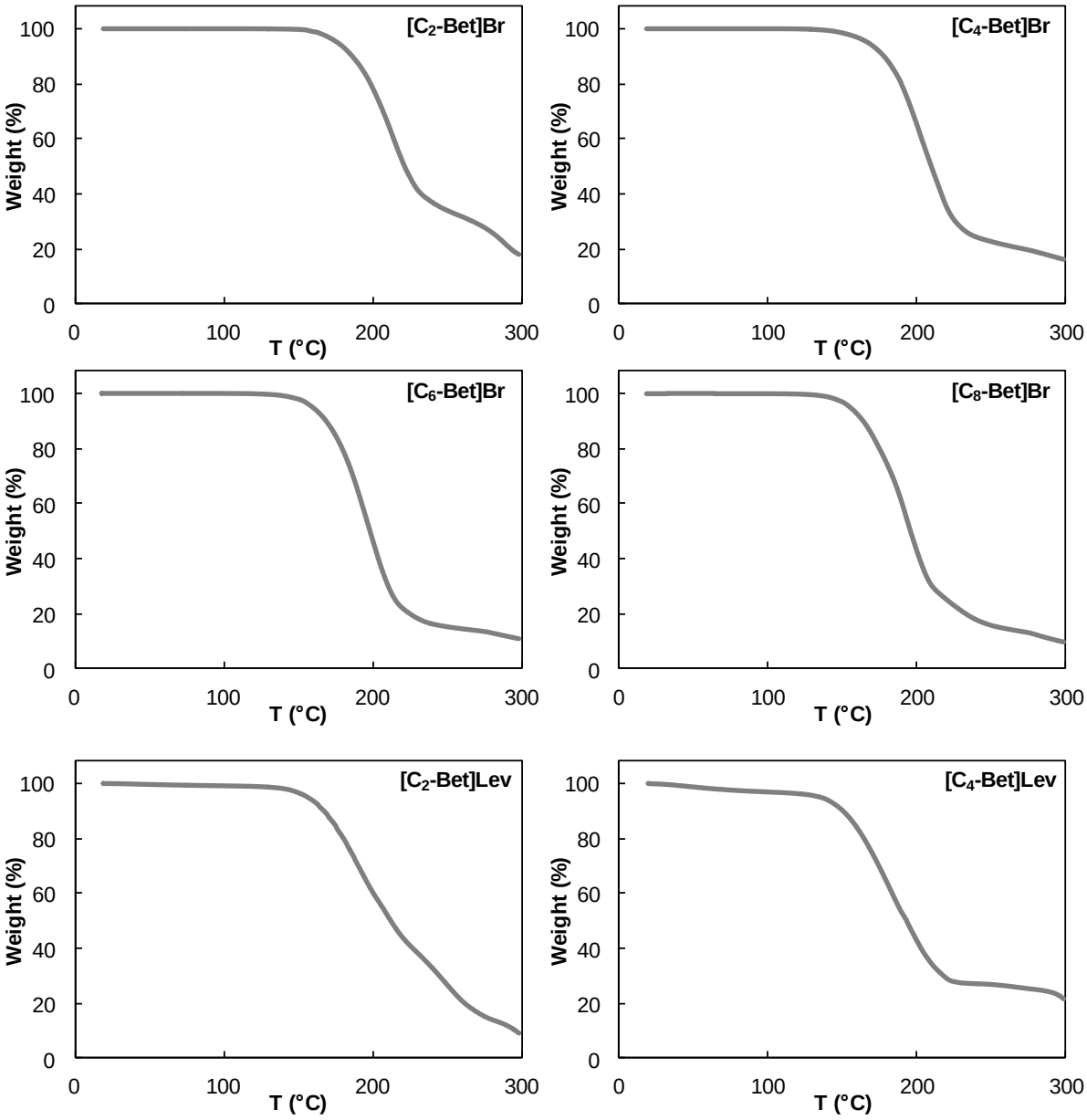

Carnitine ester compounds:

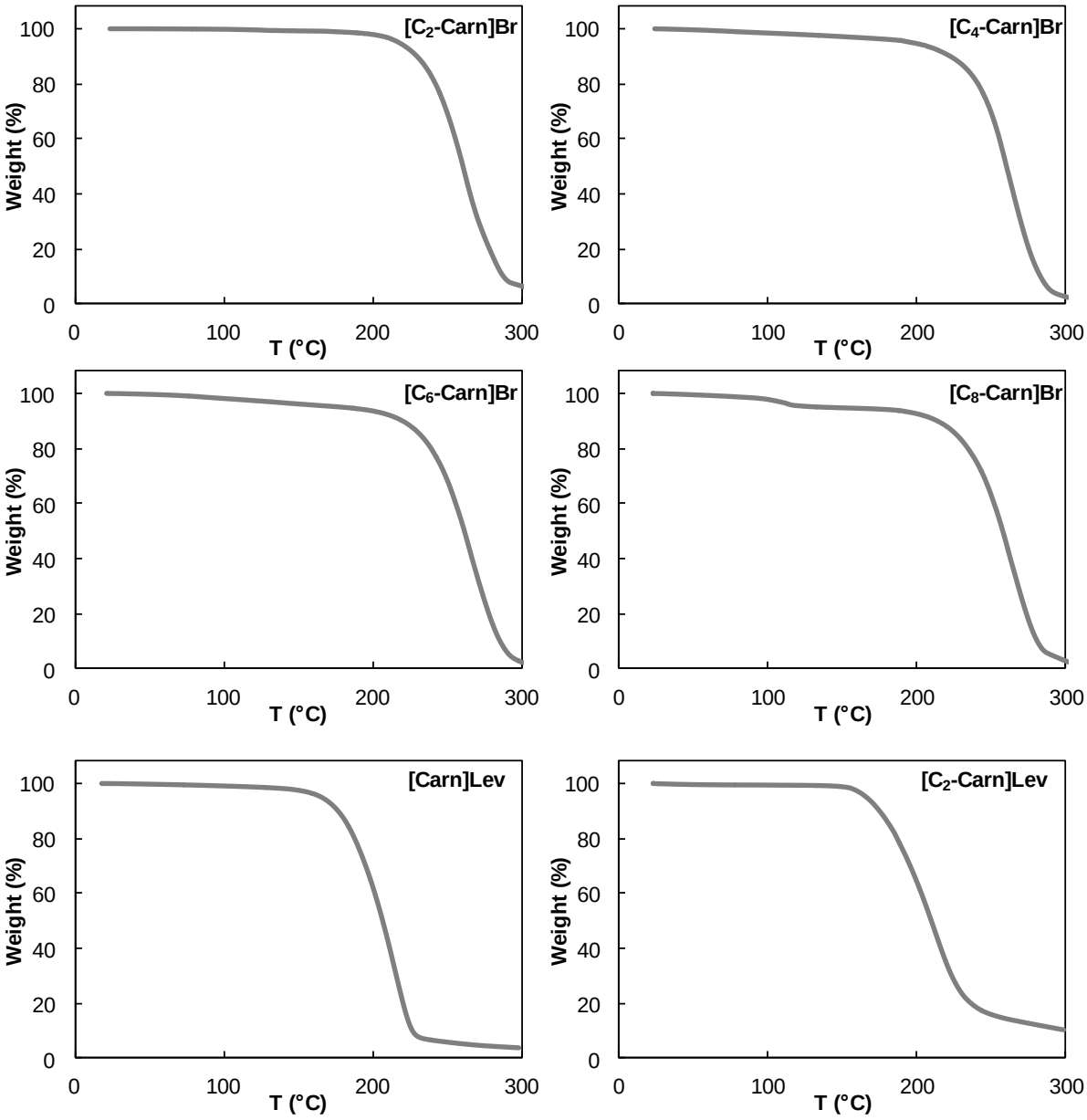

2.2) Differential scanning calorimetry (DSC)

Thermal transitions were determined by differential scanning calorimetry (DSC) as already described in the ***experimental section of chapter 2***. The DSC-curves (exo up) of **choline-, betaine- and carnitine-derivatives** are shown in the following:

Choline ether compounds:

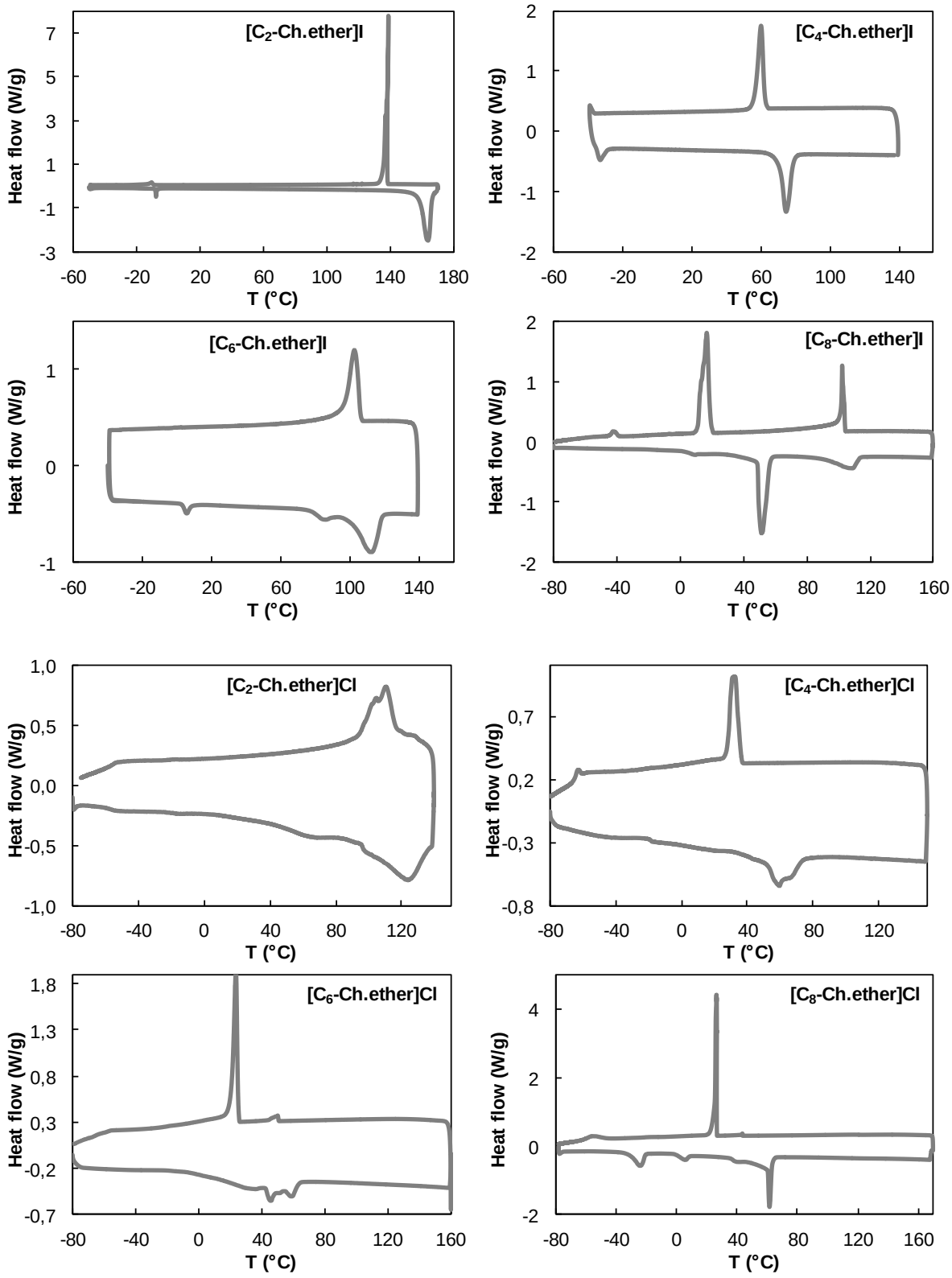

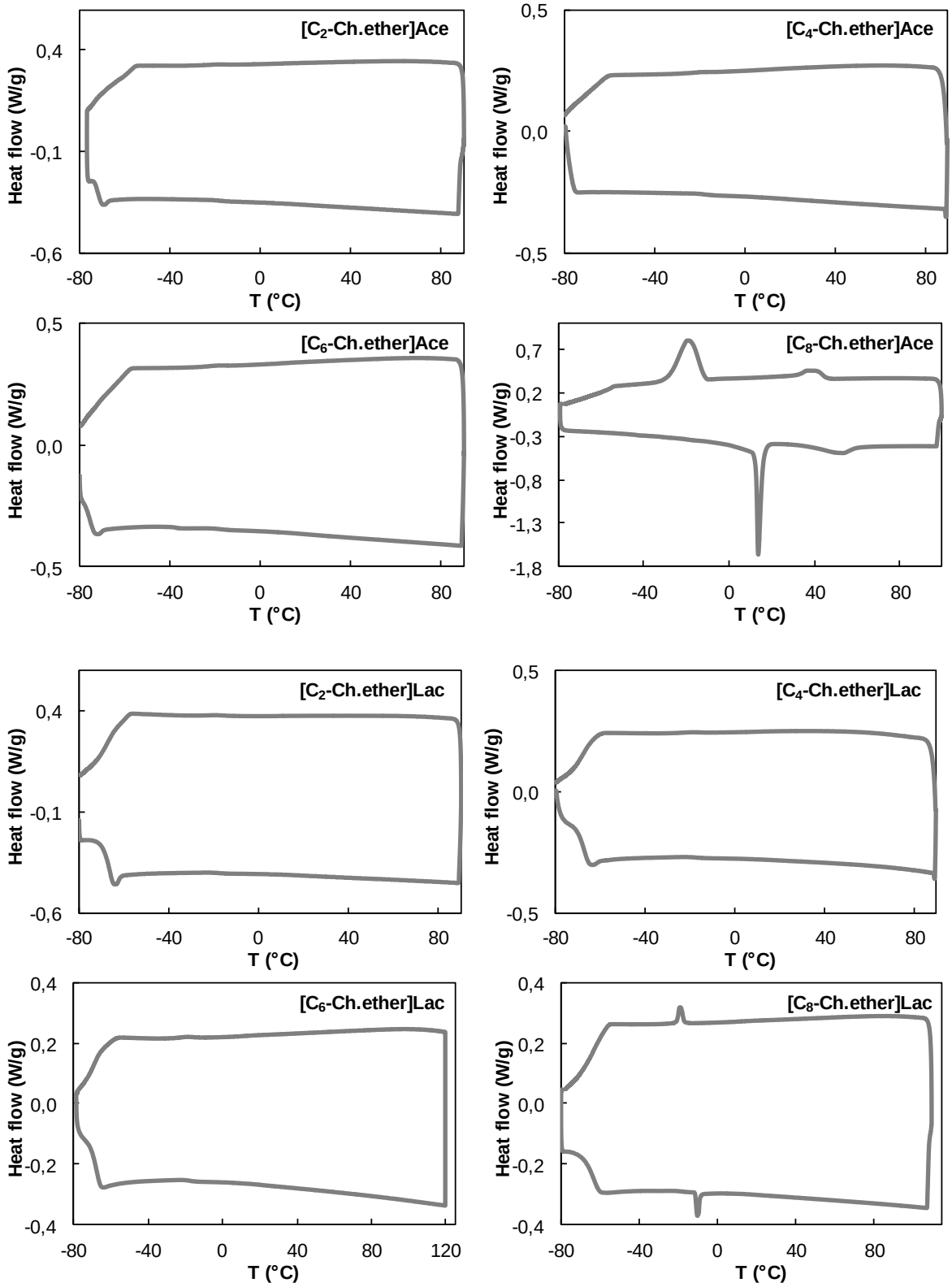
[C2-Ch.ether]Ace
[C4-Ch.ether]Ace
[C6-Ch.ether]Ace
[C8-Ch.ether]Ace
[C2-Ch.ether]Lac
[C4-Ch.ether]Lac
[C6-Ch.ether]Lac
[C8-Ch.ether]Lac
Heat flow (W/g)
T (°C)

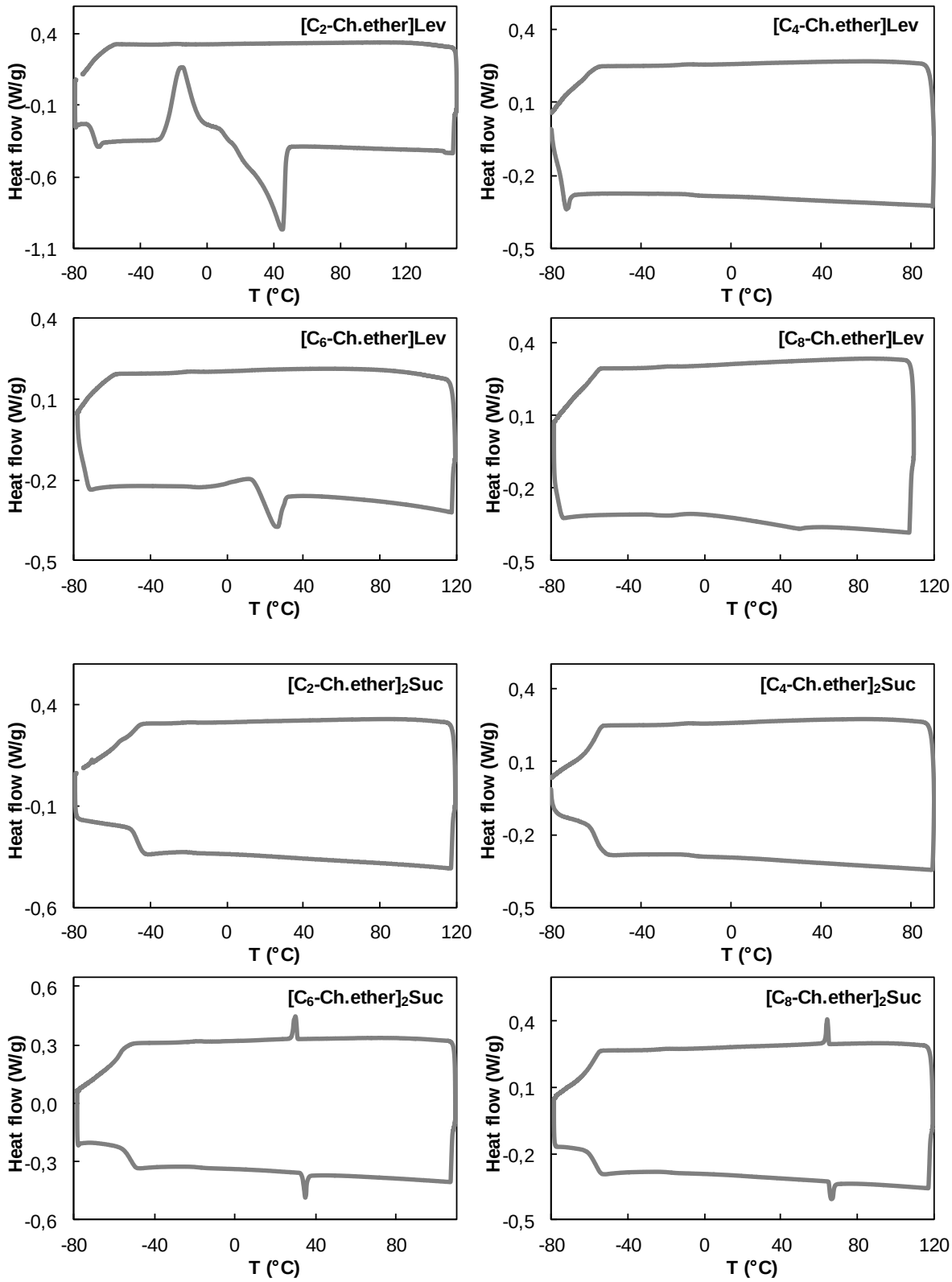
[C2-Ch.ether]Lev
[C4-Ch.ether]Lev
[C6-Ch.ether]Lev
[C8-Ch.ether]Lev
[C2-Ch.ether]2Suc
[C4-Ch.ether]2Suc
[C6-Ch.ether]2Suc
[C8-Ch.ether]2Suc
Heat flow (W/g)
T (°C)

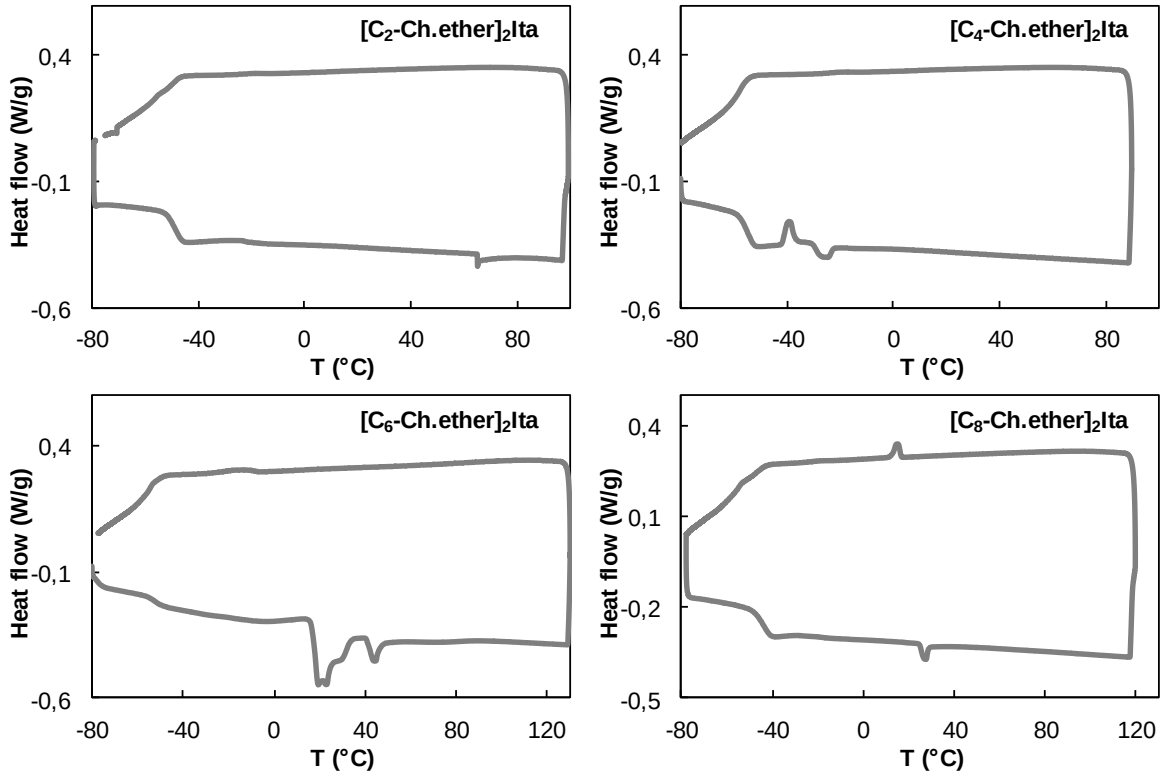

Betaine ester compounds:

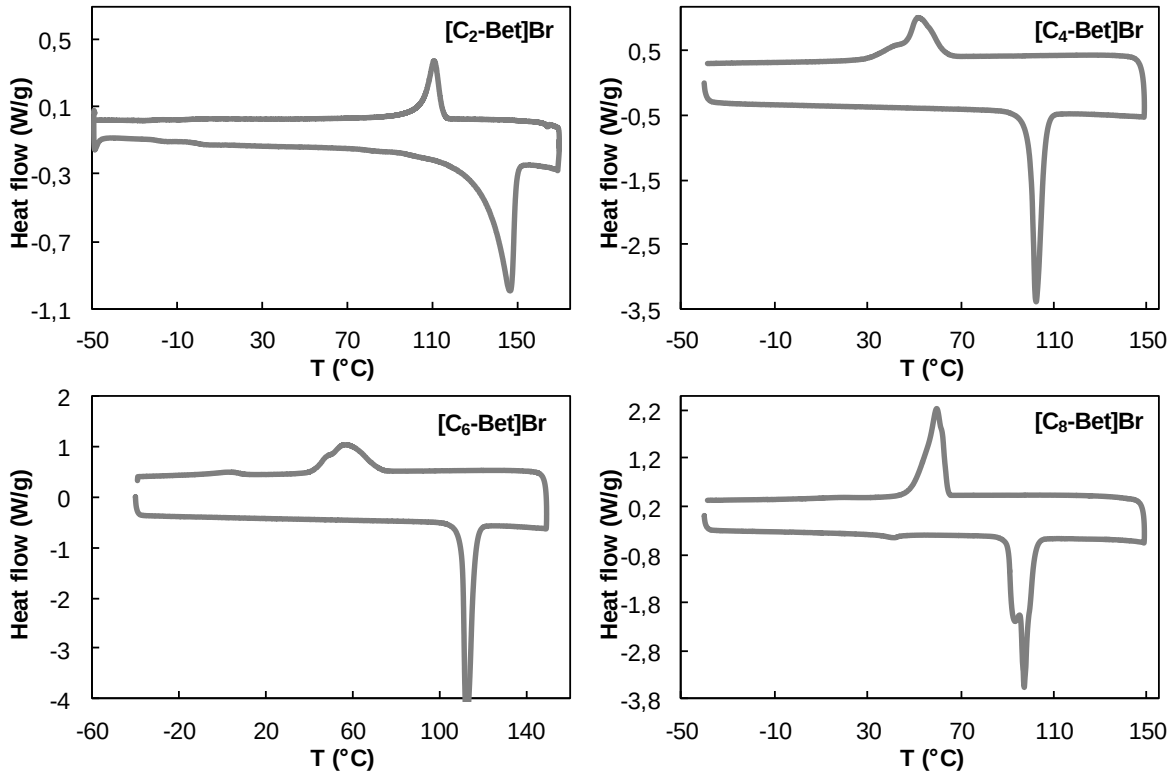

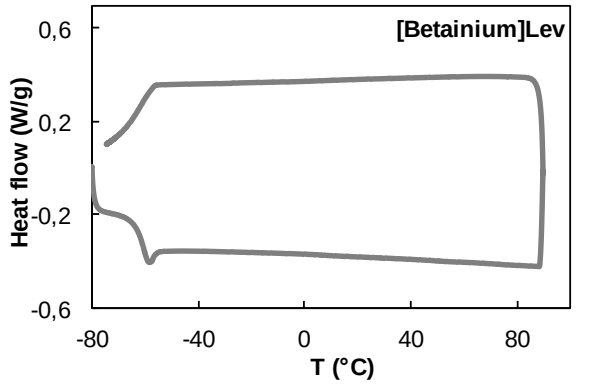

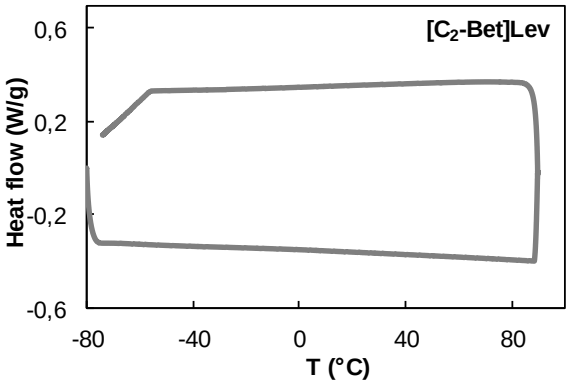

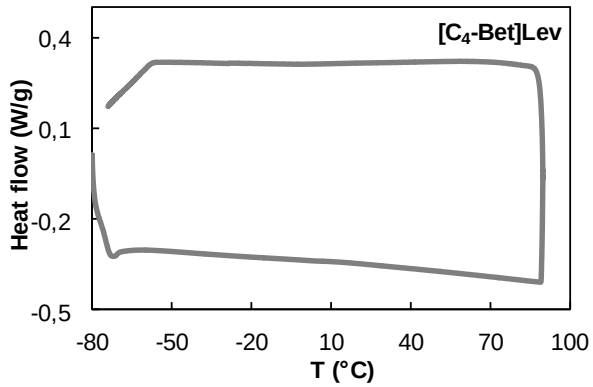

Carnitine ester compounds:

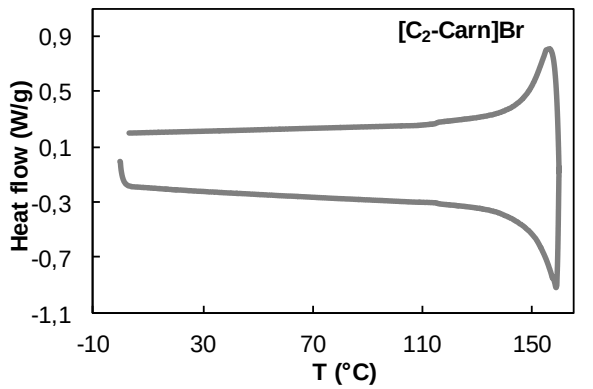

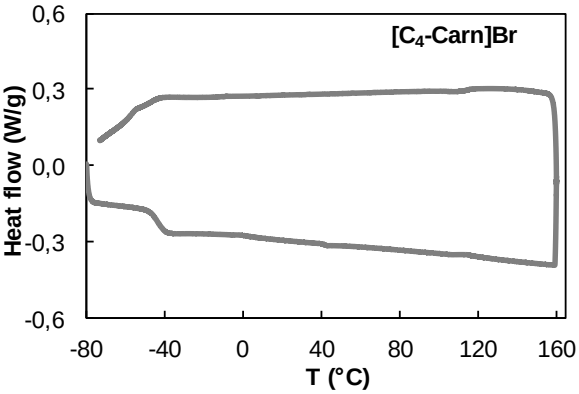

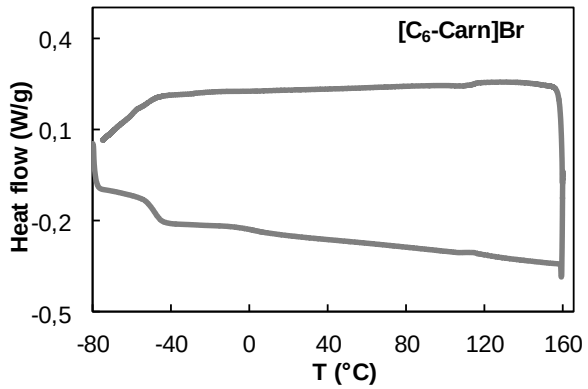

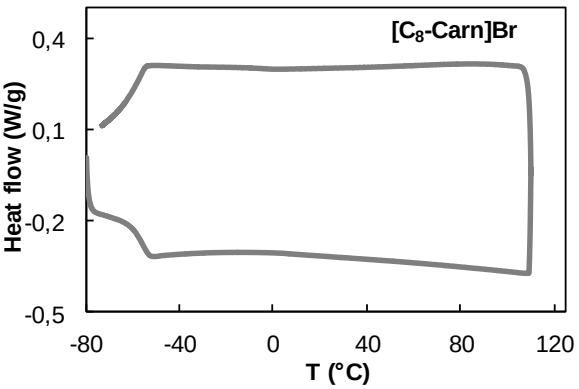

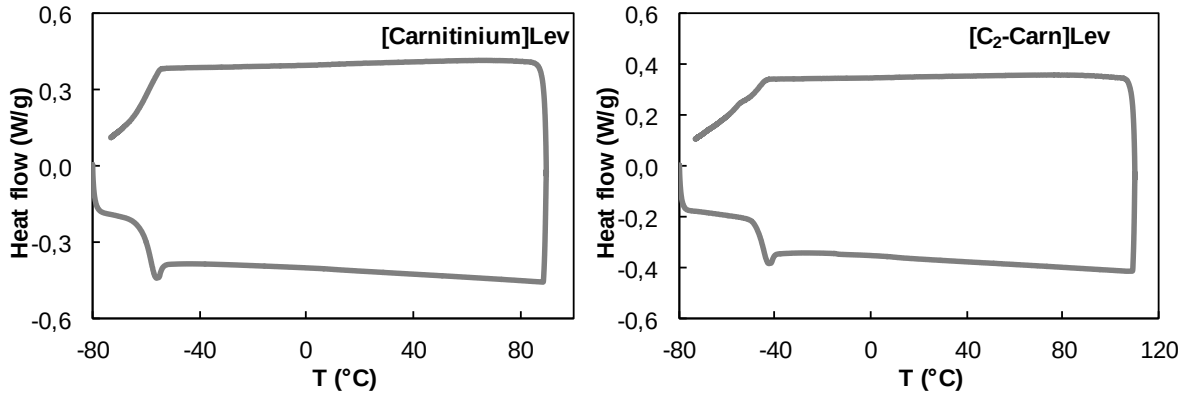

2.3) Viscosity

Viscosity measurements were carried out with the same method as described in the ***experimental section of chapter 2***.

Table 3.15 Dynamic viscosity η for choline ether levulinate ILs at 25, 40, 60, and 80 °C.

Compounds	η (Pa·s)			
	25 °C	**40 °C**	**60 °C**	**80 °C**
[C_2-Ch.ether][Lev]	0.182	0.083	0.046	0.035
[C_4-Ch.ether][Lev]	0.213	0.100	0.050	0.036
[C_6-Ch.ether][Lev]	0.299	0.145	0.078	0.053
[C_8-Ch.ether][Lev]	0.388	0.152	0.067	0.040

2.4) Tensiometry

The surface tension measurements of aqueous solutions of **choline-, betaine- and carnitine-derivatives** as a function of concentration were carried out due to the same procedure as described in the ***experimental section of chapter 2***.

2.5) Hydrotropic behavior

The solubilization of the hydrophobic dye Disperse Red 13 was measured due to the same procedure as described in the ***experimental section of chapter 2***.

3.) Biodegradation

The tests of biodegradation were carried out in the laboratory of Dr. Stefan Stolte at the *Department Sustainable Chemistry* (University of Bremen, Germany). The biological oxygen demand (BOD) of the substance was determined for 28 days using a BOD measurement system (OxiTop©, thermostatically controlled from WTW GmbH, Weilheim, Germany) with two

replicates for each test substance. Activated sewage sludge from aeration tank of wastewater treatment plant treating mostly domestic sewage in Delmenhorst (Germany) was used as a source of inoculum.

The oxygen consumption was determined manometrically. Biodegradation of the test substance was calculated by the biological oxygen uptake (BOD) for the test substance (corrected by the oxygen demand of the blank samples) with respect to the theoretical oxygen demand (ThOD) of the substance and the amount of substance present in the sample. In **Figure 3.28**, the results for the biodegradation tests are illustrated.

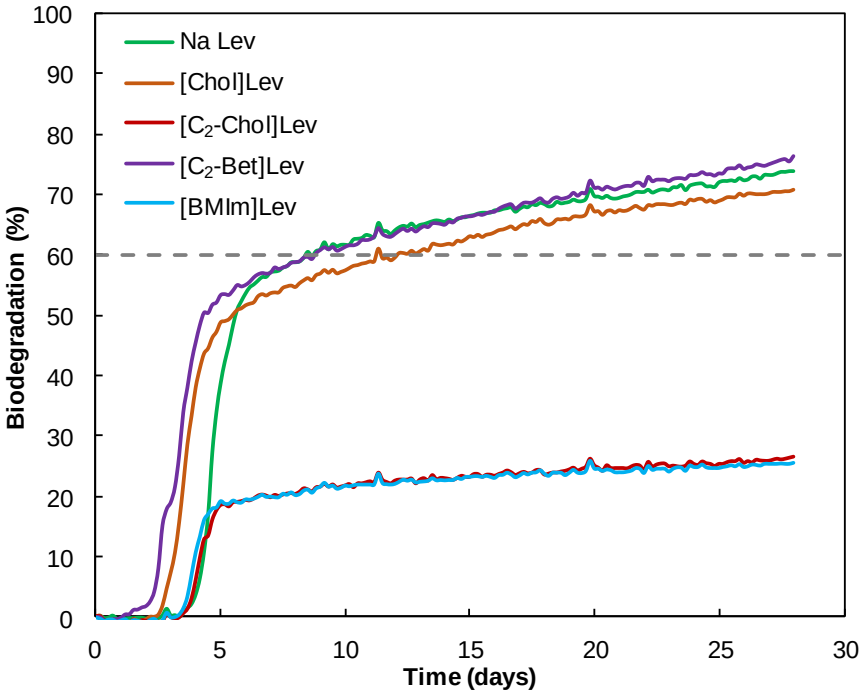

Figure 3.28 Biodegradation as a function of time of levulinate compounds during 28 days.

4.) Toxicity

All the investigations on toxicities were carried out by Marta Markiewicz in the laboratory of Dr. Stefan Stolte at the *Department Sustainable Chemistry* (University of Bremen, Germany).

4.1) Ecotoxicty test with "Daphnia magna"

The 48 h acute immobilization test with the crustacean D. magna was assessed using the commercially available Daphtoxkit F (MicroBioTest Incorporation, Gent, Belgium) referred to in OECD guideline 202 (Organisation for Economic Cooperation and Development OECD, 2004). The detailed description of how to perform this assay is given in the supplier's standard operational procedure (MicroBioTest Inc., 1996b). The tests with neonates less than 24 h old, obtained by the hatching of ephippia, were performed at 20 °C in the dark. 5 pre-fed animals

were incubated with the toxicants in a volume of 10 mL of mineral medium. For each test 5 different concentrations of the ionic liquids in 4 parallels and 4 controls were investigated. All the experiments were performed twice. The numbers of immobilised organisms were checked after 24 and 48 h.

4.2) Cytoxicty tests with IPC-81

The cytotoxicity assay using the WST-1 reagent. Briefly, promyelotic rat cells from the IPC-81 cell line are incubated for 4 h in 96-well plates with 2-(4-iodophenyl)-3-(4-nitrophenyl)-5-(2,4-disulfophenyl)-2H-tetrazolium monosodium salt (WST-1) reagent. Each plate contained blanks (no cells) and controls (no toxicant). The cell viability assays were generally carried out with a 1 : 1 dilution series. Each dose response curve was recorded for at least 9 parallel dilution series on three different 96-well plates from two different days. Positive controls with carbendazim were checked in regular intervals.

5.) Solubilization of biopolymers

The solubilization experiments of biopolymers (*e.g.* cellulose, chitin, lignin, xylan, starch) have been carried out due to the same procedure as already described for cellulose in the ***experimental section of chapter 2***. The standard deviation of the results is ±0.2 wt%.

Table 3.16 Solubility of biopolymers (cellulose, chitin, lignin, xylan, starch) in Lev-ILs at 90-100 °C.

IL	$S_{Cellulose}$ (wt%)	S_{Chitin} (wt%)	S_{Lignin}(wt%)	S_{Xylan}(wt%)	S_{Starch}(wt%)
[Mono-C_4]Lev	1.5	0	4.3	11.4	12.4
[Di-C_4]Lev	10	0	4.7	9.0	13.8
[BMIm]Lev	0	0	9.3	10.3	12.6
[Chol]Lev	0	0	6.9	8.9	0
[C_2-Chol]Lev	10	0	7.0	9.0	12.5
[Bet]Lev	0	0	6.1	0	0
[C_2- Bet]Lev	0	0	0	0	0
[Carn]Lev	0	0	6.9	0	0
[C_2- Carn]Lev	0	0	2.1	0	0

CHAPTER 4 – Deep eutectic solvents (DES) based on renewable compounds

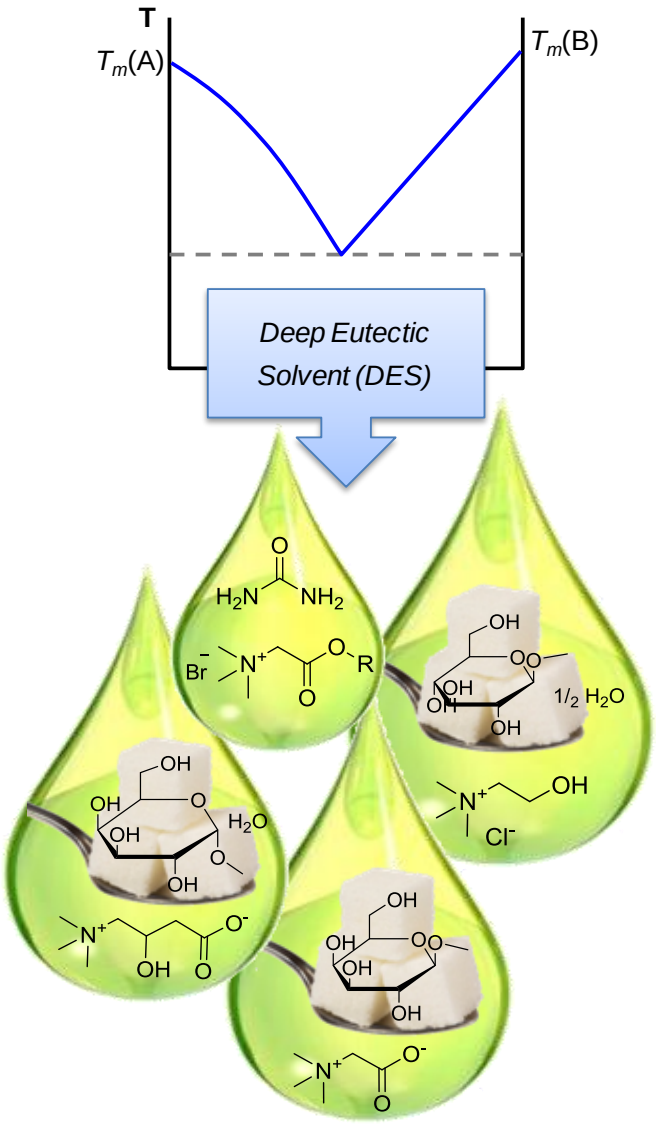

4.1 Introduction

Deep eutectic solvents (DESs) based on naturally sourced compounds represent a recent class of alternative and "green" solvents. The theory of their formation between hydrogen bond donor (HBD) and hydrogen bond acceptor (HBA) compounds, and further background information have already been described in ***chapter 1***. For the formation of DES, the choice of both compounds is an essential step, thus biosourced quaternary ammonium as HBAs and sustainable HBDs are preferred to form "green" solvents (**Figure 4.1**).

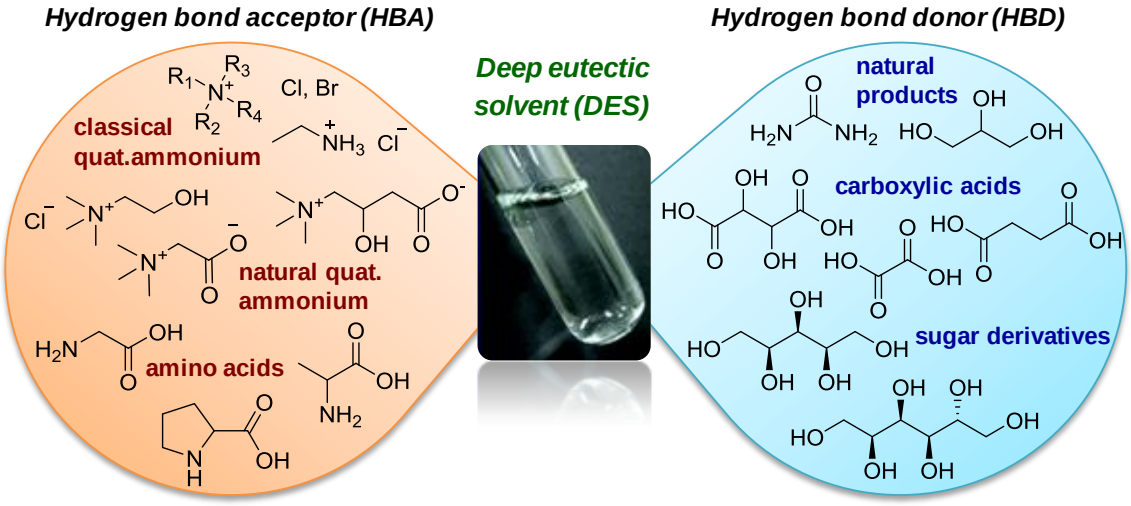

Figure 4.1 Some examples for HBAs and HBDs which can be combined for DES formation.

A first part in this study has been devoted to classical and natural quaternary ammonium combined with urea as a typical compound for DES formation. The quaternary ammonium described in ***chapter 2*** and the betaine derivatives from ***chapter 3*** were thus investigated for DES formation.

The second part of the study deals with natural quaternary ammonium, such as choline, betaine and carnitine, in combination with sugar-derivatives. Therefore, the type of sugar and the chain lengths connected to the anomeric-oxygen were varied with the aim to study these structural effects on DES formation. Hereby, the central aspect is the use of sugar-derivatives which could be obtained from natural resourced biopolymers, even from cellulose.

The main objective was the creation of "green" solvents which comprise easy preparation as the main advantage over more conventional ILs. These mixtures could be applied on polymer solubilization, but additionally their design for melting point diminution, which leads to easier handling of some compounds, is conceivable.

4.2 DES with urea

Urea, or carbamide, which plays an important role in the metabolism of nitrogen-containing compounds in mammals, is a well-known natural compound for DES formation (**Figure 4.2**).

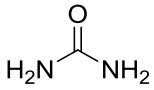

Figure 4.2 Structure of urea.

The most famous DES with urea is its mixture with choline chloride with a 2:1 mole ratio and a melting point of 12 °C.[146] Further 2:1-mixtures of urea with a variety of quaternary ammonium salts of the form $R^1R^2R^3R^4N^+X^-$ are reported in the literature (some examples in **Table 4.1**). The depression of the freezing point was explained by interactions between urea molecules and the anion of the quaternary ammonium. It was highlighted that the melting point of the mixtures decreased with reduced symmetry of the cation. The examples in **Table 4.1** comprise the following order for freezing points with the variation of the quaternary ammonium counter anion: $F^- < NO_3^- < Cl^- < BF_4^-$, which arises from their hydrogen bond strength. Furthermore, the mixture of urea with a smaller ammonium, $EtNH_3Cl$, has been studied resulting in an eutectic mixture ($EtNH_3Cl$ - urea 1:1.5) with a freezing point of ca. 30°C.[152]

Table 4.1 Freezing points of 2:1-mixtures of urea with quaternary ammonium salts.[146]

R^1	R^2	R^3	R^4	X^-	T_f (°C)
C_2H_5	C_2H_5	C_2H_5	C_2H_5	Br	113
CH_3	CH_3	CH_3	C_2H_4OH	Cl	12
CH_3	CH_3	CH_3	C_2H_4OH	BF_4	67
CH_3	CH_3	CH_3	C_2H_4OH	NO_3	4
CH_3	CH_3	CH_3	C_2H_4OH	F	1
CH_3	CH_3	$PhCH_2$	C_2H_4OH	Cl	-33
CH_3	CH_3	C_2H_5	C_2H_4OH	Cl	-38
CH_3	CH_3	C_2H_5	$PhCH_2$	Cl	26
CH_3	CH_3	C_2H_5	C_2H_4OAc	Cl	-14
CH_3	CH_3	CH_3	C_2H_4Cl	Cl	15
CH_3	$PhCH_2$	C_2H_4OH	C_2H_4OH	Cl	-6
CH_3	CH_3	CH_3	C_2H_4F	Cl	55

For the formation of completely bio-based DES, some natural quaternary ammonium have already been used to replace classical ones. Betaine monohydrate combined with urea resulted in a mixture with an eutectic point, which was reported in two different studies: T_m at 10 °C (molar ratio (betaine:urea) 2:1)[280], or T_m at 27 °C (molar ratio (betaine:urea) 15:85)[145]. The

mixture of L-carnitine and urea (2:3; wt:wt) was reported as DES with T_m at 74 °C.[281] This low-melting composition was used as a solvent for organic reactions, *e.g.* Heck cross-coupling, Diels-Alder cycloaddition. Furthermore, urea was combined with guanidine salts (guanidine hydrochloride, guanidine thiocyanate) forming eutectic mixtures at 67 mol-% urea, as for choline chloride-urea-mixtures.[282] The melting points are described at 58 °C for the guanidine hydrochloride-urea DES and at 47 °C for the DES with guanidine thiocyanate.

4.2.1 Structural aspects and preparation of mixtures

For the preparation of DESs in combination with **urea**, we have used classical quaternary ammonium, namely **[DiC$_4$]Cl** and **[DiC$_4$]Br** (from ***chapter 2***). Furthermore, "greener" quaternary ammonium were tested, such as betaine ester derivatives **[C$_n$-Bet]Br** (n = 2, 4, 6, 8; from ***chapter 3***).

The preparation of DESs is easy as described by Abbott *et al.*[141] Therefore, both components were mixed at defined mole ratios and stirred under heating until a homogeneous liquid was formed. The liquids were cooled down slowly (ca. 1 °C·min^{-1}), and the freezing point was taken at the temperature at which the first solid began to crystallize. Some systems were not only studied visually, but also by DSC measurements. Details are given in the ***experimental section***.

4.2.1.1 Simple quaternary ammonium mixtures with urea

For the formation of DES, synthesized dibutyldimethyl ammonium bromide **[DiC$_4$]Br** and chloride **[DiC$_4$]Cl** (***chapter 2***) have been mixed with urea in different molar ratios. In **Figure 4.3**, the phase diagram of quaternary ammonium salts with urea is shown. Both mixtures show an eutectic point at a 1:1 molar ratio of urea with the [DiC$_4$] salt, which was detected by DSC-measurements (curves are shown in the ***experimental section***).

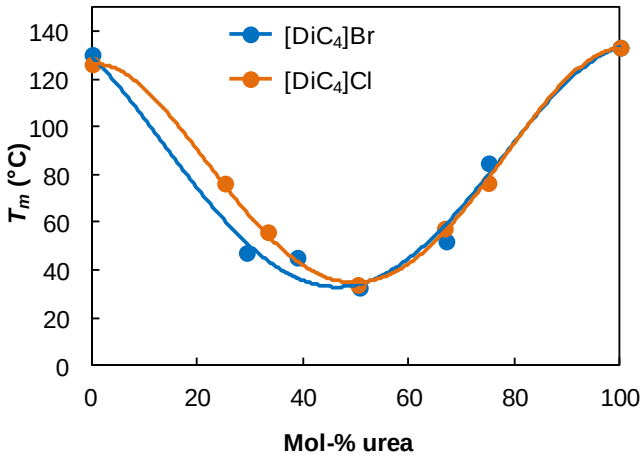

Figure 4.3 Melting point T_m of quaternary ammonium salt / urea mixtures as a function of composition.

Both **[DiC$_4$]X** (with X = Cl, Br) salts combined with urea show a similar behavior for DES formation. The eutectic point appeared for a 1:1 molar ratio at 32-33 °C. Thus, in this case the structuration is the same independently of the halogenide counter anions.

4.2.1.2 Betaine-derivatives with urea

To replace classical quaternary ammonium compounds with biosourced HBAs, betaine-derivatives **[C$_n$-Bet]Br** (with n = 2, 4, 6, 8; from ***chapter 3***) have been used in this part of the work. Therefore, their ability to form DESs in combination with urea was studied, and the results are shown in **Figure 4.4**. The melting points T_m of betaine ester / urea mixtures at different ratios have been determined by DSC-measurements (curves are shown in the ***experimental section***). The T_m of pure **[C$_2$-Bet]Br** is much higher than the T_m of pure **[C$_n$-Bet]Br** with longer alkyl chains, *i.e.* n = 4, 6, 8, because for this short-chain derivative the ionic character seems to be predominant resulting in an elevated T_m. However, the derivatives with longer chains (n = 4, 6, 8) have much lower T_m for the probable reason that their most important interactions are weak, *e.g.* van der Waals and dipolar ones.

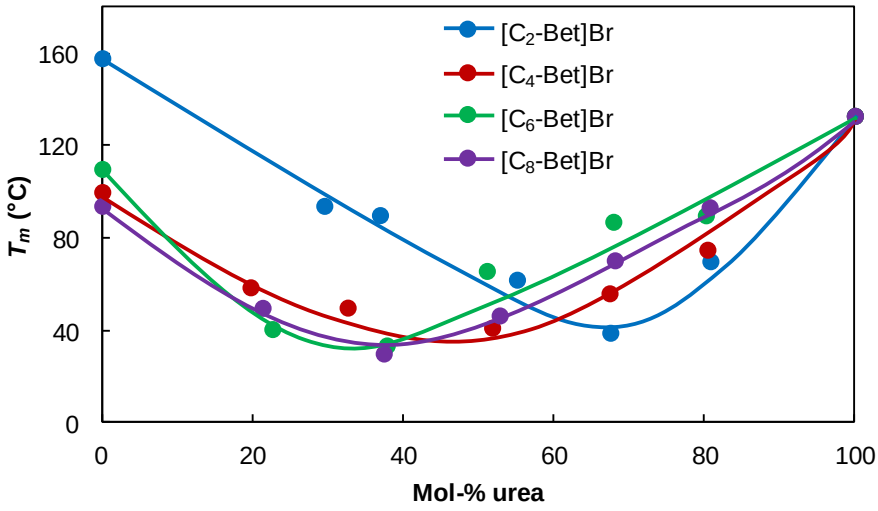

Figure 4.4 Melting point T_m of betaine ester bromides [C$_n$-Bet]Br (n = 2, 4, 6, 8) / urea mixtures as a function of composition.

All the tested **[C$_n$-Bet]Br** result in eutectic mixtures with urea with a T_m much lower than the pure compounds. The 1:2 mixture of **[C$_2$-Bet]Br** with urea had a T_m of 39 °C, the 1:1 mixture of **[C$_4$-Bet]Br** with urea had a T_m of 41 °C, **[C$_6$-Bet]Br** and **[C$_8$-Bet]Br** have formed eutectic mixtures with only 37 mol-% of urea with T_m of 33 and 30 °C respectively. Comparing the composition of DES with **[C$_n$-Bet]Br** and urea, a correlation between the mol-% of urea and the chain length n of the betaine ester bromides was noticed. As shown in **Figure 4.5**, the shorter the chain length n the more urea was necessary for DES formation. This phenomenon could be attributed to the stronger interactions between the quaternary ammonium with shorter alkyl

chains (n = 2, 4) and its counter anion (Br) due to its high ionic character. Accordingly, the anion is less accessible for interactions with the HBD, *i.e.* urea, which results in eutectic mixtures with a higher amount of urea compared to quaternary ammonium with longer alkyl chain lengths (n = 6, 8).

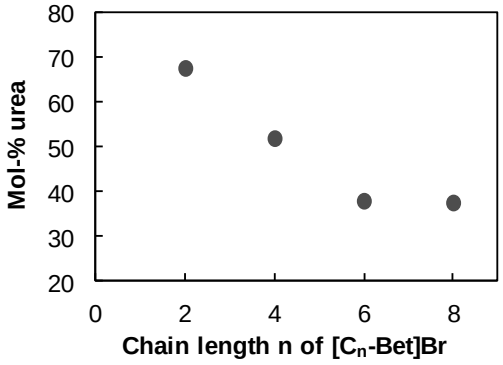

Figure 4.5 Comparison of the composition of [C_n-Bet]Br / urea mixtures at the eutectic point (≈ 40 °C) as a function of the chain length n.

4.2.2 Physicochemical properties of DESs based on urea

The thermal phase transitions of the DESs based on urea were investigated to identify the ratio giving an eutectic point and its melting temperature T_m. Furthermore, the viscosities of some systems were determined as an important property of solvents.

4.2.2.1 Melting temperature

The comparison of the eutectic mixtures of quaternary ammonium as HBA with urea as HBD is shown in **Table 4.2**.

Table 4.2 Molar ratios and melting points T_m of urea-mixtures with different quaternary ammonium hydrogen bond acceptors (HBAs).

HBA	Molar ratio (HBA : urea)	T_m (°C)
[DiC_4]Br	1 : 1	32
[DiC_4]Cl	1 : 1	33
[C_2-Bet]Br	1 : 2	39
[C_4-Bet]Br	1: 1	41
[C_6-Bet]Br	2 : 1	33
[C_8-Bet]Br	2 : 1	30

The DESs with simple quaternary ammonium [DiC_4]X (X = Br, Cl) form both 1:1 eutectics with urea with a similar T_m at 32 and 33 °C, thus the anion did not have a large influence on these

systems. The T_m of DES with [C_n-Bet]Br (with n = 2, 4, 6, 8) were in the range of 30 to 41 °C with only little differences, and it shows the following order: [C_2-Bet]Br ≈ [C_4-Bet]Br > [C_6-Bet]Br > [C_8-Bet]Br. However, the molar ratio (HBA : urea) changed with the alkyl chain length n of betaine ester bromides from 1:2 (for n = 2) to 1:1 (for n = 4) and up to 2:1 (for n = 6, 8). As already mentioned before, the amount of urea to obtain an eutectic mixture indicates the strength of interactions between the quaternary ammonium cation and its counter anion. Or more precisely, for short chain betaine ester, which have strong interactions between the cation and anion due to their predominant ionic character, more urea is necessary for the formation of DESs. Quaternary ammonium with mediocre alkyl chain lengths, *i.e.* [DiC_4], [C_4-Bet], result in DESs 1:1 ratios with urea. However, DESs based on quaternary ammonium with longer alkyl chain lengths contain less amount of urea as HBD because of the weaker interactions between the quaternary ammonium cation and its counter anion, and therefore higher accessibility of the anion to enter into intermolecular interactions with urea, and therefore DES formation.[283]

4.2.2.2 Viscosity

Generally, viscosity of DESs is found in the same range as for ILs. The viscosity of a fluid is linked to the free volume and the probability of finding holes of suitable dimensions for the solvent species (hole theory). So, the reason for relatively high viscosity of DESs or ILs is that the solvent species have relatively large radii (ca. 3-4 Å) compared to the average radius of the voids (ca. 2 Å).[152] For giving an example, Abbott *et al.* reported viscosities of 169 cP for the 1:2 mixture of choline chloride with urea and 2214 cP for acetylcholine chloride with urea at 40 °C.[152]

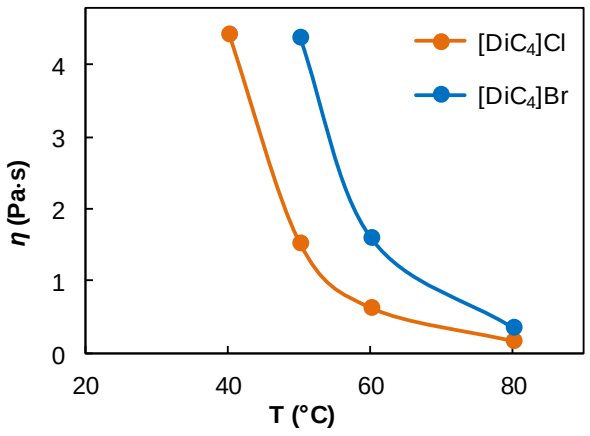

Figure 4.6 Dynamic viscosities η of 1:1 mixtures of urea and quaternary ammonium [DiC_4]X (X = Cl, Br) at different temperatures.

The dynamic viscosity η of quaternary ammonium-urea mixtures was studied at their eutectic composition with a rheometer (cone-plate geometry) as an example for DESs based on urea. As shown in **Figure 4.6**, both 1:1 mixtures with [DiC_4]-salts were very viscous at low temperatures,

i.e. 4.4 Pa·s at 40 °C for [DiC_4]Cl and the same viscosity for [DiC_4]Br at 50 °C. Below 80 °C, the DES with [DiC_4]Br is much more viscous than the one with [DiC_4]Cl. The viscosity of DESs decreased with higher temperatures, as expected.[284] At 80 °C, the viscosity amounted 0.17 Pa·s for [DiC_4]Cl and 0.35 Pa·s for [DiC_4]Br. The higher viscosity for the urea DES with [DiC_4]Br compared to [DiC_4]Cl could be attributed to the higher volume of the Br-anion, and thus the mobility is more hindered.

Abbot *et al.* have proposed the optimization of DES viscositites by reducing the free volume of both compounds.[152] Furthermore, strong intermolecular interactions should be reduced to design lower viscosities.[145] Thus, less viscous liquids could be obtained using small quaternary ammonium cations, *i.e.* ethylammonium, and fluorinated HBDs such as trifluoroacetamide.

4.3 DES with sugar-derivatives

Sugars or sugar derivatives are natural compounds which could be used as HBD compounds for DES formation due to their strong ability to build hydrogen bonds.[285] Carbohydrates form the main part of biomass (ca. 75 wt%), and they can be used directly after hydrolysis of poly- or oligosaccharides to monosaccharides.[286] Several low-melting mixtures based on sugars, which have already been reported in literature, are shown in **Table 4.3**.

König *et al.* reported DESs (or low-melting mixtures) based on sugars or sugar alcohols, urea and inorganic salts as solvents for Diels-Alder reactions[165] and further organic reactions[166] (*e.g.* hydrogenation, Suzuki reaction). In this study, natural carbohydrates (*i.e.* fructose, glucose, mannose, sorbitol, mannitol, maltose, lactose, α-cyclodextrin) were combined with urea or *N*,*N*-dimethylurea (and an inorganic salt) resulting in mixtures with $\boldsymbol{T_m}$ in the range of 65 to 89 °C. The same research group developed similar carbohydrate urea mixtures as reaction medium for the formation of sugar-urea-derivatives.[286]

Low-melting sugar-based mixtures have been reported as combinations of choline chloride with fructose or glucose at different ratios (**Table 4.3**) with $\boldsymbol{T_m}$ in the range of 10 to 37 °C for DES with fructose, and 14 to 44 °C for DES with glucose.[285,287] The most important properties of these DESs were studied, and some potential applications were proposed, such as for reactions, pharmaceutical uses, or for extraction processes. Further sugars and sugar-based polyols were combined with choline chloride giving DESs, such as glucose, mannitol, xylitol, sorbitol and isosorbide.[145,150]

Another study on natural DESs deals with numerous combinations of abundant cellular constituents (primary metabolites) such as sugars, sugar alcohols, amino acids, organic acids and choline derivatives (some examples are shown in **Table 4.3**).[155] This work was based on the theory that ILs and DES could play an important role as a liquid phase for solubilizing, storing, and transporting non-water soluble metabolites in living cells and organisms. As a result, a huge number of RT-liquid mixtures based on natural compounds were found.

Kunz *et al.* have recently reported ternary sugar-based mixtures based on choline chloride, urea and glucose or sorbitol.[151] These mixtures (**Table 4.3**) result in low glass transitions in the range of -37 to -29 °C. The most important physicochemical properties of these low-melting mixtures were determined, and they are proposed to find application as “greener” alternative to ILs due to their high biodegradability and low toxicity.

Table 4.3 Overview for DES or low-melting mixtures with sugars or sugar-derivatives.

Carbohydrate	**Urea**	**Salt**	T_m **(°C)**
Fructose (60 %) [a]	Urea (40 %)	/	65 [165]
Fructose (70 %)	Urea (20 %)	NaCl (10 %)	73 [166]
Fructose (40 %)	*N*,*N*-dimethylurea (60 %)	/	80 [166]
Glucose (50 %)	Urea (40 %)	$CaCl_2$ (10 %)	75 [165]
Glucose (60 %)	Urea (30 %)	NaCl (10 %)	78 [166]
Mannose (30 %)	*N*,*N*-dimethylurea (70 %)	/	75 [165]
Sorbitol (70 %)	Urea (20 %)	NH_4Cl (10 %)	67 [165]
Sorbitol (40 %)	*N*,*N*-dimethylurea (60 %)	/	77 [165]
Mannitol (50 %)	*N*,*N*-dimethylurea (40 %)	NH_4Cl (10 %)	89 [166]
Maltose (50 %)	*N*,*N*-dimethylurea (40 %)	NH_4Cl (10 %)	73 [165]
Lactose (50 %)	*N*,*N*-dimethylurea (40 %)	NH_4Cl (10 %)	88 [166]
α-Cyclodextrin (30 %)	*N*,*N*-dimethylurea (70 %)	/	77 [165]

[a] w/w percent of the compounds in the mixture

Carbohydrate	**Quaternary ammonium**	**Molar ratio**	T_m **(°C)**
Fructose	Choline chloride	1 : 1	20 [287]
Fructose	Choline chloride	1.5 : 1	13 [287]
Fructose	Choline chloride	2 : 1	10 [287]
Fructose	Choline chloride	2.5 : 1	37 [287]
Glucose	Choline chloride	1 : 1	31 [285]
Glucose	Choline chloride	1 : 1.5	24 [285]
Glucose	Choline chloride	2.5 : 1	44 [285]
Glucose	Choline chloride	2 : 1	14 [145], 15 [285]
Mannitol	Choline chloride	1 : 1	108 [145]
Xylitol	Choline chloride	1 : 1	liq at RT [150]
Sorbitol	Choline chloride	1 : 1	liq at RT [150]
Isosorbide	Choline chloride	2 : 1	liq at RT [150]
Xylose	Choline chloride	1 : 2, 1 : 3	liq at RT [155]
Sorbose	Choline chloride	2 : 5, 1 : 1	liq at RT [155]
Mannose	Choline chloride	2 : 5	liq at RT [155]
Galactose	Choline chloride	2 : 5	liq at RT [155]
Maltose	Choline chloride	1 : 4	liq at RT [155]
Sucrose	Betaine	1 : 2	liq at RT [155]

Mannose	Betaine	2 : 5	liq at RT [155]
Compounds for mixture		**Molar ratio**	**T_g (°C)**
Glucose – Urea – Choline chloride		1 : 1 : 1	-28.6 [151]
Glucose – Urea – Choline chloride		1 : 2 : 1	-25.9 [151]
Sorbitol – Urea – Choline chloride		1 : 1 : 1	-37.3 [151]
Sorbitol – Urea – Choline chloride		1 : 2 : 1	-35.2 [151]

4.3.1 Structural aspects of sugar-derivatives

For the formation of entirely "green" DESs based on sugar-derivatives in this study, natural-resourced quaternary ammonium, such as choline, betaine and carnitine, were used. As already mentioned in ***chapter 3***, all these three natural salts are mainly found in food, such as vegetables and meat.

The sugar-derivatives, which were chosen as biosourced HBDs for DES formation in this study, were composed of sugars with ether as functional group on the anomeric carbon. **Figure 4.7** gives an overview for the most common sugar-monomers and their different forms (pyranose, furanose with α- or β-configuration) which could be modified by etherification of the anomeric hydroxy-group with different chain-lengths R (R = C_nH_{2n+1}).

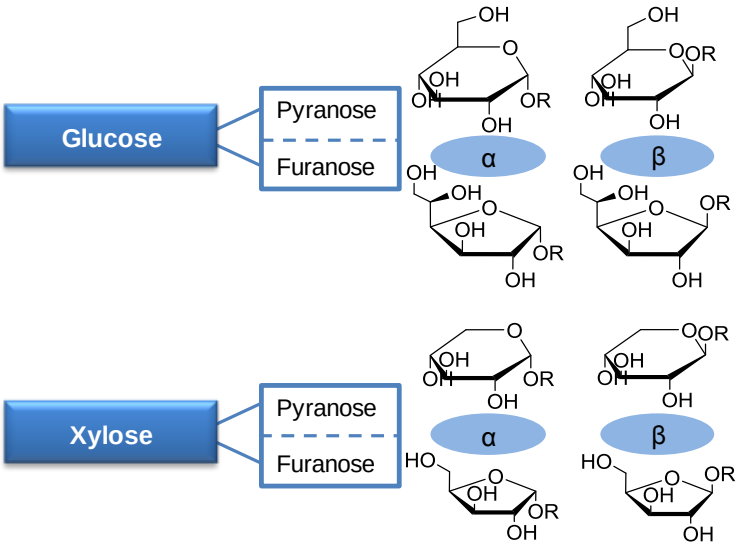

Figure 4.7 Overview for sugar-derived structures.

The used bio-resourced sugar-derivatives were either commercially available or synthesized by Dr. Sinisa Marinkovic at A.R.D, as shown in **Figure 4.8**. The form of synthesized products was influenced by reaction time, so the furanoside was the major product after 5 h reflux, while the pyranoside form was predominant after longer reaction times (*e.g.* one night). But in all cases,

the synthesized sugar-derivatives were mixtures including furanoside- and pyranoside-forms and additionally, α- and β-positions at the anomeric carbon. As these sugar isomers have highly similar structural characteristics, such as polarity and size, their separation very complicated or even impossible.[288] Thus, we have used these synthesized sugar-derivatives without further purification or separation of isomers.

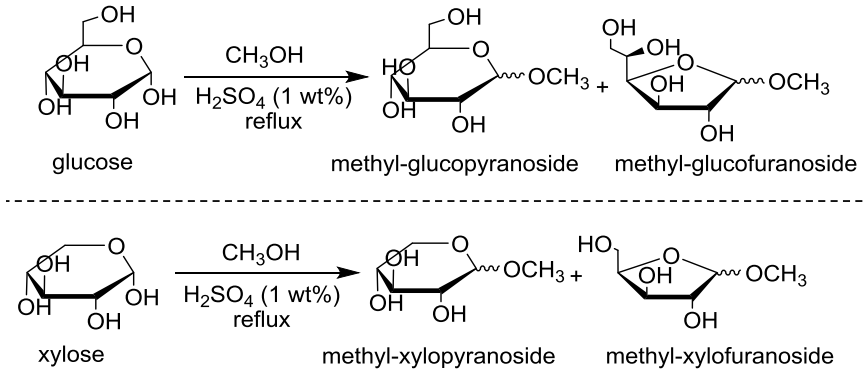

Figure 4.8 Synthesis of sugar-derivatives.

Table 4.4 gives an overview for the different ether-functionalized sugar-derivatives in this study. Some commercially available derivatives (**Table 4.4**, products **[1]** – **[7]**) were applied in DES systems in comparison to synthesized products (**Table 4.4**, products **[8]** – **[17**]; reaction time for synthesis is indicated with *5 h* or *night*), which consists of a mixture of the pyranoside-, furanoside-, α- and β-forms.

The pure products **[1]** – **[7]** are all white powders at RT with a defined melting temperature T_m. Their T_m were in the range between 102 and 196 °C with the following order: **[3]** > **[7]** > **[5]** ≥ **[2]** > **[4]** > **[1]** > **[6]**. Unfortunately, the differences of T_m cannot be explained based on their structural differences, *e.g.* sugar-monomer (glucose, xylose, mannose, arabinose) or position of the anomeric carbon (α, β). However, the sugars **[1]** and **[6]** have notably lower T_m because of their hydration water in the structure which decreases melting points due to the reduced lattice energy.[283]

However, the synthesized sugars **[8]** – **[16]** are pastes or very viscous liquids at RT with low glass transition temperatures T_g which were analyzed by DSC measurements. The graphs of thermal analysis (TGA and DSC) of synthesized sugar-derivatives are shown in the ***experimental section***. As these compounds contain mixtures of four different forms, the synthesized sugar-derivatives have not a crystalline structure, thus they are in an amorphous state with a low glass transition T_g in the range of -42 to -27 °C instead of a melting temperature T_m. The synthesized sugar **[17]** was the only one which was solid at RT and showed a melting temperature T_m (57 °C). The crystallization as thermal phase transition shows that this sugar is not amorphous, which indicates the presence of only one isomeric structure.

Table 4.4 Sugar-derivatives ([1] – [7]: commercial; [8] – [17]: synthesized by A.R.D.) with their melting point T_m or glass transition temperature T_g and molecular structure.

	Sugar-derivative	**Structure**	T_m **(°C)**
[1]	Methyl-β-D-glucopyranoside hemihydrate	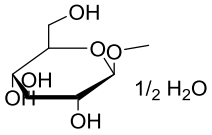	107-111
[2]	Methyl-α-D-glucopyranoside	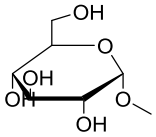	165-169
[3]	Methyl-α-D-mannopyranoside	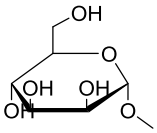	187-196
[4]	Methyl-β-D-xylopyranoside	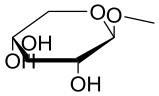	155-158
[5]	Methyl-β-L-arabinopyranoside	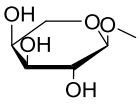	169
[6]	Methyl-α-D-galactopyranoside monohydrate	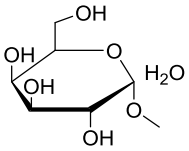	102-103
[7]	Methyl-β-D-galactopyranoside	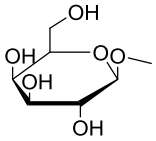	175-179
[8]	Methyl-glucopyranoside (*5 h*)	Synthesized sugar-derivatives are mixtures of: - pyranoside, - furanoside, - α, - β.	T_g -27
[9]	Methyl-xylopyranoside (*5 h*)		T_g -40
[10]	Methyl-glucopyranoside (*night*)		T_g -32
[11]	Methyl-xylopyranoside (*night*)		T_g -42
[12]	Ethyl-glucopyranoside (*5 h*)		T_g -41
[13]	Ethyl-xylopyranoside (*5 h*)		T_g -47
[14]	Ethyl-glucopyranoside (*night*)		T_g -35
[15]	Ethyl-xylopyranoside (*night*)		T_g -39
[16]	Butyl-glucopyranoside (*5 h*)		T_g -41
[17]	Butyl-xylopyranoside (*5 h*)		57

4.3.2 Low-melting mixtures

Mixtures of natural choline chloride, betaine, carnitine HBAs with commercially available and synthesized sugar-derivatives as HBDs have been prepared in different molar ratios due to the described preparation method of DES (**Figure 4.9**). Because of the huge number of combinations, the melting behavior and states of the mixtures were observed only visually.

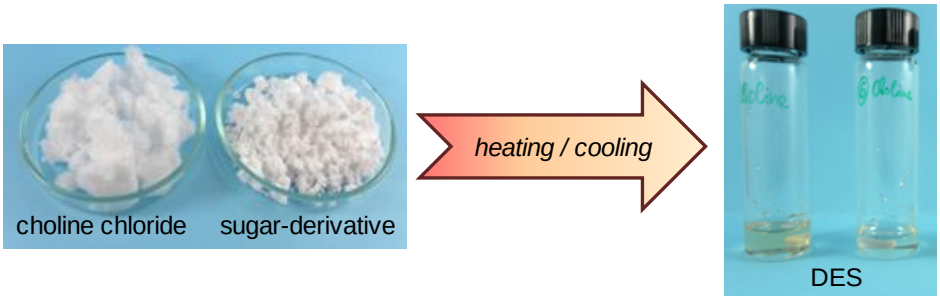

Figure 4.9 Preparation of DES based on choline chloride and sugar-derivatives.

4.3.2.1 Choline chloride as HBA

The natural quaternary ammonium choline chloride was combined with all the different sugar-derivatives **[1]** – **[17]** in different molar ratios, such as 25, 33, 50, 66 and 75 mol-% of sugar (the table with visually observed melting temperatures for each mixture is given in the ***experimental section***).

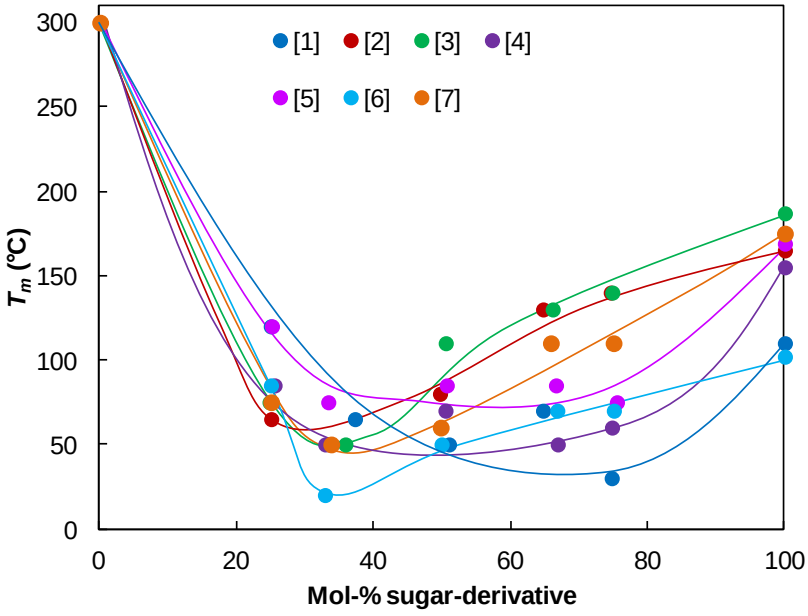

Figure 4.10 Melting points T_m of choline chloride / sugar-derivatives ([1] – [7]) mixtures as a function of their composition.

Most of the tested choline chloride mixtures with commercially available sugar-derivatives (**[1]** – **[7]**) show an eutectic point (**Figure 4.10**). However, the mixture of choline chloride with sugar

[5] (Methyl-β-L-arabinopyranoside) had the least pronounced eutectic with the lowest T_m at 75 °C. Comparing all the low-melting compositions, especially the mixtures with sugars **[1]** (Methyl-β-D-glucopyranoside hemihydrates) and **[6]** (Methyl-α-D-galactopyranoside monohydrate) show large depressions of melting points. This phenomenon could be attributed to the presence of crystallization water (monohydrate, hemihydrate) in the sugar-derivative which could play a role for loose-packed structuration resulting in low melting points, as water of hydration decreases melting points because it reduces the lattice energy.[283]

In **Figure 4.11**, the melting points of choline chloride mixtures with synthesized sugar derivatives **[8]** - **[17]** are illustrated at different molar ratios. The melting points T_m of pure sugars are not represented in the graph because they have low glass transition temperatures T_g, as already explained before. All the synthesized sugar-derivatives comprise the same effect of T_m depression on choline chloride, resulting in low-melting mixtures which are liquid at RT (represented as T_m 25 °C in **Figure 4.11**; the grey dashed line shows the general trend for all mixtures). Thus, the recrystallization of choline chloride during the process of cooling is hindered due to the different isomeric forms of sugar, which end up in a large network of structuration. These mixtures are not really DESs because the sugars are amorphous without melting temperatures. The phenomenon could be rather seen as a kind of solubilization of choline chloride in a mixture of isomeric sugar-derivatives (pyranoside, furnaoside, α, β).

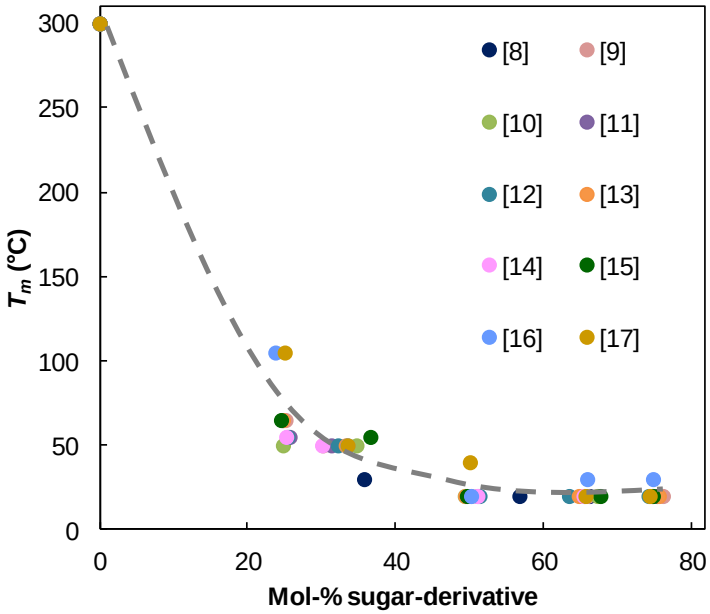

Figure 4.11 Melting points T_m of choline chloride / sugar-derivatives ([8] – [17]) mixtures as a function of their composition.

4.3.2.2 Betaine as HBA

Betaine was used as biosourced HBA for DES formation with the sugar-derivatives **[1]** – **[17]** in different molar ratios, such as 25, 33, 50, and 66 mol-% of sugar (the table with visually observed melting temperatures for each mixture is given in the ***experimental section***). The results for the mixtures with commercial sugars (**[1]** – **[7]**) are shown in **Figure 4.12**. The eutectic mixtures with the lowest melting temperatures (T_m around 30 – 45 °C) are found for betaine combined with the sugars **[1]**, **[4]**, **[6]** and **[7]**. As already mentioned for mixtures with choline chloride, sugars containing crystallization water, **[1]** and **[6]**, (hemi-, monohydrate) seems to be particularly efficient for the formation of DESs. For the other efficient sugar-derivatives, we cannot discern special structural reasons for their behavior. Some sugar-derivatives (i.d. **[2]**, **[3]**, **[5]**) have only a poor effect of melting temperature diminution on betaine. These mixtures have their lowest T_m around 65 – 75 °C for compositions with a molar ratio of 1:1.

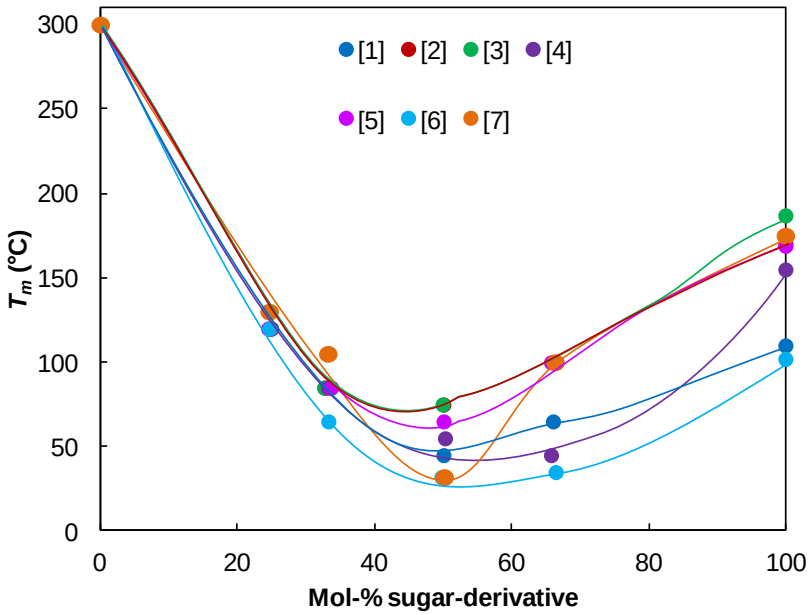

Figure 4.12 Melting points T_m of betaine / sugar-derivatives ([1] – [7]) mixtures as a function of their composition.

The results for low-melting mixtures of betaine with synthesized sugar-derivatives **[8]** - **[17]** are shown in **Figure 4.13** (the grey dashed line shows the general trend for all mixtures). All of the combinations result in eutectic mixtures for a proportion of sugar ≥ 50 mol-% with T_m around 30 °C or being liquid at RT. Thus, the synthesized sugar-derivatives, containing different isomeric forms, hold the same effect on betaine as already observed and described for choline chloride.

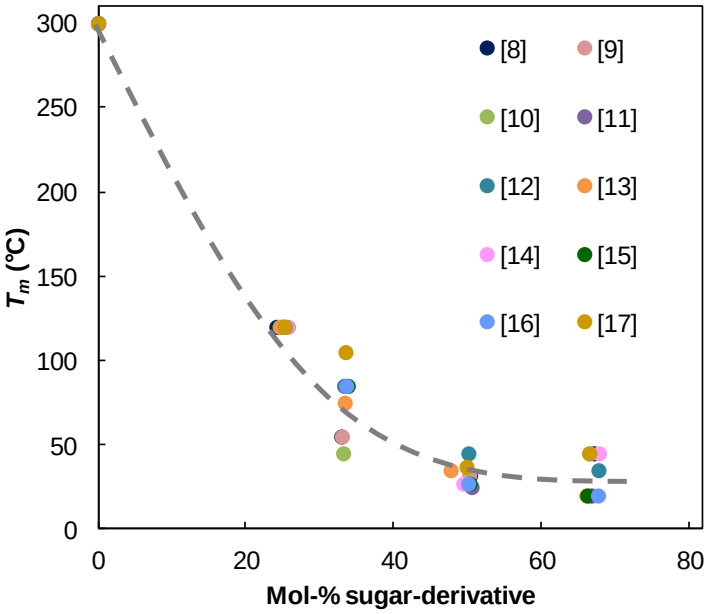

Figure 4.13 Melting points T_m of betaine / sugar-derivatives ([8] – [17]) mixtures as a function of their composition.

4.3.2.3 Carnitine as HBA

Similar as for choline chloride and betaine, the naturally resourced carnitine was combined with sugar-derivatives to study their behavior for DES formation. The results for mixtures of carnitine with the commercial sugar-derivatives **[1]** – **[7]** are presented in **Figure 4.14**.

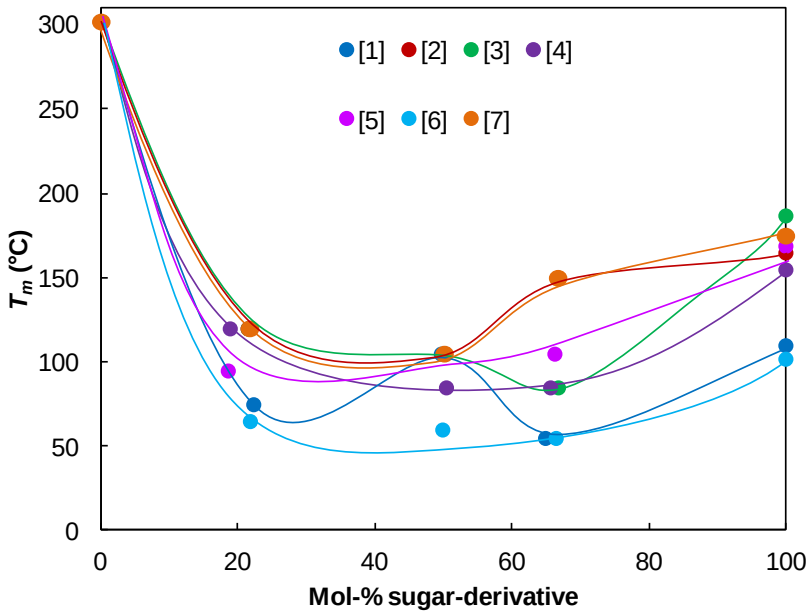

Figure 4.14 Melting points T_m of carnitine / sugar-derivatives ([1] – [7]) mixtures as a function of their composition.

The compositions with the lowest eutectic point ($\boldsymbol{T_m}$ 55 °C) were obtained with the sugars **[1]** and **[6]**. As already described for DES with choline chloride or betaine, the high efficiency of both

sugar-derivatives could be explained with the presence of crystallization water in their structure, thus the structures of mixtures are loose-packed and hold low T_m. The other sugar-derivatives had only a slight effect for melting temperature reduction of carnitine, resulting in mixtures with T_m around 85 - 105 °C.

The systems formed of carnitine and the synthesized sugar-derivatives **[8]** – **[17]** are given in **Figure 4.15** (the grey dashed line shows the general trend for all mixtures). Similar to the results for choline chloride and betaine, all mixtures show a strong effect of melting temperature depression of carnitine, which is seen as solubilization of quaternary ammonium in the isomeric sugar-derivative-mixture. Here, we have found T_m around 35 - 65 °C for systems with a molar ratio of 1:1, and even lower T_m (around 25 – 55 °C) with 66 mol-% sugar.

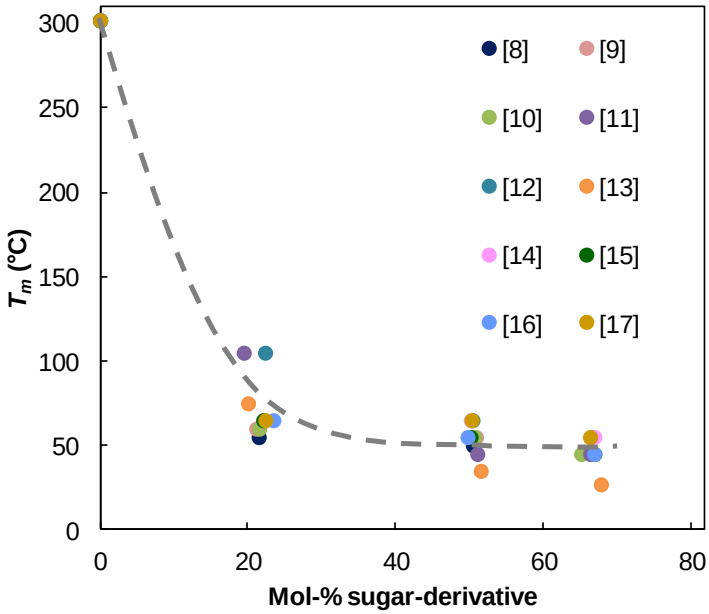

Figure 4.15 Melting points T_m of carnitine / sugar-derivatives ([8] – [17]) mixtures as a function of their composition.

4.3.3 Physicochemical properties of DESs based on sugar-derivatives

The DESs based on sugar-derivatives were compared due to their molar ratios with the lowest melting temperature T_m. In addition, the viscosities of some systems were studied as an essential property of solvents.

4.3.3.1 Thermal properties

Table 4.5 gives the overview for all eutectic mixtures formed between natural quaternary ammonium (choline chloride, betaine, carnitine) as hydrogen bond acceptor (HBA) and sugar-derivatives as hydrogen bond donor (HBD). Their composition is given as molar ratio of HBA

and HBD with the melting temperature T_m which was determined visually. Here, only the mixtures based on commercially available sugars (**[1]** – **[7]**) are reported because they are considered as real DESs. However, mixtures with synthesized sugars (**[8]** – **[17]**) are seen as solubilization of quaternary ammonium in amorphous mixtures of sugar-derivative-mixtures composed of different isomers (furanoside, pyranoside, α, β).

Table 4.5 Molar ratios and melting points T_m of DES with choline chloride, betaine and carnitine as HBAs in combination with different sugar-derivatives as HBDs.

HBA	**HBD (sugar-derivative)**	**HBA : HBD** [a]	T_m **(°C)**
Choline chloride	[1] Methyl-β-D-glucopyranoside hemihydrate	3 : 1	30
Choline chloride	[2] Methyl-α-D-glucopyranoside	2 : 1	50
Choline chloride	[3] Methyl-α-D-mannopyranoside	2 : 1	50
Choline chloride	[4] Methyl-β-D-xylopyranoside	2 : 1	50
Choline chloride	[5] Methyl-β-L-arabinopyranoside	2 : 1	75
Choline chloride	[6] Methyl-α-D-galactopyranoside monohydrate	2 : 1	lq. at RT
Choline chloride	[7] Methyl-β-D-galactopyranoside	2 : 1	50
Betaine	[1] Methyl-β-D-glucopyranoside hemihydrate	1 : 1	45
Betaine	[2] Methyl-α-D-glucopyranoside	1 : 1	75
Betaine	[3] Methyl-α-D-mannopyranoside	1 : 1	75
Betaine	[4] Methyl-β-D-xylopyranoside	1 : 2	45
Betaine	[5] Methyl-β-L-arabinopyranoside	1 : 1	65
Betaine	[6] Methyl-α-D-galactopyranoside monohydrate	1 : 1	32
Betaine	[7] Methyl-β-D-galactopyranoside	1 : 1	32
Carnitine	[1] Methyl-β-D-glucopyranoside hemihydrate	1 : 2	55
Carnitine	[2] Methyl-α-D-glucopyranoside	1 : 1	105
Carnitine	[3] Methyl-α-D-mannopyranoside	1 : 2	85
Carnitine	[4] Methyl-β-D-xylopyranoside	1 : 1, 1 : 2	85
Carnitine	[5] Methyl-β-L-arabinopyranoside	1 : 1, 1 : 2	105
Carnitine	[6] Methyl-α-D-galactopyranoside monohydrate	1 : 2	55
Carnitine	[7] Methyl-β-D-galactopyranoside	1 : 1	105

[a] molar ratio

Nearly all of the sugar-based DES with choline chloride as HBA were formed at the molar ratio (**HBA : HBD**) of 2:1. With betaine, however, the main molar ratio for sugar DES was 1:1. For carnitine, we found both ratios 1:1 and 1:2, and for some mixtures even two eutectic points (with the sugars **[4]**, **[5]**). Nevertheless, the building principles are not simple to generalize.[143]

Different to normal chemical bonds, hydrogen bonds include different contact distances and binding energies, which depend not only on the donor and acceptor nature.

Generally, the melting point T_m of the sugar-based mixtures has the following trend due to the bio-resourced quaternary ammonium: **choline chloride < betaine < carnitine**.

4.3.3.2 Viscosity

The viscosity of liquids is one of the most important physicochemical properties for the evaluation of their potential for some applications. Two sugar-based DES-systems were studied as representative examples to give an idea of their rheological behavior, *i.e.* with sugar **[16]** as synthesized derivative and sugar **[6]** as pure, commercially available one (**Figure 4.16**).

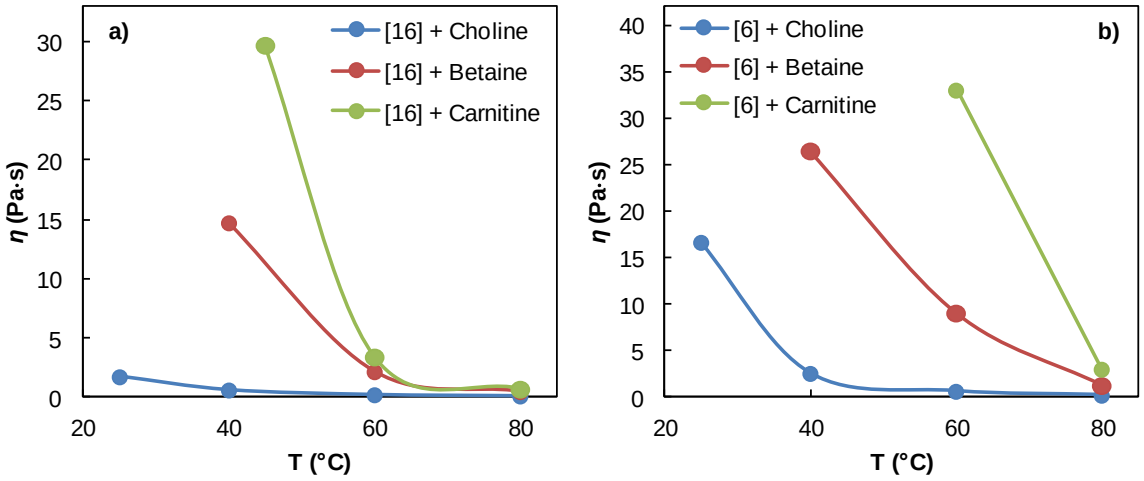

Figure 4.16 Dynamic viscosities η of DESs based on choline chloride, betaine, carnitine combined with **a)** the sugar [16], and **b)** the sugar [6] at different temperatures.

As already reported, viscosities of DESs are usually quite high compared to organic solvents due to its high interactions between the different species in the eutectic mixtures.[289] Comparing both sugar-mixtures, the general trend for dynamic viscosity η with different natural quaternary ammonium is as following: **choline chloride < betaine < carnitine** (table with the values is given in the ***experimental section***). This phenomenon could be based on the intermolecular interactions between sugar-derivatives and quaternary ammonium which are stronger for carnitine due to its carboxy- and free hydroxy-function, followed by betaine with its carboxylic group, followed by choline chloride which holds only a free hydroxyl-function.

The viscosity for sugar-DES based on the pure, commercially available derivative **[6]** is much higher for all three systems (choline chloride, betaine, carnitine) compared to the equivalent systems with the synthesized sugar-derivative **[16]**. The reason for this occurrence lies probably in the structure (mixture of isomers) and state (amorphous) of the sugar **[16]** which allows loose-packing and therefore higher mobility of the single species of the DES.

Table 4.6 gives the dynamic viscosities η of DESs composed of choline chloride and D-glucose with different molar ratios at 25 and 85 °C reported in the literature.[285]

Table 4.6 Dynamic viscosity η of DESs with different molar ratios of choline chloride to D-glucose from the literature.[285]

Abbreviation	Molar ratio	η (Pa·s) at 25 °C	η (Pa·s) at 85 °C
DES1	1 : 1	9.0371	0.2093
DES2	1.5 : 1	8.0000	0.1307
DES3	2 : 1	8.0451	0.0720
DES4	2.5 : 1	10.9100	0.1083

Comparing these values to the measured viscosities of choline chloride DESs with sugar-derivatives **[6]** and **[16]** shows that the presented results lie in between the system with the synthesized sugar **[16]** (1.720 Pa·s at 25 °C) and the system with the commercial sugar **[6]** (16.648 Pa·s at 25 °C). The inferior η of the mixture with **[16]** compared to D-glucose is based on its amorphous structure and therefore its loose packing, as already mentioned above in this section. The difference of η for DESs with sugar **[6]**, methyl-α-D-galactopyranoside monohydrate, and glucose could be explained by the slightly higher volume due to the introduced methyl-group, and therefore the molecular mobility is rather hindered.

4.4 Conclusions

DESs are innovative "green" solvents which could be real alternatives to classical organic solvents or ILs. Their "greenness" is based on the composition of naturally resourced compounds, easy and inexpensive preparation, and furthermore DESs are generally non-volatile, biodegradable and non- toxic. As they include diminution of melting temperatures at the eutectic point, these mixtures could be applied on optimization of processes and simplification of product handling.

In this project, we have focused on DESs based on two different types of biosourced hydrogen bond donors (HBDs): **urea** and **sugar-derivatives**. Urea, which is natural resourced, was combined with classical quaternary ammonium, and furthermore with betaine ester as sustainable alternative. Various sugar-derivatives, which are potentially available from cellulose transformation, were mixed with bio-based quaternary ammonium, such as choline chloride, betaine and carnitine.

Both **urea** DESs with the classical quaternary ammonium **[DiC$_4$]Br** or **[DiC$_4$]Cl** had their lowest melting temperature at 32 and 33 °C at 1:1-mixtures. Urea combined with betaine ester **[C$_n$-Bet]Br (n = 2, 4, 6, 8)** resulted in DESs with T_m in the range of 30 to 41 °C with molar ratios depending on the chain length n. Hereby, the molar ratio of urea decreased from 67% for n = 2 to 33% for n = 8 with increasing chain lengths of betaine ester.

Various **sugar-derivatives** containing an ether-functionalized anomeric carbon were studied for DES formation with **choline chloride**, **betaine** and **carnitine** as biosourced HBAs. One part of the study dealt with pure commercially available sugars resulting in moderate DES with the following general trend for T_m due to the used quaternary ammonium: **choline chloride** (liquid at RT up to 75 °C) **< betaine** (32 up to 75 °C) **< carnitine** (55 up to 105 °C). For the other part of the study, we have used synthesized, amorphous sugar-derivatives which were composed of four different isomeric structures (furanoside / pyransoide, α / β). All these products resulted in low-melting mixtures with choline chloride, betaine and carnitine which could be more seen as solubilization process than as real eutectics.

Experimental Section

1.) Preparation of DES

The preparation of DESs was carried out due to the experimental procedure described by Abbott *et al*.[141] DESs were prepared by stirring both compounds under heating (ca 120–150 °C) until a homogeneous colorless liquid was formed. The obtained liquids were cooled down slowly (rate of 1 °C·min^{-1}), and the freezing point was taken at the temperature when the first solid began to arise. The mixtures were prepared at defined mole ratios, *e.g.* 20, 33, 50, 67, and 80 Mol-% of HBD compound.

Freezing points (visual determination) of mixtures with choline chloride and sugar-derivatives:

	T_m (°C)				
	25% sugar	**33% sugar**	**50% sugar**	**66% sugar**	**75% sugar**
[1]	120	65	50	70	30
[2]	65	50	80	130	140
[3]	75	50	110	130	140
[4]	85	50	70	50	60
[5]	120	75	85	85	75
[6]	85	20 (lq)	50	70	70
[7]	75	50	60	110	110
[8]	65	30	20 (lq)	20 (lq)	20 (lq)
[9]	65	50	20 (lq)	20 (lq)	20 (lq)
[10]	50	50	20 (lq)	20 (lq)	20 (lq)
[11]	55	50	20 (lq)	20 (lq)	20 (lq)
[12]	55	50	20 (lq)	20 (lq)	20 (lq)
[13]	65	50	20 (lq)	20 (lq)	20 (lq)
[14]	55	50	20 (lq)	20 (lq)	20 (lq)
[15]	65	55	20 (lq)	20 (lq)	20 (lq)
[16]	105	50	20 (lq)	30	30
[17]	105	50	40	20 (lq)	20 (lq)

Freezing points (visual determination) of mixtures with betaine and sugar-derivatives:

	T_m (°C)			
	25% sugar	**33% sugar**	**50% sugar**	**66% sugar**
[1]	120	85	45	65
[2]	120	85	75	100
[3]	120	85	75	100
[4]	120	85	55	45
[5]	120	85	65	100
[6]	120	65	32	35
[7]	130	105	32	100
[8]	120	55	32	45
[9]	120	55	32	20 (lq)
[10]	120	45	27	45
[11]	120	85	25	20 (lq)
[12]	120	85	45	35
[13]	120	75	35	20 (lq)
[14]	120	85	27	45
[15]	120	85	27	20 (lq)
[16]	120	85	27	20 (lq)
[17]	120	105	37	45

Freezing points (visual determination) of mixtures with carnitine and sugar-derivatives:

	T_m (°C)		
	20% sugar	**50% sugar**	**66% sugar**
[1]	75	105	55
[2]	120	105	150
[3]	120	105	85
[4]	120	85	85
[5]	95	105	105
[6]	65	60	55
[7]	120	105	150
[8]	55	50	45
[9]	60	55	45
[10]	60	55	45

[11]	105	45	45
[12]	105	65	55
[13]	75	35	27
[14]	65	65	55
[15]	65	55	45
[16]	65	55	45
[17]	65	65	55

2.) DSC measurements

Thermal transitions of mixtures were determined by differential scanning calorimetry (DSC) with a DSC Q100 calorimeter (TA Instruments) unit under a nitrogen atmosphere, calibrated with a standard sample of indium. Samples between 5 and 10 mg were sealed in aluminum pans and measured over a temperature range of -80 °C until ca. 120 °C with a rate of 5 °C·min^{-1}; the samples were cooled with an intercooler. The phase transitions of the mixtures at different compositions (molar ratios) were analyzed with the software TA Universal Analysis. The DSC-curves (exo up) are shown in the following:

DSC for mixtures of urea with [DiC$_4$]Br and [DiC$_4$]Cl:

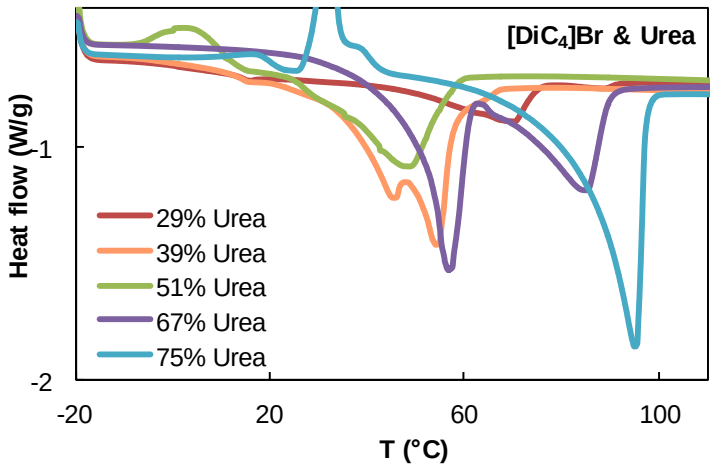

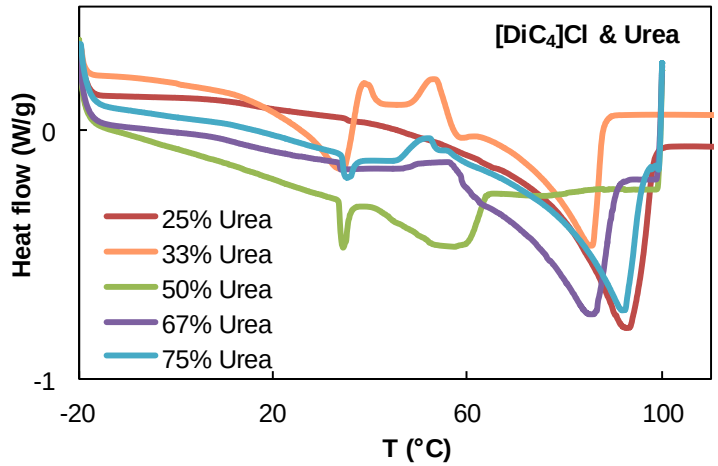

DSC for mixtures of urea with [C_n-Bet]Br (n = 2, 4, 6, 8):

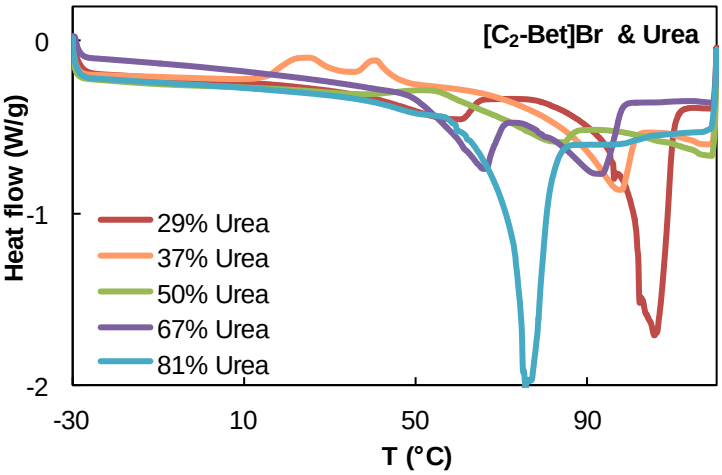

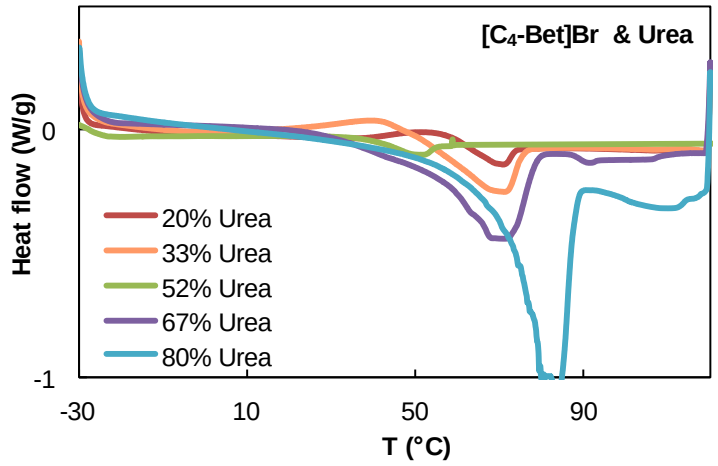

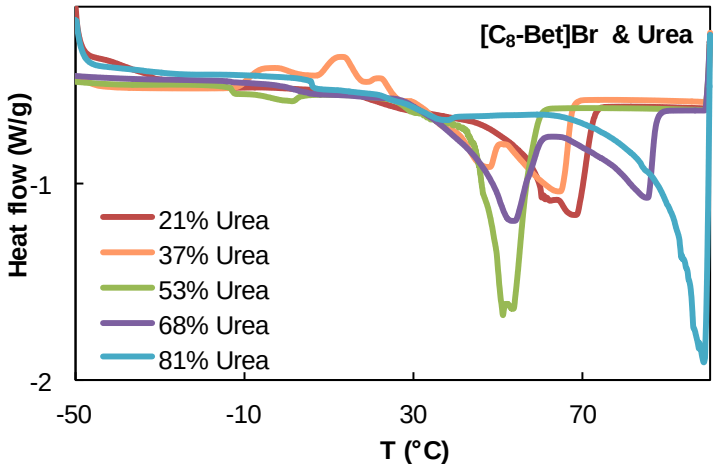

TGA and DSC for synthesized sugar-derivatives ***[8] – [17]****:*

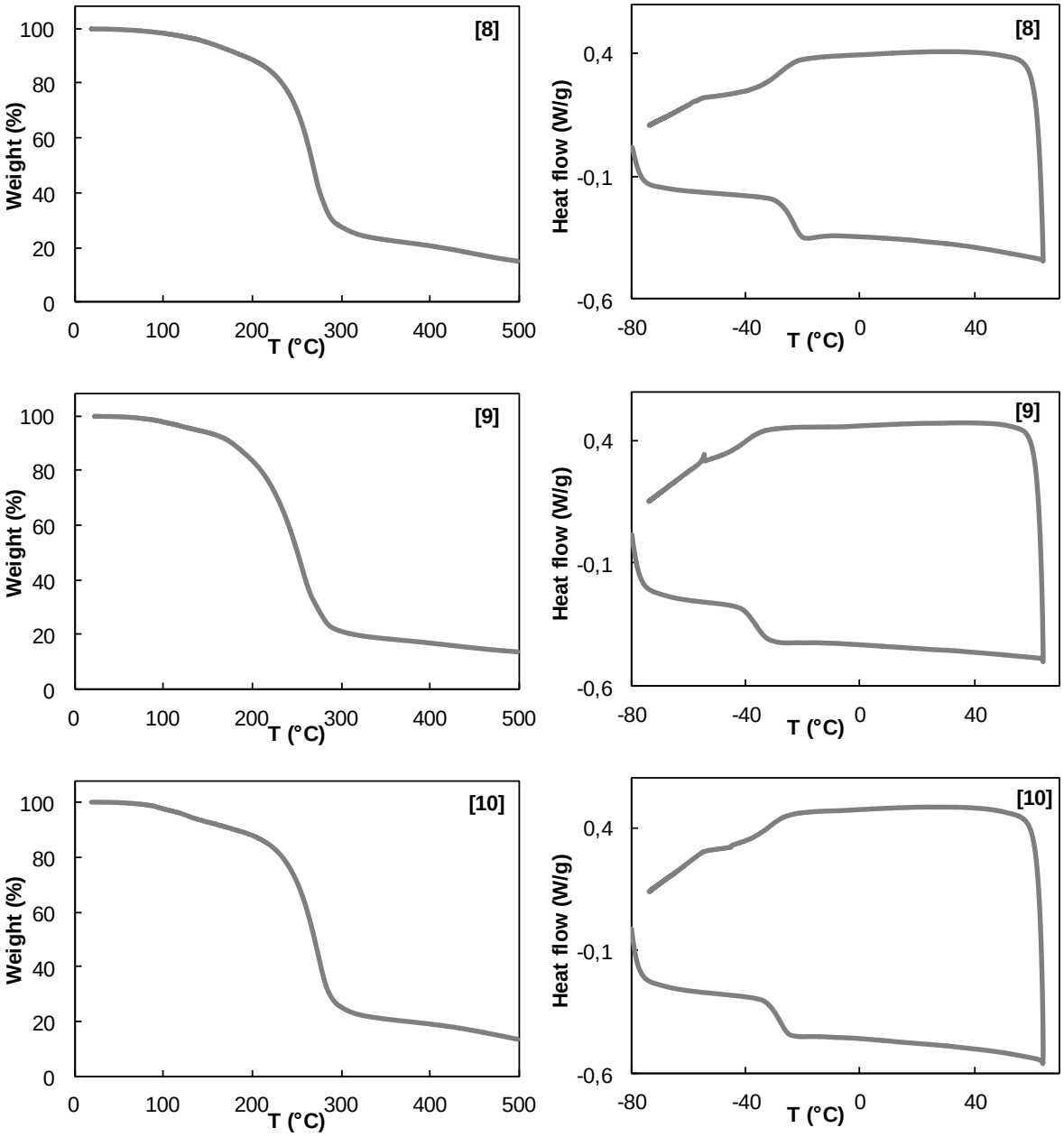

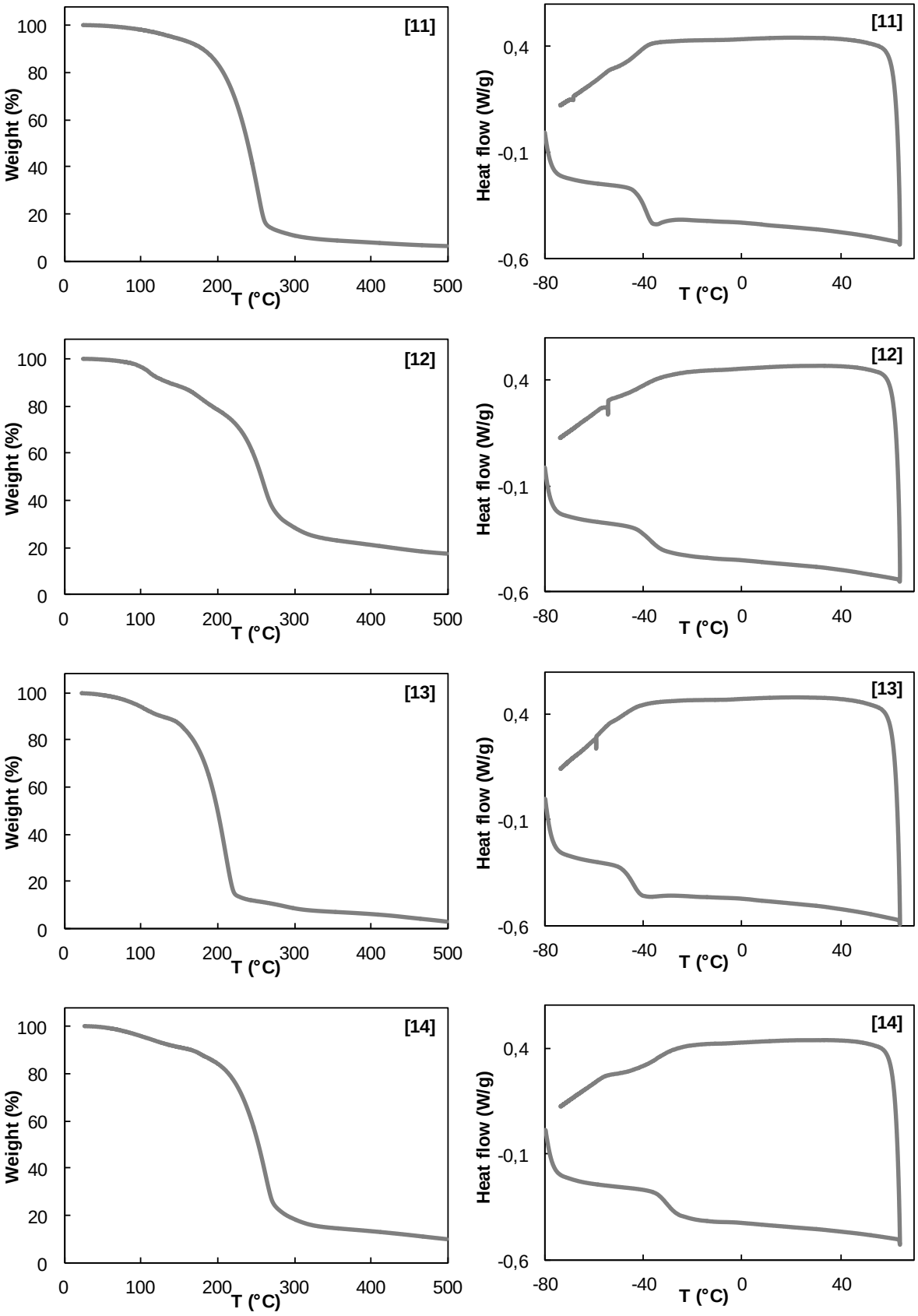
[11]
Weight (%)
T (°C)
Heat flow (W/g)
[12]
[13]
[14]

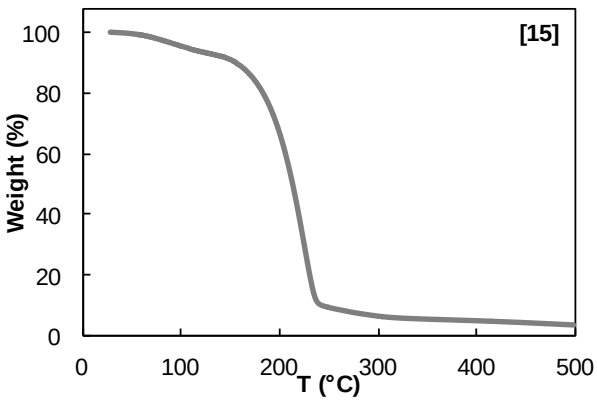
[15]
Weight (%)
T (°C)

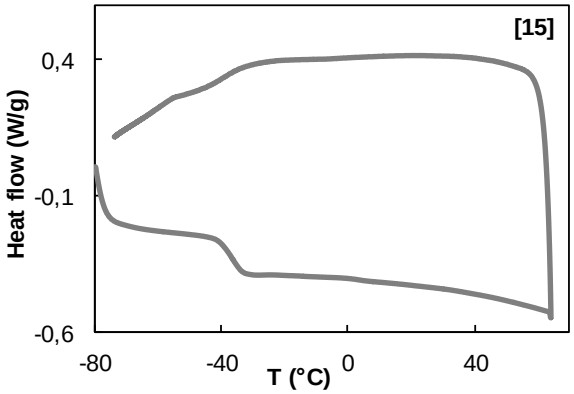
[15]
Heat flow (W/g)
T (°C)

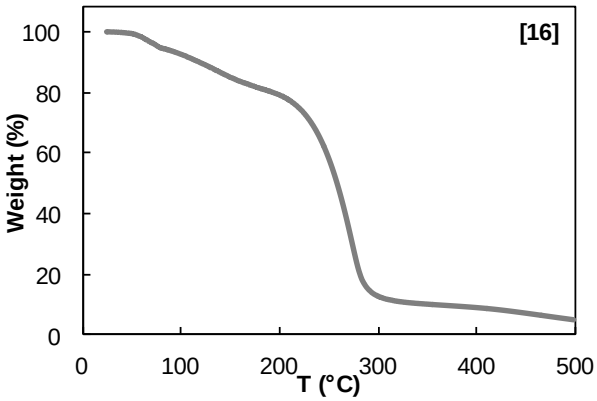
[16]
Weight (%)
T (°C)

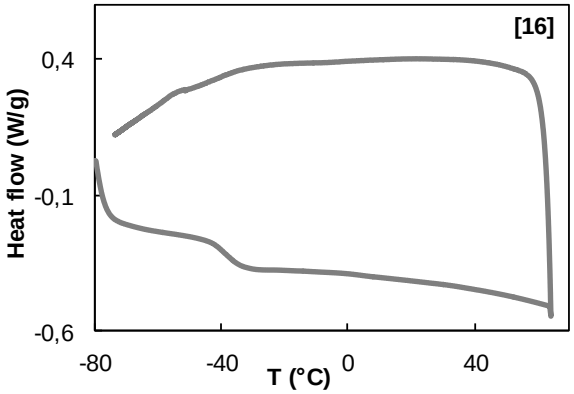
[16]
Heat flow (W/g)
T (°C)

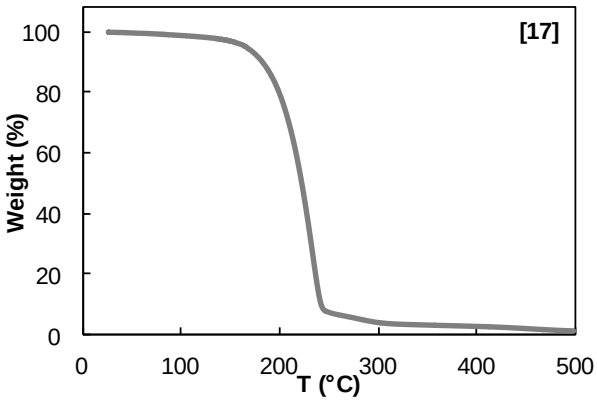
[17]
Weight (%)
T (°C)

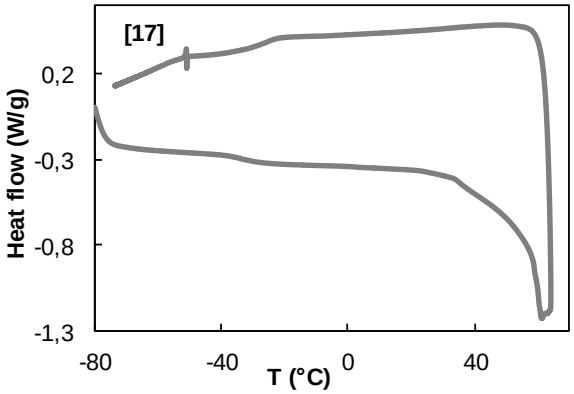
[17]
Heat flow (W/g)
T (°C)

3.) Viscosity measurements

Viscosity measurements were carried out with a Malvern Kinexus rotational rheometer with cone plate geometry (CP 20/2°), which was equipped with a Peltier temperature-controlled plate, using a sample volume of ca. 0.1 mL. Shear rates were determined over a shear stress ramp between 1 and 2000 Pa. To study the temperature dependence of the viscosity the measurements were carried out at different temperatures.

Dynamic viscosities η for sugar-based DESs (sugar [16] and [6]) with choline, betaine, carnitine at different temperatures T:

Dynamic viscosity η (Pa ·s) [T (°C)]					
[16]+Choline	**[16]+Betaine**	**[16]+Carnitine**	**[6]+Choline**	**[6]+Betaine**	**[6]+Carnitine**
1.720 [25]	/	/	16.648 [25]	/	/
0.602 [40]	14.731 [40]	29.731 [45]	2.553 [40]	26.480 [40]	/
0.203 [60]	2.151 [60]	3.393 [60]	0.628 [60]	9.042 [60]	33.017 [60]
0.100 [80]	0.467 [80]	0.674 [80]	0.210 [80]	1.247 [80]	3.003 [80]

CHAPTER 5 – Theoretical approach: modelling with COSMO-RS

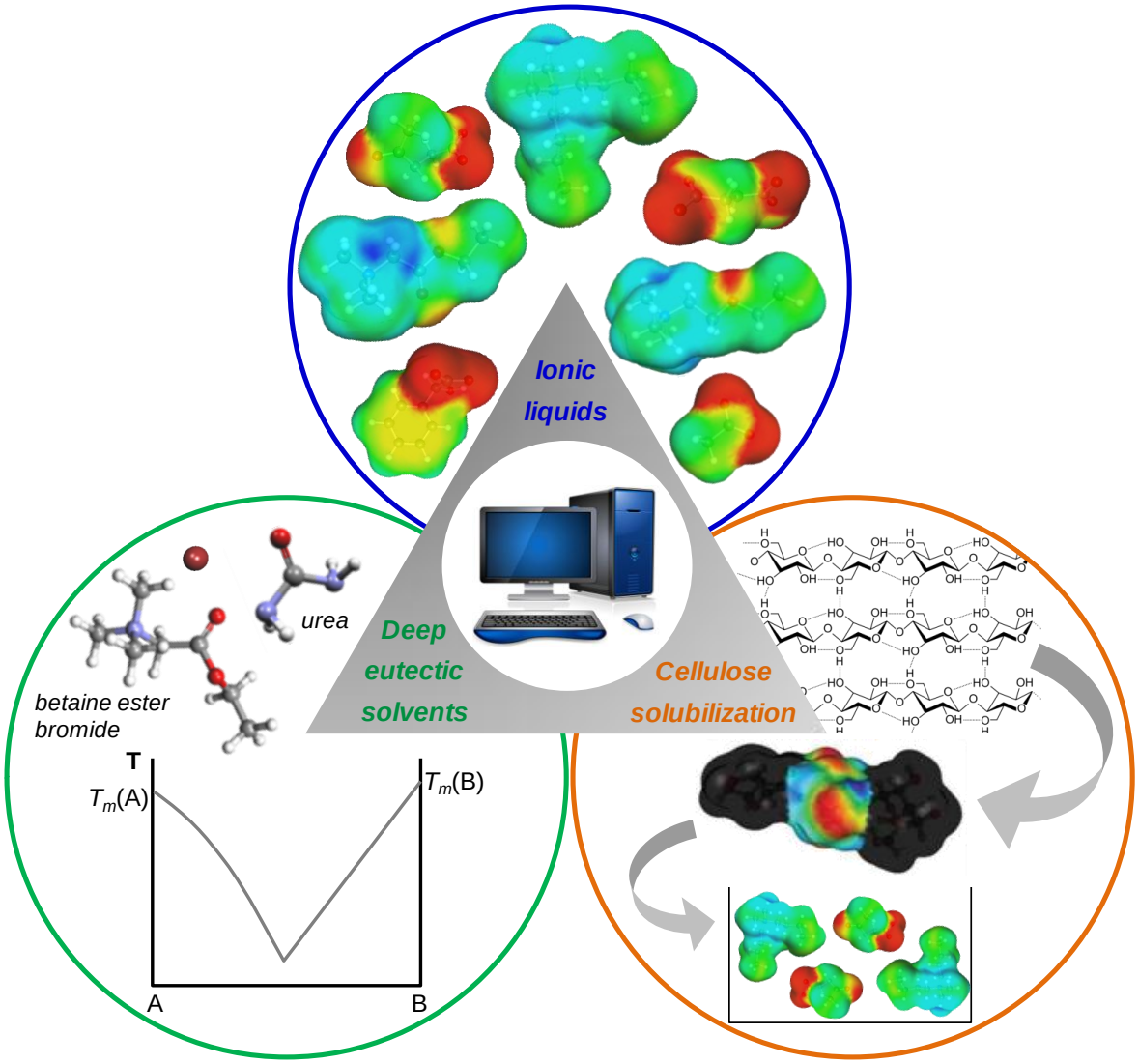

5.1 Theoretical background

Theoretical chemistry gains more and more importance with the trend of "green" chemistry because it permits the prediction of processes which could help us to reduce product and energy consumption, as well as waste production.

For chemical and biological processes, the liquid state is the most important one. There are mainly three different models for theoretical calculations which are particularly used for systems in the liquid state: simulation models based on **m**olecular **d**ynamics (MD) and **M**onte **C**arlo (MC)[290], models based on group-contribution like **uni**versal **f**unctional **a**ctivity **c**oefficients (UNIFAC)[291], and dielectric continuum solvation models, as the **co**nductor-like **s**creening **mo**del (COSMO)[292].

The properties of molecules in liquid systems are influenced by interactions with all fluctuating neighboring molecules.[293] Therefore, calculations of properties in liquid state necessitate an efficient sampling and thermodynamic averaging of all possible arrangements of solute and solvent molecules. Consequently, properties of molecules in solution need to be calculated as the combined thermodynamic and quantum mechanical expectation values of large ensembles of interacting molecules. The **co**nductor-like **s**creening **mo**del for **r**eal **s**olvents (**COSMO-RS**) was presented by Klamt in 1995 as an extension of the COSMO model.[294] This approach consists of two principal stages: one stage comprises quantum chemical calculations (COSMO) of each isolated species, followed by the second stage which includes statistical thermodynamics giving electrostatic interactions between the different species.[295] So, it permits an a-priori calculation of the chemical potential of a compound within a random number of other components or their mixtures.

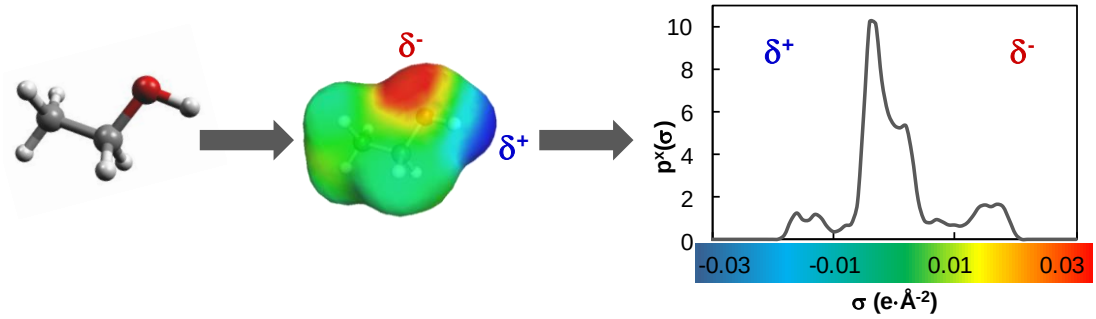

Figure 5.1 Procedure for charge density distribution (sigma-profile), p(σ), from molecular structure for ethanol.

The density of charge distribution σ on the surface of a molecule is shown with different colors as **σ-surface** (also called COSMO-surface). Hereby, green shows surface segments with no charge density, blue parts have a positive charge density δ^+, and red parts have a negative charge

density δ^-. **Figure 5.1** shows ethanol as representative example with a green zone for the hydrocarbon part, the red zone for the oxygen and the blue zone for the hydrogen. Each molecule can be represented by a histogram of surface area with respect to screening charge density, called **σ-profile p(σ)** in the framework of COSMO-RS (**Figure 5.1**). The σ-profile p(σ) is a 2D-representation of the information of the 3D σ-surface.

The σ-surface and σ-profile characterize a molecule as solute in a perfect conductor (COSMO state). However, the molecule in a perfect conductor is isolated and does not perceive the other molecules around. Thus, for molecules as solvents or molecules in solvents including their interaction energies, statistical thermodynamics has to be taken in consideration.

So, the COSMO-RS approach considers complex interaction in liquid systems as local contacts of surface segments with the charge densities σ and σ' (pair-wise interactions of surface segments), as shown in **Figure 5.2**.

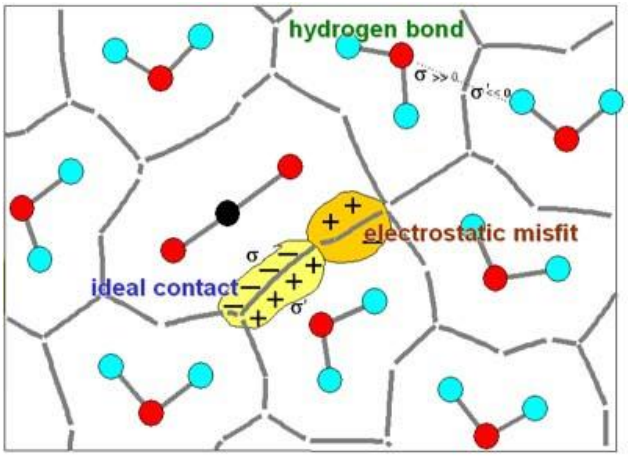

Figure 5.2 Schematic illustration of COSMO-RS view of molecular interactions in liquids.[296]

The virtual conducting molecular contact surface (double layer) is computed by the quantum chemical COSMO method. The most important contributions to the interaction energy functional are the electrostatic misfit energy, and hydrogen bonding. With the reduction of all interactions to local interactions of pairs of molecular surface pieces, the ensemble of interacting molecules could be considered as an ensemble of independently interacting surface segments.

Based on this model, the following systems can be treated with COSMO-RS calculations:[297] (a) estimation of the affinity of a molecule to another one depending on the contact charge density σ; therefore, the molecule is considered as solvent and its affinity to another molecule is represented as so-called **σ-potential $\mu_S(\sigma)$**; (b) estimation of the affinity of a molecule i in a solvent S calculated as its chemical potential μ_i^S.

The σ-potential $\mu_S(\sigma)$ of a solvent S with the polarity σ represents the chemical potential per surface area. This representation shows the affinity for a certain charge density of a molecule as

solvent S. The more the σ-potential is negative, the higher is the affinity of the solvent-molecule to the considered charge density. **Figure 5.3** shows the σ-potential of three typical solvents: ethanol, *n*-hexane and acetone.

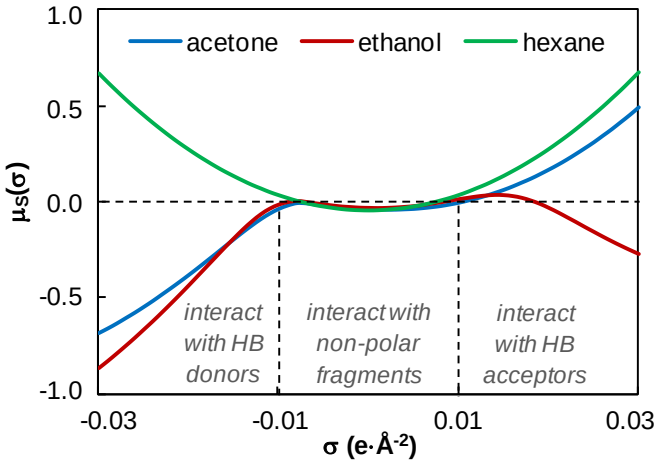

Figure 5.3 σ-Potential $\mu_S(\sigma)$ of acetone, ethanol and *n*-hexane as representative examples.

The σ-potential of ethanol highlights its affinity to positive charge densities (left side) as well as to negative charge densities (right side) indicating the character as electron donor and proton donor respectively. The σ-potential of *n*-hexane is typical of alkanes and signifies no affinity for positive or negative charge densities due to its apolar character. The solvent acetone has a σ-potential which shows affinity only for positive charge densities (left side) indicating the electron donor character.

Summing up, σ-profiles and σ-potentials can be used to qualitatively, and even quantitatively, interpret the interactions in pure liquid compounds or in mixtures.

5.2 Modelling of ionic liquids

The appropriate prediction method COSMO-RS is a very useful tool in the field of ILs.[298] Because of the enormous number of suitable cations and anions, the number of ILs increases faster than measurements of their thermodynamic properties can be performed. Thus, COSMO-RS could be a helpful technique for the selection of tailor-made ILs for a given application.

5.2.1 Sigma-surface and sigma-profile of ILs

The representation of IL cations and anions vice σ-surfaces gives a visual illustration of the charge density σ, and therefore their charge distribution.[299] **Figure 5.4** shows some examples of σ-surfaces of IL cations and anions. In this study, we have computed all the cations (ca. 20) and anions (ca. 20) except the ones which were already in the COSMO-RS IL-Database (*e.g.* Cl, Br, Ace). As already mentioned before, positive screening charge σ is colored in red, negative screening charge σ is colored in blue, whereas the green parts have rather neutral σ.

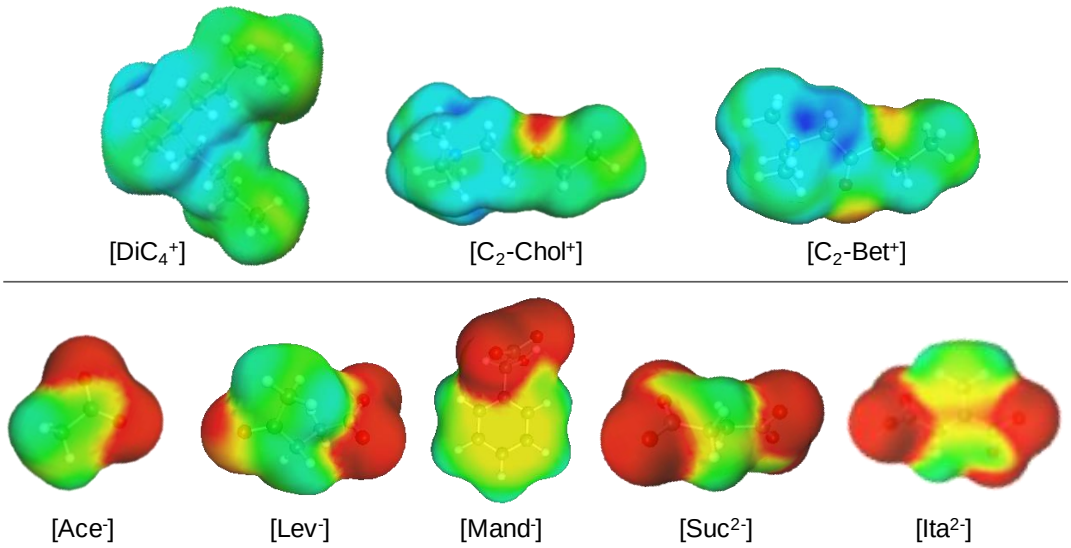

Figure 5.4 σ-Surfaces of some IL cations and anions.

Every IL can be represented as a histogram of surface area as a function of the screening charge density σ, which is called σ-profile.[299] The σ-profile of the whole system / mixture (IL) is just the sum of the σ-profiles of the components (cation and anion) weighted with their molar fraction in the mixture.[300,301] A study on ILs with classical cations (*e.g.* imidazolium, pyridinium, ammonium, phosphonium, pyrrolidinium) and anions (*e.g.* Cl^-, NTf_2^-, PF_6^-, etc.) using a quantitative structure-property relationship has been reported by the evaluation of their polarities.[302] The applied tool was quite useful for the classification of the studied ILs, as their structures were rather different.

In a same way, we have determined the σ-profiles for all the ILs in this study. Some examples for σ-profiles of quaternary ammonium carboxylate ILs (QACILs) investigated in ***Chapter 2*** are shown in **Figure 5.5**. For all [DiC_4] ILs, important peaks appear in the middle, non-polar region, which occurs mainly from large IL cations, and the anion is represented by the hydrogen-bond-acceptor region (right side). [DiC_4]Ace has a slightly lower peak in this region due to the smaller apolar part of the anion. For [DiC_4]Mand, an additional non-polar peak was detected coming from the aromatic system of the anion. Otherwise, the presented QACILs have relatively similar σ-profiles, thus their charge densities and therefore their feature of interactions are in the same range.

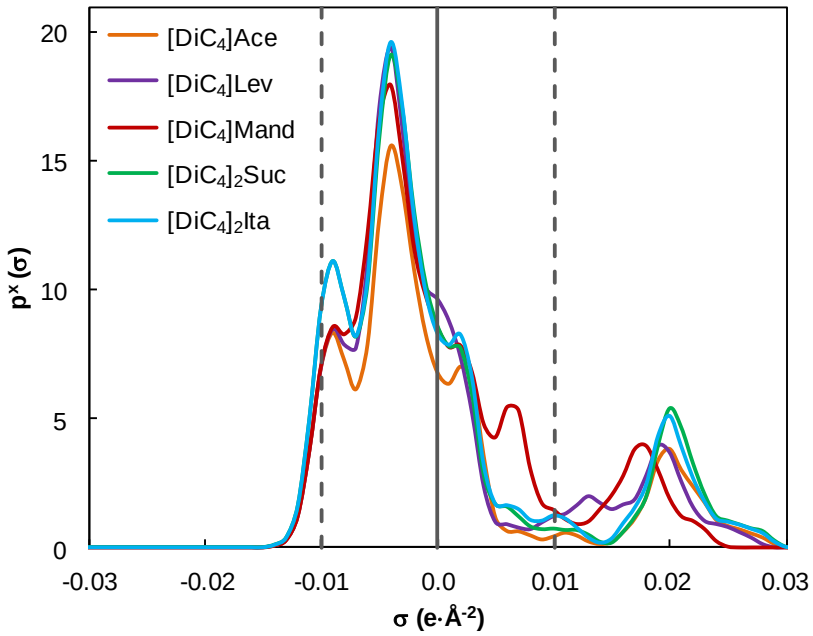

Figure 5.5 σ-Profiles of some QACILs.

Summing up, the studied ILs exhibit similar σ-profiles from the point of view of COSMO-RS which does not appear to be discriminating enough to allow a classification of their polarity and interaction ability in comparison to other conventional solvents.

5.2.2 Classification of ILs – partition coefficient

The 1-octanol-water partition coefficient (log $P_{O/W}$) could also be a useful concept for the evaluation of IL polarity, as it describes both hydrophobicity and hydrophilicity of a compound.[303]

$$\log P_{O/W} = \frac{C_i^{octanol}}{C_i^{water}} \qquad \textbf{Eq. 5.1}$$

As shown in **Eq. 5.1**, log $P_{O/W}$ is the ratio of the concentration of the solute in the 1-octanol phase to that in a juxtaposed aqueous phase at equilibrium; this is also called the Nernst distribution

law. The experimental determination of log $P_{O/W}$ values is usually carried out using the shake flask (or tube) method followed by the detection of concentration in each phase.[304] Unfortunately for ILs, the determination of log $P_{O/W}$ is easier for imidazolium-based ILs due to the easy detection of the imidazolium ring by UV-visible spectroscopy.[305] Based on these limits for experimental studies, computational predictions could be practical for having access to log $P_{O/W}$ values for different types of ILs. COSMO-RS is a convenient tool which allows the calculation of partition coefficients.[306] Spieβ *et al.* have applied COSMO-RS calculations to biocatalytic two-phase reaction systems for the prediction of solute partitioning between organic solvents and aqueous reaction medium.[307]

Therefore, we have used COSMO-RS as a prediction tool for the calculation of log $P_{O/W}$ values of the ILs synthesized in this work for their classification. **Table 5.1** represents the values of log $P_{O/W}$ calculated with COSMO-RS of ILs based on various carboxylate anions and **(a)** quaternary ammonium, **(b)** choline ethers, and **(c)** betaine esters as cations. The color code is chosen to point up highly hydrophilic ILs with blue, green ones in the middle range, and orange for highly hydrophobic ILs. The map **(a)** for quaternary ammonium shows more hydrophobic compounds than the maps **(b)** and **(c)**. This result is based on the cationic structure which has no oxygen-sites making the cation more hydrophobic. Additionally, the quaternary ammonium contains two alkyl side chains, and choline ether and betaine ester cations only one. The most hydrophilic ILs (blue parts in the map) were found for short-chain cations combined with double-charged anions, such as Suc, Fum, Male, Ita, Mala and Tar. This phenomenon could be attributed to the higher charge density in these ILs. A closer look on the influence of the anion shows that especially Sor, Sal and Mand lead to more hydrophobic ILs which is directly connected to their conjugated π-system structure. So, the partition coefficient calculations with COSMO-RS support in a good way our estimations based on ILs structural effects on polarities.

Table 5.1 Map for partition coefficients log $P_{O/W}$ of ILs based on carboxylate anions and (a) quaternary ammonium, (b) choline ether, and (c) betaine ester, determined with COSMO-RS.

(a)	[DiC$_3$]	[DiC$_4$]	[DiC$_6$]	[DiC$_8$]
For	-5.2	-4.0	-1.8	0.5
Ace	-4.4	-3.3	-1.0	1.2
Lac	-4.3	-3.1	-0.9	1.4
Gly	-5.0	-3.8	-1.6	0.7
Lev	-4.6	-3.4	-1.2	1.1
Sor	-2.7	-1.5	0.7	3.0
Sal	-1.7	-0.5	1.7	4.0
Mand	-2.7	-1.6	0.7	3.0
Suc	-10.0	-7.7	-3.3	1.3
Fum	-10.2	-7.9	-3.4	1.1
Male	-10.7	-8.4	-3.9	0.7
Ita	-9.6	-7.3	-2.8	1.7
Mala	-10.8	-8.5	-4.0	0.5
Tar	-11.6	-9.3	-4.8	-0.2
(b)	**[C$_2$-Chol]**	**[C$_4$-Chol]**	**[C$_6$-Chol]**	**[C$_8$-Chol]**
For	-6.5	-5.3	-3.7	-2.7
Ace	-5.7	-4.6	-2.9	-1.9
Lac	-5.6	-4.4	-2.8	-1.8
Gly	-6.3	-5.1	-3.5	-2.5
Lev	-5.9	-4.7	-3.1	-2.1
Sor	-4.0	-2.8	-1.2	-0.2
Sal	-3.0	-1.8	-0.2	0.8
Mand	-4.0	-2.8	-1.2	-0.2
Suc	-12.6	-10.3	-7.0	-5.0
Fum	-12.8	-10.5	-7.2	-5.2
Male	-13.3	-11.0	-7.6	-5.7
Ita	-12.2	-9.9	-6.6	-4.6
Mala	-13.4	-11.1	-7.8	-5.8
Tar	-14.2	-11.9	-8.6	-6.6
(c)	**[C$_2$-Bet]**	**[C$_4$-Bet]**	**[C$_6$-Bet]**	**[C$_8$-Bet]**
For	-5.9	-4.7	-3.7	-2.6
Ace	-5.1	-4.0	-2.9	-1.8
Lac	-5.0	-3.8	-2.8	-1.7
Gly	-5.7	-4.5	-3.5	-2.4
Lev	-5.3	-4.1	-3.1	-2.0
Sor	-3.4	-2.2	-1.2	-0.1
Sal	-2.4	-1.2	-0.2	0.9
Mand	-3.4	-2.2	-1.2	-0.1
Suc	-11.4	-9.1	-7.1	-4.8
Fum	-11.6	-9.2	-7.2	-5.0
Male	-12.1	-9.7	-7.7	-5.4
Ita	-11.0	-8.6	-6.6	-4.4
Mala	-12.2	-9.9	-7.8	-5.6
Tar	-13.0	-10.6	-8.6	-6.4

≤-10	highly hydrophilic
-9 to -4	↓
-3 to -1	
0 to 2	
≥ 2	highly hydrophobic

5.3 Solubilization of cellulose

The research on solvents, especially ILs, for the solubilization of cellulose and other natural-resourced polymers is still a growing field. Due to the huge number of combinations of cations and anions for ILs, solubilization tests for all the available ILs is product- and time-consuming. Therefore, the quantum-chemical solvation model COSMO-RS appears again as a very useful tool for solvent screening also from an ecological point of view.[308–310]

In literature, cellulose solubility in ILs has already been figured out using COSMO-RS. Kahlen *et al.* computed the activity coefficient γ to obtain a COSMO-RS-based screening of a huge number of ILs[311], and Casas *et al.* have studied the solubility of cellulose and lignin in ILs with COSMO-RS considering the activity-coefficient and excess enthalpy[312].

In this study, we have used the approach of Kahlen *et al*. as basis for our calculations.

5.3.1 Model for cellulose

As cellulose is a highly complex polymer structure building a large network based on inter- and intramolecular hydrogen-bonds, direct COMSO computation of this polymer is not feasible.[311] Thus, a small representative part of the cellulose structure including all characteristic features of the molecule should be used for calculations. Leonhard *et al*. have described their model for cellulose as the mid-monomer part of cellotriose as the representative unit which permits to determine the influence of neighboring monomeric units (**Figure 5.6**). They have found around 30 relevant structural conformers, which were taken into account for the calculations. In our study, we have used their model as structural representation for COSMO-RS calculations.

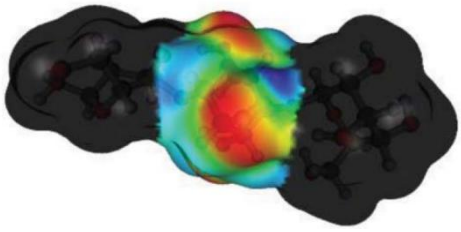

Figure 5.6 Model for cellulose as cellotriose unit.[311]

5.3.2 Calculation of cellulose solubilization via activity coefficients

The activity coefficient γ of the solute at infinite dilution is often considered as a qualitative measure for the dissolving power of the solvent.[311] Kahlen *et al.* have calculated the (residual contributions of the) activity coefficient γ of cellulose in various ILs and illustrated the predictions for 2272 ILs, as combinations of 32 anions and 71 cations (**Figure 5.7**).

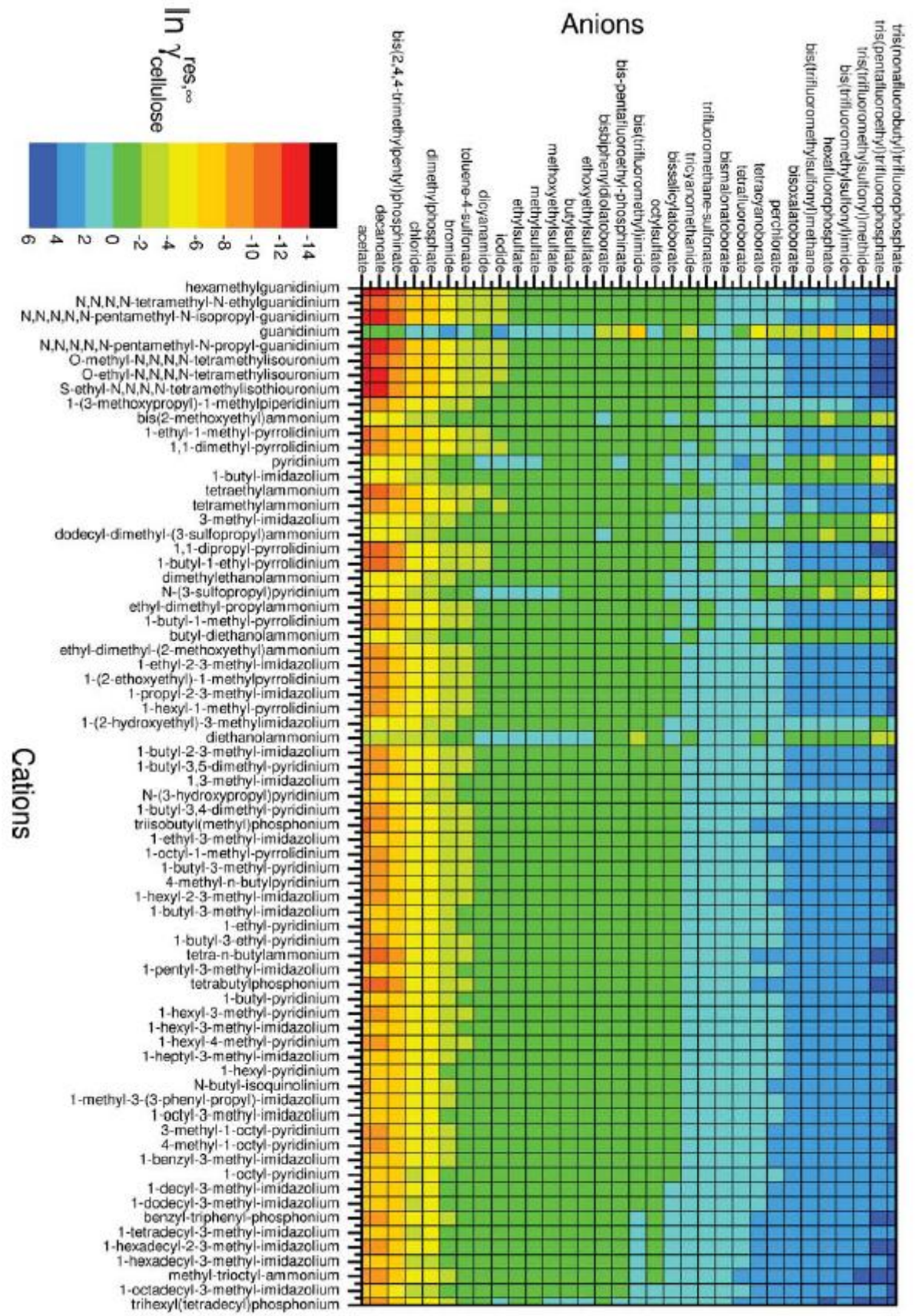

Figure 5.7 Graphical representation of the activity coefficients of cellulose in 2272 different ILs at infinite dilution from the literature.[311]

ILs with high dissolving power (strongly negative values of ln γ) are represented by red / orange colors, the weaker ones (positive values of ln γ) by blue colors. As illustrated in **Figure 5.7**, the predicted cellulose solubilization power was mainly dependent on the IL anion, with acetate, decanoate, chloride or bromide as the best ones. The predicted solubilites were compared to some experimental values for imidazolium-based ILs with Cl, Br, PF_6 and BF_4 as counter anions which fitted rather well.

In our study, similar calculations have been carried out for QACILs (see ***chapter 2***) at 100 °C, as in experiments. The ln γ values for the calculated QACILs were found to be in the range between -4.3 for [TriC_3]Ace and -1.6 for [DiC_6]Sal; all the calculated values are given in the ***experimental section*** of this chapter. So, the results are quite similar, and comparing them to the values reported in literature,[311] they are all in the same color-range (light green to green). The little difference in calculated ln γ values are rising from the similar structures of investigated IL cations (quaternary ammonium with small variations) and IL anions (carboylates). However, we have determined huge differences for cellulose solubility S_{cell} in QACILs during experimental investigations (see ***chapter 2***). The comparison of both experimental and calculated results (**Figure 5.8**) highlights no good correlation, especially for the highest (10 wt%) and the lowest (0 %) solubilities. The grey line represents the average trend which should have a slope of 1 if the correlation of experimental and calculated values would be perfect. In our case, only the middle region (solubilities between 1 and 6 wt%) were approximately well calculated (area with orange dashed line).

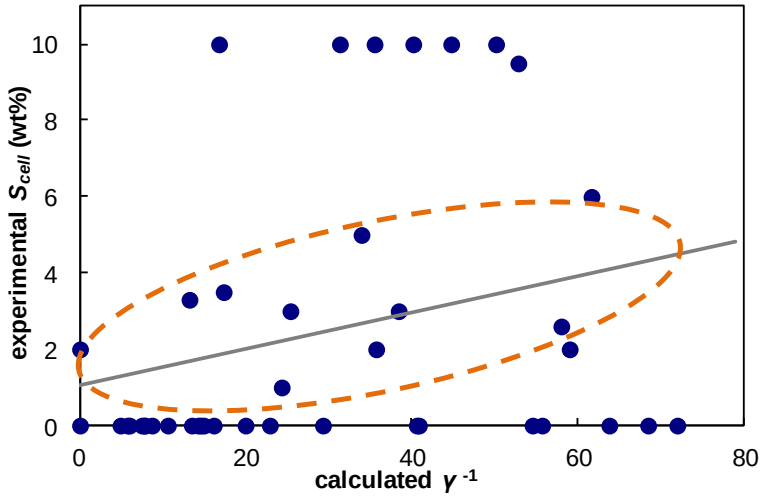

Figure 5.8 Experimental solubilization of cellulose S_{cell} in QACILs plotted against the reciprocal of the activity coefficient γ^{-1} of cellulose calculated with COSMO-RS.

Some reasons could be conceived why the prediction of cellulose solubilization in QACILs does not give good correlations with experimental results. Basically, the model of the structure of cellulose as cellotriose does not enough take into consideration all the interactions of this highly

complex polymer, so it should be further optimized. Furthermore, as the solubilization mechanism of cellulose in ILs is very complicated, and all the detailed factors are not even entirely understood, the prediction of cellulose solubilization is very difficult. Additionally, the process of cellulose solubilization in ILs is not only a thermodynamic process, but it is mainly influenced by kinetic effects. This phenomenon is perceptible with the fact that the result is not the same if cellulose is added stepwise or all in one go. Furthermore the speed of stirring plays an important role for the solubilization process. Taking all these difficulties in consideration, COSMO-RS cannot replace experimental investigations, but it could help one to gain a first idea of cellulose solubilization with ILs by this fast prediction method.

5.4 Calculation of deep eutectic mixtures

Deep eutectic solvents (DESs) are a novel generation of "green" solvents which could be obtained by mixing two salts, *i.e.* hydrogen bond donor (HBD) and hydrogen bond acceptor (HBA), in a certain (molar) ratio.[3] Details about the theory and the background have already been explained in ***chapter 1***, ***section 1.3***, and investigations of some binary systems were presented and discussed in ***chapter 4***.

As the identification of eutectic mixtures (ratio and temperature of the eutectic point) needs a detailed screening of various mixtures, a predicting method could be helpful to minimize experiments, and therefore time, product use and energy consumption. COSMO-RS permits the calculation of solid-liquid-equilibrium (SLE) which is an adapted tool for modeling DESs.[313] However, COSMO-RS is a calculation method for liquid states, thus for the SLE of solid compounds with a solvent, the Gibbs free energy of fusion of the compound, ΔG_{fus}, should be taken into account. ΔG_{fus} can be calculated from experimental data, such as the enthalpy of fusion ΔH_{fus} and the melting temperature T_m, which are accessible with DSC-measurements (**Eq. 5.2**).

$$\Delta G_{fus}(T) = -\Delta H_{fus}\left(1 - \frac{T}{T_m}\right) + \Delta Cp_{fus}\, T \ln\frac{T_m}{T} \qquad \textbf{Eq. 5.2}$$

In this study, we have calculated the SLE for some systems of ***chapter 3*** and compared to experimental results for DE mixtures. As sugars and sugar-derivatives are very problematical to treat with COSMO-RS due to its elevated number of hydroxyl-groups, mixtures based on sugar-derivatives have not been calculated. So, DESs based on **urea** in combination with **[DiC$_4$]X** (X = Cl, Br) or **[C$_n$-Bet]Br** (with n = 2, 4, 6, 8) have been computed. The comparison of experimental and calculated values for DES based on urea and **[DiC$_4$]X** (X = Cl, Br) is presented in **Figure 5.9**.

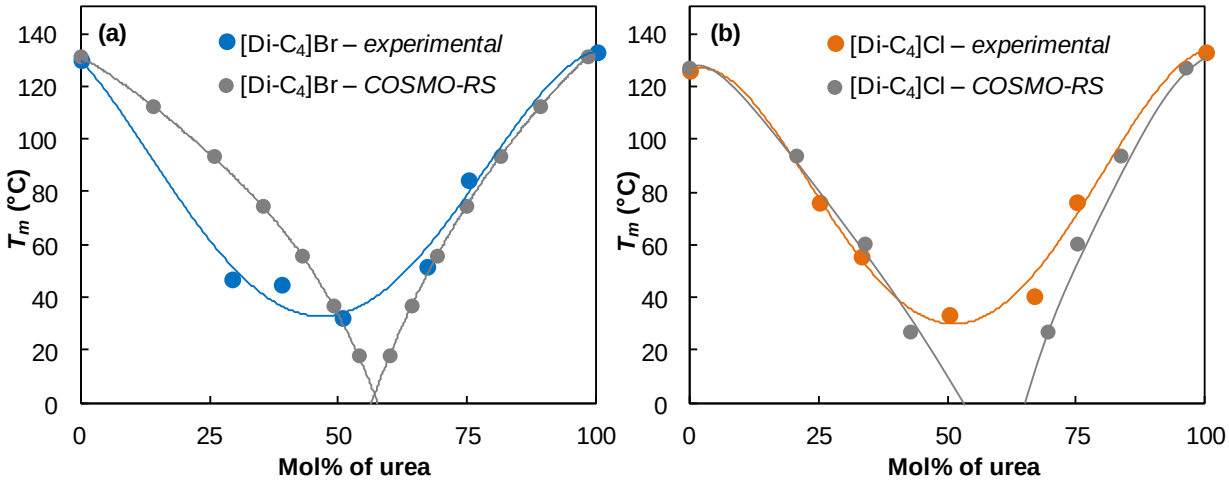

Figure 5.9 Comparison of experimental and calculated values for DES mixtures based on urea and quaternary ammonium [DiC$_4$]X with **(a)** X = Br and **(b)** X = Cl.

The COSMO-RS calculations of DESs resulted in an eutectic mixture for [DiC$_4$]Br with 57 wt% urea at a temperature of -1 °C (**Figure 5.9.a**). So, a rough trend for the ratio of the mixture was found, which could help as a first approximation to limit the quantity of experiments. The predicted temperature (-1 °C) is around 35 °C lower than the experimental value. All in all, the COSMO-RS calculation agrees not that bad with experimental findings. However, the calculations for the system of [Di-C$_4$]Cl with urea are not really fitting (**Figure 5.9.b**). The eutectic minimum seems like a gap of mixture at 60 wt% urea at -140 °C. This inadequate modeling of the system was attributed to the solid liquid equilibrium (solid solution) at the eutectic point which could not be described sufficiently by COSMO-RS which is a model for liquid states.

Figure 5.10 illustrates the comparison of experimental and calculated values for DESs based on urea and betaine ester bromides **[C$_n$-Bet]Br** (with n = 2, 4, 6, 8). For all these systems, the predicted ratio for the eutectic point was found around 55 wt% of urea. However, the experimentally determined data were quite different and showed remarkable dependence of the alkyl side chain length n of the used betaine ester bromide [C$_n$-Bet]Br.

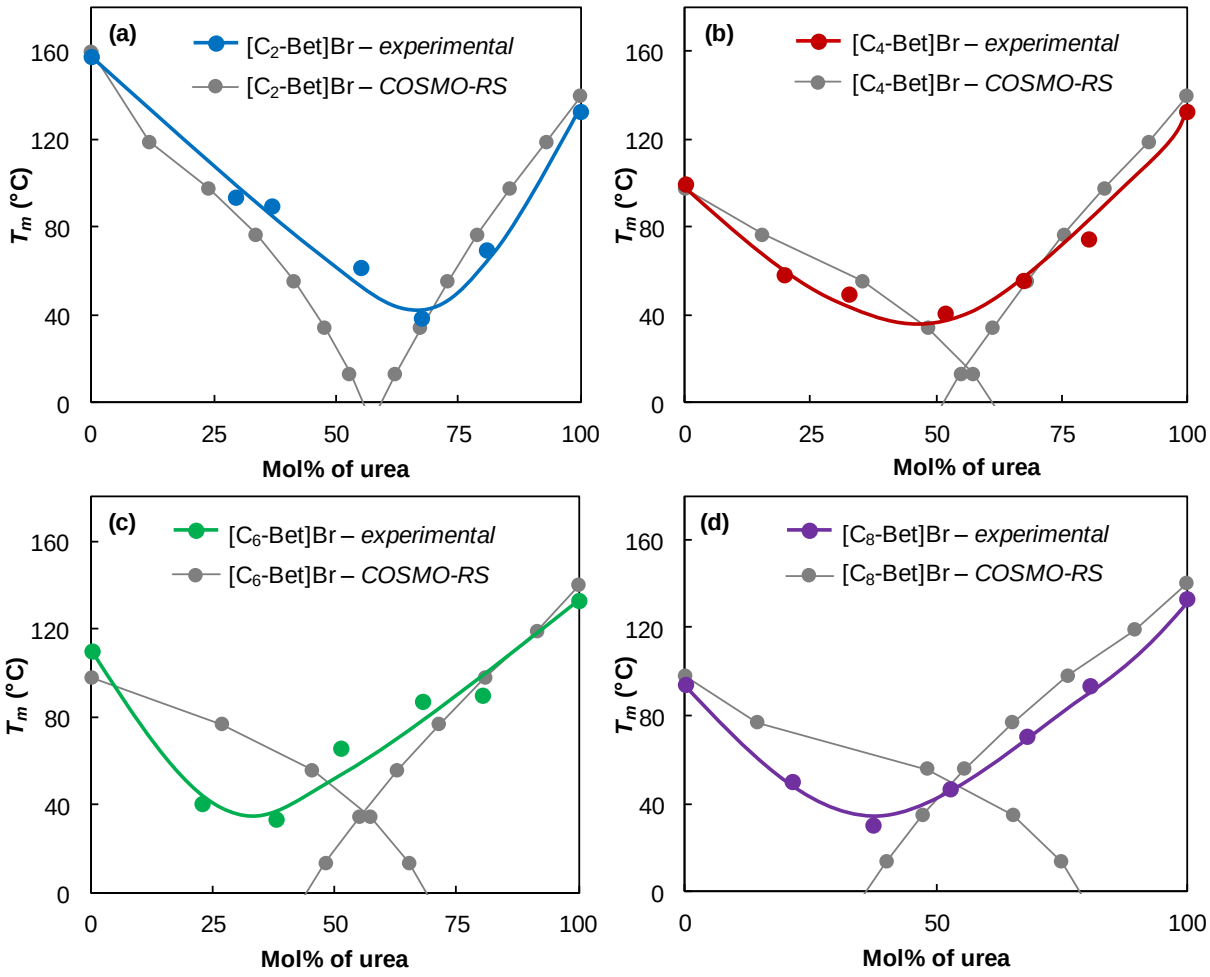

Figure 5.10 Comparison of experimental and calculated values for DES mixtures based on urea and betaine ester bromides [C$_n$-Bet]Br with **(a)** n = 2, **(b)** n = 4, **(c)** n = 6, and **(d)** n = 8.

Comparing the predicted values of the temperature of eutectic mixtures, no outstanding correlations with experimental values were found. For [C_2-Bet]Br the eutectic point was calculated for -7 °C, however experiments gave 39 °C (**Figure 5.10.a**). The modeling of [C_4-Bet]Br mixed with urea had an eutectic point at 15 °C, and in reality at 41 °C (**Figure 5.10.b**). For this system, the theoretical and experimental values were roughly well correlating. The eutectic point for [C_6-Bet]Br with urea was at 35 °C (**Figure 5.10.c**) compared to 33 °C in experiments. Thus, for this mixture the temperature was perfectly predicted, but unfortunately the ratio was not correctly predicted. The calculated eutectic point of the [C_8-Bet]Br system was found at 47 °C which matches with the experimental point at 50 wt% of urea (**Figure 5.10.d**), but this was not the mixture with minimal measured temperature.

As a conclusion, predictions for DES mixtures with COSMO-RS could be very helpful for a first estimation of ratios of HBD and HBA. But, the investigated mixtures based on urea as HBD combined with different quaternary ammonium, such as [DiC_4]X (X = Cl, Br) or [C_n-Bet]Br (n = 2, 4, 6, 8), were not perfectly calculated with COSMO-RS. Altogether, either the ratio or the temperature of the eutectic mixture was approximately predicted for some mixtures. However, this method cannot replace experimental examinations.

5.5 Conclusions

In this study, the theoretical method COSMO-RS has been applied as a tool for the support and/or prediction of experimental results. Different parts of the whole project were examined by theoretical modeling, and thus the capacity of COSMO-RS to replace experimental studies was evaluated.

First of all, synthesized ionic liquids based on simple quaternary ammonium (see ***chapter 2***), choline ether and betaine ester (see ***chapter 3***) have been modeled, *i.e.* their COSMO-surfaces and σ-profiles. As they have relatively similar structures, this information was not enough discriminating to classify these ILs due to their properties, such as polarity. Consequently, we have used the concept of the 1-octanol-water partition coefficient to get an idea about their hydrophilicity and hydrophobicity. These calculations allowed a rough estimation of the ILs polarity.

In a further step, we have tried to apply a concept from the literature for the calculation of cellulose solubilization in ILs,[311] which have already been tested experimentally in this work (see ***chapter 2***, ***3***). Unfortunately, no good correlations between experimental and theoretical investigations were obtained. This could be attributed to the lack of inter- and intermolecular interactions in the reduced model for cellulose. Furthermore, the examined ILs are structurally very similar, *i.e.* slightly varied quaternary ammonium cations and carboxylate anions, giving more or less the same results.

The last part of COSMO-RS involved in this project dealt with the modelling of deep eutectic solvents based on urea in combination with different quaternary ammonium: $[DiC_4]X$ (X = Cl, Br) or $[C_n\text{-Bet}]Br$ (n = 2, 4, 6, 8). For some of the systems, a fairly qualitative agreement with experiments, *i.e.* either the ratio or the temperature of the eutectic point, has been computed. However, COSMO-RS is not an accomplished method for the calculation of DESs, and above all it could not substitute experimental investigations.

All in all, COSMO-RS is a fairly versatile tool for theoretical calculations of various compounds, mixtures, physicochemical properties and behavior in complex systems. However, it should be used carefully and with a critical point of view based on thorough experimental results. Its application to ILs and DESs is still limited and further improvements are required to refine the information.

Experimental Section

The molecular structures of all compounds have been sketched as a three-dimensional geometry with Arguslab (http://www.arguslab.com, Release 2004), and conformational analysis has been performed using the COSMOconf script by quantum-chemical COSMO-calculations.[314] The standard quantum-chemical method for COSMO-RS has been conducted using the density functional theory (DFT) with a triple zeta valence polarized basis set (TZVP). The calculations of σ-surfaces, σ-profiles and σ-potentials, activity coefficients and eutectic mixtures were carried out with COSMOtherm (Version C21_0111).

Cellulose solubilization: experimental S_{cell} (wt%) and calculated activity coefficient γ

IL cation	IL anion	S_{cell} (wt%)	ln(γ)	γ	γ^{-1}
[Tri-C_3]	Lev	10	-3.6928	0.0249	40.1562
[Di-C_4]	Lev	10	-3.4441	0.0319	31.3166
[Di-C_3]	Lev	10	-3.5692	0.0282	35.4897
[Tri-C_4]	Lev	5	-3.5240	0.0295	33.9198
[Di-C_6]	Lev	3	-3.2329	0.0394	25.3524
[Di-C_4]$_2$	Ita	10	-3.9147	0.0199	50.1359
[Di-C_3]$_2$	Ita	6	-4.1212	0.0162	61.6335
[Di-C_6]$_2$	Ita	3	-3.6479	0.0260	38.3953
[Tri-C_3]$_2$	Ita	0	-4.2263	0.0146	68.4602
[Tri-C_4]$_2$	Ita	0	-3.9988	0.0183	54.5316
[Di-C_4]	Ace	9.5	-3.9668	0.0189	52.8136
[Tri-C_4]	Ace	2.6	-4.0604	0.0172	57.9965
[Di-C_3]	Ace	0	-4.1555	0.0157	63.7810
[Tri-C_3]	Ace	0	-4.2763	0.0139	71.9741
[Di-C_6]	Ace	0	-3.7095	0.0245	40.8329
[Di-C_4]	Lac	3.3	-2.5794	0.0758	13.1886
[Di-C_3]	Lac	0	-2.7017	0.0671	14.9054
[Tri-C_3]	Lac	0	-2.7796	0.0621	16.1123
[Di-C_6]	Lac	0	-2.3592	0.0945	10.5823
[Tri-C_4]	Lac	0	-2.6008	0.0742	13.4751
[Tri-C_4]	Cl	10	-2.8186	0.0597	16.7540
[Di-C_4]	Cl	3.5	-2.8512	0.0578	17.3079
[Di-C_3]	Cl	1	-3.1906	0.0411	24.3036
[Tri-C_3]	Cl	0	-3.1302	0.0437	22.8792
[Di-C_4]	Br	0	-2.0581	0.1277	7.8314
[Di-C_6]	Br	0	-1.7465	0.1744	5.7347
[Tri-C_4]	Br	0	-2.0090	0.1341	7.4559
[Di-C_4]	Sor	2	-3.5748	0.0280	35.6870
[Di-C_4]$_2$	Suc	2	-4.0776	0.0169	59.0025
[Di-C_4]	Gly	0	-2.6563	0.0702	14.2432
[Tri-C_4]	Gly	0	-2.6777	0.0687	14.5516

[Di-C_4]	Mand	0	-2.0454	0.1293	7.7325
[Di-C_4]$_2$	Male	0	-4.0198	0.0180	55.6873
[Di-C_4]$_2$	Fum	0	-3.7032	0.0246	40.5753
[Di-C_4]$_2$	Tar	0	-2.9931	0.0501	19.9471
[Di-C_4]	For	0	-3.3767	0.0342	29.2751
[Di-C_4]	Sal	0	-1.7847	0.1678	5.9580
[Di-C_6]	Sal	0	-1.5833	0.2053	4.8711

CONCLUSION

Today, the research on "greener" processes including biocompatible solvents, ecologically friendly techniques and naturally resourced raw materials gains more and more importance with the environmental consciousness. In the framework of this PhD thesis, novel biocompatible solvents were synthesized and characterized with the aim to apply them for biopolymer solubilization, particularly for cellulose.

In this project, novel ILs were obtained based on classical short-chain quaternary ammonium or "greener" derivatives from the natural salts choline, betaine and carnitine as cationic part. For the counter anions, we have mainly used biosourced organic carboxylates, such as acetate, levulinate, lactate, itaconate, mandelate, etc. **Figure C.1** gives an overview for the different groups of novel ILs in this study.

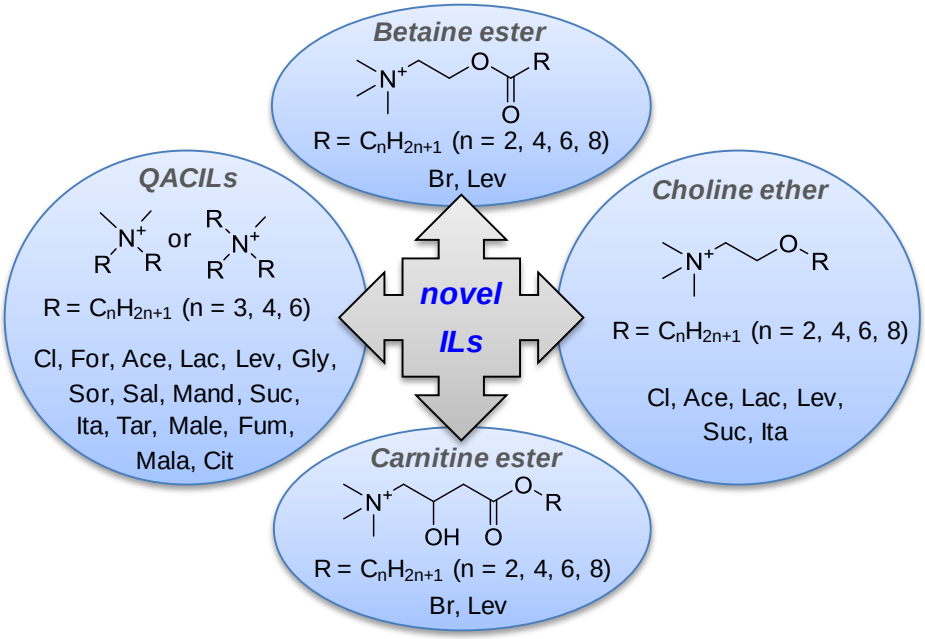

Figure C.1 Overview for the structures of the novel ILs synthesized and characterized in this project.

Besides the study of physicochemical properties of the pure ILs, such as thermal phase transitions (by DSC), thermal stability (by TGA) and viscosities, their behavior in aqueous solutions have been determined. Therefore, surface tension measurements have been carried out, and the ability to act as hydrotrope was investigated for QACILs and betaine- and carnitine-derivatives. The aqueous behavior of longer alkyl-chain **QACILs**, namely based on [DiC_6] cations, was also investigated as a function of the anion nature. In particular, itaconate-based ILs exhibited a very good aqueous solubilization capacity towards the hydrophobic dye Disperse Red 13 which was used as model for hydrophobic compounds. **[DiC_6]$_2$Ita** is even more efficient as the common hydrotrope sodium xylene sulfonate (SXS). Among **betaine-** and **carnitine-ester**, compounds, especially the ones based on [C_6-Bet], [C_8-Bet], [C_6-Carn], [C_8-Carn] cations, were surface active in aqueous solutions. We have also tested their hydrotropic behavior

resulting in high solubilization capacity towards a hydrophobic dye for [C_6-Bet]Br, [C_6-Carn]Br and [C_8-Carn]Br, as shown in **Figure C.2**. Due to their properties of solubilizing and coupling agents, hydrotropes are of great interest in industrial applications, such as formulation of cleaning products, drug solubilization and for paints and coatings.

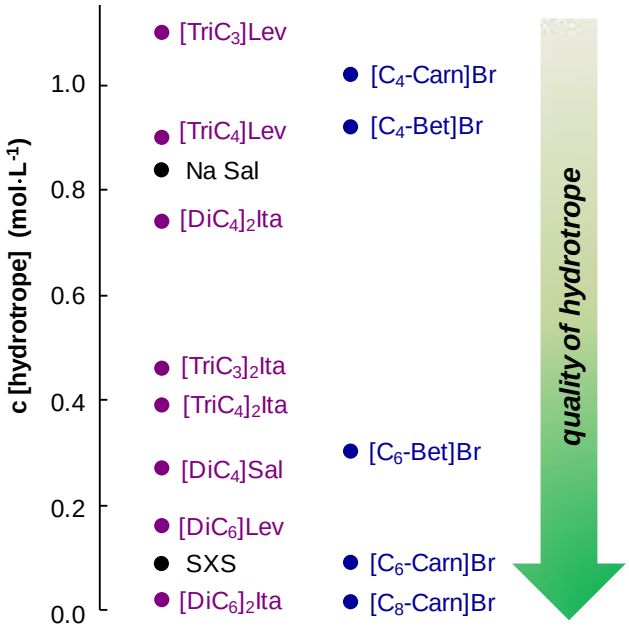

Figure C.2 ILs as hydrotropes for the aqueous solubilization of Disperse Red 13 (3.6^{E}-5 mol·L^{-1}, absorbance 1 at 503 nm) as hydrophobic model compound.

In this study we focused on quaternary ammonium as cations not only because of their structure, but also because they are less toxic than imidazolium and pyridinium compounds due to their lower lipophilicity. The additional feature to obtain ILs of high "greenness" was the use of biosourced counter anions, namely carboxylates. So, the biodegradability of **QACILs** with [DiC_4] as cation has been investigated with regard to their evaluation as "green" solvents. Most of the tested ILs, except **[DiC_4]Sor** and **[DiC_4]$_2$Ita**, have passed the limit of 60 wt% after a period of 28 days, thus they were classified as biodegradable (**Figure C.3.b**). Additionally, some ILs based on levulinate as anion have also been tested for their biodegradability (**Figure C.3.a**) identifying only **[Chol]Lev** and **[C_2-Bet]Lev** as biodegradable.

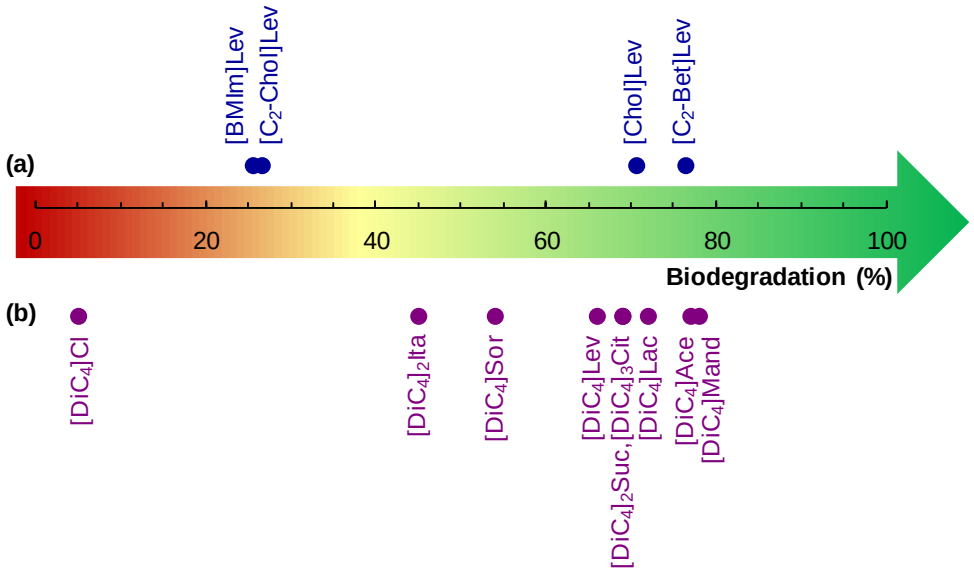

Figure C.3 Biodegradation of ILs based on **(a)** levulinate with different cations, and **(b)** the quaternary ammonium [DiC_4] with different anions.

Moreover, ecotoxicity tests were carried out showing that the levulinate IL [C_2-Bet]Lev was not toxic to aquatic systems (EC_{50} > 100 mg·L^{-1}), and [C_2-Chol]Lev, [BMIm]Lev and [Chol]Lev could not be described as having low ecotoxicities (EC_{50} < 100 mg·L^{-1}). The investigation of cytotoxicity using rat cells resulted in no toxic effects for [Chol]Lev, [C_2-Chol]Lev, [C_2-Bet]Lev and [BMIm]Lev up to the highest tested concentrations of around 1 g·L^{-1}.

DESs, which could be real alternatives to classical organic solvents or ILs, were also studied as novel "green" solvents. Therefore, two different types of biosourced hydrogen bond donors (HBDs) were examined: **urea** and **sugar-derivatives**. Urea, which is natural resourced, was combined with classical quaternary ammonium, and furthermore with betaine ester as sustainable alternative. Various sugar-derivatives, which are potentially available from cellulose transformation, were mixed with bio-based quaternary ammonium, such as choline chloride, betaine and carnitine. An overview for the studied DESs is illustrated in **Figure C.4**.

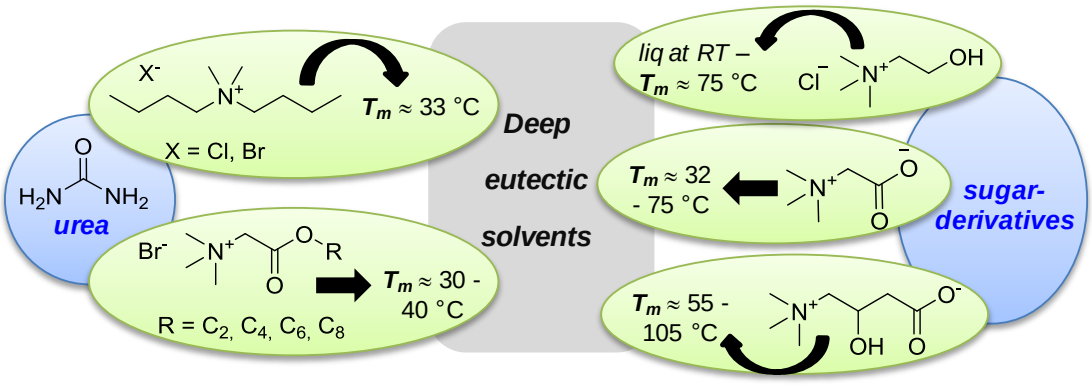

Figure C.4 Overview for DESs in this study.

In addition, DES mixtures were calculated giving rough approximations with experimental results, *i.e.* either the ratio or the temperature of the eutectic point, have been computed. Even if COSMO-RS is a highly versatile tool for theoretical calculations of various compounds, mixtures, physicochemical properties and behavior in complex systems, it should be used carefully and with a critical point of view based on thorough experimental results.

Initially, existing studies were analyzed in detail as support for the design of biocompatible cellulose solvents. Based on published estimations for the solubilization mechanism for cellulose with ILs, the first part of the project focused on quaternary ammonium, which is the simplest cation allowing a variation of the number and length of alkyl chains in order to assess the impact of the chemical structure on the physicochemical properties and power for cellulose solubilization. The most important structural effects of quaternary ammonium cations and carboxylate anions on cellulose solubilization are summarized in **Figure C.5** highlighting the following QACILs as the best ones (9 – 10 wt%): [DiC_4]Ace, [DiC_4]$_2$Ita, [DiC_3]Lev, [$TriC_3$]Lev and [DiC_4]Lev.

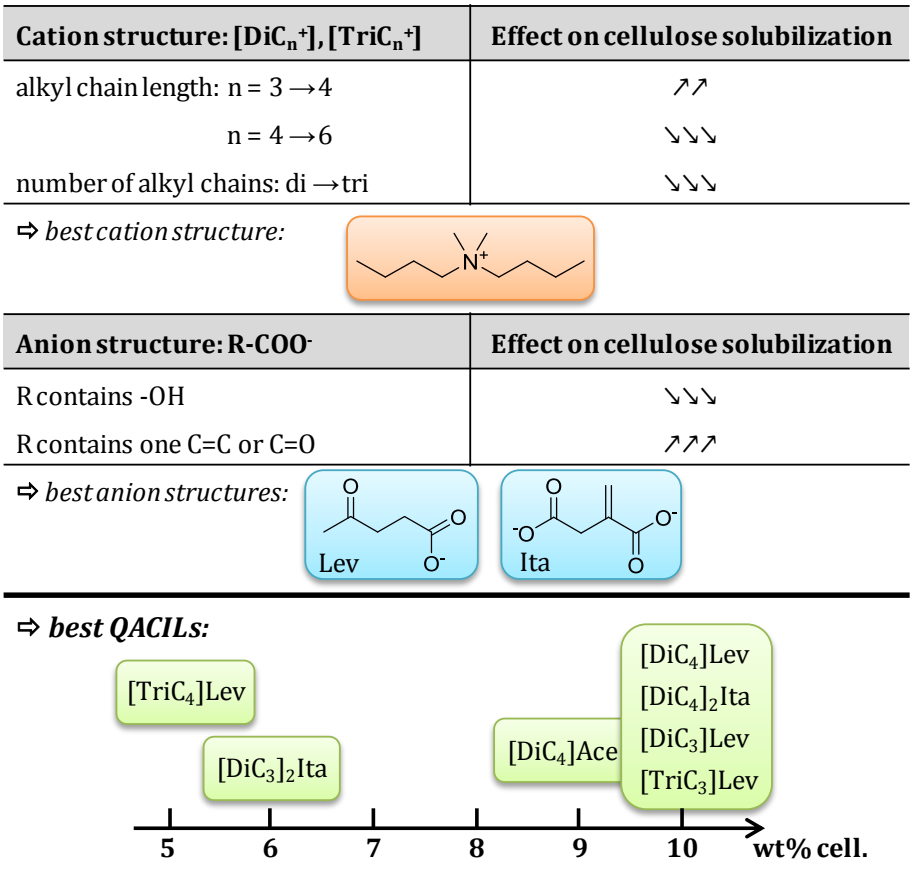

Figure C.5 Overview for the structural influence of QACILs on cellulose solubilization.

Additionally, a system of **[$TriC_3$]Lev** combined with 20 wt% **γ-valerolactone** as "green" co-solvent was able to dissolve 20 wt% of cellulose. Furthermore, the tested ILs have a high

tolerance of water (up to 15 wt% of water for [TriC_3]Lev without loss of solubilization power) which is one of the main drawbacks that common ILs are currently facing for use on a large scale.

Based on the results of QACILs for cellulose solubilization, more biocompatible ILs derived from bio-based compounds as cations, *i.e.* choline ether, betaine and carnitine esters, were designed. First, we focused on **choline ether** compounds with a variation of the alkyl side chain (ethyl, butyl, hexyl, octyl) and different natural resourced carboxylate counter anions: **acetate, lactate, levulinate, succinate** and **itaconate**. The impact of their chemical structure on cellulose solubilization was studied, resulting in **[C_2-Chol]Lev** as the only but very efficient solvent (up to 10 wt%). In addition, this IL was combined with 20 wt% **γ-valerolactone** as sustainable co-solvent resulting in 13 wt% cellulose solubilization. On the other hand, ethyl and butyl betaine and carnitine ester levulinate ILs were not efficient for the solubilization of cellulose, which could be attributed to the ester group in the cationic part. The ester group has probably an inductive effect on the IL anion which results in a poor availability for the cellulose solubilization. As an additional investigation, **[C_2-Chol]Lev** gave satisfying results for the solublization of other biopolymers at 90 - 100 °C: xylan (9 wt%), lignin (7 wt%), starch (12.5 wt%), which proves a high assessment for this novel IL.

In an additional part of this study, the theoretical method COSMO-RS has been applied as a tool for the support and/or prediction of experimental results. Unfortunately, for calculations of cellulose solubilization with ILs, no good correlations between experimental and theoretical investigations were obtained. Therefore, the calculation method should be further optimized.

Summing up, various studies on novel biocompatible solvents, such as ILs and DESs, have been carried out, including a detailed surveillance of the existing literature, the design and synthesis of ILs and DESs, their physicochemical characterization, determination of their biodegradability and finally the investigation of solubilization power of ILs for cellulose. This thesis opens up several avenues to go further in the development of greener ILs and DESs for biopolymer solubilization:

- The determination of biopolymer solubilization could be expanded by testing all presented ILs for further biopolymers, such as chitin, lignin, starch and hemicellulose, as already started for ILs based on levulinate. Furthermore, examinations on the effect of different co-solvents could be enlarged.
- The topic of betaine ester and carnitine ester depicts many possibilities for the design of various “green” compounds including ILs, DESs, hydrotropes and surfactants. Therefore,

numerous anions could be applied, especially natural carboxylates. Furthermore, the alkyl chain of the cationic part can be further varied due to the desired application. Carnitine ester, for instance, opens a new class of "green" surfactants with alkyl side chains longer than C_{10} or C_{12}.

- For DES formation, there are innumerable possible combinations of biosourced components which could give promising biocompatible solvents. For example, choline ether and carnitine ester with different alkyl chain lengths should be studied as HBAs in combination with urea. Additionally, DESs based on sugar-derivatives could still be further developed using compounds based on other sugar monomers, and their variation of alkyl chains connected to the anomeric carbon.
- In the framework of the study based on theoretical modeling, COSMO-RS calculations for the solubilization of further and/or less complicated biopolymers, *i.e.* starch or hemicellulose, could be carried out and compared to experiments. Moreover, the prediction of DESs (ratio and temperature of the eutectic mixture) could be continued with supplementary examples and evaluated with the support of experimental results.

References

(1) Anastas, P. T.; Warner, J. C. *Green Chemistry: Theory and Practice*; Oxford University Press, **2000**.

(2) Freemantle, M. *An Introduction to Ionic Liquids*; Royal Society of Chemistry: Cambridge, **2010**.

(3) Zhang, Q.; De Oliveira Vigier, K.; Royer, S.; Jérôme, F. Deep Eutectic Solvents: Syntheses, Properties and Applications. *Chem. Soc. Rev.* **2012**, *41*, 7108-1746.

(4) Pena-Pereira, F.; Namieśnik, J. Ionic Liquids and Deep Eutectic Mixtures: Sustainable Solvents for Extraction Processes. *ChemSusChem* **2014**, *7*, 1784–1800.

(5) Hon, D.-S. Cellulose: A Random Walk along Its Historical Path. *Cellulose* **1994**, *1*, 1–25.

(6) Klemm, D.; Heublein, B.; Fink, H.-P.; Bohn, A. Cellulose: Fascinating Biopolymer and Sustainable Raw Material. *Angew. Chem. Int. Ed.* **2005**, *44*, 3358–3393.

(7) Staudinger, H. Über Polymerisation. *Berichte Dtsch. Chem. Ges. B Ser.* **1920**, *53*, 1073–1085.

(8) Endres, H. J.; Siebert-Raths, A. *Technische Biopolymere: Rahmenbedingungen, Marktsitutation, Herstellung, Aufbau Und Eigenschaften*; Hanser, **2009**.

(9) Yanlong, G. Bio-Based Chemicals: A Sustainable Candidate for New Generation of Green Solvents. **2013**.

(10) JARROUX Nathalie. Les biopolymères : différentes familles, propriétés et applications. *Tech. Ing. Innov. En Matér. Avancés* **2008**, *base documentaire : TIB186DUO*.

(11) Babu, B. V. Biomass Pyrolysis: A State-of-the-Art Review. *Biofuels Bioprod. Biorefining* **2008**, *2*, 393–414.

(12) Alonso, D. M.; Bond, J. Q.; Dumesic, J. A. Catalytic Conversion of Biomass to Biofuels. *Green Chem* **2010**, *12*, 1493–1513.

(13) Fukaya, Y.; Hayashi, K.; Wada, M.; Ohno, H. Cellulose Dissolution with Polar Ionic Liquids under Mild Conditions: Required Factors for Anions. *Green Chem.* **2008**, *10*, 44–46.

(14) Agbor, V. B.; Cicek, N.; Sparling, R.; Berlin, A.; Levin, D. B. Biomass Pretreatment: Fundamentals toward Application. *Biotechnol. Adv.* **2011**, *29*, 675–685.

(15) Laurent, P.; Roiz, J.; Wertz, J.-L.; Richel, A.; Paquot, M. Le Bioraffinage, Une Alternative Prometteuse À La Pétrochimie. *Biotechnol. Agron. Société Environ.* **2011**, *15*, 597–610.

(16) Corma, A.; Iborra, S.; Velty, A. Chemical Routes for the Transformation of Biomass into Chemicals. *Chem. Rev.* **2007**, *107*, 2411–2502.

(17) Rose, M.; Palkovits, R. Cellulose-Based Sustainable Polymers: State of the Art and Future Trends. *Macromol. Rapid Commun.* **2011**, *32*, 1299–1311.

(18) Geilen, F. M. A.; Engendahl, B.; Harwardt, A.; Marquardt, W.; Klankermayer, J.; Leitner, W. Selective and Flexible Transformation of Biomass-Derived Platform Chemicals by a Multifunctional Catalytic System. *Angew. Chem.* **2010**, *122*, 5642–5646.

(19) Bozell, J. J.; Moens, L.; Elliott, D. C.; Wang, Y.; Neuenscwander, G. G.; Fitzpatrick, S. W.; Bilski, R. J.; Jarnefeld, J. L. Production of Levulinic Acid and Use as a Platform Chemical for Derived Products. *Resour. Conserv. Recycl.* **2000**, *28*, 227–239.
(20) Tian, J.; Wang, J.; Zhao, S.; Jiang, C.; Zhang, X.; Wang, X. Hydrolysis of Cellulose by the Heteropoly Acid H3PW12O40. *Cellulose* **2010**, *17*, 587–594.
(21) Takagaki, A.; Tagusagawa, C.; Domen, K. Glucose Production from Saccharides Using Layered Transition Metal Oxide and Exfoliated Nanosheets as a Water-Tolerant Solid Acid Catalyst. *Chem. Commun.* **2008**, 5363–5365.
(22) Miller-Chou, B. A.; Koenig, J. L. A Review of Polymer Dissolution. *Prog. Polym. Sci.* **2003**, *28*, 1223–1270.
(23) Wang, X.; Rinaldi, R. Solvent Effects on the Hydrogenolysis of Diphenyl Ether with Raney Nickel and Their Implications for the Conversion of Lignin. *ChemSusChem* **2012**, *5*, 1455–1466.
(24) Ji, W.; Ding, Z.; Liu, J.; Song, Q.; Xia, X.; Gao, H.; Wang, H.; Gu, W. Mechanism of Lignin Dissolution and Regeneration in Ionic Liquid. *Energy Fuels* **2012**, *26*, 6393–6403.
(25) Chakar, F. S.; Ragauskas, A. J. Review of Current and Future Softwood Kraft Lignin Process Chemistry. *Ind. Crops Prod.* **2004**, *20*, 131–141.
(26) Pinkert, A.; Marsh, K. N.; Pang, S. Reflections on the Solubility of Cellulose. *Ind. Eng. Chem. Res.* **2010**, *49*, 11121–11130.
(27) Heinze, T.; Koschella, A. Solvents Applied in the Field of Cellulose Chemistry: A Mini Review. *Polímeros* **2005**, *15*, 84–90.
(28) Fink, H. P.; Weigel, P.; Purz, H. J.; Ganster, J. Structure Formation of Regenerated Cellulose Materials from NMMO-Solutions. *Prog. Polym. Sci.* **2001**, *26*, 1473–1524.
(29) McCormick, C. L.; Dawsey, T. R. Preparation of Cellulose Derivatives via Ring-Opening Reactions with Cyclic Reagents in Lithium chloride/N,N-Dimethylacetamide. *Macromolecules* **1990**, *23*, 3606–3610.
(30) Tamai, N.; Tatsumi, D.; Matsumoto, T. Rheological Properties and Molecular Structure of Tunicate Cellulose in LiCl/1,3-Dimethyl-2-Imidazolidinone. *Biomacromolecules* **2004**, *5*, 422–432.
(31) Abou-State, M. A.; Awad, B. M. The Solvation of Cellulose by the Action of Nitrogen Tetroxide in Organic Solvents. *J. Appl. Chem. Biotechnol.* **1977**, *27*, 399–404.
(32) Ciacco, G.; Liebert, T.; Frollini, E.; Heinze, T. Application of the Solvent Dimethyl Sulfoxide/tetrabutyl-Ammonium Fluoride Trihydrate as Reaction Medium for the Homogeneous Acylation of Sisal Cellulose. *Cellulose* **2003**, *10*, 125–132.
(33) Fischer, S.; Leipner, H.; Thümmler, K.; Brendler, E.; Peters, J. Inorganic Molten Salts as Solvents for Cellulose. *Cellulose* **2003**, *10*, 227–236.
(34) Pinkert, A.; Marsh, K. N.; Pang, S.; Staiger, M. P. Ionic Liquids and Their Interaction with Cellulose. *Chem. Rev.* **2009**, *109*, 6712–6728.
(35) Heinze, T.; Liebert, T. Unconventional Methods in Cellulose Functionalization. *Prog. Polym. Sci.* **2001**, *26*, 1689–1762.
(36) Xu, A.; Wang, J.; Wang, H. Effects of Anionic Structure and Lithium Salts Addition on the Dissolution of Cellulose in 1-Butyl-3-Methylimidazolium-Based Ionic Liquid Solvent Systems. *Green Chem.* **2010**, *12*, 268–275.

(37) Kerton, F. M.; Marriott, R. *Alternative Solvents for Green Chemistry*; Second.; The Royal Society of Chemistry, **2013**.
(38) Anastas, P.; Eghbali, N. Green Chemistry: Principles and Practice. *Chem. Soc. Rev.* **2010**, *39*, 301–312.
(39) Walden, P. *Über Die Molekulargrösse Und Elektrische Leitfähigkeit Einiger Geschmolzenen Salze*; Bull Acad Imper Sci: St Petersburg, **1914**; Vol. VI serie, 8(6):405-422.
(40) Chum, H. L.; Koch, V. R.; Miller, L. L.; Osteryoung, R. A. Electrochemical Scrutiny of Organometallic Iron Complexes and Hexamethylbenzene in a Room Temperature Molten Salt. *J. Am. Chem. Soc.* **1975**, *97*, 3264–3265.
(41) Wilkes, J. S.; Levisky, J. A.; Wilson, R. A.; Hussey, C. L. Dialkylimidazolium Chloroaluminate Melts: A New Class of Room-Temperature Ionic Liquids for Electrochemistry, Spectroscopy and Synthesis. *Inorg. Chem.* **1982**, *21*, 1263–1264.
(42) Greaves, T. L.; Drummond, C. J. Protic Ionic Liquids: Properties and Applications. *Chem. Rev.* **2008**, *108*, 206–237.
(43) MacFarlane, D. R.; Seddon, K. R. Ionic Liquids—Progress on the Fundamental Issues. *Aust. J. Chem.* **2007**, *60*, 3.
(44) Krossing, I.; Slattery, J. M.; Daguenet, C.; Dyson, P. J.; Oleinikova, A.; Weingärtner, H. Why Are Ionic Liquids Liquid? A Simple Explanation Based on Lattice and Solvation Energies. *J. Am. Chem. Soc.* **2006**, *128*, 13427–13434.
(45) Xue, H.; Verma, R.; Shreeve, J. M. Review of Ionic Liquids with Fluorine-Containing Anions. *J. Fluor. Chem.* **2006**, *127*, 159–176.
(46) Huddleston, J. G.; Visser, A. E.; Reichert, W. M.; Willauer, H. D.; Broker, G. A.; Rogers, R. D. Characterization and Comparison of Hydrophilic and Hydrophobic Room Temperature Ionic Liquids Incorporating the Imidazolium Cation. *Green Chem.* **2001**, *3*, 156–164.
(47) Wasserscheid, P.; Keim, W. Ionic Liquids—New "Solutions" for Transition Metal Catalysis. *Angew. Chem. Int. Ed.* **2000**, *39*, 3772–3789.
(48) Wasserscheid, P.; Welton, T. *Ionic Liquids in Synthesis*; Wiley Online Library, **2008**; Vol. 7.
(49) Ngo, H. L.; LeCompte, K.; Hargens, L.; McEwen, A. B. Thermal Properties of Imidazolium Ionic Liquids. *Thermochim. Acta* **2000**, *357*, 97–102.
(50) Gordon, C. M.; Holbrey, J. D.; Kennedy, A. R.; Seddon, K. R. Ionic Liquid Crystals: Hexafluorophosphate Salts. *J. Mater. Chem.* **1998**, *8*, 2627–2636.
(51) Belieres, J.-P.; Angell, C. A. Protic Ionic Liquids: Preparation, Characterization, and Proton Free Energy Level Representation†. *J. Phys. Chem. B* **2007**, *111*, 4926–4937.
(52) Bonhote, P.; Dias, A.-P.; Papageorgiou, N.; Kalyanasundaram, K.; Grätzel, M. Hydrophobic, Highly Conductive Ambient-Temperature Molten Salts. *Inorg. Chem.* **1996**, *35*, 1168–1178.
(53) Yoshizawa, M.; Xu, W.; Angell, C. A. Ionic Liquids by Proton Transfer: Vapor Pressure, Conductivity, and the Relevance of ΔpKa from Aqueous Solutions. *J. Am. Chem. Soc.* **2003**, *125*, 15411–15419.

(54) Earle, M. J.; Esperança, J. M. S. S.; Gilea, M. A.; Canongia Lopes, J. N.; Rebelo, L. P. N.; Magee, J. W.; Seddon, K. R.; Widegren, J. A. The Distillation and Volatility of Ionic Liquids. *Nature* **2006**, *439*, 831–834.

(55) Viswanath, D. S.; Tushar, K. G.; Dasika, H. L. P.; Nidamarty, V. K. D.; Kalipatnapu, Y. R. *Viscosity of Liquids Theory, Estimation, Experiment, and Data*; Springer: Dordrecht, **2007**.

(56) Bandrés, I.; Alcalde, R.; Lafuente, C.; Atilhan, M.; Aparicio, S. On the Viscosity of Pyridinium Based Ionic Liquids: An Experimental and Computational Study. *J. Phys. Chem. B* **2011**, *115*, 12499–12513.

(57) Li, H.; Ibrahim, M.; Agberemi, I.; Kobrak, M. N. The Relationship between Ionic Structure and Viscosity in Room-Temperature Ionic Liquids. *J. Chem. Phys.* **2008**, *129*, 124507.

(58) Tsunamisha, K.; Sugiya, M. Physical and Electrochemical Properties of Room Temperature Ionic Liquids Based on Quaternary Phosphonium Cations. *Electrochemistry* **2007**, *75*, 734–736.

(59) Okoturo, O. O.; VanderNoot, T. J. Temperature Dependence of Viscosity for Room Temperature Ionic Liquids. *J. Electroanal. Chem.* **2004**, *568*, 167–181.

(60) Walden, P. Organic Solvents and Ionization Media. III. Interior Friction and Its Relation to Conductivity. *Z. Fuer Phys. Chem. Stoechiom. Verwandtschaftslehre* **1906**, *55*, 207–249.

(61) Fraser, K. J.; Izgorodina, E. I.; Forsyth, M.; Scott, J. L.; MacFarlane, D. R. Liquids Intermediate between "Molecular" and "Ionic" Liquids: Liquid Ion Pairs? *Chem. Commun.* **2007**, 3817–3819.

(62) Tariq, M.; Freire, M. G.; Saramago, B.; Coutinho, J. A. P.; Lopes, J. N. C.; Rebelo, L. P. N. Surface Tension of Ionic Liquids and Ionic Liquid Solutions. *Chem Soc Rev* **2012**, *41*, 829–868.

(63) Ghatee, M. H.; Zare, M.; Zolghadr, A. R.; Moosavi, F. Temperature Dependence of Viscosity and Relation with the Surface Tension of Ionic Liquids. *Fluid Phase Equilib* **2010**, *291*, 188–194.

(64) Rooney, D.; Jacquemin, J.; Gardas, R. Thermophysical Properties of Ionic Liquids. In *Ionic Liquids*; Kirchner, B., Ed.; Topics in Current Chemistry; Springer Berlin Heidelberg, **2010**; Vol. 290, pp. 185–212.

(65) Dean, J. A. *Lange's Handbook of Chemistry*; 15th ed.; McGraw-Hill: New York, 1999.

(66) Law, G.; Watson, P. R. Surface Tension Measurements of *N* -Alkylimidazolium Ionic Liquids. *Langmuir* **2001**, *17*, 6138–6141.

(67) Law, G.; Watson, P. R. Surface Orientation in Ionic Liquids. *Chem. Phys. Lett.* **2001**, *345*, 1–4.

(68) Greaves, T. L.; Weerawardena, A.; Fong, C.; Krodkiewska, I.; Drummond, C. J. Protic Ionic Liquids: Solvents with Tunable Phase Behavior and Physicochemical Properties. *J. Phys. Chem. B* **2006**, *110*, 22479–22487.

(69) Łuczak, J.; Hupka, J.; Thöming, J.; Jungnickel, C. Self-Organization of Imidazolium Ionic Liquids in Aqueous Solution. *Colloids Surf. Physicochem. Eng. Asp.* **2008**, *329*, 125–133.

(70) Bowers, J.; Butts, C. P.; Martin, P. J.; Vergara-Gutierrez, M. C.; Heenan, R. K. Aggregation Behavior of Aqueous Solutions of Ionic Liquids. *Langmuir* **2004**, *20*, 2191–2198.

(71) Dong, B.; Li, N.; Zheng, L.; Yu, L.; Inoue, T. Surface Adsorption and Micelle Formation of Surface Active Ionic Liquids in Aqueous Solution. *Langmuir* **2007**, *23*, 4178–4182.

(72) Wang, X.; Liu, J.; Yu, L.; Jiao, J.; Wang, R.; Sun, L. Surface Adsorption and Micelle Formation of Imidazolium-Based Zwitterionic Surface Active Ionic Liquids in Aqueous Solution. *J. Colloid Interface Sci.* **2013**, *391*, 103–110.

(73) Reichardt, C. Polarity of Ionic Liquids Determined Empirically by Means of Solvatochromic Pyridinium N-Phenolate Betaine Dyes. *Green Chem.* **2005**, *7*, 339–351.

(74) Carmichael, A. J.; Seddon, K. R. Polarity Study of Some 1-Alkyl-3-Methylimidazolium Ambient-Temperature Ionic Liquids with the Solvatochromic Dye, Nile Red. *J. Phys. Org. Chem.* **2000**, *13*, 591–595.

(75) Reichardt, C. Empirical Parameters of the Polarity of Solvents. *Angew. Chem. Int. Ed. Engl.* **1965**, *4*, 29–40.

(76) Reichardt, C.; Harbusch-Görnert, E. Über Pyridinium-N-Phenolat-Betaine Und Ihre Verwendung Zur Charakterisierung Der Polarität von Lösungsmitteln, X. Erweiterung, Korrektur Und Neudefinition Der ET-Lösungsmittelpolaritätsskala Mit Hilfe Eines Lipophilen Penta-Tert-Butyl-Substituierten Pyridinium-N-Phenolat-Betainfarbstoffes. *Liebigs Ann. Chem.* **1983**, *1983*, 721–743.

(77) Plechkova, N. V.; Seddon, K. R. Applications of Ionic Liquids in the Chemical Industry. *Chem. Soc. Rev.* **2008**, *37*, 123-150.

(78) Sangster, J. Octanol-Water Partition Coefficients of Simple Organic Compounds. *J. Phys. Chem. Ref. Data* **1989**, *18*, 1111–1229.

(79) Lee, S. H.; Lee, S. B. Octanol/water Partition Coefficients of Ionic Liquids. *J. Chem. Technol. Biotechnol.* **2009**, *84*, 202–207.

(80) Ropel, L.; Belvèze, L. S.; Aki, S. N. V. K.; Stadtherr, M. A.; Brennecke, J. F. Octanol Water Partition Coefficients of Imidazolium-Based Ionic Liquids. *Green Chem.* **2005**, *7*, 83-90.

(81) Hallett, J. P.; Welton, T. Room-Temperature Ionic Liquids: Solvents for Synthesis and Catalysis. 2. *Chem. Rev.* **2011**, *111*, 3508–3576.

(82) Luo, H.; Baker, G. A.; Dai, S. Isothermogravimetric Determination of the Enthalpies of Vaporization of 1-Alkyl-3-Methylimidazolium Ionic Liquids. *J. Phys. Chem. B* **2008**, *112*, 10077–10081.

(83) Jin, H.; O'Hare, B.; Dong, J.; Arzhantsev, S.; Baker, G. A.; Wishart, J. F.; Benesi, A. J.; Maroncelli, M. Physical Properties of Ionic Liquids Consisting of the 1-Butyl-3-Methylimidazolium Cation with Various Anions and the Bis(trifluoromethylsulfonyl)imide Anion with Various Cations. *J. Phys. Chem. B* **2008**, *112*, 81–92.

(84) Lee, S. H.; Lee, S. B. The Hildebrand Solubility Parameters, Cohesive Energy Densities and Internal Energies of 1-Alkyl-3-Methylimidazolium-Based Room Temperature Ionic Liquids. *Chem. Commun.* **2005**, 3469–3471.

(85) Swiderski, K.; McLean, A.; Gordon, C. M.; Vaughan, D. H. Estimates of Internal Energies of Vaporisation of Some Room Temperature Ionic Liquids. *Chem. Commun.* **2004**, 2178–2179.
(86) Ranke, J.; Stolte, S.; Stoermann, R.; Arning, J.; Jastorff, B. Design of Sustainable Chemical Products - The Example of Ionic Liquids. *Chem Rev Wash. DC U S* **2007**, *107*, 2183–2206.
(87) Earle, M. J.; Seddon, K. R. Ionic Liquids. Green Solvents for the Future. *Pure Appl. Chem.* **2000**, *72*, 1391–1398.
(88) Jessop, P. G. Searching for Green Solvents. *Green Chem.* **2011**, *13*, 1391–1398.
(89) Romero, A.; Santos, A.; Tojo, J.; Rodríguez, A. Toxicity and Biodegradability of Imidazolium Ionic Liquids. *J. Hazard. Mater.* **2008**, *151*, 268–273.
(90) Zhao, D.; Liao, Y.; Zhang, Z. Toxicity of Ionic Liquids. *CLEAN – Soil Air Water* **2007**, *35*, 42–48.
(91) Petkovic, M.; Seddon, K. R.; Rebelo, L. P. N.; Silva Pereira, C. Ionic Liquids: A Pathway to Environmental Acceptability. *Chem. Soc. Rev.* **2011**, *40*, 1383-1403.
(92) Thuy Pham, T. P.; Cho, C.-W.; Yun, Y.-S. Environmental Fate and Toxicity of Ionic Liquids: A Review. *Water Res.* **2010**, *44*, 352–372.
(93) Stolte, S.; Arning, J.; Bottin-Weber, U.; Muller, A.; Pitner, W.-R.; Welz-Biermann, U.; Jastorff, B.; Ranke, J. Effects of Different Head Groups and Functionalised Side Chains on the Cytotoxicity of Ionic Liquids. *Green Chem.* **2007**, *9*, 760–767.
(94) Gathergood, N.; Garcia, M. T.; Scammells, P. J. Biodegradable Ionic Liquids: Part I. Concept, Preliminary Targets and Evaluation. *Green Chem.* **2004**, *6*, 166-175.
(95) Garcia, M. T.; Gathergood, N.; Scammells, P. J. Biodegradable Ionic Liquids : Part II. Effect of the Anion and Toxicology. *Green Chem.* **2005**, *7*, 9-14.
(96) Stolte, S.; Arning, J.; Thöming, J. Biologische Abbaubarkeit von Ionischen Flüssigkeiten – Testverfahren Und Strukturelles Design Biodegradability of Ionic Liquids – Test Procedures and Structural Design. *Chem. Ing. Tech.* **2011**, *83*, 1454–1467.
(97) Coleman, D.; Gathergood, N. Biodegradation Studies of Ionic Liquids. *Chem. Soc. Rev.* **2010**, *39*, 600-637.
(98) Fukaya, Y.; Iizuka, Y.; Sekikawa, K.; Ohno, H. Bio Ionic Liquids: Room Temperature Ionic Liquids Composed Wholly of Biomaterials. *Green Chem.* **2007**, *9*, 1155-1157.
(99) Zhao, B.; Greiner, L.; Leitner, W. Cellulose Solubilities in Carboxylate-Based Ionic Liquids. *RSC Adv* **2012**, *2*, 2476–2479.
(100) Fukumoto, K.; Yoshizawa, M.; Ohno, H. Room Temperature Ionic Liquids from 20 Natural Amino Acids. *J. Am. Chem. Soc.* **2005**, *127*, 2398–2399.
(101) Ohno, H.; Fukumoto, K. Amino Acid Ionic Liquids. *Acc. Chem. Res.* **2007**, *40*, 1122–1129.
(102) Tao, G.; He, L.; Sun, N.; Kou, Y. New Generation Ionic Liquids: Cations Derived from Amino Acids. *Chem. Commun.* **2005**, *0*, 3562–3564.
(103) Stasiewicz, M.; Mulkiewicz, E.; Tomczak-Wandzel, R.; Kumirska, J.; Siedlecka, E. M.; Gołębiowski, M.; Gajdus, J.; Czerwicka, M.; Stepnowski, P. Assessing Toxicity and Biodegradation of Novel, Environmentally Benign Ionic Liquids (1-Alkoxymethyl-3-Hydroxypyridinium Chloride, Saccharinate and Acesulfamates) on Cellular and Molecular Level. *Ecotoxicol. Environ. Saf.* **2008**, *71*, 157–165.

(104) Coleman, D.; Gathergood, N. Biodegradation Studies of Ionic Liquids. *Chem. Soc. Rev.* **2010**, *39*, 600–637.

(105) Pernak, J.; Syguda, A.; Mirska, I.; Pernak, A.; Nawrot, J.; Prądzyńska, A.; Griffin, S. T.; Rogers, R. D. Choline-Derivative-Based Ionic Liquids. *Chem. – Eur. J.* **2007**, *13*, 6817–6827.

(106) Tseng, J. C. W.; Rondla, R.; Su, P. Y. S.; Lin, I. J. B. The Roles of Betaine-Ester Analogues of 1-N-Alkyl-3-N'-Methyl Imidazolium Salts: As Amphotropic Ionic Liquid Crystals and Organogelators. *RSC Adv.* **2013**, *3*, 25151–25158.

(107) Pârvulescu, V. I.; Hardacre, C. Catalysis in Ionic Liquids. *Chem. Rev.* **2007**, *107*, 2615–2665.

(108) Blanchard, L. A.; Hancu, D.; Beckman, E. J.; Brennecke, J. F. Green Processing Using Ionic Liquids and CO2. *Nature* **1999**, *399*, 28–29.

(109) Zhao, H.; Xia, S.; Ma, P. Use of Ionic Liquids as "green"solvents for Extractions. *J. Chem. Technol. Biotechnol.* **2005**, *80*, 1089–1096.

(110) Armand, M.; Endres, F.; MacFarlane, D. R.; Ohno, H.; Scrosati, B. Ionic-Liquid Materials for the Electrochemical Challenges of the Future. *Nat. Mater.* **2009**, *8*, 621–629.

(111) Byrne, N.; Howlett, P. C.; MacFarlane, D. R.; Forsyth, M. The Zwitterion Effect in Ionic Liquids: Towards Practical Rechargeable Lithium-Metal Batteries. *Adv. Mater.* **2005**, *17*, 2497–2501.

(112) Endres, F. Ionische Flüssigkeiten Zur Metallabscheidung. *Nachrichten Aus Chem.* **2007**, *55*, 507–511.

(113) Armel, V.; Pringle, J. M.; Forsyth, M.; MacFarlane, D. R.; Officer, D. L.; Wagner, P. Ionic Liquid Electrolyte Porphyrin Dye Sensitised Solar Cells. *Chem. Commun.* **2010**, *46*, 3146–3148.

(114) Minami, I. Ionic Liquid Lubricants. In *Encyclopedia of Tribology*; Springer, **2013**; pp. 1866–1866.

(115) Weyershausen, B.; Lehmann, K. Industrial Application of Ionic Liquids as Performance Additives. *Green Chem.* **2005**, *7*, 15–19.

(116) Bühler, G.; Zharkouskaya, A.; Feldmann, C. Ionic Liquid Based Approach to Nanoscale Functional Materials. *Solid State Sci.* **2008**, *10*, 461–465.

(117) Swatloski, R. P.; Spear, S. K.; Holbrey, J. D.; Rogers, R. D. Dissolution of Cellulose with Ionic Liquids. *J Am Chem Soc* **2002**, *124*, 4974–4975.

(118) Pu, Y.; Jiang, N.; Ragauskas, A. J. Ionic Liquid as a Green Solvent for Lignin. *J. Wood Chem. Technol.* **2007**, *27*, 23–33.

(119) Garcia, H.; Ferreira, R.; Petkovic, M.; Ferguson, J. L.; Leitao, M. C.; Gunaratne, H. Q. N.; Seddon, K. R.; Rebelo, L. P. N.; Silva Pereira, C. Dissolution of Cork Biopolymers in Biocompatible Ionic Liquids. *Green Chem.* **2010**, *12*, 367–369.

(120) Garcia, H.; Ferreira, R.; Martins, C.; Sousa, A. F.; Freire, C. S. R.; Silvestre, A. J. D.; Kunz, W.; Rebelo, L. P. N.; Silva Pereira, C. Ex Situ Reconstitution of the Plant Biopolyester Suberin as a Film. *Biomacromolecules* **2014**, *15*, 1806–1813.

(121) Xie, H.; Zhang, S.; Li, S. Chitin and Chitosan Dissolved in Ionic Liquids as Reversible Sorbents of CO2. *Green Chem.* **2006**, *8*, 630–633.

(122) Pei, Y.; Wang, J.; Wu, K.; Xuan, X.; Lu, X. Ionic Liquid-Based Aqueous Two-Phase Extraction of Selected Proteins. *Sep. Purif. Technol.* **2009**, *64*, 288–295.

(123) Maase Matthias; Massonne Klemens. Biphasic Acid Scavenging Utilizing Ionic Liquids: The First Commercial Process with Ionic Liquids. In *Ionic Liquids IIIB: Fundamentals, Progress, Challenges, and Opportunities*; ACS Symposium Series; American Chemical Society, **2005**; Vol. 902, pp. 126–132.

(124) Crowhurst, L.; Mawdsley, P. R.; Perez-Arlandis, J. M.; Salter, P. A.; Welton, T. Solvent-Solute Interactions in Ionic Liquids. *Phys. Chem. Chem. Phys.* **2003**, *5*, 2790–2794.

(125) Tan, S. S. Y.; MacFarlane, D. R.; Upfal, J.; Edye, L. A.; Doherty, W. O. S.; Patti, A. F.; Pringle, J. M.; Scott, J. L. Extraction of Lignin from Lignocellulose at Atmospheric Pressure Using Alkylbenzenesulfonate Ionic Liquid. *Green Chem.* **2009**, *11*, 339–345.

(126) Sun, N.; Rodriguez, H.; Rahman, M.; Rogers, R. D. Where Are Ionic Liquid Strategies Most Suited in the Pursuit of Chemicals and Energy from Lignocellulosic Biomass? *Chem Commun Camb. U K* **2011**, *47*, 1405–1421.

(127) Zhang, H.; Wu, J.; Zhang, J.; He, J. 1-Allyl-3-Methylimidazolium Chloride Room Temperature Ionic Liquid: A New and Powerful Nonderivatizing Solvent for Cellulose. *Macromolecules* **2005**, *38*, 8272–8277.

(128) Barthel, S.; Heinze, T. Acylation and Carbanilation of Cellulose in Ionic Liquids. *Green Chem.* **2006**, *8*, 301–306.

(129) Fukaya, Y.; Sugimoto, A.; Ohno, H. Superior Solubility of Polysaccharides in Low Viscosity, Polar, and Halogen-Free 1,3-Dialkylimidazolium Formates. *Biomacromolecules* **2006**, *7*, 3295–3297.

(130) Hermanutz, F.; Gaehr, F.; Uerdingen, E.; Meister, F.; Kosan, B. New Developments in Dissolving and Processing of Cellulose in Ionic Liquids. *Macromol Symp* **2008**, *262*, 23–27.

(131) Heinze, T.; Schwikal, K.; Barthel, S. Ionic Liquids as Reaction Medium in Cellulose Functionalization. *Macromol. Biosci.* **2005**, *5*, 520–525.

(132) Zhao, H.; Baker, G. A.; Song, Z.; Olubajo, O.; Crittle, T.; Peters, D. Designing Enzyme-Compatible Ionic Liquids That Can Dissolve Carbohydrates. *Green Chem.* **2008**, *10*, 696-705.

(133) Mäki-Arvela, P.; Anugwom, I.; Virtanen, P.; Sjöholm, R.; Mikkola, J. P. Dissolution of Lignocellulosic Materials and Its Constituents Using Ionic liquids—A Review. *Ind. Crops Prod.* **2010**, *32*, 175–201.

(134) Feng, L.; Chen, Z. Research Progress on Dissolution and Functional Modification of Cellulose in Ionic Liquids. *J. Mol. Liq.* **2008**, *142*, 1–5.

(135) Vesa Myllymäki, R. A. Dissolution Method for Lignocellulosic Materials, February 24, **2005**.

(136) Tao, F.; Song, H.; Chou, L. Catalytic Conversion of Cellulose to Chemicals in Ionic Liquid. *Carbohydr. Res.* **2011**, *346*, 58–63.

(137) Su, Y.; Brown, H. M.; Huang, X.; Zhou, X.; Amonette, J. E.; Zhang, Z. C. Single-Step Conversion of Cellulose to 5-Hydroxymethylfurfural (HMF), a Versatile Platform Chemical. *Appl. Catal. Gen.* **2009**, *361*, 117–122.

(138) Sun, Z.; Cheng, M.; Li, H.; Shi, T.; Yuan, M.; Wang, X.; Jiang, Z. One-Pot Depolymerization of Cellulose into Glucose and Levulinic Acid by Heteropolyacid Ionic Liquid Catalysis. *RSC Adv.* **2012**, *2*, 9058–9065.

(139) Villandier, N.; Corma, A. One Pot Catalytic Conversion of Cellulose into Biodegradable Surfactants. *Chem Commun Camb. U K* **2010**, *46*, 4408–4410.

(140) Corma Canos, A.; Villandier, N. D. Method for Obtaining Biodegradable Surfactants from Cellulose in a Single Reactor. WO 2011110721, September 15, **2011**.

(141) Abbott, A. P.; Boothby, D.; Capper, G.; Davies, D. L.; Rasheed, R. K. Deep Eutectic Solvents Formed between Choline Chloride and Carboxylic Acids: Versatile Alternatives to Ionic Liquids. *J. Am. Chem. Soc.* **2004**, *126*, 9142–9147.

(142) Abbott, A. P.; Capper, G.; Davies, D. L.; McKenzie, K. J.; Obi, S. U. Solubility of Metal Oxides in Deep Eutectic Solvents Based on Choline Chloride. *J. Chem. Eng. Data* **2006**, *51*, 1280–1282.

(143) Francisco, M.; van den Bruinhorst, A.; Kroon, M. C. New Natural and Renewable Low Transition Temperature Mixtures (LTTMs): Screening as Solvents for Lignocellulosic Biomass Processing. *Green Chem.* **2012**, *14*, 2153-2157.

(144) Francisco, M.; van den Bruinhorst, A.; Kroon, M. C. Low-Transition-Temperature Mixtures (LTTMs): A New Generation of Designer Solvents. *Angew. Chem. Int. Ed.* **2013**, *52*, 3074–3085.

(145) Ruß, C.; König, B. Low Melting Mixtures in Organic Synthesis – an Alternative to Ionic Liquids? *Green Chem.* **2012**, *14*, 2969.

(146) Abbott, A. P.; Capper, G.; Davies, D. L.; Rasheed, R. K.; Tambyrajah, V. Novel Solvent Properties of Choline Chloride/urea Mixtures. *Chem. Commun.* **2003**, *0*, 70–71.

(147) Shahbaz, K.; Mjalli, F. S.; Hashim, M. A.; Al Nashef, I. M. Using Deep Eutectic Solvents for the Removal of Glycerol from Palm Oil-Based Biodiesel. *J. Appl. Sci.* **2010**, *10*, 3349–3354.

(148) Hayyan, M.; Mjalli, F. S.; Hashim, M. A.; AlNashef, I. M. A Novel Technique for Separating Glycerine from Palm Oil-Based Biodiesel Using Ionic Liquids. *Fuel Process. Technol.* **2009**, *91*, 116–120.

(149) Hou, Y.; Gu, Y.; Zhang, S.; Yang, F.; Ding, H.; Shan, Y. Novel Binary Eutectic Mixtures Based on Imidazole. *J. Mol. Liq.* **2008**, *143*, 154–159.

(150) Maugeri, Z.; Domínguez de María, P. Novel Choline-Chloride-Based Deep-Eutectic-Solvents with Renewable Hydrogen Bond Donors: Levulinic Acid and Sugar-Based Polyols. *RSC Adv.* **2012**, *2*, 421-425.

(151) Fischer, V.; Kunz, W. Properties of Sugar-Based Low-Melting Mixtures. *Mol. Phys.* **2014**, *112*, 1241–1245.

(152) Abbott, A. P.; Capper, G.; Gray, S. Design of Improved Deep Eutectic Solvents Using Hole Theory. *ChemPhysChem* **2006**, *7*, 803–806.

(153) Abbott, A. P. Application of Hole Theory to the Viscosity of Ionic and Molecular Liquids. *ChemPhysChem* **2004**, *5*, 1242–1246.

(154) Abbott, A. P.; Harris, R. C.; Ryder, K. S.; D'Agostino, C.; Gladden, L. F.; Mantle, M. D. Glycerol Eutectics as Sustainable Solvent Systems. *Green Chem.* **2011**, *13*, 82–90.

(155) Dai, Y.; van Spronsen, J.; Witkamp, G.-J.; Verpoorte, R.; Choi, Y. H. Natural Deep Eutectic Solvents as New Potential Media for Green Technology. *Anal. Chim. Acta* **2013**, *766*, 61–68.

(156) Paiva, A.; Craveiro, R.; Aroso, I.; Martins, M.; Reis, R. L.; Duarte, A. R. C. Natural Deep Eutectic Solvents - Solvents for the 21st Century. *ACS Sustain. Chem. Eng.* **2014**, Ahead of Print.

(157) Abbott, A. P.; Capper, G.; Swain, B. G.; Wheeler, D. A. Electropolishing of Stainless Steel in an Ionic Liquid. *Trans. Inst. Met. Finish.* **2005**, *83*, 51–53.

(158) Abbott, A. P.; Frisch, G.; Gurman, S. J.; Hillman, A. R.; Hartley, J.; Holyoak, F.; Ryder, K. S. Ionometallurgy: Designer Redox Properties for Metal Processing. *Chem. Commun.* **2011**, *47*, 10031–10033.

(159) Abbott, A. P.; Ttaib, K. E.; Frisch, G.; Ryder, K. S.; Weston, D. The Electrodeposition of Silver Composites Using Deep Eutectic Solvents. *Phys. Chem. Chem. Phys.* **2012**, *14*, 2443–2449.

(160) Liao, H.-G.; Jiang, Y.-X.; Zhou, Z.-Y.; Chen, S.-P.; Sun, S.-G. Shape-Controlled Synthesis of Gold Nanoparticles in Deep Eutectic Solvents for Studies of Structure–Functionality Relationships in Electrocatalysis. *Angew. Chem.* **2008**, *120*, 9240–9243.

(161) Phadtare, S. B.; Shankarling, G. S. Halogenation Reactions in Biodegradable Solvent: Efficient Bromination of Substituted 1-Aminoanthra-9, 10-Quinone in Deep Eutectic Solvent (choline Chloride: Urea). *Green Chem.* **2010**, *12*, 458–462.

(162) Pawar, P. M.; Jarag, K. J.; Shankarling, G. S. Environmentally Benign and Energy Efficient Methodology for Condensation: An Interesting Facet to the Classical Perkin Reaction. *Green Chem.* **2011**, *13*, 2130–2134.

(163) Harishkumar, H. N.; Mahadevan, K. M.; Kumar, H. C. K.; Satyanarayan, N. D. A Facile, Choline Chloride/urea Catalyzed Solid Phase Synthesis of Coumarins via Knoevenagel Condensation. *Org. Commun.* **2011**, *4*, 26-32.

(164) Azizi, N.; Batebi, E.; Bagherpour, S.; Ghafuri, H. Natural Deep Eutectic Salt Promoted Regioselective Reduction of Epoxides and Carbonyl Compounds. *RSC Adv.* **2012**, *2*, 2289–2293.

(165) Imperato, G.; Eibler, E.; Niedermaier, J.; König, B. Low-Melting Sugar–urea–salt Mixtures as Solvents for Diels–Alder Reactions. *Chem. Commun.* **2005**, 1170–1172.

(166) Imperato, G.; Höger, S.; Lenoir, D.; König, B. Low Melting Sugar–urea–salt Mixtures as Solvents for Organic Reactions—estimation of Polarity and Use in Catalysis. *Green Chem.* **2006**, *8*, 1051–1055.

(167) Ilgen, F.; Ott, D.; Kralisch, D.; Reil, C.; Palmberger, A.; Konig, B. Conversion of Carbohydrates into 5-Hydroxymethylfurfural in Highly Concentrated Low Melting Mixtures. *Green Chem.* **2009**, *11*, 1948–1954.

(168) Li, X.; Hou, M.; Han, B.; Wang, X.; Zou, L. Solubility of CO2 in a Choline Chloride + Urea Eutectic Mixture. *J. Chem. Eng. Data* **2008**, *53*, 548–550.

(169) Collinet-Fressancourt, M.; Leclercq, L.; Bauduin, P.; Aubry, J.-M.; Nardello-Rataj, V. Counter Anion Effect on the Self-Aggregation of Dimethyl-Di-N-Octylammonium Cation: A Dual Behavior between Hydrotropes and Surfactants. *J. Phys. Chem. B* **2011**, *115*, 11619–11630.

(170) Gathergood, N.; Scammells, P. J.; Garcia, M. T. Biodegradable Ionic Liquids : Part III. The First Readily Biodegradable Ionic Liquids. *Green Chem.* **2006**, *8*, 156-160.

(171) Zhao, D.; Li, H.; Zhang, J.; Fu, L.; Liu, M.; Fu, J.; Ren, P. Dissolution of Cellulose in Phosphate-Based Ionic Liquids. *Carbohydr. Polym.* **2012**, *87*, 1490–1494.

(172) Pernak, J.; Kordala, R.; Markiewicz, B.; Walkiewicz, F.; Poplawski, M.; Fabianska, A.; Jankowski, S.; Lozynski, M. Synthesis and Properties of Ammonium Ionic Liquids with Cyclohexyl Substituent and Dissolution of Cellulose. *RSC Adv* **2012**, *2*, 8429–8438.

(173) Theron, M. M.; Lues, J. F. R. *Organic Acids and Food Preservation*; Taylor & Francis, **2010**.

(174) Leclercq, L.; Nardello-Rataj, V.; Rauwel, G.; Aubry, J.-M. Structure–activity Relationship of Cyclodextrin/biocidal Double-Tailed Ammonium Surfactant Host–guest Complexes: Towards a Delivery Molecular Mechanism? *Eur. J. Pharm. Sci.* **2010**, *41*, 265–275.

(175) Busi, S.; Lahtinen, M.; Mansikkamäki, H.; Valkonen, J.; Rissanen, K. Synthesis, Characterization and Thermal Properties of Small R2R′2N+X−-Type Quaternary Ammonium Halides. *J. Solid State Chem.* **2005**, *178*, 1722–1737.

(176) Tang, S.; Baker, G. A.; Ravula, S.; Jones, J. E.; Zhao, H. PEG-Functionalized Ionic Liquids for Cellulose Dissolution and Saccharification. *Green Chem* **2012**, *14*, 2922–2932.

(177) Wendler, F.; Todi, L.-N.; Meister, F. Thermostability of Imidazolium Ionic Liquids as Direct Solvents for Cellulose. *Thermochim. Acta* **2012**, *528*, 76–84.

(178) Chen, Z.; Liu, S.; Li, Z.; Zhang, Q.; Deng, Y. Dialkoxy Functionalized Quaternary Ammonium Ionic Liquids as Potential Electrolytes and Cellulose Solvents. *New J. Chem.* **2011**, *35*, 1596–1606.

(179) Erdmenger, T.; Vitz, J.; Wiesbrock, F.; Schubert, U. S. Influence of Different Branched Alkyl Side Chains on the Properties of Imidazolium-Based Ionic Liquids. *J. Mater. Chem.* **2008**, *18*, 5267–5273.

(180) Crosthwaite, J. M.; Muldoon, M. J.; Dixon, J. K.; Anderson, J. L.; Brennecke, J. F. Phase Transition and Decomposition Temperatures, Heat Capacities and Viscosities of Pyridinium Ionic Liquids. *J. Chem. Thermodyn.* **2005**, *37*, 559–568.

(181) Kobler, H.; Munz, R.; Al, G. G.; Simchen, G. A Simple Synthesis of Tetraalkylammonium Salts with Functional Anions. *Justus Liebigs Ann Chem* **1978**, 1937-1945.

(182) Grovenstein, E., Jr.; Blanchard, E. P., Jr.; Gordon, D. A.; Stevenson, R. W. Carbanions. II. Cleavage of Tetraalkylammonium Halides by Sodium in Dioxane. *J. Am. Chem. Soc.* **1959**, *81*, 4842–4850.

(183) Moura Ramos, J. J.; Afonso, C. A. M.; Branco, L. C. Glass Transition Relaxation and Fragility in Two Room Temperature Ionic Liquids. *J. Therm. Anal. Calorim.* **2003**, *71*, 659–666.

(184) Jin, Y.; Fang, S.; Chai, M.; Yang, L.; Hirano, S. Ether-Functionalized Trialkylimidazolium Ionic Liquids: Synthesis, Characterization, and Properties. *Ind. Eng. Chem. Res.* **2012**, *51*, 11011–11020.

(185) Zhou, Z.-B.; Matsumoto, H.; Tatsumi, K. Cyclic Quaternary Ammonium Ionic Liquids with Perfluoroalkyltrifluoroborates: Synthesis, Characterization, and Properties. *Chem. – Eur. J.* **2006**, *12*, 2196–2212.

(186) Alizadeh, O. H.; Parsafar, G. A.; Akbarzadeh, H. Density and Temperature Dependencies of Liquid Surface Tension. *Iran. J. Chem. Chem. Eng. IJCCE* **2011**.

(187) Freire, M. G.; Carvalho, P. J.; Fernandes, A. M.; Marrucho, I. M.; Queimada, A. J.; Coutinho, J. A. P. Surface Tensions of Imidazolium Based Ionic Liquids: Anion, Cation, Temperature and Water Effect. *J. Colloid Interface Sci.* **2007**, *314*, 621–630.

(188) Almeida, H. F. D.; Passos, H.; Lopes-da-Silva, J. A.; Fernandes, A. M.; Freire, M. G.; Coutinho, J. A. P. Thermophysical Properties of Five Acetate-Based Ionic Liquids. *J Chem Eng Data* **2012**, *57*, 3005–3013.

(189) Almeida, H. F. D.; Teles, A. R. R.; Lopes-da-Silva, J. A.; Freire, M. G.; Coutinho, J. A. P. Influence of the Anion on the Surface Tension of 1-Ethyl-3-Methylimidazolium-Based Ionic Liquids. *J. Chem. Thermodyn.* **2012**, *54*, 49–54.

(190) Restolho, J.; Mata, J. L.; Saramago, B. On the Interfacial Behavior of Ionic Liquids: Surface Tensions and Contact Angles. *J. Colloid Interface Sci.* **2009**, *340*, 82–86.

(191) Nardello-Rataj Véronique; Ho Tan Taï Louis. Formulation des détergents Produits d'entretien des articles textiles. *Tech. Ing. Élabor. Formul.* **2006**, *base documentaire : TIB335DUO*.

(192) Tadros, T. F. *Applied Surfactants: Principles and Applications*; Wiley, **2006**.

(193) Jain, N.; Trabelsi, S.; Guillot, S.; McLoughlin, D.; Langevin, D.; Letellier, P.; Turmine, M. Critical Aggregation Concentration in Mixed Solutions of Anionic Polyelectrolytes and Cationic Surfactants. *Langmuir* **2004**, *20*, 8496–8503.

(194) Lavergne, A.; Moity, L.; Molinier, V.; Aubry, J.-M. Volatile Short-Chain Amphiphiles Derived from Isosorbide: Hydrotropic Properties of Esters vs. Ethers. *RSC Adv.* **2013**, *3*, 5997–6007.

(195) Queste, S.; Bauduin, P.; Touraud, D.; Kunz, W.; Aubry, J.-M. Short Chain Glycerol 1-Monoethers-a New Class of Green Solvo-Surfactants. *Green Chem.* **2006**, *8*, 822–830.

(196) Neuberg, C. Hydrotropic Phenomena. I. *J. Chem. Soc. Abstr.* **1916**, *110*, 555.

(197) Saleh, A.; El-Khordagui, L. Hydrotropic Agents: A New Definition. *Int. J. Pharm.* **1985**, *24*, 231–238.

(198) Hodgdon, T. K.; Kaler, E. W. Hydrotropic Solutions. *Curr. Opin. Colloid Interface Sci.* **2007**, *12*, 121–128.

(199) Bauduin, P.; Renoncourt, A.; Kopf, A.; Touraud, D.; Kunz, W. Unified Concept of Solubilization in Water by Hydrotropes and Cosolvents. *Langmuir* **2005**, *21*, 6769–6775.

(200) Balasubramanian, D.; Srinivas, V.; Gaikar, V. G.; Sharma, M. M. Aggregation Behavior of Hydrotropic Compounds in Aqueous Solution. *J. Phys. Chem.* **1989**, *93*, 3865–3870.

(201) Subbarao, C. V.; Chakravarthy, I. P. K.; Sai Bharadwaj, A. V. S. L.; Prasad, K. M. M. Functions of Hydrotropes in Solutions. *Chem. Eng. Technol.* **2012**, *35*, 225–237.

(202) Friberg, S. E. Hydrotropes. *Curr. Opin. Colloid Interface Sci.* **1997**, *2*, 490–494.

(203) McKee, R. H. Use of Hydrotropic Solutions in Industry. *Ind. Eng. Chem.* **1946**, *38*, 382–384.

(204) Roy, B. .; Moulik, S. . Functions of Hydrotropes (sodium Salicylate, Proline, Pyrogallol, Resorcinol and Urea) in Solution with Special Reference to Amphiphile Behaviors. *Colloids Surf. Physicochem. Eng. Asp.* **2002**, *203*, 155–166.

(205) Agach, M.; Delbaere, S.; Marinkovic, S.; Estrine, B.; Nardello-Rataj, V. Characterization, Stability and Ecotoxic Properties of Readily Biodegradable Branched Oligoesters Based on Bio-Sourced Succinic Acid and Glycerol. *Polym. Degrad. Stab.* **2012**, *97*, 1956–1963.

(206) Stolte, S.; Steudte, S.; Areitioaurtena, O.; Pagano, F.; Thoming, J.; Stepnowski, P.; Igartua, A. Ionic Liquids as Lubricants or Lubrication Additives: An Ecotoxicity and Biodegradability Assessment. *Chemosphere* **2012**, *89*, 1135–1141.

(207) Couling, D. J.; Bernot, R. J.; Docherty, K. M.; Dixon, J. K.; Maginn, E. J. Assessing the Factors Responsible for Ionic Liquid Toxicity to Aquatic Organisms via Quantitative Structure-Property Relationship Modeling. *Green Chem.* **2006**, *8*, 82–90.

(208) Zakrzewska, M. E.; Bogel-Łukasik, E.; Bogel-Łukasik, R. Solubility of Carbohydrates in Ionic Liquids. *Energy Fuels* **2010**, *24*, 737–745.

(209) Ohno, H.; Fukaya, Y. Task Specific Ionic Liquids for Cellulose Technology. *Chem Lett* **2009**, *38*, 2–7.

(210) Wang, H.; Gurau, G.; Rogers, R. D. Ionic Liquid Processing of Cellulose. *Chem Soc Rev* **2012**, *41*, 1519–1537.

(211) Gericke, M.; Fardim, P.; Heinze, T. Ionic Liquids — Promising but Challenging Solvents for Homogeneous Derivatization of Cellulose. *Molecules* **2012**, *17*, 7458–7502.

(212) Murugesan, S.; Linhardt, R. J. Ionic Liquids in Carbohydrate Chemistry - Current Trends and Future Directions. *Curr. Org. Synth.* **2005**, *2*, 437–451.

(213) Mora-Pale, M.; Meli, L.; Doherty, T. V.; Linhardt, R. J.; Dordick, J. S. Room Temperature Ionic Liquids as Emerging Solvents for the Pretreatment of Lignocellulosic Biomass. *Biotechnol Bioeng* **2011**, *108*, 1229–1245.

(214) Pinkert, A.; Goeke, D. F.; Marsh, K. N.; Pang, S. Extracting Wood Lignin without Dissolving or Degrading Cellulose: Investigations on the Use of Food Additive-Derived Ionic Liquids. *Green Chem.* **2011**, *13*, 3124–3136.

(215) Boissou, F.; Muhlbauer, A.; De Oliveira Vigier, K.; Leclercq, L.; Kunz, W.; Marinkovic, S.; Estrine, B.; Nardello-Rataj, V.; Jerome, F. Transition of Cellulose Crystalline Structure in Biodegradable Mixtures of Renewably-Sourced Levulinate Alkyl Ammonium Ionic Liquids, [gamma]-Valerolactone and Water. *Green Chem.* **2014**, *16*, 2463–2471.

(216) Gericke, M.; Liebert, T.; Seoud, O. A. E.; Heinze, T. Tailored Media for Homogeneous Cellulose Chemistry: Ionic Liquid/Co-Solvent Mixtures. *Macromol. Mater. Eng.* **2011**, *296*, 483–493.

(217) Gericke, M.; Schlufter, K.; Liebert, T.; Heinze, T.; Budtova, T. Rheological Properties of Cellulose/Ionic Liquid Solutions: From Dilute to Concentrated States. *Biomacromolecules* **2009**, *10*, 1188–1194.

(218) Xu, A.; Zhang, Y.; Zhao, Y.; Wang, J. Cellulose Dissolution at Ambient Temperature: Role of Preferential Solvation of Cations of Ionic Liquids by a Cosolvent. *Carbohydr Polym* **2013**, *92*, 540–544.

(219) Zhao, Y.; Liu, X.; Wang, J.; Zhang, S. Insight into the Cosolvent Effect of Cellulose Dissolution in Imidazolium-Based Ionic Liquid Systems. *J. Phys. Chem. B* **2013**, *117*, 9042–9049.

(220) Andanson, J.-M.; Bordes, E.; Devémy, J.; Leroux, F.; Pádua, A. A. H.; Gomes, M. F. C. Understanding the Role of Co-Solvents in the Dissolution of Cellulose in Ionic Liquids. *Green Chem.* **2014**.

(221) Alonso, D. M.; Wettstein, S. G.; Dumesic, J. A. Gamma-Valerolactone, a Sustainable Platform Molecule Derived from Lignocellulosic Biomass. *Green Chem.* **2013**, *15*, 584–595.

(222) Hildebrand, J. H.; Scott, R. L. *The Solubility of Nonelectrolytes*; American Chemical Society monograph series; Reinhold Pub. Corp., **1950**.

(223) Hansen, C. M. The Universality of the Solubility Parameter. *Prod. RD* **1969**, *8*, 2–11.

(224) Hansen, C. M. *Hansen Solubility Parameters: A User's Handbook, Second Edition*; Taylor & Francis, **2002**.

(225) Hansen, C. M.; Abbott, S. *Hansen Solubility Parameters in Practice*; Hansen-Solubility.com, **2008**.

(226) Marciniak, A. The Solubility Parameters of Ionic Liquids. *Int. J. Mol. Sci.* **2010**, *11*, 1973–1990.

(227) Kilaru, P. K.; Condemarin, R. A.; Scovazzo, P. Correlations of Low-Pressure Carbon Dioxide and Hydrocarbon Solubilities in Imidazolium-, Phosphonium-, and Ammonium-Based Room-Temperature Ionic Liquids. Part 1. Using Surface Tension. *Ind. Eng. Chem. Res.* **2007**, *47*, 900–909.

(228) Archer, W. L. Determination of Hansen Solubility Parameters for Selected Cellulose Ether Derivatives. *Ind. Eng. Chem. Res.* **1991**, *30*, 2292–2298.

(229) Zeisel, S. H.; Blusztajn, J. K. Choline and Human Nutrition. *Annu. Rev. Nutr.* **1994**, *14*, 269–296.

(230) Craig, S. A. Betaine in Human Nutrition. *Am. J. Clin. Nutr.* **2004**, *80*, 539–549.

(231) Steiber, A.; Kerner, J.; Hoppel, C. L. Carnitine: A Nutritional, Biosynthetic, and Functional Perspective. *Carnitine* **2004**, *25*, 455–473.

(232) Likes, R.; Madl, R. L.; Zeisel, S. H.; Craig, S. A. S. The Betaine and Choline Content of a Whole Wheat Flour Compared to Other Mill Streams. *J. Cereal Sci.* **2007**, *46*, 93–95.

(233) Zicmanis, A.; Pavlovica, S.; Gzibovska, E.; Mekss, P.; Klavins, M. 2-Hydroxyethylammonium Carboxylates - Highly Biodegradable and Slightly Toxic Ionic Liquids. *Latv. J. Chem.* **2010**, *49*, 269–277.

(234) Pavlovica, S.; Zicmanis, A.; Gzibovska, E.; Klavins, M.; Mekss, P. (2-Hydroxyethyl)ammonium Lactates - Highly Biodegradable and Essentially Non-Toxic Ionic Liquids. *Green Sustain. Chem* **2011**, *1*, 103–110.

(235) Klein, R.; Zech, O.; Maurer, E.; Kellermeier, M.; Kunz, W. Oligoether Carboxylates: Task-Specific Room-Temperature Ionic Liquids. *J. Phys. Chem. B* **2011**, *115*, 8961–8969.

(236) Petkovic, M.; Ferguson, J. L.; Gunaratne, H. Q. N.; Ferreira, R.; Leitao, M. C.; Seddon, K. R.; Rebelo, L. P. N.; Pereira, C. S. Novel Biocompatible Cholinium-Based Ionic Liquids-Toxicity and Biodegradability. *Green Chem.* **2010**, *12*, 643–649.

(237) Fukaya, Y.; Iizuka, Y.; Sekikawa, K.; Ohno, H. Bio Ionic Liquids: Room Temperature Ionic Liquids Composed Wholly of Biomaterials. *Green Chem.* **2007**, *9*, 1155–1157.

(238) Muhammad, N.; Hossain, M. I.; Man, Z.; El-Harbawi, M.; Bustam, M. A.; Noaman, Y. A.; Mohamed, A., Noorjahan Banu; Ng, M. K.; Hefter, G.; Yin, C.-Y. Synthesis and Physical Properties of Choline Carboxylate Ionic Liquids. *J. Chem. Eng. Data* **2012**, *57*, 2191–2196.

(239) Restolho, J.; Mata, J. L.; Saramago, B. Choline Based Ionic Liquids. Interfacial Properties of RTILs with Strong Hydrogen Bonding. *Fluid Phase Equilibria* **2012**, *322-323*, 142–147.

(240) Shahriari, S.; Tome, L. C.; Araujo, J. M. M.; Rebelo, L. P. N.; Coutinho, J. A. P.; Marrucho, I. M.; Freire, M. G. Aqueous Biphasic Systems: A Benign Route Using Cholinium-Based Ionic Liquids. *RSC Adv.* **2013**, *3*, 1835-1843.

(241) Moriel, P.; Garcia-Suarez, E. J.; Martinez, M.; Garcia, A. B.; Montes-Moran, M. A.; Calvino-Casilda, V.; Banares, M. A. Synthesis, Characterization, and Catalytic Activity of Ionic Liquids Based on Biosources. *Tetrahedron Lett.* **2010**, *51*, 4877–4881.

(242) Hou, X.-D.; Liu, Q.-P.; Smith, T. J.; Li, N.; Zong, M.-H. Evaluation of Toxicity and Biodegradability of Cholinium Amino Acids Ionic Liquids. *PLoS One* **2013**, *8*, e59145.

(243) Sachnov, S. J.; Schneiders, K.; Schulz, P. S.; Wasserscheid, P. Chirality Transfer in Mandelate Ionic Liquids through Ion Pairing Effects. *Tetrahedron Asymmetry* **2010**, *21*, 1821–1824.

(244) Capelo, S. B.; Mendez-Morales, T.; Carrete, J.; López Lago, E.; Vila, J.; Cabeza, O.; Rodriguez, J.; Turmine, M.; Varela, L. Effect of Temperature and Cationic Chain Length on the Physical Properties of Ammonium Nitrate-Based Protic Ionic Liquids. *J. Phys. Chem. B* **2012**, *116*, 11302–11312.

(245) Seki, S.; Tsuzuki, S.; Hayamizu, K.; Serizawa, N.; Ono, S.; Takei, K.; Doi, H.; Umebayashi, Y. Static and Transport Properties of Alkyltrimethylammonium Cation-Based Room-Temperature Ionic Liquids. *J. Phys. Chem. B* **2014**, *118*, 4590–4599.

(246) Yu, G.; Zhao, D.; Wen, L.; Yang, S.; Chen, X. Viscosity of Ionic Liquids: Database, Observation, and Quantitative Structure-Property Relationship Analysis. *AIChE J.* **2012**, *58*, 2885–2899.

(247) Thalasso, F.; Van, der B., Jaap; O'Flaherty, V.; Colleran, E. Large-Scale Anaerobic Degradation of Betaine. *J. Chem. Technol. Biotechnol.* **1999**, *74*, 1176–1182.

(248) Sasaki, K.; Takao, K.; Suzuki, T.; Mori, T.; Arai, T.; Ikeda, Y. Extraction of Pd(ii), Rh(iii) and Ru(iii) from HNO3 Aqueous Solution to Betainium Bis(trifluoromethanesulfonyl)imide Ionic Liquid. *Dalton Trans.* **2014**, *43*, 5648–5651.

(249) Sasaki, K.; Suzuki, T.; Mori, T.; Arai, T.; Takao, K.; Ikeda, Y. Selective Liquid–Liquid Extraction of Uranyl Species Using Task-Specific Ionic Liquid, Betainium Bis(trifluoromethylsulfonyl)imide. *Chem. Lett.* **2014**, *43*, 775–777.

(250) Long, K.; Goff, G.; Runde, W. Unusual Redox Stability of Neptunium in the Ionic Liquid [Hbet][Tf2N]. *Chem. Commun.* **2014**, *50*, 7766–7769.

(251) Hoogerstraete, T. V.; Onghena, B.; Binnemans, K. Homogeneous Liquid-Liquid Extraction of Metal Ions with a Functionalized Ionic Liquid. *J. Phys. Chem. Lett.* **2013**, *4*, 1659–1663.

(252) Jagadeeswara Rao, C.; Venkatesan, K. A.; Tata, B. V. R.; Nagarajan, K.; Srinivasan, T. G.; Vasudeva Rao, P. R. Radiation Stability of Some Room Temperature Ionic Liquids. *Radiat. Phys. Chem.* **2011**, *80*, 643–649.

(253) Jagadeeswara Rao, C.; Venkata Krishnan, R.; Venkatesan, K. A.; Nagarajan, K.; Srinivasan, T. G. Thermochemical Properties of Some Bis(trifluoromethyl-Sulfonyl)imide Based Room Temperature Ionic Liquids. *J. Therm. Anal. Calorim.* **2009**, *97*, 937–943.

(254) Messadi, A.; Mohamadou, A.; Boudesocque, S.; Dupont, L.; Guillon, E. Task-Specific Ionic Liquid with Coordinating Anion for Heavy Metal Ion Extraction: Cation Exchange versus Ion-Pair Extraction. *Sep. Purif. Technol.* **2013**, *107*, 172–178.

(255) Zhu, J.-F.; He, L.; Zhang, L.; Huang, M.; Tao, G.-H. Experimental and Theoretical Enthalpies of Formation of Glycine-Based Sulfate/Bisulfate Amino Acid Ionic Liquids. *J. Phys. Chem. B* **2012**, *116*, 113–119.

(256) Goursaud, F.; Berchel, M.; Guilbot, J.; Legros, N.; Lemiegre, L.; Marcilloux, J.; Plusquellec, D.; Benvegnu, T. Glycine Betaine as a Renewable Raw Material to "Greener" New Cationic Surfactants. *Green Chem.* **2008**, *10*, 310–320.

(257) Varade, D.; Bahadur, P. Effect of Hydrotropes on the Aqueous Solution Behavior of Surfactants. *J. Surfactants Deterg.* **2004**, *7*, 257–261.

(258) Bremer, J. Carnitine--Metabolism and Functions. *Physiol. Rev.* **1983**, *63*, 1420–1480.

(259) Cipollone, M.; De Maria, P.; Fontana, A.; Frascari, S.; Gobbi, L.; Spinelli, D.; Tinti, M. Formation of Micelles and Liposomes from Carnitine Amphiphiles. *Eur. J. Med. Chem.* **2000**, *35*, 903–911.

(260) Patra, T.; Ghosh, S.; Dey, J. Cationic Vesicles of a Carnitine-Derived Single-Tailed Surfactant: Physicochemical Characterization and Evaluation of in Vitro Gene Transfection Efficiency. *J. Colloid Interface Sci.* **2014**, *436*, 138–145.

(261) Yu, Y.; Lu, X.; Zhou, Q.; Dong, K.; Yao, H.; Zhang, S. Biodegradable Naphthenic Acid Ionic Liquids: Synthesis, Characterization, and Quantitative Structure–Biodegradation Relationship. *Chem. – Eur. J.* **2008**, *14*, 11174–11182.

(262) Tehrani-Bagha, A. R.; Oskarsson, H.; van Ginkel, C. G.; Holmberg, K. Cationic Ester-Containing Gemini Surfactants: Chemical Hydrolysis and Biodegradation. *J. Colloid Interface Sci.* **2007**, *312*, 444–452.

(263) Neumann, J.; Steudte, S.; Cho, C.-W.; Thoming, J.; Stolte, S. Biodegradability of 27 Pyrrolidinium, Morpholinium, Piperidinium, Imidazolium and Pyridinium Ionic Liquid Cations under Aerobic Conditions. *Green Chem.* **2014**, *16*, 2174–2184.

(264) Nockemann, P.; Thijs, B.; Driesen, K.; Janssen, C. R.; Van Hecke, K.; Van Meervelt, L.; Kossmann, S.; Kirchner, B.; Binnemans, K. Choline Saccharinate and Choline Acesulfamate: Ionic Liquids with Low Toxicities. *J. Phys. Chem. B* **2007**, *111*, 5254–5263.

(265) Pernak, J.; Chwala, P. Synthesis and Anti-Microbial Activities of Choline-like Quaternary Ammonium Chlorides. *Eur. J. Med. Chem.* **2003**, *38*, 1035–1042.

(266) Dale, H. H. The Action of Certain Esters and Ethers of Choline and Their Relation to Muscarine; Wellcome Physiological Research Laboratories, **1914**.

(267) Muhammad, N.; Man, Z.; Bustam, M.; Mutalib, M. I. A.; Wilfred, C.; Rafiq, S. Dissolution and Delignification of Bamboo Biomass Using Amino Acid-Based Ionic Liquid. *Appl. Biochem. Biotechnol.* **2011**, *165*, 998–1009.

(268) Pinkert, A.; Marsh, K. N.; Pang, S. Alkanolamine Ionic Liquids and Their Inability To Dissolve Crystalline Cellulose. *Ind. Eng. Chem. Res.* **2010**, *49*, 11809–11813.

(269) Lindman, B.; Karlstroem, G.; Stigsson, L. On the Mechanism of Dissolution of Cellulose. *J Mol Liq* **2010**, *156*, 76–81.

(270) Chen, Z.; Liu, S.; Li, Z.; Zhang, Q.; Deng, Y. Dialkoxy Functionalized Quaternary Ammonium Ionic Liquids as Potential Electrolytes and Cellulose Solvents. *New J. Chem.* **2011**, *35*, 1596-1606.

(271) Rinaudo, M. Chitin and Chitosan: Properties and Applications. *Prog. Polym. Sci.* **2006**, *31*, 603–632.

(272) Teleman, A.; Larsson, P.; Iversen, T. On the Accessibility and Structure of Xylan in Birch Kraft Pulp. *Cellulose* **2001**, *8*, 209–215.

(273) Oates, C. G. Towards an Understanding of Starch Granule Structure and Hydrolysis. *Trends Food Sci. Technol.* **1997**, *8*, 375–382.

(274) Kerton, F. M.; Liu, Y.; Omari, K. W.; Hawboldt, K. Green Chemistry and the Ocean-Based Biorefinery. *Green Chem.* **2013**, *15*, 860–871.

(275) Pillai, C. K. S.; Paul, W.; Sharma, C. P. Chitin and Chitosan Polymers: Chemistry, Solubility and Fiber Formation. *Prog. Polym. Sci.* **2009**, *34*, 641–678.

(276) Biswas, A.; Shogren, R. L.; Stevenson, D. G.; Willett, J. L.; Bhowmik, P. K. Ionic Liquids as Solvents for Biopolymers: Acylation of Starch and Zein Protein. *Carbohydr. Polym.* **2006**, *66*, 546–550.

(277) Wu, Y.; Sasaki, T.; Irie, S.; Sakurai, K. A Novel Biomass-Ionic Liquid Platform for the Utilization of Native Chitin. *Polymer* **2008**, *49*, 2321–2327.

(278) Hossain, M. M.; Aldous, L. Ionic Liquids for Lignin Processing: Dissolution, Isolation, and Conversion. *Aust. J. Chem.* **2012**, *65*, 1465–1477.

(279) Lee, S. H.; Doherty, T. V.; Linhardt, R. J.; Dordick, J. S. Ionic Liquid-Mediated Selective Extraction of Lignin from Wood Leading to Enhanced Enzymatic Cellulose Hydrolysis. *Biotechnol. Bioeng.* **2009**, *102*, 1368–1376.

(280) Hertel, R. M.; Bommarius, A. S.; Realff, M. J.; Kang, Y. Deep Eutectic Solvent System Comprising Betaine Monohydrate and Hydrogen Bond Donor., October 26, **2012**.

(281) Ilgen, F.; Konig, B. Organic Reactions in Low Melting Mixtures Based on Carbohydrates and L-Carnitine-a Comparison. *Green Chem.* **2009**, *11*, 848–854.

(282) Parnica, J.; Antalik, M. Urea and Guanidine Salts as Novel Components for Deep Eutectic Solvents. *J. Mol. Liq.* **2014**, *197*, 23–26.

(283) Smith, E. L.; Abbott, A. P.; Ryder, K. S. Deep Eutectic Solvents (DESs) and Their Applications. *Chem. Rev.* **2014**.

(284) Tang, B.; Row, K. H. Recent Developments in Deep Eutectic Solvents in Chemical Sciences. *Monatshefte Fuer Chem.* **2013**, *144*, 1427–1454.

(285) Hayyan, A.; Mjalli, F. S.; AlNashef, I. M.; Al-Wahaibi, Y. M.; Al-Wahaibi, T.; Hashim, M. A. Glucose-Based Deep Eutectic Solvents: Physical Properties. *J. Mol. Liq.* **2013**, *178*, 137–141.

(286) Russ, C.; Ilgen, F.; Reil, C.; Luff, C.; Haji Begli, A.; Konig, B. Efficient Preparation of [small Beta]-D-Glucosyl and [small Beta]-D-Mannosyl Ureas and Other N-Glucosides in Carbohydrate Melts. *Green Chem.* **2011**, *13*, 156–161.

(287) Hayyan, A.; Mjalli, F. S.; AlNashef, I. M.; Al-Wahaibi, T.; Al-Wahaibi, Y. M.; Hashim, M. A. Fruit Sugar-Based Deep Eutectic Solvents and Their Physical Properties. *Thermochim. Acta* **2012**, *541*, 70–75.

(288) Hvizd, M. G.; Bailey, B.; Crafts, C.; Plante, M.; Acworth, I. Simple Separation and Detection Techniques for the Analysis of Carbohydrates, **2011**.

(289) Florindo, C.; Oliveira, F. S.; Rebelo, L. P. N.; Fernandes, A. M.; Marrucho, I. M. Insights into the Synthesis and Properties of Deep Eutectic Solvents Based on Cholinium Chloride and Carboxylic Acids. *ACS Sustain. Chem. Eng.* **2014**.

(290) Allen, P.; Tildesley, D. J. Computer Simulation of Liquids; Oxford science publications; Clarendon Press, **1987**.

(291) Fredenslund, A.; Jones, R. L.; Prausnitz, J. M. Group-Contribution Estimation of Activity Coefficients in Nonideal Liquid Mixtures. *AIChE J.* **1975**, *21*, 1086–1099.

(292) Klamt, A.; Schuurmann, G. COSMO: A New Approach to Dielectric Screening in Solvents with Explicit Expressions for the Screening Energy and Its Gradient. *J. Chem. Soc. Perkin Trans. 2* **1993**, 799–805.

(293) Klamt, A.; Eckert, F.; Arlt, W. COSMO-RS: An Alternative to Simulation for Calculating Thermodynamic Properties of Liquid Mixtures. *Annu. Rev. Chem. Biomol. Eng.* **2010**, *1*, 101–122.

(294) Klamt, A. Conductor-like Screening Model for Real Solvents: A New Approach to the Quantitative Calculation of Solvation Phenomena. *J. Phys. Chem.* **1995**, *99*, 2224–2235.

(295) Klamt, A. COSMO-RS: From Quantum Chemistry to Fluid PhaseThermodynamics and Drug Design; Elsevier, **2005**.

(296) Klamt, A.; Eckert, F. COSMO-RS: A Novel and Efficient Method for the a Priori Prediction of Thermophysical Data of Liquids. *Fluid Phase Equilibria* **2000**, *172*, 43–72.

(297) Moity, L. Conception, Modélisation et Caractérisation de Solvants Agro-Sourcés. PhD Thesis, Université Lille 1, **2013**.

(298) Klamt, Andreas. Chemical Engineering - Property prediction for ionic liquids with COSMOtherm: green solvents, vapor pressure http://www.cosmologic.de/index.php?cosId=4205&crId=4 (accessed Sep 22, 2014).

(299) Diedenhofen, M.; Klamt, A. COSMO-RS as a Tool for Property Prediction of IL Mixtures. A Review. *Fluid Phase Equilibria* **2010**, *294*, 31–38.

(300) Eckert, F.; Klamt, A. Fast Solvent Screening via Quantum Chemistry: COSMO-RS Approach. *AIChE J.* **2002**, *48*, 369–385.

(301) Torrecilla, J. S.; Palomar, J.; Lemus, J.; Rodriguez, F. A Quantum-Chemical-Based Guide to Analyze/quantify the Cytotoxicity of Ionic Liquids. *Green Chem.* **2010**, *12*, 123–134.

(302) Palomar, J.; Torrecilla, J. S.; Lemus, J.; Ferro, V. R.; Rodriguez, F. A COSMO-RS Based Guide to Analyze/quantify the Polarity of Ionic Liquids and Their Mixtures with Organic Cosolvents. *Phys. Chem. Chem. Phys.* **2010**, *12*, 1991–2000.

(303) Ropel, L.; Belveze, L. S.; Aki, S. N. V. K.; Stadtherr, M. A.; Brennecke, J. F. Octanol-Water Partition Coefficients of Imidazolium-Based Ionic Liquids. *Green Chem.* **2005**, *7*, 83–90.

(304) Andersson, J. T.; Schräder, W. A Method for Measuring 1-Octanol−Water Partition Coefficients. *Anal. Chem.* **1999**, *71*, 3610–3614.

(305) Kamath, G.; Bhatnagar, N.; Baker, G. A.; Baker, S. N.; Potoff, J. J. Computational Prediction of Ionic Liquid 1-Octanol/water Partition Coefficients. *Phys. Chem. Chem. Phys.* **2012**, *14*, 4339–4342.

(306) Klamt, A.; Eckert, F.; Hornig, M. COSMO-RS: A Novel View to Physiological Solvation and Partition Questions. *J. Comput. Aided Mol. Des.* **2001**, *15*, 355–365.

(307) Spieß, A. C.; Eberhard, W.; Peters, M.; Eckstein, M. F.; Greiner, L.; Büchs, J. Prediction of Partition Coefficients Using COSMO-RS: Solvent Screening for Maximum Conversion in Biocatalytic Two-Phase Reaction Systems. *Biothermodynamics* **2008**, *47*, 1034–1041.

(308) Padmanabhan, S.; Kim, M.; Blanch, H. W.; Prausnitz, J. M. Solubility and Rate of Dissolution for Miscanthus in Hydrophilic Ionic Liquids. *Fluid Phase Equilibria* **2011**, *309*, 89–96.

(309) Balaji, C.; Banerjee, T.; Goud, V. COSMO-RS Based Predictions for the Extraction of Lignin from Lignocellulosic Biomass Using Ionic Liquids: Effect of Cation and Anion Combination. *J. Solut. Chem.* **2012**, *41*, 1610–1630.

(310) Casas, A.; Palomar, J.; Alonso, M. V.; Oliet, M.; Omar, S.; Rodriguez, F. Comparison of Lignin and Cellulose Solubilities in Ionic Liquids by COSMO-RS Analysis and Experimental Validation. *Ind. Crops Prod.* **2012**, *37*, 155–163.

(311) Kahlen, J.; Masuch, K.; Leonhard, K. Modelling Cellulose Solubilities in Ionic Liquids Using COSMO-RS. *Green Chem.* **2010**, *12*, 2172–2181.

(312) Casas, A.; Omar, S.; Palomar, J.; Oliet, M.; Alonso, M. V.; Rodriguez, F. Relation between Differential Solubility of Cellulose and Lignin in Ionic Liquids and Activity Coefficients. *RSC Adv.* **2013**, *3*, 3453–3460.

(313) Eckert, F. COSMOtherm Users Manual. *Version C2* **2003**.

(314) Klamt, A.; Eckert, F.; Diedenhofen, M. Prediction of the Free Energy of Hydration of a Challenging Set of Pesticide-Like Compounds†. *J. Phys. Chem. B* **2009**, *113*, 4508–4510.

ANNEX

Volume 16 | Number 5 | May 2014 | Pages 2301–2888

Green Chemistry

Cutting-edge research for a greener sustainable future

www.rsc.org/greenchem

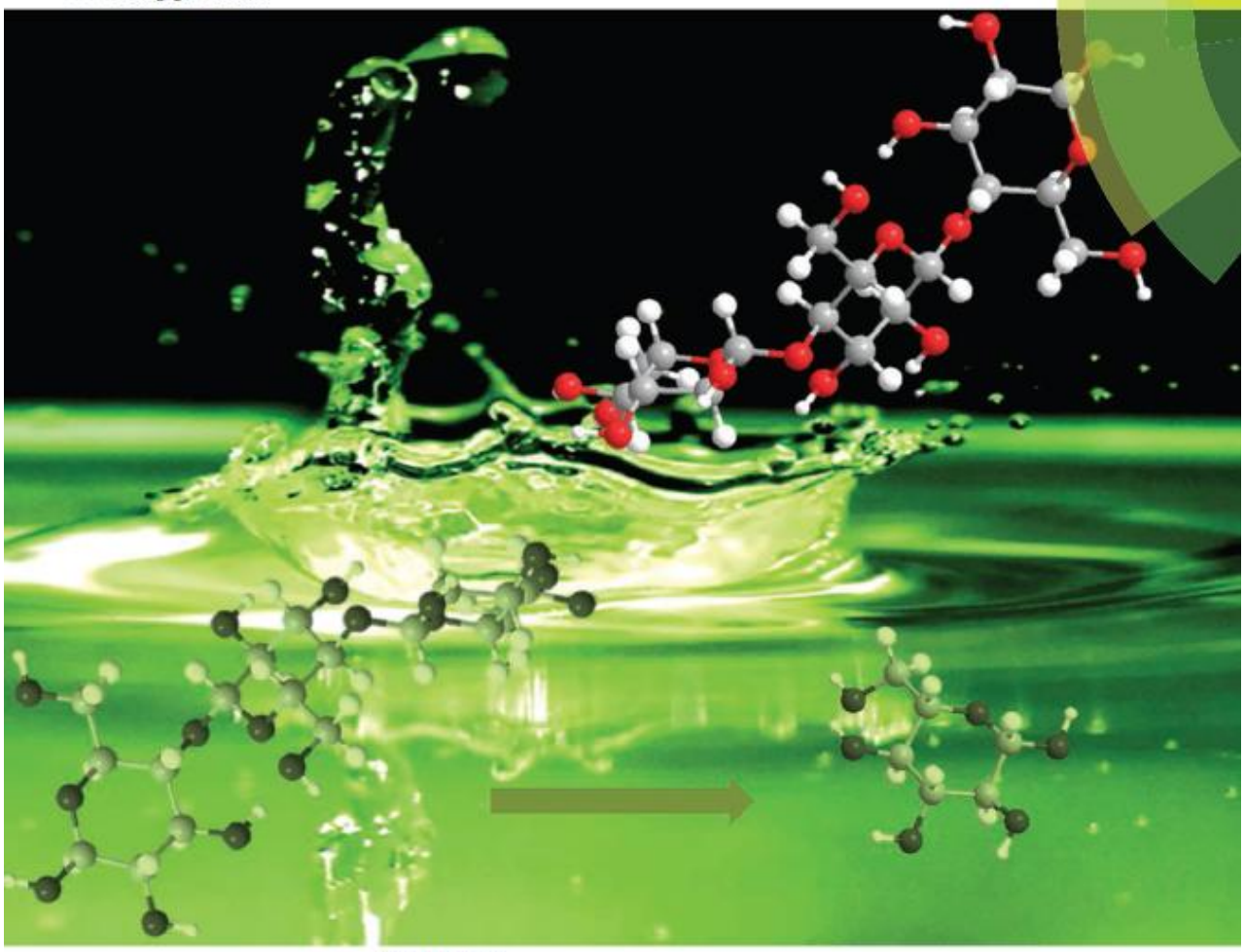

ISSN 1463-9262

ROYAL SOCIETY OF CHEMISTRY

PAPER

Véronique Nardello-Rataj, François Jérôme *et al.*

Transition of cellulose crystalline structure in biodegradable mixtures of renewably-sourced levulinate alkyl ammonium ionic liquids, γ-valerolactone and water

Green Chemistry

PAPER

View Article Online
View Journal | View Issue

Cite this: Green Chem., 2014, 16, 2463

Transition of cellulose crystalline structure in biodegradable mixtures of renewably-sourced levulinate alkyl ammonium ionic liquids, γ-valerolactone and water†

Florent Boissou,[a,b] Andrea Mühlbauer,[b,c,d] Karine De Oliveira Vigier,[a] Loïc Leclercq,[c] Werner Kunz,[d] Sinisa Marinkovic,[b] Boris Estrine,[b] Véronique Nardello-Rataj*[c] and François Jérôme*[a]

Received 22nd November 2013,
Accepted 5th February 2014

DOI: 10.1039/c3gc42396d

www.rsc.org/greenchem

In this work, we report that combination of levulinate as a renewably sourced anion with short chain alkyl ammonium as a cation yields room temperature ionic liquids that are capable of dissolving up to 10 wt% of microcrystalline cellulose. This dissolution results in a change of the cellulose crystalline structure from cellulose I to cellulose II, a pre-requisite step known to significantly improve the accessibility of cellulose to enzymes. As compared to previous methodologies, such ILs tolerate the presence of up to 18 wt% of water. Hence technical grade ILs can be used, thus avoiding the energy-consuming drying process generally required with traditional ILs before dissolution experiments. In addition, such ILs can be mixed with 20 wt% of γ-valerolactone, a renewably-sourced co-solvent, resulting in an improvement of the cellulose dissolution up to 20 wt% while concomitantly increasing the sustainability of these media. Finally, prepared ILs were proved to be biodegradable according to the OCDE 301F directive, thus opening a promising route for the pre-treatment of cellulose with a higher eco-efficiency.

Introduction

With the depletion of fossil reserves and the impact of CO_2 emissions on climate change, the use of cellulose as a renewable raw material in the chemical industry is gaining more and more interest for the production of various chemicals such as ethanol, solvents, monomers, surfactants, chemical platforms, *etc.*[1] Among the different grades of cellulose available on the market, microcrystalline cellulose (MCC) is of particular interest in fine chemistry owing to its large availability and its high content of glucose from which fuels and chemicals can be then produced. On account of this high content of glucose, MCC has a high crystallinity index. In particular, chains of MCC form two distinct allomorphs of cellulose I, I_α with a triclinic unit cell and I_β with a monoclinic cell, the fractional distribution between I_α and I_β varying according to the origin of cellulose.[2] Unfortunately, this high crystallinity of MCC hampers its accessibility to (bio)catalysts, making its deconstruction difficult. To overcome this problem, MCC is generally subjected to a pre-treatment process before its (bio)-catalytic deconstruction.[3] This pre-treatment aims at favouring better accessibility of the cellulosic backbone to (bio)catalyst by modifying its crystallinity[4] or particle size[5] or degree of polymerization[6] for instance. In this context, much effort has been recently paid to the search for innovative media capable of dissolving and thus disrupting the supramolecular organization of cellulose. Dissolution of cellulose in a non-derivatizing solvent is an interesting approach that allows the crystallinity index of cellulose to be decreased or changed from cellulose I to cellulose II. In particular, cellulose II has been proved to be more readily digested by cellulases than cellulose I, thanks to a decrease of the van der Waals interaction between hydrogen-bonded sheets.[7] After the dissolution process, cellulose is generally recovered by precipitation after addition of an anti-solvent such as ethanol or water.

Historically, mixtures of DMSO–LiCl or DMA–LiCl[8] (among other combinations) and *N*-methylmorpholine-*N*-oxide (Lyocell® process) have been used for the dissolution/decrystallization of cellulose.[9] Although these systems ensure a

[a]Institut de Chimie des Milieux et Matériaux de Poitiers, ENSIP, Université de Poitiers, 1 rue Marcel Doré, 86022 Poitiers, France
[b]ARD – Agro-industrie Recherches et Développements, Green Chemistry Department, Route de Bazancourt, F-51110 Pomacle, France
[c]Université Lille1, EA-4478 Chimie Moléculaire et Formulation, Cité Scientifique C6, F-59655 Villeneuve-d'Ascq, France. E-mail: veronique.rataj@univ-lille1.fr; Tel: +33 (0) 320 336 369
[d]University of Regensburg, Institute of Physical and Theoretical Chemistry, Universitätsstraße 31, D-93040 Regensburg, Germany
†Electronic supplementary information (ESI) available. See DOI: 10.1039/c3gc42396d

change in the crystallinity index of cellulose, their recycling is difficult and rather expensive. Recently, ionic liquids (ILs) have received considerable attention owing to their ability to dissolve and thus to decrease the crystallinity index of cellulose.[4] Dissolution of cellulose in ILs was first demonstrated at the beginning of the 20th century, in particular using ethyl ammonium nitrate.[10] With the recent emergence of room temperature ILs (RTILs), the use of ILs for the dissolution of cellulose is now witnessing a sort of renaissance. Since the pioneering investigations of Rogers and co-workers,[11] plenty of work has been reported in this field of chemistry and this topic is too large to be summarized here. Complementary information to this section can be found in the excellent recent reviews.[4,12]

Although elucidation of the exact mechanism governing the dissolution and change of the cellulose crystallinity in ILs is still not really clear, it has been demonstrated in the current literature that ionic liquids can provide adapted physical and chemical properties such as tunable hydrophilic–lipophilic balance and basic properties that play an important role in the dissolution process of cellulose. It is more or less accepted that the cation has the role of sliding open the cellulose fibrils and transporting the anion within the cellulose backbone where it interacts with the hydrogen bond network.[13] To date, 1-butyl-3-methyl-imidazolium chloride and 1-ethyl-3-methyl-imidazolium acetate have been considered as the best ILs for the dissolution of cellulose. Despite the remarkable ability of these ILs to dissolve cellulose (up to 15–20 wt%), their industrial emergence is unfortunately hampered by their high cost, toxicity and high viscosity. Additionally, the presence of water (an important contaminant of biomass) is known to have a negative effect on the dissolution of cellulose in ILs. As a consequence, most of the ILs require to be dried prior to dissolving cellulose, which dramatically raises their price to an unacceptable level for use on a large scale. Nevertheless, RTILs are excellent models to understand the mechanism governing the dissolution/decrystallization of cellulose.

Here we wish to report a new generation of water-tolerant ILs for the dissolution of MCC and the transition of cellulose I crystalline structure to cellulose II. In particular, we designed promising ILs for the dissolution of cellulose using various alkyl quaternary ammonium salts as cations, and levulinate as a renewably-sourced anion. We found that this specific anion greatly enhanced the rate and cellulose dissolution ability of ILs but also allows cellulose to be dissolved in the presence of up to 18 wt% of water. To our knowledge, this is the first time that cellulose could be dissolved in a relatively short time in ionic liquids containing a large amount of water, paving the way for a potential application in the industry, as water tolerance of ILs is an important bottleneck for their industrial development. In addition, these levulinate-derived alkyl ammonium ILs have been efficiently associated with 20 wt% of renewably-sourced γ-valerolactone as a co-solvent and have been proved to be biodegradable which considerably increase the attractiveness of such media for industrial use.

Results and discussion

The procedure for the synthesis of all ILs discussed in this manuscript was inspired by previous methods. Typically, the quaternary ammonium $[(C_nH_{2n+1})_2N(CH_3)_2][X]$ or $[(C_nH_{2n+1})_3N(CH_3)][X]$ (n = 3, 4, 6; X = Br, I) salts were first prepared *via* an alkylation of *N*,*N*-alkyldimethylamines or *N*,*N*-dialkylmethylamines with 1-haloalkanes followed by an anion metathesis with OH^- (anion exchange over Amberlite® IRA-400) and neutralization with the desired bio-sourced acid.[14] For the sake of clarity, prepared ILs as well as their abbreviations are summarized in Scheme 1. Because some of the prepared ILs are not described in the current literature, a list of the main physicochemical properties of ILs is provided in Table 1. The phase transitions of the prepared ILs were determined by differential scanning calorimetry (DSC). Except for $[DiC_4][Sor]$ which exhibits a melting temperature of 51.9 °C, all other prepared technical grade ILs are liquid at room temperature (see water content in Table 2). The glass transition (T_g) and the melting temperature (T_m) of all ILs are provided in Table 1.[15,16] Thermogravimetric analysis (TGA) was carried out to determine the decomposition temperature and therefore the

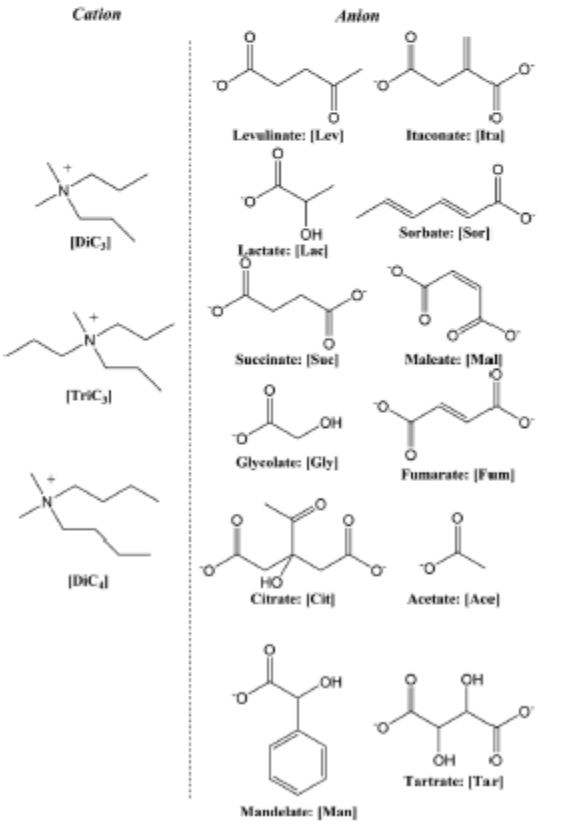

Scheme 1 List of ILs prepared in this work.

Table 1 Main physicochemical properties of prepared ILs

ILs	T_d (°C)	T_g (°C)	T_m (°C)	η/Pa s at 25 °C (80 °C)	γ/mN m^{-1} at 25 °C (80 °C)
[DiC_3][Ace]	140–228	−68.1	—	0.231 (0.032)	39.4 (36.2)
[DiC_3][Lac]	156–263	−69.6	—	0.284 (0.037)	41.5 (34.1)
[DiC_3][Lev]	143–254	−13.0	—	0.194 (0.031)	34.6 (30.2)
[DiC_3]$_2$[Ita]	150–260	−55.3	—	1.683 (0.082)	46.8 (44.4)
[$TriC_3$][Ace]	140–260	−64.0	—	0.374 (0.037)	39.2 (37.2)
[$TriC_3$][Lac]	150–256	−68.4	—	0.196 (0.036)	42.8 (41.6)
[$TriC_3$][Lev]	140–250	−66.8; −11.9	—	0.218 (0.031)	35.5 (25.1)
[$TriC_3$]$_2$[Ita]	136–252	−47.4; −12.2	—	4.372 (0.099)	42.6 (39.0)
[DiC_4][Ace]	138–248	−67.8	—	0.177 (0.041)	34.7 (32.7)
[DiC_4][Lac]	162–262	—	14.6	0.428 (0.048)	37.2 (35.0)
[DiC_4][Gly]	155–272	−62.4; 0.6	—	0.585 (0.058)	41.6 (39.4)
[DiC_4][Lev]	140–258	—	—	0.172 (0.043)	36.4 (28.6)
[DiC_4][Sor]	144–245	−64.3	51.9	Solid (0.064)	Solid (30.6)
[DiC_4][Mand]	173–281	−52.0; −16.6	—	0.448 (0.071)	40.9 (nd)
[DiC_4]$_2$[Suc]	146–276	−54.7; −7.2	—	16.790 (0.307)	39.9 (40.1)
[DiC_4]$_2$[Ita]	142–260	−53.4; 5.4	—	0.676 (0.052)	38.6 (30.5)
[DiC_4]$_2$[Male]	140–250	−56.6	—	3.317 (0.092)	38.4 (37.3)
[DiC_4]$_2$[Fum]	153–262	−53.5; 3.1	—	2.974 (0.139)	42.3 (40.6)
[DiC_4]$_2$[Tar]	170–260	−36.9	—	6.525 (0.209)	30.5 (41.4)
[DiC_4]$_3$[Cit]	135–250	−41.8; −1.1	—	19.185 (0.316)	36.3 (36.6)

Table 2 Dissolution of cellulose in prepared ILs

Anion	Cation	Water content (wt%)	Dissolution (wt%)	Dissolution rate[a] (g h^{-1})
[Lev]	[$TriC_3$]	3.5	10	5.0
	[$TriC_3$]	15.5	10	5.0
	[DiC_4]	2.5	10	2.0
	[DiC_4]	14	10	2.0
	[DiC_3]	2.6	10	2.0
	[$TriC_4$]	6.7	5	1.7
[Ita]	[DiC_4]	12.8	10	1.4
	[DiC_3]	5.9	6	0.9
	[$TriC_3$]	8.3	0	—
	[$TriC_4$]	6.6	0	—
[Ace]	[DiC_4]	10.8	9.5	2.4
	[DiC_4]	16.8	9.5	1.3
	[$TriC_4$]	6.5	2.6	0.4
	[DiC_3]	10.0	0	—
	[$TriC_3$]	7.7	0	—
[Lac]	[DiC_4]	2.8	3.3	1.7
	[$TriC_3$]	2.6	0	—
[Sor]	[DiC_4]	5.5	2	0.7
[Suc]	[DiC_4]	5.3	2	0.2
[Cit]	[DiC_4]	7.3	2	0.1
[Gly]	[DiC_4]	5.0	0	—
	[$TriC_4$]	1.6	0	—
[Man]	[DiC_4]	1.1	0	—
[Mal]	[DiC_4]	11.5	0	—
[Fum]	[DiC_4]	9.8	0	—
[Tar]	[DiC_4]	4.1	0	—

[a] Dissolution experiments were performed within a temperature range of 90–110 °C.

thermal stability of the prepared ILs. For all compounds, thermal decomposition occurred between 140 and 170 °C. Note that viscosity (η) and surface tension (γ) of prepared ILs are discussed later in the manuscript.

Dissolution ability of prepared ILs

All cellulose dissolution experiments were performed using a microcrystalline cellulose (MCC) of the type AVICEL PH 200. AVICEL PH 200 has a glucose content higher than 99% along with a degree of polymerization of 200, a particle size of 150 μm and a water content of 5 wt%. In a typical experiment, a solution of IL containing 2 wt% of MCC was heated at 90–115 °C. When MCC was dissolved, an extra amount of MCC was progressively added until the limit of solubility was reached.

Considering that the total removal of water from ILs is a costly and energy consuming step, we decided here to not extensively dry ILs prior to dissolving cellulose and to evaluate their performances as collected after synthesis. Results on solubility measurements are summarized in Table 2. Among all tested renewably-sourced anions, it appears that levulinate is the most promising one allowing up to 10 wt% of MCC to be dissolved within only 2 h of stirring at 90 °C. In a first approximation, efficiency of anions for cellulose dissolution can be classified as follows: levulinate > itaconate, acetate > lactate > sorbate, succinate, citrate > glycolate, mandelate, maleate, fumarate, tartrate. As a general trend, it appears that anions bearing a hydroxyl group such as tartrate, citrate, mandelate, glycolate and lactate are not favourable for the dissolution of cellulose. The presence and substitution of a carbon–carbon double bond on the structure of anions also exerted an influence on the cellulose dissolution. Whereas anions with disubstituted C=C bonds such as maleate and fumarate are incapable of dissolving cellulose, 10 wt% of cellulose can be dissolved in the presence of itaconate which exhibits a terminal C=C bond.

For all eligible anions, it is noteworthy that the difference in dissolution ability was obviously observed according to the nature of the cation, confirming that the cation also participates in the dissolution mechanism. Except levulinate which was able to dissolve rather large amounts of cellulose whatever the cation, the [DiC_4] cation afforded the best result in terms of both dissolution ability and dissolution rate for all tested anions.

As mentioned above, water contained in commonly used imidazolium-derived ILs has an inhibiting effect on cellulose dissolution, thus requiring an extensive and energy-consuming drying of ILs before dissolution experiments. In this context, the water content of prepared ILs and its effect on the cellulose dissolution have been investigated (Table 2). The water content of each IL was determined by means of Karl–Fischer titrations. Most of the ILs contain water within a range of 1.1–12.8 wt%. Although [$TriC_3$][Lev] (the best IL in terms of dissolution ability and rate) has a lower water content than the average of tested ILs, there is no clear relationship between the water content of ILs and their ability to dissolve cellulose. For instance, [DiC_4]$_2$[Ita] and [DiC_4][Ace] exhibited a high water content of 12.8 and 10.8 wt%, respectively, and are capable of dissolving 10 and 9.5 wt% of cellulose whereas with a similar water content [DiC4]$_2$Mal and [DiC_4]$_2$[Fum] are not able to dissolve cellulose (Table 2). These results suggest that the dissolution of cellulose is more dependent on the molecular structure of the alkylammonium carboxylate ILs than on the water content of ILs.

Considering that the water-tolerance of the best ILs, *i.e.* [$TriC_3$][Lev] and [DiC_4][Ace], is a remarkable advantage over imidazolium-derived ILs, we then checked their ability to dissolve cellulose when the water content was increased (Fig. 1, Table 2). Remarkably, we were pleased to see that [$TriC_3$][Lev] and [DiC_4][Ace] were still able to dissolve a similar amount of cellulose (10 wt% and 9.5 wt%, respectively) at a water content of 15.5 wt% and 16.8 wt%, respectively. Interestingly, in the case of [$TriC_3$][Lev], the dissolution rate of cellulose was not affected by the presence of water whereas this was the case with [DiC_4][Ace] for which an increase of the water content from 10.8 wt% to 16.8 wt% dramatically reduced the cellulose dissolution rate from 2.4 g L^{-1} to 1.3 g L^{-1} (Table 2). Note that in both cases, cellulose was not dissolved anymore when the water content was higher than 18 wt%, which represents here the maximum tolerance of these ILs to water. When [BMIM]Cl was used as a reference IL, we found that a water content higher than 4 wt% totally inhibited the dissolution process, showing the remarkable efficiency of [$TriC_3$][Lev] and [DiC_4]-[Ace] in the dissolution of cellulose. Note that a similar conclusion can be drawn with the [DiC_4][Lev] IL that can dissolve up to 10 wt% of cellulose at a water content of 14 wt% (similar dissolution rate = 2 g h^{-1}, Table 2).

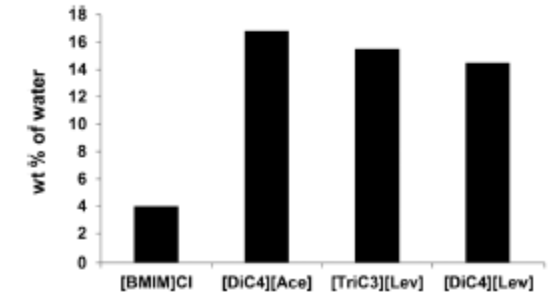

Fig. 1 Water-tolerance of tested ILs (results collected at 90 °C).

The temperature obviously plays also a pivotal role in the ability of ILs to dissolve cellulose. Similarly to common ILs such as [BMIM]Cl (solid up to 70 °C) or [BMIM]Ace (RTIL), below 70 °C no dissolution occurred. The dissolution process started at 70 °C and was complete only at a temperature within the range of 90–110 °C.

At this stage one may conclude that the [$TriC_3$][Lev] IL appears to be a promising IL for the dissolution of cellulose. In particular, the tolerance of [$TriC_3$][Lev] to water is a noticeable advantage over imidazolium-derived ILs for use on a large scale.

Physicochemical properties of ILs

To better understand the difference of dissolution ability observed between the alkylammonium ILs, we focused on the viscosity (η) and surface tension (γ) of ILs.

Viscosity is an important physical property considering the application of ILs because of its strong effect on the rate of mass transport.[17,18] Because dissolution experiments were performed at 80–110 °C, the variation of the viscosity *versus* temperature was investigated over a temperature range of 25 to 80 °C for the different ILs. As expected, the viscosities decreased with an increase of the temperature. However, at 80 °C, one should notice that most of the ILs exhibit viscosities in a similar range (0.030–0.099 Pa s). Only [DiC_4]$_2$[Suc], [DiC_4]$_2$[Tar] and [DiC_4]$_3$[Cit] exhibited a slightly higher viscosity at 80 °C (0.2–0.3 Pa s). Hence, one may conclude that viscosity of ILs is not a good descriptor to explain the greatest ability of levulinate-derived ILs to dissolve cellulose.

Next, we focused on the surface tension which provides information on the cohesive forces between liquid molecules at the surface.[19] All prepared ILs have higher surface tensions than most of the common molecular solvents (*e.g.* ethanol: 22.0, acetone: 23.5, diethyl ether: 16.6 mN m^{-1}), but lower than water (72 mN m^{-1} at 25 °C) (Table 1). Generally, the surface tension at the liquid–air interface decreases with an increase of the temperature as a result of the change of the internal cohesive energy (sum of molecular interactions, like electrostatic and van der Waals interactions).[19] All of the investigated ILs show this expected behavior: the reduction of the surface tension values at high temperature is noticeable and the temperature effect on average is the same for the different ILs (Table 1). Although surface tension of ILs is by far the only parameter governing the dissolution of cellulose in ILs, we experimentally observed a relationship between the ability of ILs to dissolve cellulose and their surface tensions measured at 80 °C. As a general trend, the dissolution of cellulose in ILs is higher for ILs exhibiting the lowest surface tension ([DiC_3]$_2$[Ita] is the only exception). In particular, whatever the cation ([DiC_4], [DiC_3] or [$TriC_3$]), we noticed that ILs exhibiting a surface tension lower than 35 mN m^{-1} dissolved the highest amount of cellulose (Fig. 2a). The same trend was also observed on the dissolution rate of cellulose, *i.e.* the lower the surface tension, the higher the dissolution rate (Fig. 2b). In a

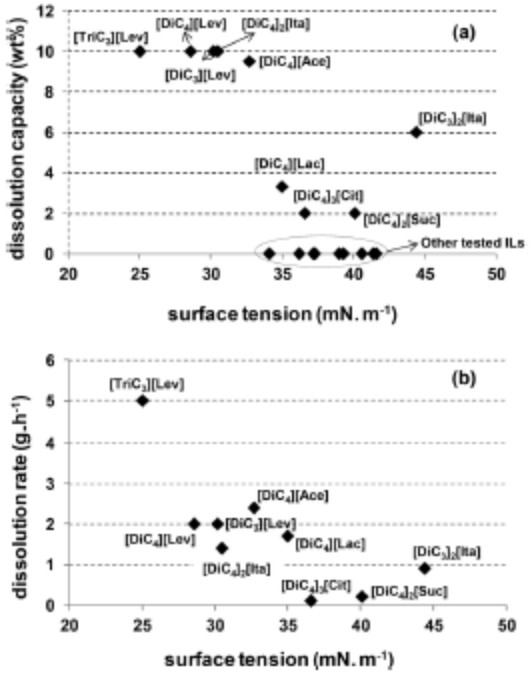

Fig. 2 Relationship between the surface tension of ILs at 80 °C and (a) their cellulose dissolution ability and (b) cellulose dissolution rate.

first approximation, one may hypothesize that ILs with a low surface tension (main feature of levulinate-derived ILs) has a low cohesive energy and are thus more prone to interact with the hydrogen bond network of cellulose.

Contribution of GVL as a renewable-sourced co-solvent

In order to benchmark the levulinate to the chloride anion, we then compared the ability of $[DiC_4][Lev]$ and $[TriC_3][Lev]$ to dissolve cellulose with that of $[DiC_4]Cl$ and $[TriC_4]Cl$. Comparison was also carried out with the well-known [BMIM]Cl often used as a reference in the current literature. Results are summarized in Table 3.

$[TriC_4]Cl$ and [BMIM]Cl are capable of dissolving similar amounts of cellulose (10 wt%) to $[TriC_3][Lev]$ and $[DiC_4][Lev]$ while the solubility of cellulose in $[DiC_4]Cl$ is much lower (3.5 wt%). The difference of dissolution rate was however clearly observed between chloride and levulinate-derived alkyl ammonium ILs (only [BMIM]Cl approached the performances of $[TriC_3][Lev]$). In particular, dissolution of cellulose in levulinate-derived alkyl ammonium ILs is faster than in chloride-derived alkyl ammonium ILs. For instance, the dissolution of cellulose is 8 times faster in $[TriC_3][Lev]$ than in $[TriC_4]Cl$ (Table 3, entries 1, 3). This result might be here ascribed to the high viscosity of chloride-derived alkyl ammonium ILs (solid at room temperature) as compared to $[TriC_3][Lev]$ and $[DiC_4][Lev]$ (RTILs), making the stirring of the solution rather difficult. For instance, using $[TriC_4]Cl$, we noticed that a gel was rapidly formed after the progressive addition of cellulose, which obviously impacts not only the dissolution rate but also the cellulose dissolution ability of $[TriC_3]Cl$. This effect is even more pronounced using $[DiC_4]Cl$. Whereas $[DiC_4]Cl$ dissolved cellulose at a higher rate than $[TriC_3]Cl$, only 3.5 wt% of cellulose can be dissolved in such IL. Here again, the system is limited by the formation of a highly viscous gel during the dissolution process that prevent the stirring of the mixture and thus the dissolution of a larger amount of cellulose. To circumvent this problem, the $[DiC_4]Cl$ was diluted with an organic solvent to overcome mass transfer limitation. Although dimethylsulfoxide can be used as a non-protic polar organic solvent to fluidify the system, we focused our attention on the use of γ-valerolactone (GVL), a sustainable chemical derived from levulinic acid.[20] Interestingly, addition of GVL to the $[DiC_4]Cl$ IL helped not only to fluidify the medium but also to increase the cellulose dissolution ability of $[DiC_4]Cl$. In particular, in a mixture $[DiC_4]Cl$–γ-valerolactone (15/1 *i.e.* 18 wt% of γ-valerolactone), 10 wt% of cellulose with a dissolution rate of 3.3 g h^{-1} was observed *vs.* 3.5 wt% at a rate of 1.6 g h^{-1} without the assistance of GVL (Table 3, entries 4, 6). Note that a higher content of GVL led to a decrease of the dissolution ability of the mixture. Promoting the effect of GVL on the dissolution of cellulose was then checked using $[TriC_3][Lev]$. Remarkably, using GVL as a co-solvent (20 wt%) allowed also the dissolution ability of $[TriC_3][Lev]$ to be improved from 10 wt% to 20 wt% while the dissolution rate remained constant (5 g h^{-1}) (Table 3, entry 7). It is worth noting that this is one of the highest dissolution capacities ever reported for ILs, demonstrating the efficiency of the proposed system. One should comment that after regeneration of cellulose (see procedure below), analysis of the reaction medium by ^1H NMR revealed that GVL remained unaltered and may be thus recycled. In addition, IR spectrum of regenerated cellulose did not reveal the presence of a carbonyl group further confirming the chemical inertness of GVL in our conditions (Fig. S1†).

Table 3 Comparison of levulinate anion with chloride anion

Entry	ILs	*T* (°C)	Wt% dissolution	Dissolution rate (g h^{-1})
1	$[TriC_3][Lev]$	90	10	5
2	$[DiC_4][Lev]$	90	10	2
3	$[TriC_4]Cl$	110	10	0.6
4	$[DiC_4]Cl$	115	3.5	1.6
5	[BMIM]Cl	90	10	4
6	$[DiC_4]Cl$/GVL	100	10	3.3
7	$[TriC_3][Lev]$/GVL	90	20	5
8	GVL	100 °C	—	—

Regeneration of cellulose and recycling experiments

Next, we have investigated the regeneration of cellulose. In this study, $[TriC_3][Lev]$ was selected. Same experiments were also conducted with $[TriC_4]Cl$ to show the beneficial effect of the levulinate anion (as compared to the chloride anion) on the regeneration of cellulose. By means of TGA analyses, we found that these two ILs are stable up to 140–150 °C, which should

also facilitate their long term recycling. Once dissolved, cellulose was regenerated from the IL by precipitation with addition of an anti-solvent which is generally ethanol, water or acetone as described in the current literature. Whereas in the case of [TriC$_4$]Cl, more than 95 wt% of cellulose was conveniently recovered by addition of acetone, water or ethanol, all attempts to recover cellulose from the [TriC$_3$][Lev] using acetone or ethanol failed mainly due to the very high solubility of cellulose in this system. Use of an excess of water was however found much more efficient to regenerate cellulose from [TriC$_3$][Lev]. In particular, addition of 10 mL of water to 1.5 g of [TriC$_3$][Lev] containing 10 wt% of cellulose led to more than 95 wt% of recovery of cellulose.

XRD analyses of regenerated cellulose (from [TriC$_3$][Lev]) confirmed that its dissolution/regeneration led to a change of its crystallinity index from 74% to 64%. XRD patterns of AVICEL PH 200 (cellulose I) is composed of three peaks.[21] The main peak observed at 22.5° corresponds to the distance between hydrogen-bonded sheets. Additionally, a broad peak located at ~16° (overlap of two peaks resulting from the contribution of I_β and I_α) is also observed together with a third peak at 34.5° stemming from the ordering along the fiber direction. After dissolution/regeneration of cellulose I (MCC) in [TriC$_3$][Lev], XRD analyses revealed that cellulose II was obtained, which is typically characterized by a broad peak at 12.1° and two main peaks at 20.5° and 22.0° (Fig. 3).[22] Change in the crystallinity from cellulose I to cellulose II was also typically observed using the mercerization process[23] or the treatment of MCC in subcritical water[24] or ball-milling in the presence of water.[25]

The change of the cellulose crystalline structure from I to II was also confirmed by ^{13}C CP/MAS NMR (Fig. S5†).[26] It should be noted that ^{13}C CP/MAS NMR also confirmed the slight decrease in crystallinity when changing cellulose I (MCC) to II. However, crystallinity values determined by NMR are lower than those determined by XRD (54% for cellulose I and 45% for cellulose II).

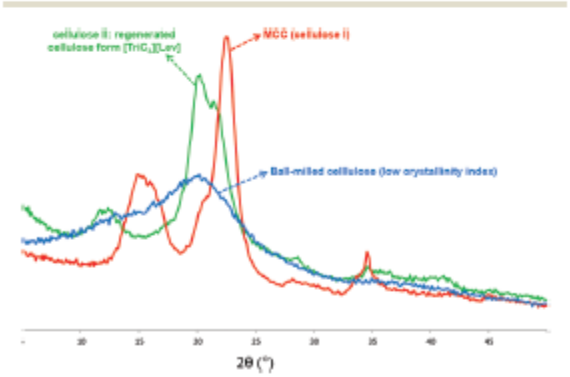

Fig. 3 XRD patterns of MCC (cellulose I), regenerated cellulose from [TricC$_3$][Lev] (cellulose II) and ball-milled cellulose ("amorphous" cellulose).

Regeneration of cellulose II after the pre-treatment of MCC in [TriC$_3$][Lev] is of huge interest for industrial application since cellulose II is known to be more readily digested than MCC or "amorphous" cellulose (commonly obtained by dry ball-milling), thus increasing again the attractiveness of such IILs.[2]

On the other hand, FT-IR of regenerated cellulose II was very similar to that of MCC (cellulose I), suggesting that glucose units were not damaged or functionalized during the dissolution process (Fig. S1†). The surface area and porous volume was also determined. Although a slight increase of the porous volume and surface area was observed after the dissolution/regeneration process, it should be however noted that results were within the uncertainty of measurements and thus were not included in this manuscript. Finally, viscosimetry analyses revealed that the degree of polymerization of cellulose remained unchanged after the dissolution process.

After removal of the anti-solvent, the recycling of [TriC$_3$][Lev] and [TriC$_4$]Cl was then attempted. Curiously, in the case of [TriC$_4$]Cl, no dissolution occurred in the second cycle when cellulose was regenerated either with water or ethanol as an anti-solvent. Analysis of the used [TriC$_4$]Cl by ^{1}H NMR (in DMSO-d$_6$) revealed that the chemical structure of the IL was preserved during the dissolution process. However, we noticed by ^{1}H NMR that it was very difficult to fully remove water or ethanol from the used [TriC$_4$]Cl, even when freeze-drying was employed (Fig. S2†). We suspect that the difficulty to remove ethanol from [TriC$_4$]Cl may be attributed to the formation of a deep eutectic or azeotropic mixture between ethanol as a hydrogen bond donor and [TriC$_4$]Cl as a hydrogen bond acceptor. At this stage we have however no evidence to support this hypothesis. To confirm the negative effect of ethanol on the dissolution of cellulose, [TriC$_4$]Cl was first dissolved in ethanol which was then removed under vacuum prior to dissolving cellulose. After this treatment, all attempts to use [TriC$_4$]Cl in the dissolution of cellulose failed, supporting the inhibiting effect of ethanol in the dissolution of cellulose. When a non-protic polar solvent such as acetone was used as an anti-solvent instead of water or ethanol, [TriC$_4$]Cl was successfully recycled at least four times without appreciable decrease of its dissolution ability, further demonstrating the "poisoning effect" of protic solvents such as ethanol and water during the recycling experiments of [TriC$_4$]Cl. These results suggest that use of polar protic solvents to regenerate cellulose from [TriC$_4$]Cl is detrimental for its recyclability, which represents a serious limitation to the use of this IL.

Conversely, as mentioned above, [TriC$_3$][Lev] is tolerant to the presence of water. Thereby, recyclability of this levulinate-derived IL is not affected by water and can be thus successfully recycled at least 4 times without intermediate purification (Fig. S3† for ^{1}H NMR spectrum of reused [TriC$_3$][Lev]). Note that NMR analysis of used [TriC$_3$][Lev] confirmed its stability.

Biodegradability

Biodegradability is a key parameter in the hazard assessment of chemicals. When new industrial chemical products are

developed, the question of sustainability is a major concern. High biodegradability is thus required to reduce bioaccumulation or persistence in the environment and to limit any possible adverse effects. Biodegradation tests were performed following the OECD 301 F procedures (Organisation for Economic Cooperation and Development OECD, 2006) by measuring the oxygen uptake.

Although the tolerance of tested ILs to the presence of water and GVL definitely contributes to increase the sustainability of this system, we evaluated the impact of the anion on the biodegradation of ILs, which is one of the main obstacles that current ILs are facing. Biodegradation is defined as the weight percent of ILs converted to CO_2 after 10 and 28 days. For the sake of clarity, the $[DiC_4]$ cation has been selected in these experiments. Results are summarized in Table 4. As expected, in the presence of a Cl^- anion, the corresponding ILs exhibited a poor biodegradability, which is also consistent with previous reports on [BMIM]Cl. However, the presence of a renewably-sourced anion greatly enhanced the biodegradation of ILs. After 28 days, biodegradation of renewably-derived ILs can be classified as follows $[DiC_4][Ace] > [DiC_4][Lac] > [DiC_4]_3[Cit]$ and $[DiC_4]_2[Suc] > [DiC_4][Lev] > [DiC_4][Sor] > [DiC_4]_2[Ita]$. Interestingly, we observed that the anion is not the only part of the IL to enter into the biodegradation process. In particular, we noticed that the anion also exerted an influence on the biodegradation of the quaternary ammonium cation. Indeed, if one may consider that only the renewably-sourced anion is biodegraded, then the biodegradability would have followed the wt% proportion of the anion in the IL (Table 4). For most of the investigated ILs in our study, the biodegradation exceeds the wt% of the anions, implying that the cation is concomitantly biodegraded. In particular, this is clearly highlighted by the good biodegradation of $[DiC_4][Ace]$, keeping in mind that the reference material of the test is sodium acetate (Table 4, entry 2). In the literature, very few studies or data are available on the biodegradation of organic acid-derived quaternary ammonium. The short set of data available attest that the biodegradation of the ammonium cation also obviously depends on the cation structure (such as the number of methylene groups or the length of some alkyl groups)[27] but also on the absence of toxicity generated by the biodegradation of the anions. According to the OCDE 301F directive, $[DiC_4]$-[Lev] and $[DiC_4][Ace]$ are thus considered as biodegradable solvents, further increasing the sustainability of these systems.

Table 4 Biodegradation of selected ILs

		% Biodegradation		
Entry	ILs	10 days	28 days	Wt% of the anion
1	$[DiC_4]Cl$	5	5	—
2	$[DiC_4][Ace]$	65	77	28
3	$[DiC_4][Lev]$	21	66	42
4	$[DiC_4]_2[Ita]$	36	45	29
5	$[DiC_4][Lac]$	41	72	36
6	$[DiC_4]_3[Cit]$	65	69	29
7	$[DiC_4][Sor]$	16	54	41
8	$[DiC_4]_2[Suc]$	65	69	43

Experimental

Dissolution of cellulose. In a typical experiment, 1.5 g of IL (or a mixture of the IL with GVL or water) was first heated under stirring in a sealed glass vial at the desired temperature (see Table 2). Then, 2 wt% of cellulose AVICEL PH200 was added into the IL and the heating time was prolonged until complete dissolution of cellulose was observed. When cellulose was completely dissolved, extra amounts of cellulose were then progressively added until the limit of solubility was reached. Please note that cellulose needs to be added progressively, otherwise the dissolution ability of ILs becomes lower. ILs that are unable to dissolve at least 2 wt% of cellulose within 10 h of heating were considered as not efficient.

Please note that all attempts to dissolve wheat straw or poplar wood in such ILs failed, indicating that use of these ILs is at the moment only restricted to cellulose.

Regeneration of cellulose. After complete dissolution of cellulose in the IL, cellulose was regenerated by addition of an antisolvent, preferentially water when using levulinate-derived ILs. In a typical procedure involving $[TriC_3][Lev]$, 10 mL of water was added to the hot solution of $[TriC_3][Lev]$ (1.5 g) containing 10 wt% of cellulose. Note that for some of the ILs described in the manuscript (mostly chloride-derived ILs), acetone or ethanol were also used to regenerate cellulose. The regenerated cellulose was then filtered off and successively washed with water and acetone to remove residual ILs. Crystallinity and degree of polymerization of regenerated cellulose was then checked by XRD and FTIR analyses, respectively.

Recycling of cellulose. After regeneration and filtration of cellulose II, water was removed under reduced pressure. Then, the recovered IL was directly reused without any further purification using the same procedure as described above for dissolution experiments. Although tested ILs were recycled at least five times without appreciable decrease of their dissolution ability, we would like to point out that the long term recycling of ILs is more problematic like it is also observed with imidazolium-derived ILs (accumulation of impurities stemming from the slight degradation of cellulose).

Conclusions

Here we report that the use of levulinate as a renewably-sourced anion allowed designing various technical grade room temperature short chain (C_3 and C_4) alkyl ammonium-derived ILs that are capable of dissolving cellulose AVICEL with a high efficiency. In particular, the best systems are capable of dissolving up to 20 wt% of cellulose at a dissolution rate of 5 g h^{-1}, which is among the highest dissolution capacity reported in the current literature. After regeneration, the crystalline structure of MCC was changed from I to II, a key point known to improve the digestibility of cellulose by cellulases. Although the concept of cellulose decrystallization in ionic liquids is

known, it is our opinion that our work offers significant scientific breakthroughs in this field of chemistry as compared to the previous methodologies such as (1) their tolerance to the presence of up to 18 wt% of water which is one of the main drawbacks that common ILs are currently facing for use on a large scale, (2) their tolerance to the presence of 20 wt% of GVL as a renewably-sourced co-solvent and (3) their biodegradability which dramatically increases the eco-efficiency of these systems.

Among the different combinations, a mixture composed of technical grade [TriC$_3$][Lev] and 20 wt% of GVL afforded similar results in terms of both dissolution ability and dissolution rate to imidazolium-based IL. Combination of levulinate with other cations as well as the evaluation of these mixtures in lignocellulosic biomass pre-treatment is now under investigation in our groups.

Acknowledgements

The authors are grateful to the CNRS, the French Ministry of Research and ARD for their financial support. The authors gratefully acknowledge the financial support by the Champagne-Ardenne Region and FEDER for this project (Innobioref program). Florent Boissou and Andrea Mühlbauer also thank ARD for the funding of their PhD.

Notes and references

1 (*a*) S. V. de Vyver, J. Geboers, P. A. Jacobs and B. F. Sels, *ChemCatChem*, 2011, **3**, 82–94; (*b*) P. Gallezot, *Chem. Soc. Rev.*, 2012, **41**, 1538–1558; (*c*) A. Corma, S. Iborra and A. Velty, *Chem. Rev.*, 2007, **107**, 2411–2502; (*d*) M. Stöcker, *Angew. Chem., Int. Ed.*, 2008, **47**, 9200–9211; (*e*) M. Mascal and E. B. Nikitin, *Angew. Chem., Int. Ed.*, 2008, **47**, 7924–7926.

2 A. J. Sugiyama, R. Vuong and R. Chanzy, *Macromolecules*, 1991, **24**, 4168–4175.

3 (*a*) N. Mosier, C. Wyman, B. Dale, R. Elander, Y. Y. Lee, M. Holtzapple and M. Ladisch, *Bioresour. Technol.*, 2005, **96**, 673–686; (*b*) L. C. Sousa, S. P. Chundawat, V. Balan and B. E. Dale, *Curr. Opin. Biotechnol.*, 2009, **20**, 339–347; (*c*) M. FitzPatrick, P. Champagne, M. F. Cunningham and R. A. Whitney, *Bioresour. Technol.*, 2010, **101**, 8915–8922.

4 As selected recent review see: H. Tadesse and R. Luque, *Energy Environ. Sci.*, 2011, **4**, 3913–3929.

5 (*a*) Q. Zhang, M. Benoit, K. De Oliveira Vigier, J. Barrault, G. Jégou, M. Philippe and F. Jérôme, *Green Chem.*, 2013, **13**, 963–969; (*b*) J. Mikkola, A. Kirilin, J. Tuuf, A. Pranovich, B. Holmbom, L. M. Kustov, D. Y. Murzin and T. Salmi, *Green Chem.*, 2007, **9**, 1229–1237; (*c*) R. Sun and J. Tomkinson, *Ultrason. Sonochem.*, 2002, **9**, 85–93; (*d*) R. Sun and J. Tomkinson, *Carbohydr. Polym.*, 2002, **50**, 263–271; (*e*) R. Velmurugan and K. Muthukumar, *Bioresour. Technol.*, 2011, **102**, 7119–7123; (*f*) P. C. S. F. Tiescher, M. R. Sierakowski, H. Westfahl and C. A. Tischer, *Biomacromolecules*, 2010, **11**, 1217–1224.

6 (*a*) N. Meine, R. Rinaldi and F. Schüth, *ChemSusChem*, 2012, **5**, 1449–1454; (*b*) S. M. Hick, C. Griebel, D. T. Restrepo, J. H. Truitt, E. J. Buker, C. Bylda and R. G. Blair, *Green Chem.*, 2010, **12**, 468–474; (*c*) M. Benoit, A. Rodrigues, Q. Zhang, E. Fourré, K. De Oliveira Vigier, J.-M. Tatibouët and F. Jérôme, *Angew. Chem., Int. Ed.*, 2011, **50**(38), 8964–8967; (*d*) Q. Zhang and F. Jérôme, *ChemSusChem*, 2013, **6**(11), 2042–2044.

7 A. Pinkert, K. N. Marsh and S. Pang, *Ind. Eng. Chem. Res.*, 2010, **49**, 11121–11130.

8 S. Chrapava, D. Touraud, T. Rosenau, A. Potthast and W. Kunz, *Phys. Chem. Chem. Phys.*, 2003, **5**, 1842–1847.

9 M. Wada, M. Ike and K. Tokuyasu, *Polym. Degrad. Stab.*, 2010, **95**, 543–548.

10 (*a*) P. Walden, *Bull. Acad. Imper. Sci.*, 1914, 1800. C. Graenacher, *US Patent* 1943176, 1934.

11 P. R. R. Swatloski, S. K. Spear, J. D. Holbrey and R. D. Rogers, *J. Am. Chem. Soc.*, 2002, **124**, 4974–4975.

12 As selected articles only see: (*a*) S. D. Zhu, Y. X. Wu, Q. M. Chen, Z. Yu, C. Wang, S. Jin, Y. Ding and G. Wu, *Green Chem.*, 2006, **8**(4), 325–327; (*b*) A. Pinkert, K. N. Marsh, S. Pang and M. P. Staiger, *Chem. Rev.*, 2009, **109**(12), 6712–6728.

13 (*a*) B. Lindman, G. Karlström and L. Stigsson, *J. Mol. Liq.*, 2010, **156**, 76–81 and references cited therein; (*b*) H. Wang, G. Gurau and R. D. Rogers, *Chem. Soc. Rev.*, 2012, **41**, 1519.

14 L. Leclercq, V. Nardello-Rataj, G. Rauwel and J.-M. Aubry, *Eur. J. Pharm. Sci.*, 2010, **41**, 265–275.

15 T. Erdmenger, J. Vitz, F. Wiesbrock and U. S. Schubert, *J. Mater. Chem.*, 2008, **18**, 5267–5273.

16 J. M. Crosthwaite, M. J. Muldoon, J. K. Dixon, J. L. Anderson and J. F. Brennecke, *J. Chem. Thermodyn.*, 2005, **37**, 559–568.

17 D. Rooney, J. Jacquemin and R. Gardas, in *Ionic Liquids*, ed. B. Kirchner, Springer, Berlin, Heidelberg, 2010, vol. 290, pp. 185–212.

18 Z.-B. Zhou, H. Matsumoto and K. Tatsumi, *Chem.–Eur. J.*, 2006, **12**, 2196–2212.

19 M. Tariq, M. G. Freire, B. Saramago, J. A. P. Coutinho, J. N. C. Lopes and L. P. N. Rebelo, *Chem. Soc. Rev.*, 2012, **41**, 829–868.

20 D. M. Alonso, S. G. Wettstein and J. A. Dumesic, *Green Chem.*, 2013, **15**(3), 584–595.

21 M. Wada, T. Kondo and T. Okano, *Polym. J.*, 2003, **35**, 155–159.

22 G. Cheng, P. Varanasi, C. li, H. Liu, Y. B. Melnichenko, B. A. Simmons, M. S. Kent and S. Singh, *Biomacromolecules*, 2011, **12**, 933–941.

23 A. C. O'sullivan, *Cellulose*, 1997, **4**, 173–207.

24 S. Kumar, R. Gupta, Y. Y. Lee and R. B. Gupta, *Bioresour. Technol.*, 2010, **101**, 1337–1347.

25 M. Ago, T. Endo and T. Hirotsu, *Cellulose*, 2004, **11**, 163–167.

26 For comparative data on ^{13}C CP/MAS NMR of cellulose II, please refer to: (*a*) G. Zuckerstätter, G. Schild, P. Wollboldt,

T. Röder, H. K. Weber and H. Sixta, *Lenzinger Berichte*, 2009, **87**, 38–46; (*b*) R. H. Newman and T. C. Davidson, *Cellulose*, 2004, **11**, 23–32.

27 S. Stolte, S. Steudte, O. Areitioaurtena, F. Pagano, J. Thöming, P. Stepnowski and A. Igartua, *Chemosphere*, 2012, **89**, 1135–1141.